ARTICLE IN PRESS Available online http://jopr.mpob.gov.my/category/article-in-press/

Journal of Oil Palm Research

Vol. 36 (3) • September 2024



REVIEW ARTICLE

Autonomous Harvesting Robot for Oil Palm Plantation: A Review



eISSN 2811-4701

MPOB

JOURNAL OF OIL PALM RESEARCH (formerly known as ELAEIS)

JOURNAL OF OIL PALM RESEARCH (JOPR), an international refereed journal, carries full-length original research papers, short communications and scientific review papers on various aspects of oil palm and palm oil and other palms. JOPR is published four times per year, *i.e.* March, June, September and December.

© Malaysian Palm Oil Board (MPOB), 2024

All rights reserved. No part of this publication may be reproduced in any form or by any means without the written permission of MPOB.

Impact Factor:
1.2
data from *2023 Journal Citation Report*® Science Edition
– A Clarivate Analytics product.

For more information on advertisement for the JOPR, please write to:

Editor-in-Chief
Journal of Oil Palm Research
Malaysian Palm Oil Board
6, Persiaran Institusi, Bandar Baru Bangi
43000 Kajang, Selangor, Malaysia

Tel: *+603-8769 4400*
E-mail: *jopr.admin@mpob.gov.my*
Website: *jopr.mpob.gov.my*

DISCLAIMER
Views of writers expressed in this publication are not necessarily endorsed by or represent the views of MPOB.

MPOB Press
Malaysian Palm Oil Board
6, Persiaran Institusi, Bandar Baru Bangi
43000 Kajang, Selangor, Malaysia
Tel: +603-8769 4400 | Fax: +603-8925 9446
E-mail: *jopr.admin@mpob.gov.my*

JOURNAL OF OIL PALM RESEARCH

Vol. 36 (3) September 2024

CONTENTS

REVIEW ARTICLES

349 Autonomous Harvesting Robot for Oil Palm Plantation: A Review
Teoh Kean Hao and Lai Nai Shyan

RESEARCH ARTICLES

367 The Influence of Flowering Beneficial Plant, *Turnera subulata* on the Insect Natural Enemies' Abundance in Relation to Oil Palm Bagworm Occurrence in Bagan Datuk, Perak, Malaysia
Siti Nurulhidayah Ahmad; Saharul Abillah Mohamad; Othman Arshad and Mohamed Mazmira Mohd Masri

380 Performance of Selfed and Intercrossed Oil Palm Deli Ulu Remis Progenies Based on Selected Agronomic Traits
Norziha, A; Zamri, Z; Zulkifli, Y; Fadila, A M; Marhalil, M and Mohd Din, A

393 Biology and Population Dynamics of Adult *Sagalassa valida* Walker, 1856 (Lepidoptera: Brachodidae), the Oil Palm Root Borer in Colombia
Carlos Andrés Sendoya-Corrales; José Luis Pastrana-Sanchez; Jesús Arvey Matabanchoy Solarte; Álex Enrique Bustillo Pardey; Miriam Rosero Guerrero and Anuar Morales Rodríguez

409 Pollination Activity of *Elaeidobius kamerunicus* Faust in Oil Palm and Cocoa (*Theobroma Cacao* L.) Intercropping System in India
L Saravanan; V Suchitra and T Phanikumar

420 Oil Palm Pollen Compatibility with OxG Hybrids in Ecuador
María Raquel Meléndez-Jácome; Andrés Alejandro Galvis-Correa; Pamela Elizabeth Mantilla-Valdivieso; Franco Estéfano-Tobar; Mauricio Andrés Racines-Oliva; Trevor Anthony Jackson and Wilson Vasquez-Castillo

432 Identification of the Oil Palm Bagworm, *Mahasena corbetti* Tams (Lepidoptera: Psychidae) via Molecular Techniques and Its Biocontrol Assay Using *Bacillus thuringiensis*
Mohd Shawal Thakib Maidin; Amalia Mohd Hashim; Noorhazwani Kamarudin; Siti Nurulhidayah Ahmad; Mohamed Mazmira Mohd. Masri; Raha Abdul Rahim and Syari Jamian

445 Effect of Graphite Microparticles as Additive in an Indirect Diesel Engine Fuelled with Pure Palm Oil
Rico Aditia Prahmana; Prihadi Setyo Darmanto; Iman Kartolaksono Reksowardojo; Teuku Meurah Indra Riayatsyah; Achmad Gus Fahmi; Firman Bagja Juangsa; Tirto Prakoso; Abdi Hanra Sebayang; Muhammad Syaukani; Zido Yuwazama and Wiagil Tunku Nastiti Widoyoko

456 Renewable Energy and Greenhouse Gases Emission Reduction Potential of Biogas from Palm Oil Mill Effluent
Abu Bakar Nasrin; Abdul Aziz Abdul Raman; Mohamad Azri Sukiran; Nurul Adela Bukhari; Archina Buthiyappan; Vijaya Subramaniam; Astimar Abdul Aziz and Soh Kheang Loh

469 Evaluation of Oil Palm Frond for Biobutanol Production by Different *Clostridia* Species
Abdurrahman Abubakar; Madihah Md Salleh; Adibah Yahya; Huszalina Hussin; Chong Chun Shiong; Shaza Eva Mohamad and Suraini Abd Aziz

484 Effect of Reaction Time on Various Properties of Palm Oil Biodiesel in Continuous Biodiesel Reactor
V Palaniselvam; S Sindhuja Rajan; S Sriramajayam and D Ramesh

495 Selective Cytotoxicity Effects of *R*-Glycidol and *S*-Glycidol on Vero and HCT 116 Cells in Evaluating the Incidence of Glycidyl Esters in Edible Oils and Fats
Siti Nur Syahirah Nor Mahiran; Nanthini Ravi; Alam Mahboob and Nurul Huda Abd Kadir

510 Comparative Study of Palm-based Milk Yoghurt with Dairy and Coconut Milk Yoghurt Based on Proximate, Texture and Amino Acid Analysis
Hadi Akbar Dahlan and Norrakiah Abdullah Sani

524 N-Alkane Profiles of Lard and Vegetable Oils, and Their Chemometrics Differentiation
Nur Ain Syaqirah Sapian; Muhamad Aidilfitri Mohamad Roslan; Amalia Mohd Hashim; Yanty Noorzianna Abdul Manaf; Mohd Nasir Mohd Desa; Murni Halim; Muhamad Shirwan Abdullah Sani; Mohd Termizi Yusof; Mohd Sabri Pak Dek and Helmi Wasoh

SHORT COMMUNICATION

534 Palm Oil Mill Effluent (POME) as a Source of Biofuels and Value-added Products via Oil Recovery: A Review
Yee Mun Tang; Kok Tat Tan and Lai Peng Wong

Cover picture:
1. A terrain mapping robot prototype.
2. MPOB's prototype of an articulated harvesting machine.

EDITORIAL BOARD

(1 January 2024 – 31 December 2025)

Datuk Dr. Ahmad Parveez Ghulam Kadir
Malaysia (Editor-in-Chief)

Dr. Carl Traeholt
Malaysia

Prof. Dr. Matthias Finkbenier
Germany

Prof. Dr. Dirk Prufer
Germany

Prof. Dr. Douglas G Hayes
USA

Prof. Dr. Tan Chin Ping
Malaysia

Prof. Dr. Takashi Hirano
Japan

Dr. Ahmad Aldrie Amir
Malaysia

Prof. Jonathan Wong Woon Chung
Hong Kong

Dr. Tristan Durand Gasselin
France

Prof. Fikret Isik
USA

Prof. Dr. Jan Stenlid
Sweden

PUBLICATION COMMITTEE

CHAIRPERSON
Datuk Dr. Ahmad Parveez Ghulam Kadir

SECRETARY
Dr. Anita Taib

MANAGING EDITOR
Ts. Dr. Gan Sin Yee

PRODUCTION EDITOR
Dr. Laziana Ahmad

COMMITTEE MEMBERS
Dr. Zainab Idris
Dr. Ramle Moslim
Dr. Sivaruby Kanagaratnam
Dr. Astimar Abdul Aziz
Dr. Rajinder Singh
Dr. Meilina Ong Abdullah
Dr. Aki @ Zaki Aman
Dr. Zafarizal Aldrin Azizul Hasan
Ruba'ah Masri
Johari Minal
Mohd Saufi Awang
Iptisam Abdul Wahab

REVIEW ARTICLE

Journal of Oil Palm Research Vol. 36 (3) September 2024 p. 349-366
DOI: https://doi.org/10.21894/jopr.2024.0008

AUTONOMOUS HARVESTING ROBOT FOR OIL PALM PLANTATION: A REVIEW

TEOH KEAN HAO[1]* and LAI NAI SHYAN[1]

ABSTRACT

Due to the continuous labour crisis, the oil palm industry in Malaysia has lost an estimated worth of RM10.46 billion unharvested fruit in the first five months of the year 2022. A robotic system in automating the harvesting process of the oil palm fresh fruit bunches (FFB) is proposed to solve the existing problems related to oil palm harvesting and further enhance the development of oil palm harvesting technologies. This article aims to review the six identified key technologies for solving the technological challenges in the development of this robotic system. The key technologies are as follows: (1) Oil palm ripeness detection; (2) oil palm cutting mechanism; (3) tree climbing mechanism; (4) motion trajectory planning for fruit harvesting manipulator; (5) localisation; (6) navigation and obstacle avoidance. Six criteria for successful implementation of the proposed harvesting robot are discussed followed by recommendations on the type of technology used. The integration of these technologies as a complete robotic system is analysed. Prediction on the trend of technological development in oil palm harvesting is discussed.

Keywords: climbing mechanism, motion trajectory planning, navigation, oil palm harvesting mechanisation, ripeness detection.

Received: 28 May 2023; **Accepted:** 17 November 2023; **Published online:** 23 January 2024.

INTRODUCTION

Overview of the Oil Palm Industry

The oil palm industry is one of most significant commodity crops in Malaysia, with exports totalling more than RM64.84 billion in 2019 (Parveez *et al.*, 2020). With estimated oil palm plantation area of 5.9 million hectares, the industry is working harder than ever to address concerns about sustainability and safety that have been raised on a worldwide scale. Furthermore, the oil palm plantation in Malaysia is accountable for the employment of 428 000 workers as of May 2017 (Tang and Al Qahtani, 2019). According to Meijaard *et al.* (2020), palm oil is subjected to about 40% of the present global yearly demand for vegetable oil for use in food and fuel. Therefore, improving the overall efficiency in oil palm industry will provide huge positive impact to the world.

[1] School of Engineering,
Asia Pacific University of Technology and Innovation,
Technology Park Malaysia, Bukit Jalil,
57000 Kuala Lumpur, Malaysia.

* *Corresponding author e-mail: TP044741@mail.apu.edu.my*

Problems Related to Oil Palm Harvesting

Labour shortage. According to FMT Reporters, (2022), the oil palm plantation was short of 28 940 workers, each of whom could pick 2 t of fresh fruit bunches (FFB) every day. Due to the continuous labour crisis, the oil palm industry in Malaysia has lost an estimated worth of RM10.46 billion unharvested FFB from January to May of year 2022. In Malaysia, foreign workers make up more than 75% of the total workforce in oil palm plantations (Channel News Asia, 2022). The difficulty in hiring foreign workers, particularly those from Indonesia, occurs because of immigration restrictions brought on by COVID-19 pandemic.

The work environment in oil palm plantations is considered as 4-Ds (dirty, difficult, dangerous, demeaning) by Malaysians (SOPPOA, 2021). According to the study conducted by Bhuanantanondh *et al.* (2021), 88% of oil palm harvesting workers suffered a prevalence of musculoskeletal disorders (MSDs) in year 2020. The most affected body parts of MSDs for oil palm harvesting workers include the lower back, shoulder, neck, upper back, and hand. The common risk factors of MSDs in oil palm harvesting include lifting and

carrying heavy FFB, extended or repeated stooping, and repetitive muscle movements. Moreover, the lack of ergonomics in the oil palm harvesting process has caused high rates of developing MSDs on workers in oil palm plantations as compared with other agricultural sectors (Bhuanantanondh *et al.*, 2021).

Most oil palm plantations have uneven terrain, which is usually located in rough and sloping areas (Sowat *et al.*, 2018). Therefore, accessibility by workers to the oil palm plantation is the biggest factor limiting the use of mechanised harvesting equipment. Therefore, manual labour harvesting is still regarded as the most effective choice.

FFBs of tall oil palm trees are difficult to harvest. The older oil palm trees can grow up to 20 m in height (Britannica, 2021). Highly skilled workers are required to harvest the FFB at this height. Despite the high yield of these older oil palm trees, it is claimed to be not economical to harvest them. Therefore, the tall oil palm trees will be left unharvested in the plantation and pending to be replanted. This issue has been solved by planting the dwarf variant of the oil palm, which can grow up to 6 m in height (Bernama, 2021). However, replanting the oil palm trees takes time and there is still large percentage of tall oil palm tree that remains unharvested.

Trends in Development of Oil Palm Harvesting Method

Malaysia has progressed through several harvesting technologies, from manual to semi-mechanised to fully mechanised. The manual harvesting process is usually done by using two types of tools: Chisel and sickle. Chisels are normally used for harvesting FFB from shorter trees, which are below 3 m in height. For taller trees, a sickle with long pole is used. Handling these tools, especially those with long flexible pole, is a very difficult and dangerous task (Sowat *et al.*, 2018). Therefore, the workers must possess exceptional tool handling skills in addition to having sufficient energy to complete the cutting task for taller oil palm trees.

To solve the issues related to manual harvesting, semi-mechanised tools are developed which are more economical and efficient. The Cantas motorised cutter was developed by the Malaysian Palm Oil Board (MPOB), capable of harvesting FFB at 4.5-6.0 m in height (Zahid and Firdaus, 2018). Cantas enables 37% faster cutting than using a traditional manual sickle with pole, while productivity increased from 4.19 to 11.60 t FFB/day (Sowat *et al.*, 2018). Although Cantas had demonstrated to boost harvesting effectiveness, however this technology possesses various limitations. Firstly, the maximum reach for Cantas is only 6.0 m while the height of oil palm trees can go up to 20.0 m. Secondly, the workers using this mechanised cutter are exposed to a high magnitude of vibrations. Exposure to these vibrations for an extended period may cause the development of Hand-Arm Vibration Syndrome (HAVS), affecting the health of the workers (CCOHS, 2017) (*Figure 1*).



Source: Shuib *et al.* (2011).

Figure 1. FFB harvesting operation with Cantas motorised cutter.

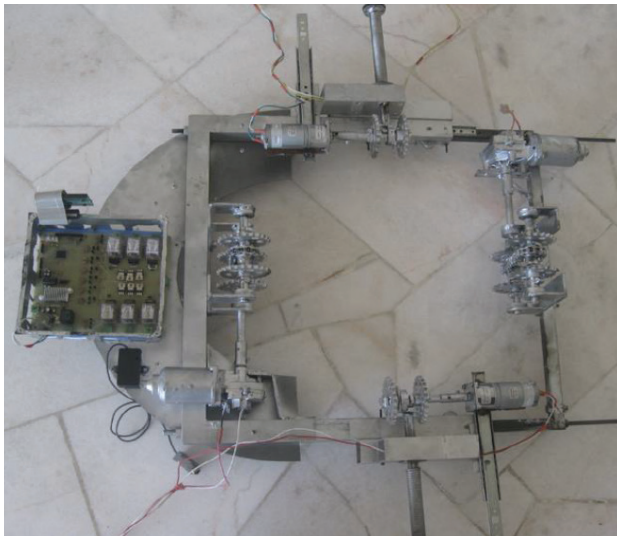
Other than semi-mechanised harvesting, there are several attempts that have been made on fully mechanised harvesting techniques (*Figure 2*). One of the techniques is using a harvesting machine with a cutting mechanism mounted to the end effector of a boom (Sowat *et al.*, 2018). These cutting mechanisms included hydraulic scissors, circular blades and wire-cutting mechanism. The boom of the harvesting machine was mounted onto a tracked vehicle powered by a 31.5 hp diesel engine with a loading capacity of 500 kg (Shuib *et al.*, 2011). This technique achieved the productivity of harvesting 4 to 6 t FFB/day. However, it had a limited maximum height that the cutting mechanisms could reach. Increase in the maximum reach would require the use of longer boom, which would be heavier, larger in size and less cost-effective. Moreover, the relatively large size of the vehicle also caused accessibility issues, especially on narrow and rough terrain. Furthermore, heavy vehicles, which are 10 to 30 t in weight, often cause soil compaction when running through the oil palm estate (Sowat *et al.*, 2018). This would in turn degrade the soil quality and reduce the crop yields.



Source: Shuib *et al.* (2011).

Figure 2. Fully mechanised harvesting machine.

Another approach to fully mechanised harvesting is by using a tree climbing robotic harvester (Shokripour *et al.*, 2010). This climbing robot was designed to be as light as possible, hence, reducing the amount of energy required to reach the top of the tree as shown in *Figure 3*. Further details on the tree climbing mechanisms are discussed under the "*Tree Climbing Mechanism*" section. The advantage of using climbing robot in oil palm FFB harvesting is that it can reach the top of the oil palm tree regardless of the height, which solves the limitations of other harvesting methods. According to Sowat *et al.* (2018), the current climbing robots could only climb trees with smooth surfaces. However, oil palm trees are usually full of frond stubs, which is the results of pruned fronds and forms irregular surface on the entire trunk. Hence, a reliable tree climbing mechanism for oil palm tree has not been fully developed to this date.



Source: Shokripour *et al.* (2010).

Figure 3. Oil palm climbing robot.

Research Problem

A robotic system in automating the harvesting process of the oil palm FFB is proposed to further enhance the development of harvesting technologies and solve the existing problems. The technological challenges for developing this robotic system are discussed as follows.

Difficulty of a mobile robot to manoeuvre autonomously in oil palm plantation. The terrain of oil palm plantations can be categorised into four major types: Flat, hilly, peat and sandy (Teoh, 2000). The hilly terrains are less accessible to the mobile robot especially on wheels or tracks due to the limited climbing angles. Besides, the terrains with peat soil are soft, damp, and uneven. This will cause the mobile robot to have a high chances of getting stuck when manoeuvring through this area. Moreover, the existence of largely grown vegetation on the ground in oil palm plantations will cause difficulty for sensors to detect the available path.

Inaccuracy of existing robot localisation technology for oil palm plantation. Localisation refers to the ability of the robot to determine its location on the plantation. Most of the existing robot localisation technology revolves around the use in urban areas (Georgiev and Allen, 2004), unmanned aerial vehicles (Back *et al.*, 2020) or ships (Medina *et al.*, 2018). Since the working conditions of these areas differ from the oil palm plantation, direct implementation of the existing localisation techniques will cause incompatibility and inaccuracies in the result. Therefore, adaptation and modification of these localisation techniques are required before implementing them in the oil palm plantation.

Non-robust climbing mechanism for climbing robot to move up and down the oil palm tree. Most of the existing climbing mechanisms are designed for climbing trees with relatively circular shape of trunk. Furthermore, these mechanisms are very limited to climbing the trees with a specified range of diameter. Since the trunks of oil palm trees have irregular shapes and the diameter variation is relatively large between each tree, the existing tree climbing mechanisms are not robust enough to be implemented for the oil palm tree (Tan *et al.*, 2014). Therefore, modifications and improvements to the

existing climbing mechanisms must be made so that it is feasible to be used on oil palm trees.

Non-existence of robotic harvesting manipulator that can detect and harvest the oil palm FFB autonomously. As discussed earlier, all the existing solutions for oil palm harvesting require manpower to harvest manually or operate on the semi-mechanised equipment. Thus, high labour cost is still required for oil palm harvesting. This problem can be solved by implementing the state-of-the-art robotic manipulator technology such that robots are used to harvest the oil palm FFB autonomously, hence, minimising the labour cost. Inaccuracy of ripeness classification for oil palm FFB in field conditions. Human judgement is the current way of determining the oil palm FFB ripeness in the plantation. As the judgement varies between individuals, there is a lack of consistency in the classification of oil palm FFB ripeness (Rismen *et al.*, 2020). Furthermore, there is a lack of existing research on the development of techniques that can classify the FFB ripeness with high accuracy and consistency in the field conditions.

Purpose of this Review

Six key technologies are identified to solve the technological challenges stated in previous section. These technologies are (1) oil palm ripeness detection; (2) oil palm cutting mechanism; (3) tree climbing mechanism; (4) motion trajectory planning for fruit harvesting manipulator; (5) localisation; and (6) navigation and obstacle avoidance. The aim of this article is to review the state-of-the-art development of these key technologies towards the development of autonomous robots for harvesting oil palm FFB. Besides, a set of criteria for the successful implementation of these technologies will be discussed. Further analysis is conducted on the integration of these technologies as a complete robotic system followed by predicting the trend of technological development in oil palm harvesting.

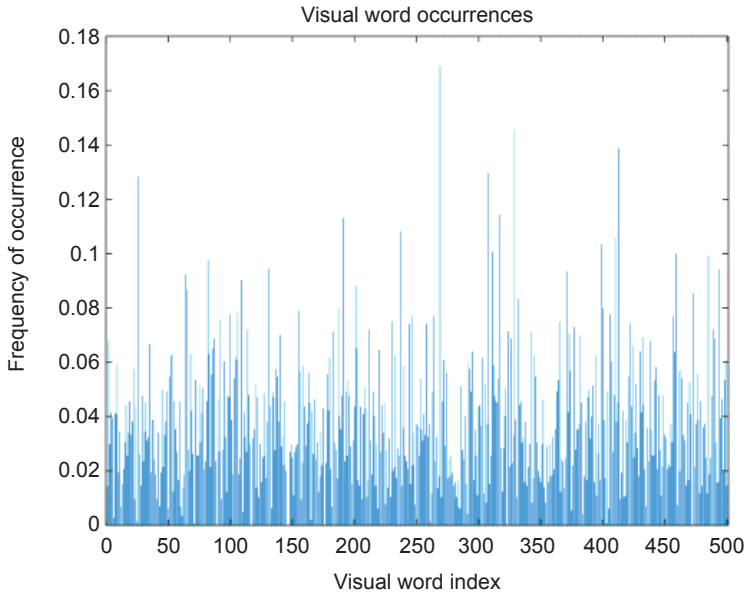
KEY TECHNOLOGIES ON AUTONOMOUS OIL PALM HARVESTING

Oil Palm FFB Ripeness Detection

In general, the ripeness of the oil palm FFB can be classified into five categories: Unripe, underripe, ripe, overripe, and rotten. The ripeness level has significant relationships with the quality and oil content of the oil palm FFB. The oil content of the FFB is highest at the ripe stage while it reduces when reaching the overripe stage. Therefore, it is crucial to determine the FFB ripeness and only harvest the ripe FFB to ensure the maximum quality and yield of palm oil (*Table 1*).

Dan *et al.* (2018) proposed a technique of identifying the oil palm FFB ripeness through Raman spectroscopy. This technique worked by measuring the vibrational characteristics of molecules while exposing the oil palm FFB samples with laser light. The result from this study showed that the Raman intensity at identified wavenumbers was the highest at the ripe stage, with the trend of increasing value from unripe to ripe stage, then decreasing from ripe to rotten stage. Raj *et al.* (2021) further implemented this finding with the use of machine learning methods to classify the ripeness automatically. This research achieved a classification accuracy of 100% by using fine k-nearest neighbours (KNN) classifier. One of the advantages of using Raman spectroscopy to determine the oil palm FFB ripeness was that it can provide sensitive, fast, and significant amounts of data for classifying the fruit ripeness level. However, the results obtained from this study were done in a controlled environment, where the outcome was not verified under field conditions. Furthermore, using Raman spectroscopy to classify the oil palm FFB ripeness requires the fruit to be sliced before measuring the Raman intensity, which is impractical to use in field conditions.

The oil palm FFB ripeness can also be classified through image analysis methods. According to Shuwaibatul *et al.* (2019), the ripeness stages of oil palm fruit could be classified by using colour features and bag of visual words (BOVW). In the colour features method, the image dataset was segmented by using the K-mean clustering algorithm to filter out the fruit and spikes from the image. Hue measurements from the segmented images were used as the input feature for support vector machine (SVM) to classify the ripeness of oil palm FFB. The BOVW method used the speeded up robust features (SURF) algorithm to convert the images into feature vectors. The BOVW was formed after clustering the feature vectors by using K-means Clustering algorithm. The BOVW was the frequency representation of the visual word occurrences in an image as illustrated in *Figure 4*. The SVM classifier was developed to classify the oil palm FFB ripeness based on the extracted BOVW feature. This study obtained average classification accuracy of 57% and 70% by using the colour features and BOVW methods respectively. Using the image analysis method to classify the oil palm FFB ripeness has the advantage of relatively long-distance classification. Besides, preparation of the oil palm fruit samples was not required in this method. However, the classification accuracy of this method was relatively low as the classification algorithms were sensitive to ambient light when taking the images.



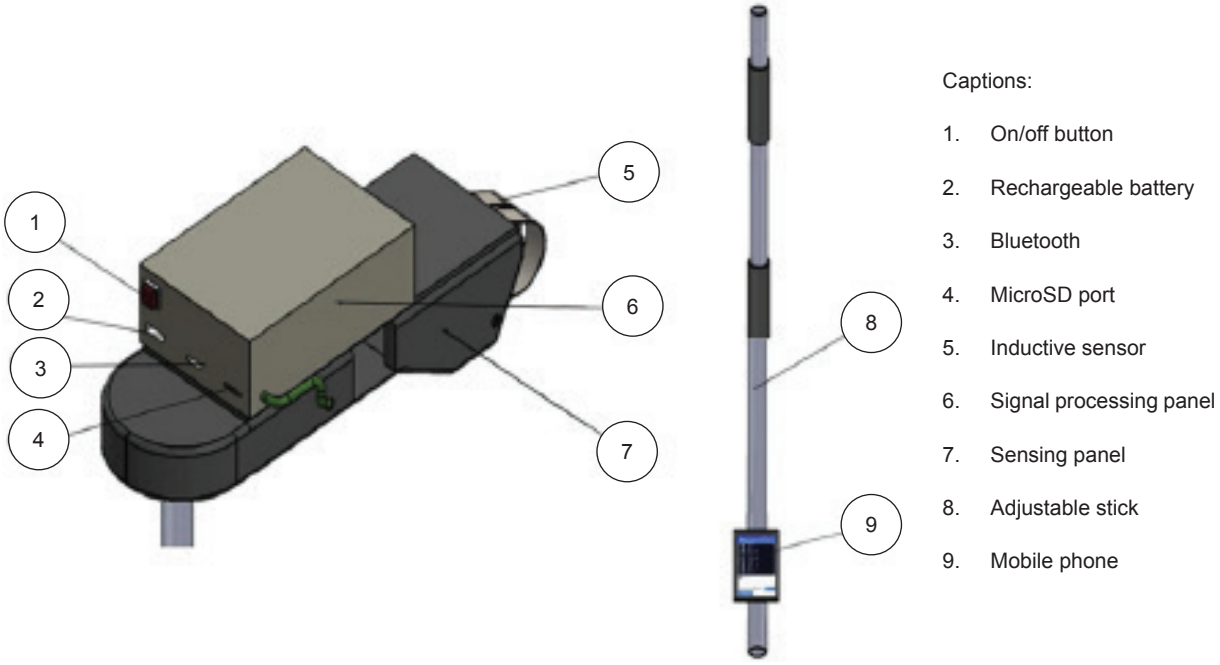
Source: Shuwaibatul *et al.* (2019).

Figure 4. Histogram of visual word occurrences used in the bag of visual word method.

According to Herman *et al.* (2020), the ripeness of oil palm fruit could be classified by using computer vision based on deep learning and visual attention techniques. The residual attention mechanism allowed the classification algorithm to recognise small details between images. Combining the residual attention mechanism with deep learning techniques, the proposed model was called ResAtt DenseNet. This paper utilised a Ten Crop pre-processing method to increase the number of images in the dataset, by cropping each image from different orientations with horizontal flipping. This technique achieved the test F1 score of 0.6929. This technique had higher classification accuracy compared to the machine learning method based on colour features and BOVW. However, deep learning algorithms are more computationally complex than machine learning algorithms.

Other than computer vision-based classification, Rismen *et al.* (2020) proposed a technique for identifying and forecasting the oil palm ripeness by using an inductive sensor system as shown in *Figure 5*. The inductive sensor was used to obtain the resonant frequency data for the target oil palm FFB. Discriminant analysis algorithm was applied to classify the fruit ripeness based on the sampled resonance frequency values. It was found that the value of resonant frequency decreased as the fruit ripened. Therefore, the age of ripeness of the fruit from anthesis could be estimated by using polynomial regression. This research successfully achieved the test result of 100% classification accuracy and 13.45 days of root-mean-square error in estimating the age of ripeness. Using inductive sensor to classify the oil palm FFB ripeness had higher classification accuracy over the other classification methods. Besides, this method was non-invasive, where the fruit sample was not damaged when detecting ripeness. Since the inductive sensor provided continuous range of resonant frequency data, estimation of the age of fruit ripeness could be achieved through regression technique, solving the limitation of machine vision techniques. One of the disadvantages of using inductive sensor was the relatively low sensing range, where the sensor must be physically in-contact with the fruit.

Tuerxun *et al.* (2020) proposed the use of optical sensors to detect the ripeness of oil palm FFB. This method used light emitting diode (LED) to emit light at different wavelengths towards the FFB. The spectral data of the reflected light from the FFB was captured by the optical spectrometer. By using the Lazy KStar classifier, this research achieved 63.0% of classification accuracy. Setiawan *et al.* (2019) obtained a better result of 88.2% accuracy by using a similar approach but the accuracy was determined based on oil content measurement rather than grader evaluation. Therefore, the results obtained from Setiawan *et al.* (2019) had higher validity as grader evaluation tends to be inconsistent. Besides, KNN and discriminant analysis algorithm were used as the classifiers in this research, while both obtained the same classification results. Using optical sensors to detect the ripeness of oil palm FFB has the advantage of non-destructive testing, where the FFB is not damaged in the detection process. However, the accuracy of classification might be affected by external lighting especially when implementing under field conditions.



Source: Rismen *et al.* (2020).

Figure 5. Inductive sensor system to detect the oil palm FFB ripeness.

TABLE 1. SUMMARY OF REVIEW ON OIL PALM FFB RIPENESS DETECTION

Author	Detection technique	Classifier type	Predictors	Accuracy (%)	F1 score
Raj *et al.* (2021)	Raman spectroscopy	KNN	4 peaks intensity and 2 peaks positions at different wavenumbers	100.0	-
Shuwaibatul *et al.* (2019)	Computer vision	SVM	BOVW	70.0	-
Herman *et al.* (2020)	Computer vision	ResAtt DenseNet	RGB value	-	0.69
Rismen *et al.* (2020)	Inductive sensor	Discriminant analysis	Resonance frequency	100.0	-
Tuerxun *et al.* (2020)	Optical sensor	Lazy KStar	Reflected light spectrum	63.0	-
Setiawan *et al.* (2019)	Optical sensor	KNN and discriminant analysis	Reflected light spectrum	88.2	-

Oil Palm Cutting Mechanism

During the harvesting process, the oil palm FFB may be located behind the fronds and obstruct the reach of the cutting mechanism. Therefore, the fronds must be trimmed before the cutting mechanism can reach the FFB. The design of the cutting mechanism must serve two purposes: Trimming the fronds and harvesting the FFB (*Table 2*).

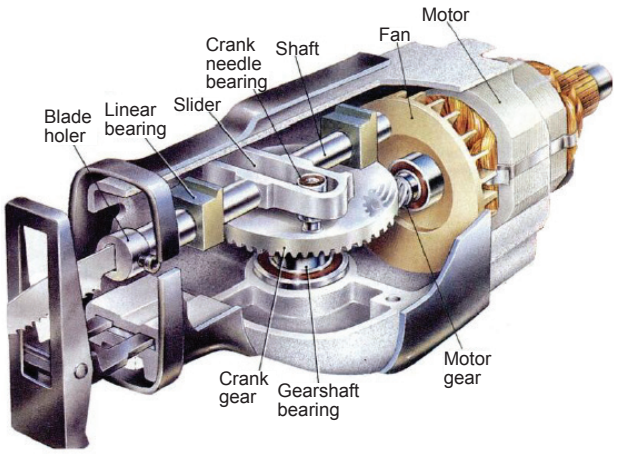
Shuib *et al.* (1988) developed an oil palm FFB harvesting machine with scissor and grapple mechanisms as shown in *Figure 6*. The scissor mechanism was used to cut the fruit bunch while the grapple mechanism held the fruit bunch to prevent it from falling. Both mechanisms were hydraulically powered. Using scissor cutting mechanism to harvest the oil palm FFB had the advantage of low mechanical vibration compared to the reciprocating mechanism. Besides, there was no reaction force induced on the manipulator during the cutting process, minimising the risk of damaging the mechanism of the manipulator. However, this mechanism was relatively heavy as the structure must be rigid enough to withstand the high cutting force on the fruit bunch.



Source: Shuib *et al.* (2011).

Figure 6. Oil palm FFB harvesting machine with grapple and scissor cutting mechanism.

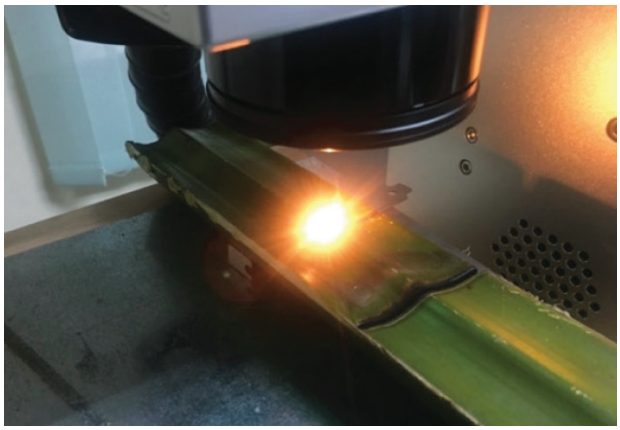
The cutting mechanism for harvesting oil palm FFB could be done by using a cutting blade with a reciprocating mechanism (Shokripour *et al.*, 2012). This mechanism replicated the back-and-forth motion of conventional hacksaw to cut the fruit bunch. This reciprocating motion was produced from a rotary motor with gear mechanism as shown in *Figure 7*. Using reciprocating cutting mechanism had advantage of smaller blade size which made it easier to be aligned properly to the target during the cutting process. However, the reciprocating motion caused intense vibration on the manipulator, potentially damaging the mechanism over time and reducing the accuracy of the cut.



Source: Shokripour *et al.* (2012).

Figure 7. Reciprocating mechanism with saw blade.

Azaman *et al.* (2022) had proposed a method for harvesting the oil palm FFB by using pulse fibre laser system. This method worked by emitting a 50 W laser beam at frequency of 500 kHz and focal length of 63 mm at the target object. This method achieved the average cutting time of 342 s on cutting the oil palm frond, which was very long compared to other cutting mechanisms. Moreover, a small scale of combustion on the palm fronds surface was observed during the cutting process, indicating the possibility of the frond to catch fire. The use of laser cutting method had the advantage of requiring lesser mechanical parts, reducing the weight and maintenance needed. Besides, no vibration would be induced on the manipulator during the cutting process. This research shows a promising alternative method for cutting the oil palm FFB, where the use of higher power laser can further reduce the cutting time (*Figure 8*).



Source: Azaman *et al.* (2022).

Figure 8. Laser cutting process of oil palm frond in laboratory condition.

Tree Climbing Mechanism

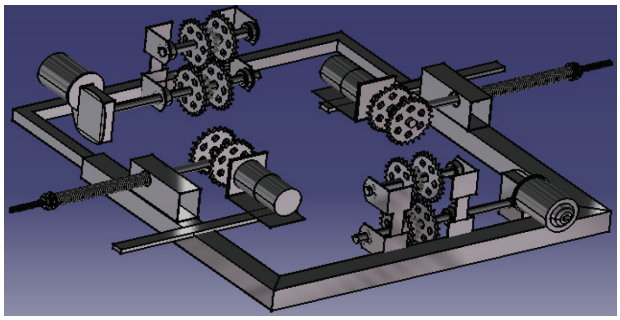
The use of harvesting machine with boom to reach the top of the oil palm tree has limitations on the maximum vertical reach due to instability. While increasing the maximum vertical reach, the weight of the harvesting machine must be increased to ensure stability. Therefore, it is not feasible to use the harvesting machine with boom for taller trees. This issue can be solved by using tree climbing robot to reach the top of the oil palm tree (*Table 3*).

Shokripour *et al.* (2010) designed a four-wheeled climbing robot for oil palm tree as shown in *Figure 9*. This robot utilised passive spring mechanism to ensure the wheels were clamped tightly on the tree. The clamping force on the wheels could be calibrated manually by using the lead screw to adjust the initial position of the wheels. Sprockets were used as the wheels to increase the adhesion on the tree. This climbing mechanism required a control system to balance the tilt angle of the robot on the tree. This could be achieved by controlling the individual motor on each side of the wheels. The advantage of using this climbing mechanism was that it can climb

TABLE 2. SUMMARY OF REVIEW ON OIL PALM CUTTING MECHANISM

Author	Cutting method	Advantages	Limitations
Shuib *et al.* (1988)	Hydraulic scissor	• Low mechanical vibration. • No reaction force induced on the manipulator.	• Entire structure of mechanism is relatively heavy.
Shokripour *et al.* (2012)	Reciprocating blade	• Small blade size. • Easy to align the blade to the target.	• Causes intense vibration on the manipulator.
Azaman *et al.* (2022)	Pulse fibre laser	• Requires fewer mechanical parts. • Relatively lightweight. • No vibration induced on the manipulator.	• Very slow cutting speed. • Potentially cause fire on the target object.

up and down the tree relatively fast while the entire robot was relatively lightweight. However, this climbing mechanism requires the operator to assemble and calibrate the robot on the tree manually, which is impractical for autonomous harvesting.



Source: Shokripour *et al.* (2010).

Figure 9. Four-wheeled climbing robot for oil palm tree.

Mustapa *et al.* (2018) developed a spiral tree climbing robot for pole-like tree. This robot had three modules: Steering, driving and support module. The steering module consisted of two motors to change the angle of the driving module. The driving module had two wheels with springs inside the shaft for clamping the wheels on the tree. The support module consisted of four-ball castors to guide the movement of the robot. The advantage of using spiral tree climbing mechanism was that it allows the robot to rotate around the tree, allowing the manipulator with a cutting mechanism to harvest oil palm FFB around the tree. Besides, the use of a support module eliminated the need to use active control system for balancing the tilt of the robot. However, this climbing mechanism required the operator to assemble and calibrate the robot on the tree manually, which was impractical for autonomous harvesting.

Bionic climbing robot inspired by primates had proven to have more flexibility than wheel-based climbing robot (Wang *et al.*, 2020). This climbing robot composed of four legs and a body frame as shown in *Figure 10*. The four legs were designed to realise the motion of clamping and loosening on the tree. A total of eight degree-of-freedom (DOF) was required to imitate the tree climbing posture of the primate. The actuators of this robot were coordinated based on the forward and inverse kinematics mathematical models. By tuning the mathematical models, this climbing mechanism could be applied to trees with different diameters, increasing the flexibility of the climbing mechanism. However, it required a complex control system as compared with wheel-based climbing mechanisms. Besides, the climbing speed of the bionic climbing robot was slower than wheel-based climbing robot.

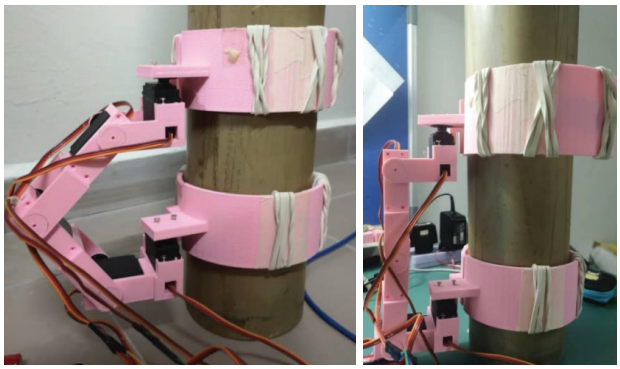


Source: Wang *et al.* (2020).

Figure 10. Climbing robot inspired by primates.

Khairam *et al.* (2021) developed a clamp-based pole climbing robot as shown in *Figure 11*. This robot consisted of three parts: Top clamp, bottom clamp, and body. The two clamps opened and closed to tighten and loosen the grip on the pole respectively. The body of the robot consisted of three servo motors. These servo motors were coordinated with a control system to realise the upward and downward movements of the robot. The advantage of using

clamp-based climbing mechanism was that the robot can be attached and detached to and from the tree easily as compared with wheel-based mechanism. However, this mechanism had issues where the clamps did not adhere properly to the tree due to the absence of spring mechanism. Besides, the climbing speed of the clamp-based climbing robot was slower than wheel-based climbing robot.



Source: Khairam *et al.* (2021).

Figure 11. Low-cost pole climbing robot.

Motion Trajectory Planning for Fruit Harvesting Manipulator

The motion trajectory planning is a crucial technology in enabling precise and efficient movements of the robotic manipulator for harvesting the oil palm FFB. The motion trajectory planning algorithm must be able to identify the fronds that obstruct the cutting path of the FFB. Hence, trimming of the fronds can be conducted, if necessary, before harvesting the FFB (*Table 4*).

One of the motion trajectory planning methods for fruit harvesting manipulators was an improved multi-objective particle swarm optimisation (GMOPSO) algorithm (Cao *et al.*, 2021). This method was divided into three steps: Path planning, B-spline parameterisation, and trajectory optimisation. The optimised rapidly exploring random tree (RRT) algorithm was used to produce the path points to be taken by the manipulator. The generated path points were connected by using multiple sections of B-spline curve to create a smooth motion trajectory. To ensure the generated trajectory meets the dynamic and kinematic limitations of the manipulator, the pulsation, energy consumption, and motion time of the manipulator must be optimised. This could be achieved by using the proposed GMOPSO algorithm to obtain the Pareto optimal solution set. This algorithm was used to solve all the constraints and optimise the trajectory taken by the manipulator. This method achieved 96.67% success rate in harvesting apples with an average motion time of 25.5 s.

Tang *et al.* (2020) proposed a path planning method for picking citrus fruits by using an improved immune algorithm (IIA). This method used a binocular camera to detect the location of the target fruits. The proposed IIA method was used to plan the optimised path for harvesting multiple fruits detected from the binocular camera. The IIA algorithm was an improvement of basic immune algorithm (BIA), which was an optimisation algorithm inspired by the biological immune system. BIA could obtain a global optimal solution with high probability, making it suitable for generating the shortest path on multiple target fruits. However, BIA had long runtime. To reduce the runtime, IIA algorithm combined the tabu search strategy with BIA algorithm. This reduced the runtime by 21.49% as compared with the BIA algorithm. However, since then the number of ripened oil palm FFB that present at the same time on a tree is usually not more than two, and the implementation of a path planning algorithm on multiple fruits are not required.

TABLE 3. SUMMARY OF REVIEW ON TREE CLIMBING MECHANISM

Author	Climbing mechanism	Advantages	Limitations
Shokripour *et al.* (2010)	Wheel-based with four wheels	• Relatively fast in climbing speed. • Entire climbing mechanism is relatively lightweight.	• Requires an active control system to balance the tilt angle of the robot, increasing complexity.
Mustapa *et al.* (2018)	Wheel-based with two wheels and support modules	• Relatively fast in climbing speed. • Allows the robot to rotate around the tree.	• The climbing mechanism is more complex.
Wang *et al.* (2020)	Bionic climbing mechanism inspired by primates	• Very flexible, can be applied on trees with different diameters.	• The climbing mechanism is very complex. • Slower climbing speed than wheel-based climbing mechanism.
Khairam *et al.* (2021)	Clamp-based with top and bottom clamps	• Can be attached and detached to and from the tree easily.	• Has issues where the clamps do not adhere properly to the tree. • Slower climbing speed than wheel-based climbing mechanism.

Therefore, a simpler path planning algorithm can be used for harvesting oil palm FFB to further reduce the required runtime.

You *et al.* (2020) proposed a motion planning framework capable of sequencing cut points while avoiding obstacles in real-time. This method used an RGB-D (Red Green Blue-Depth) camera to map and construct a 3D representation of the tree. The cut points for trimming the tree were manually selected by a human operator. The motion of the manipulator was generated by using Fast Reliable and Efficient Database Search Motion Planner (FREDS-MP) framework. The FREDS-MP framework precomputed the motion trajectories into a database. The precomputed motion trajectories were used to further optimise the trajectory while moving the manipulator in real-time. This method had achieved overall success rate of 75% on tree pruning tasks. However, the requirements of pre-mapping and manual cut point selection were impractical for the autonomous harvesting process.

Wang *et al.* (2022) proposed a trajectory planning method based on offline and online smoothing algorithms. The collision-free trajectory was initially generated by using sample-based planners, which represented the paths with segmented polygonal lines. These segmented paths caused the manipulator to stop at the vertex, causing jerky motion and reducing the motion speed. This problem could be solved by smoothing the trajectory. The proposed offline smoothing algorithm utilised short-cutting heuristic method to generate collision-free trajectory, described by using cubic polynomial functions. The trajectory was generated based on the kinematic constraints of the manipulator. This method can also be used in online smoothing, where the trajectory is optimised in real-time during execution. However, it was found that the short-cut construction in online smoothing might fail due to insufficient computational iteration, resulting in the jerky movement of the manipulator. Therefore, hardware with higher computing speed is required for online smoothing.

Localisation

Localisation refers to the process by which the robot determines its position and orientation within the oil palm plantation. This technology is an important component of navigation, ensuring that the robot is harvesting the targeted oil palm tree at the right location. Robot localisation typically involves using various sensors and algorithms to estimate the position of a robot relative to a known or previously mapped reference point (*Table 5*).

According to Georgiev and Allen, (2004), a combination of Global Positioning System (GPS), digital compass and odometry were used for real-time localisation in open-space outdoor environments. An extended Kalman filter was used to estimate the location of robot by combining these sensors data obtained in real-time. This technique strongly depended on the quality of the absolute position obtained from the GPS. Therefore, the reduction in GPS quality would reduce the accuracy of estimating the robot location. To solve this limitation, a visual pose-estimation algorithm was proposed to produce a more accurate estimation of the location of the robot. This technique used the linear features of the surrounding image obtained from a camera to compute the pose of the robot. This could be achieved by matching the linear features with the environmental model consisting of a database of small-scale facade models. By combining the GPS, compass and odometry localisation with the visual pose-estimation technique, this research was able to achieve the mean error of 0.2865 m relative to the exact location of the robot. However,

TABLE 4. SUMMARY OF REVIEW ON MOTION TRAJECTORY PLANNING FOR FRUIT HARVESTING MANIPULATOR

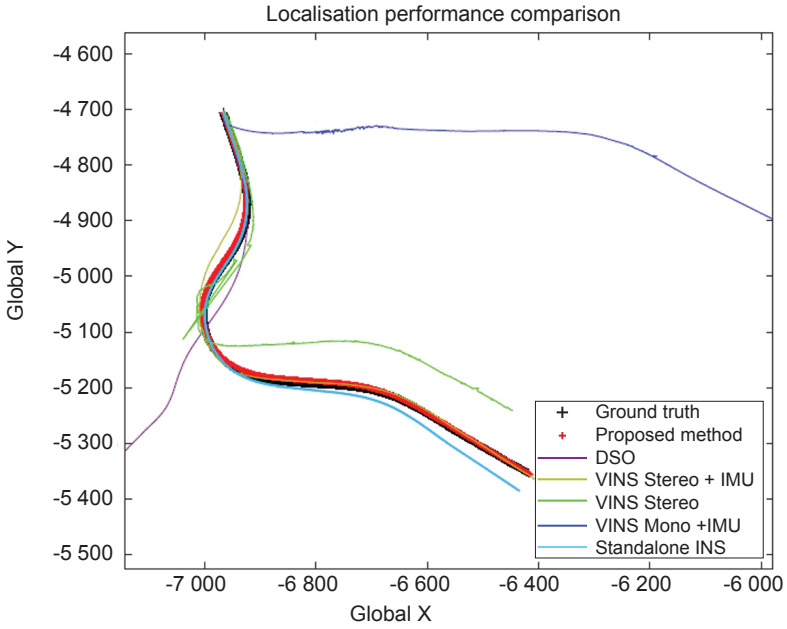
Author	Path finding algorithm	Trajectory optimisation algorithm	Findings
Cao *et al.* (2021)	Rapidly exploring random tree (RRT)	Improved multi-objective particle swarm optimisation (GMOPSO)	• Able to optimise pulsation, motion time and energy consumption of the trajectory based on kinematic constraints of the manipulator. • Achieved 96.67% success rate on harvesting apple with the average motion time of 25.5 s.
Tang *et al.* (2020)	Improved immune algorithm (IIA)	-	• Reduces the runtime by 21.49% as compared with the BIA algorithm. • Able to provide path planning for harvesting multiple fruits.
You *et al.* (2020)	Fast reliable and efficient database search motion planner (FREDS-MP)	-	• Requires pre-mapping of the tree structure. • Achieved overall success rate of 75.00% on tree pruning tasks.
Wang *et al.* (2022)	Sample-based planners	Smoothing algorithm based on short-cutting heuristic method	• Able to generate collision-free trajectory based on the kinematic constraints of the manipulator. • Can plan trajectory in real-time to avoid collision on dynamic obstacles.

the requirement of an environment model reduced the feasibility of applying this technique to different environments.

Hamer and Dandrea, (2018) proposed a localisation system using an Ultra-Wideband (UWB) Network. This method enabled numerous robots to localise themselves simultaneously within a defined area. This could be achieved by equipping the area with a stationary radio modules network, which is also called as anchors, synchronised with a distributed clock synchronisation scheme. An algorithm was also developed by utilising the time-difference of arrival (TDOA) concept to allow both the transmitting anchors and receiving robots to determine their location within the area. The TDOA algorithm worked by computing the time difference in receiving data packets from multiple anchors, which is proportional to the distance of robot between each of the anchors. This localisation technique had achieved the localisation error range of ±100 mm on the horizontal plane. One of the advantages of this localisation technique was that it allows multiple robots to locate themselves independently and anonymously. However, the actively transmitting anchors required power supply to operate, which was not available across the oil palm plantation.

Another global localisation method for mobile robots is to use radio frequency identification (RFID) technology (Tao *et al.*, 2020). This method combined phase difference and readability information from RFID signals to allow mobile robots to determine their position and attitude angle within an area. This could be done by installing two RFID reader antennas on the mobile robot and distributing RFID reference tags on the floor in a square pattern. One of the advantages of this localisation method was the high positioning accuracy, with an average precision of 5.9 cm. Besides, this method also allowed the mobile robots to determine their orientation with mean accuracy of 2.1°. One of the limitations in this localisation method was that it requires the RFID reference tag to be placed with a fixed pattern across the floor, which was impractical for outdoor environments.

To further improve the dead reckoning localisation based on inertia navigation system (INS), Jeon *et al.* (2021) had proposed a learning-based lane detection model to aid in the localisation of the vehicle. This technique worked by combining the sensor data obtained from INS with the lane detection network. The INS system provided the position, velocity and heading of the vehicle, while the lane detection network obtained the feature points describing the lane positions. An unscented Kalman Filter (UKF) was being used to combine the INS and lane points data to estimate the location of the vehicle. This research also compared the proposed method with other localisation methods as shown in *Figure 12*, showing promising results of the proposed method on estimating the vehicle location in GNSS denied area. This localisation technique could effectively minimise the error drifting problem found in standalone INS, hence, providing a more accurate estimation of the robot location. Furthermore, a learning-based lane detection model increased the robustness of the system and allowed the system to be implemented on different road geometry and environments. However, this method did not include the localisation based on rolling and pitching motion of the vehicle, which might cause errors in the localisation results.



Source: Jeon *et al.* (2021).

Figure 12. Comparisons of the localisation methods.

The proposed method is lane-aided dead-reckoning system, being compared with other systems such as direct sparse odometry (DSO), Visual-aided Inertia Navigation System (VINS) with stereo and monocular vision and standalone INS based dead reckoning system.

Navigation and Obstacle Avoidance

The navigation and obstacle avoidance allow the robot to manoeuvre through the oil palm plantation autonomously with the desired path while avoiding the obstacles. There are several approaches to navigation and obstacle avoidance in autonomous systems such as sensor-based, map-based, hybrid and machine learning-based navigations. The processes of navigation and obstacle detection involve mapping, localisation, path planning, obstacle detection and control (*Table 6*).

The generation of the shortest path for mobile robot navigation while avoiding obstacles could be done by using improved breadth first search (Tripathy *et al.*, 2021). This technique worked in a grid-based environment where the mobile robot was localised by using RFID tags placed equally in a square grid. Greedy algorithm was used to trace out the shortest and most optimal path found from the breadth first search technique. This technique allowed the mobile robot to move in four directions: Up, down, left, and right. The advantage of using this technique for navigation and obstacle avoidance was that very less computational power was required to determine the shortest and most optimal path. However, since that the mobile robot could only move in four directions, the motion of the mobile robot was not optimised especially on areas with multiple turning points.

To solve the inflexibility of grid-based environment, Ajeil *et al.* (2020) had proposed a navigation algorithm that worked in both static and dynamic environments. This algorithm was a hybrid of Particle Swarm Optimisation with Modified Frequency Bat algorithm (Hybrid PSO-MFB). The Modified Frequency Bat (MFB) algorithm worked by mimicking the echolocation behaviour of microbats during its search operation, where path searching was done by altering pulse rates and loudness of sound emission. The Particle Swarm Optimisation (PSO) algorithm helped to optimise the path generation process during navigation. Therefore, combining MFB with PSO could balance the exploration and exploitation process when generating the path for navigation. As a result, the Hybrid PSO-MFB algorithm had outperformed the MFB algorithm in terms of path optimisation. However, the computational complexity was higher for Hybrid PSO-MFB algorithm than MFB algorithm.

Back *et al.* (2020) had proposed a vision-based trail detection navigation and obstacle avoidance technique. This technique worked by combining together three methods: Trail following, disturbance recovery and obstacle avoidance. The trail following method worked by using two convolutional neural networks (CNN), one for determining the head direction of mobile robot while the other detected the lateral position offset of the mobile robot from the trail. The disturbance recovery method was used when the mobile robot loses track of the trail due to disturbances. This method utilised the past outputs from the CNN to control the heading direction of the mobile robot for recovering back to the trail. Besides, the proposed obstacle avoidance method worked based on optical flow estimation with CNN. The advantage of using this technique for navigation

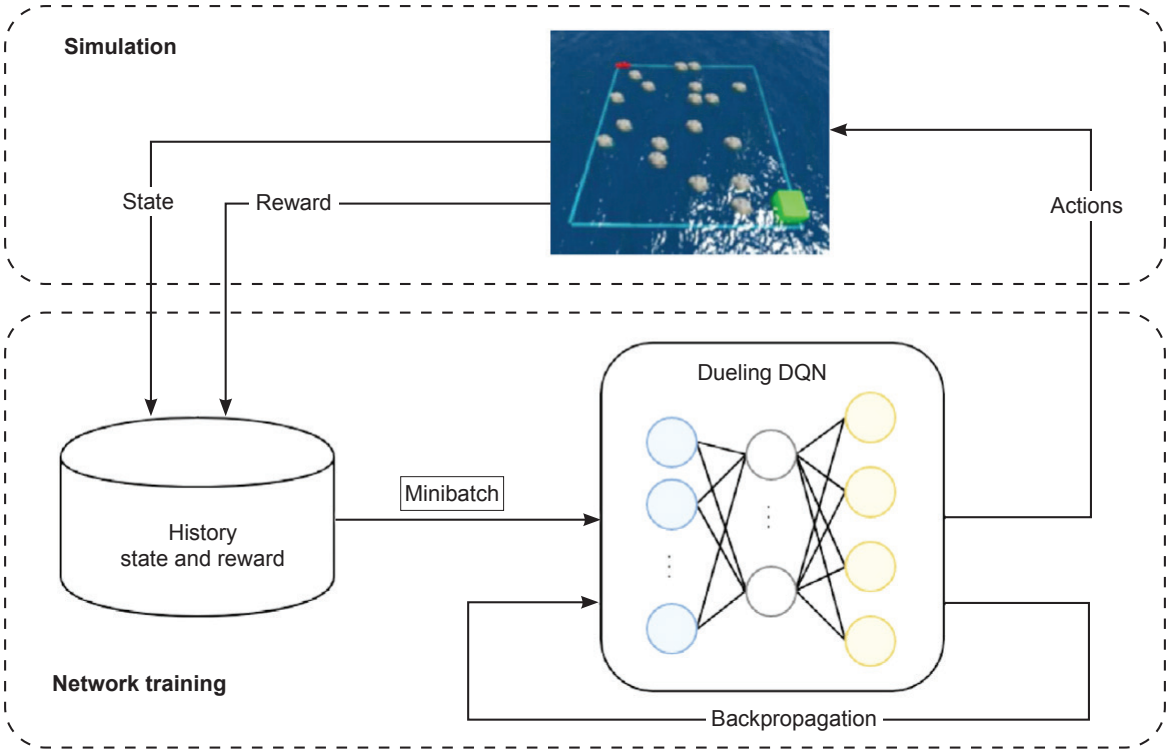
TABLE 5. SUMMARY OF REVIEW ON LOCALISATION

Author	Localisation technique	Advantages	Limitations
Georgiev and Allen (2004)	GNSS, odometry and visual pose estimation	• Obtain relatively accurate localisation with the mean error of 0.2865 m. • Can be used on areas where the GNSS signal is lost.	• Requires the preparation of environment model before using, reducing the feasibility for using on different environments.
Hamer and Dandrea (2018)	Ultra-wideband (UWB) network	• Allows multiple robots to locate themselves independently and anonymously.	• Requires power supply for multiple active transmitting anchors.
Tao *et al.* (2020)	Radio frequency identification (RFID)	• High positioning accuracy, with average precision of 5.9 cm. • Can determine the orientation of the robot with mean accuracy of 2.1°.	• Placing RFID reference tags across the floor is impractical for outdoor environment.
Jeon *et al.* (2021)	Inertia navigation system (INS) with learning-based lane detection model	• High localisation accuracy on GNSS denied area. • Can be implemented on different road geometry and environments.	• Rolling and pitching motion of the vehicle may cause errors in the localisation results.

and obstacle avoidance was that the computational cost is relatively low as the whole system could be implemented in a low power single-board computer. However, this technique only worked in known and trained environments, which was not robust to be applied in complex environments.

Other than deep learning, deep reinforcement learning (DRL) method called Autonomous Navigation and Obstacle Avoidance (ANOA) was proposed by Wu *et al.* (2020). The DRL algorithm worked by exploring the environment based on rewards mechanism to optimise the actions for completing the tasks. ANOA was based on Q-learning, where the algorithm learns the value of an action to estimate obtainable rewards known as Q values. The Q values were used for discrete decision making on controlling the mobile robot. The ANOA deep reinforcement learning framework is shown in *Figure 13*. Comparing with different Q-learning algorithm such as deep Q-network (DQN) and Deep Sarsa, ANOA used a duelling DQN which was proven to be the fastest in optimising the actions. In contrast with ANOA, heuristic-based navigation methods such as path planning and swarm intelligence algorithms were computationally slow and unable to avoid dynamic obstacles in real-time. However, Wu *et al.* (2020) had noted that implementing the DRL methods from simulation to real world was difficult as the algorithm tended to be overfitted to the simulated environment when training, which led to poor generalisation.

To solve the problem associated with poor generalisation of deep reinforcement learning (DRL) in navigation, Liu *et al.* (2021) proposed a self-improving navigation technique called lifelong learning for navigation (LLfN). To improve the navigation results in different environments, gradient episodic memory (GEM) was used when training the DRL model. GEM algorithm prevents catastrophic forgetting of the DRL model, which is the result of overwriting old knowledge when adapting to the new environment. GEM works by ensuring the update process of the navigation model will not increase the loss of previous tasks. The training process was done on three different simulated environments. The training result had shown that LLfN was capable of learning in new environments while avoiding catastrophic forgetting. In comparison with LLfN, the Sequential Training technique had shown improvement of navigation performance in present environment but reduced the previous ones. Therefore, LLfN technique had proven to be effective in multiple environment usage without the need of additional parameter tuning and calibration. However, this technique increased the total time required for training the navigation model as compared with Sequential Training.



Source: Wu *et al.* (2020).

Figure 13. Block diagram of the ANOA algorithm.

TABLE 6. SUMMARY OF REVIEW ON NAVIGATION AND OBSTABLE AVOIDANCE

Author	Methodology	Dynamic obstacle avoidance	Findings
Tripathy *et al.* (2021)	Path finding using improved breadth first search with RFID tags distributed equally in a square grid for localisation	No	• Very less computational power is required. • Allows the mobile robot to move in only 4 directions, which is not optimised for environment with multiple turning points.
Ajeil *et al.* (2020)	Hybrid PSO-MFB	Yes	• Outperformed the MFB algorithm in terms of path optimisation. • The computational complexity is higher for hybrid PSO-MFB algorithm than MFB algorithm
Back *et al.* (2020)	Deep learning based on vision-based trail detection navigation and obstacle avoidance	Yes	• Can be implemented in a low power single-board computer. • Computational cost is relatively low. • Only works in known and trained environments.
Wu *et al.* (2020)	Deep reinforcement learning using duelling deep Q-network	Yes	• Proven to be the fastest in optimising the actions compared to deep Q-network and Deep Sarsa. • Algorithm tends to be overfitted to the simulated environment when training, which leads to poor generalisation.
Liu *et al.* (2021)	Deep reinforcement learning with self-improvement technique	Yes	• Proven to be effective in multiple environment usage. • Increases the total time required for training the navigation model.

DISCUSSION

The use of autonomous robotic system in harvesting oil palm FFB is proposed to solve the existing problems in harvesting operation. A successful deployment of this robotic system requires solving all the technological challenges as stated in this review. This can be achieved by implementing and integrating the six identified key technologies.

Criteria for Successful Implementation on the Key Technologies

To further assist on the future research in this proposed robotic harvesting system, a set of criteria for successful implementation of these key technologies are discussed in this section.

The harvesting robot must have the capability to detect the ripeness of the oil palm FFB accurately with minimal human supervision. This process is crucial as the detection result is required for the robot to decide which oil palm FFB to harvest. Besides, the detection result can also be used by the robot to locate the position of the fruit for planning the motion trajectory and harvest the FFB. As reviewed in the previous section, the existing methods for identifying the ripeness of oil palm FFB can be categorised into four types: Raman spectroscopy, computer vision, inductive sensor, and optical sensor. Based on the advantages and limitations of these methods, the use of computer vision is recommended due to the relatively long sensing range.

The harvesting robot must be equipped with an efficient cutting tool to harvest the oil palm FFB. Since that the kinematics of the robotic manipulator are different from human body, the cutting tool must be redesigned to fit the usage for the robotic manipulator. This is essential to increase the cutting efficiency and maximise productivity of the harvesting robot. The existing cutting mechanisms are chisel, sickle, mechanised chisel, mechanised sickle, reciprocating saw, scissor, and laser. Modification and experimentation on these cutting tools are required to find the best fit of use on the robotic manipulator.

The harvesting robot must have a motion trajectory planning algorithm to control the robotic manipulator on harvesting the oil palm FFB. The motion trajectory of the robotic manipulator highly depends on the position and orientation of the fruit on the tree, type of cutting tools being used and the mechanics of the robotic manipulator. Therefore, the motion trajectory planning algorithm used must be robust to be used in different situations and configurations. The existing motion trajectory planning methods are mainly based on optimisation techniques such as improved multi-objective particle swarm optimisation (GMOPSO) algorithm, improved immune algorithm (IIA), Fast Reliable and Efficient Database Search Motion Planner (FREDS-MP) framework, and motion smoothing algorithms. Adaptation of these algorithms based on the configuration of robot is required to ensure the motion trajectory for harvesting the oil palm FFB is optimised.

The harvesting robot must have the ability to climb up and down the oil palm tree efficiently.

Since the oil palm trees can grow up to an average height of 15 m, it will be impractical for the robot to harvest the fruit with structural support from the ground level due to instability. Therefore, the use of climbing mechanism is recommended for the robot to reach the top of the tree. This is because the climbing mechanism allows the robot to utilise the tree trunk as the structural support, hence, minimising the vertical reach required for the robotic manipulator. The existing tree climbing mechanism are categorised as follows: Clamp-based, wheel-based, and bio-inspired climbing mechanisms. The major challenge on implementing these climbing mechanisms on oil palm tree is the existence of frond base on the tree trunk. The frond base reduce the roundness and smoothness of the tree trunk, which increases the complexity of the climbing mechanisms required to move up and down the tree effectively. Removal of the frond base from the tree trunk is recommended to overcome this challenge.

The harvesting robot must be able to determine its location in the oil palm plantation. The ability of the robot to localise is crucial such that the robot will not move randomly in the oil palm plantation. Furthermore, it allows the robot to harvest the oil palm FFB within the plantation with a planned path for maximising productivity. The existing technologies for robot localisation are global navigation satellite system (GNSS), inertia measurement unit (IMU), radio frequency identification (RFID), visual odometry and active beaconing system. Each of these localisation technologies have their own advantages and limitations, implementing a combination of these technologies is recommended.

The harvesting robot must be capable of manoeuvring through the oil palm plantation autonomously while avoiding obstacles. This allows the robot to harvest the oil palm FFB from tree to tree without the need for human supervision. There are several approaches to navigation and obstacle avoidance in autonomous systems such as sensor-based, map-based, hybrid and machine learning-based navigations. The sensor-based navigation and obstacle avoidance uses various sensors, such as cameras, lidars, and radars, to perceive the environment and detect obstacles in the path of the robot. The map-based navigation and obstacle avoidance technique uses a pre-built map of the environment to plan a path that avoids obstacles. The hybrid navigation and obstacle avoidance technique use both sensor-based and map-based navigation. Machine learning-based navigation and obstacle avoidance use machine learning algorithms to train robots to navigate through the environment and avoid obstacles. Since that the trees are planted in a grid manner, hybrid navigation and obstacle avoidance is recommended.

Interconnectivity Between the Key Technologies as a Complete System

The proposed robotic system must be integrated with the six key technologies to achieve autonomous harvesting process. Localisation provides the essential spatial awareness required for the robot to pinpoint its exact position within the oil palm plantation. This positional data is then employed by navigation systems to plan optimal paths, enabling the robot to move from tree to tree efficiently. The obstacle avoidance technology ensures the navigation path remains clear and collision-free. Besides, having a robust climbing mechanism allows the robot to reach the top of the tree efficiently. After climbing to the top of the tree, the ripeness detection technology allows the robot to identify and distinguish ripe FFB from unripe ones accurately. After the ripe FFB is detected, the robotic manipulator with cutting tool can harvest the FFB with the right trajectory by implementing the motion trajectory planning algorithms. Finally, the robot climbs down the tree and the harvesting process repeats.

The use of Robot Operating System (ROS) as the middleware to integrate the robot control is recommended. ROS is widely used in complex robotic systems due to its versatility, modularity, and robustness. It provides a framework that simplifies the development and integration of various components within a robot, making it easier to implement the six key technologies as a complete system.

Prediction on the Trend of Technological Development in Oil Palm Harvesting

Driven by the need to increase efficiency, reduce labour costs, and address various challenges in the oil palm plantation, the use of autonomous harvesting robots can serve as the long-term solution to these problems. This solution is feasible based on the following arguments.

Increased adoption of artificial intelligence and machine learning. These technologies will enable the harvesting robots to better understand their environment, make real-time decisions, and adapt to changing conditions.

Advancements in sensor technology. The cost of sensors, including LiDAR, cameras, GPS, and other environmental sensors, is steadily decreasing. This reduction in sensor prices makes it more economically viable to equip the harvesting robots with the necessary sensing capabilities, enabling robots to navigate, perceive their surroundings, and make informed decisions more effectively.

Improved battery technology. Battery technology is a crucial factor in the development of autonomous harvesting robots, as they need

reliable power sources for extended operation in the field. Advances in battery technology, including higher energy densities, faster charging, and longer lifespans, will lead to robots with extended runtimes and reduced downtime for recharging or battery replacement.

Increasing computing power. The increase in computing capabilities enables robots to process larger volumes of data and perform complex computations in real time. It also facilitates the use of more sophisticated artificial intelligence algorithms, allowing robots to adapt and make decisions more rapidly and accurately.

CONCLUSION

To solve the existing problems related to oil palm harvesting, a robotic system in automating the harvesting process of the oil palm FFB is proposed. The technological challenges for developing this robotic system are (1) difficulty of a mobile self-driving unit to manoeuvre autonomously in oil palm plantation; (2) inaccuracy of existing robot localisation technology for oil palm plantation; (3) non-robust climbing mechanism for climbing robot to move up and down the oil palm tree; (4) non-existence of robotic harvesting module that can detect and harvest the oil palm FFB autonomously and (5) inaccuracy of ripeness classification for oil palm FFB in field conditions.

Six key technologies for developing this robotic system are reviewed. These technologies include: (1) Oil palm ripeness detection; (2) oil palm cutting mechanism; (3) tree climbing mechanism; (4) motion trajectory planning for fruit harvesting manipulator; (5) localisation; (6) navigation and obstacle avoidance. Future work for implementation and integration of these key technologies onto oil palm harvesting process are necessary to further enhance the development of oil palm industry.

Six criteria for successful implementation of the proposed autonomous robotic system in harvesting oil palm are discussed. Recommendations on the technology used for fulfilling these criteria are made. Interconnectivity between the key technologies as a complete system is analysed. The trend of technological development in oil palm harvesting is predicted.

ACKNOWLEDGEMENT

The authors would like to acknowledge Asia Pacific University of Technology and Innovation for supporting the publication of this review article. Special thanks to Mr. Dennis Tan for providing important ideas and feedback to make this review article a success.

REFERENCES

Ajeil, F H; Ibraheem, I K; Azar; A T and Humaidi, A J (2020). Autonomous navigation and obstacle avoidance of an omnidirectional mobile robot using swarm optimization and sensors deployment. *Int. J. Adv. Robotic Sys., 17(3)*: 1-5. DOI: 10.1177/1729881420929498.

Azaman, M I H; Ramli, A S; Mdradzi, M K F; Ahmad, M R; Ramdhan, M; Azwan, M; Kamil, Y M and Mahdi, M A (2022). Feasibility study of oil palm harvesting using pulse fibre laser system with different lenses. *J. Oil Palm Res., 34(3)*: 488-489. DOI: 10.21894/jopr.2022.0005.

Back, S; Cho, G; Oh, J; Tran, X T and Oh, H (2020). Autonomous UAV trail navigation with obstacle avoidance using deep neural networks. *J. Intell. Robot. Syst.: Theory Appl., 100(3-4):* 1195-1211. DOI: 10.1007/s10846-020-01254-5.

Bernama (2021). Malaysia developing a dwarf variety of oil palm tree. Free Malaysia Today. https://www.freemalaysiatoday.com/category/nation/2021/04/25/malaysia-developing-a-dwarf-variety-of-oil-palm-tree/, accessed on 17 April 2023.

Bhuanantanondh, P; Buchholz, B; Arphorn, S; Kongtip, P and Woskie, S (2021). The prevalence of and risk factors associated with musculoskeletal disorders in thai oil palm harvesting workers: A cross-sectional study. *Public Health, 18*: 5474. DOI: 10.3390/ijerph.

Britannica (2021). Oil palm. Encyclopedia Britannica. https://www.britannica.com/plant/oil-palm, accessed on 3 October 2023.

Cao, X; Yan, H; Huang, Z; Ai, S; Xu, Y; Fu, R and Zou, X (2021). A multi-objective particle swarm optimization for trajectory planning of fruit picking manipulator. *Agronomy, 11(11):* 2286. DOI: 10.3390/agronomy11112286.

CCOHS (2017). Vibration - Health effects. Canadian centre of occupational health and safety. https://www.ccohs.ca/oshanswers/phys_agents/vibration/vibration_effects.html, accessed on 3 March 2023.

Channel News Asia (2022). Malaysia labour crunch cost palm oil sector $2 billion between Jan-May. https://www.channelnewsasia.com/business/malaysia-labour-crunch-cost-palm-oil-sector-2-billion-between-jan-may-2820346, accessed on 3 March 2023.

Dan, S A M; Hashim, F H; Raj, T; Huddin, A B and Hussain, A (2018). Classification of oil palm fresh fruit bunches (FFB) using Raman spectroscopy.

Int. J. Engine. Technol., 7(4): 184-188. DOI: 10.14419/ijet.v7i4.11.20798.

FMT Reporters (2022). RM10.46 bil lost in unpicked oil palm fruit due to labour shortage. Free Malaysia Today (FMT). https://www.freemalaysiatoday.com/category/nation/2022/07/19/rm10-46bil-lost-in-unpicked-oil-palm-fruit-due-to-labour-shortage/, accessed on 3 March 2023.

Georgiev, A and Allen, P K (2004). Localization methods for a mobile robot in urban environments. *IEEE Trans. Robot., 20(5)*: 851-864. DOI: 10.1109/TRO.2004.829506.

Hamer, M and Dandrea, R (2018). Self-calibrating ultra-wideband network supporting multi-robot localization. *IEEE Access, 6*: 22292-22304. DOI: 10.1109/ACCESS.2018.2829020.

Herman; Susanto, A; Cenggoro, T W; Suharjito and Pardamean, B (2020). Oil palm fruit image ripeness classification with computer vision using deep learning and visual attention. *J. Telecomm. Electron. Comput. Eng. (JTEC), 12(2)*: 21-27.

Jeon, J; Hwang, Y; Jeong, Y; Park, S; Kweon, I S and Choi, S B (2021). Lane detection aided online dead reckoning for GNSS denied environments. *Sensors, 21(20)*: 6805. DOI: 10.3390/s21206805.

Khairam, H; Choong, Y M; Ismadi, N S N; Othman, W A F W; Wahab, A A A and Alhady, S S N (2021). Design and development of a low-cost pole climbing robot using arduino mega. *J. Phys.: Conf. Ser., 1969(1)*: 012008. DOI: 10.1088/1742-6596/1969/1/012008.

Liu, B; Xiao, X and Stone, P (2021). A lifelong learning approach to mobile robot navigation. *IEEE Robot. Autom. Lett., 6(2)*: 1090-1096. DOI: 10.1109/LRA.2021.3056373.

Medina, D; Heselbarth, A; Buscher, R; Ziebold, R and Garcia, J (2018). On the Kalman filtering formulation for RTK joint positioning and attitude quaternion determination. *IEEE/ION Position, Locat. Navig. Symp., 2018*: 597-604. DOI: 10.1109/PLANS.2018.8373432.

Meijaard, E; Brooks, T M; Carlson, K M; Slade, E M; Garcia-Ulloa, J; Gaveau, D L A; Lee, J S H; Santika, T; Juffe-Bignoli, D; Struebig, M J; Wich, S A; Ancrenaz, M, Koh; L P, Zamira, N; Abrams, J F; Prins, H H T; Sendashonga, C N; Murdiyarso, D; Furumo, P R and Sheil, D (2020). The environmental impacts of palm oil in context. *Nature Plants, 6(12)*: 1418-1426. DOI: 10.1038/s41477-020-00813-w.

Mustapa, M A; Othman, W A F W; Abu Bakar, E and Othman, A R (2018). Development of pole-like tree spiral climbing robot. *ICCSCE, 2015*: 285-293. DOI: 10.1007/978-981-10-8788-2_26.

Parveez, G K A; Hishamuddin, E; Loh, S K; Ong-Abdullah, M; Salleh, K M; Bidin, M N I Z; Sundram, S; Hasan, Z A A and Idris, Z (2020). Oil palm economic performance in Malaysia and R&D progress in 2019. *J. Oil Palm Res., 32(2)*: 159-190. DOI: 10.21894/jopr.2020.0032.

Raj, T; Hashim, F H; Huddin, A B; Hussain, A; Ibrahim, M F and Abdul, P M (2021). Classification of oil palm fresh fruit maturity based on carotene content from Raman spectra. *Sci. Rep., 11(1)*: 18315. DOI: 10.1038/s41598-021-97857-5.

Rismen, S; Tineke, M; Dewa, M S and Wawan, H (2020). Application of an inductive sensor system for identifying ripeness and forecasting harvest time of oil palm. *Scientia Horticulturae, 265*: 109231. DOI: 10.1016/j.scienta.2020.109231.

Setiawan, A W; Mengko, R; Putri, A P H; Danudirdjo, D and Ananda, A R (2019). Classification of palm oil fresh fruit bunch using multiband optical sensors. *Int. J. Electr. Comput. Eng., 9(4)*: 2386-2393. DOI: 10.11591/ijece.v9i4.pp2386-2393.

Shokripour, H; Ishak, W and Karimi, Z M (2010). Development of an automatic self balancing control system for a tree climbing robot. *African J. Agric. Res., 5(21)*: 2964-2971.

Shokripour, H; Ishak, W; Shokripour, R and Moezkarimi, Z (2012). Development of an automatic cutting system for harvesting oil palm fresh fruit bunch (FFB). *African J. Agric. Res., 7(17)*: 2683-2688. DOI: 10.5897/ajar11.1648.

Shuib, A R; Hassan, A H and Hitam, A (1988). Development of harvesting machines for oil palm. National Oil Palm/Palm Oil Conference: 11-15.

Shuib, A R; Khalid, M R and Deraman, M S (2011). Innovation and technologies for oil palm mechanization. https://www.researchgate.net/publication/280134906, accessed on 2 February 2023.

Shuwaibatul, A G; Hazlin, S; Zai, O and Rubiya, Y (2019). Image analysis techniques for ripeness detection of palm oil fresh fruit bunches. *J. Electr. Eng., 18(3)*: 57-62. DOI: 10.11113/elektrika.v18n3.192.

SOPPOA (2021). Oil palm plantation 4Ds work still shun by locals despite offered good wages.

http://soppoa.org.my/archives/highlights/oil-palm-plantation-4ds-work-still-shun-by-locals-despite-offered-good-wages.php, accessed on 3 March 2023.

Sowat, S N; Ishak, W; Mahadi, M R; Bejo, S K; Saufi, M and Kassim, M (2018). Trend in the development of oil palm fruit harvesting technologies in Malaysia. *Sci. Eng., 80(2)*: 2180-3722. DOI: 10.11113/jt.v80.11298.

Tan, K P; Kasturi, D K and Cracknell, A P (2014). On the upstream inputs into the MODIS primary productivity products using biometric data from oil palm plantations. *Int. J. Remote Sens., 35(6)*: 2215-2246. DOI: 10.1080/01431161.2014.889865.

Tang, K H D and Qahtani, H M S (2019). Sustainability of oil palm plantations in Malaysia. *Environ. Dev. Sustain., 22(6)*: 4999-5023. DOI: 10.1007/s10668-019-00458-6.

Tang, Z; Xu, L and Xie, H (2020). Picking trajectory planning of citrus based on improved immune algorithm and binocular vision. *2020 IEEE International Conference on Artificial Intelligence and Computer Applications (ICAICA)*. IEEE, Dalian. p. 6-10. DOI: 10.1109/ICAICA50127.2020.9182606.

Tao, B; Wu, H; Gong, Z; Yin, Z and Ding, H (2020). An RFID-based mobile robot localization method combining phase difference and readability. *IEEE Transactions on Automation Science and Engineering, 18(3):* 1406-1416. DOI: 10.1109/TASE.2020.3006724.

Teoh, C H (2000). *Land Use and the Oil Palm Industry in Malaysia*. WWF Malaysia. Kuala Lumpur. 102 pp.

Tripathy, H K; Mishra, S; Thakkar, H K and Rai, D (2021). CARE: A collision-aware mobile robot navigation in grid environment using improved breadth first search. *Comput. Electr. Eng., 94*: 107327. DOI: 10.1016/j.compeleceng.2021.107327.

Tuerxun, A; Shariff, A R M; Janius, R; Abbas, Z and Mahdiraji, G A (2020). Oil palm fresh fruit bunches maturity prediction by using optical spectrometer. *IOP Conf. Ser.: Earth Environ. Sci., 540(1)*: 012085. DOI: 10.1088/1755-1315/540/1/012085.

Wang, H; Zhao, Q; Li, H and Zhao, R (2022). Polynomial-based smooth trajectory planning for fruit-picking robot manipulator. *Inf. Process. Agric., 9(1)*: 112-122. DOI: 10.1016/j.inpa.2021.08.001.

Wang, R G; Huang, H B; Li, Y and Yuan, J W (2020). Design and analysis of a novel tree climbing robot mechanism. DOI: 10.21203/rs.3.rs-55599/v1.

Wu, X; Chen, H; Chen, C; Zhong, M; Xie, S; Guo, Y and Fujita, H (2020). The autonomous navigation and obstacle avoidance for USVs with ANOA deep reinforcement learning method. *Knowledge-Based Systems, 196*: 105201. DOI: 10.1016/j.knosys.2019.105201.

You, A; Sukkar, F; Fitch, R; Karkee, M and Davidson, J R (2020). An efficient planning and control framework for pruning fruit trees. *IEEE International Conference on Robotics and Automation (ICRA)*. IEEE, Paris. p. 3930-3936. DOI: 10.1109/ICRA40945.2020.9197551.

Zahid, M and Firdaus, M (2018). Mechanization in oil palm harvesting. *Int. J. Acad. Research Business Soc. Sci., 8(5)*: 246-255. DOI: 10.6007/IJARBSS/v8-i5/4098.

RESEARCH ARTICLES

Journal of Oil Palm Research Vol. 36 (3) September 2024 p. 367-379
DOI: https://doi.org/10.21894/jopr.2023.0017

THE INFLUENCE OF FLOWERING BENEFICIAL PLANT, *Turnera subulata* ON THE INSECT NATURAL ENEMIES' ABUNDANCE IN RELATION TO OIL PALM BAGWORM OCCURRENCE IN BAGAN DATUK, PERAK, MALAYSIA

SITI NURULHIDAYAH AHMAD[1]*; SAHARUL ABILLAH MOHAMAD[1]; OTHMAN ARSHAD[1] and MOHAMED MAZMIRA MOHD MASRI[1]

ABSTRACT

The devastating infestation of bagworms in Malaysia had significant impact on oil palm production. The influence of beneficial plant, Turnera subulata *on the natural enemies' abundance in relation to bagworm,* Pteroma pendula *occurrence in an oil palm plantation located in Bagan Datuk, Perak was investigated. Sampling techniques (yellow sticky trap and sweep net) were employed in each of the sampling areas: (i)* T. subulata *groves, and (ii) oil palm inter-row. A total of 1035 individuals of insect natural enemies representing four orders and nine families were collected. The highest diversity was found in the* T. subulata *groves, with Shannon-Wiener index (H') of 1.747 compared to inter-rows (1.447). These values are supported by the higher abundance of natural enemies on* T. subulata *groves that indicated 82% of total individuals captured, dominated by Chalchidae (580 individuals). Overall, the interaction between the techniques and locations was significant (F = 9.125; df = 1;* P *= 0.003). A significant positive correlation was observed between natural enemies and pupal stage of* P. pendula *(r = 0.659; r^2 = 0.434;* P*<0.001). The findings from this study suggest that the propagation of insect natural enemies can be effectively achieved by the establishment of beneficial plants such as* T. subulata.

Keywords: bagworm, beneficial plant, natural enemies, oil palm.

Received: 26 October 2022**; Accepted:** 16 March 2023**; Published online:** 13 April 2023.

INTRODUCTION

Numerous pests threaten crops throughout the world, imposing significant economic losses in the case of a lack of effective control. It is also important to note that using chemical pesticides to manage pests frequently fails to offer effective conventional control and causes serious environmental harm (Wood and Norman, 2019; Ziolkowska *et al*., 2021). For instance, excessive pesticide use can result in pest resurgence such as *Galerucella birmanica* (Singhara beetle) and cereal aphids (Krauss *et al*., 2011; Parameswari *et al*., 2020), as well as a decline in the population of beneficial insects such as natural enemies (Janssen and van Rijn, 2021) (*e.g., Chrysoperla rufilabris* and *Coccinella septempunctata*), and pollinators such as bumblebees (Siviter *et al*., 2018). A successful management of insect pests at local and global scales is a prerequisite for a sustainable oil palm agriculture system. In Southeast Asia, notably in Malaysia, palm oil is a significant export commodity and a major economic driver. The export revenues amounting to approximately RM108.52 billion was reported by Parveez *et al*. (2022). The entire area of land used

[1] Malaysian Palm Oil Board,
6, Persiaran Institusi, Bandar Baru Bangi,
43000 Kajang, Selangor, Malaysia.

* *Corresponding author e-mail: nurulhidayah@mpob.gov.my*

for oil palm cultivation, including those owned by the smallholders, has reached 5.74 million hectares (Parveez *et al*., 2022). Oil palm-cultivated lands are known to be particularly blessed with several ecosystem services (Aulia *et al*., 2020; Norman *et al*., 2019). Insects provide a variety of ecosystem services, including pollination and natural enemies for pest control, that are particularly important for both natural habitations and agriculture (Sáenz-Romo *et al*., 2019).

As an ecosystem function benefits people economically, insect natural enemies play a crucial role in pest control (Koh and Holland, 2015). Implementing beneficial plants in the oil palm landscape can increase the populations of natural enemies as a way to aid biological control conservation (Norman and Othman, 2016). It has been demonstrated that natural enemies such as parasitic and predatory insects are beneficial in suppressing pest species (Basri *et al*., 1995; Siti Nurulhidayah and Norman, 2016; Siti Nurulhidayah *et al*., 2020). These species coexist in natural ecosystems and may interact with one another in ways that affect the effectiveness of pest regulation (Dainese *et al*., 2017). Norman *et al.* (2017) have identified hymenopterans as a prominent insect order that was known to be the natural enemies of bagworms and other oil palm leaf-eating caterpillars. Parasitoids, specifically hymenopterans, although small in size, are important ecologically and economically (LaSalle and Gould, 1993). Due to their special adaptations toward host concealment, parasitoids perform a unique function in pest population reduction. For example, Cerambycid wood borers were suppressed by generalist parasitoids in the forest industry (Wang *et al*., 2021). Habitat manipulation, in conjunction with conservation biological control implementation in agriculture settings, is known to be instrumental in fostering the populations of natural enemies, while suppressing the pest population (Fiedler *et al*., 2008; Gurr *et al*., 2017).

Bagworm (Lepidoptera: Psychidae) infestations have significantly impacted the oil palm yield, particularly for smallholders (Nur Robaatul Adhawiyah *et al*., 2021; Nurul Afiah *et al*., 2022). Severe infestation can result in yield reductions of up to 43% (Basri, 1993; MPOB, 2016). Bagworms were recorded in over 12% of the estate areas (7811 ha) by 2000, according to a later survey by Ho *et al*. (2011). Malaysia has experienced outbreaks for over five decades (Cheong and Tey, 2012). Currently, outbreaks are still reported, particularly in Perak and Johor (Noorhazwani *et al*., 2017; Nur Robaatul Adhawiyah *et al*., 2021). Despite the existence of efficient control techniques, this problem persists. The current integrated pest management (IPM) strategy for bagworms in Malaysia comprises the aerial application of bio-insecticides and the use of natural pheromone traps (Norman *et al*., 2019). Another technique to increase the populations of predators and parasitoids is habitat manipulation. This includes offering shelter habitat, substitute hosts or prey, or food plants from which nectar and pollen can be acquired (Baggen *et al*., 1999; Shakeel *et al*., 2022). Shelter habitats within the field may consist of plants selected to be beneficial for the natural enemies (Nilsson *et al*., 2016). These plants attract parasitoids and predators by offering a source of nectar to prolong their lifespan and lay eggs (Norman and Othman, 2016).

In the oil palm ecosystem, four species of nectar-producing plants, including *Cassia cobanensis, Euphorbia heterophylla, Antigonon leptopus* and *Turnera subulata*, were observed to be beneficial to the natural enemies of bagworms (Basri *et al*., 2001; Ho *et al*., 2003; Jamian *et al*., 2020). Basri *et al.* (2001) evaluated several beneficial plants in the field for their attraction to main bagworm parasitoids. Parasitism was more prevalent near the flowers. This study investigated three plants: *C. cobanensis*, *E. heterophylla* and *Crotalaria usaramoensis*. Ho *et al*. (2003) explored the topic in greater depth. They tested *C. cobanensis* and *E. heterohylla*, as well as *A. leptopus, C. zanzibarensis, T. subulata* and *Asystasia gangetica*, and a control of mixed grasses. It was observed that the parasitism was more abundant near *C. cobanensis* and *E. heterophylla*. Around the year 2000, it became regular practice to plant *C. cobanensis, E. heterophylla, A. leptopus*, and/or *T. subulata* in open spaces in Malaysian oil palm plantations (Siti Ramlah *et al*., 2005). Yusdayati *et al.* (2014) later concluded that *Turnera* spp. were more recommended since flowering is continuous compared to other species. *Turnera subulata* (Turneraceae) is a perennial herb which is up to 0.8 m tall with a woody stem base and growing from a thick taproot, with darker bases, thick herb and dark green foliage (Saravanan *et al*., 2018). Its dark-eyed flowers have five obovate cream-colored petals with a yellow base or are pure yellow. Flowers cannot self-pollinate and must rely on another flower to generate seeds. However, the impact of *T. subulata* on the populations of natural enemies and pests has received little attention. As such, this study aimed to address the influence of the flowering beneficial plants on the abundance of the natural enemies and subsequently, their relation to the occurrence of bagworms in the oil palm plantation.

MATERIALS AND METHODS

Study Site

The research location was an oil palm plantation in Bagan Datuk, Perak, Malaysia 3º48′22.13″N, 101º06′8.68″E; (*Figure 1*) that was reported to

have a mild infestation with the bagworm, *Pteroma pendula*. The 10 ha site on shallow peat soil comprised 12-year-old DxP plantings, with generally uniform palm growth. The selection of the sampling location was based on the existence of beneficial plants and with infestation levels exceeding the recommended economic threshold (*i.e.*, more than 10 live larvae per oil palm frond), being given priority (MPOB, 2016; Noorhazwani *et al.*, 2017; Wood and Norman, 2019). *Turnera subulata* was selected as the subject plant, as the groves are easy to establish in the oil palm plantation setting as stated by Yusdayati *et al*. (2014). A total of six oil palm planting blocks were selected with each block approximately 1 hectare and with *T. subulata* planted around it as an adjacent plant along the road. The distance between each block was 500 m. Three sampling plots were designated inside each block, ranging from the block's edge to its interior. Ten recording palms made up each sampling plot as described by Norman and Basri (2010) in their study of *C. cobanensis* plant. The sampling was conducted for 24 months, from June 2014 to June 2016.

The characteristic of the inter-row area is non-harvesting paths within oil palm rows with approximately nine metres distance between facing palms and covered ten facing palms with approximately 45 m distance, for each sampling plot. While for the *T. subulata* groves area, the size of its planting plot was 2.0 × 0.5 m with a 1.0 m distance between planting plots and planted along the main road and drain. *Turnera subulata* was already planted and maintained by the estate management as one of their management requirements. According to them, 10 g phosphate fertiliser was used during the planting for each plant cutting and empty fruit bunches (EFB) were used to mulch the soil for soil moisture conservation. Propagation was performed through the use of seeds and stem cuttings. Sufficient sunlight is an important factor in maintaining flower production (*Personal communication*).

Evaluation of the Bagworm Population

A monthly census was conducted to assess the field population of *P. pendula*. *Pteroma pendula* were sorted, counted, and recorded according to their life stage. Ten palms were randomly chosen per hectare as census palms. Fronds with a 45° inclination or the upper fronds showing signs of bagworm attack were cut down. Each census palm had at least one frond assessed.

Insect Sampling Techniques and Preservation

In this study, two beneficial insect guilds which consisted of predators and parasitoids, were sampled at *T. subulata* groves and in the oil palm inter-rows. Two sampling techniques were utilised in each plot as follows: i) A sweep net made of muslin cloth with a diameter of 30 cm at the opening and a length of 60 cm, and ii) a yellow sticky trap. Sweep net samplings were carried out inside each planting block by sweeping four times over the grove and along the path, from 9.00 am to 12.00 pm. The yellow sticky trap was mostly used

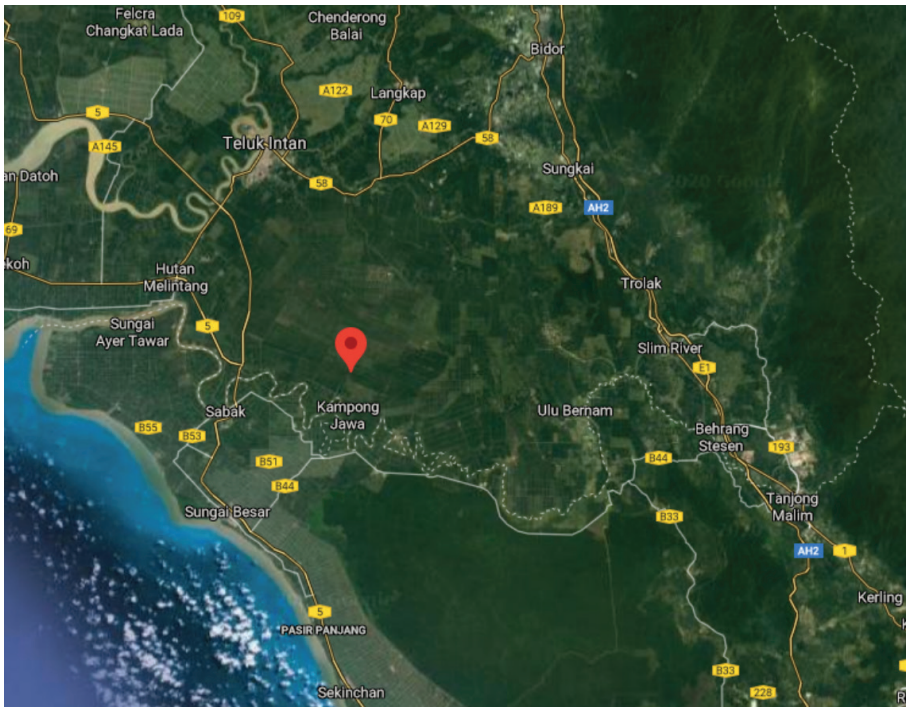


Figure 1. Map of study site in Bagan Datuk, Perak.

to catch flying insects. This square trap measured 48 × 48 cm. It was made of plywood, painted yellow, wrapped in a clear plastic sleeve and sprayed with polybutene gum (Neopeace brand; containing polybutene 16% w/w). The trap was positioned about 1.5 m from the ground. The traps were then placed randomly at the *T. subulata* grove in the study plot and left there for two days. For two consecutive days, the data was collected at 9.00 am on the following morning, each day. The sticky traps were replicated three times inside each plot, in the inter-rows between the oil palm trees (at the non-harvesting path) and *T. subulata* groves. Both sampling techniques were replicated three times each, following the procedure recommended by Norman and Basri (2010). Samplings were carried out monthly. The sampling was conducted in the bright middle of the morning when most insects began to become active. The insects captured by using sweep nets were put into jars containing cotton that had been soaked in ethyl acetate. Meanwhile, the insects captured by sticky traps were carefully collected and transferred into bottles. Since most of the specimens adhered to the sticky trap, some of them were photographed using a digital camera for counting and identification purposes.

In order to assess parasitoid emergence, live bagworm samples (larvae and pupae) were also collected from each block monthly and brought to the laboratory. Thirty recording palms were randomly chosen from each sampling block. Dead specimens were put into plastic vials individually until the emergence of parasitoids, while the live bagworms were reared on oil palm leaflets in transparent cylindrical cages (12.5 cm in diameter x 23.5 cm in height) with ventilated lids until the emergence of parasitoids at a temperature of 24 ± 1°C and 60%-70% relative humidity. Daily observations and records of the emergence were made. The collected parasitoids were stored and preserved in 70% alcohol for further identification. Identification of samples up to the family or species level was conducted using a stereo-zoom microscope by referring to "The Handbook of Common Parasitoids and Predators Associated with Bagworms and Nettle Caterpillars in Oil Palm Plantations" by Norman *et al.* (2017).

Statistical Analysis

The two-way ANOVA analysis was carried out to determine whether there were significant differences in the number of natural enemies captured by different sampling techniques in relation to sampling locations. All pairwise multiple comparison procedures (Holm-Sidak method) of significance testing at 5% levels were used for mean comparisons. The correlation coefficient (r) analysis was also carried out to determine the relationship between bagworm occurrence and natural enemies abundance by using SigmaPlot 12.5 software. The figures showing the bagworm population, emergence and monthly captures of insect natural enemies were generated using Microsoft Excel.

RESULTS AND DISCUSSION

It had been observed that the population of the bagworm, *P. pendula*, fluctuated in relation to the abundance of its natural enemies throughout the study duration. *Figure 2* shows the *P. pendula* population fluctuated from undetectable levels to as high as 106.8 ± 13.723 live bagworms per frond (BPF), which exceeded the economic threshold level (ETL). The ETL for *P. pendula* is ten live larvae per oil palm frond (MPOB, 2016; Noorhazwani *et al*., 2017; Wood and Norman, 2019). Two main peaks of the infestation were recorded in November 2014 (90.2 ± 21.653 BPF) and in November 2015 (106.8 ± 13.723 BPF), before fluctuating to a low density and remaining below ETL of less than 10 BPF in the following months.

In September and October 2014, the live larval population of *P. pendula* increased, reaching a peak of 90.2 BPF in November 2014. The sudden increase in the pest population coincided with a lack of parasitoids emerging between September and October 2014 (*Figure 2*). Similar circumstances had been observed before the second peak (highest peak) in November 2015, while no emergence of parasitoids was recorded from August to October 2015. Basri *et al*. (1995) suggested that due to their short life span, the abundance of the parasitoids in the field can fluctuate heavily. After a peak period of abundance, their population can reduce greatly within a short period. Thus, when their abundance is not in sync with the bagworms' life cycle, a subsequent generation of bagworms may evade full natural control, leading to a sudden surge in the infestation.

Although the bagworm population was observed to be fluctuating in this study, a vastly decreasing trend was recorded from the peak bagworm population of 106.8 BPF in November 2015 to less than the ETL (<10 BPF), at 4.31 BPF in December 2015. Thereafter, the population continued to fluctuate at low levels until it reached a non-detectable level during July 2016 and later samplings. According to Cheong *et al*. (2010), the parasitoid community has also been highlighted as one of the mortality mechanisms that has contributed to a nearly 36.7% decrease in the population of bagworms. This suggests that the natural mortality factors by insect natural enemies with the presence of the beneficial plant were sufficient to achieve control.

The activities of natural enemies were monitored based on captures of sticky traps and sweep net (Böckmann and Meyhöfer, 2017; Norman and Basri, 2010; Pobozniak *et al.*, 2020; Shweta and Rajmohana, 2016). Using both techniques, various species of the insect's natural enemies were captured during sampling. The outcomes of the current study revealed that a total of 1035 individuals belonging to at least 20 insect species of two trophic guilds were present in *T. subulata* groves, while at oil palm inter-rows a total of 182 individuals belonging to at least 10 insect species of two trophic guilds were present. A total of 20 parasitoid species (including three unknown species) belonging to seven families namely Ichneumonoidae, Braconidae, Chalcididae, Eurytomidae, Eulophidae, Elasmidae, and Tachinidae (*Table 1*) were captured. As for the predators, three species were recorded belonging to two families, Reduviidae and Cleridae. The reduviid predator species found were *Sycanus dichotomus* and *Cosmolestes picticeps* while the clerid predator found was *Callimerus arcufer* (*Table 1*).

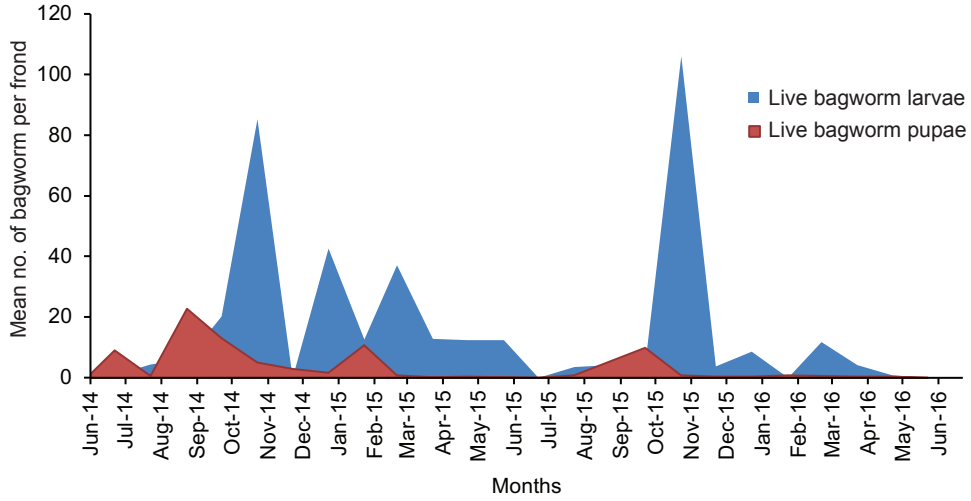


Figure 2. The bagworm, Pteroma pendula *population density at the study area in Bagan Datuk, Perak.*

TABLE 1. THE LIST OF NATURAL ENEMIES SPECIES AND THEIR ABUNDANCE IN *Turnera subulata* GROVES AND OIL PALM INTER ROWS CAPTURED USING STICKY TRAP AND SWEEP NET

Trophic guild	Order	Family	Species	No. of individuals		
				Turnera subulata groves	Oil palm inter rows	Total
Parasitoid	Hymenoptera	Ichneumonoidae	*Spinaria spinator*	26	8	34
			Paraphylax varius	6	6	12
			Buysmania oxymora	4	0	4
			Unidentified	8	0	8
		Eulophidae	*Pediobius anomalus*	2	0	2
			Tetrastichus sp.	4	0	4
			Sympiesis sp.	24	2	26
			Pediobius imbreus	2	0	2
		Braconidae	*Dolichogenidae metesae*	22	6	28
			Apanteles aluella	2	0	2
			Aulosaphes psychidivorus	2	0	2
		Chalcididae	*Brachymeria lugubris*	150	14	164
			Brachymeria carinata	384	32	416
		Elasmidae	*Elasmus* sp.	6	0	6
			Unidentified	2	0	2
		Eurytomidae	*Eurytoma* sp.	4	0	4
	Diptera	Tachinidae	Unidentified	4	2	6
Predator	Hemiptera	Reduviidae	*Cosmolestes picticeps*	199	102	301
			Sycanus dichotomus	2	2	4
	Coleoptera	Cleridae	*Callimerus arcufer*	2	8	10
Total individuals				853	182	1 035

The abundance of natural enemies in *T. subulata* groves revealed that *B. carinata* represented the largest percentage with 45% (384 individuals). *Cosmolestes picticeps* and *Brachymeria lugubris* represented 24% (199 individuals) and 18% (150 individuals), respectively. Other parasitoids and predators were recorded at low levels (<4%) within each species. Based on the findings in this study, it is revealed that *B. carinata* represented the highest number of individuals captured and present in all sampling plots (*Figure 3*).

Meanwhile, at oil palm inter-row plots, a total of 182 individuals comprising 70 parasitoids and 112 predators, were captured using sticky traps and sweep nets. There were seven different parasitoid species in all, and they were divided into five different families: Ichneumonoidae, Braconidae, Chalcididae, Eulophidae, and Tachinidae. Whereas, three species of predators, from two families (Reduviidae and Cleridae) were recorded. Contrasting to *T. subulata* groves, *C. picticeps* was discovered to be the most prominent species, representing 58% of all captures (102 individuals), followed by *B. carinata* (18%: 32 individuals), *B. lugubris* (7%: 14 individuals). Other species were recorded at lower levels (<5%) (*Figure 3*). The occurrence of more predators than parasitoids in inter-row plots was in contrast with the finding in *T. subulata* plots. In the inter-row plots, where there were no beneficial plants, the predators appear to predominate over the parasitoids. The predators have frequently been discovered residing around the ground covers, which was also suggested by Norman and Basri (2010). While the parasitoid prefers to dwell on *T. subulata* due to the shelter and nectar source. The lack of parasitoids in the oil palm inter-row could occur in an area with palms that are physically uniform in height and size. According to Mohd Hanysyam *et al*. (2013), this situation might not be ideal for the parasitoids' activities due to insufficient intense sunlight or availability of food. However, it might provide sustenance for naturally occurring interactions with bagworms, which act as hosts for their reproduction.

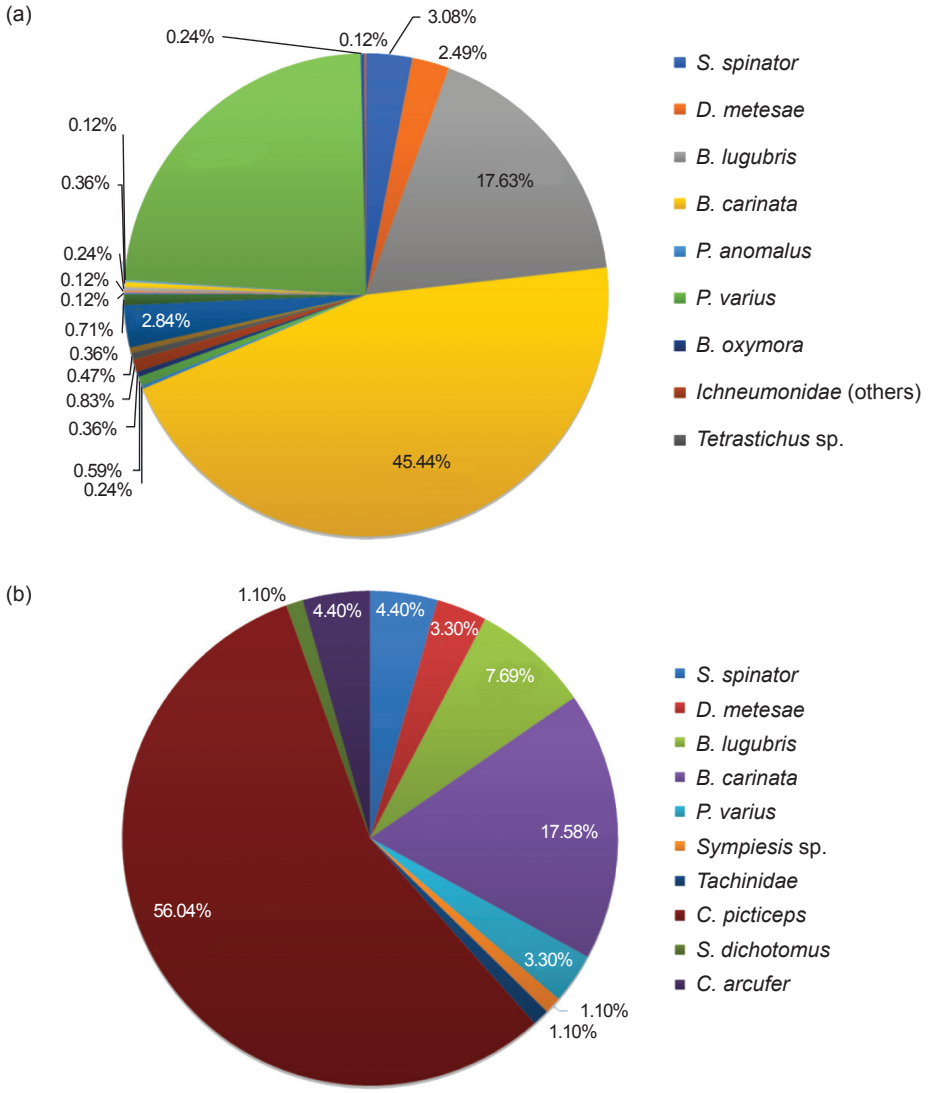


Figure 3. The percentage of natural enemies species captured at (a) Turnera subulata *groves and (b) oil palm inter-rows.*

A greater presence of both parasitoids and predators was recorded in *T. subulata* groves compared to the oil palm inter-rows (*Figure 4* and *5*). The increase in the observation of the natural enemies in the groves of *T. subulata* coincided with the negligible presence of bagworms on the oil palm fronds. The insect natural enemies are drawn to the groves by the abundance of incentives (*i.e.*, nectar and shelter). As pointed out by Jonsson *et al*. (2010), habitat manipulation, in this case, by offering shelters and resources limited in the agroecosystems, has proven to be effective in conserving the natural enemies.

Besides the reduviid predator *C. picticeps*, the prominent parasitoids found at all sampling sites were mostly chalcids (*B. lugubris* and *B. carinata*) and braconids (*Dolichogenidea metesae*). The results showed that the sweep net consistently captured a wider range of natural enemies than the sticky trap, as shown in *Figure 5* and *6*. According to Shweta and Rajmohana (2016), this could be due to the majority of the natural enemies being the resident population. Sweep nets are regarded as one of the most simple and effective ways to catch hymenopteran parasitoids as well as other types of insects (Daniel *et al*., 2018). Results showed that the overall effect of the sampling technique on natural enemies' capture was highly significant ($F = 15.969$; $df = 1$; $P<0.001$). Similarly, the sampling location also exhibited a highly significant effect on the natural enemy captures ($F = 13.252$; $df = 1$; $P<0.001$). Overall, the interaction between the sampling technique and sampling locations was significant ($F = 9.125$; $df = 1$; $P = 0.003$) (*Table* 2). These findings demonstrate that the natural enemies' activities shifted to the *T. subulata* plant groves due to the

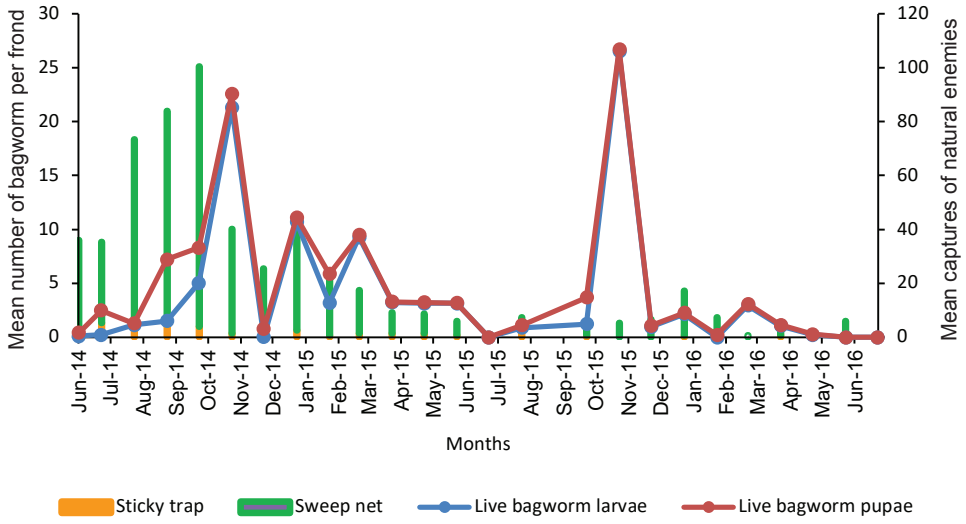


Figure 4. Mean of monthly captures of insect natural enemies using sticky trap and sweep net on Turnera subulata *groves in relation to bagworm population.*

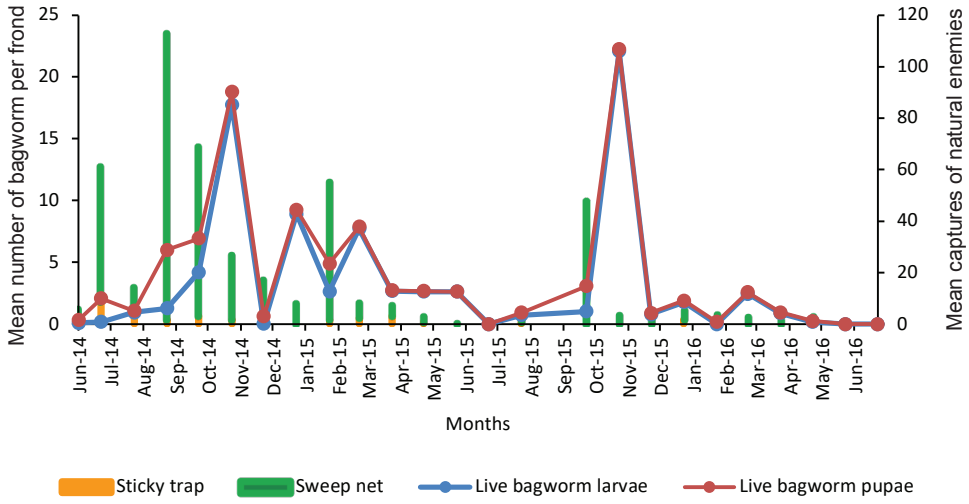


Figure 5. Mean of monthly captures of insect natural enemies using sticky trap and sweep net in oil palm inter-row in relation to bagworm population.

low and fluctuated number of bagworm hosts in the oil palm inter-rows. This also implies that the parasitoids tended to congregate around their food sources (in *T. subulata*). This situation can be seen in the sampling where *T. subulata* grove plots had recorded a constantly higher number of captures compared to oil palm inter-rows (*Table 1*).

The observation of natural enemies' emergence was also conducted in the laboratory. Overall, 222 natural enemies from six species of Hymenopteran parasitoids and one species of Coleopteran predator were associated and found to have emerged from *P. pendula* that had been sampled throughout the sampling period in all experimental blocks (*Figure 6*). The most prominent family was Eulophidae, which included three species (*Pediobius imbrues*, *Pediobius anomalus* and *Pediobius elasmi*) and 191 individuals, which constituted 86% of the total individuals found emerging from the bagworms, followed by Ichneumonidae (7.2%), Cleridae (5.9%) and Chalcididae (0.9%). The most abundant parasitoid species was *P. imbrues* (74.8%), followed by *P. anomalus* (10.8%), *P. varius* (5.0%), an unidentified Ichneumonid (2.3%), *B. carinata* (2.9%), and *P. elasmi* (0.5%). A species of Clerid predator, *C. arcufer* (representing 5.9%) was also found to emerge from the bagworm. The percentage of natural enemies' species is displayed in *Figure 6*.

While the correlation analysis between natural enemies (from emergence, sweep net and sticky trap data) and larval stages of *P. pendula* gave a low coefficient (r) value, a significant positive correlation was observed between natural enemies (captured by sweep net and sticky trap) and pupal stage of *P. pendula* ($r = 0.659$; $r^2 = 0.434$; $P<0.001$) (*Table 3*). This indicates a higher occurrence of the emergence of parasitoids from the pupal stage of *P. pendula* compared to larval stages, this finding was supported by earlier finding by Basri *et al.* (1995). This is explained by the fact that different parasitoid species have different life spans, some of which may not be synced with the duration of

TABLE 2. TWO-WAY ANOVA ANALYSIS ON THE NUMBER OF NATURAL ENEMIES CAPTURED BY DIFFERENT SAMPLING TECHNIQUES IN RELATION TO SAMPLING LOCATIONS

Source of variation	Degree of freedom	Sum of squares	Mean square	F-value	*P*-value
Sampling technique	1	173.925	173.925	15.969	<0.001
Sampling location	1	144.325	144.325	13.252	<0.001
Sampling technique x Sampling location	1	99.381	99.381	9.125	0.003
Residual	92	1 001.987	10.891		
Total	95	1 419.618	14.943		

Note: Numbers in bold font indicate a significant difference ($P< 0.05$).

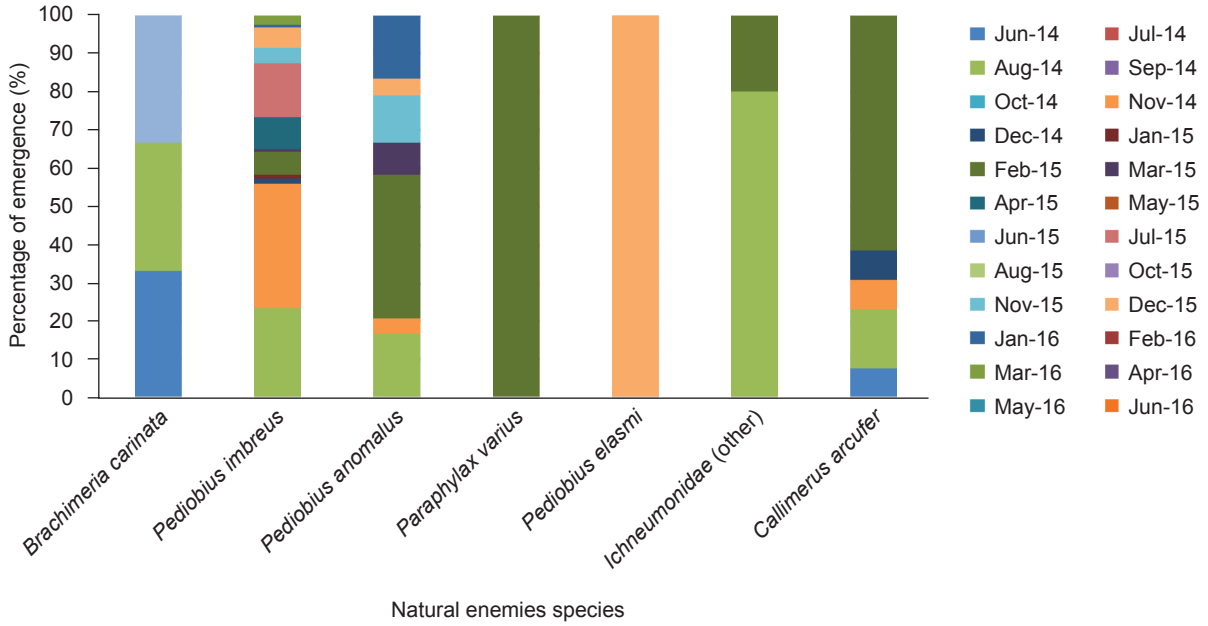


Figure 6. The percentage of species accumulation emergence for natural enemies throughout the study duration.

their preferred host stages. This did not represent the entire degree of parasitism because the parasitoids' life span was only a fraction of that of the bagworm, and sampling was done in a short time per sampling activity. Factors such as direct disturbances, pesticide spraying, unpredictable humidity and temperature can also influence parasitism activity, resulting in a decrease in fauna diversity in oil palm plantations (Mohd Hanysyam *et al*., 2013).

The overall diversity and species richness of natural enemies recorded were calculated with several diversity indices and presented in *Table 4*. The S′, D′, H′ and E′ values varied between the sampling locations. The highest natural enemies' diversity was found in the *T. subulata* groves, which has a Shannon-Wiener index diversity of 1.747 as compared to oil palm inter-rows (1.447). The index trend is similar to Simpson's index, which is higher on *T. subulata* groves (0.406). These values are supported by the dominant and higher abundance of natural enemies on *T. subulata* groves (*Table 1*) that indicated that 82% of total individuals captured using both sampling techniques was dominated by Chalchidae family (580 individuals). Evennes index provides information on composition and richness, with oil palm inter-rows having the greatest value (0.628) as compared to *T. subulata* groves (0.583). In terms of species richness, *T. subulata* groves were twice as rich as oil palm inter-rows. The greater value of H′ in the *T. subulata* area is influenced by the values of E′ (E = 0.583) and D′ (D = 0.406). In the case of oil palm inter-rows, the decreased value of H (H = 1.447) is attributable to less insect diversity since the area was shaded by the oil palm canopy. This finding demonstrated that the practices of establishing the beneficial plants in the oil palm plantation were able to exploit the natural enemies (parasitoids and predators) in regulating the bagworm population, as supported by Mohd Hanysyam *et al.* (2013).

Different parasitoid species were discovered in this study. Some behaved as primary parasitoids, hyperparasitoids, and some species might fit into both categories, such as *P. anomalus, P. imbrues, Elasmus* sp. and *Tetrastichus* sp. These similar species have also been found on other species of bagworms, such as *Metisa plana* and *Mahasena corbetti* (Basri *et al.,* 1995). According to Basri *et al*. (1995), the primary parasitoids were the dominant cause of host mortality from the third to the final instar, proving that they were the predominant main cause of bagworm decline. These are the ecosystem service providers whose agents are crucial in keeping bagworm populations below threshold levels.

Apart from the commonly found *C. picticeps*, other predatory species with the capacity to prey on the bagworms include *S. dichotomus* (Hemiptera: Reduviidae) and *C. arcufer* (Coleoptera: Cleridae) (Siti Nurulhidayah *et al*., 2020). This shows that while the presence of the bagworms' natural enemies is often scarce, they have the potential to multiply and impose natural control. Nevertheless, the presence of alternative hosts may also aid in maintaining the population, particularly for the primary parasitoids (Basri *et al*., 1995). As stated by Basri *et al*. (1995), in addition to the natural control provided by predators and parasitoids, bagworm mortality can also be caused by infertility, empty bags, desiccation and disintegration, fungal infection, host feeding, and incomplete pupation.

TABLE 3. THE CORRELATION COEFFICIENT BETWEEN BAGWORM AND NATURAL ENEMIES

	Natural enemies (captured by sticky trap and sweep net)			Natural enemies (emergence)		
	r	r^2	*P*-value	R	r^2	*P*-value
Bagworm (all stages)	0.176	0.0310	0.411	0.237	0.0564	0.264
Bagworm (larval stage)	0.0399	0.00159	0.853	0.245	0.0599	0.249
Bagworm (pupal stage)	0.659	0.434	<0.001*	0.0189	0.000358	0.930

Note: r = correlation coefficient value; r^2 = linear regression value; * = significant value at $P< 0.01$.

TABLE 4. COMPARISON OF NATURAL ENEMIES AT THE SAMPLING LOCATIONS USING DIFFERENT DIVERSITY INDICES

Sampling location	Number of individuals	Species richness (S′)	Simpson's index (D′)	Shannon-wiener index (H′)	Evenness (E′)
Turnera subulata groves	853	20	0.406	1.747	0.583
Oil palm inter-rows	182	10	0.247	1.447	0.628
Total	1 035	30	0.653	3.194	1.211

Natural enemies such parasitoids and predator groups have a significant role in population regulation and fluctuation of the bagworm population in oil palm (Halim *et al*., 2017; Siti Nurulhidayah *et al*., 2020). In order to maintain the population of natural enemies for the long-term control of bagworms, Norman and Mohd Basri (2010) strongly recommends the need of planting beneficial plants inside the vicinity of oil palm plantations. The presence of beneficial plants that were planted along the roadside within the plantation enhanced the availability and abundance of the natural enemies in the plantations.

Other beneficial flowering plants, including *C. cobanensis, A. leptosus* and *T. ulmifolia*, have been proven to be effective in natural insect pest management in oil palm environments, particularly in Malaysia (Basri *et al.,* 1999). The constant establishment of these beneficial plants in the plantations can greatly reduce the presence of the bagworm or other insect pest population in the long run as a crucial part of integrated pest management (IPM) and as an ecosystem service, as stated by Norman *et al.* (2019). The natural flowering weed species found in the experimental plots were represented by shrubs, such as *Asystasia intrusa* and *Nephrolepis* fern species. The findings indicate that planting suitable flowering species of beneficial plants as adjacent planting in patches may be useful in promoting the presence of beneficial insects in oil palm surroundings and could be part of a sustainable oil palm ecosystem. Thus, it is strongly recommended that the planting of beneficial plants within the surroundings of the oil palm landscape in order to sustain the population of natural enemies for long-term control of bagworms. The rationale behind planting nectar-producing, beneficial plants is to increase the lifespan of insect natural enemies and retain them in the field to suppress the population of the leaf-eating pest. These studies demonstrated that low populations of bagworms are maintained below their threshold levels with the presence of natural enemies, which contribute to an ecological balance.

Additionally, the size and life stage of the host may also have an impact on the natural enemies' acceptance of the host, particularly parasitoids. A study by Harvey *et al.* (2013) demonstrated that it is possible that competition between parasitoids of the same species or different species will attack a similar host, and that they will be competing for dominance of host resources, which will result in host suppression. It is proven that parasitoids and predators communities with the presence of beneficial plants enrolled as successful biological control agents for bagworms in oil palm plantations.

CONCLUSION

According to the research findings, it can be concluded that the interaction between the sampling technique and sampling locations was significant (p<0.05). The highest natural enemies diversity index and species richness were found in the *T. subulata* groves. This study represents that the higher natural enemies' abundance obtained by the establishment of *T. subulata* in the landscape surrounding the oil palm plantation enhanced the conservation biological control of the *P. pendula*. The finding suggests that *T. subulata* as ground cover in patches could be established to encourage the propagation of natural enemies and could be part of a sustainable oil palm management system. This information will help us understand whether there are adequate natural enemies to maintain an equilibrium in the bagworm population. The environmental alteration would be appropriate for bagworm control since improving the environment is better to ensure that the natural enemies continue to survive and thrive therein.

ACKNOWLEDGEMENT

We would like to thank the Director-General, Director of Biology and Sustainability Research Division, and extend our appreciation for the assistance given by the entire team of the Entomology and Ecology Laboratory (Noor Hasan Mohd Yob, Hajijah Shamsuddin, Tunku Akhirudin T. Aris, Zuriahti Khamis and Dr. Norman Kamarudin).

REFERENCES

Aulia, A F; Sandhu, H and Millington, A C (2020). Quantifying the economic value of ecosystem services in oil palm dominated landscapes in Riau province in Sumatra, Indonesia. *Land, 9(6)*: 194. DOI: 10.3390/land9060194.

Baggen, L R; Gurr, G M and Meats, A (1999). Flowers in tri-trophic systems: Mechanisms allowing selective exploitation by insect natural enemies for conservation biological control. *Entomol. Exp. Appl., 91(1)*: 155-161. DOI: 10.1046/j.1570-7458.1999.00478.x.

Basri, M W (1993). *Life history, ecology and economic impact of the bagworm,* Metisa plana *Walker (Lepidoptera: Psychidae), on the oil palm,* Elaeis guineensis *Jacquin (Palmae), in Malaysia*. Ph.D thesis, University of Guelph. 231 pp.

Basri, M W; Norman, K and Hamdan, A B (1995). Natural enemies of the bagworm *Metisa plana*

(Lepidoptera: Psychidae) and their impact on host population regulation. *Crop Prot., 14(8)*: 637-645. DOI: 10.1016/0261-2194(95)00053-4.

Basri, M W; Simon, S; Ravigadevi, S and Othman, A (1999). Beneficial plants for the natural enemies of the bagworm in oil palm plantations. *Proc. of the 1999 PORIM International Palm Oil Congress – Emerging Technologies and Opportunities in the Next Millennium.* PORIM, Bangi. p. 441-455.

Basri, M W; Norman, K and Othman, A (2001). Field impact of beneficial plants on the parasitism levels of the bagworm, *Metisa plana* (Lepidoptera: Psychidae). *Proc. of the PIPOC 2001 International Palm Oil Congress - Cutting-edge Technologies for Sustained Competitiveness*: *Module 1 - Agriculture, Biotechnology and Sustainability Conference (unedited)*. MPOB, Bangi. p. 441-445.

Böckmann, E and Meyhöfer, R (2017). Sticky trap monitoring of a pest-predator system in glasshouse tomato crops: are available trap colours sufficient? *J. Appl. Entomol., 141(5)*: 339-351. DOI: 10.1111/jen.12338.

Cheong, Y L; Sajap, A P; Hafidzi, M N; Omar, D and Abood, F (2010). Outbreaks of bagworms and their natural enemies in an oil palm, *Elaeis guineensis*, plantation at Hutan Melintang, Perak, Malaysia. *J. Entomol., 7(3)*: 141-151. DOI: 10.3923/je.2010.141.151.

Cheong, Y L and Tey, C C (2012). Understanding pest biology and behaviour for effective control of oil palm bagworms. *The Planter, 88(1039)*: 699-715.

Dainese, M; Schneider, G; Krauss, J and Steffan-Dewenter, I (2017). Complementarity among natural enemies enhances pest suppression. *Sci. Rep., 7*: 8172. DOI: 10.1038/s41598-017-08316-z.

Daniel, J A; Ramaraju, K; Kumar, S M; Jeyaprakash, P and Chitra, N (2018). A study on five sampling methods of parasitic hymenopterans in the rice ecosystem. *J. Biol. Control, 32(3)*: 187-192. DOI: 10.18311/jbc/2018/22104.

Fiedler, A K; Landis, D A and Wratten, S D (2008). Maximizing ecosystem services from conservation biological control: The role of habitat management. *Biol. Control, 45*: 254-271. DOI: 10.1016/j.biocontrol.2007.12.009.

Gurr, G M; Wratten, S D; Landis, D A and You, M (2017). Habitat management to suppress pest populations: Progress and Prospects. *Annu. Rev. Entomol., 62*: 91-109. DOI: 10.1146/annurev-ento-031616-035050.

Halim, M; Muhaimin, A M D; Syarifah Zulaikha, S A; Nor Atikah, A R; Masri, M M M and Yaakop, S (2017). Evaluation of infestation in parasitoids on *Metisa plana* Walker (Lepidoptera: Psychidae) in three oil palm plantations in Peninsular Malaysia. *Serangga, 22(2)*: 135-149.

Harvey, A J; Poelman, E H and Tanaka, T (2013). Intrinsic inter- and intraspecific competition in parasitoid wasps. *Annu. Rev. Entomol., 58*: 333-351. DOI: 10.1146/annurev-ento-120811-153622.

Ho, C T; Ibrahim, Y and Khoo, K C (2011). Infestations by the bagworms *Metisa plana* and *Pteroma pendula* for the period 1986-2000 in major oil palm estates managed by Golden Hope Plantation Berhad in Peninsular Malaysia. *J. Oil Palm Res., 23*: 1040-1050.

Ho, C T; Khoo, K C; Yusof, I and Dzolkhifli, 0 (2003). Comparative studies on the use of beneficial plants for the natural suppression of bagworm infestation in oil palm plantations. *Proc. of the 1999 PORIM International Palm Oil Congress – Agriculture Conference*. MPOB, Bangi. p. 372-424.

Jamian, S; Adam, N A; Noor, H M; Zulperi, D; Asib, N; Muhamad, R; Mokhtar, A S; Abdul Wahab, M A; Azhar, B; Sidi, M and Maamor, A (2020). The effect of plant volatiles on plant preference by the predatory insect, *Sycanus dichotomus* Stal. (Hemiptera: Reduviidae) in oil palm plantation. *J. Oil Palm Res., 32(3)*: 471-479. DOI: 10.21894/jopr.2020.0053.

Janssen, A and van Rijn, P C J (2021). Pesticides do not significantly reduce arthropod pest densities in the presence of natural enemies. *Ecol. Lett., 24*: 2010-2024. DOI: 10.1111/ele.13819.

Jonsson, M; Wratten, S D; Landis, D A; Tompkins, J M L and Cullen, R (2010). Habitat manipulation to mitigate the impacts of invasive arthropod pests. *Biol. Invasions, 12(9)*: 2933-2945. DOI: 10.1007/s10530-010-9737-4.

Koh, I and Holland, J D (2015). Grassland plantings and landscape natural areas both influence insect natural enemies. *Agric. Ecosyst. Environ., 199*: 190-199. DOI: 10.1016/J.AGEE.2014.09.007.

Krauss, J; Gallenberger, I and Steffan-Dewenter, I (2011). Decreased functional diversity and biological pest control in conventional compared to organic crop fields. *PLoS ONE, 6(5)*: e19502. DOI: 10.1371/journal.pone.0019502.

LaSalle, J and Gould, I D (1993). Hymenoptera: Their biodiversity, and their impact on the diversity of other organisms. CAB International. Wallingford, UK. p. 1-26.

Mohd Hanysyam, M N; Fauziah I; Siti Kahiriyah, M H; Fairuz, K; Mohd Rasdi, Z; Nurul Zfarina; Ismail, R and Norazliza, R (2013). Assessment on the diversity of parasitoids of bagworms (Lepidoptera: Psychidae) in FELDA Gunung Besout 6, Sungkai, Perak. *2013 IEEE Symposium on Humanities, Science and Engineering Research (SHUSER)*. IEEE, Adelaide. p. 130-135.

MPOB (2016). *Standard Operating Procedures (SOP) Guidelines for Bagworm Control*. 1st edition. MPOB, Bangi. 32 pp.

Nilsson, U; Rännbäck, L M; Anderson, P; Björkman, M; Futter, M and Rämert, B (2016). Effects of conservation strip and crop type on natural enemies of *Delia radicum*. *J. Appl. Entomol.*, *140(4)*: 287-298.

Noorhazwani, K; Siti Ramlah, A A; Mazmira, M M M; Najib, Che Ahmad Hafiz, C M and Norman, K (2017). Controlling *Metisa plana* Walker (Lepidoptera: Psychidae) outbreak using *Bacillus thuringiensis* at an oil palm plantation. *J. Oil Palm Res.*, *29(1)*: 47-54. DOI: 10.21894/jopr.2017.2901.05.

Norman, K; Basri, M W and Zulkefli, M (2017). *Handbook of Common Parasitoids and Predators Associated with Bagworms and Nettle Caterpillars in Oil Palm Plantations*. MPOB, Bangi. 30 pp.

Norman, K and Basri, M W (2010). Interactions of the bagworm, *Pteroma pendula* (Lepidoptera: Psychidae), and its natural enemies in an oil palm plantation in Perak. *J. Oil Palm Res.*, *22(1)*: 758-764.

Norman, K and Othman, A (2016). Diversity and activity of insect natural enemies of the bagworm (Lepidoptera: Psychidae) within an oil palm plantation in Perak, Malaysia. *J. Oil Palm Res.*, *28(3)*: 296-307.

Norman, K; Idris, A S and Mazmira, M M M (2019). Prospects in sustainable control of oil palm pests and diseases through the enhancement of ecosystem services - The way forward. *J. Oil Palm Res.*, *31(3)*: 381-393.

Nurul Afiah, S M J; Khairunniza-Bejo, S; Rashid, A M; Nur Azuan, H; Mazmira, M M M and Noorhazwani, K (2022). Identification of bagworm (*Metisa plana*) instar stages using hyperspectral imaging and machine learning techniques. *Comput. Electron. Agric.*, *194*: 106739. DOI: 10.1016/j.compag.2022.106739.

Nur Robaatul Adhawiyah, M A N; Noorhazwani Kamarudin; Mohd Fahmi Keni; Mohd Najib Ahmad and Mohamed Mazmira Mohd Masri (2021). Impact of multiple aerial spraying of *Bacillus thuringiensis* on bagworm control in oil palm smallholdings in Johor, Malaysia. *Serangga, 26(4)*: 113-123.

Parameswari, E; Davamani, V; Ilakiya, T; Arulmani, S and Prithiv Raj, V (2020). Impact of pesticides on environment. *Biotica Research Today, 2(5)*: 136-138.

Parveez, G K A; Kamil, N N; Zawawi, N Z; Ong-Abdullah, M; Rasuddin, R; Loh, S K; Selvaduray, K R; Hoong, S S and Idris, Z (2022). Oil palm economic performance in Malaysia and R&D progress in 2021. *J. Oil Palm Res.*, *34(2)*: 185-218. DOI: 10.21894/jopr.2022.0036.

Pobozniak, M; Tokarz, K and Musynov, K (2020). Evaluation of sticky trap colour for thrips (Thysanoptera) monitoring in pea crops (*Pisum sativum* L.). *J. Plant Dis. Prot., 127*: 307-321. DOI: 10.1007/s41348-020-00301-5.

Sáenz-Romo, M G; Veas-Bernal, A; Martínez-García, H; Campos-Herrera, R; Ibáñez-Pascual, S; Martínez-Villar, E; Pérez-Morenoa, I and Marco-Mancebón, V S (2019). Ground cover management in a Mediterranean vineyard: Impact on insect abundance and diversity. *Agric. Ecosyst. Environ., 283*: 106571. DOI: 10.1016/j.agee.2019.106571.

Saravanan, M; Senthilkumar, P; Kalimuthu, K; Rajalakshmi, G and Vajjiram, M C (2018). Regeneration of plants from derived callus of *Turnera subulata* SM - An important medicinal herb. *J. Biosci., 5(2)*: 64-70.

Shakeel Q; Ali, S; Raheel, M; Bajwa, R T; Aqueel, M A; Iftikhar, Y; Ajmal, S and Tariq, K (2022). Habitat manipulation in crops for integrated insect pest and disease management. *Adv. In Integrated Pest Management Technology.* Springer, Cham. p. 83-120. DOI: 10.1007/978-3-030-94949-5_5.

Shweta, M and Rajmohana, K (2016). A comparison of efficiencies of sweep net, yellow pan trap and malaise trap in sampling Platygastridae (Hymenoptera: Insecta). *J. Exp. Zool. India, 19(1)*: 393-396.

Siti Nurulhidayah, A and Norman, K (2016). Growth and longevity of the insect predator, *Sycanus dichotomus* Stal. (Hemiptera: Reduviidae) fed on live insect larvae. *J. Oil Palm Res., 28(4)*: 471-478.

Siti Nurulhidayah, A; Mazmira, M M M and Norman, K (2020). Assessment on voracity and predation by predator, *Sycanus dichotomus* Stal. (Hemiptera: Reduviidae) to oil palm bagworm, *Pteroma pendula*. *J. Oil Palm Res.*, *32(3)*: 480-487. DOI: 10.21894/jopr.2020.0040.

Siti Ramlah, A A; Basri, M W; Mohd Najib, A and Mazmira, M M M (2005). Integrated pest management: Terakil-1, *Cassia cobanensis* and beneficial insects for controlling of bagworms infestation in Malaysia. *Proc. of the PIPOC 2005 International Palm Oil Congress: Technologies Breakthroughs and Commercialization the Way Forward*. MPOB, Bangi. p. 660-690.

Siviter, H; Brown, M J F and Leadbeater, E (2018). Sulfoxaflor exposure reduces bumblebee reproductive success. *Nature, 561(7721)*: 109-112. DOI: 10.1038/s41586-018-0430-6.

Wang, X; Wang, X Y; Kenis, M; Cao, L M; Duan, J J; Gould, J R and Hoelmer, K A (2021). Exploring the potential for novel associations of generalist parasitoids for biological control of invasive woodboring beetles. *Biol. Control, 66:* 97-112. DOI: 10.1007/s10526-020-10039-6

Wood, B J and Norman, K (2019). Bagworm (Lepidoptera: Psychidae) infestation in the centennial of the Malaysian oil palm industry – A review of causes and control. *J. Oil Palm Res., 31(3):* 364-380. DOI: 10.21894/jopr.2019.0032.

Yusdayati, R; Ahmad, A H and Hamid, N H (2014). Diversity and distribution of natural enemies (predators and parasitoids) of bagworms (Lepidoptera: Psycidae) on selected host plants in an oil palm plantation. *The Planters, 90*: 91-101.

Ziolkowska, E; Topping, C J; Bednarska, A J and Laskowski (2021). Supporting non-target arthropods in agroecosystems: Modelling effects of insecticides and landscape structure on carabids in agricultural landscapes. *Sci. Total Envi., 774*: 145746. DOI: 10.1016/j.scitotenv.2021.145746.

Journal of Oil Palm Research Vol. 36 (3) September 2024 p. 380-392
DOI: https://doi.org/10.21894/jopr.2023.0023

PERFORMANCE OF SELFED AND INTERCROSSED OIL PALM DELI ULU REMIS PROGENIES BASED ON SELECTED AGRONOMIC TRAITS

NORZIHA, A[1]*; ZAMRI, Z[2]; ZULKIFLI, Y[1]; FADILA, A M[1]; MARHALIL, M[1] and MOHD DIN, A[1]

ABSTRACT

Deli is considered the best dura *material for breeding and seed production. The Deli* dura *is predominantly utilised as the maternal parent in all commercial* dura *x* pisifera *(DxP) hybrid seed production programmes. This study evaluated the selfed and intercrossed Deli Ulu Remis oil palm progenies at the Malaysian Palm Oil Board (MPOB) Research Station in Kluang, Johor, Malaysia. Performance of the selfed and intercrossed progenies in the bunch yield and bunch quality components were assessed. We also estimated the variance components and heritability for selected agronomic traits, based on the parental types. Intercrossed progenies produced significantly higher yields compared to selfed progenies. Broad-sense heritability estimates were higher in selfed compared to intercrossed progenies for most of the agronomic characters. In summary, this study identified the most promising* dura *progeny and individual palms as the female parents for commercial oil palm seed production, as well as a source for further genetic improvement via ongoing breeding programmes.*

Keywords: breeding, deli *dura*, heritability, yield.

Received: 6 October 2022**; Accepted:** 9 April 2023**; Published online:** 30 May 2023.

INTRODUCTION

The oil palm (*Elaeis guineensis* Jacq.) is the most productive oil crop in terms of oil yield per hectare compared to other vegetable oils (Kome *et al*., 2020). Although the maximum theoretical oil yield has been predicted to be 18.2 t/ha/yr (Corley, 1998), stagnation in the oil yields of between 3.5 to 3.9 t/ha has been observed for more than two decades (Kushairi *et al.,* 2010). Therefore, increasing productivity through high-yielding planting materials is a feasible approach as such materials are available in the industry. In 2020, the Malaysian oil palm industry produced 19.14 million tonnes of crude palm oil (CPO), where the average fresh fruit bunch (FFB) yield was 16.73 t/ha with an oil extraction rate (OER) of 19.92% (MPOB, 2021). This performance was slightly lower, compared to the previous year due to the outbreak of the global COVID-19 pandemic.

Commercial seed production programmes in Malaysia currently use the Deli *dura*s as the female parents (Kushairi *et al*., 2011; Kushairi and Mohd Din, 2020). The Deli type is still considered the best *dura* for breeding and seed production which originated from the four palms planted at the Botanical Garden in Bogor (1848) (Hartley 1988; Rajanaidu *et al*., 2000). Compared to the *tenera* fruit form and the African *dura*s, Deli *dura*s produce fewer but heavier bunches. The fruit colour is darker, larger, and have a high mesocarp content, with higher oil to bunch ratio compared to African *dura*s. Despite their

[1] Malaysian Palm Oil Board,
6, Persiaran Institusi, Bandar Baru Bangi,
43000 Kajang, Selangor, Malaysia.

[2] Institute of Systems Biology,
Universiti Kebangsaan Malaysia,
43600 Bangi, Selangor, Malaysia.

* *Corresponding author e-mail: norziha.abdullah@mpob.gov.my*

narrow genetic base, Sparnaaij and van der Vossen (1980) in their review, provided justifications for the continuous exploitation of Deli populations in breeding programmes.

Oil palm has a long breeding cycle of 10 to 12 years. It is therefore of utmost importance to understand the variability, inheritance and genetic pattern of the materials studied. This information would be useful in designing breeding programmes for selection and improvement. Oil palm breeding programmes and selection in the Malaysian Palm Oil Board (MPOB) adopt a two-pronged approach, which includes prospecting new germplasm apart from fully utilising the traditional Deli *dura* and AVROS *pisifera* collections (Marhalil *et al*., 2016; Noh *et al*., 2012). Studies on the performance of (Deli x Deli) and (Deli x AVROS) progenies have been carried out extensively to identify the outstanding progenies to increase oil production.

In this study, the performance of 28 intercrossed and 35 selfed progenies from Deli Ulu Remis *dura* were evaluated in terms of bunch yield and bunch quality components. Analyses were conducted to estimate the genetic components and heritability of these agronomic traits and to identify the potential progenies and individual palms for breeding and seed production.

MATERIALS AND METHODS

The materials used in this study comprise two groups, *i.e.,* Deli *dura* (Ulu Remis) progenies: intercrossed (28 progenies) and selfed (35 progenies). The intercrossed and selfed progenies were field planted on inland soil in trials 0.484 and 0.488 respectively, at MPOB Kluang Research Station, Johor, Malaysia. Both trials (0.484 and 0.488) were initiated in August 2008, in a Randomised Complete Block Design (RCBD) with four and three replications for intercrossed and selfed progenies respectively, and at 16 palms per progeny per replication. The total number of palms evaluated in this study was 2553.

Data Collection

Harvesting and FFB yield recording were initiated by MPOB in August 2011. FFB yield data were recorded for each individual palm, at each harvesting round (2 to 3 rounds per month), starting from 36 months after field planting. The yield record was summarised over 12 months, between January and December for each year until December 2020. Summarised bunch yields for the four best consecutive years (*i.e.,* 2016 to 2019 or 7.5 to 10.5 years old) were used for data analysis. Meanwhile, bunch and fruit quality components were analysed for nine years (2012-2020). Bunch quality components were estimated using the bunch analysis method (Rao *et al*., 1983), to determine the oil extraction and fruit quality components. For this purpose, three bunches were sampled from each palm. To avoid seasonal variation, ripe bunches with one to 10 loose fruits were randomly sampled at intervals of at least three months (Rao, 1987).

Data Analysis

Data on bunch yield and bunch quality characters was based on individual palms and computed using the Statistical Analysis System (SAS) program. Analysis of variance (ANOVA) and comparison between progeny means was carried out using Fisher's Least Significant Difference (LSD) procedure at the minimum 5% level of probability. Broad-sense heritability statistics were estimated for each character using variance components. Variance analysis for the estimation of broad-sense heritability was processed from the variance component procedure (PROC VARCOMP) of SAS version 9.2 using Equation (1):

$$h^2_B = \frac{a^2 f}{a^2 f + a^2 wf} \quad (1)$$

where α^2f = variance between progenies, α^2wf = variance within progenies. In full-sib progenies, $2h^2_B$ equals broad sense heritability (Falconer and Mackay, 1996).

RESULTS AND DISCUSSION

Yield Performance of DxD Intercrossed and Selfed Progenies

The progeny factor in both intercrossed and selfed progenies was highly significant for all yield traits (*Table 1*). It is widely known that many factors affect oil palm yield components including uncontrollable aspects, such as its growing environment and the genetic background of the planting materials. High heritability values were observed for the bunch number (BNO), with a higher value of 0.34 for selfed progenies compared to 0.22 for intercrossed progenies. Our results further revealed that genetic variation contributed to 0.16-0.34 of the phenotypic variation in yield, *i.e.,* FFB, BNO and average bunch weight (ABW), suggesting stronger uncontrolled factors that include environmental influence on the expression of these characters.

Moreover, heritability estimates for yield characters vary depending on location, suggesting

that the environment may exert a stronger influence on yield (Mohd Din *et al*., 2015).

The best performing progeny among the intercrossed progenies is PK4687, producing FFB of 218.77 kg/palm/yr (*Table 2*), *i.e.*, ~25% above the trial mean of 175.59 kg/palm/yr. This high FFB yield was likely contributed by its high BNO (13.91 bunches/palm/yr). Selecting for high BNO may also lead to a high sex ratio. In comparison, PK4669 produced the lowest FFB yield of only 146.28 kg/palm/yr, *i.e.*, 16.7% below the trial mean. PK4654 recorded the highest ABW of 18.0 kg/bunch, with a moderate FFB yield of 155.91 kg/palm/yr, likely resulting from its low BNO (8.80 bunches/palm/yr). On the other hand, evaluation of the DxD selfed progenies revealed that PK4587 produced the highest FFB yield with 182.67 kg/palm/yr but this was not significantly different from the yields of seven other progenies, PK4341, PK4378, PK4386, PK4440, PK4452, PK4497 and PK4554. The lowest FFB yield in PK4677 progeny was likely due to its lower BNO of 7.56 bunches/palm/yr and producing a modest ABW (14.49 kg/bunch/yr). Improvements on various *dura* lines such as Banting, Elmina and Ulu Remis have shown that Elmina *dura*s provide the best FFB yield with oil to bunch (O/B) of 24.09% (Marhalil *et al*., 2016). However, only a small improvement was observed from the F4 to F5 Elmina *dura* generations, which may be due to several factors including inbreeding. Selection improvement for FFB yield in the second and subsequent generations has been estimated to be 10%-15% per generation (Hardon *et al*., 1987).

TABLE 1. MEAN SQUARES, VARIANCE COMPONENTS AND HERITABILITIES FOR YIELD AND YIELD COMPONENTS IN 28 DxD INTERCROSSED AND 35 DxD SELFED PROGENIES

Source	df	Mean squares		
		FFB (kg/palm/yr)	BNO (bunches/palm/yr)	ABW (kg/palm/yr)
		DxD intercrossed progenies		
Replication (R)	3	57 015.91**	171.25**	61.13**
Progenies (P)	27	13 933.44**	63.65**	39.20**
RxP	77	4 395.53**	13.84**	19.72**
Within palms	1 192	1 765.89	7.20	6.16
Progeny variance (σ^2_p)		167.66	0.92	0.72
RxP variance (σ^2_{gr})		162.76	0.41	0.84
Within palms variance (σ^2_w)		1 765.90	7.20	6.16
Broad-sense heritability, h^2_B		**0.16**	**0.22**	**0.19**
		DxD selfed progenies		
Replication (R)	2	3 831.09*	2.45^{ns}	23.41**
Progenies (P)	34	15 299.72**	95.44**	50.00**
RxP	65	4 019.88**	23.21**	18.97**
Within palms	1 151	1 369.20	6.25	4.95
Progeny variance (σ^2_p)		246.09	1.58	0.67
RxP variance (σ^2_{gr})		214.69	1.37	1.14
Within palms variance (σ^2_w)		1 369.20	6.25	4.95
Broad-sense heritability, h^2_B		**0.27**	**0.34**	**0.20**

Note: FFB - fresh fruit bunch; BNO - bunch number; ABW - average bunch weight; *, ** Significant at $P \leq 0.05$ and $P \leq 0.01$ respectively, otherwise not significant.

TABLE 2. PROGENY MEANS OF 28 DxD INTERCROSSED AND 35 DxD SELFED DELI ULU REMIS PROGENIES FOR YIELD AND YIELD COMPONENTS

No.	Progeny	Pedigree	N	FFB (kg/palm/yr)	BNO (bunches/palm/yr)	ABW (kg/palm/yr)
			DxD intercrossed progenies			
1.	PK4419	0.332/451 x 0.332/83	49	186.16b-e	11.32e-i	16.48c-e
2.	PK4494	0.332/83 x 0.332/215	44	159.31j-n	10.95g-i	14.75g-k

TABLE 2. PROGENY MEANS OF 28 DxD INTERCROSSED AND 35 DxD SELFED DELI ULU REMIS PROGENIES FOR YIELD AND YIELD COMPONENTS (continued)

No.	Progeny	Pedigree	N	FFB (kg/palm/yr)	BNO (bunches/palm/yr)	ABW (kg/palm/yr)
3.	PK4515	0.332/83 x 0.332/451	37	173.81e-l	11.99b-g	14.41i-k
4.	PK4520	0.332/190 x 0.332/451	47	203.18ab	13.04ab	15.71d-g
5.	PK4536	0.332/190 x 0.332/157	46	165.43g-m	11.41e-i	14.61h-k
6.	PK4566	0.332/382 x 0.332/451	48	179.09d-n	11.04g-i	16.36c-f
7.	PK4567	0.332/451 x 0.332/382	50	156.82 l-n	10.45i-k	15.08g-i
8.	PK4571	0.332/382 x 0.332/83	45	167.14f-m	12.20b-f	13.81jk
9.	PK4572	0.332/157 x 0.332/83	43	178.08d-i	11.73c-h	15.39f-i
10.	PK4588	0.332/360 x 0.332/83	50	186.87b-e	12.71bc	14.84g-j
11.	PK4597	0.332/330 x 0.332/83	49	192.11b-d	11.72c-h	16.86bc
12.	PK4602	0.332/360 x 0.332/157	48	156.36l-n	11.52d-i	13.78k
13.	PK4603	0.332/83 x 0.332/190	49	175.24d-k	11.46d-i	15.56e-h
14.	PK4612	0.332/360 x 0.332/45	48	178.13d-i	11.38e-i	15.68e-g
15.	PK4615	0.332/190 x 0.332/83	50	185.25c-e	12.54b-d	14.85g-j
16.	PK4618	0.332/157 x 0.332/382	49	163.22h-n	11.23f-i	14.70g-k
17.	PK4619	0.332/83 x 0.332/45	12	160.69i-n	11.88c-h	13.74k
18.	PK4628	0.332/446 x 0.332/83	55	186.81b-e	12.04b-g	15.62e-h
19.	PK4634	0.332/190 x 0.332/382	54	182.95c-g	12.39b-e	14.84g-j
20.	PK4641	0.332/360 x 0.332/215	50	151.13mn	9.21 l	16.52c-e
21.	PK4642	0.332/215 x 0.332/45	39	158.26k-n	9.59kl	16.75b-d
22.	PK4654	0.332/451 x 0.332/215	44	155.91mn	8.80l	18.00a
23.	PK4665	0.332/360 x 0.332/330	44	175.76d-k	11.71c-h	15.57e-h
24.	PK4669	0.332/330 x 0.332/215	44	146.28n	9.79j-l	15.25g-i
25.	PK4680	0.332/360 x 0.332/451	47	199.21bc	11.37e-i	17.68ab
26.	PK4687	0.332/45 x 0.332/83	44	218.77a	13.91a	15.68e-g
27.	PK4688	0.332/330 x 0.332/382	54	183.90c-f	10.78h-j	17.31a-c
28.	PK4718	0.332/382 x 0.332/45	58	176.37d-j	12.19b-f	14.72g-k
	Mean			**175.59**	**11.46**	**15.53**
	LSD			17.88	1.12	1.05
			DxD selfed progenies			
1.	PK4232	0.332/382 x 0.332/382	40	138.10jk	11.40f-j	11.99p
2.	PK4244	0.332/214 x 0.332/214	47	119.75l	9.45mn	12.68n-p
3.	PK4260	0.332/203 x 0.332/203	41	143.31h-k	10.32j-n	13.95d-j
4.	PK4289	0.332/19 x 0.332/19	38	169.42a-e	11.39f-j	15.01bc
5.	PK4291	0.332/370 x 0.332/370	31	168.99a-e	12.55b-e	13.89e-k
6.	PK4297	0.332/277 x 0.332/277	41	141.73i-k	10.83h-l	13.21h-o
7.	PK4309	0.332/100 x 0.332/100	31	172.31a-c	12.68b-d	14.32c-g
8.	PK4336	0.332/363 x 0.332/363	40	148.56f-k	10.58i-m	14.19c-h
9.	PK4337	0.332/133 x 0.332/133	45	165.24b-f	10.07l-n	16.60a
10.	PK4341	0.332/224 x 0.332/224	22	176.16ab	14.22a	12.42op
11.	PK4342	0.332/285 x 0.332/285	42	159.70b-h	11.26g-k	14.25c-g
12.	PK4343	0.332/275 x 0.332/275	43	144.88g-k	10.68i-l	13.67g-n
13.	PK4378	0.332/247 x 0.332/247	31	171.61a-c	11.65d-i	14.76c-f
14.	PK4385	0.332/2 x 0.332/2	41	111.213l	8.18o	13.63g-n
15.	PK4386	0.332/329 x 0.332/329	37	171.21a-d	11.40e-j	14.97b-d

TABLE 2. PROGENY MEANS OF 28 DxD INTERCROSSED AND 35 DxD SELFED DELI ULU REMIS PROGENIES FOR YIELD AND YIELD COMPONENTS (continued)

No.	Progeny	Pedigree	N	FFB (kg/palm/yr)	BNO (bunches/palm/yr)	ABW (kg/palm/yr)
16.	PK4395	0.332/330 x 0.332/330	42	144.54g-k	10.01l-n	14.65c-g
17.	PK4435	0.332/317 x 0.332/317	34	147.83g-k	9.34n	15.88ab
18.	PK4440	0.332/413 x 0.332/413	34	171.08a-e	13.39a-c	12.95j-p
19.	PK4443	0.332/124 x 0.332/124	44	159.72b-h	11.84d-h	13.73g-m
20.	PK4447	0.332/153 x 0.332/153	39	141.54i-k	10.13k-n	14.09c-i
21.	PK4448	0.332/47 x 0.332/47	40	154.69d-j	10.69h-l	14.59c-g
22.	PK4452	0.332/369 x 0.332/369	31	172.84a-c	12.44c-f	14.14c-h
23.	PK4487	0.332/222 x 0.332/222	26	138.38jk	10.11k-n	13.80f-l
24.	PK4497	0.332/144 x 0.332/144	37	173.18a-c	13.62ab	12.84l-p
25.	PK4514	0.332/451 x 0.332/451	17	150.62f-k	10.13k-n	15.00bc
26.	PK4544	0.332/107 x 0.332/107	39	154.36e-j	11.32f-j	13.79f-l
27.	PK4554	0.332/83 x 0.332/83	37	175.67ab	13.48a-c	13.10i-o
28.	PK4559	0.332/416 x 0.332/416	35	137.08k	11.38f-j	12.04p
29.	PK4585	0.332/215 x 0.332/215	41	136.91k	9.43mn	14.61c-g
30.	PK4587	0.332/114 x 0.332/114	31	182.67a	11.56d-i	16.38a
31.	PK4633	0.332/9 x 0.332/9	28	156.36c-i	12.37c-g	12.70m-p
32.	PK4649	0.332/135 x 0.332/135	38	157.84c-i	11.05h-l	14.37c-g
33.	PK4676	0.332/394 x 0.332/394	22	158.75c-h	10.68i-l	14.85b-e
34.	PK4677	0.332/378 x 0.332/378	41	108.38l	7.56o	14.49c-g
35.	PK4678	0.332/45 0.332/45	27	160.25b-g	12.56b-d	12.90k-p
	Mean			**152.60**	**11.04**	**14.00**
	LSD			16.83	1.16	1.04
	Parent mean (0.332)			**160.86**	**14.42**	**11.21**

Note: FFB - fresh fruit bunch; BNO - bunch number; ABW - average bunch weight; N - number of individual palms. Means with the same letter in superscript are not significantly different at $P \leq 0.05$ based on the Least Significant Difference (LSD) test.

Performance of DxD Intercrossed and Selfed Progenies on Bunch Quality Components

Bunch quality components for the oil palm are related to the oil content and variability in bunch composition. Substantial genetic variations on these traits were observed (*Table 3*), which may be exploited for further selection and improvements. There was a statistically significant interaction between the replicates and progeny factors (R×P) on all the evaluated traits except kernel to fruit ratio (K/F) in selfed progenies. This suggested that there may be irregularities in the performance of these traits across the replicates. The results contrasted with Noh *et al.* (2014) where these five traits showed no significant difference in R×P interaction among 12 introgressed progenies of Nigerian *dura* x Deli *dura*. It is not usual to observe R×P interactions for bunch components. Many reasons can be investigated. The main suggestion should be to verify the identity of the crossings in each replicate, to eliminate the risk of mistakes.

Alvarado and Escobar (2016) reported that a mesocarp to fruit ratio (M/F) of 60.7% to 67.8% was observed in 33 DxD progenies planted in Costa Rica. They also observed that the percentage of O/B varied from 23.0% to 26.0% which was higher than the industry standard for *dura* palms. In DxD intercrossed progenies, PK4619 provided the highest M/F (67.71%) while PK4232 from the selfed progenies produced the highest M/F (68.07%), likely due to its lowest S/F among the selfed progenies (*Table 4*). The M/F for the intercrossed progenies ranged from 59.46%-67.71% while a slightly wider range was observed for selfed progenies (57.27%-68.07%). The O/B varied from 18.84%-23.57% for the intercrossed progenies and 15.21%-22.26% for the selfed progenies, which is lower than the O/B range reported for the DxD progenies in Costa Rica (Alvarado and Escobar, 2016). O/B is a derived character comprising of fruit to bunch, mesocarp to fruit and oil to wet mesocarp ratios. Thus, the O/B differences observed between the DxD progenies in Alvarado

and Escobar (2016) and this study may be due to the other contributing parameters to the O/B, such as the oil to wet mesocarp and fruit to bunch values, in addition to environmental and genotypic differences.

O/B is a significant character used for oil palm breeding and selection (Noh *et al*., 2010). In this study, the highest achieving intercrossed progeny in terms of O/B was PK4612 (0.332/360 x 0.332/45) (23.57%) and may thus be selected for oil improvement through breeding. Among the selfed progenies, PK4678 (0.332/45 x 0.332/45) recorded the highest O/B (22.26%) which was slightly lower than PK4612's O/B of 23.57%. Based on these results, the parent palm of PK4612 and PK4678 (palm no. 0.332/45) may possess a good genetic control for the O/B character. A previous evaluation of 10 DxD progenies means of 22.19% O/B and 62.73% M/F (Burhanuddin *et al*., 2017), suggested that the O/B and M/F means of the selfed and intercrossed DxD progenies obtained in this study are comparable.

Based on several parameters, most of the material evaluated displayed mean values higher than the commercial minimum standard requirement. The main objective in establishing these trials was to select potential palms for use as female parents for commercial seed production. To ensure production authenticity for desired productivity and sustainability of the oil palm industry, a Malaysian Standard (MS) was developed for DxP hybrid seeds. Based on this Malaysian standard, the *dura* to be used as a female parent must meet certain criteria and be differentiated based on the pedigree and performance (SIRIM, 2017). Malaysian Standard (MS 157) issued by the Department of Standards Malaysia (STANDARDS MALAYSIA) is developed by a committee which consists of a representative from oil palm breeders, producers and planters. The standard, *Oil Palm Seeds for Commercial Planting -Specification,* was first published in 1973 and has been reviewed periodically and the latest (fourth) edition (MS 157:2017) was published in 2017. The standard includes a minimum FFB yield of 150 kg/palm/yr, a minimum mesocarp to fruit ratio of 57%, a maximum shell to the fruit of 33%, a minimum kernel to fruit ratio of 5%, a minimum oil to dry mesocarp of 75% and a minimum oil to a bunch of 19%. However, Kandha *et al*. (2017) reported that many commercial oil palm seed producers have progressed from simple two-way crosses to more complicated multi-way crosses, with the expectation of increasing the hybrid vigour and hence developing a higher yield potential.

TABLE 3. MEAN SQUARES, VARIANCE COMPONENTS AND HERITABILITIES FOR BUNCH QUALITY COMPONENTS IN 28 DxD INTERCROSSED PROGENIES AND 35 DxD SELFED PROGENIES

Source	df	Mean squares				
		M/F (%)	K/F (%)	S/F (%)	O/DM (%)	O/B (%)
		DxD intercrossed progenies				
Replication (R)	3	146.62**	4.91^{ns}	193.51**	13.71^{ns}	12.08^{ns}
Progenies (P)	27	167.85**	31.24**	133.58**	44.39**	67.39**
RxP	77	24.57*	4.88**	20.17**	1.86**	17.25**
Within palms	1 192	16.28	2.05	11.56	4.60	9.50
Progeny variance (σ^2_p)	-	2.92	0.53	2.30	0.72	0.99
RxP variance (σ^2_{gr})	-	0.56	0.19	0.58	0.26	0.52
Within palms variance (σ^2_w)	-	16.28	2.05	11.56	4.60	9.50
Broad-sense heritability		**0.30**	**0.38**	**0.32**	**0.26**	**0.18**
		DxD selfed progenies				
Replication (R)	2	68.10**	27.03**	10.71^{ns}	6.76^{ns}	14.86^{ns}
Progenies (P)	34	283.65**	41.08**	185.33**	62.79**	93.95**
RxP	65	42.33**	6.85	31.98**	11.92**	14.41**
Within palms	1 151					
Progeny variance (σ^2_p)		5.94	0.84	3.77	1.25	1.96
RxP variance (σ^2_{gr})		2.47	0.43	1.80	0.69	0.60
Within palms variance (σ^2_w)		15.61	2.16	12.49	4.45	7.88
Broad-sense heritability		**0.49**	**0.49**	**0.42**	**0.39**	**0.38**

Note: M/F - mesocarp to fruit; K/F - kernel to fruit; S/F - shell to fruit; O/DM - oil to dry mesocarp; O/B - oil to bunch. *, ** Significant at $P \leq 0.05$ and $P \leq 0.01$, respectively. Otherwise, non-significant.

TABLE 4. PROGENY MEANS OF 28 DxD INTERCROSSED AND 35 DxD SELFED PROGENIES FOR BUNCH QUALITY COMPONENTS

No.	Progeny	Pedigree	N	M/F (%)	K/F (%)	S/F (%)	O/DM (%)	O/B (%)
			DxD intercrossed progenies					
1.	PK4419	0.332/451 x 0.332/83	49	63.59e-i	6.41d-f	30.00f-k	79.81a	22.98ab
2.	PK4494	0.332/83 x 0.332/215	44	62.29hi	5.87f-j	31.85cd	76.66j	18.84m
3.	PK4515	0.332/83 x 0.332/451	37	62.36g-i	5.79g-j	31.85cd	78.53d-f	20.38h-l
4.	PK4520	0.332/190 x 0.332/451	47	60.37jk	6.82b-d	32.81bc	79.32a-d	20.92g-k
5.	PK4536	0.332/190 x 0.332/157	46	60.35jk	5.26j-l	34.40a	77.00ij	19.55lm
6.	PK4566	0.332/382 x 0.332/451	48	65.31b-e	5.98e-i	28.71k-n	78.78c-f	21.64c-h
7.	PK4567	0.332/451 x 0.332/382	50	64.31c-f	6.42d-f	29.27h-m	79.75ab	22.35a-e
8.	PK4571	0.332/382 x 0.332/83	45	66.87ab	4.75lm	28.38l-n	77.91f-i	20.96g-k
9.	PK4572	0.332/157 x 0.332/83	43	64.01d-h	4.76lm	31.24d-f	78.55d-f	21.14e-k
10.	PK4588	0.332/360 x 0.332/83	50	66.72ab	5.12kl	28.16mn	78.01fg	21.59c-h
11.	PK4597	0.332/330 x 0.332/83	49	59.46k	7.19a-c	33.36ab	78.84b-f	20.21i-l
12.	PK4602	0.332/360 x 0.332/157	48	65.83bc	4.77lm	29.41h-m	76.97j	20.39h-l
13.	PK4603	0.332/83 x 0.332/190	49	62.62f-i	5.87f-j	31.52c-e	77.97f-h	21.11e-k
14.	PK4612	0.332/360 x 0.332/45	48	65.31b-e	6.08e-i	28.61k-n	79.66a-c	23.57a
15.	PK4615	0.332/190 x 0.332/83	50	63.99d-h	5.30j-l	30.72d-h	78.07fg	21.10e-k
16.	PK4618	0.332/157 x 0.332/382	49	64.67c-e	4.38m	30.95d-g	77.51g-j	19.99j-m
17.	PK4619	0.332/83 x 0.332/45	12	67.71a	4.72lm	27.57n	79.59a-c	22.79a-c
18.	PK4628	0.332/446 x 0.332/83	55	64.77c-e	6.59c-e	28.64k-n	79.61a-c	22.14b-g
19.	PK4634	0.332/190 x 0.332/382	54	63.98d-h	5.50i-k	30.52d-i	78.49d-f	21.01f-k
20.	PK4641	0.332/360 x 0.332/215	50	65.21b-e	5.66h-k	29.13i-m	78.19fg	21.33d-i
21.	PK4642	0.332/215 x 0.332/45	39	63.69d-i	7.32ab	29.00j-n	79.27a-d	23.46ab
22.	PK4654	0.332/451 x 0.332/215	44	65.05ij	7.59a	30.36e-j	79.17a-e	20.67h-l
23.	PK4665	0.332/360 x 0.332/330	44	65.31b-e	5.51i-k	29.19i-m	78.07fg	21.26d-j
24.	PK4669	0.332/330 x 0.332/215	44	62.92f-i	5.59h-k	31.50c-e	77.06h-j	19.86k-m
25.	PK4680	0.332/360 x 0.332/451	47	64.02d-g	6.44d-f	29.54g-m	79.50a-c	22.31a-f
26.	PK4687	0.332/45 x 0.332/83	44	64.17c-f	6.14e-h	29.70g-l	79.94a	23.56a
27.	PK4688	0.332/330 x 0.332/382	54	64.10c-f	6.12e-i	29.78f-l	78.26e-g	20.43h-l
28.	PK4718	0.332/382 x 0.332/45	58	65.41b-d	6.38d-g	28.21mn	79.66a-c	22.55a-d
	Mean			**63.98**	**5.86**	**30.16**	**78.53**	**21.32**
	LSD			1.74	0.62	1.48	0.93	1.33
			DxD selfed progenies					
1.	PK4232	0.332/382 x 0.332/382	40	68.07a	4.77l-o	27.16m	77.00d-j	19.35f-i
2.	PK4244	0.332/214 x 0.332/214	47	65.64bc	5.22j-n	29.15j-l	77.70d-f	19.31f-i
3.	PK4260	0.332/203 x 0.332/203	41	63.36e-h	5.21j-n	31.43e-h	76.66g-l	19.19g-j
4.	PK4289	0.332/19 x 0.332/19	38	58.83n-q	6.80c-f	34.3ab	75.70lm	16.75o-q
5.	PK4291	0.332/370 x 0.332/370	31	63.07f-i	5.48i-l	31.45e-h	75.86k-m	19.39e-i
6.	PK4297	0.332/277 x 0.332/277	41	59.24l-p	6.84c-f	33.92a-c	76.59g-l	17.49l-o
7.	PK4309	0.332/100 x 0.332/100	31	63.08f-i	7.32a-d	29.61i-l	79.34ab	22.08ab
8.	PK4336	0.332/363 x 0.332/363	40	61.13j-l	6.93b-e	31.94e-g	76.96d-j	18.26i-n

TABLE 4. PROGENY MEANS OF 28 DxD INTERCROSSED AND 35 DxD SELFED PROGENIES FOR BUNCH QUALITY COMPONENTS (continued)

No.	Progeny	Pedigree	N	M/F (%)	K/F (%)	S/F (%)	O/DM (%)	O/B (%)
9.	PK4337	0.332/133 x 0.332/133	45	63.97c-f	4.65m-o	31.39e-h	76.12j-l	18.18i-n
10.	PK4341	0.332/224 x 0.332/224	22	64.37c-f	4.82l-o	30.82g-j	76.84f-k	18.35h-n
11.	PK4342	0.332/285 x 0.332/285	42	59.75k-p	4.97k-n	35.29a	73.18o	16.15p-r
12.	PK4343	0.332/275 x 0.332/275	43	60.89j-m	7.60ab	31.51e-g	77.78c-f	19.61d-h
13.	PK4378	0.332/247 x 0.332/247	31	60.00j-o	7.04b-e	32.96b-e	77.15d-i	18.38h-m
14.	PK4385	0.332/2 x 0.332/2	41	60.70j-n	5.60i-k	33.70a-d	77.70d-f	15.21r
15.	PK4386	0.332/329 x 0.332/329	37	58.70o-q	6.60d-g	34.70a	76.53h-l	17.97j-o
16.	PK4395	0.332/330 x 0.332/330	42	61.33i-k	6.33e-h	32.35c-g	76.44h-l	19.02g-j
17.	PK4435	0.332/317 x 0.332/317	34	63.42d-h	5.89g-j	30.70g-k	78.73bc	20.51c-f
18.	PK4440	0.332/413 x 0.332/413	34	61.54h-k	5.76h-j	32.71b-f	76.19i-l	18.83h-k
19.	PK4443	0.332/124 x 0.332/124	44	57.99pq	7.65ab	34.37ab	77.03d-j	17.24m-p
20.	PK4447	0.332/153 x 0.332/153	39	64.77b-f	5.91g-j	29.32j-l	77.68d-f	18.13i-n
21.	PK4448	0.332/47 x 0.332/47	40	64.02c-f	6.55e-g	29.43j-l	75.06mn	17.05n-p
22.	PK4452	0.332/369 x 0.332/369	31	64.49c-f	5.93g-j	29.58i-l	77.38d-h	18.35h-n
23.	PK4487	0.332/222 x 0.332/222	26	60.48j-o	7.57ab	31.95e-g	77.93cd	19.12g-j
24.	PK4497	0.332/144 x 0.332/144	37	61.72g-j	6.19f-i	32.09d-g	77.87c-e	18.70h-l
25.	PK4514	0.332/451 x 0.332/451	17	65.00b-e	6.36e-h	28.64lm	79.75a	21.67a-c
26.	PK4544	0.332/107 x 0.332/107	39	63.06f-i	5.76h-j	31.19f-i	76.88e-j	19.28f-j
27.	PK4554	0.332/83 x 0.332/83	37	65.57bc	4.62no	29.82h-l	77.43d-h	20.69c-e
28.	PK4559	0.332/416 x 0.332/416	35	66.42ab	4.67m-o	28.92l	77.57d-g	20.82b-d
29.	PK4585	0.332/215 x 0.332/215	41	65.31b-d	5.54i-k	29.14j-l	77.12d-j	18.67h-l
30.	PK4587	0.332/114 x 0.332/114	31	65.15b-e	5.35j-m	29.51i-l	77.33d-h	20.23d-g
31.	PK4633	0.332/9 x 0.332/9	28	59.14m-q	7.86a	33.00b-e	76.61g-l	15.70qr
32.	PK4649	0.332/135 x 0.332/135	38	63.28e-h	5.34j-m	31.38e-h	76.50h-l	18.19i-n
33.	PK4676	0.332/394 x 0.332/394	22	60.45j-o	4.22o	35.34a	74.06no	17.55k-o
34.	PK4677	0.332/378 x 0.332/378	41	57.27q	7.59ab	35.14a	77.86c-e	18.43h-m
35.	PK4678	0.332/45 0.332/45	27	63.60d-g	7.33a-c	29.07kl	79.36ab	22.26a
	Mean			**62.31**	**6.10**	**31.60**	**76.92**	**18.58**
	LSD			1.90	0.72	1.69	1.01	1.32
		Parent mean (0.332)		**62.07**	**6.53**	**31.40**	**77.39**	**19.38**

Note: M/F - mesocarp to fruit; K/F - kernel to fruit; S/F - shell to fruit; O/DM - oil to dry mesocarp, O/B - oil to bunch. N - number of individual palms. Means with the same letter are not significantly different at $P \leq 0.05$ based on Least Significant Difference (LSD).

Yield Performance of Selected DxD Selfed and Their Intercrossed Reciprocal Progenies

Yield performance from three sets of selected selfed and reciprocal intercrossed oil palm Deli Ulu Remis progenies was evaluated in detail (*Table 5*). Mean FFB values for set A indicated that PK4687 (0.332/45 x 0.332/83) with 218.77 kg/palm/yr was the best performer, compared to its reciprocal cross and selfed progenies. The high FFB yield was contributed by its BNO (13.91 bunches/palm/yr) and ABW (15.68 kg/bunch), which were also the highest among the progenies. For set B, the highest FFB yield

was recorded by PK4419 (0.332/451 x 0.332/83) which was significantly higher than the FFB of its selfed progeny PK4514 (selfed 0.332/451). For the third set (C), the intercrossed progeny PK4566 (0.332/382 x 0.332/451) had achieved the best FFB yield, likely contributed by its high ABW, the highest among the progenies in the set. These effects from selfings and intercrossings are in agreement with Fadila *et al*. (2015) who suggested that intercrosses of MPOB Deli *dura*s may broaden the genetic base of Deli *dura* in Malaysia. The highest FFB-producing progeny from each set (*Table 5*) are indeed intercrosses, which were higher yielding than their selfings. The narrow genetic diversity coupled with intensive selection has reduced the variability of yield components of oil palm breeding populations (Maizura *et al*., 2022). Selfing may have led to inbreeding depression among the evaluated traits as can be seen from the inferior FFB yield performance among the selfed progenies. Furthermore, intercrossed Deli *dura* progenies were also more tolerant to *Ganoderma* infection than selfed Deli *dura* progenies in Kluang, Malaysia (Norziha *et al*., 2012). Meanwhile, a lower incidence was reported among Deli x Yangambi crosses than pure Deli *dura* (Durand-Gasselin *et al*., 2005). The introduction of new genetic resources into the *dura* populations is therefore highly recommended. Such efforts could help breeders to strategise crossing schemes to avoid inbreeding and preserve sufficient variability in their effort to produce more resilient progenies against diseases and climate change.

For bunch quality components, the highest M/F (67.71%) reported in set A was from progeny PK4619 (0.332/83 x 0.332/45) (*Table 6*). The progeny had the highest M/F, due to its lowest S/F of less than 28%. Similar findings had been observed by Schmole (1930), whereby Deli *dura* fruit has on average, 62%-63% mesocarp, 30% shell, and 7%-8% kernel. Selfed progeny, PK4554 (0.332/83 x 0.332/83) had reported the highest S/F (29.82%) and the lowest K/F (4.62%), O/DM (77.43%) and O/B (20.69%). Among the set B progenies, the lowest M/F was obtained by intercrossed progeny, PK4515 (0.332/83 x 0.332/451), and also had the lowest O/B (20.38%), and the highest S/F (31.85%). On the other hand, PK4554 (0.332/83 x 0.332/83) was found significantly different from intercrossed progenies (PK4419 and PK4515). The selfed progeny recorded the lowest K/F (4.62%) and O/DM (77.43%). Based on set C, a significant difference was observed between selfed progeny, PK4232 (0.332/382 x 0.332/382) and selfed progeny, PK4514 (0.332/451 x 0.332/451). However, PK4514 was not significantly different from their reciprocal crosses. PK4232 obtained the lowest K/F (4.77%), S/F (27.16%), O/DM (77.0%) and O/B (19.35%). The best O/B was reported in intercrossed progeny, PK 4567 (0.332/451 x 0.332/382) which also had the highest K/F (6.42%), S/F (29.27%) and O/DM (79.75%). The findings from these results could serve as supplementary information for breeders during their crossing designs, assisting in a more precise decision on the selection of parental materials for seed production and inbred line development.

The mean values observed for each bunch quality component within each set were not significantly different from one another. This suggested that selfings and intercrossing do not affect these components. The highest O/B obtained was generally not significantly different from the other selfings or intercrossing in the same set though it was generally exhibited by an intercrossed progeny. Therefore, the reciprocal intercrosses and selfings appear to significantly influence the yield components and not the bunch quality components. Some studies were reported on maternal effects evaluated in oil palm progenies. Rajanaidu and Jalani (1994) mentioned that the kernel to bunch ratio is highly heritable and maternally inherited. Norziha *et al*. (2012) reported that the yield components may have a strong maternal influence on the production of oil palm progenies. The information on the genetic contribution of each parent is important and this type of analysis may serve as a guide for the breeders on the use of a *dura* palm as the male or female parent in intercrossing programmes to obtain higher yields from their progenies.

Identifying good and promising *dura* combinations is one of the measures taken to improve current DxD planting materials. This improvement can only be realised if breeders have the knowledge and access to quality breeding materials. The breeding strategy carried out by MPOB went through more generations of improvement either through selfing of Deli *dura* or intercrossing of Deli *dura* from different sub-populations (Tey *et al*., 2018). Progress was made in using the remaining variability available in Deli populations which resulted in a new *dura* which is now used for seed production. The selected *dura*s may subsequently be progeny tested with *pisifera*s from the advanced breeding population such as AVROS, Yangambi, La Me and Nigeria. The AVROS *pisifera* progenies, for example, produce more BNO which is the most heritable trait and exhibits a high M/F ratio. Besides, a high M/F implied a high O/B. Swaray *et al.* (2020) reported that Deli Ulu Remis × AVROS was the most outstanding progeny, producing mean values above the trial means in all bunch fruit quality components, except in kernel-related components. Deli Ulu Remis was found to be a good associate with AVROS *pisifera* due to its overall performance in bunch quality components.

TABLE 5. MEAN PERFORMANCE FOR SELFED AND INTERCROSSED RECIPROCAL PROGENIES FOR YIELD AND ITS COMPONENTS

Set	No.	Progeny	Pedigree	Type	N	FFB (kg/palm/yr)		BNO (bunches/palm/yr)		ABW(kg/palm/yr)	
						Mean	CV	Mean	CV	Mean	CV
A	1	PK4554	0.332/83 x 0.332/83	self	37	175.67b	25.87	13.48ab	21.34	13.10b	18.70
	2	PK4678	0.332/45 x 0.332/45	self	31	160.25b	28.28	12.56ab	26.67	12.90b	20.64
	3	PK4619	0.332/83 x 0.332/45	intercross	12	160.69b	19.71	11.88b	18.43	13.74b	19.92
	4	PK4687	0.332/45 x 0.332/83	intercross	44	218.77a	23.69	13.91a	18.50	15.68a	12.94
				Mean		**185.66**	**25.18**	**13.25**	**21.49**	**14.03**	**17.07**
				LSD		**26.62**		**1.62**		**1.36**	

Set	No.	Progeny	Pedigree	Type	N	FFB (kg/palm/yr)		BNO (bunches/palm/yr)		ABW (kg/palm/yr)	
						Mean	CV	Mean	CV	Mean	CV
B	1	PK4514	0.332/451 x 0.332/451	self	15	153.34b	20.10	10.37c	14.38	14.87b	16.98
	2	PK4554	0.332/83 x 0.332/83	self	37	175.67ab	25.87	13.48a	21.34	13.10c	18.70
	3	PK4419	0.332/451 x 0.332/83	intercross	53	186.16a	27.16	11.32bc	24.68	16.48a	13.41
	4	PK4515	0.332/83 x 0.332/451	intercross	39	173.81ab	31.21	11.99b	25.56	14.41b	15.23
				Mean		**176.70**	**27.58**	**11.96**	**23.36**	**14.88**	**15.47**
				LSD		**25.32**		**1.45**		**1.20**	

Set	No.	Progeny	Pedigree	Type	N	FFB (kg/palm/yr)		BNO (bunches/palm/yr)		ABW (kg/palm/yr)	
						Mean	CV	Mean	CV	Mean	CV
C	1	PK4232	0.332/382 x 0.332/382	self	48	138.10b	31.38	11.40a	24.72	11.99c	13.76
	2	PK4514	0.332/451 x 0.332/451	self	15	153.34b	20.10	10.37a	14.38	14.87b	16.98
	3	PK4566	0.332/382 x 0.332/451	intercross	48	179.09a	25.75	11.04a	23.53	16.36a	16.82
	4	PK4567	0.332/451 x 0.332/382	intercross	50	156.82b	32.18	10.45a	29.6	15.08b	15.29
				Mean		**160.04**	**28.52**	**10.91**	**25.06**	**14.73**	**16.03**
				LSD		**22.25**		**1.33**		**1.15**	

Note: FFB - fresh fruit bunch; BNO - bunch number; ABW - average bunch weight; N - number of individual palms. Means with the same letter are not significantly different at $p \leq 0.05$ based on Least Significant Difference (LSD).

TABLE 6. MEAN PERFORMANCE FOR SELFED AND INTERCROSSED RECIPROCAL PROGENIES FOR BUNCH QUALITY COMPONENTS

Set	No.	Progeny	Pedigree	Type	N	M/F (%)		K/F (%)		S/F (%)		O/DM (%)		O/B (%)	
						Mean	CV	Mean	CV	Mean	CV	Mean	CV	Mean	CV
A	1	PK4554	0.332/83 x 0.332/83	self	34	65.57ab	7.85	4.62c	28.46	29.82a	14.49	77.43b	2.76	20.69b	12.89
	2	PK4678	0.332/45 x 0.332/45	self	27	63.60b	8.64	7.33a	22.26	29.07a	19.21	79.36a	2.38	22.26a	14.59
	3	PK4619	0.332/83 x 0.332/45	intercross	11	67.71a	4.62	4.72c	15.57	27.58a	11.40	79.59a	1.63	22.79a	11.34
	4	PK4687	0.332/45 x 0.332/83	intercross	40	64.17b	4.31	6.14b	18.16	29.70a	8.30	79.94a	1.51	23.56a	7.76
				Mean		**64.80**	**6.73**	**5.82**	**22.17**	**29.38**	**13.75**	**79.01**	**2.17**	**22.30**	**11.47**
				LSD		**2.61**		**0.77**		**2.42**		**1.03**		**1.53**	

Set	No.	Progeny	Pedigree	Type	N	M/F (%)		K/F (%)		S/F (%)		O/DM (%)		O/B (%)	
						Mean	CV	Mean	CV	Mean	CV	Mean	CV	Mean	CV
B	1	PK4514	0.332/451 x 0.332/451	self	15	65.10a	6.26	6.36a	29.01	28.54b	10.68	79.71a	1.58	21.92ab	14.25
	2	PK4554	0.332/83 x 0.332/83	self	34	65.57a	7.85	4.62b	28.46	29.82b	14.89	77.43c	2.76	20.69b	12.89
	3	PK4419	0.332/451 x 0.332/83	intercross	50	63.59ab	5.41	6.41a	18.97	30.00ab	10.22	79.81a	1.93	22.98a	10.32
	4	PK4515	0.332/83 x 0.332/451	intercross	35	62.36b	7.49	5.79a	41.52	31.85a	13.26	78.53b	2.85	20.38b	20.81
				Mean		**63.94**	**6.76**	**5.79**	**29.29**	**30.28**	**12.33**	**78.86**	**2.39**	**21.6**	**14.4**
				LSD		**1.98**		**0.9**		**1.99**		**1.00**		**1.66**	

Set	No.	Progeny	Pedigree	Type	N	M/F (%)		K/F (%)		S/F (%)		O/DM (%)		O/B (%)	
						Mean	CV	Mean	CV	Mean	CV	Mean	CV	Mean	CV
C	1	PK4232	0.332/382 x 0.332/382	self	48	68.07a	7.10	4.77b	44.20	27.16b	15.79	77.00b	3.33	19.35b	17.02
	2	PK4514	0.332/451 x 0.332/451	self	15	65.10b	6.26	6.36a	29.01	28.54ab	10.68	79.71a	1.58	21.92a	14.25
	3	PK4566	0.332/382 x 0.332/451	intercross	48	65.31b	6.55	5.98a	24.57	28.71ab	12.09	78.78a	2.79	21.64a	13.78
	4	PK4567	0.332/451 x 0.332/382	intercross	41	64.31b	6.74	6.42a	23.08	29.27a	11.43	79.75a	2.62	22.35a	12.45
				Mean		**65.84**	**6.75**	**5.78**	**29.66**	**28.39**	**12.91**	**78.59**	**2.83**	**21.18**	**14.36**
				LSD		**2.22**		**0.86**		**1.83**		**1.11**		**1.52**	

Note: M/F - mesocarp to fruit; K/F - kernel to fruit; S/F - shell to fruit; O/DM - oil to dry mesocarp; O/B - oil to bunch; N - number of individual palms. Means with the same letter are not significantly different at $p \leq 0.05$ based on Least Significant Difference (LSD).

CONCLUSION

In this study, intercrossed *dura* progenies were found to produce higher yields compared to selfed progenies. Parental lines of advanced breeding materials are continuously being improved at MPOB, where crossing programmes involving palms with different economic characters, are being routinely conducted. The best materials obtained from the new combinations are further evaluated to develop the next generation of parental lines for commercial seed production which is necessary for the sustainable development of the Malaysian oil palm industry.

ACKNOWLEDGEMENT

The authors would like to thank the Director-General of MPOB for permission to publish this article. Special thanks also go to the Breeding and Genetics Group for their assistance in the laboratory and field work.

REFERENCES

Alvarado, A and Escobar, R (2016). Seed production and oil palm breeding in ASD Costa Rica. *Proc. of International Seminar on Oil Palm Breeding and Seed Production.* Medan, Indonesia. p. 21-38.

Burhanuddin, S; Aslim, R and Herman, A (2017). Progeny evaluation of *dura* x *dura* crosses to be utilized for female parents in oil palm (*Elaeis guineensis* Jacq.) seed production. *Proc. of PERIPI-2017 International Seminar.* 2 October 2017. Bogor, Indonesia. p. 121-127.

Corley, R H V (1998). What is the upper limit to oil extraction ratio? *Proc. Oil and Kernel Production in Oil Palm - A Global Perspective.* PORIM, Bangi. p. 256-269.

Department of Standard Malaysia (2017). Malaysian Standard, MS 157:2017. Oil palm seeds for commercial planting - Specification (Fourth revision). Standard and Industrial Research Institute of Malaysia Berhad, Selangor.

Durand-Gasselin, T; Asmady, H; Flori, A; Jacquemard, J C; Hayun, Z; Breton, F and de Franqueville, H (2005). Possible sources of genetic resistance in oil palm (*Elaeis guineensis* Jacq.) to basal stem rot caused by *Ganoderma boninense* - Prospects for future breeding. *Mycopathologia, 159*: 93-100.

Fadila, A M; Mohd Din, A; Rajanaidu, N; Marhalil, M; Norziha, A and Kushairi, A (2015). Bunch yield and bunch components of MPOB Deli *dura* intercrosses based on different Deli populations. *MPOB International Palm Oil Congress and Exhibition.* Kuala Lumpur, Malaysia. p. 91-99.

Falconer, D S and Mackay, T F C (1996). Introduction to quantitative genetics genetics. 4th edition. *Trends in Genetics*, *12(7)*: 280 pp.

Hardon, J J; Corley, R H V and Lee, C H (1987). Breeding and selecting the oil palm. *Improving Vegetatively Propagated Crops* (Abbott, A J and Atkin, R K eds.). Academic Press. 63 pp.

Hartley, C W S (1988). The botany of oil palm. *The Oil Palm*. 3rd edition. Longman, London. p. 47-94.

Kandha, S; Mohan, S; Xaviar, A and Rafii, M Y (2017). Yield and bunch quality component comparison between two-way crosses and multi-way crosses of DxP oil palm progenies. *Sains Malaysiana*, *46(9)*: 1587-1595.

Kome, G; Tabi, F; Enang, R and Silatsa, F (2020). Land suitability evaluation for oil palm (*Elaeis guineensis* Jacq.) in Coastal Plains of Southwest Cameroon. *Open J. Soil Sci.*, *10*: 257-273. DOI: 10.4236/ojss.2020.107014.

Kushairi, A and Mohd Din, A (2020). Development of new oil palm cultivars in Malaysia. *J. Oil Palm Res., 32(3)*: 420-426.

Kushairi, A; Mohd Din, A and Rajanaidu, N (2011). Oil palm breeding and seed production. *Further Advances In Oil Palm Research* (2000-2010) (Mohd Basri, W; Choo, Y M and Chan, K W eds). MPOB, Bangi. p. 47-101.

Kushairi, A; Tarmizi, A H; Zamzuri, I; Ong-Abdullah, M; Samsul Kamal, R; Ooi, S E and Rajanaidu, N (2010). Production, performance and advances in oil palm tissue culture. *Proc. of the International Seminar on Advances in Oil Palm Tissue Culture*. Yogyakarta, Indonesia. 29 May 2010. p. 1-23.

Maizura, I; Rajanaidu, N; Singh, R and Kushairi, A (2022). An assessment of the Malaysian oil palm breeding populations using AFLP markers. *J. Oil Palm Res., 36(1)*: 27-39. DOI: 10.21894/jopr.2022.0073.

Marhalil, M; Rajanaidu, N; Mohd Din, A; Suzana, M; Zulkifli, Y; Fadila, A M; Saleh, G B and Kushairi, A (2016). Oil palm breeding for seed production in MPOB and introduction of Nigerian-based DxP population. *Proc. of the International Seminar on Oil Palm Breeding - Oil Palm Breeding and Seed Production.* Medan, Indonesia. p. 64-77.

Mohd Din, A; Rajanaidu, N and Sukaimi, J (2015). Genetic variation and heritability estimate for bunch yield, bunch components, and vegetative traits in oil palm interspecific hybrids. *J. Agri. Sci. Technol., 5*: 162-173.

MPOB (2021). Overview of the Malaysian oil palm industry 2020. http://bepi.mpob.gov.my/images/overview/Overview_of_Industry_2021.pdf., accessed on 31 March 2022.

Noh, A; Rafii, M Y; Saleh, G and Kushairi, A (2010). Genetic performance of 40 Deli *dura* × AVROS *pisifera* full-sib families. *J. Oil Palm Res., 22(2)*: 781-795.

Noh, A; Rafii, M Y; Saleh, G; Kushairi, A and Latif, M A (2012). Genetic performance and general combining ability of oil palm deli *dura* x AVROS *pisifera* tested on inland soils. *Sci. World J., 2012*: 1-8.

Noh, A; Rafii, M Y; Mohd Din, A; Kushairi, A; Norziha, A; Rajanaidu, N; Latif, M A and Malek, M A (2014). Variability and performance evaluation of introgressed Nigerian *dura* x Deli *dura* oil palm progenies. *Genet. Mol. Res., 13(2)*: 2426-2437.

Norziha, A; Fadila, A M; Zulkifli, Y and Mohd Din, A (2012). A preliminary study on maternal inheritance of reciprocal crosses in oil palm. *Proc. UMT 11th International Annual Symposium on Sustainability Science and Management.* Terengganu Malaysia. p. 1488-1490.

Norziha, A; Noh, A; Fadila, A M; Zulkifli, Y; Mohd Din, A; Rajanaidu, N and Kushairi, A (2012). *Ganoderma* infection studies in selfed and intercrossed Deli *dura* progenies. *Proc. International Seminar on Breeding for Oil Palm Disease Resistance.* Bogota, Colombia.

Rajanaidu, N; Rao, V; Halim, A H and Ong, S H (1990). Genetic resources: New developments in oil palm breeding. *Elaeis, 1*: 1-10.

Rajanaidu, N and Jalani, B S (1994). Potential sources of lauric oils for the oleochemical industry. *Proc. of the World Conference and Exhibition on Lauric Oils*: Sources, Processing and Applications (Applewhite, T H ed.). AOCS, Manila, Philippines. p. 47-50.

Rajanaidu, N; Kushairi, A; Rafii, M; Mohd Din, A; Maizura, I and Jalani, B S (2000). Oil palm breeding and genetic resources. *Advances in Oil Palm Research* (Yusof, B; Jalani, B S and Chan, K W eds.). MPOB, Bangi. p. 171-237.

Rao, V (1987). Important traits in oil palm selection. *Proc. of the Colloquium onBreeding and Selection for Clonal Oil Palms*. PORIM, Kuala Lumpur. p. 21-33.

Rao, V; Soh, A C; Corley, R H V; Lee, C H; Rajanaidu, N; Tan, Y P; Chin, C W; Lim, K C; Tan, S T; Lee, T P and Ngui, M (1983). A critical re-examination of the method of bunch quality analysis in oil palm breeding. *PORIM Occasional Paper, 9*: 28 pp.

Schmole, J F (1930). The selection of oil palm (*Elaeis guineensis* Jacq.). *Proc. of the 4th Pacific Scientific Congress*. p. 185.

Sparnaaij, L D and van der Vossen, H A M (1980). Development in oil palm breeding: A reappraisal of present and future breeding procedures in light of results from the Nigerian Institute for Oil Palm Research breeding programme. *Oil Palm News, 24*: 4-11.

Swaray, S; Mohd Din, A; Rafii, M Y; Jamian, S; Ismail, M F; Jalloh, M; Marhalil, M; Mustakim, M M and Yusuff, O (2020). Influence of parental *dura* and *pisifera* genetic origins on oil palm fruit set ratio and yield components in their DxP progenies. *Agronomy, 10(11)*: 1793.

Tey, C C; Chua, K L; Lee, C H; Cheah, S C; Jakim, B; Au, W F; Mohd Fuad, A and Tan, S G (2018). Genetic diversity and inbreeding level in Deli *dura* and AVROS advanced breeding materials in oil palm (*Elaeis guineensis* Jacq.) using microsatellite markers. *J. Oil Palm Res., 30*: 366-379.

Journal of Oil Palm Research Vol. 36 (3) September 2024 p. 393-408
DOI: https://doi.org/10.21894/jopr.2023.0034

BIOLOGY AND POPULATION DYNAMICS OF ADULT *Sagalassa valida* WALKER, 1856 (Lepidoptera: Brachodidae), THE OIL PALM ROOT BORER IN COLOMBIA

CARLOS ANDRÉS SENDOYA-CORRALES[1]; JOSÉ LUIS PASTRANA-SANCHEZ[2]*; JESÚS ARVEY MATABANCHOY SOLARTE[3]; ÁLEX ENRIQUE BUSTILLO PARDEY[2]; MIRIAM ROSERO GUERRERO[2] and ANUAR MORALES RODRÍGUEZ[2]

ABSTRACT

Sagalassa valida *is a pest of economic importance because the larval stage feeds on the root system of the oil palm. In this investigation, the life cycle, the population dynamics of the adults, and their natural enemies were determined through biweekly samplings for 43 months in two lots of oil palm; located in the Central and Western Zone of Colombia. It was determined that the life cycle of* S. valida *is 64.1 days on average; the duration of each stage was: Egg 9.2 ± 0.5 days, larva 38.1 ± 4.9 days (five instars), prepupa 2.9 ± 1.1 days, pupa 13.9 ± 1.1 days and adult 12.3 ± 4.3 days. The adults of* S. valida *were present in the two zones during the study; using Spearman's correlation index, it was determined that in the Central Zone, the precipitation presented a direct and significant correlation with the variables: number of males (ρ = 0.24;* P *= 0.023) and the total number of adults (ρ = 0.21;* P *= 0.044). Ten natural enemies of* S. valida *and 14 weeds were identified in the study areas. This information is essential to implement an efficient management strategy for* S. valida *in plantations.*

Keywords: *Elaeis guineensis,* interspecific hybrid, life cycle, predators, weeds.

Received: 19 August 2022**; Accepted:** 15 May 2023**; Published online:** 8 August 2023.

INTRODUCTION

Colombia has 595 723 ha planted with African oil palm (*Elaeis guineensis* Jacq.) and interspecific hybrid (*Elaeis oleifera* x *Elaeis guineensis*) (*Figure 1*), the total planted is distributed in four palm zones (*Table 1*) (Fedepalma, 2022a; 2022b).

Oil palm agroecosystems are home to a great diversity of insects, some species are classified as pests of economic importance, and others are considered beneficial species in the crop (natural enemies and pollinators) (Aldana *et al.,* 2010; Bustillo-Pardey, 2014b; Montes *et al.,* 2018). Currently, five species of borer habits pest have been registered; each species affects a specific part of the oil palm, causing significant damage to the roots, the stipe, the inflorescences and the fruits (Aldana *et al.,* 2010; Barrios-Trilleras *et al.,* 2020). Among the most relevant species, the root borer, *Sagalassa valida* Walker, 1856 (Lepidoptera: Brachodidae), causes damage of economic importance in the Central and Western zones.

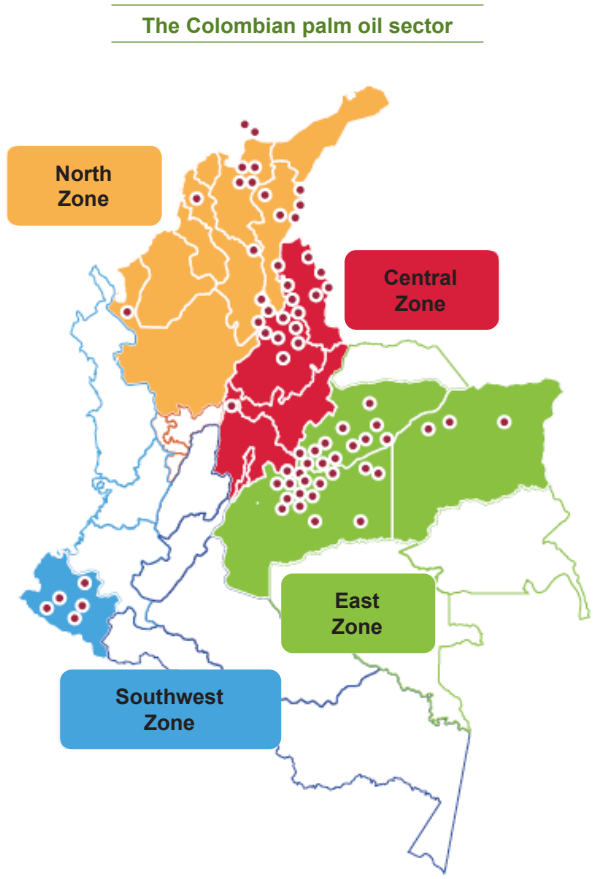
Sagalassa valida is a native species of South America that is present in Brazil, Colombia, Ecuador, Panama, Peru, Suriname and Venezuela. In Colombia, this borer is present in all oil palm areas. However, *S. valida* has caused significant economic loss in *E. guineensis* cultivars and the interspecific

[1] National University of Colombia, (Universidad Nacional de Colombia – UNAL), Ave Cra 30, 45-3, Bogota, Colombia.

[2] Colombian Oil Palm Research Centre, (Corporación Centro de Investigación en Palma de Aceite – Cenipalma), Calle 21, 42-55, Bogota, Colombia.

[3] National Federation of Coffee Growers of Colombia, (Federación Nacional de Cafeteros – FNC), Calle 73, 8-13, Bogota, Colombia.

* *Corresponding author e-mail: jpastrana@cenipalma.org*



Source: Fedepalma (2022b).

Figure 1. Oil palm growing zones in Colombia.

TABLE 1. DISTRIBUTION OF OIL PALM PLANTED AREA IN COLOMBIA BY ZONE

Zone	Area planted (ha)	Production area (ha)	Growth area (ha)
Northern	111 789	101 177	10 612
Central	182 438	161 402	21 036
Eastern	278 513	216 672	61 841
Western	22 983	20 113	2 870
Total	**595 723**	**499 364**	**96 359**

Source: Fedepalma (2022a).

hybrid OxG (Coari x La Mé), in the Central and Western zones, respectively (Aldana *et al.*, 2000; Corredor *et al.*, 2016; Peña and Jiménez, 1994; Pinzón, 1995).

The larval stage of *S. valida* feeds on the root system of oil palms, feeding initially on the quaternary and tertiary roots. As it grows, pierces through the secondary and primary roots (Peña and Jiménez, 1994; Sáenz and Olivares, 2008a). While *S. valida* larvae are distributed throughout the entire root system and can be located at any distance and depth that the root system reaches, they are normally located close to the stipe in young oil palms and at 1.0-1.5 m from the base of the stipe in adult oil palms (Aldana *et al.*, 2000).

Due to the damage caused by the larval stage in the roots, physiological changes occur in the palm that is reflected by poor development, slow growth, yellowing, drying of the basal leaves, continuous emission of male inflorescences, as well as a decrease in bunch size and weight, in severe attacks can overturn the palm (Aldana *et al.*, 2000; Peña and Jiménez, 1994). Chávez *et al.* (2000) determined that economic damage could occur in the crop from 5% fresh damage to the oil palm roots. Aldana *et al.* (2000) recorded losses that can exceed 50% of the root system of 6 and 10 year old palms. In 10-year-old palms, the worst damage occurred at 1.50 m from the stipe, while in 6-year-old oil palms, damage occurred at all sampling distances. Corredor *et al.* (2016) estimated decrease in yield, ranging from 50%-83% of fresh fruit bunch weight, in areas of the interspecific hybrid OxG (Coari x La Mé) infested with *S. valida*.

Sagalassa valida management is based on cultural, biological and chemical crop control practices. The cultural control consists of using available ground plant covers, such as empty fruit bunches (EFB), pruned fronds, rice husks, or crop residues, to cover the base of the oil palm and prevent direct oviposition by *S. valida* females on oil palm roots (Pinzón, 1995). Biological control can be performed using nematodes of the genera *Heterorhabditis* and *Steinernema*, native to the zones where oil palms are grown in Colombia (Bustillo, 2014b; Sáenz *et al.*, 2005). These nematodes are produced for research and are sprayed on the ground around the base of the oil palm (Sáenz *et al.*, 2006). However, these native nematodes are not commercially available due to their high production costs. In addition, the oil palm crop agroecosystem contains various weeds visited by natural enemies of *S. valida*, which control its population (Barrios *et al.*, 2018; Mexzón, 1997; Sendoya and Bustillo, 2016). Lastly, chemical control involves the application of insecticides to the base of the palm (Sáenz and Ospino, 2007); however, this measure is not very effective in controlling its population and has a negative impact on populations of natural enemies.

Some studies on the biology of *S. valida* have been published, such as Genty *et al.* (1978) and Pinzón (1995). However, considering this insect's economic impact and importance on the oil palm crop, the biology, population dynamics, habits of the adults, and the main natural enemies of *S. valida* in the oil palm crop agroecosystem, must be assessed.

MATERIALS AND METHODS

Study Area

The biological study of *S. valida* was carried out under laboratory conditions at the La Providencia experimental station of the Colombian Oil Palm Research Centre, located in the Western Oil Palm Zone of Colombia in the Municipality of Tumaco (Nariño) (1°33'3.705"N, 78°41'38.213"W, 29 m asl). The population dynamics of *S. valida* adults, their habits, and their natural enemies were studied in two agroecological oil palm zones of Colombia; the first plot was selected in the Western Zone located in the municipality of Tumaco - Nariño (1°27'54.05"N, 78°38'14.13"W, 31 m asl), planted in 2008 with the interspecific hybrid OxG cultivar Coari x La Mé in a soil with a clay loam texture (FA) and the second plot in the Central Zone, in the Palmar de la Vizcaína Experimental Station (CEPV), located in the municipality of Barrancabermeja - Santander (06°59'1.15"N, 73°41'43.5"W, 100 m asl), was planted in 2007 with *Elaeis guineensis* cultivar Deli *dura* - Patuca x Deli *dura* - Pepilla, in a soil with a clay loam texture (FA). In each area, a plot of oil palm was selected bordering wooded areas, where the presence of *S. valida* was confirmed.

Taxonomic Verification of Adults of *S. valida*

Adult collections were made with the help of an entomological sweep net (40 cm wide, with a 60 cm long handle); in the two study areas. The insects were placed in a lethal chamber with ethyl acetate, and dry mounts were made to confirm their taxonomic identification. The specimens collected were identified up to the species level and confirmed by Erika Valentina Vergara Navarro of AGROSAVIA Colombia, following the morphological key proposed by Heppner and Duckworth (1981). The extraction of the genitalia of the adult specimens was carried out following the morphological key proposed by Heppner and Duckworth (1981) for the identification and confirmation of the species.

Biology of *S. valida*

The colony was established under laboratory conditions at 25.3 ± 0.6°C and 67.6 ± 9.6% RH. *S. valida* adults were collected from 08:00 to 11:00 hr in oil palm plots near wooded areas using a sweep net (40 cm wide, with a 60 cm long handle), placed in 50 mL conical polystyrene tubes, and transferred to the laboratory. Subsequently, 20 oviposition units, consisting of five females and one male, were arranged in a 3.7 L glass jar containing a damp paper towel, *Pueraria phaseoloides* (Roxb.) Benth (Fabales: Fabaceae) leaves as an oviposition substrate (*Figure 3a*). *Melanthera aspera* (Jacq.) (Asterales: Asteraceae) flowers and a cotton ball soaked in a 1:2 solution of water and sugar as a food source. The top of the jar was covered with tulle; to prevent adults from leaving.

A cohort of 193 eggs of the colony was collected and placed in glass Petri dishes (10 cm diameter) containing a wet filter paper. The eggs were monitored daily to determine their development time and viability.

Two hundred newly emerged first instar larvae were individualised in 10 cm Petri dishes containing moist paper towels and a freshly cut primary root of the interspecific hybrid OxG (Coari x La Mé) used as a food source and changed daily. The Petri dishes were covered with Kraft paper to simulate dark environmental conditions and maintained until pre-pupation. The presence of cephalic capsules coming from the molts was the criterion taken to record the instar change (Dyar, 1890; Gaines and Campbell, 1935) (*Figure 4f*). The width of the cephalic capsules was measured using a trinocular stereoscope (Olympus SZ2-ST, Tokyo, Japan) with a 14MP 1/2.3" digital camera (UCMOS14000KPA, Nanjing Amada Instrument Co., China) and the ToupView program (x 86, ToupTek Photonics, China).

In total, 135 pre-pupae and 127 pupae were counted in 16 oz plastic jars, covered with Kraft paper to simulate natural dark conditions, and monitored daily. The sex of the adults that emerged in each container was identified. Lastly, 18 oviposition units were established in 3.7 L glass jars following the method described above, with one pair of adults placed in each unit. The plant material was changed daily, the adult longevity was recorded, and the number of eggs oviposited per female was counted daily.

Habits of *S. valida* Adults and Associated Weeds

The behaviour of the adults of *S. valida* was determined by observations every hour for 30 min, from 07:00 to 18:00 hr; these were carried out on a 50 m transect between a forest area and the oil palm plantation. Observations were made every biweekly for 43 months.

To identify the plants visited by the adults of *S. valida*, a simple W-shaped transect samplings were carried out (five observations/sampling units), for determination of the presence or absence of these individuals on the predominant weeds in the same transect mentioned above. This sampling was made every hour for 30 min, from 07:00 to 18:00 hr, biweekly for 43 months. The plants frequently visited by adults of *S. valida* were photographed and kept in the herbarium. The plant samples were also sent to the Colombian National Herbarium (*Herbario Nacional Colombiano* – COL) for identification.

Natural Enemies of *S. valida*

The natural enemies of *S. valida*, were collected between 07:00 and 18:00 hr, at biweekly intervals for 43 months. In the weeds, the natural enemies observed preying on the adults of *S. valida* were recorded and their frequency was annotated. Roots of the oil palms close to the forest area of the study plots were sampled while the larval predators were observed. For this purpose, the method proposed by Chávez *et al*. (2000) was used, with a pit made in the area with the greatest presence of roots. For *E. guineensis*, a pit (30 × 20 × 15 cm) was dug from the base of the stipe. The size of the pit in interspecific hybrids OxG was determined after considering the distribution of the root system, as proposed by Torres *et al*. (2004). The 35 x 30 cm deep pit was dug at 50 cm from the base of the stipe. Once the position of the pit was marked, the existing vegetation was removed. Subsequently, the soil was loosened using a trenching shovel and a stake, revealing the primary and secondary roots of the oil palm, which were checked for *S. valida* larvae and their beneficial species. The collected invertebrates were taken to the laboratory for identification using taxonomic keys (Fernández and Sharkey, 2006).

Population Dynamics of *S. valida*

Simple random samplings were performed between 09:00 and 11:00 hr in the plots of the two selected oil palm zones, every fortnight for 43 months. Samplings were performed in a 50 m transect close to a wooded area. *Sagalassa valida* adults were captured by marking four transects per plot and completing 60 double passes in each transect with a sweep net (40 cm wide, with a 60 cm long handle). The captured adults were quantified and placed in 50 mL polystyrene conical tubes containing ethanol (70%). Subsequently, the species was corroborated, and the sex was determined in the laboratory. The precipitation and temperature records were retrieved from the meteorological station closest to each study area.

Statistical Analysis

Data recorded to determine the biology of *S. valida* were analysed using descriptive statistics. Information on the population behaviour of *S. valida* adults were plotted in population dynamics graphs for the two agroecological zones during the 43 months of sampling. The Spearman's rank correlation coefficient of the population of *S. valida* adults was calculated using the climatical variables to determine the relationship between meteorological factors (precipitation and average temperature) with the populations of the adults using the statistical software SAS 9.4 (SAS Institute Inc., Cary, NC).

RESULTS AND DISCUSSION

Taxonomic Verification of Adults of *S. valida*

The specimens collected in the two study zones were identified as *S. valida* Walker, 1856 (Lepidoptera: Brachodidae) (*Figure 2*). Insects are present in all oil palm areas of Colombia, with economic importance in oil palm crops in the Central and Western Zone.

Biology of *S. valida*

The life cycle of *S. valida* from egg to adult emergence lasted 64.2 ± 7.6 days (average ± standard deviation), with 53.5% mortality under laboratory conditions. The egg stage lasted 9.2 ± 0.5 days with 5.7% mortality (*Table 2*). Newly oviposited eggs were white (*Figure 3b*). As these eggs developed and were close to hatching, they became dark yellow, with their chorion showing dots and forming vertical lines (*Figure 3c*).

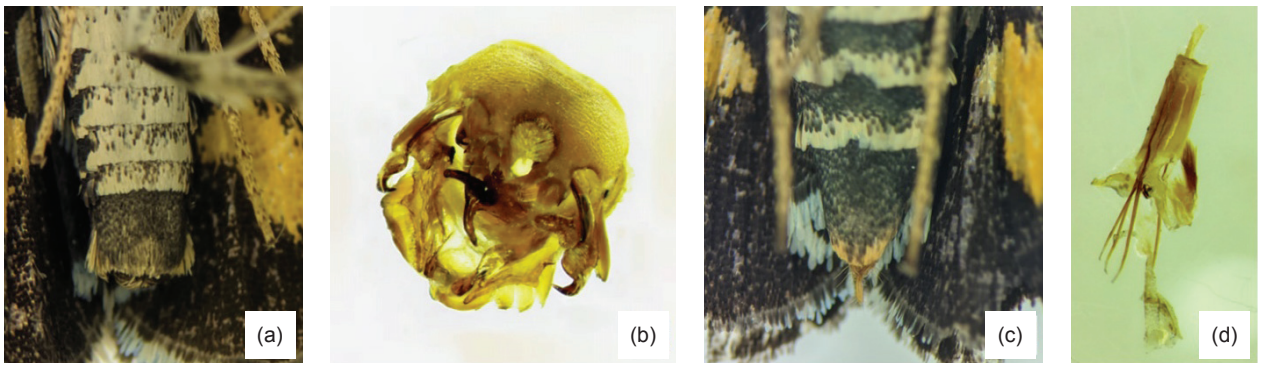


Figure 2. Sexual dimorphism and genitalia of S. valida *Walker, (a) male, last conical abdominal segment, (b) male, genitalia with aedeagus in situ, (c) female, last straight abdominal segment, and (d) female, genitalia.*

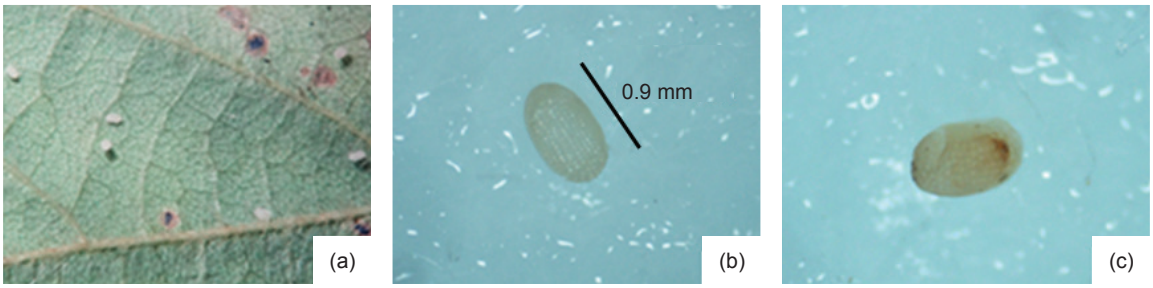


Figure 3. Sagalassa valida *eggs, (a)* S. valida *eggs on* Pueraria phaseoloides *leaves, (b) Recently oviposited* S. valida *egg on* P. phaseoloides *leaves, and (c)* S. valida *egg near hatching.*

TABLE 2. DEVELOPMENT TIME OF THE DIFFERENT STAGES OF THE OIL PALM ROOT BORER *Sagalassa valida* UNDER LABORATORY CONDITIONS (25.3 ± 0.6°C and 67.6 ± 9.6% relative humidity)

Stage		Number of repetitions	Stage duration (days)	Survival (%)
Egg		193	9.2 ± 0.5	94.3
Larva	I Instar	200	5.3 ± 0.7	82.0
	II Instar	164	4.2 ± 0.7	74.5
	III Instar	149	4.5 ± 0.9	74.0
	IV Instar	148	6.3 ± 1.1	74.0
	V Instar	135	17.9 ± 4.8	67.5
	VI Instar	26	8.7 ± 4.2	92.3
Pre-pupa		135	2.9 ± 1.1	63.5
Pupa		127	13.9 ± 1.1	46.5
Adult	Male	48	12.3 ± 4.8	
	Female	45	12.3 ± 4.3	
Total*			**76.4 ± 12.1**	

Note: * The 6th larval instar was omitted from the total.

The larval stage underwent five instars with an average development time of 38.1 ± 4.9 days (*Table 2*). Only 19.3% of the total population larvae presented six instars, with an average duration of 8.7 ± 4.2 days. Neonate larvae had a hyaline body and an amber head. As they developed, their body turned pale yellow and their head dark brown (*Figure 4*). The mortality was 32.5% and peaked in the first instar at 18.0%, followed by the second instar (7.5%). The third, fourth, and fifth stage larval were the most active and voracious.

The cephalic capsule width increased with each change in the larval instar (*Table 3*). The average cephalic capsule of the first instar larvae was 0.20 ± 0.02 mm, while the cephalic capsule of the fourth instar larvae reached 0.91 ± 0.07 mm; that is, their size was approximately four times greater than their initial measurement (*Figure 4f*). The pre-pupal period (*Figure 5a*) was 2.9 ± 1.1 days, with 4% mortality. The pupal stage lasted 13.9 ± 1.1 days, with 17% mortality. The pupa was light brown or amber (*Figure 5b*) (*Table 2*).

TABLE 3. MEAN (± SD) CEPHALIC CAPSULE WIDTH AND GROWTH RATE OF THE DIFFERENT LARVAL INSTARS OF *Sagalassa valida*

Larval instars	Width (mm)	Relationship between instars
I	0.20 ± 0.02	1.65
II	0.33 ± 0.03	1.69
III	0.56 ± 0.05	1.62
IV	0.91 ± 0.07	1.31
V	1.19 ± 0.13	1.04
VI	1.24 ± 0.06	-

Adult longevity was 12.3 ± 4.5 days, with no differences between male and female longevity (*Table 2*). Newly emerged adults were olive green, changing to ochre over time, had a black transverse band on the forewings (*Figure 5c*), and showed discrete sexual dimorphism. The last abdominal segment was conical in males (*Figure 2a*) and straight in females (*Figure 2c*). The antennae were

filiform and smooth in males but contained sensory setae in females, which could be identified under a stereoscope or magnifying glass. The sex ratio was 1:1, and the females laid an average of 51.2 ± 42.5 eggs.

Habits of *S. valida* Adults and Associated Weeds

Sagalassa valida adults were found to be diurnal insects and made short and erratic flights over the nectariferous plants in the oil palm agroecosystem, on which they fed. They visited shady areas on the boundaries of the oil palm plots near the wooded areas and were also usually found near streams or pools of water that formed in the plantation while remaining hidden in low light hours during rainy periods. Between 07:00 and 09:00 hr, *S. valida* adults landed on the selected host plant species, with their antennae held along their body, but this behaviour may vary with climatic conditions. From 09:00-11:00 hr, the adults extended their antennae and flew over these plants to feed (*Figure 6a*) and copulate (*Figure 6b*). Subsequently, the females descend to the base of the palm and land on grooves in the ground, using their wings and abdomen to sweep the soil surface, later ovipositing near the tertiary and quaternary roots of the palm. In the afternoon, the activity of *S. valida* adults decreased as they sheltered within the nectariferous plants (*Figure 7*).

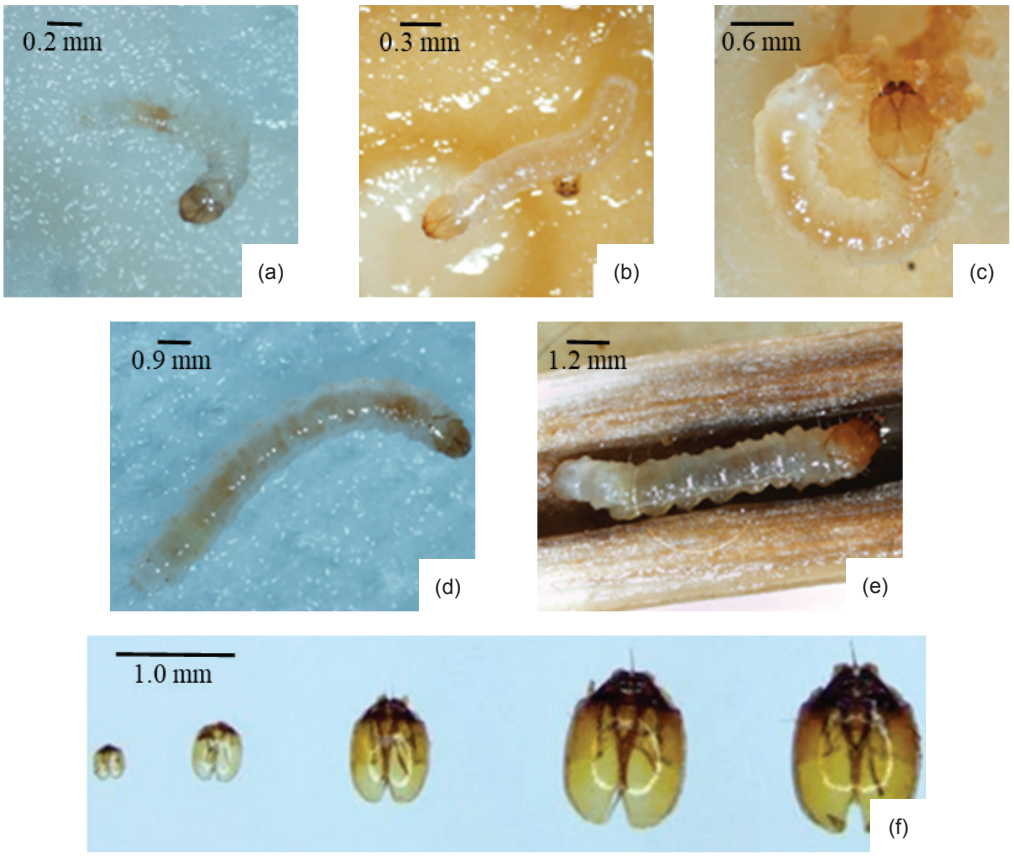


Figure 4. Larval stages of S. valida*: (a) 1st, (b) 2nd, (c) 3rd, (d) 4th, and (e) 5th instars, and (f) cephalic capsules of the different larval instars of* S. valida.

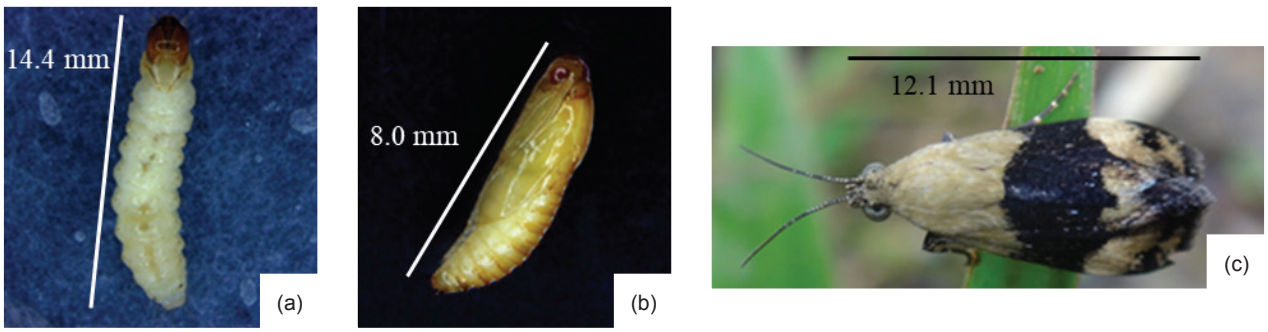


Figure 5. (a) Pre-pupa, (b) pupa, and (c) adult S. valida.

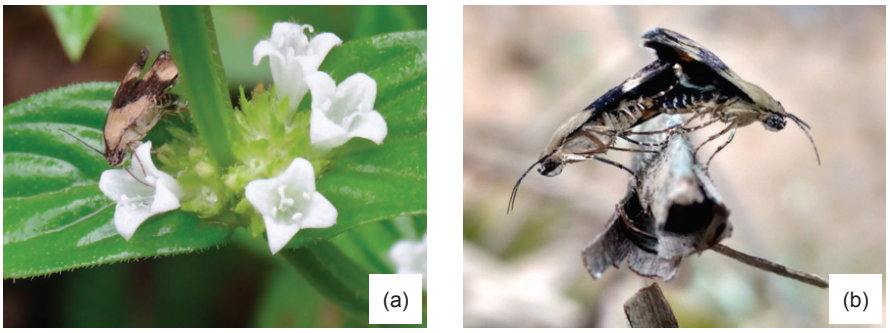
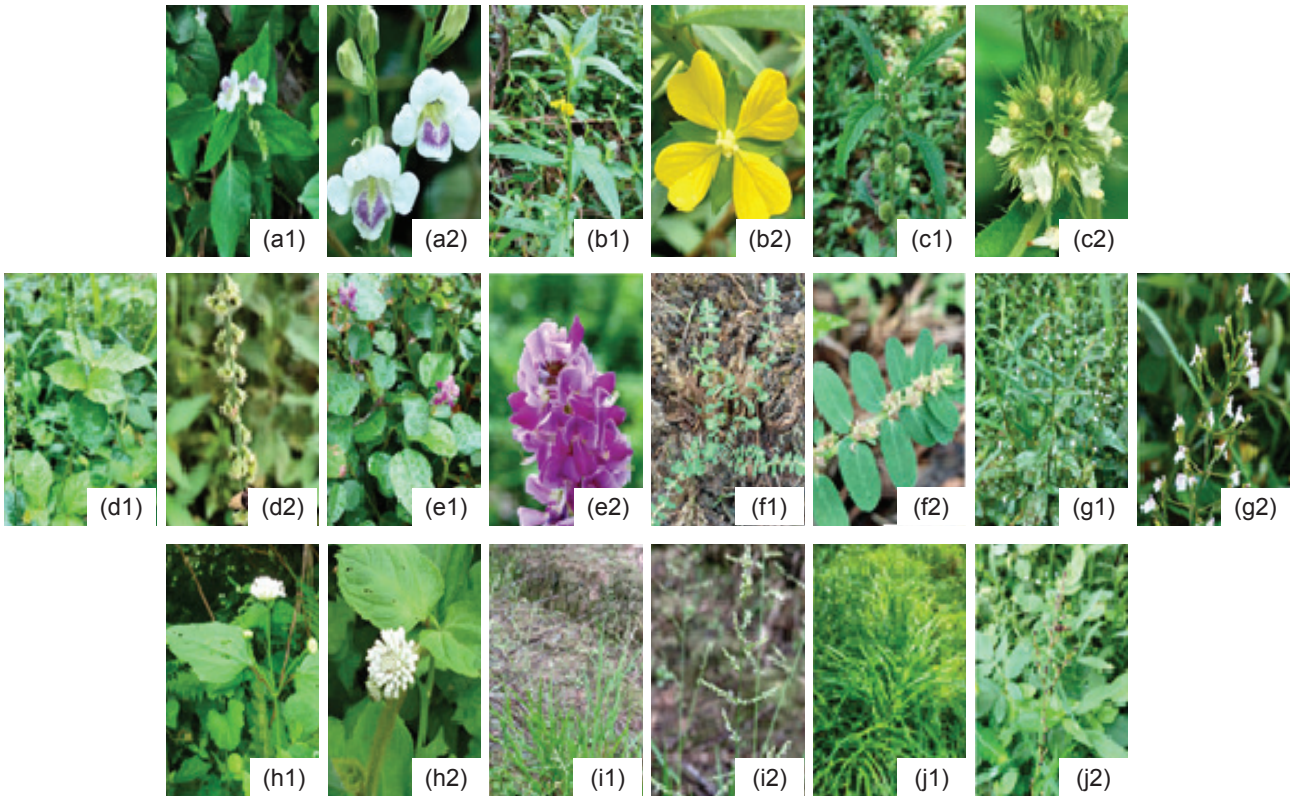


Figure 6. S. valida *adult (a) feeding on a* Spermacoce *sp. flower (09:00 to 11:00 hr), (b) copulating (between 10:00 and 12:00 hr).*



Note: 1 - Plant (full view); 2 - Flower/inflorescence (detail).

Figure 7. Weed species visited by S. valida *adults and their natural enemies: (a)* Asystasia intrusa, *(b)* Ludwigia decurrens, *(c)* Hyptis brevipes, *(d)* Cyathula prostrata, *(e)* Desmodium heterocarpon, *(f)* Chamaesyce *sp., (g)* Justicia comata, *(h)* Melanthera aspera, *(i)* Panicum laxum, *and (j)* Scleria melaleuca.

In the two agroecological zones, the weeds visited by *S. valida* adults for nectar feeding and sheltering during the day were recorded. However, this habitat was also a niche for predatory arthropods of *S. valida* and other beneficial insects of the oil palm agroecosystem. *Sagalassa valida* and their natural enemies frequently visited the nectariferous plants, such as *Asystasia intrusa* Blume (Lamiales: Acanthaceae) (*Figure 7a*), *Ludwigia decurrens* Walter (Myrtales: Onagraceae) (*Figure 7b*), *Hyptis brevipes* Poit (Lamiales: Lamiaceae) (*Figure 7c*), *Hyptis recurvata* Poit (Lamiales: Lamiaceae), *Justicia comata* (L.) Lam. (Lamiales: Acanthaceae) (*Figure 7g*), *Cyathula prostrata* L. (Caryophyllales: Amaranthaceae) (*Figure 7d*), *Desmodium heterocarpon* L. (Fabales: Fabaceae) (*Figure 7e*), *Spermacoce* sp. L. (Gentianales: Rubiaceae), *Stachytarpheta cayennensis* Vahl (Lamiales: Verbenaceae), *Chamaesyce* sp. L. (Malpighiales: Euphorbiaceae) (*Figure 7f*), *Pueraria phaseoloides* (Roxb.) Benth (Fabales: Fabaceae), and *Melanthera aspera* Rohr (Asterales: Asteraceae) (*Figure 7h*). The grass *Panicum laxum* L. (Poales: Poaceae) (*Figure 7i*) and the Cyperaceae *Scleria melaleuca* (Bergius) (Poales: Cyperaceae) (*Figure 7j*) were also identified (*Table 4*).

TABLE 4. WEED SPECIES VISITED BY *Sagalassa valida* ADULTS AND THEIR NATURAL ENEMIES IN TWO AGROECOLOGICAL ZONES OF OIL PALM IN COLOMBIA

Species	Presence in oil palm zone	
	Central	Western
Asystasia intrusa (Acanthaceae)	×	
Chamaesyce sp. (Euphorbiaceae)	×	×
Cyathula prostrata (Amaranthaceae)	×	×
Desmodium heterocarpon (Fabaceae)	×	×
Hyptis brevipes (Lamiaceae)	×	×
Hyptis recurvata (Lamiaceae)	×	×
Justicia comata (Acanthaceae)	×	
Ludwigia decurrens (Onagraceae)	×	
Melanthera aspera (Asteraceae)	×	×
Panicum laxum (Poaceae)	×	×
Pueraria phaseoloides (Fabaceae)	×	×
Scleria melaleuca (Cyperaceae)	×	×
Spermacoce sp. (Rubiaceae)		×
Stachytarpheta cayennensis (Verbenaceae)	×	×

Natural Enemies of *S. valida*

There was no evidence of parasitoids or entomopathogenic microorganisms affecting *S. valida* larvae during the sampling period in both study areas. Arachnids (Araneae) and a species of Odonata (Coenagrionidae), present within the weeds had preyed upon the *S. valida* adults (*Figure 8*). Spiders and ants were the only predators that attacked *S. valida* larvae. Among the ants (Hymenoptera: Formicidae), *Ectatomma ruidum* (Roger, 1861), *Odontomachus brunneus* (Patton, 1894), *Pachycondyla harpax* (Fabricius, 1804), *Pachycondyla obscuricornis* (Emery, 1890), and *Neoponera villosa* Fabricius (1804), were found active at the base of the palms (*Figure 9*).

Population Dynamics of Adults of *S. valida*

The abundance of *S. valida* adults was higher in the Central Zone than in the Western Zone (*Figure 10-13*). Adults were present in both zones throughout the year. The largest populations were recorded in March, April, May, August and November in the Central Zone plot (*Figure 10-11*) and in August, October and November in the Western Zone plot (*Figure 12-13*). The monthly average catches of *S. valida* adults were 121.9 ± 62.1 *S. valida* adults in the Central Zone plot and 38.4 ± 37.6 in the Western Zone plot. The male-to-female ratio of the captured adults of *S. valida* was 0.9:1.1 in the Central Zone plot and 1.2:0.8 in the Western Zone plot. There was no monthly trend of population peaks of *S. valida* in the Western Zone, in contrast to the Central Zone.

In the Central Zone plot, precipitation had significant positive correlations with the following population variables: the number of captured females ($\rho = 0.24$; $P = 0.02$) and the total number of insects captured ($\rho = 0.21$; $P = 0.04$); however, no significant correlations were found between precipitation, and the number of males captured ($\rho = 0.13$; $P = 0.22$), that is to say, that in conditions of precipitation, the activity of the females is greater in comparison to the males in this study area. No significant correlation was found between temperature and the numbers of males, females, and the total of insects captured (*Table 5*). In contrast, the Western Zone plot, recorded no significant correlations between climate and the population variables (*Table 5*).



Figure 8. Natural enemies of S. valida *adults. (a) Arachnid preying on* S. valida *on* A. intrusa, *(b)* M. aspera, *and (c)* Pueraria phaseoloides.



Source: Jhon David Cardenas.

Figure 9. Natural enemies of S. valida *larvae, (a)* Ectatomma ruidum, *(b)* Odontomachus brunneus, *and (c)* Neoponera villosa.

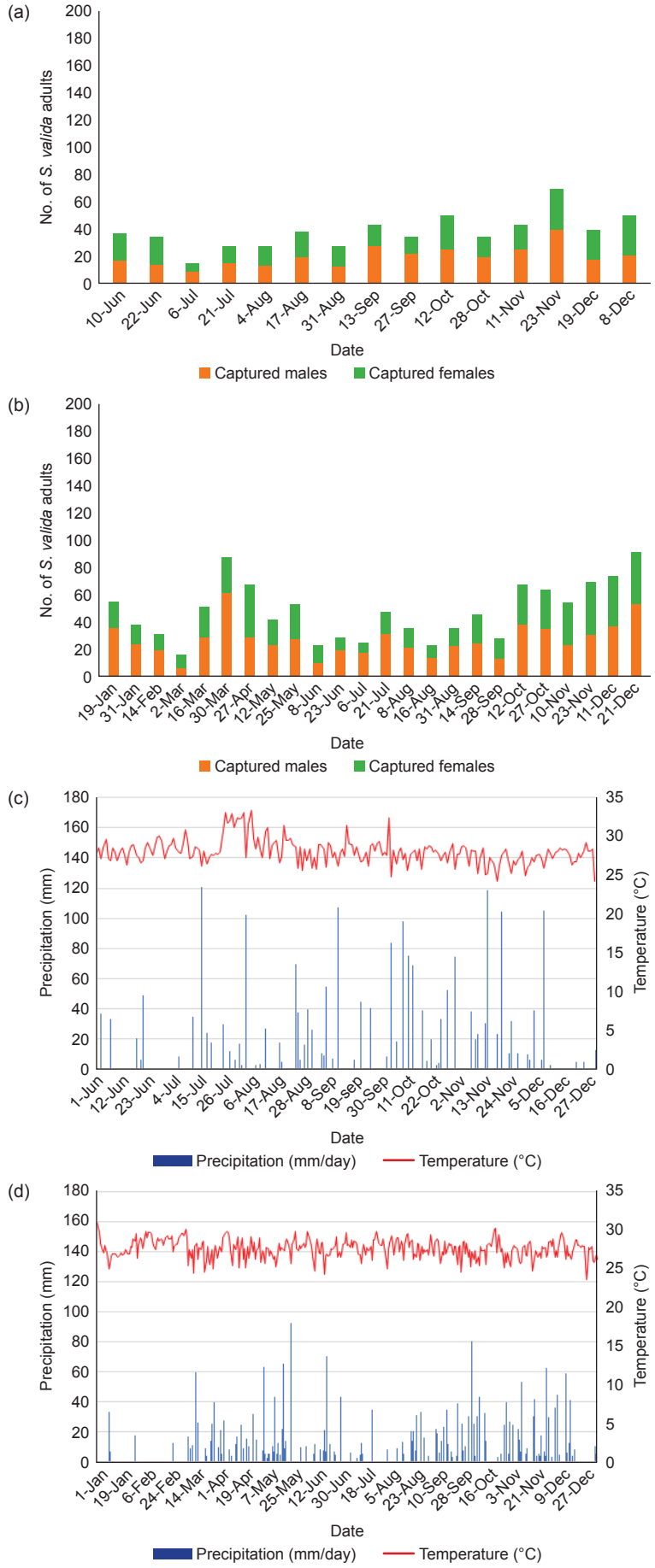


Figure 10. Population dynamics of S. valida *adults in the Central Zone in (a) year 1 and (b) year 2, and temperature and precipitation in (c) year 1, and (d) year 2.*

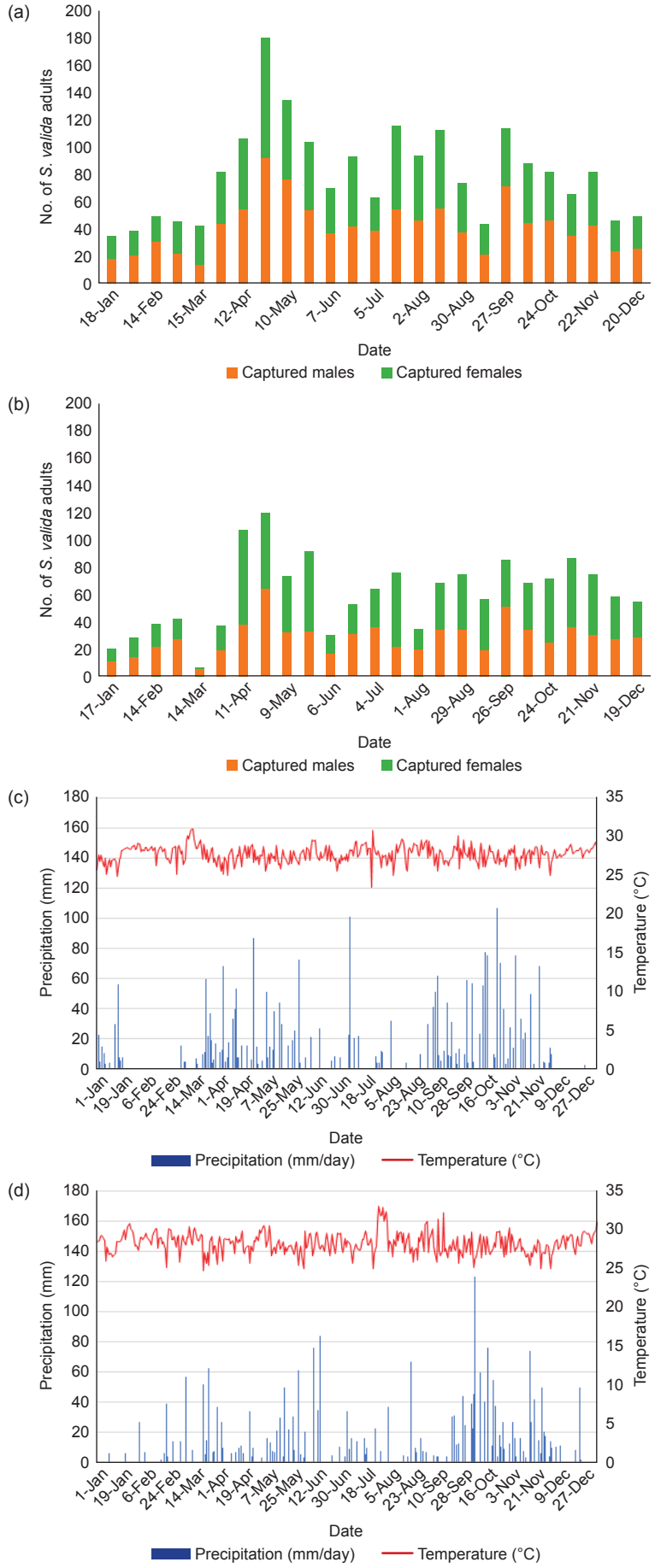


Figure 11. Population dynamics of S. valida *adults in the Central Zone in (a) year 3 and (b) year 4, and temperature and precipitation in (c) year 3, and (d) year 4.*

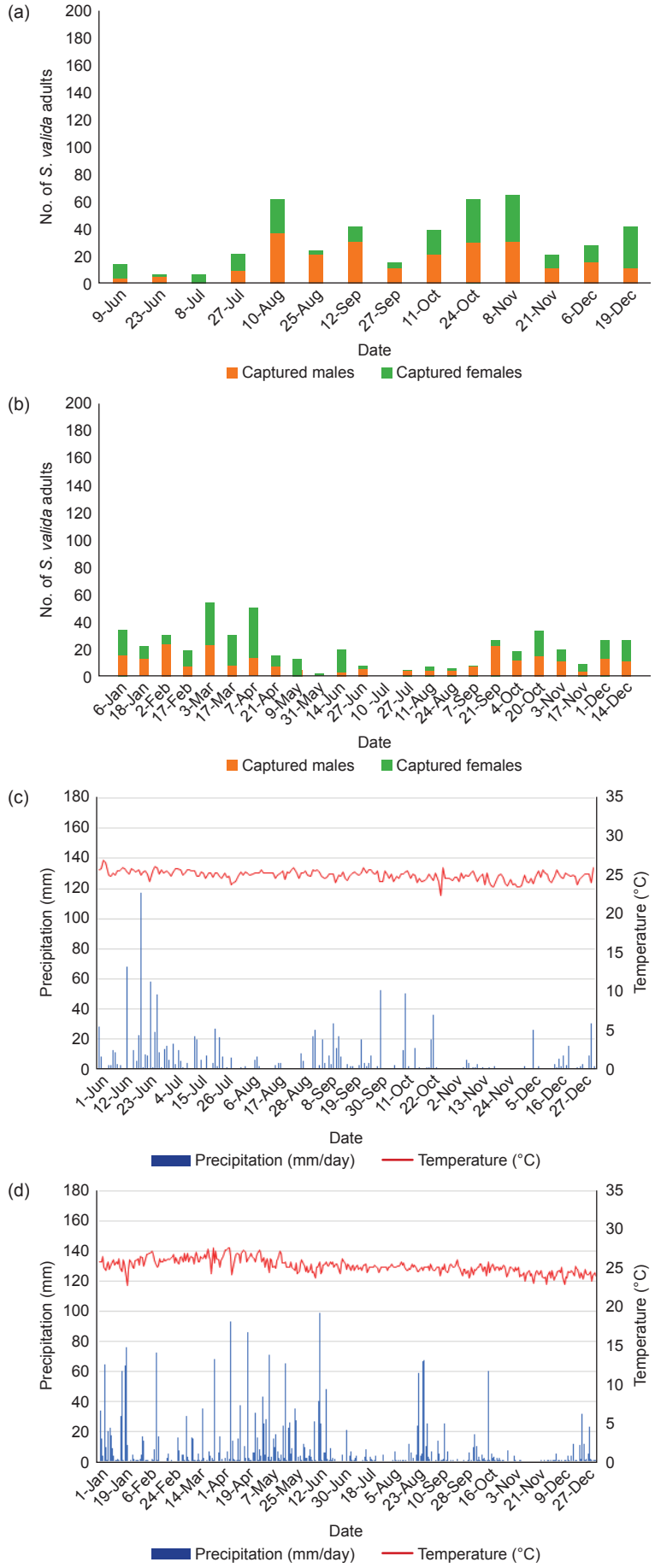


Figure 12. Population dynamics of S. valida *adults in the Western Zone in (a) year 1 and (b) year 2, and temperature and precipitation in (c) year 1, and (d) year 2.*

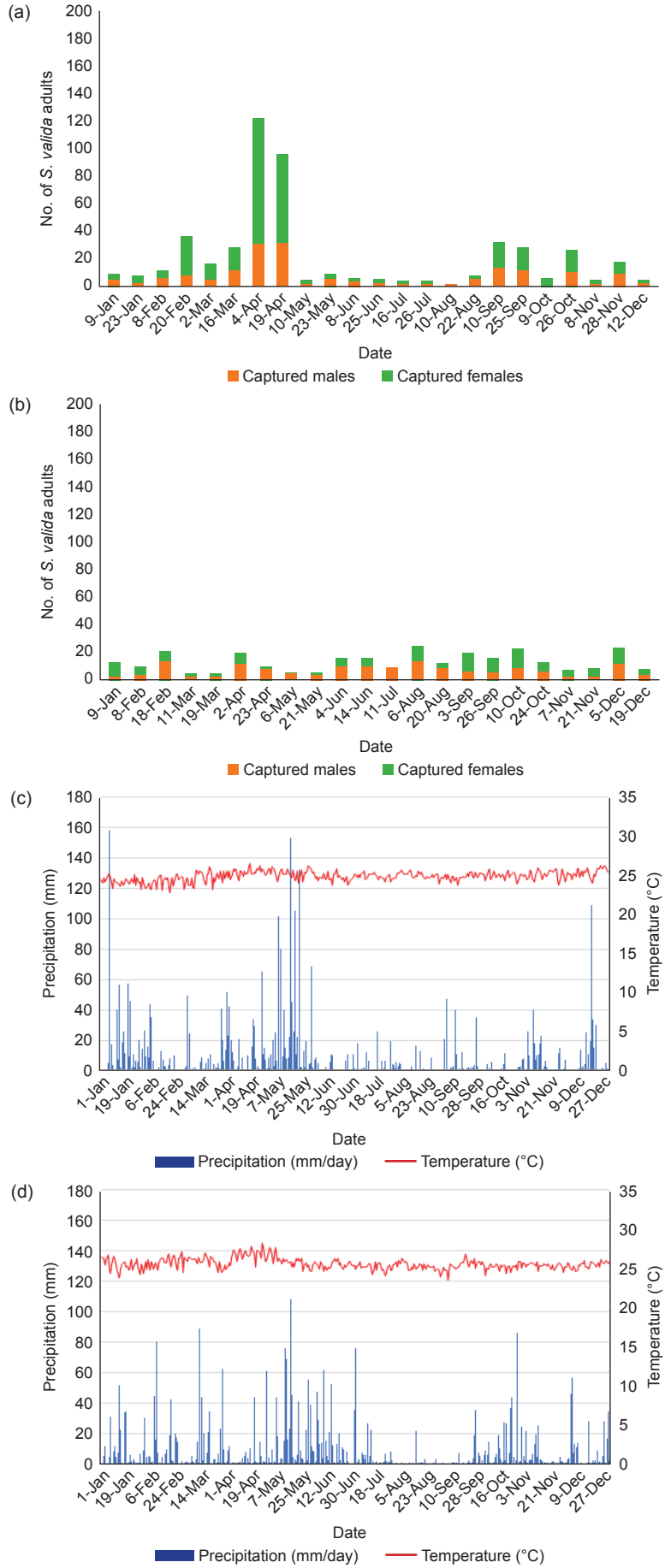


Figure 13. Population dynamics of S. valida *adults in the Western Zone in (a) year 3 and (b) year 4, and temperature and precipitation in (c) year 3, and (d) year 4.*

TABLE 5. SPEARMAN'S RANK CORRELATIONS BETWEEN ENVIRONMENTAL CONDITIONS AND POPULATION DYNAMICS OF *Sagalassa valida* ADULTS IN EACH AGROECOLOGICAL ZONE

Study area	Climate conditions	Population of *S. valida* adults		
		Females	Males	Total
Central Zone	Precipitation (mm)	*ρ:* 0.240 *P:* 0.023	*ρ:* 0.131 *P:* 0.220	*ρ:* 0.214 *P:* 0.044
	Temperature (°C)	*ρ:* -0109 *P:* 0.310	*ρ:* -0.043 *P:* 0.690	*ρ:* -0.095 *P:* 0.377
Western Zone	Precipitation (mm)	*ρ:* 0.068 *P:* 0.542	*ρ:* 0.080 *P:* 0.470	*ρ:* 0.064 *P:* 0.563
	Temperature (°C)	*ρ:* -0.029 *P:* 0.798	*ρ:* 0.066 *P:* 0.554	*ρ:* 0.009 *P:* 0.933

Note: Significant Spearman's rank correlations indicated by $P \leq 0.05$.

Discussion

The development time of the egg stage of *S. valida* is 9.2 ± 0.5 days (*Table 2*), a duration similar to that reported by Pinzón (1995); who recorded that the egg stage lasts from 8 to 9 days. The viability of the eggs was 94.3% (*Table 2*), while Pinzón (1995) reports a viability of 73%. These differences could be due to unfavourable environmental conditions related to temperature and relative humidity.

The larval stage of *S. valida* lasted 38.1 ± 4.9 days (*Table 2*) and went through five instars; however, 19.3% of the larval population presented a sixth instar. On the other hand, these results differ from those recorded by Pinzón (1995), who, under an average temperature of 29°C, recorded six larval instars with a duration of 45 to 48 days. These differences could be due to temperature variations and cultivars used as food resources. Pinzón (1995) used *E. guineensis* roots to feed larvae, whereas the interspecific hybrid OxG (Coari x La Mé) were used in the current study. Biological studies in other Lepidopteran species, such as *Spodoptera litura* (Fabricius) (Lepidoptera: Noctuidae), highlight differences in larval development as a function of diet, temperature, and relative humidity, with this species presenting six larval instars when fed lettuce (*Lactuca sativa* L.), while 52% of individuals showed six larval instars and the rest showing seven instars when the larvae were fed Perilla (*Perilla frutescens* L. Britton), possibly due to the differences in temperature and chemical composition of these host plants (Esperk *et al.*, 2007; Mo *et al.*, 2013).

The width of the cephalic capsules was studied using Dyar's law (1890); which means that the width of the capsule increases according to a regular geometric progression. The relationship between larval instars remained between 1.0 and 1.7 (*Table 3*); these values are within the tolerance range of Dyar's Law: 1.1 to 1.9. Through the size of the cephalic capsule, the larval instars of populations of *S. valida* can be estimated in the field.

The pupal stage lasted 13.9 ± 1.1 days, similar to those found by Pinzón (1995), who recorded developmental time from 12.0 to 18.0 days. The longevity of *S. valida* adults was recorded at 12.3 ± 4.5 days, while Pinzon (1995) reported between 5.0 to 6.0 days duration. In this study, the differences were also evident in the oviposition rate of the females, at an average of 51.2 ± 42.5 eggs per female, in contrast to Pinzon (1995), who recorded an average of eight eggs and a maximum of 30 eggs per female. These differences may be due to the place and environmental conditions in which the adults were kept; unfortunately, these factors were not reported in previous studies. The same occurs with fertility, which can be affected by the type of food consumed by the insect, as observed in *Conogethes punctiferalis* Guenée, 1854 (Esperk *et al.*, 2007) (Lepidoptera: Crambidae), where fecundity was the highest (282.3 eggs/female) when the larvae were reared on Chinese chestnut trees (*Castanea mollissima* Blume) and the lowest (19.2 eggs/female) when reared on apple trees (*Malus domestica* Miller) (Chen *et al*., 2018).

Regarding behaviour, *S. valida* adults were active diurnally and visited the woody areas near the oil palm plantations. During the day (09:00-11:00 hr), they fed and copulated on weeds within the oil palm agroecosystem. This behaviour matched that reported by Pinzón (1995), who recorded that *S. valida* adults copulated between 10:00 and 12:00 hr, with the number of adults decreasing in hours of low light and hiding when it rained; however, in one of the study areas (Central Zone), rainfall had presented a direct and significant effect, which correlated with the number of females and the total number of adults ($r = 0.24$; $P = 0.023$ and $r = 0.21$; $P = 0.044$, respectively). This same author observed that the females were more abundant within the forest, while the males were more abundant near the forested areas at the boundary of the oil palm plots. However, in this study, there was a male and female ratio of 0.9:1.1 in the Central Zone and 1.2:0.8 in the Western Zone, between the forest and the oil palm plantation.

The weeds identified in this study (*Table 4*, *Figure 7*) helped to attract other beneficial invertebrates, such as parasitoids and predators, which use these plant species for food and shelter. The plant species such as *Hyptis capitata*, *Chamaesyce* sp., *C. prostrata*, and *M. aspera* attract Hymenoptera of the families Braconidae, Chalcididae, Ichneumonidae, Scelionidae, Vespidae, Evaniidae, and Formicidae, Diptera of the families Syrphidae, Tachinidae, and Asilidae, and Hemiptera of the families Pentatomidae and Reduviidae (Aldana *et al*., 1997; Mexzón, 1997; Sendoya and Bustillo, 2016), which play key roles in controlling populations of the lepidopteran oil palm pests such as *Stenoma impressella* Busck, 1914, *Stenoma cecropia* Meyrick, 1916 (Lepidoptera: Elachistidae), *Opsiphanes cassina* Felder, 1862 (Lepidoptera: Nymphalidae), *Euprosterna elaeasa* Dyar, 1906 (Lepidoptera: Limacodidae), and other defoliators that attack the oil palm crop (Aldana *et al*., 2010; Escalante, 2007; Sendoya and Bustillo, 2016).

Ants were the only predators observed that affected *S. valida* larvae in the oil palm (*Figure 11*). Löhr and Narváez (2021) determined that *E. ruidum* was the dominant ant species within the oil palm crop in the Western Zone of Colombia, with a dominance of 84.5%. Studies conducted by Coral *et al*. (2004) calculated inverse correlations of 76.7% (P = 0.0096) and 58.0% (P = 0.0786) between populations of the larval stages of *S. valida* and populations of *P. harpax* and *P. obscuricornis* present in the oil palm plantations, respectively. In contrast, Sarmiento *et al.* (2005) found that, under laboratory conditions, *P. harpax* and *P. obscuricornis* predation did not surpass 10% of the exposed population of *S. valida*. Furthermore, these biological controllers showed no preference for preying on *S. valida* larvae or eggs. Regarding entomopathogenic microorganisms, no infected insects were identified in this study; however, Pinzón (1995) demonstrated the pathogenicity of *Metarhizium anisopliae* (Metsch) Sorokin to *S. valida* larvae. Sáenz *et al.* (2005) reported observations of larvae infected with this fungus in the field. Other studies have demonstrated entomopathogenic nematodes efficacy in controlling *S. valida* larvae (Sáenz *et al*., 2005; Sáenz and Olivares, 2008b).

CONCLUSION

The life cycle and the adult longevity of *S. valida* span a total of 76.4 ± 12.1 days, which suggests that this insect pest may undergo four to five cycles a year in the oil palm crops. Due to the overlap between generations of *S. valida*, adults were found throughout the year in the two study zones. Therefore, the integrated management of *S. valida* must be based on an opportunistic diagnosis through monitoring of the adult populations, especially in lots that adjoin the wooded areas. The growth of plant species such as those recorded in this study should also be promoted to help establish and maintain populations of natural enemies that contribute to the biological control of *S. valida* and other oil palm pests.

ACKNOWLEDGEMENT

The authors thank Erika Valentina Vergara Navarro, curator of the National Taxonomic Collection of Insects "Luis Maria Murillo" - AGROSAVIA Colombia, for identifying the specimens. The plantations technicians for their logistical support, the Agricultural Engineer Janis Jacqueline Piza de la Hoz for assisting with laboratory tests, and the Statistician Liseth Estefanía Vargas Medina for her help with the statistical analysis. Also, the Oil Palm Development Fund (*Fondo de Fomento Palmero* – FFP, administered by the National Federation of Oil Palm Growers (*Federación Nacional de Cultivadores de Palma de Aceite* – Fedepalma) for funding this study. CAS-C, JLP-S, and JAM-S conducted the experiments. CAS-S, JLP-S, JAM-S, and MR-G wrote the manuscript with the help of AEB-P and AM-R. All authors provided critical comments and helped shape the research, analysis, and manuscript. AEB-P supervised the project.

REFERENCES

Aldana, J; Calvache, H; Escobar, B and Castro, H (1997). Las plantas arvenses benéficas dentro de un programa de manejo integrado de *Stenoma cecropia* Meyrick, en palma de aceite. *Revista Palmas* (C*olombia)*, *18*: 11-21.

Aldana, R; Calvache, H and Zambrano, J (2000). Determinación del daño de *Sagalassa valida* Walker (Lepidoptera: Glyphipterigidae) en el sistema radical de la palma de aceite. *Revista Palmas* (C*olombia)*, *21*: 74-179.

Aldana, R; Aldana, J; Calvache, H and Franco, P (2010). *Manual de plagas de la palma de aceite en Colombia*. Cuarta Edición. Bogotá-Colombia. 198 pp.

Barrios, C E; Aldana, R C; Bustillo- Pardey, A E; Castillo, N J; Pulgarín, J A and Lozano, M (2018). Plantas nectaríferas asociadas a plantaciones de palma de aceite, que favorecen la fauna benéfica de este ecosistema. Guía de bolsillo. Convenio BID Fedepalma ATN/FM-13216-CD. Conservación

de la biodiversidad en zonas de cultivo de palma. *Cenipalma*. 59 pp.

Barrios-Trilleras, C E; Bustillo-Pardey, A E and Morales-Rodriguez, A (2020). *Caphys bilineata* (Lepidoptera: Pyralidae), una plaga que afecta los frutos de híbridos OxG de la palma de aceite en Colombia. *Ceniavances*, *193*: 1-4.

Bustillo-Pardey, A E (2014a). Nematodos entomopatógenos y sus posibilidades para el control de plagas de la palma de aceite. *Revista Palmas, 35*(2): 53-58.

Bustillo-Pardey, A E (2014b). Manejo de insectos-plaga de la palma de aceite con énfasis en el control biológico y su relación con el cambio climático. *Revista Palmas*, *35*(4): 66-77.

Chávez, C; Ortiz, L; Salamanca, J and Peña, R (2000). Muestreo de *Sagalassa valida* en plantaciones de palma de aceite de la zona Tumaco (Nariño), Colombia. *Revista Palmas* (*Colombia*), *21*: 181-184.

Chen, G M; Chi, H; Wang, R C; Wang, Y P; Xu, Y Y; Li, X D; Yin, P and Zheng, F Q (2018). Demography and uncertainty of population growth of *Conogethes punctiferalis* (Lepidoptera: Crambidae) reared on five host plants with discussion on some life history statistics. *J. Econ. Entomol., 111*(*5*): 2143-2152. DOI: 10.1093/jee/toy202.

Coral, J; Calvache, H; Salamanca, J; Aldana, R and Chávez, C (2004). Reconocimiento de insectos depredadores del barrenador de raíces *Sagalassa valida* Walker en la palma de aceite. *Revista Palmas (Colombia), 25 (especial)*: 232-239.

Corredor, M; Mosquera, M; Fontanilla, D and Ruiz, A (2016). *Sagalassa valida* Walker y el paradigma de los platos limpios. *Revista Palmas* (*Colombia*), *37*: 123-131.

Dyar, H G (1890). The number of molts of Lepidopterous larvae. *Psyche, 5*: 420-422.

Emery, C (1890). Formicides (Voyage de M E Simon au Venezuela ed.). *Annales de la Societe Entomologique de France*, *6(10)*: 55-76.

Escalante, M (2007). Insectos y hongos que afectan a *Opsiphanes cassina* en palma aceitera del sur del Lago de Maracaibo, estado Zulia, Venezuela. *Revista Palmas (Colombia), 20*: 339-344.

Esperk, T; Tammaru, T and Nylin, S (2007). Intraspecific variability in number of larval instars in insects. *J. Econ. Entomol., 100*: 627-645. DOI: 10.1093/jee/100.3.627.

Fabricius, J C (1804). *Systema* Piezatorum secundum *ordines, genera, species, adjectis synonymis, locis, observationibus, descriptionibus* (C. Reichard ed.). Brunswick, Central America. 30 pp.

Fedepalma (2022a). *Anuario estadístico 2022: Principales cifras de la agroindustria de la palma de aceite en Colombia y en el mundo 2017-2021*. Federación Nacional de Cultivadores de Palma de Aceite. 256 pp.

Fedepalma (2022b). *Sustainability report of the Colombian palm oil sector 2018-2021*. Federación Nacional de Cultivadores de Palma de Aceite. 6 pp.

Fernández, F and Sharkey, M (2006). *Introducción a los Hymenoptera de la región Neotropical*. Sociedad Colombiana de Entomología y Universidad Nacional de Colombia, Bogotá. 893 pp.

Gaines, J C and Campbell, F L (1935). Dyar's rule as related to the number of instars of the corn ear worm, *Heliothis obsoleta* (Fab.), collected in the field. *Ann. Entomol. Soc. Am., 28(4)*: 445-461. DOI: 10.1093/aesa/28.4.445.

Genty, P; Desmier De Chenon, R and Morin, J P (1978). Las Plagas de la palma aceitera en América Latina. *Oleagineux, 33(7)*: 326-420.

Heppner, J and Duckworth, W (1981). *Classification of the superfamily Sesioidea (Lepidoptera: Ditrysia)*. Smithsonian Institution, City of Washington. 152 pp.

Löhr, B and Narváez, A (2021). Land use and terrestrial arthropods at the Colombian Pacific coast. *Revista Colombiana de Entomología, 47(1)*: 1-8. DOI: 10.25100/socolen.v47i1.7640.

Mexzón, R (1997). Pautas de manejo de las malezas para incrementar las poblaciones de insectos benéficos en el cultivo de palma aceitera (*Elaeis guineensis* Jacq). *Agronomía mesoamericana, 8*: 21-32.

Mo, H H; Jang, K B; Park, J J; Lee, S E; Shin, K I; Lee, J H and Cho, K (2013). Interactive effect of diet and temperature on instar numbers in *Spodoptera litura*, with reference to head capsule width and weight. *J. Asia-Pacific Entomol., 16(4)*: 521-525. DOI: 10.1016/j.aspen.2013.08.007.

Montes, L G; Sánchez, L Á; Prada, F; Daza, E S; Bustillo, A E and Romero, H M (2018). Relationships between inflorescences and pollinators and their effects on bunch components in *Elaeis guineensis*, in Colombia. *J. Entomol. Sci.*, *53(4)*: 554-568.

Patton, W H (1894). Habits of the leaping-ant of southern Georgia. *Am. Nat., 28*: 618-619.

Peña, R and Jiménez, O (1994). Distribución del daño del insecto *Sagalassa valida* Walker en el sistema radical de la palma de aceite (*Elaeis guineensis* Jacq.) en la zona de Tumaco. *Revista Palmas (Colombia), 15*: 19-23.

Pinzón, Y (1995). Aspectos generales sobre la biología y manejo de *Sagalassa valida* Walker, barrenador de las raíces de la palma de aceite en palmas de Tumaco. *Revista Palmas* (*Colombia), 16*: 17-23.

Roger, J (1861). Die Ponera-artigen Ameisen I. *Berl. Entomol. Z., 4*: 278-312.

Sáenz, A; Benítez, E and De Haro, E (2005). Patogenicidad y signos en larvas del barrenador de raíces de palma de aceite, *Sagalassa valida*, por nematodos entomopatógenos. *Ceniavances (Colombia), 127*: 1-4.

Sáenz, A; Mosquera, M; Fajardo, M and Pulido, C (2006). Comparación de costos para el manejo de *Sagalassa valida* Walker en la Zona Occidental de Colombia. *Revista Palmas* (*Colombia), 27*: 47-51.

Sáenz, A and Ospino, J (2007). Efectividad de insecticidas para el control del barrenador de raíces de palma *Sagalassa valida* Walker. *Revista Palmas* (*Colombia), 28*: 31-38.

Sáenz, A and Olivares, W (2008a). Velocidad de desplazamiento del primer instar de *Sagalassa valida* (Lepidoptera: Glyphipterigidae). *Revista Colombiana de Entomología, 34(1)*: 57-61.

Sáenz, A and Olivares, W (2008b). Capacidad de búsqueda del nematodo entomopatógeno *Steinernema* sp. SNIO 198 (Rhabditida: Steinernematidae). *Revista Colombiana de Entomología, 34(1)*: 51-56.

Sarmiento, A; Benítez, E and Aldana, R (2005). Descripción de la capacidad depredadora de las hormigas *Pachycondyla harpax* y *Pachycondyla obscuricornis*, sobre *Sagalassa valida* Walker, barrenador de raíces en la palma de aceite. *Revista Palmas* (*Colombia), 26*: 23-38.

Sendoya, C and Bustillo, A (2016). Enemigos naturales de *Stenoma cecropia* (Lepidoptera: Elachistidae) en palma de aceite, en el suroccidente de Colombia. *Revista Colombiana de Entomología, 42*: 146-154. DOI: 10.25100/socolen.v42i2.6685.

Torres, V; Rey, B; Gelves, R and Santacruz, L (2004). Evaluación del comportamiento de los híbridos interespecíficos *Elaeis oleifera* x *Elaeis guineensis*, en la plantación de Guaicaramo S.A. *Revista Palmas* (*Colombia), 25*: 350-357.

Journal of Oil Palm Research Vol. 36 (3) September 2024 p. 409-419
DOI: https://doi.org/10.21894/jopr.2023.0035

POLLINATION ACTIVITY OF *Elaeidobius kamerunicus* FAUST IN OIL PALM AND COCOA (*Theobroma cacao* L.) INTERCROPPING SYSTEM IN INDIA

L SARAVANAN[1]*; V SUCHITRA[2] and T PHANIKUMAR[1]

ABSTRACT

Pollinating activity of Elaeidobius kamerunicus *Faust (Coleoptera: Curculionidae) was studied in oil palm-cocoa intercrop conditions in Andhra Pradesh, India. The study showed a high abundance of* E. kamerunicus *on anthesising as well as post-anthesised male inflorescences for a greater part of the year* i.e.*, 62.2 to 162.2 and 39.3 to 87.3 weevils/spikelet respectively. Although, pollinator density declined during summer months, it was sufficient for effecting satisfactory fruit sets. Peak activity was noticed in February. Pearson correlation analysis showed highly significant negative correlations between pollinator population and minimum, maximum and mean temperatures. Pollinator population peaked on 3rd day of anthesis on male inflorescences, and on 2nd day of anthesis on female inflorescences. Weevil activity recorded on the day of highest abundance during anthesis revealed a peak activity between 10:00-12:00 hr and 10:00-13:00 hr on male and female inflorescences respectively. Rat predation on the pollinator was noticed throughout the year with a higher level of predation during summer months. In spite of negative effects posed by abiotic and biotic factors,* E. kamerunicus *density and pollinating efficiency were high throughout the year for the purpose of achieving a higher fruit set (79.6%-93.6%). The practical implications of this knowledge are discussed.*

Keywords: *Elaeidobius kamerunicus*, fruit set, oil palm-cocoa intercrop, pollinating activity, rat predation.

Received: 30 December 2022**; Accepted:** 14 June 2023**; Published online:** 8 August 2023.

INTRODUCTION

Oil palm (*Elaeis guineensis* Jacquin) is known to be the highest edible oil yielding perennial crop, capable of yielding 4.0-5.0 million tonnes of palm oil and 0.4-0.5 million tonnes of palm kernel oil with good planting material, irrigation and proper management (Ministry of Agriculture and Farmers Welfare, 2018). In India, it is grown in an area of 0.32 million hectares under both rainfed and irrigated conditions (ICAR, 2019). Oil palm, being a monoecious crop and seldom both male and female inflorescences of the same plant simultaneously receptive, demands cross pollination. Several insect species are reported as natural pollinating agents, of which, *Elaeidobius kamerunicus* Faust (Coleoptera: Curculionidae), is the most efficient insect pollinator of oil palm (Syed, 1979). It was introduced from Cameroon (West Africa) to Malaysia (Syed *et al.*, 1982) and subsequently to other oil palm growing regions of Southeast Asia, South Pacific Islands and India resulting in a significant increase in fruit set (Basri *et al.*, 1983; Dhileepan and Nampoothri, 1989). However, there have been reports of poor fruit set and decline in oil palm yield after few years of introduction, from many parts of the world due to population fluctuation of *E. kamerunicus*. It has been reported that poor fruit formation

[1] ICAR-National Bureau of Plant Genetic Resources, Regional Station, Hyderabad, Telangana State, India.

[2] Horticultural Research Station, Sri Konda Laxman Telangana State Horticultural University, Adilabad, Telangana State, India.

* *Corresponding author e-mail: laxmansaravanars@gmail.com*

indicates insufficient pollination due to the low population of the oil palm pollinating weevil (Prasetyo *et al*., 2014). The population is affected by hot and dry weather conditions (Dhileepan, 1994; Prasetyo *et al.,* 2014; Syed, 1984), rainfall (Sugih *et al.,* 1996), lower male inflorescence density per hectare (Bulgarelli *et al.,* 2002; Rao and Law, 1998) and predation by rats, spiders (Ponnamma *et al.,* 2006; Siswanto and Soetopa, 2020) and parasitism by nematodes (Krantz and Poinar, 2004). Cropping systems normally play a vital role in the arthropod population dynamics. Conventional oil palm monoculture system is characterised with increased fluctuations in microclimate (Luskin and Potts, 2011), which can influence arthropod population density and diversity. Changes in air temperature within an area can influence the physiological conditions of arthropods, in particular, for specialist species like *E. kamerunicus,* preventing them from colonisation (Cornelissen, 2011) and affecting their activity either positively or negatively. Manipulating microclimatic conditions in oil palm plantations might bring a favourable environment for enhanced pollinator activity and thereby decrease bunch failure. Alley cropping in oil palm may have the potential to ameliorate unfavourable microclimate and increase the pollinator efficiency and oil palm yield. Several trials on oil palm intercropping systems with reference to profitability, compatibility and pest status are conducted globally (Bawa *et al.,* 2011; Dissanayake and Palihakkara, 2019; Gawankar *et al*., 2018; Reddy and Suresh, 2009; Van Leeuwen, 2019), yet, to date, no study is undertaken aiming to know the activity and pollinating efficiency of *E. kamerunicus* in oil palm intercropping systems in India. Globally too, such studies are scarce. Oil palm-cocoa (*Thebroma cacao* Linnaeus) intercropping is a popular cropping system owing to its multiple advantages in India (Bhagya and Suresh, 2018). However, there is a common biological threat caused by rats in this system. For instance, on oil palm, rats gnaw post-anthesised male inflorescences in search of immature stages of the pollinator and predate them, thereby reducing the pollinator density (Siswanto and Soetopa, 2020). On cocoa, rats damage ripe cocoa pods either directly by making holes and consuming cocoa beans or indirectly by biting and scratching the pods (Asunbo, 2021; Smith and Nott, 1988). So far, no attempts are made to know the rat activity and its predation on pollinating weevil in this system. Therefore, this study aimed to determine the seasonal and diurnal activity of *E. kamerunicus*; to know seasonal activity of rats and their predation on the pollinators; and to quantify the pollinator efficiency in terms of oil palm fruit set in spite of effect of abiotic and biotic factors in the oil palm-cocoa intercropping.

MATERIALS AND METHODS

Study Site

The study was conducted in a farmer's field at Suryaraopeta village, West Godavari District, Andhra Pradesh, India having oil palm (seven years old) intercropped with cocoa (six years old) in 10 ha of land. In this system, palm trees were planted in a triangular spacing of 9.0 m while, cocoa was planted in a spacing of 3.0 m in and between oil palm rows. The GPS coordinates for the study site is as follows: 16°49'35.0"N and 81°05'12.1"E.

Seasonal Variation of *E. kamerunicus* Population on Male Inflorescences

Number of weevils per male inflorescences were determined at monthly intervals from January 2014 to December 2015. Weevil population was recorded on 10 randomly selected male inflorescences from the first day of the anthesis and continued until it was complete. From each inflorescence, 15 spikelets (five each from the top, the middle and the bottom of the inflorescence) were selected, gently cut and placed individually in plastic bag and number of weevils congregating on each spikelet was then counted.

Seasonal Variation in Progeny Emergence

Ten post-anthesised male inflorescences (7-10 days after opening) were randomly selected each month from January 2014 to December 2015. From each inflorescence, 15 spikelets (five each from the top, the middle and the bottom of the inflorescence) were collected and placed in perforated transparent plastic containers (20 x 15 cm size) and maintained in the laboratory for progeny emergence. The number of weevil progeny emerging from the spikelets was recorded daily until no further emergence.

Activity of *E. kamerunicus* on Male and Female Inflorescences During Anthesis

Observations on the population of *E. kamerunicus* on both male and female inflorescences during the time of anthesis were taken on each five male and female inflorescences separately and the experiments were repeated twice at different periods to know the effect of stages of anthesis on weevil activity. Inflorescences that were about to enter anthesis were covered with cotton cloth bags of 60 x 40 cm size and firmly tied with twine around the collar portion of the inflorescence to prevent the entry of weevils into the inflorescences (*Figure 1*). To determine the number of weevils that visited inflorescences during the anthesis, the weevils that congregate on the surface of cotton

bag were collected between 09:00 hr and 18:30 hr every day at every 2 hr interval using camel brush, secured in transparent polythene bag, labelled and counted in the laboratory later. Observations were continued from the first day of anthesis until the seventh day in case of male inflorescences and until the fifth day in case of female inflorescences.



Figure 1. Congregation of E. kamerunicus *on the surface of cotton bag covered on inflorescence.*

Diurnal Variation of *E. kamerunicus*

To understand the diurnal variation of *E. kamerunicus* visiting male and female inflorescences, weevils that congregate on the surface of cotton bag were collected gently on the third day and second day of anthesis for male and female inflorescences respectively (as initial observations revealed, the weevils visited in large numbers) at every hour from 08:00 hr to 18:30 hr. Collections were brought to the laboratory and the number of males and females were determined.

Effect of Rat Activity on *E. kamerunicus* Population

For estimating the rat damage, 20 palms were selected randomly every month starting from January 2014 to December 2015 and observations were recorded on rat incidence (number of palms with damaged male inflorescences/total number of palms x 100) and percent rat damage based on visual estimation in the scale of 5%, 10%, 25%, 50%, 75% and 100% damage on male inflorescences.

Effect of *E. kamerunicus* Population on Fruit Set

Ten post anthesis female inflorescences were randomly selected and marked on every month from January to December 2015 at the time of taking census of *E. kamerunicus* on male inflorescences. Marked ripe bunches were harvested at about five to six months later. All the harvested bunches were subjected to normal bunch analysis and the fruit set (the ratio of the total number of normal fruits, divided by the total number of fruits in the bunch, expressed as percentage) was estimated according to the method described by Rao *et al.* (1983).

Recording of Weather Parameter

Weather parameters like minimum and maximum temperature, morning and evening relative humidity and rainfall were recorded daily by the automatic weather station located at Indian Institute of Oil Palm Research, Andhra Pradesh, India. The data were combined on the basis of meteorological weeks and used for statistical analyses.

Analyses

Data collected during January 2014 to December 2015 (two years) on seasonal population of *E. kamerunicus* on male inflorescences during anthesis, progeny emergence and rat activity were cumulated for the analyses and presentation in the study. Cumulative data on seasonal population of *E. kamerunicus* on male inflorescences during anthesis, progeny emergence and rat activity on inflorescences was used for Pearson correlation co-efficient analysis to know their relationships with weather parameters. Bunch characters were correlated with weevil population to understand the effect of weevil activity on fruit set. Percentage values were subjected to arcsine transformations before statistical analyses. Regression analyses were carried out for factors which showed significance in order to understand the strength of relationships and contribution of various factors to the population variation of *E. kamerunicus* and its influence on bunch characters. Analyses were performed using SAS version 9.3 software.

RESULTS AND DISCUSSION

Seasonal Activity of *E. kamerunicus* on Anthesising and Post-anthesised Male Inflorescences in Relation to Weather Factors

Results of seasonal variation in *E. kamerunicus* population is depicted in *Figure* 2. *Elaeidobius kamerunicus* was active throughout the year in the study site with noticeable seasonal fluctuation within the range of 32.7 to 162.2 weevils/spikelet. During summer months, *i.e.*, April, May and June, weevil population was low on male inflorescences (35.7, 32.7 and 46.3 weevils/spikelet respectively). In spite of this decline, weevils recovered rapidly since end of June and maintained higher for a

greater part of the year. *Elaeidobius kamerunicus* population was higher during dry seasons, *i.e.*, January, February, November and December with a peak population during February (162.2 weevils/spikelet). Rainy period (from July to early November) did not cause any adverse effect on the multiplication and activity of *E. kamerunicus*, rather, the population was being built up steadily.

Pearson co-efficient of correlation analysis between weevil population and weather parameters like minimum, maximum and mean temperature indicated a highly significant negative correlation, *i.e.*, r = -0.905, $p \leq 0.01$; r = -0.974, $p \leq 0.01$ and r = -0.973, $p \leq 0.01$ respectively. Relative humidity did not exert significant effect on the weevil activity. Although, rainfall had negative effect on the weevil activity, it did not influence significantly during the study period (*Table 1*). Results of regression analysis indicated that minimum, maximum and mean temperature exerted 81.80%, 94.80% and 94.60% role respectively on *E. kamerunicus* population variation on anthesising male inflorescences (*Table 2*).

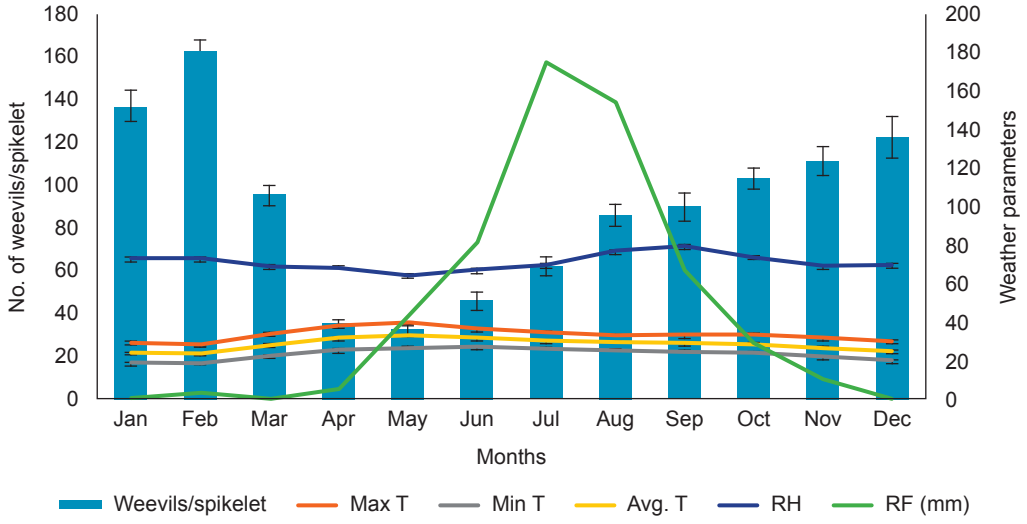
TABLE 1. CORRELATIONS OF ACTIVITY OF *Elaeidobius kamerunicus* POPULATION IN RELATION TO ABIOTIC AND BIOTIC FACTORS AND BUNCH CHARACTERS

Weather parameters	Weevil activity during anthesis	Progeny emergence
Max. temperature (°C)	-0.974**	-0.905**
Min. temperature (°C)	-0.905**	-0.966**
Average temperature (°C)	-0.973**	-0.965**
Average RH (%)	0.469 ^{NS}	0.246 ^{NS}
Rainfall (mm)	-0.410 ^{NS}	-0.549*
Rat incidence	-0.593*	-
Percent rat damage	-0.333^{NS}	-
Fruit set (%)	0.726**	-
Bunch weight (kg)	0.620*	-
Sterile fruits (%)	-0.726**	-

Note: ** - $P \leq 0.01$; * - $P \leq 0.05$; N - 12; NS - non significant.

TABLE 2. REGRESSION MODELS DEPICTING *Elaeidobius kamerunicus* ACTIVITY IN RELATION TO ABIOTIC AND BIOTIC FACTORS AND BUNCH CHARACTERS

Details	Regression equation	r	100R^2
Weevil population *vs.* minimum temperature	Y = -12.217x + 377.008	0.905	81.80
Weevil population *vs.* maximum temperature	Y = -11.804 + 485.448	0.974	94.80
Weevil population *vs.* mean temperature	Y = -12.858x + 456.536	0.973	94.60
Weevil progeny emergence *vs.* minimum temperature	Y = -6.499x + 205.874	0.966	93.20
Weevil progeny emergence *vs.* maximum temperature	Y = -5.466x + 236.387	0.905	81.90
Weevil progeny emergence *vs.* mean temperature	Y = -6.367x + 234.736	0.966	93.40
Weevil progeny emergence *vs.* rainfall	Y = -0.181x + 62.050	0.549	30.10
Rat incidence *vs.* weevil population	Y = -0.805x + 102.133	0.593	35.10
Weevil population *vs.* fruit set	Y = 0.086x + 62.919	0.726	52.70
Weevil population *vs.* bunch weight	Y = 0.030x + 76.560	0.620	38.50



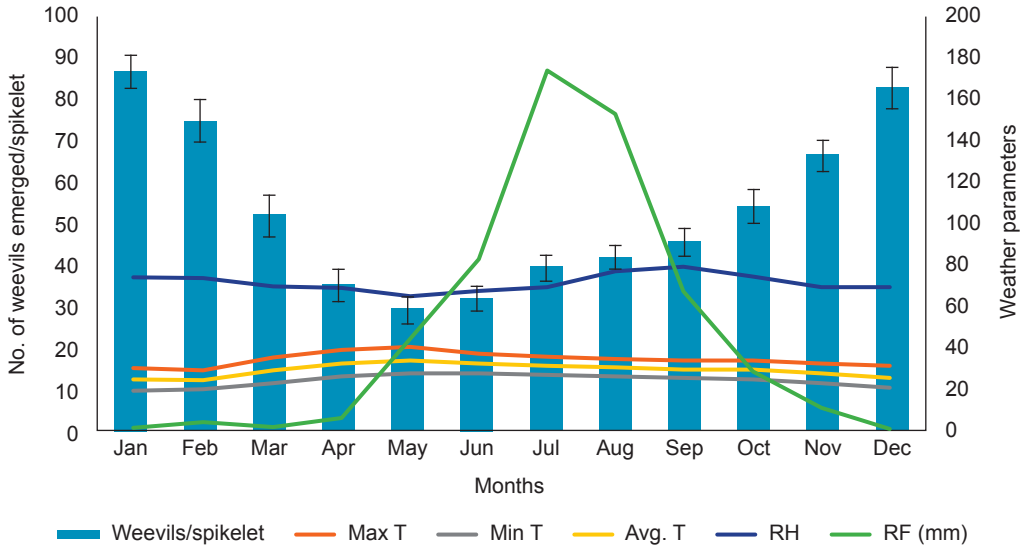
Note: Each data point in the figure is presented as mean ± SE.
RH - relative humidity (%); RF - rainfall.

Figure 2. Seasonal variation of E. kamerunicus *on anthesising male inflorescences (cumulative data of two years).*

Progeny emergence was noticed throughout the year from the post-anthesised male inflorescences with considerable variation in weevil population between the seasons (*Figure 3*). It ranged from 35.0 to 87.3 weevils/spikelet with peak emergence on January. There was a remarkable reduction in the progeny emergence during summer months, *i.e.*, April, May and June (35.0, 29.1 and 31.7 weevils/spikelet respectively). During dry seasons, *i.e.*, January, February, November and December, progeny emergence was consistently higher (ranging 66.8 to 87.3 weevils/spikelet) compared to wet seasons, *i.e.*, July, August, September and October (ranging 39.3 to 54.4 weevils/spikelet). The number of female weevils was always greater than that of the males.

Pearson co-efficient correlation analysis between weevil progeny versus minimum, maximum and mean temperature and rainfall indicated a highly significant negative correlation, *i.e.*, r = -0.966, $p \leq 0.01$; r = -0.905, $p \leq 0.01$; r = -0.965, $p \leq 0.01$ and r = -0.549, $p \leq 0.05$, respectively. Relative humidity did not exert significant effect on the progeny (*Table 1*). Results of regression analysis indicated that minimum, maximum and mean temperature and rainfall exerted 93.20%, 81.90%, 93.40% and 30.10% role respectively in causing variation in the progeny emergence of *E. kamerunicus* (*Table 2*).

Conventional oil palm plantations use a monoculture management system, experiencing higher temperatures and reduced humidity (Sabajo *et al.*, 2017). Greater canopy openness in oil palm plantations results in greater penetration of sunlight to the ground, thus, leading to a hotter and drier micro-climate (Comte *et al.*, 2012; Luskin and Potts, 2011), which affect the population dynamics of the insects severely and paves way for bunch failure in oil palm. On the other hand, Ashraf *et al.* (2019) reported that oil palm alley-cropping system can promote greater vegetation heterogeneity and improve micro-climate compared to the monoculture system by increasing vegetation cover, reducing sun exposure, reducing drying and buffering extreme temperature; and creating the habitat that is required to enhance biodiversity and ecosystem functions such as nutrient cycling, pest regulation and pollination, *etc*. In the present investigation, it was found that there was a high abundance of *E. kamerunicus* on anthesising as well as post-anthesised male inflorescences for a greater part of the year, *i.e.*, 62.2 to 162.2 weevils/spikelet and 39.3 to 87.3 weevils/spikelet, compared to the studies reported elsewhere in sole oil palm conditions (Chinchilla and Richardson, 1991; Dhileepan, 1994; Mohamad *et al.*, 2021; Siswanto and Soetopo, 2020; Syed, 1981). Moreover, it was found that, although hot dry summer [maximum temperature ranging from 36.1°C-39.4°C; minimum temperature 25.1°C-27.1°C; mean temperature 31.6°C-33.2°C and relative humidity (RH) 64.1%-68.6%] caused a decline in the pollinator population, interestingly, both the anthesising and post-anthesised male inflorescences were not devoid of the pollinators during this period, but were found with 32.7 to 46.3 and 29.1 to 35.0 weevils/spikelet, respectively. On the contrary, in sole oil palm cropping situation, Bulgarelli *et al.* (2002) reported that during April and May months, although anthesising male inflorescences were found, these were completely



Note: Each data point in the figure is presented as mean ± SE.
RH - relative humidity (%); RF - rainfall.

Figure 3. Seasonal variation of E. kamerunicus *progeny on post-anthesised male inflorescences (cumulative data of two years).*

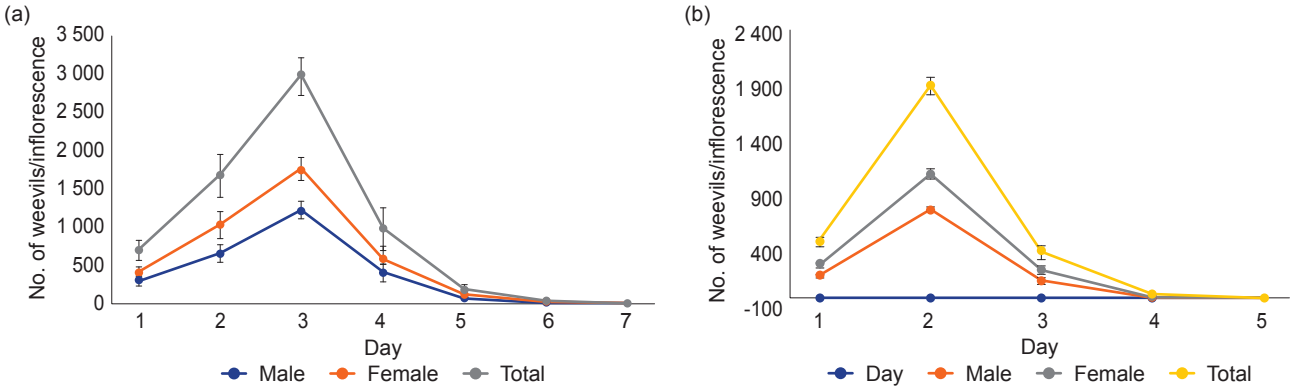
free of *E. kamerunicus* and caused bunch failure in Costa Rica. Dhileepan (1992) and Syed (1982) also reported that very hot and dry summer weather caused a severe decline in the weevil population in West Africa and India. Findings of Sugih *et al.* (1996) also showed that population of the pollinating weevil declined sharply to its lowest level in April in Riau, Sumatra due to very low rainfall coupled with hot temperature and caused bunch failure. Similarly, from India, Kalidas (2020) reported that high temperature coupled with low relative humidity could be the reason for poor pollinator population during the summer months leading to poor fruit set in oil palm. Hence, it is conveniently assumed that the favourable micro-climate created in oil palm-cocoa intercrop conditions, might be one of the reasons for the increased, unceasing and satisfactory weevil activity during most part of the year including during summer. Findings of Ashraf *et al.* (2019) revealed that oil palm intercropped with black pepper and cocoa had lower air and surface temperatures, *i.e.*, 1.3°C and 1.2°C of air temperature and 2.1°C and 2.0°C surface temperature respectively, which may alter the insect activity positively. Oil palm intercropped with cacao plants have diversified vegetation structure with a high ground vegetation cover; such as grass or ground litter, and a wider canopy cover for cacao (Somarriba and Beer, 2011). These vegetation structure characteristics influence not only the air temperature, but also the interception of solar radiation to the ground. In addition, physical characteristics of cacao such as wider canopy cover will act as a wind barrier and reduces the vertical mixing of warm air due to the longer distance for the wind to reach the ground surface (Hardwick *et al*., 2015). Therefore, increasing relative humidity and lowering air temperature (Ashraf *et al*., 2019), which create a favourable environment for enhanced activity and efficiency of the oil palm pollinator. The present findings are in conformity with the results of Bawa *et al.* (2011), who reported that *Elaeidobius* sp. was abundant in oil palm-cocoa intercrop than in sole oil palm due to crop diversity. Studies of Huber *et al.* (2022) also revealed that intercropping led to the increase in activity of pollinators like bumble bees and honey bees and improve the species richness. Further, these results are in conformity with one of our observations of field surveys conducted during summer. In which, in one of oil palm gardens, located in Nellore district of Andhra Pradesh, (where the mean daily maximum temperature is normally about 38°C and RH less than 50% in May) having banana (*Musa paradoxica*) as intercrop, the weevil activity was observed satisfactorily, while the sole oil palm plantations were devoid of weevils in same area (data unpublished).

Activity of *E. kamerunicus* on Male and Female Inflorescences During Anthesis

Adults of *E. kamerunicus* congregated on male inflorescences from the first to the sixth day of anthesis. Population increased with progress in anthesis and was highest during the third day of anthesis when all the florets had opened. There were about 698.7 weevils on male inflorescences on the first day of the anthesis when about 25% of the florets had opened. The number increased on the second day (1673.7 weevils) when 50% of the florets had opened and reached a maximum of 2970.1 adults on the third day, when all the flowers had opened. Thereafter, the number of adult weevils progressively declined until the sixth day due to emigration. No weevils were collected on the seventh day (*Figure 4a*). By this time, male inflorescences started withering. While, on female inflorescences, weevils visited from the first to the fourth day of anthesis. On the first day, 508.2 weevils visited the female inflorescence. On the second day, when maximum florets had opened, the total number of weevils reached a maximum of 1911.3. Thereafter, the number of weevils declined sharply on the third and the fourth day of anthesis to 414.4 and 22.4 respectively (*Figure 4b*). Later, no weevils were attracted to female inflorescences, as the florets turned to pink colour indicating the end of receptivity. The number of females visiting inflorescences was always greater than that of males on both male and female inflorescences. The present findings are more or less similar to the findings reported elsewhere in sole oil palm conditions (Dhileepan, 1994; Ponnamma, 1999; Sambathkumar and Ranjith, 2011; Syed, 1982; Yue *et al.*, 2015).

Diurnal Activity of *E. kamerunicus*

On the third day of anthesis, the weevil population varied remarkably on male inflorescences. Weevils began to visit inflorescences between 08:00 and 09:00 hr and were very active between 10:00 and 12:00 hr. Maximum weevils (455.1) visited at around 11:00 hr, of which 298.1 were females and 163.0 were males. After 14:00 hr, weevil population declined sharply and began to be active again between 17:00 and 18:00 hr (*Figure 5*). While, on female inflorescences, on the second day of anthesis, weevils began to visit and increase in number at 09:00 hr. They were very active between 10:00 and 13:00 hr and reached a maximum number of 377.6 at 12:00 hr, of which 220.5 were females and 157.1 were males. Weevil population sharply declined after 14:00 hr and again began to congregate between 17:00 and 18:00 hr (*Figure 6*). The difference in peak activity of weevils between male and female



Note: Each data point in the figure is presented as mean ± SE.

Figure 4. Number of E. kamerunicus *weevils visiting inflorescences during the anthesis on (a) male inflorescence and (b) female inflorescence.*

inflorescences is because of the emigration of overcrowded weevils from male inflorescences to female inflorescences due to competition for food and oviposition. Reduced weevil activity in the afternoon and slightly increased activity in the evening could be explained as the weevils were reluctant to fly from the shelter or settlement to the field during hot hour of the day and resumed the activity as the temperature drop down in the evening (17:00-18:00 hr). Although some variations are reported in the timing of weevil activity by various researchers (Ponnamma, 1999; Sambathkumar and Ranjith, 2011; Syed *et al*., 1982) under sole oil palm crop conditions, in general, they conform to the basic pattern of activity in intercropping situation too.

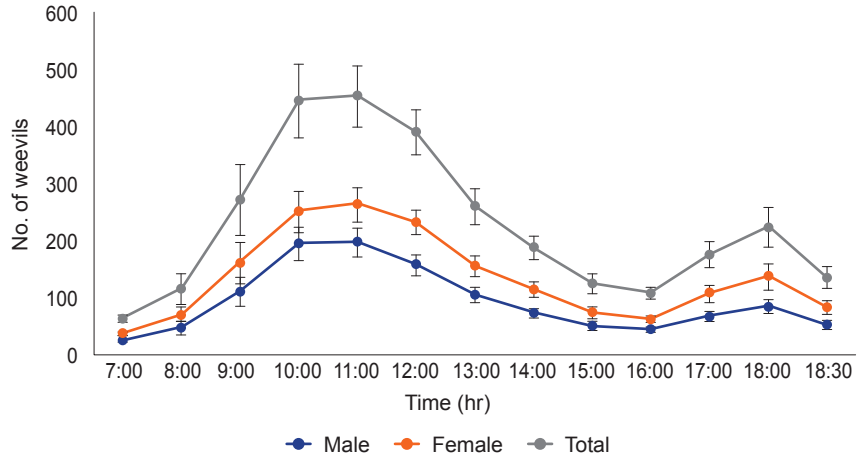
Rat Predation on *E. kamerunicus*

Rats gnawed post-anthesised male inflorescences and damaged them for search of eggs, larvae, pupae and imago of *E. kamerunicus* and preyed upon them. Rat incidence and damage on male inflorescences varied over the months and they ranged from 47.2% to 85.4% and 44.2% to 67.1% respectively. Although rat incidence and damage were noticed throughout the year, maximum incidence (March-June) and damage (April-June) were recorded during summer months (*Figure 7*). Pearson correlation analysis indicated that rat incidence had significant negative influence on the weevil population (r = -0.593; $p \leq 0.05$) (*Table 1*). Regression analysis showed that rat incidence exerted 35.1% variation on the population density of *E. kamerunicus* in the study site (*Table 2*).

There are reports of poor fruit set and yield decline in oil palm due to predation of rats on weevils apart from weather factors (Chiu *et al*., 1985; Yusdayati and Hamid, 2015). Although rat predation was noticed throughout the year, the level of predation was higher during summer months (April-June) due to less or non-availability of the right stage of cocoa pods. Rat predation might be one of the causes for decline in *E. kamerunicus* population during summer, in addition to hot weather conditions. A high degree of rat damage recorded in the present study site could be due to cocoa as intercrop. The study revealed that the two crops have common problem of rat damage and their association will compound rat problems of either crop, if rat management practices are ignored. Interestingly, even in the face of rat predation, weevil population was still maintained for effecting satisfactory pollination as reported in the study.

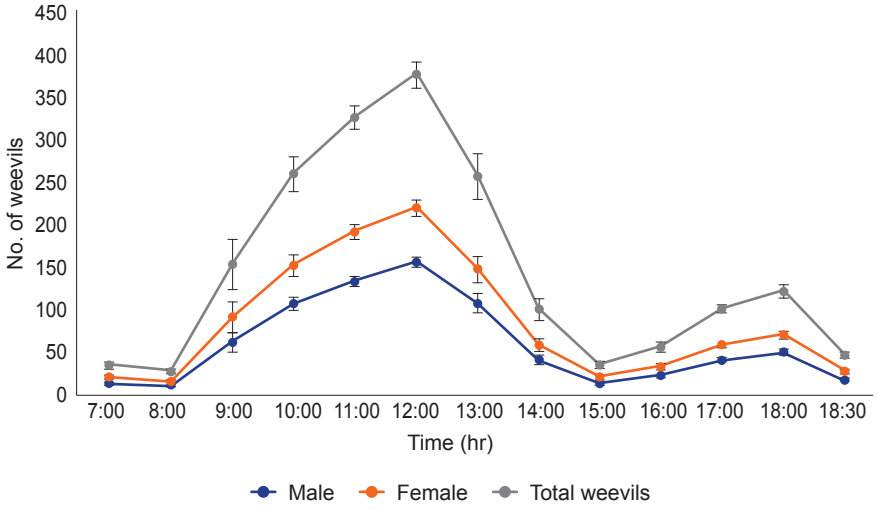
***E. kamerunicus* and its Relation to Fruit Set**

In this study, it was observed that the average fruit set oscillated between 79.6% and 93.6% during the year 2015-2016. Fruit set (at harvest time) was lowest in October (79.6%). It was a response associated with a reduction in the pollinating weevil population that occurred about five months earlier, *i.e*., May 2015 (38.8 weevils/spikelet). Fruit set was comparatively less in November, January, February and March (ranging from 80.1% to 85.9%) when compared to April to September months (≥90.0% fruit set). It was a response associated with wet months about five months earlier (June, July, August and September) (*Figure 8*). Norman *et al.* (2018) also found that wet weather of between 200 to 400 mm seemed to cause low fruit set and low oil extraction rate (≤18.0%) in several oil palm estates in Sarawak, Malaysia. Pearson correlation analysis indicated that activity of *E. kamerunicus* on male inflorescences during anthesis was contributing positively and significantly towards fruit set (r = 0.726; $p \leq 0.01$) and bunch weight (r = 0.620; $p \leq 0.05$). There was an existence of significant positive correlation between fruit set and bunch weight (r = 0.668; $p \leq 0.01$) too (*Table 1*). Regression analysis indicated that weevil population contributed 52.7% and 38.5% of variation in the fruit set and bunch weight respectively (*Table 2*).



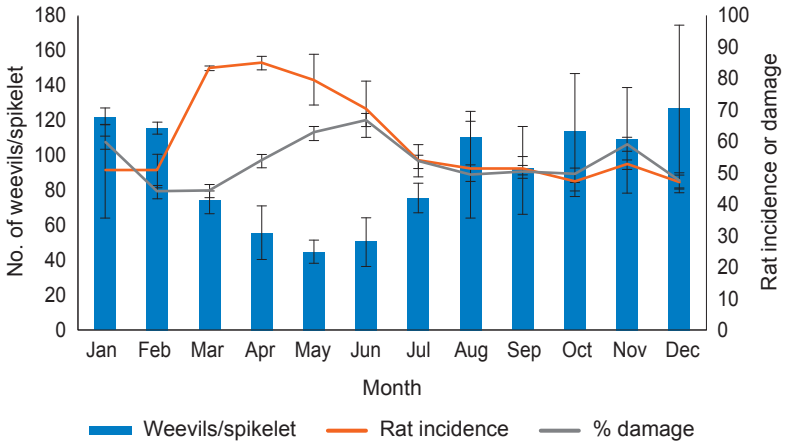
Note: Each data point in the figure is presented as mean ± SE.

Figure 5. Diurnal variation of E. kamerunicus *population on male inflorescences on the 3rd day of anthesis.*



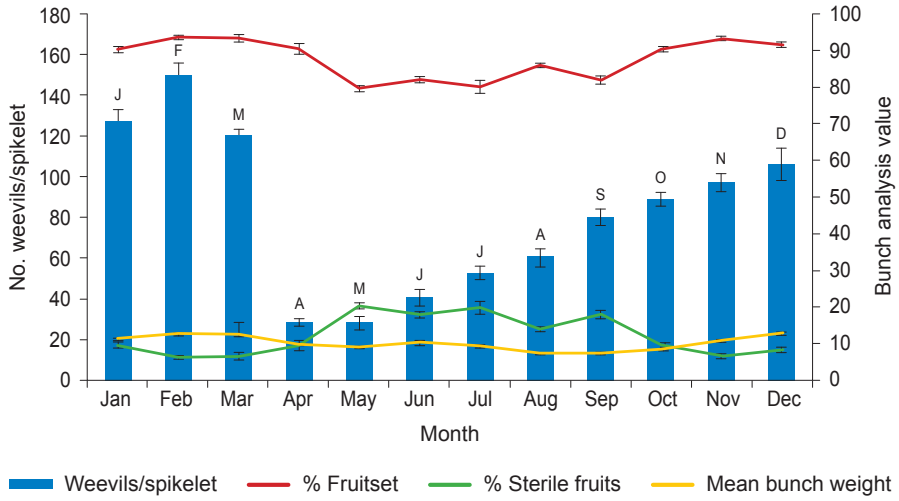
Note: Each data point in the figure is presented as mean ± SE.

Figure 6. Diurnal variation of E. kamerunicus *population on female inflorescences on the 2nd day of anthesis.*



Note: Each data point in the figure is presented as mean ± SE.

Figure 7. Rat incidence and damage on male inflorescences (cumulative data of two years).



Note: Each data point in the figure is presented as mean ± SE.

Figure 8. Relationship between E. kamerunicus *population and fruit set.*

The study showed that fruit set values were higher (around more than 80%) throughout the year. Higher fruit set values could be attributed to adequate weevil population and increased pollinating efficiency of the weevil in the altered micro-climatic conditions under oil palm-cocoa intercrop as discussed earlier. It was found that *E. kamerunicus* population was satisfactory throughout the year even during summer months for the purpose of achieving a higher fruit set, as evidenced by the level of fruit set which was always above 60%; the minimum considered adequate indicating that there was sufficient pollination activity (Syed, 1984). Furthermore, the present results are in conformity with the findings of Dissanayake and Palihakkara (2019), who reported that oil palm yield in intercropping system was significantly increased every year with yield increment of 36.40% than sole crop due to addition of biomass into the system.

CONCLUSION

This study showed a satisfactory pollinator activity and pollination efficiency throughout the year in spite of biotic (hot temperature) and abiotic stresses (rat predation). Since, it is understood that oil palm-cocoa intercrop conditions can provide not only additional income to oil palm growers, but also can improve vegetation cover, increase faunal and floral biodiversity, reduce sun exposure, and reduce drying and mitigate extreme micro-climate; thereby increasing pollinating activity of *E. kamerunicus* and oil palm yield, it should be considered as a key strategy in sustainable and climate smart oil palm production. Further, based on the information obtained from the present study, future line of research should be conducted in different oil palm intercropping systems *vis-a-vis* oil palm monoculture to know their effect on arthropod biodiversity, including pollinator activity and natural enemies of the pests.

ACKNOWLEDGEMENT

Authors are thankful to the Director, Indian Institute of Oil Palm Research, Pedavegi 534 450, India for providing necessary facilities and support during the study periods.

REFERENCES

Ashraf, M; Sanusib, R; Zulkiflia, R; Tohirana, K A; Moslim, R; Butt, A A and Azhar, B (2019). Alley-cropping system increases vegetation heterogeneity and moderates extreme microclimates in oil palm plantations. *Agric. For. Meteorol.*, *276-277*: 107632.

Asunbo, O (2021). Impacts of rodent pests on cocoa (*Theobroma cacao* L): A mini review. *J Agric. Ecol. Res. Intl.*, *22(3)*: 72-81. DOI: 10.973/jaer/2021/v22i330192.

Basri, M W; Halim, A H and Hitam, A H (1983). Current status of *Elaeidobius kamerunicus* Faust and its effects on the oil palm industry in Malaysia. *PORIM occasional Paper, 6*: 39.

Bawa, A S; Yawson, G K; Ofori, S E; Appiah, S O and Afreh-Nuamah, K (2011). Relative abundance of insect species in oil palm-cocoa intercrop at Kusi in the Eastern Region of Ghana. *Agric. Sci. Res. J.*, *1*: 238-247.

Bhagya, H P and Suresh, K (2018). Carbon sequestration potential in oil palm-cocoa cropping system grown in Andhra Pradesh under irrigated conditions. *Int. J. Curr. Microbiol. App. Sci*., *7*: 358-362.

Bulgarelli, J; Chinchilla, C and Rodríguez, R (2002). Male inflorescences, population of *Elaeidobius kamerunicus* and pollination in young commercial oil palm plantation in a dry area of Costa Rica. *ASD Oil Palm Papers (Costa Rica), 24*: 32-37.

Chinchilla, C and Richardson, D L (1991). Pollinating insects and the pollination of oil palm in Central America. *ASD Oil Palm papers (Costa Rica), 2*: 1-18.

Chiu, S; Khoo, K C and Mohmmed Yusoff, H (1985). Extent of rat predation on *Elaeidobius kamerunicus* Faust the pollinating weevil of oil palm. *The Planter, 61*: 101-112.

Comte, I; Colin, F; Whalen, J K; Grünberger, O and Caliman, J P (2012). Agricultural practices in oil palm plantations and their impact on hydrological changes, nutrient fluxes and water quality in Indonesia: A review. *Adv. Agron*., *116*: 71-124.

Cornelissen, T (2011). Climate change and its effects on terrestrial insects and herbivory patterns. *Neotrop. Entomol*., *40*: 155-163.

Dhileepan, K (1992). Pollen carrying capacity, pollen load and pollen transferring ability of the oil palm pollinating weevil, *Elaeidobius kamerunicus* Faust in India. *Oleagineux*, *47*: 55-61.

Dhileepan, K (1994). Variation in populations of the introduced pollinating weevil, (*Elaeidobius kamerunicus,* Coleoptera: Cucurlionidae) and its impact on fruit set of oil palm in India. *Bull. Entomol. Res*., *84*: 477-485.

Dhileepan, K and Nampoothri, K V K (1989). Pollination potential of introduced weevil, *Elaeidobius kamerunicus* in oil palm plantations. *Indian J. Agric. Sci*., *59*: 517-521.

Dissanayake, S M and Palihakkara, I R (2019). A review on possibilities of intercropping with immature oil palm. *Int. J. Res. Appl. Sci. Biotechnol., 6*: 23-27.

Gawankar, M S; Haldankar, P M; Salvi, B R; Haldavanekar, P C; Malshe, K V and Maheshwarappa, H P (2018). Intercropping in young oil palm plantation under Konkan region of Maharashtra, India. *Int. J. Curr. Microbiol. App. Sci*., *7*: 2752-2761.

Hardwick, S R; Toumi, R; Pfeifer, M; Turner, E C; Nilus, R and Ewers, R M (2015). The relationship between leaf area index and microclimate in tropical forest and oil palm plantation: Forest disturbance drives changes in microclimate. *Agric. For. Meteorol*., *201*: 187-195.

Huber, C; Zettl, F; Hartung, J and Lindenlauf, M M (2022). The impact of maize-bean intercropping on insect biodiversity. *Basic Appl. Ecol., 6*: 1-9.

ICAR (2019). *Annual Report*. ICAR-Indian Institute of Oil Palm Research, Pedavegi, Andhra Pradesh, India. p. 1-14.

Kalidas, P (2020). Management of oil palm bunch failure in high sex ratio palms. *The Planter*, *96*: 707-715.

Krantz, G W and Poinar, G O (2004). Mites, nematode and the multimillion-dollar weevil. *J Nat. Hist*., *38*: 135-141.

Luskin, M S and Potts, M D (2011). Microclimate and habitat heterogeneity through the oil palm lifecycle. *Basic Appl. Ecol*., *12*: 540-551.

Mohamad, S A; Ahmad, S N; Syarif, M N Y; Sulaiman, M R; Hung, K T; Mohammed, M A and Masri, M M M (2021). Population abundance of oil palm pollinating weevil, *Elaeidobius kamerunicus* Faust and its relation to fruit set formation in mineral and peat soil areas in Peninsular Malaysia. *Serangga, 26*: 107-117.

Ministry of Agriculture and Farmers Welfare (2018). Status paper on oil palm. Oilseeds Division, Department of Agriculture, Cooperation and Farmers Welfare, Ministry of Agriculture and Farmers Welfare, Government of India. 24 pp.

Norman, K; Moslim, R; Mohamad, S A and Sulaiman, M R (2018). Fruit set and weevil population issues in oil palm. *The Planter*, *94*: 565-578.

Ponnamma, K N (1999). Diurnal variation in the population of *E. kamerunicus* on the anthesising male inflorescences of oil palm. *The Planter, 75*: 405-410.

Ponnamma, K N; Sanjeeb Khan, A and Asha Vijayan (2006). Adverse factors affecting the population of pollinating weevil, *Elaeidobius kamerunicus* F and fruit set on oil palm in India. *The Planter, 82*: 555-557.

Prasetyo, A K; Purba, W O and Susanto, A (2014). *Elaeidobius kamerunicus*: Application of Hatch and carry technique for increasing oil palm fruit set. *J. Oil Palm Res*., *26*: 195-202.

Rao, V and Law, I H (1998). The pattern of poor fruit set in parts of East Malaysia. *The Planter, 74*: 463-483.

Rao, V; Soh, A C; Corley, R H V; Lee, C H; Rajanaidu, N; Tan, Y P; Chin, C W; Lim, K C; Tan, S T; Lee, T P and Ngui, M (1983). A critical examination of the method of bunch analysis in oil palm breeding. *PORIM Occasional Paper, 9*: 28.

Reddy, V M and Suresh, K (2009). Oil palm based cropping system under irrigated conditions-Indian scenario. *Proceedings of National Conference on Oil Palm. SOPOPRAD*, Pedavegi, Andhra Pradesh, India. p. 155-161.

Sabajo, C R; Le Maire, G; June, T; Meijide, A; Roupsard, O and Knohl, A (2017). Expansion of oil palm and other cash crops causes an increase of the land surface temperature in the Jambi province in Indonesia. *Biogeosciences*, *14*: 4619.

Sambathkumar, S and Ranjith, A M (2011). Insect pollinators of oil palm in Kerala with special reference to African weevil, *Elaeidobius kamerunicus* Faust. *Pest Manage. Hortic. Ecsyst., 17*: 14-18.

Siswanto and Soetopo, D (2020). Population of oil palm pollinator insect (*Elaeidobius kamerunicus* Faust) at PTP Nusantara VIII Cisalak Baru, Rangkasbitung - Banten. *IOP Conf. Ser.: Earth Environ. Sci., 418*: 012045.

Smith, R H and Nott, H M R (1988). Rodent damage to cocoa in Equatorial Guinea. *FAO Plant Prot. Bull*., *36*: 119-124.

Somarriba, E and Beer, J (2011). Productivity of *Theobroma cacao* agroforestry systems with timber or legume service shade trees. *Agrofor. Syst*., *81*: 109-121.

Sugih, W; Heru, S; Achmad, F and Thiagarajan, S (1996). Influence of rainfall, palm age and assisted pollination on oil palm fruit set Riau, Indonesia. *Proceedings of the International Palm Oil Congress (Agriculture) 1996 (PIPOC, 1996)*, Kuala Lumpur. p. 207-220.

Syed, A (1979). Studies on oil palm pollination by insects. *Bull. Entomol. Res*., *69*: 213-224.

Syed, R A (1981). Insect pollination of oil palm feasibility of introducing *Elaeidobius* spp. into Malaysia. *Oil Palm News*, *25*: 2-16.

Syed, R A (1982). Insect pollination of oil palm: Feasibility of Introducing *Elaeidobius* sp. into Malaysia. *The Oil Palm in Agriculture in the Eighties Vol. 1*. (Pushparajah, E and Chew Pol Soon eds.). Malaysian Palm Oil Research Institute, Malaysia. p. 263-289.

Syed, R A (1984). Insect pollinators of African oil palm. *Palmas, 5*: 19-64.

Syed, R A; Law, I H and Corley, R H V (1982). Insect pollination of oil palm: Introduction, establishment and pollinating efficiency of *Elaeidobius kamerunicus* in Malaysia. *The Planter, 58*: 547-561.

Van Leeuwen, S K (2019). Analysis of a pineapple-oil palm intercropping system in Malaysia. MSc Thesis, Wageningen University. 93 pp.

Yue, J; Yan, Z; Bai, C; Chen, Z; Lin, W and Jiao, F (2015). Pollination activity of *Elaeidobius kamerunicus* (Coleoptera: Curculionidae) on oil palm on Hainan Island. *Fla. Entomol*., *98*: 499-505.

Yusdayati, R and Hamid, N H (2015). Effect of several insecticides against oil palm pollinator weevil, *Elaeidobius kamerunicus* (Coleoptera: Curculionidae). *Serangga, 20*: 27-35.

Journal of Oil Palm Research Vol. 36 (3) September 2024 p. 420-431
DOI: https://doi.org/10.21894/jopr.2023.0041

OIL PALM POLLEN COMPATIBILITY WITH OxG HYBRIDS IN ECUADOR

MARÍA RAQUEL MELÉNDEZ-JÁCOME[1]; ANDRÉS ALEJANDRO GALVIS-CORREA[1]; PAMELA ELIZABETH MANTILLA-VALDIVIESO[1]; FRANCO ESTÉFANO-TOBAR[1]; MAURICIO ANDRÉS RACINES-OLIVA[1]; TREVOR ANTHONY JACKSON[2] and WILSON VASQUEZ-CASTILLO[1]*

ABSTRACT

*The spread of bud rot disease in oil palm-growing regions of South America has led to the uptake of interspecific hybrids which show some resistance to the disease, but require assisted pollination. A study was carried out to assess pollen viability from commercial oil palm species [*Elaeis guineensis *(G), interspecific hybrids (OxG)] and* Elaeis oleifera *(O) from the Pacific coast and Amazon regions of Ecuador.* Elaeis guineensis *consistently produced pollen of high viability in the Amazon region (95.0%) and Pacific coast (94.0%), while pollen from* E. oleifera *had high viability when produced in the Amazon region (93.7%) but lower viability from the Pacific coast (53.2%). Pollen from oil palm hybrids had very low viability on the Pacific coast. Another objective was to determine the impact of applying pollen from* E. guineensis *and hybrids on fruit set and parthenocarpy by means of assisted pollination trials in both regions. The application of* E. guineensis *pollen resulted in a higher fruit set in comparison with assisted pollination using hybrid's pollen. A low fruit set was compensated by greater production of parthenocarpic fruits in the hybrids, which increased the final bunch weight. The study provides a guide to pollination in both regions.*

Keywords: *Elaeis guineensis*, *Elaeis oleifera*, fruit set, interspecific hybrids, parthenocarpic.

Received: 5 January 2023; **Accepted:** 14 June 2023; **Published online:** 29 August 2023.

INTRODUCTION

Oil palm (*E. guineensis*) is an important commercial crop in humid tropical regions for the production of vegetable oil. The plant requires deep soils, stable high temperatures and high humidity throughout the whole year (Verheye, 2010). There are two geographical origins of *Elaeis* species: 1) The tropical Americas, and 2) West Africa (Durand-Gasselin *et al*., 2009; Hayati *et al*., 2004). In Latin America, the most important producers of oil palm are Brazil, Colombia, Costa Rica, Venezuela and Ecuador having a total plantation area of around 257 120 ha (Fedepalma, 2021).

Oil palm production in Latin America is currently threatened by the spread of bud rot disease (BRD), known locally as '*pudrición del cogollo*' which is causing severe losses of plants in commercial crops in Ecuador, Colombia, Brazil, Panama and Suriname (Durand-Gasselin *et al.*, 2009; Müller *et al., 2006*). A well-documented review was published by Meléndez and Ponce (2016). Hybrids of *E. oleifera* x *E. guineensis* (OxG) can show good agronomic characteristics and tolerance to BRD (Franqueville, 2001), which seems to be inherited from *E. oleifera*, the oil palm native to America (Barba and Baquero, 2012). Hybrid research has been carried out since 1953 (Botelho and Rocha, 1983), with many breeding options studied using Ecuadorian, Panamanian and Brazilian genetic materials (Barba and Baquero, 2012; Teixeira, 2013; Vieira and Lopes, 2010). Hybrid productivity has been shown to be superior to *E. guineensis* species; some hybrids have achieved fresh fruit bunch (FFB) yield of 20-30 t ha^{-1} yr^{-1} with an oil rate extraction of between 18% and 20% (Vieira and Lopes, 2010)

[1] Ingeniería Agroindustrial, Universidad de las Américas, UDLA. Av. de los Granados E12-41 y Colimes, EC170125 Quito, Ecuador.

[2] AgResearch, Lincoln Research Centre Christchurch, New Zealand.

* *Corresponding author e-mail: wilson.vasquez@udla.edu.ec*

or even up to 10 t oil ha^{-1} yr^{-1} (Romero and Ayala, 2021). Nevertheless, nutritional studies have been performed to improve yield (Rosero *et al*., 2013) and more studies covering field management to improve bunch yield and quality have been published (Astorkia *et al*., 2019; Ochoa-C and Palacio-Mahecha, 2021; Romero *et al*., 2021; Ting *et al*, 2020). The OxG hybrids could be a promising solution for oil palm production; however, they have limitations through poor fruit set due to a lack of pollen fertility or low level of insect pollination in commercial plantations (Kumar *et al*., 2015; Swaray *et al*., 2021). This problem has been overcome by assisted pollination by hand and using phytohormones (Daza *et al*., 2020). Nevertheless, these practices have high costs for commercial production and need high numbers of workers that are not always available or well-trained (Li *et al*., 2019; Ruiz-Alvarez *et al*., 2021). In Ecuador, commonly used assisted pollination is based on the application of *E. guineensis* pollen to achieve commercial fruit sets; nonetheless, the current use of hybrids raises opportunities to study the compatibility of alternative donor sources and female plant material.

Assisted pollination has been adopted as a systematic practice for increasing productivity in commercial oil palm plantations. Protocols and pollen dosage for increasing yields have been described by Arnaud (1980). However, a low fruit set and productivity of hybrids on commercial plantations have led to pollen studies comparing *E. guineensis*, *E. oleifera* and their interspecific hybrids OxG. A study presented by Sánchez and Romero (2013) showed that the pollen of OxG hybrids achieved only 21.9%-26.3% germination, attributed not only to weather conditions but also to morphological and physiological aspects of the hybrid's pollen grains. In contrast, pollen from *E. guineensis* and *E. oleifera* showed 88% germination (Sánchez and Romero, 2013). The current effect of environmental conditions or the effect of climate change on pollen germination remains to be investigated by the scientific community.

Pollen has been evaluated for its capacity to fertilise female flowers and produce fruit sets. Commercial plantations of the hybrid OxG have always used *E. guineensis* as the pollen donor for assisted pollination, even though there has been limited research on alternatives, such as *E. oleifera* or OxG hybrids, as pollen donors and their effects on fruit set. Previous studies in Latin America on the influence of weather on pollen viability and its capacity to fertilise female flowers were inconclusive (Corrado, 1984). In Asia, pollination using an introduced insect, *Elaeidobius kamerunicus*, increased fruit set and the production of seeded fruits of *E. guineensis* in commercial plantations (Swaray *et al*., 2021; Syed, 1986).

The pollination of OxG hybrids in commercial plantations in Ecuador has depended on pollen provided by *E. guineensis* and hand pollination (Alvarado *et al*., 2013; Prasetyo *et al*., 2014). Alvarado *et al*. (2013) mention that the "Amazon" hybrid in Central America depends on the pollen input of ancient *E. guineensis* palms nearby. Pollen compatibility can be evaluated after the manually assisted pollination of adult palms. Alvarado *et al*. (2013) also showed that the fruit set was higher using *E. guineensis* as the pollen donor compared with using an Amazonian hybrid as the pollen donor. Their research demonstrated the importance of pollen quality and viability and showed that pollen viability of between 15% and 20% limited fertile fruits in the fruit bunch.

The introduction of the bud rot disease has led to research for new resistant/tolerant hybrids, and growers have been encouraged to replant with OxG hybrids, but this is exacerbating the problem of poor fruit set and raises the need for urgent research to address the problem. With high genetic variability among the new hybrids, there is a lack of information about their behaviour and their responses to pollen compatibility. As new hybrids are used for commercial production, there is a need to understand pollen compatibility between species to avoid dependence on only one source of pollen: *E. guineensis*.

The present study was carried out to assess pollen percentage germination rate in vitro, from commercial oil palm species (*E. guineensis* (G), interspecific hybrids (OxG) and *E. oleifera* (O) from the Ecuadorian Amazon region and Pacific coastal region.

In this research, the objective was to determine the effect of different pollen sources on pollination and oil palm yield was examined with experiments in two locations: The Pacific coastal plains and Amazon region headwaters, where flowers from a selection of OxG hybrid oil palm were treated, by assisted pollination, with pollen from different sources. The knowledge of fruit set behaviour submitted to different pollen sources will allow us to understand the impact of assisted pollination and analyse present agronomic management practices in commercial oil palm production. It is expected that the results of this study will guide the selection of donors for artificial pollination for hybrid oil palms in Ecuador and other regions where hybrids are grown.

MATERIALS AND METHODS

Location of Experimental Sites

Studies of pollen germination and compatibility were established in two distinct geographical regions.

Site 1 was the Ecuadorian Amazon region (El Coca, Francisco de Orellana province) at Palmar del Río plantation of 10 000 ha (GPS location: 0° 19´ S, 77° 04´ W at 290 masl, 3392 mm of annual precipitation, 1327 light hours, maximum temperature: 33.4°C, and minimum temperature: 18.2°C). Site 2 was the Ecuadorian Pacific coast, specifically a 3000 ha site at Energy & Palma plantation, located in San Lorenzo, Esmeraldas province (GPS location: 1° 07´ N, 78° 45´ 50" W at 500 masl, with 1500-1800 mm of annual precipitation, 1380 light hours, 400 W m^2 of irradiation, maximum temperature: 34.0°C, and minimum temperature: 27.0°C). Both sites had a plant density of 146 plants ha^{-1} for *E. guineensis*, *E. oleifera* and OxG hybrids. These two regions were chosen due to the prevalence of bud rot disease (BRD) in oil palm plantations where many growers are cropping OxG hybrids as a possible solution to control the disease. This research was developed with commercial and native species of five-year-old palms in both regions. In the first phase of this study, pollen germination percentage was evaluated in OxG hybrids with commercial oil palm species (*E. guineensis* and *E. oleifera*) as controls. In the second phase, pollen compatibility, fruit set, and production were compared within OxG hybrids.

Determination of Pollen Grain Germination in OxG Hybrids

The pollen germination (%) of three hybrids in Site 1: Coarí x LaMé (CxL), Taisha x AVROS (TxA), and Taisha x LaMé (TxL) and three hybrids in Site 2: Coarí x LaMé (CxL), Taisha x AVROS (TxA) and Unipalma – were evaluated. Unipalma is only cultivated in the Pacific coastal region, and (TxL) only in the Amazon region. Male inflorescences from each of *E. guineensis*, *E. oleifera* and hybrid plants (Taisha x AVROS, Taisha x LaMé and Coarí x LaMé) were selected during the first spate of the opening stage, early on and before the anthesis, corresponding to stage 607 BBCH scale (Moreno and Romero, 2012). No insects were present on the male inflorescences, which avoided contamination with foreign pollen grains from other palm species. The inflorescences were isolated using a double-layer bag (MANGLAR GP-004 (63x83 cm), Green Putumayo) and tied at the peduncle base with a cotton thread (Arnaud, 1980). The bag was revisited every two days to adjust its tightness to the inflorescence peduncle when needed. The male inflorescences were collected during the anthesis phase, then immediately transported to the laboratory located in the plantation site and placed in a chamber at 22°C, 33% RH for 4 hr. After storage, spikes were cut off and gently shaken to liberate pollen. The collected pollen was placed in envelopes and dried in an oven at 37°C for 12 hr. The pollen was sieved through a 40 µm mesh to separate impurities and then packed in glass tubes (10 mL) and stored for less than two weeks at -20°C, according to the methodology described by Turner and Gillbanks (1974). To evaluate germination, pollen grains were scattered onto Petri dishes containing a simple culture medium (saccharose: 11 g; agar: 1.2 g; distilled water 100 mL). Petri dishes were incubated at 37°C for 12 hr. After incubation, 100 pollen grains were observed under the microscope per sample (Optical Olympus microscope BX51 model), photographed with a camera attached to the microscope (Infinity 2, applying 1:10 fold), and assessed for the presence of a pollen tube emerging from the grain, indicating germination (Myint *et al.*, 2012). Pollen germination was determined for each palm species and the hybrid plants. Pollen was considered germinated when the pollen tube was equal to or greater than the size of the pollen grain.

Statistical Methods

To analyse the germination percentage of pollen grains, a completely randomised block design (CRBD) was applied and an analysis of variance with 95% of reliability was performed. The results were obtained in the statistical software MINITAB 2016. A total of 18 male inflorescences from each species and hybrid were isolated to collect pollen in Site 1, and 25 male inflorescences from each species and hybrid were isolated in Site 2 for comparison. Germination was compared between species and, in the case of *E. guineensis*, *E. oleifera* and (TxA), the differences were estimated according to the sampling region as well. Tukey's test (5%) was performed where appropriate when statistical differences were presented in the Analysis of Variance.

Determination of Fruit Set in OxG Hybrids by Selective Assisted Pollination

Selective assisted pollination was carried out in the two regions (Amazon region and the Pacific coast). In both regions, there are specialised people who work daily only in pollination activities, using standardised practices, and they contributed to this study with their skills. Pollen from selected hybrids (Site 1: Taisha x AVROS, Taisha x LaMé, Coarí x LaMé; Site 2: Unipalma, Taisha x AVROS and Coarí x LaMé) and *E. guineensis* were applied to female inflorescences from oil palms hybrids (OxG) as shown in *Table 1*.

Female flowers were bagged (MANGLAR GP-004 (63x83 cm), Green Putumayo) individually and pollen was applied according to the standard method for assisted pollination of OxG hybrids described by Turner and Gillbanks (1974). Female flowers during pre-anthesis I (Hormaza *et al.*, 2012) were treated with pollen (10 g of pollen and talcum powder in

a 1:10 mixture), applied with a sprayer inside the bag, which was then sealed. After hand pollination, female inflorescences remained bagged for 110 days. On Site 1, three female flowers from different plants were pollinated with each male treatment; a total of 12 bunches were evaluated. On Site 2, five female flowers were pollinated with pollen from each donor to evaluate a total of 20 bunches.

The total weight of the bunch was recorded on a digital scale, then the fruits were extracted from the bags and classified into seeded, parthenocarpic, and undeveloped fruits. Seeded fruits had seeds, and contained a nut made up of a shell, a kernel, and a mesocarp, while parthenocarpic fruits were formed without pollination, so they did not present an almond. Finally, undeveloped fruits were considered those with white pigmentation, no almond, and no mesocarp, or were one of those that fell from the cluster (Corley and Tinker, 2016; Hormaza *et al*., 2012). The weight of each category was measured to differentiate the proportions of useable fruits.

Statistical Methods

To compare the results of the fruit set, a randomised complete block design (RCBD) in factorial arrangement 3x4 (female flowers and pollen donors) was carried out on each site and later an analysis of variance (ANOVA) with 95% reliability was performed. The results were obtained using the statistical software MINITAB 2016. A total of 5 male inflorescences from each species were isolated to collect pollen from Site 1 and Site 2 to use as pollen donors for female flowers from oil palm species and hybrids. Three female inflorescences in the anthesis of each oil palm species, present in each site (1 and 2), were used as pollen receptors (*Table 1*). The analysis was performed to compare total bunch weight along with the percentage of normal, parthenocarpic, and undeveloped fruits according to the pollen donor. If the ANOVA (p<0.05) presented statistical differences, Tukey's test (p<0.05%) was performed to determine groups of similar behaviour.

RESULTS AND DISCUSSION

Pollen Germination Rate

The germination rate of pollen collected from commercial oil palm species in the Amazon region was high, with 95.0% germination recorded for *E. guineensis* and 93.7% for *E. oleifera* (*Figure 1*). High germination percentages (75%-85%) for pollen from these species collected from the Amazon region have also been reported by Myint *et al*. (2012).

Pollen germination rates for OxG hybrids (TxA (12.2%), CxL (9.7%) and TxL (16.9%)) were significantly lower than for the species (*Figure 1*), although TxL pollen germination was significantly higher than the other hybrids. Low pollination germination from hybrids was also found in Brazil by Sánchez (2008) and Alvarado *et al*. (2000).

Pollen germination rates from commercial and hybrid materials grown on the Pacific coast are also presented in *Figure 1*. The pollen germination rate of *E. guineensis* was 94.0%, similar to that attained in the Amazon region, whereas the pollen

TABLE 1. POLLEN APPLIED AS TREATMENTS TO FEMALE OIL PALM HYBRID (OxG) INFLORESCENCES

Pollen donor	*E. guineensis*	Taisha x AVROS	Taisha x LaMé	Coarí x LaMé	Unipalma
Female inflorescences					
Amazon region (Site 1)					
Taisha × AVROS	(TxA) × *E. guineensis*	(TxA) × (T×A)	(T×A) × (T×L)	(T×A) × (C×L)	-
Taisha × LaMé	(TxL) × *E. guineensis*	(TxL) × (T×A)	(T×L) × (T×L)	(T×L) × (C×L)	-
Coarí × LaMé	(CxL) × *E. guineensis*	(CxL) × (T×A)	(C×L) × (T×L)	(C×L) × (C×L)	-
Pacific coast (Site 2)					
Taisha × AVROS	(TxA) × *E. guineensis*	(TxA) × (T×A)	-	(T×A) × (C×L)	(T×A) × Unipalma
Coarí × LaMé	(CxL) × *E. guineensis*	(CxL) × (T×A)	-	(C×L) × (C×L)	(C×L) × Unipalma
Unipalma	Unipalma × *E. guineensis*	Unipalma × (T×A)	-	Unipalma × (C×L)	Unipalma × Unipalma

Note: Oil palm hybrids: Taisha x AVROS (TxA); Taisha x LaMé (TxL); Coarí x LaMé (CxL). Coarí- pure *oleifera* from Brazil; Taisha- pure *oleifera* from Ecuador; LaMé- L10T x L2T; AVROS- SP 540 (Compact Seeds and Clones ASD, 2004; INIAP, 2013).

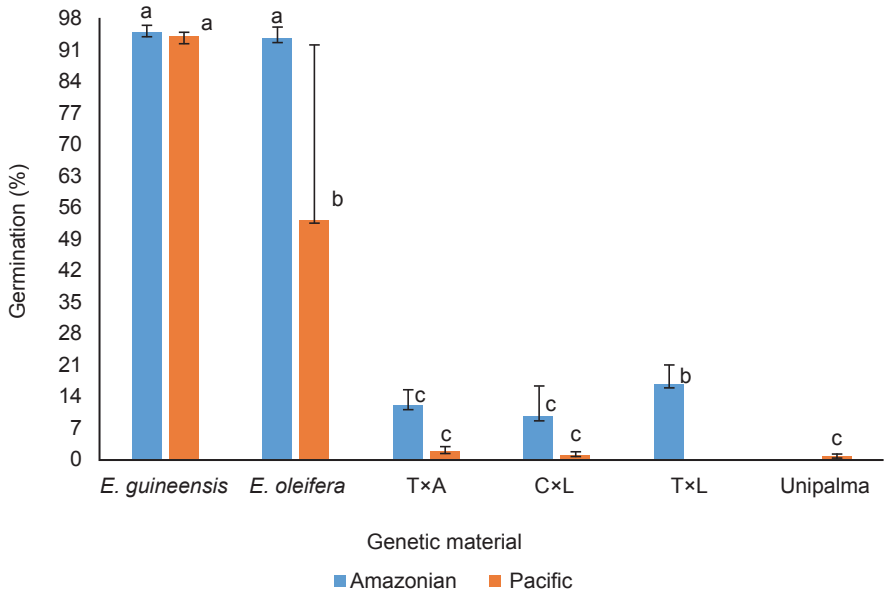


Figure 1. Oil palm pollen germination before storage for commercial species or hybrids in the Amazon region and Pacific coast (Tukey grouping CI 95%).

germination of *E. oleifera* was significantly lower (53.2%). These results agree with those reported by Criollo and Dominguez (2018), where *E. guineensis* showed better pollen quality. Pollen germination from the three hybrids on the Pacific coast was very low (TxA: 1.9%; CxL: 1.1% and Unipalma 0.7%) when compared to the Amazon region. The results indicate that there is a higher percentage of pollen germination in the Amazon region than on the Pacific coast, possibly due to the interaction between climate and genetic composition of plant material, as suggested by Lin *et al*. (2017) and Davarynejad *et al*. (1995) and this study. While the Amazon is consistently humid (annual average precipitation of 3392 mm), the Pacific coast's humidity and temperature can oscillate widely, and rainfall is lower with 1500-1800 mm yr^{-1} (INAMHI, 2016).

The low germination rate for pollen produced from hybrids indicates the need for manual pollination (Haniff and Noor, 2002) and illustrates the importance of choosing a good pollen donor. One indicator of pollen germination potential might be the morphology of pollen grains and genetic characteristics (Sánchez and Romero, 2013), which was observed by microscopy (*Figure 2* and *3*). Pollen grain was considered germinated when the pollen tube was longer than the diameter of the grain (*Figure 2*).

The 10-fold increase in size is due to the microscope settings allowing a better resolution in the measurements. If this is considered, the pollen size is similar to those published by Forero *et al*. (2012) and Sánchez and Romero (2013), ranging from approximately 30.0 to 39.1 µm (*Figure 3*) in size from both species and hybrids,

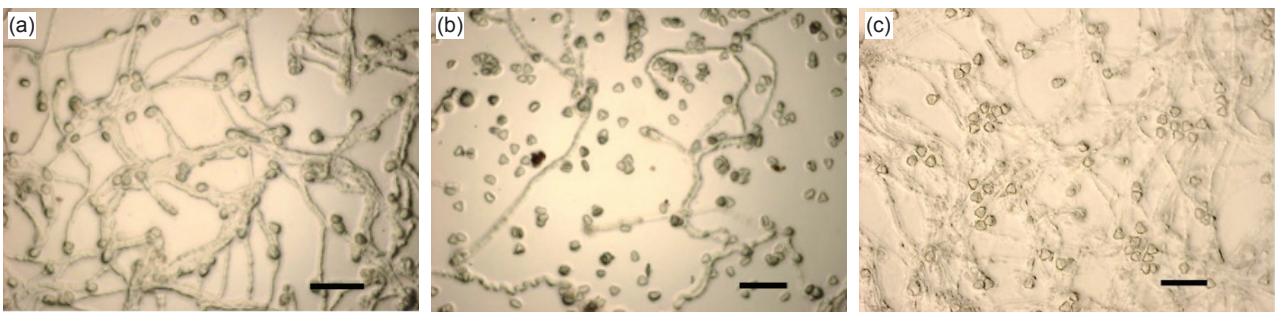


Figure 2. Oil palm pollen germination under optical microscope observation: (a) E. guineensis*; (b)* E. oleifera*; and (c) Hybrid OxG. Scale bar in black = 2 mm.*

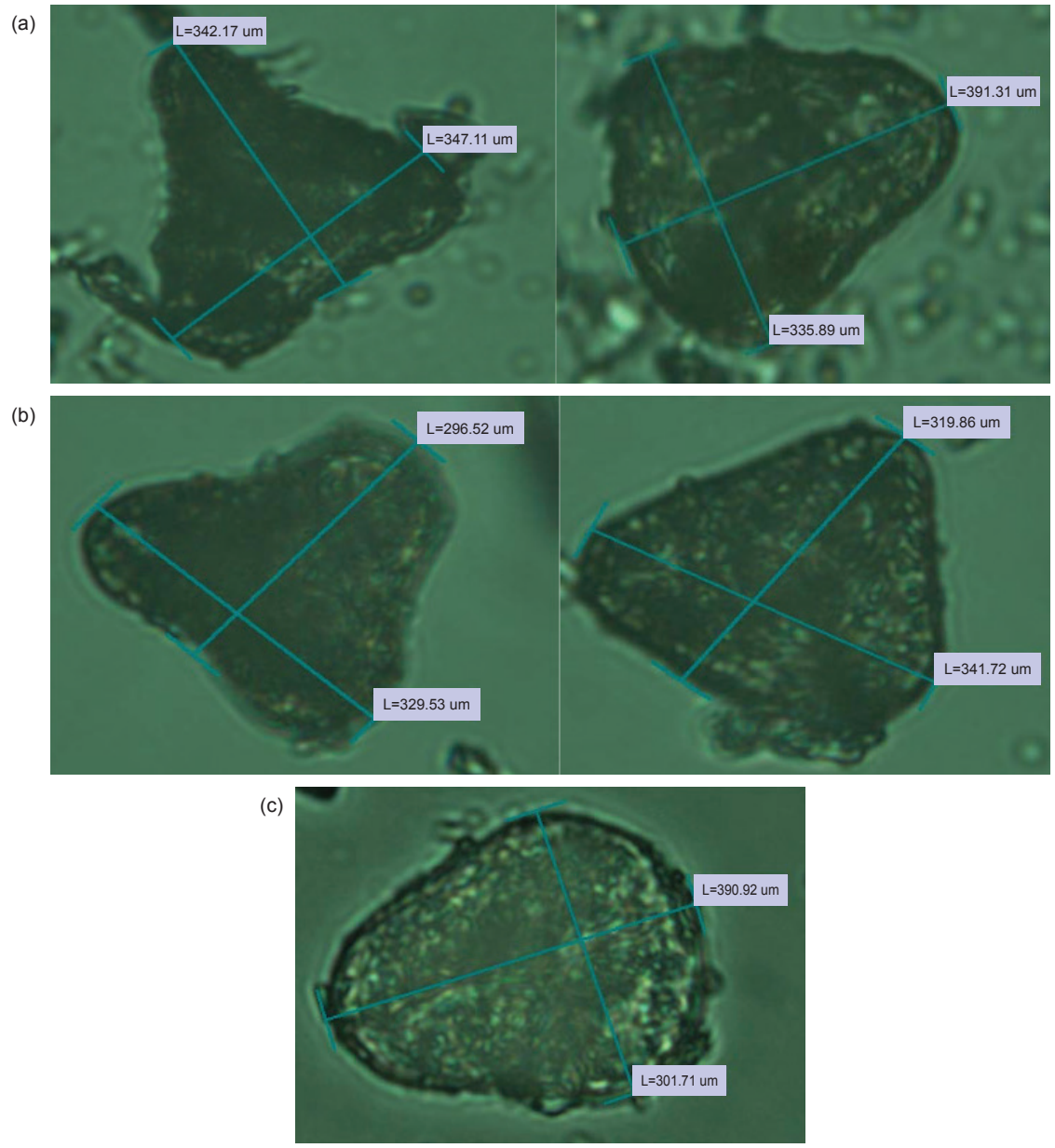


Figure 3. Size and morphology of Hybrids OxG pollen grains 100x: (a) Unipalma, (b) CxL and TxA, and (c) E. oleifera.

nevertheless, the morphology of oil palm pollen varied. Hybrids pollen was triangular in shape: *Figure 3a* and *3b* in comparison with *E. oleifera*¸ which produced elliptical pollen grains (*Figure 3c*). Similar pollen morphology characteristics in *E. guineensis* were reported in other studies (Myint *et al*., 2012; Sánchez and Romero, 2013; Tandon *et al*., 2001). However, pollen from hybrids presented a mixture of pollen shapes and shared morphological attributes from *E. oleifera* and *E. guineensis*, which was also found by Sánchez and Romero (2013). This might suggest a level of incompatibility between parental plants, which would affect germination.

Fruit Set and Yield Obtained After Oil Palm Cultivar Pollination with Hybrid and *E. guineensis* Materials

In the Amazon region, palm flowers from three hybrid palm cultivars (TxA, TxL, and CxL) were treated with four pollen sources (*E. guineensis*, TxA, TxL, and CxL) (*Table 1*). The highest bunch weight was obtained in the CxL variety (10.79 kg), but all hybrid varieties had high proportions of parthenocarpic and undeveloped fruits. The highest proportion of fertilised fruits was obtained in the TxL hybrid, with 37.9% seeded (*Table 2*).

TABLE 2. THE EFFECTS OF FEMALE FLOWERS AND POLLEN DONORS ON BUNCH CHARACTERISTICS IN THE AMAZON REGION

Female flower effect on					
	Bunch weight (kg)	**Seeded fruits (weight %)**	**Parthenocarpic fruits (weight %)**	**Seeded + parthenocarpic fruits (weight %)**	**Undeveloped fruits (weight %)**
C×L	10.79 a	17.82 b	–	42.04 b	14.34 b
T×A	8.9 ab	24.25 b	–	34.94 c	22.92 a
T×L	7.15 b	37.92 a	–	57.62 a	11.35 b
Pollen donor effect on					
E. guineensis	10.41 a	43.47 a	10.55 b	54.02 a	10.79 b
C×L	9.39 ab	27.7 b	21.94 a	49.64 a	15.44 a
T×L	8.89 ab	20.4 b	18.77 ab	39.17 b	19.82 a
T×A	7.19 b	15.08 b	21.55 a	36.62 b	18.77 a

Note: Means followed by the same letter are not significantly different using Tukey's test (p=5%).

When pollen source is considered, pollen from *E. guineensis* produced the greatest bunch weight, but this was not significantly (p<0.05) greater than that obtained from CxL and TxL pollen donors (*Table 2*). While bunches treated with *E. guineensis* pollen contained significantly (p<0.05) more fertilised (seeded) fruits and less undeveloped fruits, bunches treated with hybrid pollen compensated for fertilisation failure by producing greater proportions of parthenocarpic fruits (18.77%-21.94%), contributing to the overall bunch weight (*Table 2*).

On the Pacific Coast, flowers from the hybrid palm varieties (TxA, CxL, and Unipalma) were treated with four pollen sources (*E. guineensis*, TxA, CxL, and Unipalma) (*Table 1*). A significantly (p<0.05) high bunch weight was obtained with the TxA variety (11.68 kg), as shown in *Table 3,* whereas for the rest of the studied variables, there were no statistical differences. Pollen from *E. guineensis* produced the highest proportion of seeded fruits by weight (34.84%), significantly (p<0.05) greater than CxL (21.24%) (*Table 3*).

TABLE 3. THE EFFECTS OF FEMALE FLOWERS AND POLLEN DONORS ON BUNCH WEIGHTS AND SEEDED FRUIT IN THE PACIFIC COAST

Female flower type	**Bunch weight (kg)**	**Seeded fruit (weight %)**	**Parthenocarpic fruits (weight %)**
T×A	11.68 a	28.42	24.52
C×L	8.05 b	27.91	20.15
Unipalma	6.03 b	25.51	22.72
Pollen donor			
E. guineensis	9.56	34.84 a	18.03
T×A	7.31	27.17 ab	23.72
Unipalma	8.24	25.88 ab	26.09
C×L	9.25	21.24 b	22.01

Note: Means followed by the same letter are not significantly different using Tukey's test (p=5%). Means without letters belong to the same statistical group.

For oil palm, successful commercial production depends on achieving adequate fruit bunch weight and oil extraction. Both factors are affected by pollination in the Amazon region and the Pacific coast. Pollen germination percentage is an essential factor in determining seeded fruit production (Ruiz-Alvarez *et al.,* 2021), and seeded fruits present an advantage in weight over parthenocarpic fruits (Daza *et al*., 2020). A higher percentage of seeded fruits is also a desired characteristic for industry, as it facilitates the oil extraction process (Fernández, 2013).

Pollination is a challenge in Ecuador, where the bud rot disease (named PC, for its abbreviation in Spanish) is causing enormous damage to *E. guineensis* commercial plantations. Hence the species is being replaced by the OxG hybrid, which may result in a lack of *E. guineensis* pollen. However, the hybrids require assisted pollination and alternatives to *E. guineensis* pollen are sought.

This study shows that *E. guineensis* pollen achieved the best commercial performance in both the Amazon region and the Pacific coast. As shown in *Table 2, 3* and *4*, *E. guineensis* is always the best pollen donor in order to obtain a good percentage of seeded fruits and useful commercial fruits. Our results suggest that CxL and TxA could be good candidates for replacing *E. guineensis* as a pollen donor for commercial plantations in the Amazon region, as long as yield is maintained. If there were a lack of availability of *E. guineensis* pollen on the Pacific coast, TxA and Unipalma could be a good alternative pollen donor, as they maintained a high percentage of seeded fruits without significant yield loss, aided by parthenocarpic fruits (Kumar *et al*., 2015).

On the Pacific coast, the highest yield was obtained from TxA hybrids. In contrast, in the Amazon region, CxL was one of the best materials. Possibly the Brazilian origin of the hybrids CxL and Unipalma explains their better adaptation to local weather conditions, as these were the first OxG hybrids planted in the Ecuadorian Amazon region (Arias, *et al*., 2015; Barba *et al*., 2010), and nowadays is the most prevalent one.

When examined by region, the interaction between female flower and pollen donor (*Table 4*) shows that high proportions of industrially useable fruits (Seeded + parthenocarpic fruits) can be produced in the Amazon region, but the results are highly variable (67.9% to 23.4% of useable fruits), indicating pollen incompatibility. The highest proportions of useable fruits were achieved from hybrids treated with *E. guineensis* pollen. This can be seen in two crosses: (TxL) x (*E. guineensis*) with 67.9% and (CxL) x (*E. guineensis*) with 53.57%. In the Coastal region, bunch weight presented statistical differences between treatments: (TxA) x *E. guineensis* with 15% in comparison with Unipalma x Unipalma and Unipalma x (CxL) with 4.74% and 5.80%, respectively.

However, there are no differences in the other two parameters (Seeded + parthenocarpic fruits and Seeded fruits), these results suggest that the pollen donor does not influence the percentage of seeded fruits.

The behaviour of oil palm plants depends upon the genetic variability of the parents and the effect of the environmental conditions in each site (Rosero and Santacruz, 2014). Pollen viability and pollination success are probably affected by weather conditions (temperature) and other abiotic aspects that characterise each region, such as relative humidity, the availability of water and sunshine, and soil type (Murugesan *et al.,* 2017), as suggested by various results from the Amazon and Pacific coastal regions. Hence, the information presented in this article is vital for future applications carried out by the industry.

TABLE 4. EFFECT OF THE INTERACTION BETWEEN DIFFERENT OIL PALM MATERIALS WITH VARIOUS POLLEN DONORS ON PRODUCTION (SEEDED + PARTHENOCARPIC FRUITS) IN THE AMAZON REGION AND PACIFIC COAST

Female flowers × Pollen donors	Bunch weight (kg)	Seeded + parthenocarpic fruits (weight %)	Seeded fruit (weight %)
Amazon region			
(T×L) × (*E. guineensis*)	8.17	67.9 a	60.52 a
(T×L) × (C×L)	6.65	55.48 ab	36.19 abc
(T×L) × (T×A)	6.58	54.95 ab	25.75 bc
(C×L) × (*E. guineensis*)	11.03	53.57 ab	40.24 ab
(T×L) × (T×L)	7.23	52.15 ab	29.23 bc
(T×A) × (*E. guineensis*)	12.04	48.28 b	29.65 bc
(C×L) × (T×L)	11.73	41.97 bc	21.80 bc

TABLE 4. EFFECT OF THE INTERACTION BETWEEN DIFFERENT OIL PALM MATERIALS WITH VARIOUS POLLEN DONORS ON PRODUCTION (SEEDED + PARTHENOCARPIC FRUITS) IN THE AMAZON REGION AND PACIFIC COAST (continued)

Female flowers × Pollen donors	Bunch weight (kg)	Seeded + parthenocarpic fruits (weight %)	Seeded fruit (weight %)
Amazon region			
(T×A) × (C×L)	9.87	40.60 b	29.65 bc
(T×A) × (T×A)	6.25	27.47 cd	10.64 bc
(C×L) × (T×A)	8.75	27.45 cd	8.84 bc
(T×A) × (T×L)	7.71	23.40 d	10.18 bc
Pacific coast			
(T×A) × (Unipalma)	12.84 ab	27.81	27.00
(Unipalma) × (T×A)	6.38 ab	26.79	23.44
(T×A) × (C×L)	10.15 ab	25.85	22.35
(C×L) × (Unipalma)	7.13 ab	25.56	27.46
(T×A) × (T×A)	8.73 ab	25.34	26.00
(Unipalma) × (Unipalma)	4.74 b	24.92	23.15
(Unipalma) × (C×L)	5.80 b	23.61	17.54
(C×L) × (*E. guineensis*)	6.47 ab	19.46	28.34
(T×A) × (*E. guineensis*)	15.00 a	19.07	38.27
(C×L) × (T×A)	6.82 ab	19.02	32.00
(C×L) × (C×L)	11.74 ab	16.56	23.83
(Unipalma) x (*E. guineensis*)	7.20 ab	15.57	37.91

Note: Means followed by the same letter are not significantly different using Tukey's test (p=5%). Means without letters belong to the same statistical group.

CONCLUSION

The germination rate was high for *E. guineensis* pollen collected from both the Amazon region and the Pacific coast (95% and 94%) and *E. oleifera* pollen collected from Amazon region (93.7%), whereas *E. oleifera* pollen collected from the Pacific coast site showed a lower germination rate (53.2%). The germination of pollen collected from hybrids was low in both regions. In the Amazon region, germination from hybrids ranged from 9.7% to 16.9%, while on the Pacific coast, the germination was even lower at 1%-2%. The results indicate that the production of viable pollen from *E. oleifera* or hybrids is challenging on the Pacific coast, but viable pollen can be collected in the Amazon region from hybrids, although at lower levels of germination. The results showed that especially for *E. oleifera* and hybrids, the Pacific coast was detrimental to pollen viability, which might be due to climatic conditions. This has important implications for assisted pollination and the selection of pollen donors on the Pacific Coast. Nevertheless, further studies are needed to confirm the climate hypothesis.

Pollination and bunch yield are affected by both the female flower and the pollen donor. Without assisted pollination, the rate of fruit set in oil palm hybrids is poor. In these trials, the assisted application of *E. guineensis* pollen produced the highest fruit set, but the lack of pollination was, to some extent, compensated for by the production of parthenocarpic fruit. When *E. guineensis* pollen is unavailable, due to the death of plants caused by *E. guineensis* susceptibility to bud rot, our results suggest that new pollen sources such as CxL in the Amazon region and TxA in the Pacific coast could be used to assist pollination in commercial plantations, by virtue of the tolerance that they present to bud rot and the fact that they induce good levels of fruit set at same pollen doses as *E. guineensis*. Moreover, the capacity of oil palm to produce parthenocarpic fruits permits it to have a commercially acceptable bunch weight. This alternative should be analysed to offer new agronomic management alternatives to oil palm producers.

ACKNOWLEDGEMENT

The authors would like to thank the growers for their support in realising this study, as well as ANCUPA of Ecuador for financing part of this study.

REFERENCES

Alvarado, A; Bulgarelli, J and Moya, B (2000). Germinación del polen en poblaciones derivadas de un híbrido entre *Elaeis guineensis* Jacq. y *E. oleifera* HBK, Cortes. *ASD Oil Palm Papers*, *20*: 35-36.

Alvarado, A; Escobar, R and Henry, J (2013). El híbrido OxG Amazon: Una alternativa para regiones afectadas por pudrición del cogollo en palma de aceite. *Revista Palmas*, *34*: 305-314.

Arias, D; González, M; Prada F; Ayala-Diaz, I; Montoya, C; Daza, E and Romero, H M (2015). Genetic and phenotypic diversity of natural American oil palm (*Elaeis oleifera* (H.B.K.) Cortés) accessions. *Tree Genetics and Genomes*, *(11)*: 122.

Arnaud, F (1980). Fertilité pollinique de l'hybride *Elaeis melanococca* × *Elaeis guineensis* et des espèces parentales. *Oléagineux*, *35(3)*: 121-127.

Astorkia, M; Hernandez, M; Bocs, S; Lopez de Armentia, E; Herran, A; Ponce, K and Ritter, E (2019). Association mapping between candidate gene SNP and production and oil quality traits in interspecific oil palm hybrids. *Plants*, *8(10)*: 377.

Barba, J; Orellana, F; Vallejo, G and Manzano, R (2010). Evaluación agronómica de híbridos interespecíficos de palma de aceite OxG (*Elaeis oleifera* × *Elaeis guineensis*) provenientes de diversos orígenes americanos y su tolerancia a la pudrición del cogollo. Primera parte. *Palma*, *3*: 11-15.

Barba, J and Baquero, Y (2012). Híbridos OxG obtenidos a partir de oleíferas Taisha Palmar del Río - (Ecuador) - Variedad - PDR (Taisha x Avros). *Revista Palmas*, *38(1)*: 1-13.

Botelho, E and Rocha, J (1983). Avaliação de híbridos interespecíficos de *Elaeis guineensis* × *Elaeis oleifera*. Belém: Embrapa, Brazil.

Criollo-Escobar, H and Dominguez, J (2018). Germinabilidad y viabilidad del polen de cuatro cultivares mejorados de palma aceitera bajo condiciones de laboratorio. *Rev. Fac. Nac. Agron. Medellín*, *71(1)*: 8395-8405. DOI: 10.15446/rfna.v71n1.69587.

Corrado, F (1984). La conformación de los Racimos de la Palma Africana en las Plantaciones de Colombia. *Revista Palmas., 5(3)*: 66-87.

Compact Seeds and Clones ASD (2004). Semillas y clones de palma aceitera de alto rendimiento, San Jose, Costa Rica. 18 pp.

Corley, R and Tinker, P (2016). *The Oil Palm*. Chichester, West Sussex, Reino Unido: Wiley Blackwell.

Davarynejad, G H; Szabó, Z; Váci Felhösné, E; Kun, Z and Nyéki, J (1995). Anther and pollen grain characteristics of apricot cultivars. *Acta Horticulturae*, *384*: 351-354. DOI: 10.17660/actahortic.1995.384.54.

Daza, E; Ayala-Díaz, I; Ruiz-Romero, R and Romero, H M (2020). Effect of the application of plant hormones on the formation of parthenocarpic fruits and oil production in oil palm interspecific hybrids (*Elaeis oleifera* Cortés × *Elaeis guineensis* Jacq.). *Plant Prod. Sci., 24(3):* 1-9. DOI: 10.1080/1343943X.2020.1862681.

Durand-Gasselin, T; Corredor, J; Sanz, J; De Franqueville, H and Amblard, P (2009). Future vision of oil palm genetic improvement in Latin America. Several resolutions on cooperation in Colombia for planting material improvement. *16th International Oil Palm Conference and Expopalma. Challenges in sustainable oil palm development, 22 to 25 September 2009, Cartegena de Indias, Colombia*. Bogota: FEDEPALMA, (21 vues). International Oil Palm Conference and Expopalma. 16.

FEDEPALMA (2021). Balance económico del sector palmero colombiano en el primer trimestre de 2021.

Fernández, C (2013). Experiencias en el procesamiento de racimos de fruta fresca de híbridos oleifera por guineensis, en la Zona Suroccidental. *Palmas, 34(4)*: 109-113.

Franqueville, H (2001). Oil palm bud rot in Latin America: Preliminary review of established facts and achievements. CIRAD. p. 33.

Forero, D; Hormaza, P; Moreno, L and Ruíz, R (2012). *Generalidades sobre la morfología y fenología de la palma de aceite.* Centro de Investigación en Palma de Aceite (Cenipalma). Bogotá, Colombia. 149 pp.

Haniff, M and Noor, M (2002). Fruit set and oil palm bunch components. *J. Oil Palm Res., 14*: 24-33.

Hayati, A; Wickneswari, R; Maizura, I and Rajanaidu, N (2004). Genetic diversity of oil palm (*Elaeis guineensis* Jacq.) germplasm collections from Africa:

Implications for improvement and conservation of genetic resources. *TAG. 108(7*): 1274-1284. DOI: 10.1007/s00122-003-1545-0.

Hormaza, P; Fuquen, E and Romero, H (2012). Phenology of the oil palm interspecific hybrid *Elaeis oleifera* × *Elaeis guineensis*. *Scientia Agricola*, *69*: 275-280.

Instituto Nacional de Meteorología e Hidrología (INAMHI) (2016). Anuario Meteorológico. Quito, Ecuador.

Instituto Nacional de Investigaciones Agropecuarias (INIAP) (2013). Informe anual del Programa de Palma Aceitera. Estación Experimental Santo Domingo, La Concordia, Ecuador.

Kumar, K; Mathur, R and Sparjanbabu, D (2015). Efficacy of organic solvents for medium-term storage of oil palm (*Elaeis guineensis* Jacq.) pollen. *Indian J. Agric. Res.*, *49*: 516-521.

Li, K; Tscharntke, T; Saintes, B; Buchori, D and Grass, I (2019). Critical factors limiting pollination success in oil palm: A systematic review. *Agric., Ecosyst. Environ., 280*: 152-160. DOI: 10.1016/j.agee.2019.05.001.

Lin, Y; Wang, Y; Iqbal, A; Shi, P; Li, J; Yang, Y and Lei, X (2017). Optimization of culture medium and temperature for the *in vitro* germination of oil palm pollen. *Scientia Horticulturae, 220*: 134-138. DOI: 10.1016/j.scienta.2017.03.040.

Meléndez, R and Ponce, P (2016). Pollination in the oil palms *Elaeis guineensis*, *E. oleifera* and their hybrids (OxG), in tropical America. *Pesq. Agropec. Trop. Goiânia*, *46*: 102-110. DOI: 10.1590/1983-40632016v4638196.

Moreno, L and Romero, H (2012). Escala BBCH para la descripción del desarrollo reproductivo de *Elaeis oleifera* Cortes H.B.K. in Generalidades sobre la morfología y fenología de la palma de aceite. Cenipalma. Bogotá, Colombia. 150 pp.

Murugesan, P; Aswathy, G; Sunil Kumar, K; Masilamani P; Vinod Kumar and Ravi, V (2017). Oil palm (*Elaeis guineensis*) genetic resources for abiotic stress tolerance: A review. *Indian J. Agric. Sci., 87(5)*: 571-579.

Müller, A; Furlan, J and Celestino, P (2006). Contribuições da Embrapa Amazônia Oriental para o agronegócio do dendê. Belém: Embrapa. Brazil.

Myint, K A; Rafii, M Y; Sheikh-Abdullah, S A; Lwin, N M; Din, A M and Latif, M A (2012). Determination of the optimum pollen germination medium for different fruit forms of oil palm (*Elaeis guineensis*). *J. Anim.Plan Sci., 14*, *14*: 1855-1865.

Ochoa-C, I E and Palacio-Mahecha, N (2021). Contribución al diseño de racimos con ácido α-naftalenacético (ANA). *Revista Palmas*, *42(1)*: 107-118.

Prasetyo, A E; Purba, W O and Susanto, A (2014). *Elaeidobius kamerunicus*: Application of hatch and carry technique for increasing oil palm fruit set. *J. Oil Palm Res.*, *26*: 195-202.

Romero, H M and Ayala, I M (2021). Cómo alcanzar 10 toneladas de aceite por hectárea: tecnologías de manejo de los híbridos interespecíficos OxG hacia una producción altamente eficiente. *Revista Palmas*, *42(1*): 55-64.

Romero, H M; Daza, E; Ayala-Díaz, I and Ruiz-Romero, R (2021). High-oleic palm oil (HOPO) production from parthenocarpic fruits in oil palm interspecific hybrids using naphthalene acetic acid. *Agronomy, 2021*(*11)*: 290. DOI: 10.3390/agronomy11020290.

Rosero, G; Santacruz, L and Cristancho, A (2013). Caracterización de las variables de crecimiento, niveles foliares y de rendimiento en dos materiales genéticos de palma OxG y DxP en diferentes edades de desarrollo de la plantación Guaicaramo S.A. *Revista Palma*s, *34(4)*: 99-108.

Rosero, G and Santacruz, L (2014). Efecto de la polinización asistida en la conformación del racimo en material híbrido OxG en la plantación Guaicaramo S.A. *Revista Palmas*, *35(4)*: 11-19.

Ruiz-Alvarez, E; Daza, E; Caballero-Blanco, K and Mosquera-Montoya, M (2021). Complementing assisted pollination with assisted pollination in oil palm crops planted with interspecific hybrids OxG (*Elaeis guineensis* × *Elaeis oleifera*): Is it profitable? *OCL, 28*: 27. DOI: 10.1051/ocl/2021014.

Sánchez, A and Romero, H (2013). Viabilidad y morfología del polen de diferentes materiales de palma de aceite. *Ceniavances-cenipalma.* Bogot*á.* 4 pp.

Sánchez, G (2008). *Dissertacao_Gilson_Chia 2008 diferencias racimo oleifera*. Manaus: Instituto Nacional de Pesquisas da Amazônia, Universidade Federal do Amazonas. Brazil.

Swaray, S; Rafii, M; Din Amiruddin, M; Firdaus, M; Jamian, S; Jalloh, M; Oladosu, Y; Mustakim Mohamad, M; Marjuni, M and Kolapo, O K

(2021). Assessment of oil palm pollinating weevil (*Elaeidobius kamerunicus*) population density in biparental *dura* × *pisifera* hybrids on deep peat-soil in Perak State, Malaysia. *Insects*, *12*: 221. DOI: 10.3390/insects12030221.

Syed, R (1986). Factibilidad de la introducción de *E. kamerunicus* en Colombia. *Revista Palmas*, *1*: 11-15.

Tandon, R; Manohara, T N; Nijalingappa, B H and Shivanna, K R (2001). Pollination and pollen-pistil interaction in oil palm, *Elaeis guineensis*. *Ann. Bot.*, *87(6)*: 831-838. DOI: 10.1006/anbo.2001.1421.

Teixeira Souza Júnior, M (2013). Enfoque y avances del programa de mejoramiento genético de la palma de aceite en Embrapa. *Revista Palmas.*, *34(1*): 168-173.

Ting, N C; Sherbina, K; Khoo, J S; Kamaruddin, K; Chan, P and Chan, K L (2020). Expression of fatty acid and triacylglycerol synthesis genes in interspecific hybrids of oil palm. *Sci. Rep.*, *10*: 16296. DOI: 10.1038/s41598-020-73170-5.

Turner, P D and Gillbanks, R A (1974). Oil palm cultivation and management. Oil palm cultivation and management. CABI. p. 672.

Verheye, W (2010). Growth and production of oil palm, land use, land cover and soil sciences. *Encyclopedia of Life Support Systems (EOLSS*). UNESCO-EOLSS Publishers, Oxford, UK. p. 1-24.

Vieira, R and Lopes, R (2010). BRS Manicoré: híbrido interespecífico Caiaué e do dendezeiro africano recomendado para áreas de incidência de amarelecimento fatal. Manaus, Embrapa, Brazil.

Journal of Oil Palm Research Vol. 36 (3) September 2024 p. 432-444
DOI: https://doi.org/10.21894/jopr.2023.0036

IDENTIFICATION OF THE OIL PALM BAGWORM, *Mahasena corbetti* TAMS (LEPIDOPTERA: PSYCHIDAE) VIA MOLECULAR TECHNIQUES AND ITS BIOCONTROL ASSAY USING *Bacillus thuringiensis*

MOHD SHAWAL THAKIB MAIDIN[1,2]*; AMALIA MOHD HASHIM[2,3]; NOORHAZWANI KAMARUDIN[1]; SITI NURULHIDAYAH AHMAD[1]; MOHAMED MAZMIRA MOHD. MASRI[1]; RAHA ABDUL RAHIM[2,4] and SYARI JAMIAN[5]

ABSTRACT

The larvae of the bagworm Mahasena corbetti *Tams (Lepidoptera: Psychidae) cause significant yield losses by defoliation of the oil palm crop in Malaysia. This necessitates the development of an effective and sustainable control strategies against this pest. The objective of this study was to identify* M. corbetti *via molecular techniques and evaluate the potential of a local strain of* Bacillus thuringiensis *(MPOB Bt1), as a biocontrol agent for the pest. Morphological and molecular analysis was performed to identify* M. corbetti*, using the mitochondrial cytochrome oxidase I (COI) gene for genetic identification. The results showed that* M. corbetti *isolate SH01 (GenBank accession number MN373269) had a high degree of similarity (98.52%, 0.0 E-value) with the COI gene of* M. corbetti *voucher GB270DN1795 (GenBank accession number MG574312) collected in India and 100% BOLD similarities with the COI gene of* M. corbetti *from Singapore (BOLD ID PSYCH113-12). Laboratory bioassay showed 100% mortality of* M. corbetti *larvae three days after treatment with MPOB Bt1 (10^8 spores/mL). The results demonstrate the potential of MPOB Bt1 as an environmentally friendly biopesticide against* M. corbetti *in oil palm, but optimisation and efficacy in other pests require further research. Furthermore, biocontrol can be used as part of an integrated pest management program against bagworms and other lepidopteran pests.*

Keywords: *Bacillus thuringiensis*, COI gene, *Mahasena corbetti*, molecular identification, oil palm pest.

Received: 1 March 2023**; Accepted:** 21 June 2023**; Published online:** 8 August 2023.

[1] Malaysian Palm Oil Board,
6, Persiaran Institusi, Bandar Baru Bangi,
43000 Kajang, Selangor, Malaysia.

[2] Faculty of Biotechnology and Biomolecular Sciences,
Universiti Putra Malaysia,
43400 Serdang, Selangor, Malaysia.

[3] Halal Products Research Institute,
Universiti Putra Malaysia,
43400 Serdang, Selangor, Malaysia.

[4] National Institutes of Biotechnology Malaysia,
C/O MARDI Headquarters,
43400 Serdang, Selangor, Malaysia.

[5] Faculty of Agriculture,
Universiti Putra Malaysia,
43400 Serdang, Selangor, Malaysia.

* *Corresponding author e-mail: shawal@mpob.gov.my*

INTRODUCTION

Mahasena corbetti Tams (Jones and Park, 1928), a bagworm moth which belongs to the family Psychidae, and Superfamily Tineoidea, is a polyphagous insect and can also be a pest of the oil palm *Elaeis guineensis*. This species is recorded mainly in Malaysia, Indonesia, and among a number of oil palm growers in Southeast Asia (Lelana *et al*., 2022; Leong and Lim, 2012; Lepesme, 1947; Norman *et al.*, 1994; Robinson *et al.*, 2011; Syed, 1978). *M. corbetti* has been reported as an important defoliating pest in Sarawak (Tiong, 1979), East Sabah (Basri *et al.*, 1988), and in Perak and Johor, but is rarely documented in a serious outbreak (Norman and Basri, 2007). It typically

attacks all growth stages of the oil palms, with it causing more severe damage and spreading easily in mature palms via the overlapping fronds (Basri *et al.,* 2003; Lelana *et al*., 2022). A moderate infestation of *M. corbetti* can cause leaf damage of between 10%-50% and can result in crop losses of over 40%-50% in two subsequent years (Basri *et al.,* 2003; Liau, 1987; Priwiratama *et al*., 2023).

Various morphological traits such as the case or bag length and wing span have been used to identify *M. corbetti* (Lelana *et al*., 2022; Norman *et al.,* 1994; Robinson *et al.,* 1994). It takes a lot of work and extensive taxonomic expertise to complete this procedure. In general, only males can be distinguished (Firake *et al*., 2018; Niitsu *et al*., 2017; Norman *et al*., 1994; Robinson *et al*., 1994). Apart from this, morphological identification has the disadvantage of requiring whole adult specimens, which is difficult when identifying fragmentary bodies, early morphological structures (eggs, larvae and pupae), and related species (Kondo *et al*., 2008; Utsugi *et al*., 2011).

Taxonomists are gradually turning to molecular approaches to overcome the complexity of the morphological approach (Firake *et al.,* 2018; Firake and Behere, 2021; Hebert *et al.,* 2003; Nagoshi *et al.,* 2011). In this technique, the mitochondrial cytochrome c oxidase subunit I gene region was used to discriminate between organisms (Hebert *et al*., 2003). Due to its maternal lineage, great stability and longevity, the insect mtDNA COI gene has emerged as one of the most important molecular markers in insect taxonomy (Firake *et al*., 2018; Nagoshi *et al*., 2011). Alternative markers such as 16S, 12S rDNA (Aliabadian *et al.,* 2009; Kappner and Bieler, 2006; Vences *et al.,* 2005), ribosomal DNA internal transcribed spacer region 2 (ITS -2) (Kumar *et al.,* 2009), NADH dehydrogenase subunit 1 (nadh1) (Jalali *et al.,* 2015) and cytochrome b (cytb) (Bradley and Baker, 2001; Desalle, 2006; Jalali *et al.,* 2015; Pfunder *et al.,* 2004) can also be used when no mitochondrial DNA sequence is generated.

Identifying and characterising genetic diversity in insect populations is an important topic for improving pest management strategies because the evolution of insect species that are becoming increasingly resistant to insecticides depends on the occurrence of resistant alleles, resistance inheritance, the relative cost of fitness and gene flow (Ali *et al*., 2018; 2019; Khan *et al*., 2020; Leon *et al*., 2021; Zaynab *et al*., 2019). In agriculture, bioinsecticides can be used to control insects, with *Bacillus thuringiensis* (Bt) being the most popular active ingredient because it contains a particular insecticidal protein (Kumar *et al*., 2021; Li *et al*., 2022). It has long been known that the toxins produced by Bt are effective against caterpillars feeding on leaves because they act as pure stomach poison. Ecobac-1, Terakil-1 and Bafog-1 are three Bt products which were developed to control the oil palm pests *Metisa plana* and *Pteroma pendula* (Najib *et al.,* 2013; Noorhazwani *et al.,* 2017; Ramlah *et al.,* 2005). Information on the susceptibility of *M. corbetti* to Bt is limited. A significant difference in toxicity of commercial Bt strains for *M. corbetti* and *M. plana* was discovered in 1996 by Basri *et al*. When a sufficiently high dose of the insecticide trichlorfon was administered, bagworm mortality was comparable to that of trichlorfon.

This study was conducted with the aim of firstly, confirming the species of the bagworm *M. corbetti* that infested the oil palm plantation in Johor, Malaysia, by COI gene sequencing. Secondly, its genetic diversity was investigated using the available COI gene sequences of *M. corbetti*, *M. plana* and *P. pendula*. Finally, the antagonistic activity of the Bt strain MPOB Bt1, which was developed by Ramlah and Basri (1997) against the *M. corbetti* isolate SH01 will be determined. The results of this study would contribute to the preliminary knowledge of the genetic diversity and distribution of the bagworms, to facilitate future strategies for the management and control of bagworms in Malaysian oil palms.

MATERIALS AND METHODS

Study Location, Sample Collection at Different Growth Stages

The bagworm infestation was discovered in March 2019, in an oil palm plantation in Johor (2°12′38.778″N and 103°20′22.830″E), at the southern part of Peninsular Malaysia. Bagworms on the infested palm were examined a total of 300 multistage bagworm samples with randomly collected from the infested palms and later reared on oil palm leaves in insect cages (measuring 45 x 45 x 45 cm). The larvae were reared under laboratory conditions (temperature: Day 27°C ± 1°C, night 24°C ± 1°C; relative humidity 35%-50%; photoperiod, light:dark = 12:12 hr) for molecular and taxonomic characterisation. The developmental stages of *M. corbetti* were recorded and photographed using an Olympus DP12 microscope digital camera connected to a trinocular stereo zoom microscope (model: Olympus SZ61). The life cycle of the bagworm *(Figure 1*) was based on a report by Syed (1978) and MPOB (2016). The remaining larval samples were subjected to a laboratory bioassay with the entomopathogenic bacteria, *Bacillus thuringiensis* MPOB Bt1 (Ramlah and Basri, 1997).

Amplification of Mitochondrial Cytochrome Oxidase 1 (COI) Gene

A total of three larval samples was randomly selected for genomic DNA (gDNA) extraction. Extraction of gDNA was performed according to the manufacturer's instructions using the Trans Direct Animal Tissue PCR Kit (Trans, Beijing, China). The standard barcoding region of the cytochrome oxidase 1 (COI) gene of mtDNA was amplified as described by Firake *et al.* (2018). Amplifications were performed using the standard barcoding primer set LepF1 (5'-ATTCAACCAATCATAAAGATATTGG-3') and LepR1 (5'-TAAACTTCTGGATGTCCAAAA AATCA-3'). The PCR reaction was performed in a total volume of 25 µL containing 10 pmol of each primer, 100 mM dNTP, 1X PCR buffer, 50 mM $MgCl_2$, 0.3% BSA, 2.5 units of Taq polymerase, and 50 ng/µL genomic DNA and was performed using a thermocycler (Eppendorf, Germany). Thermocycler conditions included an initial denaturation at 94°C for 2 min, followed by 35 cycles of 94°C for 30 s, 50°C for 40 s, 72°C for 1 min, and a final extension at 72°C for 10 min. The PCR amplification product was verified by running a 10 µL aliquot of the amplified products together with 100 bp Plus DNA Ladder Marker (TransGen Biotech, China) on 1.5% agarose gels at 140 V for 30 min, stained with GelRed (Biotium, USA), and visualised on the Omega Fluor™ Plus Imaging System (Aplegen, USA). The amplified 724 bp PCR products of the COI gene sequence was purified using QIAquick gel extraction kits (QIAGEN), Inc., Valencia, CA) according to the manufacturer's instruction. The purified DNA was sent to Apical Scientific Sdn. Bhd. Laboratory (Malaysia) for sequencing. The raw pair end DNA sequence reads were assembled using Clone Manager 9 (Sci-Ed Software, Denver, CO, USA) and the unknown nucleotide, "N" was trimmed, resulting in a sequence length of 607 bp. The sequence similarity search was performed using the GenBank BLASTn at the National Center for Biotechnology Information (NCBI) (https://www.ncbi.nlm.nih.gov/) and BOLD Identification System (IDS). The analysed COI gene sequence was then submitted to GenBank (NCBI) (Genbank Accession Number: MN373269).

Phylogenetic Analysis

The 607 bp of COI gene sequence of *M. corbetti* isolate SH01 (Genbank accession number: MN373269) was aligned with other registered COI gene sequences of *M. corbetti* deposited in NCBI and Barcode of Life Data System databases (BOLD) using ClustalW. The neighbourhood tree was based on the Kimura 2 parameter (K2P) model of nucleotide substitution (Kimura, 1980) to determine the relationships among the sequences in the study. The K2P model is the most commonly used model for DNA barcoding (Chevasco *et al.*, 2014; Jin *et al.*, 2013; Park *et al.*, 2011; Ruiz-Lopez *et al.*, 2012). The tree was constructed using the MEGA (5.2) package (Tamura *et al.*, 2011) and gaps were removed by complete deletion. The topological stability of the neighbourhood tree was assessed using 1000 bootstraps indicated by values over the nodes (Felsenstein, 1985).

***B. thuringiensis* Strain and Culture Conditions**

The Bt, MPOB Bt1 (Ramlah and Basri, 1997) that produces insecticidal crystal proteins specific to Lepidoptera (Ramlah *et al.*, 2003), was obtained from the culture collection of the Entomology and Integrated Pest Management Unit (EIPM), Malaysian Palm Oil Board (MPOB), Malaysia. This bacterium was isolated from soil by several isolation steps. The strain was maintained at -80°C in nutrient broth (Oxoid, Basingstoke, UK) containing 20% (v/v) glycerol. The isolated bacterium was aseptically propagated three times at 30°C in nutrient broth for activation before use. Incubation of the culture was performed at 150 rpm, 30°C for 48 hr to sporulate MPOB Bt1 (Mazmira *et al.*, 2021).

Laboratory Bioassay of MPOB Bt1 Against *M. corbetti*

The number of MPOB Bt1 spores per mL of water was counted using the Neubauer chamber to a standard concentration of approximately 1 x 10^9 spores/mL (Ramlah *et al.*, 2003). From the standard concentration, five serial dilutions were prepared at 10^8, 10^7, 10^6, 10^5 and 10^4 spores/mL. A total of five replicates were used with a sample size of 10 larvae per dilution, while MiliQ water served as a control. The effectiveness of the MPOB Bt1 was determined by calculating the percentage of mortality in the group exposed to the aforementioned bacteria compared to the mortality rate in the control group (Ismail *et al.*, 2022). The efficacy of MPOB Bt1 against *M. corbetti* isolate SH01 was analysed using Abbott's controlled mortality (Abbott, 1925) for day 3, 7 and 12 after treatments (DAT), which calculates the corrected mortality as Equation (1):

$$\frac{(\%\ \text{test mortality} - \%\ \text{control mortality})}{(100\% - \%\ \text{control mortality})} \times 100 \quad (1)$$

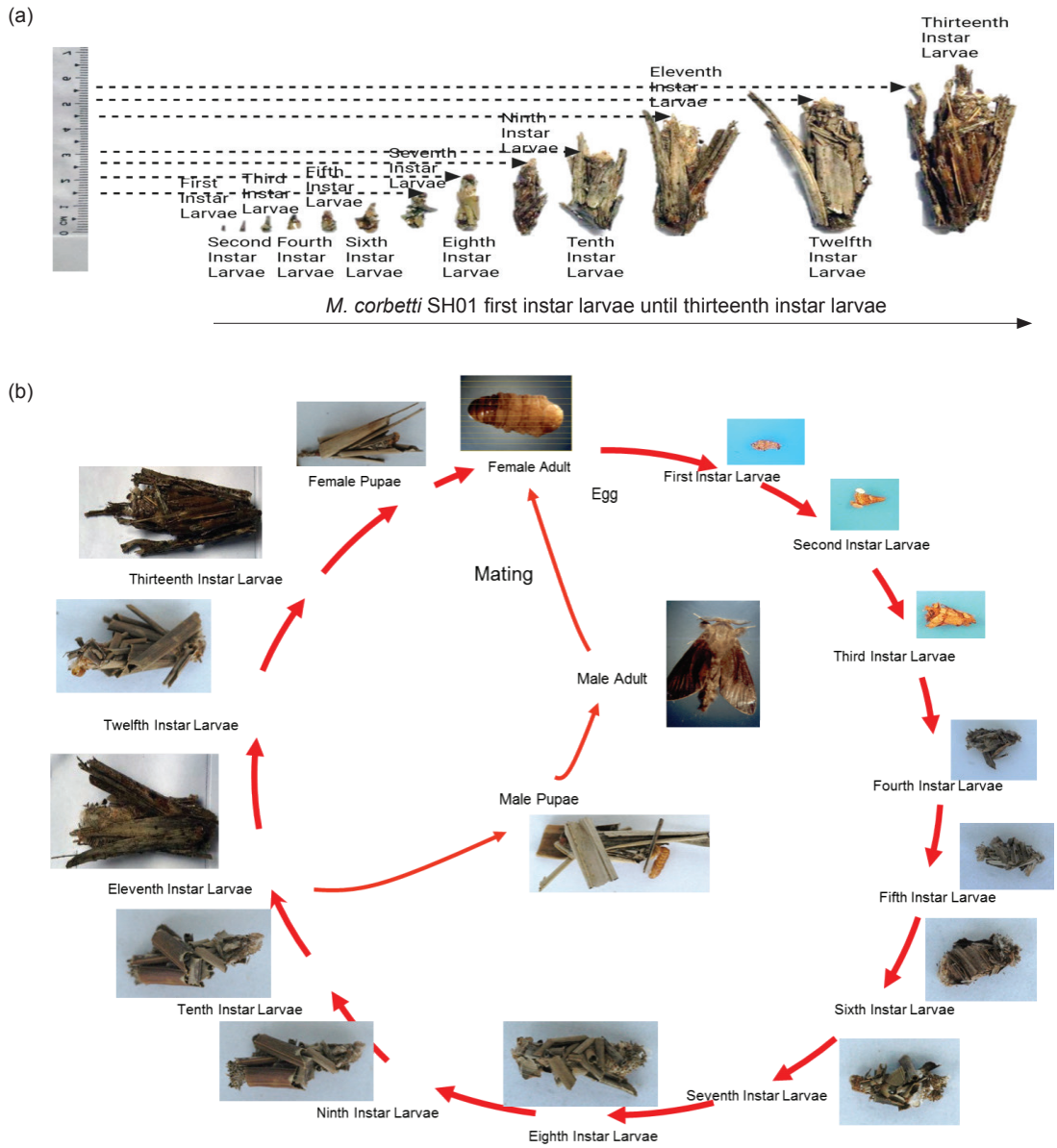
Data were then subjected to analysis of variance (ANOVA), and means were compared with Tukey's test at the 5% probability level.

RESULTS AND DISCUSSION

Morphological and Life Cycle Characterisation of *M. corbetti*

The bagworms are moths of which their larval stages construct protective bags, made from silk and plant material. These bags accommodate their developing body size as they grow and molt. In this study, the multiple life stages of *M. corbetti* were observed at the sampling site and the larvae collected were divided into 13 larval stages, based on its measured bag length (*Figure 1a*). The sizes of larvae ranged from 2 to 56 mm body length, from larval stage 1 (first instar larvae) to larval stage 13 (thirteenth instar larvae), while the male only passes up through instar stage 11 (Syed, 1978).

The morphological characteristics of the collected bagworm larvae were consistent with those previously described by Syed (1978), Basri (1993), Norman *et al*., 1994, Cheong and Tey (2012), Firake *et al*., (2018) and Lelana *et al*., (2022) and followed the life cycle of *M. corbetti* as shown in *Figure 1b* (MPOB, 2016). These characteristics included a large and robust male moth with a wingspan of about 21 to 25 mm, a thorax with dense, elongate, hair-like scales, and a stout and conical abdomen (*Figure 2*). The forewings and hindwings were dark brown in colour. These findings confirm the morphological identity of *M. corbetti* as the species infesting the oil palm plants in Johor.



Source: MPOB (2016).

Figure 1. Life cycle and larval stage sizes of M. corbetti, *as observed at Kluang, Johor. (a) Larvae were divided into 13 stages based on bag length measurements, ranging from 2 to 56 mm in body length. The female passes through instar stage 13, while the male passes through instar stage 11. (b) The life cycle of* M. corbetti *was used as a reference for the multistage larvae collected in this study.*



Figure 2. A detailed image of an adult male M. corbetti *moth in stretched wing, emphasising its stout, conical abdomen and robust body. The distinct features of this bagworm species help distinguish it from other moths and aid in its identification as a pest of oil palm.*

The larvae of *Mahasena corbetti*, were observed feeding on leaves of oil palms in Johor, Malaysia. *M. corbetti* was previously known to infest coconuts and was rarely found on oil palms in Peninsular Malaysia (Corbett, 1927; Gater, 1925; Wood and Norman, 2019). This species of bagworm was more commonly recorded in Sabah, Malaysia, where the first outbreak had occurred in 1965 (Wood, 1968; Wood and Norman, 2019). *M. corbetti* individuals are comparatively larger than *M. plana* or *P. pendula*, and the biology of *M. corbetti* is also less well known (Lelana *et al*., 2022; Wood, 1968). The life cycle duration of *M. corbetti* is up to 15 weeks (Wood and Nesbit, 1969) and 110-140 days by some estimates (Cheong and Tey, 2012). Generally, the eggs of bagworm are soft, yellow creamy to pale in colour, with less than 1 mm long and oblong or barrel shaped (*Figure 1*). These observations were also consistent with other studies by Basri and Kevan (1995) and Ho (2002). *M. corbetti* typically lays an average of 3000 eggs within the pupal case of the adult female (Cheong and Tey, 2012; Lelana *et al*., 2022). The larvae of *M. corbetti* are unable to support their case upright due to their increased weight during development. Therefore, the pendulous case is supported by silk threads connecting the upper edge of the bag to the plant, or by clinging to its thoracic legs (Jones and Park, 1928). The life cycle of *M. corbetti* sampled in this study was divided into 13 larval instars for the female, and only up to 10 or 11 larval instars for the male. In contrast, *M. plana* displays seven larval instars for the female and five or six larval instars for the male, and only three larval instars for male and female *P. pendula*, respectively (MPOB, 2016). Successful laboratory rearing was only achieved up to the eighth larval instar (Syed, 1978). Techniques for identifying male *M. corbetti* have been detailed, including keys for identification based on wing scales and veins, genital structure, and adult morphology (Norman *et al*., 1994). These identification techniques have yielded tremendous benefits in identifying bagworms, particularly those infesting oil palms in Malaysia.

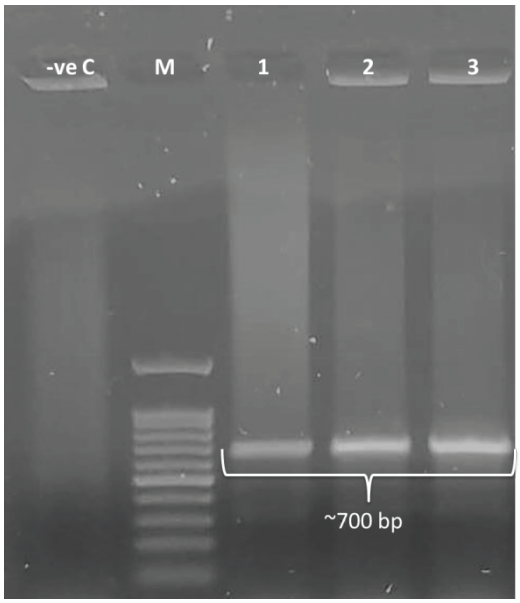
Molecular Identification Using Mitochondrial Cytochrome Oxidase 1 (COI) Gene

The PCR amplification of the bagworm sample's partial COI gene was successful (*Figure 3a*), and the resulting DNA sequence is presented in *Figure 3b*. To identify the species, molecular identification using BLAST and BOLD systems was performed. The bagworm isolate showed a high percentage of identities with COI gene sequences of other bagworms, ranging from 91.14% to 100.00% (*Table 1*). The isolate showed 98.52% and 98.51% identity, respectively, with *M. corbetti* voucher GB270DN1795 collected in India (Genbank Accession Number: MG574312) (Firake and Behere, 2021; Firake *et al*., 2018) and 100.00% similarity with *M. corbetti* from Singapore (BOLD ID: SYCH113-12) (Leong and Lim, 2012). The DNA of the other three *Mahasena* sp. collected in China showed about 91.00% identity and similarity. Therefore, the bagworm isolate was then designated as *M. corbetti* isolate SH01.

Accurate identification of bagworm species is critical for implementing an effective integrated pest management program (IPM) (Egonyu *et al*., 2022; Tahir *et al*., 2018). However, conventional morphological identification methods can be challenging (Barrett and Hebert 2005), particularly when identifying pest species based on morphological characteristics like eggs and instars (Ball and Armstrong, 2006). Additionally, females are more difficult to identify morphologically because they lack wings and other important organs (Chevasco *et al*., 2014; Firake *et al*., 2018). For this reason, DNA barcoding is used to swiftly and precisely identify organisms (Ball and Armstrong 2006; Blagoev *et al*.,; Dona *et al*., 2015; Firake *et al*., 2018; Firake and Behere, 2021; Hebert *et al*., 2004; Leong and Lim 2012; 2013; Raso *et al*., 2014; Xu *et al*., 2015). Furthermore, the evolutionary relationship between genera and species within the family Psychidae can indicate genetic and phenotypic relatedness between them.

In this study, the search against BLASTn and the BOLD database for *M. corbetti* COI DNA sequences detected only one *M. corbetti* voucher GB270DN1795 in BLASTn (Genbank Accession Number: MG574312) and one *M. corbetti* BOLD: ABV9843 in BOLD (BOLD ID: PSYCH113-12), while other closely related sequences were the three *Mahasena* sp. from China (*Table 1*). The 100% similarity between the *M. corbetti* isolate SH01 from Johor and *M. corbetti* BOLD: ABV9843 from Singapore can be explained by the small geographical distances between the Malaysian state of Johor and Singapore.

(a)



(b)

1 taaacttctg gatgtccaaa aaatcaaaat aaatgtnnnn nnnntgatat aaaataggat

61 ctccaccacc tgcaggatca aagaatgaag tatttaaatt tcgatctgtt aaaagtatag

121 taattgctcc tgctaaaaca ggtaaagata gtaataataa taaagcagta ataattacag

181 ctcaaacaaa taaaggtatt tgatctaatg atatattatt tatccgtata ttaatagctg

241 ttgtaataaa attcacagct cctaaaattg atgaaattcc tgctaaatgt aaagaaaaaa

301 tagctaaatc aactgaacta ccattatgag caatattaga tgaaagtgga gggtacactg

361 ttcatccggt tcctacacca ttttctacta gacttcttgc agttagtaat aacaatgagg

421 ggggtaaaag tcaaaacctt atattattta ttcgggggaa agctatatca ggggctccta

481 atattaaagg tactaatcaa tttccaaatc ctccaattat aataggtatt actataaaaa

541 aaattataat aaaagcatga gcagtgacaa tagtattata aatttgatca tttccaatta

601 atgatctagg ggtactcaat tctgctcgaa ttagcactct taaagaggtt ccaattaatc

661 cagatcaaat tcctaaaata annannnnng taaagagttc caatatcttt atgattggtt

721 gaat

Figure 3. Molecular identification of M. corbetti *SH01 using cytochrome c oxidase I (COI) sequence. (a) Agarose gel electrophoresis image showing the PCR product of COI from* M. corbetti *isolate SH01. Lane M represents 100 bp DNA ladder, and individual bagworm samples are labeled with numbers. (b) The DNA sequence of approximately 700 bp with the binding sites of primers LepF1 and LepR1 underlined.*

TABLE 1. LIST OF *Mahasena corbetti* ISOLATE SH01 IDENTIFICATION PERCENTAGE (%) IN BLAST AND SIMILARITIES IN BOLD

Species identified in BLAST/BOLD	BLAST (%)	BOLD (%)	GenBank Accession	BOLD ID	Origin
M. corbetti	98.52	98.51	MG574312	GBGL32880-19	India
M. corbetti	Not deposited	100.00	Unavailable	PSYCH113-12	Singapore
Mahasena sp.	91.35	91.33	MN132311	BEFCN1124-19	China
Mahasena sp.	91.15	91.14	MN131212	BEFCN025-19	China
Mahasena sp.	90.96	91.34	MN132201	BEFCN1014-19	China

This study has demonstrated the utility for species identification, particularly within a family that shares similar morphology despite different geographical distances. This method is specific and simpler than traditional morphological diagnosis, and provides rapid results at lower cost (Atikah *et al.*, 2019; Jinbo *et al.*, 2011; Zhu *et al*., 2022). However, further research is necessary to obtain more COI DNA sequences from various geographical regions to fully investigate the distribution and migration patterns of this bagworm species in Malaysia. Additionally, other information, such as bacterial and host dynamics across the life stages, should also be considered since the microbiome can also affect host fitness and immunity (Ali *et al*., 2019).

Phylogenetic Analysis

After trimming the raw DNA sequence (*Figure 3a*) of the 724 bp COI gene, a partial 607 bp sequence of *M. corbetti* isolate SH01 (Genbank accession number: MN373269) was aligned using ClustalW (*Figure 4a*) with other COI gene sequences of *M. corbetti* available in NCBI and Barcode of Life Data System databases (BOLD) (Thompson *et al*., 1994). The NJ tree (*Figure 4b*) in this study revealed two main clusters, with *M. corbetti* isolate SH01 being closely related to *M. corbetti* from Singapore (BOLD ID: PSYCH1 13-12) (Leong and Lim, 2012) and *M. corbetti* (GB270DN1795) from India (Genbank Accession Number: MG574312) (Firake *et al.*, 2018), indicating a close genetic relationship despite geographic separation. *Mahasena* spp. formed a separate group, while *M. plana* isolate BT1 and *P. pendula* isolate OP05 8 were selected as outgroups. These findings highlight the genetic diversity among bagworm pests and the importance of distinguishing between different species for effective pest management.

The phylogenetic relationships observed in this study had generally supported traditional classification methods (Che *et al.*, 2012; Chevasco *et al.*, 2014; Hebert *et al.*, 2004) and were constructed using the Kimura-2 parameter (K2P) model of nucleotide substitution (Kimura 1980; Suresh *et al*., 2022), which is recommended for barcoding using

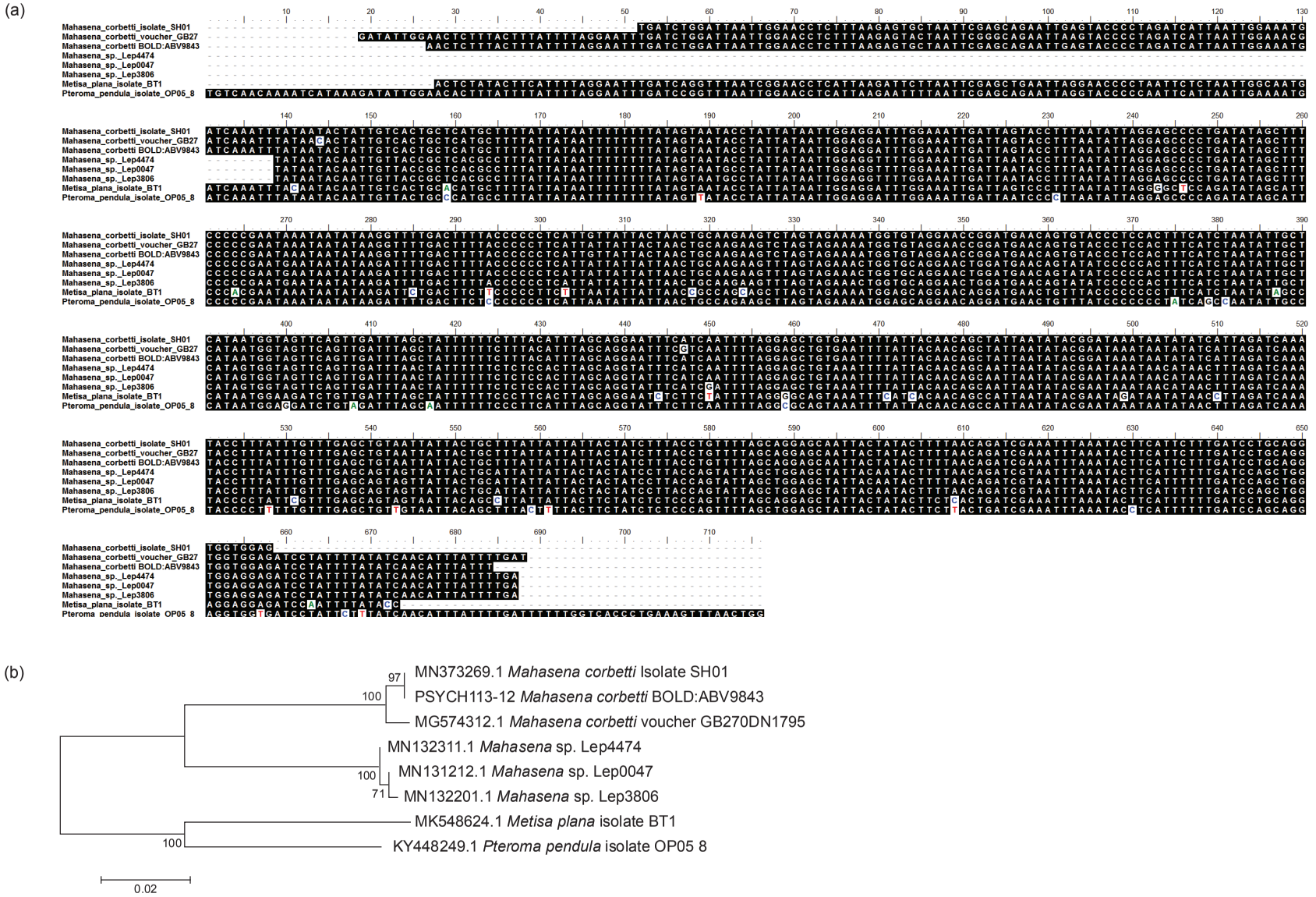


Figure 4. Molecular phylogenetic analysis of cytochrome c oxidase I (COI) sequence of M. corbetti *collected from Johor, Malaysia. (a) ClustalW alignment of* M. corbetti *isolate SH01 with other registered COI gene sequences deposited in NCBI and BOLD databases. (b) Phylogenetic tree was drawn using the neighbour-joining method within the MEGA (5.2) package based on multiple sequence alignment of nucleotide sequences generated by ClustalW. Data were analysed using the Kimura 2 parameter (K2P) algorithm and gaps were removed by complete deletion. The topological stability of the neighbour-joining tree was evaluated by 1000 bootstrapping replications, and the bootstrapping values are indicated by numbers at the nodes. The number of the sequences in this tree refers to the GenBank Accession Number, except for PSYCH113-12, which refer to the BOLD systems. MN373269.1 is the* M. corbetti *analysed in this study (underlined). The scale bar indicates 1.0% sequence variation.*

COI gene sequences (Che *et al.*, 2012; Chevasco *et al.*, 2014; Hebert *et al.*, 2004). The COI sequence of *M. corbetti* isolate SH01 was deposited in GenBank (Genbank Accession Number: MN373269). This study represents the first phylogenetic analysis of *M. corbetti* species based on molecular data in Malaysia. The phylogenetic analysis also revealed the monophyletic group formation of the family Psychidae with good support, consistent with the morphological observations of the larval stage indicating the family's monophyly (Chang *et al.*, 2023; Rhainds *et al.*, 2009). The study highlights the usefulness of COI fragments for species distinction and the consistency of molecular identification with the morphological analysis performed. However, more extensive studies using COI gene sequences from different geographical regions would be necessary to better understand the distribution and genetic diversity of the bagworm species in Malaysia.

MPOB Bt1 Toxicity

The corrected mortality of *M. corbetti* isolate SH01 at different concentrations of MPOB Bt1 spores (10^8, 10^7, 10^6, 10^5, and 10^4 spores/mL) on different treatment days (3 DAT, 7 DAT, and 12 DAT) was assessed and recorded in *Figure 5*. The results showed that the larval mortality varied with different concentrations and days after treatment. At the highest concentration of MPOB Bt1 (10^8 spores/mL) for 3 DAT, 7 DAT, and 12 DAT, no significant differences in larval mortality were detected by one-way analysis ANOVA with Tukey's analysis (P>0.05). All larvae died at 3 DAT at a concentration of 10^8 spores/mL, which is within the normal range observed for concentrated Bt effects on bagworm (Ramlah and Basri, 1997). Concentrations of 10^5 and 10^4 spores/mL resulted in corrected mortality rates of 80% and 60%, respectively, at 12 DAT compared to 10^8, 10^7, and 10^6 spores/mL, which achieved a corrected mortality rate of 100% at similar DAT.

The results revealed that the *M. corbetti* isolate SH01 was susceptible to Bt, with the 10^8 spore/mL being the strongest concentration and showing 100% mortality from as little as 3 DAT. This suggests that high concentrations of Bt spores may contain virulence factors such as a high δ-endotoxin concentration, making them highly toxic to the *M. corbetti* isolate SH01. MPOB Bt1, a Bt isolate from the laboratory, has been successfully used as an active ingredient for biopesticide application to control bagworm infestation in Malaysian oil palm plantations (Mazmira *et al.*, 2010; Najib *et al.*, 2009; Noorhazwani *et al.*, 2017; Ramlah and Basri, 1997; Ramlah *et al.*, 2003). The toxins produced by Bt are generally safe for human health and the environment due to their specific mode of action that requires specific receptors, enzymes, and a basic pH (Azizoglue, 2023; de Maagd *et al.*, 2001). According to Najib *et al.* (2011), Bt-based products are virtually nontoxic and specifically target lepidopteran pests such as bagworms and nettle caterpillars.

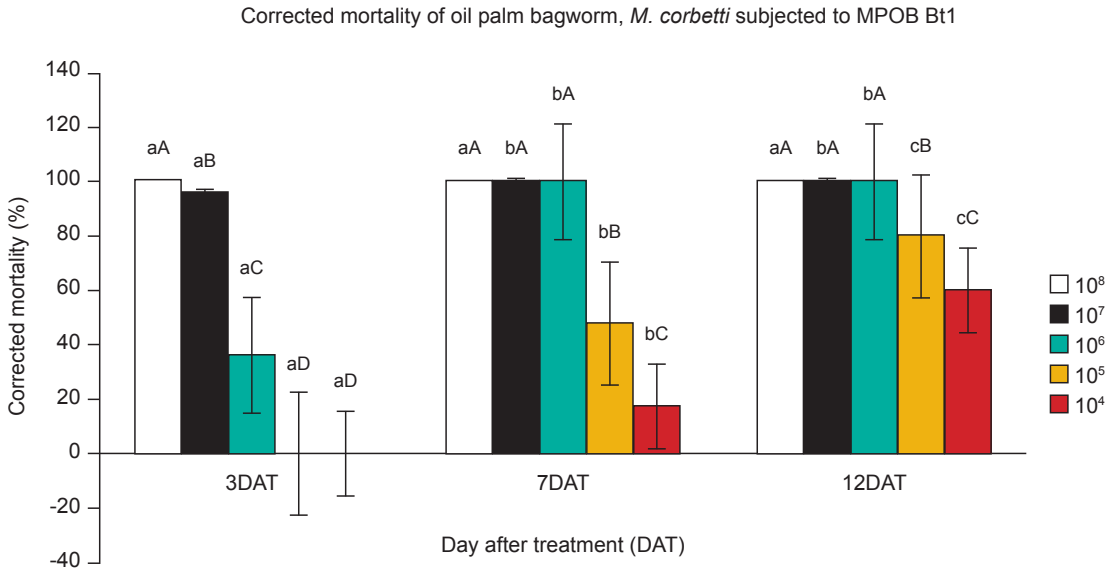


Figure 5. Corrected mortality of M. corbetti *isolate SH01 after 12 days of exposure to Bt. Bars with different letters are significantly different* (P<0.05) *analysed in one-way ANOVA using Tukey HSD test. Percentage of mortality is calculated by comparing the number of dead insects treated with MPOB Bt1 to the number of dead insects in the control group. Small letters indicate statistical comparison between days of treatment (DAT) within Bt spore concentrations, whereas capital letters indicate statistical comparison between different spore concentrations of the same day of treatment (DAT) at 10^8, 10^7, 10^6, 10^5 and 10^4. Standard Error of the Mean (SEM) was constructed for each spore concentration of 10^8, 10^7, 10^6, 10^5 and 10^4. Corrected mortality was determined using Abbott's formula (Abbott 1925).*

CONCLUSION

This study characterised and confirmed the bagworm, found in an oil palm plantation in Johor, Malaysia as *M. corbetti*, a notorious oil palm pest. The larval stage *of M. corbetti* was divided into 13 larval instars for females and 10-11 larval instars for males, and laboratory rearing up to the eighth instar larva was achieved in previous work by Syed (1978). The study also described the morphology of the adult *M. corbetti*, highlighting its stout and conical abdomen and robust body. Molecular identification using the COI gene confirmed the identity of the collected bagworm larvae as *M. corbetti* with high COI gene sequence similarity to other bagworms. These findings are valuable for identifying and managing *M. corbetti* infestations and can serve as a basis for studying other pests and beneficial insects in oil palm plantations. Moreover, gathering detailed information on the distribution, ecology, and development of oil palm related insects can help develop an integrated strategy to control *M. corbetti* infestations in oil palm plantations more effectively in the future.

ACKNOWLEDGEMENT

We thank the MPOB Director-General and the Director of Biology and Sustainability Research Division for permission to post this manuscript online. We would also like to thank the head and staff of Entomology and Integrated Pest Management Unit for their guidance and support during the experiment and preparation of the manuscript.

REFERENCES

Abbott, W S (1925). A method of computing the effectiveness of an insecticide. *J. Econ. Entomol., 18(2)*: 265-266. DOI: 10.1093/jee/18.2.265a.

Aliabadian, M; Kaboli, M; Nijman, V and Vences, M (2009). Molecular identification of birds: Performance of distance-based DNA barcoding in three genes to delimit parapatric species. *PLoS ONE, 4*: 1-8. DOI: 10.1371/journal.pone.0004119.

Ali, H; Muhammad, A; Islam, S U; Islam, W and Hou, Y (2018). A novel bacterial symbiont association in the hispid beetle, *Octodonta nipae* (Coleoptera: Chrysomelidae), their dynamics and phylogeny. *Microb. Pathog., 118*: 378-386. DOI: 10.1016/j.micpath.2018.03.046.

Ali, H; Muhammad, A; Sanda, N B; Huang, Y and Hou, Y (2019). Pyrosequencing uncovers a shift in bacterial communities across life stages of *Octodonta nipae* (Coleoptera: Chrysomelidae). *Front. Microbiol., 10*: 466. DOI: 10.3389/fmicb.2019.00466.

Atikah, A N; Halim, M; Zulaikha, S S and Yaakop, S (2019). Molecular identification and first documentation of seven species of *Carpophilus stephens* (Nitidulidae: Carpophilinae) in oil palm ecosystem, Peninsular Malaysia. *J. Asia Pac. Entomol., 22(2)*: 619-624. DOI: 10.1016/j.aspen.2019.04.010.

Azizoglu, U; Salehi Jouzani, G; Sansinenea, E and Sanchis-Borja, V (2023). Biotechnological advances in *Bacillus thuringiensis* and its toxins: Recent updates. *Rev. Environ. Sci. Biotechnol., 22*: 1-30. DOI: 10.1007/s11157-023-09652-5.

Ball, S L and Armstrong, K F (2006). DNA barcodes for insect pest identification: A test case with tussock moths (Lepidoptera: Lymantriidae). *Can. J. Forest Res., 36(2)*: 337-350. DOI: 10.1139/x05-276.

Barrett, R D H and Hebert, P D N (2005). Identifying spiders through DNA barcodes. *Can J. Zool., 83*: 481-491. DOI: 10.1139/z05-024.

Basri, M W (1993). *Life History, Ecology and Economic Impact of the Bagworm,* Metisa plana *Walker (Lepidoptera: Psychidae) on the oil palm,* Elaeis guineensis *Jacquin (Palmae) in Malaysia*. Ph.D. thesis, University of Guelph, Canada.

Basri, M W and Kevan, P G (1995). Life history and feeding behaviour of the oil palm bagworm, *Metisa plana* Walker (Lepidoptera: Psychidae). *Elaeis, 7*: 18-34.

Basri, M W; Hassan, A H and Zulkefli, M (1988). Bagworms (Lepidoptera: Psychidae) of oil palm in Malaysia. *PORIM Occasional Paper, 23*: 37.

Basri, M W; Norman, K; Idris, A S; Ariffin, D; Shamala, S; Ramle, M and Ramlah, S A A (2003). *Handbook of Pests and Diseases of Oil Palm*. MPOB, Bangi. p. 5-7.

Basri, M W; Ramlah, S A A; Ramle, M and Othman, A (1996). Biological efficacy of three commercial products of *Bacillus thuringiensis* for the control of bagworms, *Metisa plana* and *Mahasena corbetti* (Lepidoptera: Psychidae) of oil palm. *Proc. of the 1996 PORIM International Palm Oil Congress – Competetiveness for the 21st Century* (Ariffin, D; Basri, M W; Rajanaidu, N; Tayeb, M D; Paranjothy, K; Cheah, S C; Chang, K C; Ravigadevi, S eds). PORIM Bangi. p. 369-378.

Blagoev, G A; Nikolova, N I; Sobel, C N; Hebert, P D N and Adamowicz, S J (2013). Spiders

(Araneae) of Churchill, Manitoba: DNA barcodes and morphology reveal high species diversity and new Canadian records. *BMC Ecol., 13*: 44-44. DOI: 10.1186/1472-6785-13-44.

Chang, H; Guo, J; Li, M; Gao, Y; Wang, S; Wang, X and Liu, Y (2023). Comparative genome and phylogenetic analysis revealed the complex mitochondrial genome and phylogenetic position of *Conopomorpha sinensis* Bradley. *Sci. Rep., 13(1)*: 4989. DOI: 10.1038/s41598-023-30570-7.

Cheong, Y L and Tey, C C (2012). Understanding pest biology and behavior for effective control of oil palm bagworms. *The Planter, 8(1039)*: 699-715.

Cheong, Y L; Sajap, A S; Hafidzi, M N; Dzolkifli, O and Faizah, A (2010). Demography of the bagworm, *Pteroma pendula* Joannis on an exotic tree, *Acacia mangium* Willd in Malaysia. *The Malaysian Forester, 73(1)*: 77-85.

Che, J; Chen, H M; Yang, J X; Jin, J Q; Jiang, K; Yuan, Z Y; Murphy, R W and Zhang, Y P (2012). Universal COI primers for DNA barcoding amphibians. *Mol. Ecol. Resour., 12*: 247-258. DOI: 10.1111/j.1755-0998.2011.03090.x.

Chevasco, V; Elzinga, J A; Mappes, J and Grapputo, A (2014). Evaluation of criteria for species delimitation of bagworm moths (Lepidoptera: Psychidae). *Eur. J. Entomol., 111(1)*: 121-136. DOI: 10.14411/eje.2014.013

Corbett, G H (1927). Insect pests of the oil palm in Malaya. *Malay. Agric. J., 15(9-10)*: 338-342.

de Maagd, R A; Bravo, A and Crickmore, N (2001). How *Bacillus thuringiensis* has evolved specific toxins to colonize the insect world. *Trends Genet., 17*: 193-199. DOI: 10.1016/s0168-9525(01)02237-5.

Desalle, R (2006). Species discovery versus species identification in DNA barcoding effort, response to Rubinoff. *Conserv. Biol., 20*: 1545-1547. DOI: 10.1111/j.1523-1739.2006.00543.x.

Dona, J; Diaz-Real, J; Mironov, S; Bazaga, P; Serrano, D and Jovani, R (2015). DNA Barcoding and minibarcoding as a powerful tool for feather mite studies. *Mol. Ecol. Resour., 15*: 1216-1225. DOI: 10.1111/1755-0998.12384.

Felsenstein, J (1985). Confidence limits of phylogenies: An approach using the bootstrap. *Evolution, 39*: 783-791.

Firake, D M and Behere, G T (2021). Molecular approaches in insect pest management: Relevance and reality. *Indian J. Entomol., 83(1)*: 126-132. DOI: 10.5958/0974-8172.2021.00008.0.

Firake, D M; Behere, G T; Arnscheid, W R; Kumar, R and Ngachan, S V (2018). First report of coconut case caterpillar, *Mahasena corbetti* Tams (Lepidoptera: Psychidae) from India. *Phytoparasitica, 46(3)*: 355-364. DOI: 10.1007/s12600-018-0673-7.

Gater, B A R (1925). Insects on African oil palms. *Malay. Agric. J., 13(8)*: 250-256.

Hebert, P D N; Penton, E H; Burns, J M; Janzen, D H and Hallwachs, W (2004). Ten species in one: DNA barcoding reveals cryptic species in the neotropical skipper butterfly *Astraptes fulgerator. Proc. Natl. Acad. Sci. USA, 101*: 14812-14817. DOI: 10.1073/pnas.0406166101.

Hebert, P D N; Ratnasingham, S and De Waard, J R (2003). Barcoding animal life: Cytochrome c oxidase subunit 1 divergences among closely related species. *Proc. Royal Soc. Lond B Biol. Sci, 270(1)*: 96-99. DOI: 10.1098/rsbl.2003.0025.

Ho, C T (2002). *Ecological studies on* Pteroma pendula *Joannis and* Metisa plana *Walker (Lepidoptera: Psychidae) towards improved integrated management of infestations in oil palm*. Ph.D. thesis, Universiti Putra Malaysia.

Ismail, S A; Abed, M; El Sayed, A M and Elakhrasy, F I (2022). Efficacy appraisement of some compounds against *Monacha cartusiana* snail using various application techniques, under laboratory and field conditions. *J. Plant Prot. Pathol., 13(11)*: 273-276. DOI: 10.21608/jppp.2022.170760.1108.

Jalali, S K; Rakshit, O and Venkatesan, T (2015). DNA barcoding for identification of agriculturally important insects. New horizons in insect science: Towards sustainable pest management (Chakravarthy, A K ed.). *New Dehli: Springer*. p. 13-23. DOI: 10.1007/978-81-322-2089-3_2.

Jin, Q; Han, H; Hu, X; Li, X; Zhu, C; Ho, S Y; Ward, R D and Zhang, A (2013). Quantifying species diversity with a DNA barcoding-based method: Tibetan moth species (Noctuidae) on the Qinghai-Tibetan Plateau. *PLoS ONE, 8*: e64428. DOI: 10.1371/journal.pone.0064428.

Jinbo, U; Kato, T and Ito, M (2011). Current progress in DNA barcoding and future implications for entomology. *Entomol. Sci., 14*: 107-124. DOI: 10.1111/j.1479-8298.2011.00449.x.

Jones, F M and Parks, H B (1928). The bagworm of Texas. *Bulletin of Texas Agricultural Experiment Station, 382*: 5-26.

Kalshoven, L G E (1981). *Pest of Crops in Indonesia* (Van Der Laan, P A; Ichtiar Baru, P T and Van Hoeve eds.). Ichtiar Bain, Jakarta. 701 pp.

Kappner, I and Bieler, R (2006). Phylogeny of venus clams (Bivalvia: Venerinae) as inferred from nuclear and mitochondrial gene sequences. *Mol. Phylogenet. Evol., 40*: 317-313. DOI: 10.1016/j.ympev.2006.02.006.

Khan, K A; Al-Ghamdi, A A; Ghramh, H A; Ansari, M J; Ali, H; Alamri, S A; Al-Kahtani, S N; Adgaba, N; Qasim, M and Hafeez, M (2020). Structural diversity and functional variability of gut microbial communities associated with honey bees. *Microb. Pathog.*, *138*: 103793. DOI: 10.1016/j.micpath.2019.103793.

Kimura, M (1980). A simple method for estimating evolutionary rates of base substitutions through comparative studies of nucleotide sequences. *J. Mol. Evol., 16*: 111-120. DOI: 10.1007/BF01731581.

Kondo, T; Gullan, P J and Williams, D J (2008). Coccidology: The study of scale insects (Hemiptera: Sternorrhyncha: Coccoidea). *Tecnologia Agropecuaria, 9*: 55-61.

Kumar, A G; Jalali, S K; Venkatesan, T; Stouthamer, R; Niranjana, P and Lalitha, Y (2009). Internal transcribed spacer-2 restriction fragment length polymorphism (ITS-2-RFLP) tool to differentiate some exotic and indigenous trichogrammatid egg parasitoids in India. *Biol. Control, 49*: 207-213. DOI: 10.1016/j.biocontrol.2009.02.010.

Kumar, P; Kamle, M; Borah, R; Mahato, D K and Sharma, B (2021). *Bacillus thuringiensis* as microbial biopesticide: Uses and application for sustainable agriculture. *Egypt. J. Biol. Pest Control*, *31(1)*: 1-7. DOI: 10.1186/s41938-021-00440-3.

Lelana, N E; Utami, S; Darmawan, U W; Nuroniah, H S; Haneda, N F; Darwiati, W and Anggraeni, I (2022). Bagworms in Indonesian plantation forests: Species composition, pest status, and factors that contribute to outbreaks. *Diversity*, *14(6)*: 471. DOI: 10.3390/d14060471.

Leon, R G; Dunne, J C and Gould, F (2021). The role of population and quantitative genetics and modern sequencing technologies to understand evolved herbicide resistance and weed fitness. *Pest Manag. Sci.*, *77(1)*: 12-21.

Leong, T M and Lim, K K (2012). Record of the bagworm moth, *Mahasena corbetti* tams in Singapore (Lepidoptera: Psychidae). *Nat. Singap., 5*: 1-5.

Lepesme, P (1947). Les insects des palmiers. Paris: Paul Lechevalier. p. 346.

Li, Y; Wang, C; Ge, L; Hu, C; Wu, G; Sun, Y; Song, L; Wu, X; Pan, A; Xu, Q and Shi, J (2022). Environmental behaviors of *Bacillus thuringiensis* (Bt) insecticidal proteins and their effects on microbial ecology. *Plants, 11(9)*: 1212. DOI: 10.3390/plants11091212.

Liau, S S (1987). Problems and control of bagworms (Lepidoptera: Psychidae) and rats (Rodentia: Muridae) in the oil palm. *Proc. of the Second Chemara Workshop*. p. 46-59.

Mazmira, M M M; Ramlah, S A A; Najib, M A; Norman, K; Kushairi, A D and Basri, M W (2010). Integrated pest management (IPM) of bagworms in Southern Perak via aerial spraying of *Bacillus thuringiensis*. *Oil Palm Bull., 63*: 24-33.

Mazmira, M M M; Shawal, M T M and Arbakariya, A (2021). Impact of single and two-phase dissolved oxygen tension control on *Bacillus thuringiensis* cultivation and delta endotoxin production. *Malays. Appl. Biol., 50*: 1-12. DOI: 10.55230/mabjournal.v50i1.14.

MPOB (2016). Standard Operating Procedures (SOP) Guidelines for Bagworm Control. MPOB, Bangi. p. 6.

Nagoshi, R N; Brambila, J and Meagher, R L (2011). Use of DNA barcodes to identify invasive armyworm *Spodoptera* species in Florida. *J. Insect Sci., 11*: 154-111. DOI: 10.1673/031.011.15401.

Najib, M A; Ramlah, S A A; Mazmira, M M M and Basri, M W (2009). Effect of *Bacillus thuringiensis*, Terakil-1® and Teracon-1® against oil palm polinator *Elaeidobius camerunicus*, and beneficial insects associated with *Cassia cobanensis*. *J. Oil Palm Res., 21*: 667-674.

Najib, M A; Ramlah, S A A; Mazmira, M M M and Basri, M W (2011). Ecotoxicity of *Bacillus thuringiensis*, Terakil-1® and Teracon-1® against freshwater fish, *Tilapia nilotica*. *J. Oil Palm Res., 23*: 1036-1039.

Najib, M A; Ramlah, S A A; Mazmira, M M M and Basri, M W (2013). Efficacy of Bafog-1, formulated local *Bacillus thuringiensis* for controlling bagworm *Pteroma pendula* (Lepidoptera: Psychidae). *J. Oil Palm Res., 25(2)*: 228-234.

Niitsu, S; Sugawara, H and Hayashi, F (2017). Evolution of female-specific wingless forms in bagworm moths. *Evol. Dev., 19*: 9-16. DOI: 10.1111/ede.12213.

Noorhazwani, K; Ramlah, S A A; Mazmira, M M M; Najib, M A; Hafiz, C A C M and Norman, K (2017). Controlling *Metisa plana* Walker (Lepidoptera: Psychidae) outbreak using *Bacillus thuringiensis* at an oil palm plantation in Slim River Perak, Malaysia. *J. Oil Palm Res., 29(1)*: 47-54. DOI: 10.21894/jopr.2017.2901.05.

Norman, K and Basri, M W (2007). Status of common oil palm insect pests in relation to technology adoption. *The Planter, 83(975)*: 371-385.

Norman, K; Robinson, G S and Basri, M W (1994). Common bagworm pests (Lepidoptera: Psychidae) of oil palm in Malaysia with notes on related South-east Asian species. *Malayan Nature J., 48(2)*: 93-123.

Park, D; Foottit, R; Maw, E and Hebert, P D (2011). Barcoding bugs: DNA-based identification of the true bugs (Insecta: Hemiptera: Heteroptera). *PLoS ONE, 6*: 18749. DOI: 10.1371/journal.pone.0018749.

Pfunder, M; Holzgang, O and Frey, J (2004). Development of microarray based diagnostics of voles and shrews for use in biodiversity monitoring studies and evaluation of mitochondrial cytochrome oxidase I vs. cytochrome b as genetic markers. *Mol. Ecol., 13*: 1277-1286. DOI: 10.1111/j.1365-294X.2004.02126.x.

Priwiratama, H; Rozziansha, T A P and Prasetyo, A E (2023). Potential application of spinetoram as an alternative insecticide for controlling oil palm bagworm *Mahasena corbetti*. *IOP Conference Series: Earth and Environmental Science*. IOP Publishing. p. 012025.

Ramlah, S A A and Basri, M W (1997). A local *Bacillus thuringiensis* SRBT1 with potential for controlling *Metisa plana* (Wlk). *Elaeis 9(1)*: 34-45.

Ramlah, S A A; Basri, M W and Mahadi, M N (2003). IPM of bagworms and nettle caterpillars using *Bacillus thuringiensis*-towards understanding and increasing efficacy. *Proc. of the PIPOC 2003 International Palm Oil Congress – Agriculture Conference.* MPOB, Bangi. p. 449-474.

Ramlah, S A A; Mazmira, M M M; Najib, M A and Basri, M W (2005). *Bacillus thuringiensis*, Terakil 1 (WP) for biological control of bagworms. *MPOB Information Series,* 1511-7871.

Raso, L; Sint, D; Rief, A; Kaufman, R and Traugott, M (2014). Molecular identification of adult and juvenile Linyphiid and Theridiid spiders in Alpine Glacier Foreland communities. *PLoS ONE, 9*: 101755. DOI: 10.1371/journal.pone.0101755.

Rhainds, M; Davis, D R and Price, P W (2009). Bionomics of bagworms (Lepidoptera: Psychidae). *Annu. Rev. Entomol., 54*: 209-226. DOI: 10.1146/annurev.ento.54.110807.090448.

Robinson, G S; Ackery, P R; Kitching, I J; Beccaloni, G W and Hernández, L M (2011). *Hosts - a database of the World's Lepidopteran Hostplants.* London: Natural History Museum.

Robinson, G S; Tuck, K R and Shaffer, M (1994). *A Field Guide to the Smaller Moths of South-East Asia*. London: Natural History Museum.

Ruiz-Lopez, F; Wilkerson, R C; Conn, J E; Mckeon, S N; Levin, D M; Quiñones, M L; Póvoa, M M and Linton, Y (2012). DNA barcoding reveals both known and novel taxa in the Albitarsis group (Anopheles: Nyssorhynchus) of Neotropical malaria vectors. *Paras. Vect., 5*: 1-12. DOI: 10.1186/1756-3305-5-44.

Suresh, E; Rathipriya, A; Shanmugam, S A; Hamsavalli, R and Kathirvelpandian, A (2022). Character-based diagnostic keys, molecular identification and phylogenetic relationships of threadfin breams (family: Nemipteridae) based on mitochondrial genes from the Southern coromandel Coast, India. *Animal Biotechnology.* Taylor and Francis Online. p. 1-13. DOI: 10.1080/10495398.2022.2040522.

Syed, R A (1978). Bionomic of the three important species of bagworms on oil palm. *Malays. Agric. J., 51*: 392-398.

Tahir, H M; Noor, A; Mehmood, S; Sherawat, S M and Qazi, M A (2018). Evaluating the accuracy of morphological identification of insect pests of rice crops using DNA barcoding. *Mitochondrial DNA Part B, 3(2)*: 1220-1224. DOI: 10.1080/23802359.2018.1532334.

Tamura, K; Peterson, D; Peterson, N; Stecher, G; Nei, M and Kumar, S (2011). MEGA5: Molecular evolutionary genetics analysis using maximum likelihood, evolutionary distance, and maximum parsimony method. *Mol. Biol. Evol., 28*: 2731-2739. DOI: 10.1093/molbev/msr121.

Tiong, R H C (1979). Some predators and parasites of *Mahasena corbetti* (Tams) and those a asigna (Moore) in Sarawak. *The Planter, 55(639)*: 279-289.

Utsugi, J B; Toshihide, K T and Motomi, I T O (2011). Current progress in DNA barcoding and future implications for entomology. *Entomol. Sci., 14*: 107-124. DOI: 10.1111/j.1479-8298.2011.00449.x.

Vences, M; Thomas, M; Bonett, R M and Vieites, D R (2005). Deciphering amphibian diversity through DNA barcoding: Chances and challenges. *Philos. Trans. R. Soc. Lond. B. Biol. Sci., 360*: 1859-1868. DOI: 10.1098/rstb.2005.1717.

Wood, B J (1968). *Pest of Oil Palms in Malaysia and Their Control*. Incorporated Society of Planters, Kuala Lumpur. p. 204.

Wood, B J and Nesbit, D P (1969). Caterpillar outbreak on oil palms in Eastern Sabah. *The Planter, 45(518)*: 285-299.

Wood, B J (1971). Development of integrated control programmes for pests of tropical perennial crops in Malaysia. *Biol. Control (Huffaker CB)*. p. 422-457.

Wood, B J and Norman, K (2019). Bagworm (Lepidoptera: Psychidae) infestation in the centennial of the oil palm industry a review of causes and control. *J. Oil Palm Res., 31(3)*: 364-380. DOI: 10.21894/jopr.2019.0032.

Xu, X; Liu, F; Chen, J; Li, D and Kuntner, M (2015). Integrative taxonomy of the primitively segmented spider genus *Ganthela* (Araneae: Mesothelae: Liphistiidae): DNA barcoding gap agrees with morphology. *Zool. J. Linnean Soc., 175*: 288-306. DOI: 10.1111/zoj.12280.

Zaynab, M; Fatima, M; Sharif, Y; Zafar, M H; Ali, H and Khan, K A (2019). Role of primary metabolites in plant defense against pathogens. *Microbial Pathogenesis, 137*: 103728. DOI: 10.1016/j.micpath.2019.103728.

Zhu, L; Ma, Q; Chen, J and Zhao, G (2022). Current progress on innovative pest detection techniques for stored cereal grains and thereof powders. *Food Chemistry*, 133706. DOI: 10.1016/j.foodchem.2022.133706.

Journal of Oil Palm Research Vol. 36 (3) September 2024 p. 445-455
DOI: https://doi.org/10.21894/jopr.2023.0030

EFFECT OF GRAPHITE MICROPARTICLES AS ADDITIVE IN AN INDIRECT DIESEL ENGINE FUELLED WITH PURE PALM OIL

RICO ADITIA PRAHMANA[1,2]*; PRIHADI SETYO DARMANTO[3]; IMAN KARTOLAKSONO REKSOWARDOJO[3,10]; TEUKU MEURAH INDRA RIAYATSYAH[2,4]; ACHMAD GUS FAHMI[5]; FIRMAN BAGJA JUANGSA[3]; TIRTO PRAKOSO[6]; ABDI HANRA SEBAYANG[7,11]; MUHAMMAD SYAUKANI[2]; ZIDO YUWAZAMA[8] and WIAGIL TUNKU NASTITI WIDOYOKO[9]

ABSTRACT

Research lately has shown the prospects of graphite as an additive for diesel engines due to its favourable characteristics. Moreover, using pure palm oil (PPaO) as the primary fuel in diesel engines is not recommended because of numerous disadvantages. To overcome such a problem, the effect of graphite oxide (GO) and graphite powder (GP) microparticle as an additive on PPaO was investigated by analysing the diesel engine combustion performance and emissions. GO was prepared using the Hummers method. The use of PPaO as a single fuel led to a significant increase in opacity by up to 127.0% compared to diesel fuel (DF). However, adding GO and GP as fuel additives can significantly reduce opacity by up to 63.9%, improve thermal efficiency by up to 20.4%, and increase specific fuel consumption by up to 40.1% compared to DF. These results indicate that GO and GP have promising potential as effective fuel additives for PPaO, leading to increased combustion efficiency, and reduced hazardous emissions in diesel engine applications.

Keywords: diesel engine performance, graphite oxide, graphite powder, pure palm oil.

Received: 5 December 2022**; Accepted:** 21 May 2023**; Published online:** 18 July 2023.

[1] Doctoral Program of Mechanical Engineering, Faculty of Mechanical and Aerospace Engineering, Institut Teknologi Bandung, 40132 Bandung, Indonesia.

[2] Program Study of Mechanical Engineering, Department of Production and Industrial Technology, Institut Teknologi Sumatera, 35365 South Lampung, Indonesia.

[3] Department of Mechanical Engineering, Faculty of Mechanical and Aerospace Engineering, Institut Teknologi Bandung, 40132 Bandung, Indonesia.

[4] Department of Mechanical Engineering, National Yunlin University of Science and Technology, Touliu, Yunlin 64002 Taiwan.

[5] Program Study of Cosmetic Engineering, Department of Production and Industrial Technology, Institut Teknologi Sumatera, 35365 South Lampung, Indonesia.

[6] Department of Chemical Engineering, Faculty of Industrial Technology, Institut Teknologi Bandung, 40132 Bandung, Indonesia.

[7] Department of Mechanical Engineering, Politeknik Negeri Medan, 20155 Medan, Indonesia.

[8] Master Program of Mechanical Engineering, Faculty of Mechanical and Aerospace Engineering, Institut Teknologi Bandung, 40132 Bandung, Indonesia.

[9] Undergraduate Program of Mechanical Engineering, Faculty of Mechanical and Aerospace Engineering, Institut Teknologi Bandung, 40132 Bandung, Indonesia.

[10] Program Study of Mechanical Engineering, Faculty of Industrial Technology, Universitas Pertamina, 12220 Jakarta, Indonesia.

[11] Center of Renewable Energy, Department of Mechanical Engineering, Politeknik Negeri Medan, 20155 Medan, Indonesia.

* *Corresponding author e-mail: rico.aditia@ms.itera.ac.id*

INTRODUCTION

Diesel fuel is versatile and has applications in many industries, including transportation, locomotives, construction, mining, maritime, agriculture, military and stationary power generation (Ooi *et al*., 2016; Yilmaz *et al*., 2022a; 2022b). Moreover, alternative fuels for diesel engines have been widely developed by researchers, the most popular of which is biodiesel with various raw materials, followed by natural gas, LPG, methane, propane, hydrogen and others (Atmanli and Yilmaz, 2021; Geng *et al*., 2017; Kegl *et al*., 2013; Ropandi *et al*., 2022). Some of these fuels can be used directly in diesel engines, and some require other methods, such as dual fuel, blending and emulsification (Atmanli, 2020; Hoang *et al*., 2022; Kegl *et al*., 2021). Palm oil is one of the most popular biofuel sources to replace conventional diesel fuel derived from the oil palm tree. Palm oil is generally useful as the feedstock for food and cosmetics (Harahap *et al*., 2020; Xin *et al*., 2022). Indonesia is the largest palm oil producer in the world, with a production of up to 46.9 million tonnes in 2022 and has an excellent potential to utilise palm oil as an alternative fuel in diesel engines (Farobie and Hartulistiyoso, 2021; Sani *et al*., 2018).

Palm oil biodiesel (POB) which is produced from crude palm oil (CPO), is a clean, renewable fuel characterised by higher flash points, lubricity, combustion efficiency, cetane number, biodegradability, and non-toxicity compared to conventional diesel fuel (Dey *et al*., 2021). However, the development of POB has several obstacles, particularly the production process, which could be more complicated (Pipitone and Costanza, 2018). Moreover, using CPO directly in a diesel engine is not recommended because it prompts several undesirable consequences, including increased fuel consumption, decreased engine power performance and forming carbon deposits in the combustion chamber (Syarif *et al*., 2017; Yilmaz *et al*., 2017). Besides, many studies have been conducted over the last two decades to evaluate the use of pure palm oils as diesel fuel. The high viscosity of PPaO limits fuel atomisation and enhances fuel spray penetration, leading to engine deposits and the thickening of lubricating oil (De Almeida *et al*., 2002).

Several works have been done to enhance engine performance and emissions, such as combustion treatments, engine configuration options, biofuel utilisation, and fuel additive (Atmanli, 2016; Sebayang *et al*., 2022; Zhao *et al*., 2023). Fuel additives are one of the most cost-effective methods for mitigating the rising diesel pollution emissions and increasing engine performance. Substantial research is currently being conducted into using nanoscale materials as fuel additives for diesel engines (Ooi *et al*., 2016). Multiwall carbon nanotube (MWCNT), carbon nanotube (CNT), aluminium oxide (Al_2O_3), silicon oxide (SiO_2), alumina, graphite oxide (GO), graphene and many other nanomaterials were utilised as additives in diesel fuel. MWCNT and alumina had been used as additives in jatropha biodiesel. It was found that adding MWCNT reduced the ignition delay and improved combustion performance (Sonara and Rathod, 2022).

A numerical investigation of MWCNT as a fuel additive in diesel fuel has been reported (Sa *et al*., 2021). The result showed that the addition of MWCNT and graphene nanoplatelets (GNP) could increase the coefficient of heat transfer rate and pressure drop. Vellaiyan (2019) performed research applying CNT additions in soybean biodiesel in diesel engines. It was found that soybean biodiesel and its mix promote a shorter ignition delay time, reduced in-cylinder pressure and net heat release rate compared to diesel fuel.

Chen *et al.* (2018) used CNT to compare the effects of using nanoparticles of Al_2O_3, CNT, and silicon oxide (SiO_2) as additives in diesel engines. It was found that CNT has better brake-specific fuel consumption (BSFC), high brake thermal efficiency (BTE) and low CO emission compared to Al_2O_3 and SiO_2. Razzaq *et al.* (2021) employed B30 palm biodiesel with GNP and dimethyl carbonate (DMC) as fuel additives. The results show improved BTE and BSFC at all engine speeds, significantly reducing HC emissions (Ooi *et al*., 2016; 2017) examine GO using as a fuel additive. In this investigation, GO was found to be highly efficient in enhancing the combustion properties of diesel fuel and lower pollutant emissions.

However, there is no published research to investigate PPaO as primary fuel with GP and GO microparticles as fuel additives in indirect diesel engines, most of them focus on additive nanoparticles and use biodiesel and diesel fuel as the primary fuel. Thus, this topic is becoming quite interesting to explore. Hence, the current study aims to investigate the performance and emission characteristics of the indirect diesel engine fuelled with PPaO with GO and GP microparticles as fuel additives. The fuel was prepared by blending PPaO with GO and GP using ultrasonic methods. The baseline fuels for comparing engine performance and emissions were diesel fuel and PPaO.

MATERIALS AND METHODS

Experimental Apparatus

The schematic layout of the engine bench is illustrated in *Figure 1*. The engine power

performance was calculated and analysed. The exhaust smoke was measured utilising a smoke meter. *Table 1* shows the test engine's specifications. To ensure the experiment's validity and the precision of the data, each component of equipment and item of equipment was checked and adjusted to its proper settings before performing the experiments. Each operational point was measured several times to reduce error. After more than 10 min of stable operation, the data were collected thrice under identical operating conditions.

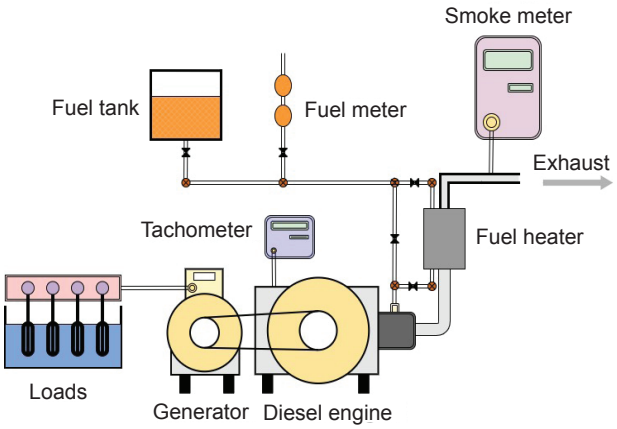


Figure 1. Schematic of engine test.

TABLE 1. SPECIFICATION OF THE TEST ENGINE

Specification	Dafeng S195
Type	Four stroke, indirect injection, single cylinder
Bore × Stroke	95 × 115 mm
Cylinder volume	0.815 L
Compression ration	22 : 1
Engine max power rate	14 hp/2200 rpm
Generator rated power	7500W at 1500 rpm

Test Fuel

In this study, diesel fuel (DF) was utilised as the baseline fuel for comparison. PPaO was prepared as the primary fuel for the diesel engine. Preheating of PPaO was conducted in fuel lines at temperatures 60°C-100°C to lower the viscosity of PPaO and avoid clogging in the fuel line and injector. A similar approach was used by (De Almeida *et al*., 2002). The additive material utilised in this study was GP. The Hummer technique was used to synthesise GO, and the procedure was continued by mixing PPaO with GP and GO. The sonication method is utilised in this process to provide a medium for the mixing of fuel, as seen in *Figure 2*, the formulation of test fuel can be seen in *Table 2*. The test fuel properties of DF, PPaO and PPaO blended of additives of GP and GO are presented in *Table 3*.

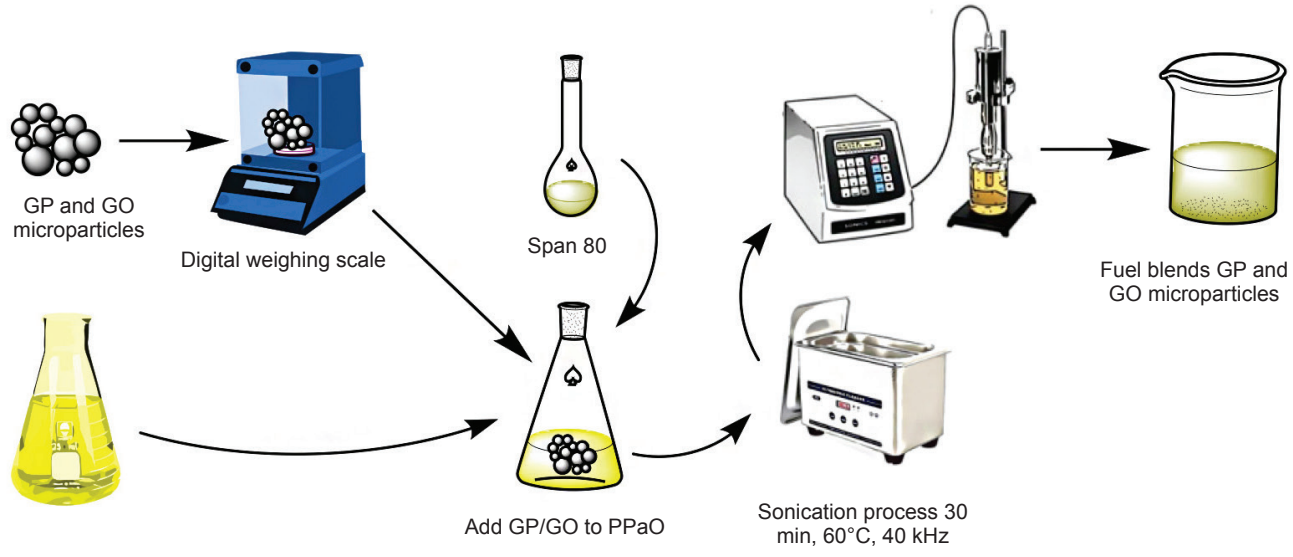


Figure 2. The mixing process of PPaO with additives of graphite powder and graphite oxide.

TABLE 2. THE PREPARATION OF THE FUEL SAMPLE

Formulation	Dosage of additive	Dosage of surfactant	Label
Diesel fuel	-	-	DF
Pure palm oil	-	-	PPaO
PPaO + Graphite powder	Graphite powder (150 ppm)	-	PPaOG
PPaOG + Span 80	Graphite powder (150 ppm)	Span 80 (20 mL)	PPaOGS
PPaO + Graphite oxide powder	Graphite oxide (150 ppm)	-	PPaOGO
PPaOGO+ Span 80	Graphite oxide (50 ppm)	Span 80 (20 mL)	PPaOGOS

Note: PPaOG - Pure palm oil graphite powder; PPaOGO - Pure palm oil graphite oxide.

TABLE 3. TEST FUEL PROPERTIES

Formulation label	Lower heating value (kcal/kg)	Viscosity (cP)	Density (kg/m^3)	Flash point (°C)
DF	10 536	2.852	844.4	28
PPaO	9 735	49.740	908.8	56
PPaOG	9 420	46.832	912.4	38
PPaOGS	9 432	48.841	909.2	50
PPaOGO	9 462	46.114	906.9	42
PPaOGOS	9 485	49.273	908.9	40

Note: PPaOGS - Pure palm oil graphite powder surfactant; PPaOGO - Pure palm oil graphite oxide; PPaOGOS - Pure palm oil graphite oxide surfactant.

Material Characterisation

The particle size distribution was measured using particle size analysis based on light scattering (Horiba SZ-100). The Fourier transform infrared spectroscopy (FTIR) of the sample was obtained. Scanning electron microscope (SEM) was used to study the morphologies of GP and GO and energy dispersive X-ray spectroscopy (EDS) analysis was utilised to determine the elemental composition of GP and GO as well as their distribution. Both of SEM and EDS were performed on HITACHI SU3500. The crystal structure of materials was analysed using X-ray diffractometer (XRD) Bruker D8 Advance diffractometer with Cu Kα radiation (λ =1:54060Å).

Engine Performance Analysis

Several characteristics, such as engine power, torque, specific fuel consumption and thermal efficiency, are required to determine engine power performance.

Engine power (Pe).

$$Pe = \frac{V.I.\cos\phi}{1000.\eta_{generator}} (kW) \quad (1)$$

where V is voltage (V), I is ampere (I), cos ϕ is power factor for one single phase is 1 and $\eta_{generator}$ is electric generator efficiency for engines under 50 kVA is 87%-89%; for generators employing V belts, the power generated is divided by 0.96 (Belt efficiency) (Khairil *et al*., 2020).

Engine torque (Te).

$$Te = \frac{6000.\ Pe}{2.Phi.\ N} (kW) \quad (2)$$

where Pe is the engine power, Phi is 3.14 and N is the engine rotation (RPM).

The specific fuel consumption (SFC). The specific fuel consumption (SFC) is described as the quantity of fuel the engine uses to generate power, expressed in kW/h. The SFC may be computed using the following equation (Khairil *et al*., 2020).

$$SFC = \frac{\dot{m}fuel}{Pe} \quad (3)$$

where SFC is the specific fuel consumption (kg/kWh), $\dot{m}fuel$ is fuel mass flow (kg/hr) and Pe is the engine power (kW).

Thermal efficiency. The heat-use efficiency of fuel to be transformed into mechanical work is characterised as thermal efficiency. The equation may be used to compute the thermal efficiency (Khairil *et al*., 2020).

$$\eta th = \frac{Pe \,.632{,}5}{\dot{m}\, fuel \,.\ \mathrm{LHV}} \qquad (4)$$

where ηth is the thermal efficiency (%) and LHV is the lower heating value (kcal/kg).

RESULTS AND DISCUSSION

Microparticles of GP and GO

Particle size analysis (PSA). It is a critical technique in materials science and engineering for understanding the physical properties of materials. PSA provides information about the size distribution of particles in a sample, which is essential for understanding the behaviour of the material. PSA is used to analyse various materials, including powders, suspensions, emulsions, and aerosols. PSA techniques include light scattering, sedimentation, and microscopy-based methods. Each technique has its advantages and disadvantages, and the choice of technique depends on the properties of the material being analysed. Particle size analysis based on light scattering is a method of determining the velocity of Brownian motion by analysing the fluctuations of scattered light by particles in suspension when illuminated with a laser. This velocity can then be used to calculate the hydrodynamic size of particles using the Stokes-Einstein relationship (Hussain *et al.*, 2020). According to the measurements illustrated in *Figure 3a*, the average particle size of graphite powder is 1.8 µm, mean 2.3 µm, standard deviation 2.8 µm with medium dispersion viscosity of 0.896 mPa.s.

Fourier transform infrared (FTIR) spectroscopy. It is a powerful analytical technique used to identify and characterise materials. FTIR is a method for identifying and quantifying some material constituents, including fuel and the chemical composition of the environment. FTIR is one of the analytical methods that is frequently applied due to the factors such as cost, speed, and screening quality. This procedure uses a molecular "fingerprinting" technique (Riayatsyah *et al.*, 2021). *Figure 3b* shows the results of the FTIR synthesised from graphite powder to graphite Oxide as an additive. As seen in *Table 4*, the FTIR results of the additive effect, such as wavenumber, group attribution, absorption intensity, and vibration type of the absorption peaks, have been detected. The graphite spectrum tends not to have a typical absorption from the oxide functional group unless there is absorption in the wave number region of 1800-2200 cm^{-1}, a characteristic of chemical precursors (refined oil) with molecular vibrations of C=O stretching. As for the graphite oxide spectrum, a new broad spectrum is formed at a wave number of 3653 cm^{-1}, a stretching vibration, and at 1000-1300 cm^{-1}, a bending vibration for the O-H functional group.

Scanning electron microscope (SEM). It is a powerful tool that has revolutionised the field of materials science by enabling high-resolution imaging of surface morphology and microstructure. SEM in this study was used to investigate the morphology and microstructure of GP and GO, as seen in *Figure 4a* and *4b*, it was found that GP exhibited a layered structure, with thin and flat graphite flakes stacked on top of each other. The SEM images revealed that the flakes had irregular edges and a

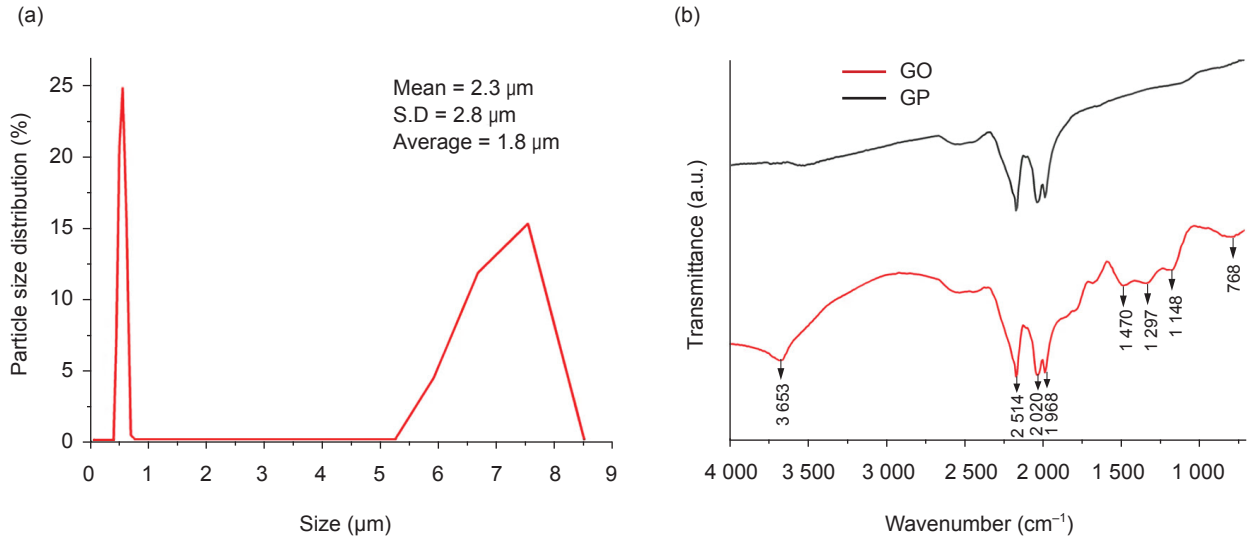


Figure 3. (a) Particle size analysis based on light scattering of graphite powder and (b) the FTIR Spectra synthesised from graphite powder to graphite oxide.

TABLE 4. THE FTIR OF THE ADDITIVE

Wavenumber (cm^1)	Group attribution	Vibration type	Absorption intensity
3 653	O–H	Stretching	Broad, Strong
2 154	C=O carbonyl	Stretching	Sharp, Strong
2 020	C=O	Stretching	Sharp, Strong
1 968	O–H	Bending	Sharp, Strong
1 470	C–H	Bending	Broad, Strong
1 297	C–OH	Stretching	Broad, Weak
1 148	C–O–C	Stretching	Broad, Weak
768	CH2	Stretching	Broad, Weak

size range of 5-10 µm. The microstructure analysis showed that the graphite flakes had a crystalline structure with well-defined basal planes and high aspect ratios. *Figure 4c* and *4d* showed that GO exhibited a flake-like morphology, with a size range of 0.1-5.0 µm. The SEM images revealed that the surface of the GO flakes was rough and porous, with many wrinkles and folds. The microstructure analysis showed that the GO flakes had a layered structure with an interlayer spacing of 0.8 nm, consistent with the presence of oxygen-containing functional groups. The average thickness of the GO flakes was found to be approximately 10 nm. The layered structure of GO is due to the oxidation of the graphite layers, which results in the formation of oxygen functional groups on the surface. The crumpled and wrinkled morphology of GO is believed to be caused by the interactions between the oxygen functional groups and the surrounding environment. The irregular edges of the GO flakes are consistent with the presence of oxygen functional groups, which can cause structural defects and irregularities.

Energy-dispersive X-ray spectroscopy (EDS). EDS is a widely used analytical technique for elemental analysis of materials. EDS is a non-destructive technique that can be performed on a wide range of materials, including metals, ceramics, polymers and biological samples. The technique involves the detection and measurement of X-rays emitted from a sample when it is bombarded with an electron beam. The energy and intensity of the X-rays are used to identify and quantify the elements present in the sample. EDS has several advantages over other analytical techniques, including high sensitivity, rapid analysis and non-destructive analysis (Hernandez C *et al*., 2022). The EDS analysis of GO, as seen in *Figure 5a* was found to contain carbon, oxygen, and traces of other elements. The atomic percent composition of carbon and oxygen in GO was found to be 55.63% and 39.43%, respectively. These results are consistent with the expected composition of GO based on its chemical structure and properties. The EDS analysis of GO confirmed the presence of carbon and oxygen, which are the main elements in GO. The atomic percent composition of carbon and oxygen in GO was consistent with previous studies that used different techniques to analyse the elemental composition of GO. The traces of other elements detected in the EDS analysis may be due to impurities in the GO sample or contamination during the sample preparation.

X-ray diffraction (XRD). XRD analysis is a widely used technique for determining the crystal structure of materials. XRD analysis was conducted on GP to investigate its crystal structure and identify its characteristic peaks. The GP sample was prepared as powder. XRD analysis was performed using a Bruker D8 Advance X-ray diffractometer with Cu Kα radiation (λ=1.5406 Å) in the 2θ range of 10° to 80° with a step size of 0.02° and a scanning rate of 0.5°/min. The XRD pattern of graphite powder is shown in *Figure 5b*. The diffraction peaks at 2θ angles are 26.55°, 44.30°, 54.60° and 77.50° which correspond to the (002), (100), (004) and (110) planes of the hexagonal crystal structure of graphite, respectively. The results show that the graphite powder has a typical hexagonal crystal structure with characteristic diffraction peaks at 2θ angles of 26.50°, 44.30°, 54.70° and 77.50° are matching with The International Centre for Diffraction Data (ICDD) Graphite 00-008-0415. The obtained XRD pattern was compared with research done by Ahmad Daud *et al*. (2017), and the results confirmed the identification of the sample as graphite.

Power Performance

Engine power and torque are important parameters that determine the performance of an engine. Power is the rate at which work is done, while torque is the twisting force produced by the engine. Based on the experiment, the engine power and torque were estimated. A comparison chart with an error bar of the engine power and torque

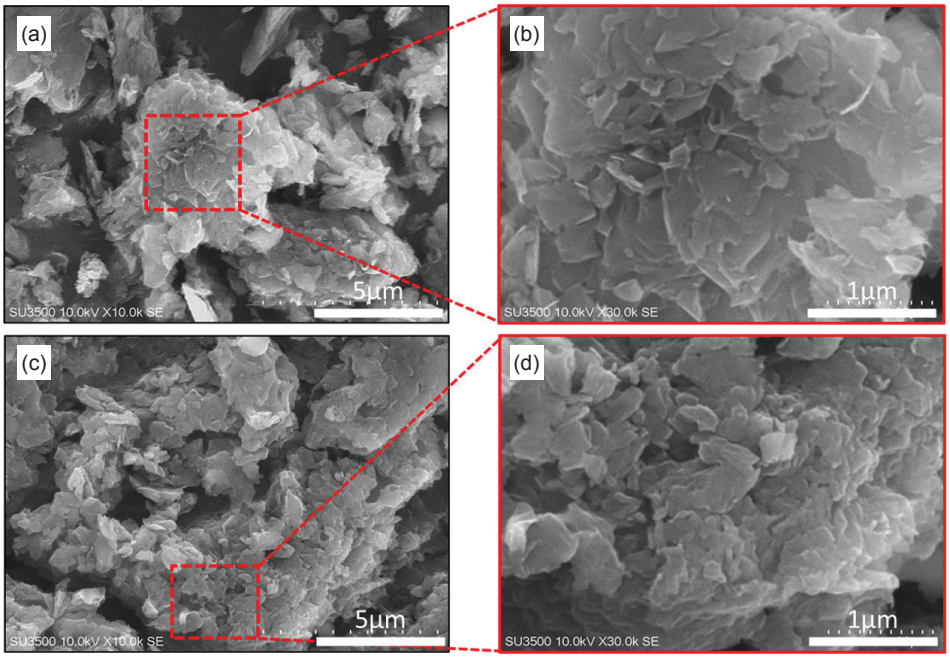


Figure 4. SEM images of (a and b) graphite powder and (c and d) graphite oxide.

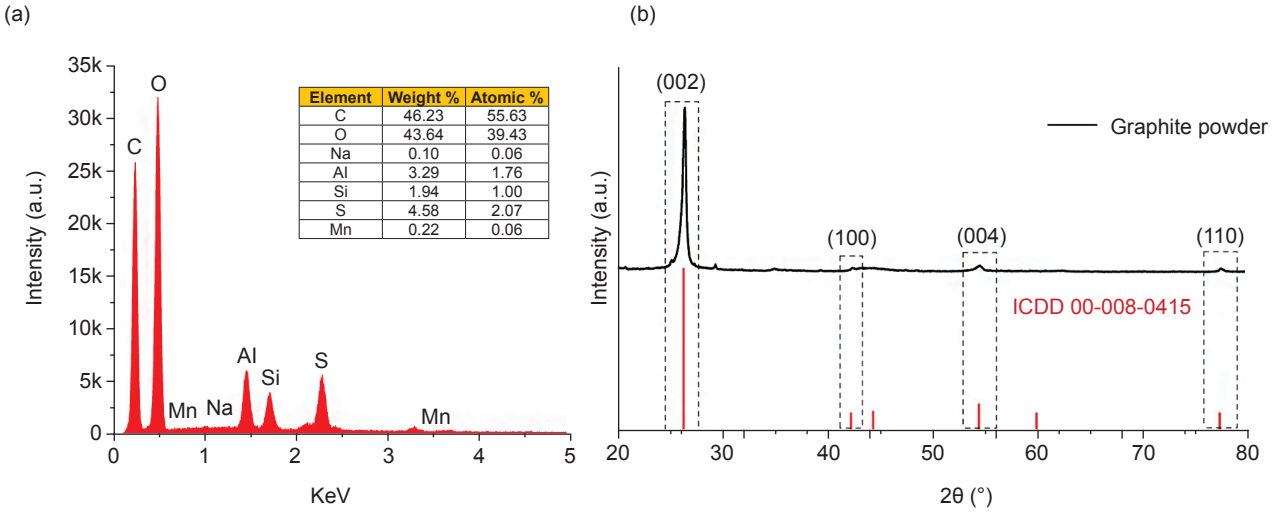


Figure 5. (a) EDS spectra and element analysis of graphite oxide, and (b) XRD spectra of graphite powder.

is illustrated in *Figure 6*. The result showed that the engine fuelled with pure palm oil graphite powder (PPaOG) produced lower power and torque than other fuels. The maximum engine power and torque decreased using PPaOG was 18.0% at 100.0% load, with the highest average power loss was 29.5% compared to DF. The increase in engine power and torque may be ascribed to the energy created in the cylinder because of an increase in the surface-to-volume ratio of the additive, as well as an increase in the heat transfer coefficient owing to the additives in the fuels (Heidari-Maleni *et al.*, 2020). The low heating value is one of the factors that contributes to the decreased engine power and torque that occurs when PPaO is used. *Figure 6* illustrates an important finding that the use of pure palm oil graphite oxide surfactant (PPaOGOS) leads to engine power and torque that are comparable to those produced by DF. This indicates that PPaOGOS has the potential to achieve similar performance levels as DF in terms of engine power and torque. Utilising PPaOGOS as the main fuel may increase the combustion rate due to the quick burning of PPaOGOS during the premixed

combustion stage. Other causes for the increase in engine power and torque are oxygen content in PPaOGOS, and a similar result was conducted by (Hoseini *et al.*, 2020).

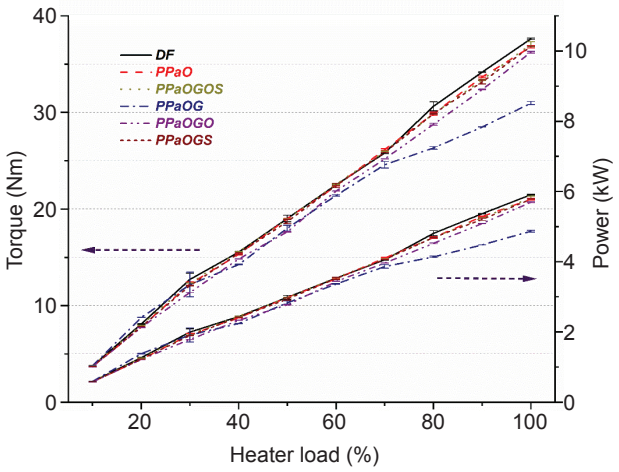


Figure 6. Comparison of power and torque with engine load.

Fuel Economy

Specific fuel consumption (SFC) and thermal efficiency are important performance parameters of an engine, which significantly impact its operation. SFC represents the amount of fuel consumed per unit of power output, while thermal efficiency is the ratio of the useful work output to the heat input. The engine load has a noticeable effect on both SFC and thermal efficiency, as shown in *Figure 7*. The findings demonstrate that at a load of 73.0%, PPaOG exhibits the highest increase in SFC, with a rise of 40.1%, and an average SFC of about 12.6% compared to DF. This is attributed to the fact that DF has a lower density and higher calorific value than PPaOG and other fuels, causing PPaOG to consume more fuel to produce the same amount of power as DF. Similar results were observed for other fuels blended with PPaO. These findings align with prior research conducted by (Radhakrishnan *et al.*, 2018; Syarif *et al.*, 2017).

In addition, the thermal efficiency of PPaO and PPaO blended with GP and GO was discovered to be higher than that of DF. The most significant increase in thermal efficiency was observed in PPaOG at an 82.0% load, with a rise of 20.4%. This is because PPaO has a lower calorific value than DF, resulting in a smaller energy input to the system while still delivering comparable engine power. Moreover, using GO as an additive enhances thermal efficiency more than GP, since the oxygen in PPaO combined with GO results in better fuel and air mixing, leading to increase efficiency. These findings are consistent with those of Syarif *et al.* (2017), who also reported a similar increase in thermal efficiency.

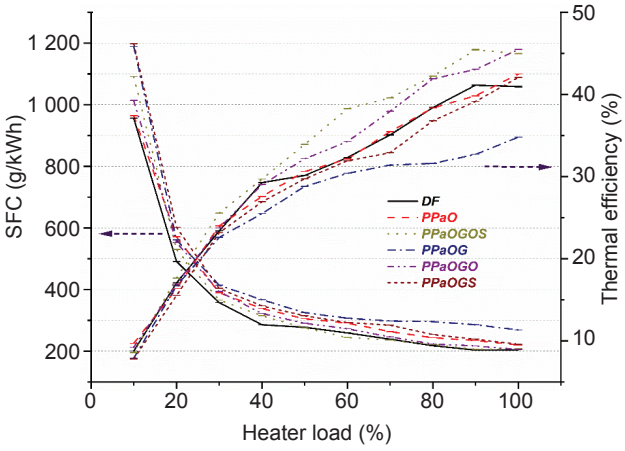


Figure 7. Comparison of SFC and thermal efficiency with engine load.

Smoke Emission

Diesel engines are known to emit significant amounts of particulate matter, which can have adverse effects on human health and the environment. Smoke opacity is a crucial indicator of the level of particulate matter emissions from diesel engines. Factors such as inadequate oxygen levels, longer oxidation residence time, and high in-cylinder temperatures all contribute to higher exhaust emissions, negatively impacting human health and the environment (Lv *et al.*, 2022). As illustrated in *Figure 8*, the use of PPaO resulted in a 127.0% increase in opacity, which is significantly higher compared to DF fuel. This can be attributed to the fact that PPaO has a much higher viscosity, ten times higher than DF, which leads to the formation of larger droplets that are difficult to burn and could result in incomplete combustion when entering the combustion chamber. On the other hand, the addition of GP and GO to PPaO significantly reduced the opacity, with the highest decrease observed for PPaOGOS by 63.9% compared to DF. Previous studies (Gavhane *et al.*, 2021; Prabu, 2018; Shaafi and Velraj, 2015) reported that adding nanomaterial additives to diesel and biodiesel can effectively reduce CO emissions. The addition of graphite and graphite oxide additives can serve as a fuel catalyst, which helps to smoothen the fuel droplets and leads to micro-explosions, making them more flammable and producing a better combustion process. Interestingly, Appavu and Venkata Ramanan (2020) found that the emissions of fuel containing nanoparticles are significantly lower than those of diesel at full load, as the nanoparticles can boost the atomisation rate and redox properties of the fuel, leading to complete combustion. In summary, the addition of GP and GO to PPaO has proven to be an effective method for reducing diesel engine opacity and improving combustion efficiency. Moreover, the use of alternative fuels, including those with

nanomaterial additives, could potentially contribute to long-term reductions in urban pollution and fossil fuel consumption.

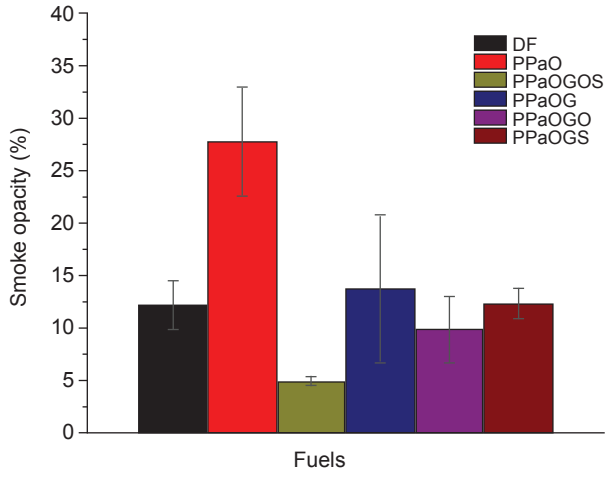


Figure 8. Smoke opacity emission.

CONCLUSION

The effects of adding fuel additives of GO and GP to diesel fuel and PPaO were investigated. It was found that the addition of GO and GP in PPaO improved the fuel properties such as LHV, flash point, viscosity. The SEM images revealed that the GO and GP particles were uniformly distributed in the fuel matrix, facilitating the heat transfer, and promoting the formation of a stable flame front.

In this study, the viscosity of diesel fuel was reduced through preheating, and the effects of adding GP and GO to PPaO were investigated. The results showed that the addition of GP and GO to PPaO significantly increased opacity by 127.0% compared to DF. Interestingly, the use of PPaOGOS resulted in a lower opacity, with a reduction of 63.9% compared to PPaO. The observed differences in opacity could be attributed to the varying sizes and shapes of the graphite particles, which affect light scattering in the fuel.

The study also evaluated the thermal efficiency of the fuels, with the highest thermal efficiency observed for PPaOG at a load of 82.0%, with an increase of 20.4% compared to DF, and an average increase of 0.3% with the use of the additive. However, it is worth noting that an increase in SFC was observed, with PPaOG showing the maximum increase at a load of 73.0%, with a rise of 40.1% compared to DF, and an average increase of about 12.6%. This increase in SFC may be due to the additional energy required to break down the larger graphite particles, which reduces the overall fuel energy efficiency.

Overall, the addition of graphite powder and graphite oxide to PPaO was found to be an effective approach to reduce diesel engine opacity and increase thermal efficiency compared to DF. These findings suggest that alternative fuels for diesel engines, such as PPaO with graphite powder and graphite oxide additives, could potentially contribute to the long-term reduction of urban pollution and fossil fuel consumption. Further research is needed to fully evaluate the potential benefits and drawbacks of alternative fuels and additives for diesel engines.

ACKNOWLEDGEMENT

The authors would like to thank Research and Community Service Program (PPMI), Institut Teknologi Bandung (ITB) for financial support and the undergraduate student in mechanical engineering program at Institut Teknologi Sumatera (ITERA) for their technical support for this research.

REFERENCES

Ahmad Daud, N; Chieng, B W; Ibrahim, N A; Talib, Z A; Muhamad, E N and Abidin, Z Z (2017). Functionalizing graphene oxide with alkylamine by gamma-ray irradiation method. *Nanomaterials, 7*: 135. DOI: 10.3390/nano7060135.

Appavu, P and Venkata Ramanan, M (2020). Study of emission characteristics of a diesel engine using cerium oxide nanoparticle blended pongamia methyl ester. *Int. J. Ambient Energy, 41*: 524-527. DOI: 10.1080/01430750.2018.1477063.

Atmanli, A (2016). Effects of a cetane improver on fuel properties and engine characteristics of a diesel engine fueled with the blends of diesel, hazelnut oil and higher carbon alcohol. *Fuel, 172*: 209-217. DOI: 10.1016/j.fuel.2016.01.013.

Atmanli, A (2020). Experimental comparison of biodiesel production performance of two different microalgae. *Fuel, 278*: 118311.

Atmanli, A and Yilmaz, N (2021). Comparative assessment of different diesel engines fueled with 1-pentanol and diesel blends. *Environ. Prog. Sustain. Energy, 40*: e13663. DOI: 10.1002/ep.13663.

Chen, A F; Adzmi, M A; Adam, A; Othman, M F; Kamaruzzaman, M K and Mrwan, A G (2018). Combustion characteristics, engine performances and emissions of a diesel engine using nanoparticle-diesel fuel blends with aluminium oxide, carbon nanotubes and silicon oxide. *Energy Convers. Manag., 171*: 461-477. DOI: 10.1016/j.enconman.2018.06.004.

De Almeida, S C; Belchior, C R; Nascimento, M V; Dos Sr Vieira, L and Fleury, G (2002). Performance of a diesel generator fuelled with palm oil. *Fuel., 81*: 2097-2102. DOI: 10.1016/S0016-2361(02)00155-2.

Dey, S; Reang, N; Das, P and Deb, M (2021). A comprehensive study on prospects of economy, environment, and efficiency of palm oil biodiesel as a renewable fuel. *J. Clean. Prod., 286*: 124981. DOI: 10.1016/j.jclepro.2020.124981.

Farobie, O and Hartulistiyoso, E (2021). Palm oil biodiesel as a renewable energy resource in Indonesia: Current status and challenges. *Bioenerg. Res., 15:* 1-19. DOI: 10.1007/s12155-021-10344-7.

Gavhane, R; Kate, A; Soudagar, M E M; Wakchaure, V; Balgude, S; Rizwanul Fattah, I; Nik-Ghazali, N N; Fayaz, H; Khan, T Y and Mujtaba, M (2021). Influence of silica nano-additives on performance and emission characteristics of soybean biodiesel fuelled diesel engine. *Energ., 14*: 1489. DOI: 10.3390/en14051489.

Geng, P; Cao, E; Tan, Q and Wei, L (2017). Effects of alternative fuels on the combustion characteristics and emission products from diesel engines: A review. *Renew. Sustain. Energ. Rev., 71*: 523-534. DOI: 10.1016/j.rser.2016.12.080.

Harahap, F; Leduc, S; Mesfun, S; Khatiwada, D; Kraxner, F and Silveira, S (2020). Meeting the bioenergy targets from palm oil based biorefineries: An optimal configuration in Indonesia. *Appl. Energ., 278*: 115749. DOI: 10.1016/j.apenergy.2020.115749.

Heidari-Maleni, A; Gundoshmian, T M; Karimi, B; Jahanbakhshi, A and Ghobadian, B (2020). A novel fuel based on biocompatible nanoparticles and ethanol-biodiesel blends to improve diesel engines performance and reduce exhaust emissions. *Fuel, 276*: 118079. DOI: 10.1016/j.fuel.2020.118079.

Hernandez, C L A; Cedeno, E; Rojas T, J B; Alvarado, S; Isidro, O M A; Vargas, E; Calderon, A; Marin, E and Mansanares, A M (2022). A comparison between thermal lens and conventional optical spectroscopy for monitoring of a photo catalytic process. *Rev. Mex. de Fis., 68*: 1-7. DOI: 10.31349/RevMexFis.68.021303.

Hoang, A T; Le, M X; Nižetić, S; Huang, Z; Ağbulut, Ü; Veza, I; Said, Z; Le, A T; Tran, V D and Nguyen, X P (2022). Understanding behaviors of compression ignition engine running on metal nanoparticle additives-included fuels: A control comparison between biodiesel and diesel fuel. *Fuel, 326*: 124981. DOI: 10.1016/j.fuel.2022.124981.

Hoseini, S; Najafi, G; Ghobadian, B; Ebadi, M; Mamat, R and Yusaf, T (2020). Biodiesels from three feedstock: The effect of graphene oxide (GO) nanoparticles diesel engine parameters fuelled with biodiesel. *Renew. Energ., 145*: 190-201. DOI: 10.1016/j.renene.2019.06.020.

Hussain, R; Alican Noyan, M; Woyessa, G; Retamal Marín, R R; Antonio Martinez, P; Mahdi, F M; Finazzi, V; Hazlehurst, T A; Hunter, T N and Coll, T (2020). An ultra-compact particle size analyser using a CMOS image sensor and machine learning. *Light: Sci. Appl., 9*: 21. DOI: 10.1038/s41377-020-0255-6.

Kegl, B; Kegl, M and Pehan, S (2013). *Green Diesel Engines.* Springer. London. p. 5-50.

Kegl, T; Kralj, A K; Kegl, B and Kegl, M (2021). Nanomaterials as fuel additives in diesel engines: A review of current state, opportunities, and challenges. *Prog. Energy Combust. Sci., 83*: 100897. DOI: 10.1016/j.pecs.2020.100897.

Khairil; Riayatsyah, T M I; Bahri, S; Sofyan, S E; Jalaluddin, J; Kusumo, F; Silitonga, A S; Padli, Y; Jihad, M and Shamsuddin, A H (2020). Experimental study on the performance of an SI engine fueled by waste plasticpyrolysis oil-gasoline blends. *Energies, 13*: 4196.

Lv, J; Wang, S and Meng, B (2022). The effects of nano-additives added to diesel-biodiesel fuel blends on combustion and emission characteristics of diesel engine: A Review. *Energies, 15*: 1032. DOI: 10.3390/en15031032.

Ooi, J B; Ismail, H M; Swamy, V; Wang, X; Swain, A K and Rajanren, J R (2016). Graphite oxide nanoparticle as a diesel fuel additive for cleaner emissions and lower fuel consumption. *Energy & Fuels., 30*: 1341-1353. DOI: 10.1021/acs.energyfuels.5b02162.

Ooi, J B; Rajanren, J R; Ismail, H M; Swamy, V and Wang, X (2017). Improving combustion characteristics of diesel and biodiesel droplets by graphite oxide addition for diesel engine applications. *Int. J. Energy Res., 41*: 2258-2267. DOI: 10.1002/er.3787.

Pipitone, E and Costanza, A (2018). An experimental investigation on the long-term compatibility of preheated crude palm oil in a large compression ignition diesel engine. *Biofuel Res. J., 5(4)*: 900-908. DOI: 10.18331/BRJ2018.5.4.5.

Prabu, A (2018). Nanoparticles as additive in biodiesel on the working characteristics of a DI

diesel engine. *Ain Shams Eng. J., 9*: 2343-2349. DOI: 10.1016/j.asej.2017.04.004.

Radhakrishnan, S; Munuswamy, D B; Devarajan, Y and Mahalingam, A (2018). Effect of nanoparticle on emission and performance characteristics of a diesel engine fueled with cashew nut shell biodiesel. *Energy Sources, Part A: Recovery, Utilization and Environmental Effects, 40*: 2485-2493. DOI: 10.1080/15567036.2018.1502848.

Razzaq, L; Mujtaba, M; Soudagar, M E M; Ahmed, W; Fayaz, H; Bashir, S; Fattah, I R; Ong, H C; Shahapurkar, K and Afzal, A (2021). Engine performance and emission characteristics of palm biodiesel blends with graphene oxide nanoplatelets and dimethyl carbonate additives. *J. Environ. Manag., 282*: 111917. DOI: 10.1016/j.jenvman.2020.111917.

Riayatsyah, T M I; Thaib, R; Silitonga, A S; Milano, J; Shamsuddin, A H; Sebayang, A H; Sutrisno, J and Mahlia, T M I (2021). Biodiesel production from *Reutealis trisperma* oil using conventional and ultrasonication through esterification and transesterification. *Sustainability, 13*: 3350. DOI: 10.3390/su13063350.

Ropandi, M; Hayawin, Z N; Astimar, A; Noorshamsiana, A; Ridzuan, R and Zawawi, I (2022). Effect of biofuel on light-duty vehicles engine performance and lube oil degradation. *J. Oil Palm Res., 34*: 104-115. DOI: 10.21894/jopr.2021.0023.

Sa, B; Markov, V; Liu, Y; Kamaltdinov, V and Qiao, W (2021). Numerical investigation of the effect of multi-walled carbon nanotube additive on nozzle flow and spray behaviors of diesel fuel. *Fuel, 290*: 119802. DOI: 10.1016/j.fuel.2020.119802.

Sani, K; Siallagan, M; Putro, U S and Mangkusubroto, K (2018). Indonesia energy mix modelling using system dynamics. *Int. J. Sustain. Energy Plan. Manag., 18*: 29-51. DOI: 10.5278/ijsepm.2018.18.3.

Sebayang, A; Milano, J; Alfansuri, M; Silitonga, A; Kusumo, F; Prahmana, R A; Fayaz, H and Zamri, M (2022). Modelling and prediction approach for engine performance and exhaust emission based on artificial intelligence of sterculia foetida biodiesel. *Energ. Rep., 8*: 8333-8345.

Shaafi, T and Velraj, R (2015). Influence of alumina nanoparticles, ethanol and isopropanol blend as additive with diesel-soybean biodiesel blend fuel: Combustion, engine performance and emissions. *Renew. Energy, 80*: 655-663. DOI: 10.1016/j.renene.2015.02.042.

Sonara, V D and Rathod, P P (2022). Droplet combustion and ignition analysis of carbon multiwall nanotube and alumina blended jatropha biodiesel. *Materials Today: Proceedings, 59(1)*: 101-106.

Syarif, A C; Reksowardojo, I K and Harjono, J E (2017). Uji prestasi dan emisi diesel berbahan bakar minyak nabati murni untuk pembangkitan daya di daerah terpencil. *Jurnal Power Plant, 8*: 18-23. DOI: 10.33322/powerplant.v5i1.115.

Vellaiyan, S (2019). Enhancement in combustion, performance, and emission characteristics of a diesel engine fueled with diesel, biodiesel, and its blends by using nanoadditive. *Environ. Sci. Pollut. Res., 26*: 9561-9573. DOI: 10.1007/s11356-019-04356-2.

Xin, Y; Sun, L and Hansen, M C (2022). Oil palm reconciliation in Indonesia: Balancing rising demand and environmental conservation towards 2050. *J. Clean. Prod., 380*: 135087. DOI: 10.1016/j.jclepro.2022.135087.

Yilmaz, N; Atmanli, A and Trujillo, M (2017). Influence of 1-pentanol additive on the performance of a diesel engine fueled with waste oil methyl ester and diesel fuel. *Fuel, 207*: 461-469. DOI: 10.1016/j.fuel.2017.06.093

Yilmaz, N; Atmanli, A; Hall, M J and Vigil, F M (2022a). Determination of the optimum blend ratio of diesel, waste oil derived biodiesel and 1-pentanol using the response surface method. *Energies, 15*: 5144.

Yilmaz, N; Vigil, F M; Atmanli, A and Donaldson, B (2022b). Detailed analysis of PAH formation, toxicity and regulated pollutants in a diesel engine running on diesel blends with n-propanol, n-butanol and n-pentanol. *Energies, 15*: 6487. DOI: 10.3390/en15176487.

Zhao, Y; Li, T; Niu, T; Zheng, W; Xie, Y and Weibo, E (2023). Performance and emissions of a diesel engine fueled by coal-based diesel fuels and their blends with polyoxymethylene dimethyl ethers. *Sci. Rep., 13*: 1053. DOI: 10.1038/s41598-023-28283-y.

Journal of Oil Palm Research Vol. 36 (3) September 2024 p. 456-468
DOI: https://doi.org/10.21894/jopr.2023.0032

RENEWABLE ENERGY AND GREENHOUSE GASES EMISSION REDUCTION POTENTIAL OF BIOGAS FROM PALM OIL MILL EFFLUENT

ABU BAKAR NASRIN[1,2]; ABDUL AZIZ ABDUL RAMAN[1]*; MOHAMAD AZRI SUKIRAN[2]; NURUL ADELA BUKHARI[2]; ARCHINA BUTHIYAPPAN[3]; VIJAYA SUBRAMANIAM[2]; ASTIMAR ABDUL AZIZ[2] and SOH KHEANG LOH[2]

ABSTRACT

Emissions of biogas from palm oil mill effluent (POME) via anaerobic digestion is a greenhouse gas (GHG) that can be mitigated by capturing and utilising as renewable energy (RE). Huge energy potential of biogas has been reported, but none has specifically explored this potential based on actual scenario of mills equipped with biogas plants in the Malaysian palm oil industry. This study analyses the potential of biogas from POME for RE and GHG emissions reduction from two scenarios: Overall (nationwide) and mills having biogas plants. The overall potential of biogas volume, electricity generation and bio-compressed natural gas (Bio-CNG) production from all palm oil mills in 2021 were estimated at 1648 million m^3, 508 MW and 988 million m^3 Bio-CNG, respectively. With 135 mills having biogas capturing facilities, 33% of the country's overall potential energy from POME could be harnessed and utilised to potentially mitigate 4.96 million tonnes CO_2eq GHG annually. The study indicated that electricity generation is the major use of biogas in the country, particularly for grid connection. Activities of biogas capture and utilisation have thus demonstrated a feasible approach in addressing sustainable issue of the palm oil industry, which contribute to RE and GHG reduction targets in Malaysia.

Keywords: bio-compressed natural gas, biogas utilisation, electricity, palm oil, sustainability.

Received: 18 October 2022; **Accepted:** 1 June 2023; **Published online:** 2 August 2023.

INTRODUCTION

Fossil fuels such as crude oil, natural gas and coal contributed about 93% to the primary energy supply in Malaysia in 2018 (Suruhanjaya Tenaga, 2021). Heavy dependence on fossil fuels may lead to an energy crisis as well as an increased environmental problem such as global warming. Over the past years, two detrimental global threats, *i.e.*, COVID-19 pandemic and Russia-Ukraine crisis had seriously attributed to energy crisis with positive impact on greenhouse gases (GHG) emission. This unprecedented phenomenon serves as a catalyst for boosting the world to transition from fossil fuels to renewable energy (RE) while focusing on economic recovery measures. RE has been placed as a long-term solution for cushioning energy security and climate change in line with the Sustainable Development Goals 7 and 13 established by the United Nations in 2015 (United Nations, 2022). Under the Malaysia Renewable Energy Roadmap 2035, the Government targets to increase RE share in the national power installed capacity to 31% by 2025 with foreseeable reduction in GHG emissions (SEDA, 2022). Biomass including biogas generated from the palm oil industry could play a vital role in supporting the country's RE development and GHG mitigation targets.

Malaysia is the world's second largest producer and exporter of palm oil, producing 19.14 million tonnes of crude palm oil (CPO) which contributed 34.3% to the total palm oil traded worldwide in 2020

[1] Sustainable Process Engineering Centre (SPEC), Department of Chemical Engineering, Faculty of Engineering, University Malaya, 50603 Kuala Lumpur, Malaysia.

[2] Malaysian Palm Oil Board, 6, Persiaran Institusi, Bandar Baru Bangi, 43000 Kajang, Selangor, Malaysia.

[3] Institute of Ocean and Earth Sciences, C308, Institute for Advanced Studies Building, University of Malaya, 50603 Kuala Lumpur, Malaysia.

* *Corresponding author e-mail: azizraman@um.edu.my*

(Parveez *et al.*, 2021). As a result, an abundance of non-oil biomass by-products is also generated, including approximately 100 million tonnes (wet basis) of oil palm biomass annually in solid and liquid forms from palm oil mills (POMs) alone. These resources have been commercially used as fuel while many opportunities still exist for RE, in particular biogas from palm oil mill effluent (POME).

POME is the liquid by-product generated from palm oil milling activities, at an estimated volume of >60 million m^3 annually in Malaysia (Loh *et al.*, 2022). It is characterised as a highly polluted wastewater with high value of biological oxygen demand (25 000 mg L^{-1}) and chemical oxygen demand (COD) (51 000 mg L^{-1}) (Bello and Raman, 2017). The conventionally deployed open ponding systems or tanks via anaerobic digestion (AD) for POME is less environmentally-friendly with release of biogas to the atmosphere (Loh *et al.*, 2013). Uncaptured biogas consists of mainly 60%-70% methane (CH_4) and 30%-40% carbon dioxide (CO_2), in which both are GHG that cause global warming and major threat to sustainable palm oil production. Biogas capture and utilisation appears to be a promising way to address these issues and add value to POME treatment.

Economic and environmental benefits and potential of biogas from POME in the Malaysian palm oil industry are widely available in the literature. Few studies indicated that POMs equipped with biogas plant generate lower GHG of 134-196 kg CO_2eq t^{-1} CPO, compared to 814-896 kg CO_2eq t^{-1} CPO from conventional mill (Lim and Biswas, 2019; Subramaniam *et al.*, 2010). Lim and Biswas (2019) also reported that an increase of 2.3% annual mill revenue could be achieved by selling the raw biogas to nearby factory. A life cycle cost benefits analysis indicated that energy generation from POME-based biogas using digester tank technology has higher life cycle cost and cost benefits compared to that via covered lagoon technology (Sharvini *et al.*, 2022). In this regard, it is highly potential to encourage more biogas capturing and utilisation activities through policy intervention. Chia *et al.* (2020) reported that 510 000 t of CH_4 were generated from 58.5 million tonnes of POME in 2018. Recently, a computed potential of 3.5 million MWhr of electricity could be anticipated from 1789 million m^3 of biogas in POMs nationwide (Loh *et al.*, 2022). These reported potentials vary significantly as the feedstock availability was only estimated based on the total fresh fruit bunches (FFB) processed nationwide plus standard biomass (feedstock) to FFB extraction rate, regardless of biogas plant status in POMs. To date, biogas actual potential (RE and GHG savings) can only be gauged based on limited assessment, which is theoretical at large, without determining from actual scenario of POMs installed with biogas plants. As current scenario of the industry focuses on sustainable development and income maximisation, an up-to-date biogas status from POME, its roles and contribution for RE and GHG mitigations need to be reviewed and reassessed.

In this study, a systematic reassessment was performed on the RE and GHG savings potential of biogas capture and utilisation in the Malaysian POMs. A series of formulas was constructed and used to determine these potentials based on the latest total number of biogas plants operated in POMs. A survey was carried out to consolidate the status of national biogas development by millers focusing on technology used and utilisation pathway deployed. This study is original and novel in reciting the biogas potentials based on a systematic analysis of actual annual FFB process sourced from the respective mills plus national distribution in biogas pathway including a further breakdown in electricity end-uses and their installed capacity. This kind of information will be the first of its kind in the country that serves to reflect actual progress on the ground. The resulted up-to-date information on biogas development, potential RE plus the associated GHG emissions and potential savings will strengthen national reporting and shed light on future biogas endeavours and improvements gearing towards sustainable palm oil production.

MATERIALS AND METHODS

Potential Biogas and Renewable Energy (RE) from Palm Oil Mill Effluent (POME)

Potential of biogas and RE generation from POME was assessed based on two different scenarios, namely overall technical potential and actual potential. The former refers to the country's total potential of biogas calculated from all POMs while the latter analyses the actual potential of biogas generated from the total number of mills installed with biogas capture facilities. The overall technical potential for production year of 2019-2021 was determined based on the actual FFB processed annually (*Table 1*). The amount of FFB processed by 135 mills equipped with biogas plant in 2021 was used to estimate the actual potential of biogas and RE from the respective mills.

Table 1 summarises the primary data used for this study. FFB processing capacity and total amount of FFB processed of the mills from 2019-2021 were sourced from the Economic Industry Development Division, Malaysian Palm Oil Board (MPOB) (MPOB, 2022).

The amount of biogas generated and its potential for various applications such as electricity and bio-compressed natural gas (Bio-CNG) or biomethane could be calculated based on the availability of POME. It is estimated that 1 t of FFB could produce

TABLE 1. APPROVED FRESH FRUIT BUNCHES (FFB) CAPACITY AND AMOUNT OF FFB PROCESSED OF THE MALAYSIAN PALM OIL MILLS (2019-2021)

Year	2019	2020	2021	Mills with biogas plant (2021)
No. of mills	452	457	451	135
Approved FFB capacity, million tonnes	112.91	116.81	116.72	40.10
FFB processed, million tonnes	98.28	96.09	90.53	29.93
[a]Capacity utilisation, %	87.0	82.3	77.6	74.6

Note: [a]FFB processed / approved FFB capacity.

0.65 m^3 POME (Akhbari *et al.*, 2020) with biogas generation rate of 28 m^3 biogas for every m^3 POME (Loh *et al.*, 2017). Equations (1) and (2) as reported in Sarwani *et al.* (2019) were used to calculate the potential amount of $POME_{volume}$ (m^3) and $Biogas_{volume}$ (m^3) from the FFB processed in POMs.

$$POME_{volume} = 0.65 \times FFB_{processed} \quad (1)$$

where 0.65 is the generation rate of POME per t FFB processed (m^3 t^{-1}) (Akhbari *et al.*, 2020) and $FFB_{processed}$ is the amount of FFB processed by the mills (t).

$$Biogas_{volume} = 28 \times POME_{volume} \quad (2)$$

where 28 is the production rate of biogas, m^3 m^{-3} POME (Loh *et al.*, 2017).

The potential of heat energy from biogas: $Energy_{potential}$ (MJ) and $Electricity_{potential}$ (MW), *i.e.*, electricity installed capacity were calculated based on Equation (3) and (4) (Loh *et al.*, 2017) as follows:

$$Energy_{potential} = Biogas_{volume} \times CV_{biogas} \quad (3)$$

$$Electricity_{potential} = Biogas_{volume} \times CV_{biogas} \times \frac{1}{3600} \times \eta_{gas\ engine} \times \frac{1}{7200} \quad (4)$$

where CV_{biogas} is the calorific value of biogas, 20 MJ m^{-3} (Loh *et al.*, 2017), $\frac{1}{3600}$ refers to conversion factor of 1 MJ to MWhr, $\frac{1}{7200}$ is the annual average operation hour (hr^{-1}) of biogas power plant, and $\eta_{gas\ engine}$ refers to 40% efficiency of the gas engine (Chin *et al.*, 2013).

The equivalent potential of diesel and natural gas from the potential energy available from biogas could be determined based on calorific values of diesel and natural gas, which are 35.14 MJ L^{-1} (Chin *et al.*, 2013) and 35 MJ m^{-3} estimated from Lee *et al.* (2019), respectively using Equations (5) and (6) which were developed according to Chin *et al.* (2013):

$$Diesel_{equivalent} = Energy_{potential} \div CV_{diesel} \quad (5)$$

$$Natural\ gas_{equivalent} = Energy_{potential} \div CV_{natural\ gas} \quad (6)$$

Assuming the mean composition of CH_4 in biogas is 60% (Loh *et al.*, 2017), the potential conversion of biogas into Bio-CNG, $BioCNG_{potential}$ (m^3) could be determined using Equation (7) (Sarwani *et al.*, 2019) as follows:

$$BioCNG_{potential} = 0.6 \times Biogas_{volume} \quad (7)$$

where 0.6 is the average ratio of CH_4 to biogas. Since the energy content of natural gas is measured in MMBTu, the equivalent conversion factor used is 1 MMBTu = 28.26 m^3 Bio-CNG (Mundi, 2021).

Greenhouse Gases Emissions and Potential Savings from Biogas Capture and Utillisation

The amount of GHG emissions from biogas of POME could be determined from the amount of CH_4 generated, $CH_{4volume}$ as shown in Equation (8) (Hasanudin and Haryanto, 2018), which is estimated using default value of CH_{4yield}, 0.25 kg CH_4 kg^{-1} COD removed (Chin *et al.*, 2013) as follows:

$$CH_{4volume} = POME_{volume} \times COD_{POME} \times 1000\ (L) \times CH_{4yield} \quad (8)$$

where $CH_{4volume}$ is the amount of CH_4 generated (t) from POME via AD, volume conversion (m^3 to L) of 1000 and COD_{POME} is the mean value of COD for POME, 51 000 mg L^{-1} (Bello and Raman, 2017).

As the global warming potential of CH_4, GWP_{CH_4} is 25 times that of CO_2 (Subramaniam *et al.*, 2021), the associated GHG emissions could be determined using Equation (9) (Loh *et al.*, 2017) as follows:

$$GHG_{emissions} = CH_{4volume} \times GWP_{CH_4} \quad (9)$$

where $GHG_{emissions}$ is the amount of GHG emitted from AD of POME (t CO_2eq), and GWP_{CH_4} is 25.

The potential of GHG savings, $GHG_{savings}$ (t CO_2eq) from biogas capture activities in POMs could be calculated using Equation (10) (Subramaniam *et al.*, 2021) based on an overall 80% of plant efficiency (assumed based on COD removal from POME during AD and also biogas capturing efficiency) as follows:

$$GHG_{savings} = GHG_{emissions} \times 0.8 \quad (10)$$

The potential GHG savings, ($GHG_{electricity}$, t CO_2eq) made from the use of biogas for electricity generation could be determined using Equation (11) according to Subramaniam *et al.* (2021). It was calculated based on an average emission factor (EF) of grid electricity system for Peninsular Malaysia, Sabah and Wilayah Persekutuan Labuan, and Sarawak.

$$GHG_{electricity} = Electricity_{potential} \times 7200 \times EF \quad (11)$$

where $Electricity_{potential}$ is the installed capacity of electricity from biogas for each region (MW), 7200 is the annual operating hours (hr) of biogas plant, and EF is the CO_2 emission factor as follows:

Baseline EF: Peninsular Malaysia, 0.585 t CO_2 $MWhr^{-1}$; Sabah and Wilayah Persekutuan Labuan, 0.522 t CO_2 $MWhr^{-1}$ and Sarawak, 0.330 t CO_2 $MWhr^{-1}$ (MGTC, 2019).

Status of Biogas Capture and Utilisation

Analysis on status of biogas capturing facilities and their utilisation approaches in the Malaysian POMs was conducted via a survey using previously collected database in 2021. *Table 2* shows the location of the biogas plant installed in 135 POMs nationwide. Status and information of these biogas plants were collected and verified via a phone call to either the millers directly, representative of mill's parent company or RE developers that have successfully built, owned and operated the biogas plants. Questions to respondents were on status of biogas plant, technology used, type of utilisation, installed capacity (MW) and future planning, if any for those biogas plants currently on flaring option. The findings were summarised as number of mills plus percentage biogas utilisation or number of mills plus total installed capacity (MW).

TABLE 2. NUMBER OF BIOGAS PLANT IN PALM OIL MILLS (BY STATE) IN 2021

State	No. of mills with biogas plant	State	No. of mills with biogas plant
Johor	23	Perak	17
Kedah	4	Pulau Pinang	1
Kelantan	1	Sabah	34
Melaka	1	Sarawak	14
Negeri Sembilan	6	Selangor	6
Pahang	25	Terengganu	3

RESULTS AND DISCUSSION

Volume of Wastewater (POME)

As of December 2021, there were 451 POMs in operation nationwide with a total approved annual FFB processing capacity of 112.91 million tonnes. The total FFB processed in 2019 (425 mills), 2020 (457 mills) and 2021 (451 mills) were 98.28, 96.09 and 90.53 million tonnes, respectively, and thus a depreciation trend observed nationally in milling capacity utilisation from 87.0%, 82.3% to 77.6%. The approved annual FFB processing capacity and actual FFB processed by the mills equipped with biogas plant in 2021 was 40.10 and 29.93 million tonnes, respectively. *Figure 1* and *Table 3* show the estimated amount of POME generated from the Malaysian POMs from 2019 to 2021.

The POME generation decreased from 63.88 to 58.84 million m^3, with mean value of 61.72 million m^3 during these periods, 2019-2021 (*Figure 1*). This big volume is indicative of a huge availability of POME as reported in previous years; 60.88 and 58.50 million m^3 in 2015 and 2018, respectively (Chia *et al.*, 2020; Choong *et al.*, 2018). For 135 mills equipped with biogas plant, 19.45 million m^3 of POME were anaerobically treated in closed digesters in 2021 (*Table 3*). The higher POME generation in 2019 was attributed to higher FFB yield and the subsequent processed fruits which consumed more water during the milling process, compared to the lower FFB productivity for the two consecutive years associated with COVID-19 pandemic. Generation of POME is dependent on the amount of FFB processed. Restricted movement of COVID-19 and labour shortage have significantly contributed to the declining trend of FFB yield and FFB processed in 2020 and 2021 (Parveez *et al.*, 2021). Such occurrence brought about lesser amount of water used for milling activities, and thus lower POME generation compared to 2019. The COVID-19 pandemic has also caused immediate and adverse impact to the country's POME-based biogas development.

A conventional mill requires an average of 1.0-1.2 m^3 water for every tonnes of FFB processed (Kospa *et al.*, 2017), where >50% of water is discharged as POME (Loh *et al.*, 2013). The annual trend of FFB processed, either at national or individual mill level, is an important parameter needed to plan, forecast and design appropriate biogas plant capacity and its potential utilisation options.

Biogas Production from Palm Oil Mill Effluent

Figure 1 and *Table 3* also show the estimated total volume of biogas production via business-as-usual scenario, *i.e.*, AD of POME in all POMs nationwide in 2019-2021. Based on 28 m^3 m^{-3} POME, the biogas production potential significantly decreased from 1789 to 1648 million m^3 during these periods. Similarly, as biogas production is proportionate to the amount of FFB processed, the total volume of POME also showed downward trend for the past three years. The biogas yield of 28 m^3 m^{-3} POME, for estimating biogas potential, is an established biogas generation rate for POME obtained from comprehensive experimental and field monitoring data; as demonstrated by previous studies (Lim and Biswas, 2019; Muzzammil and Loh, 2020). The range of biogas yield is 24-32 m^3 m^{-3} POME using various

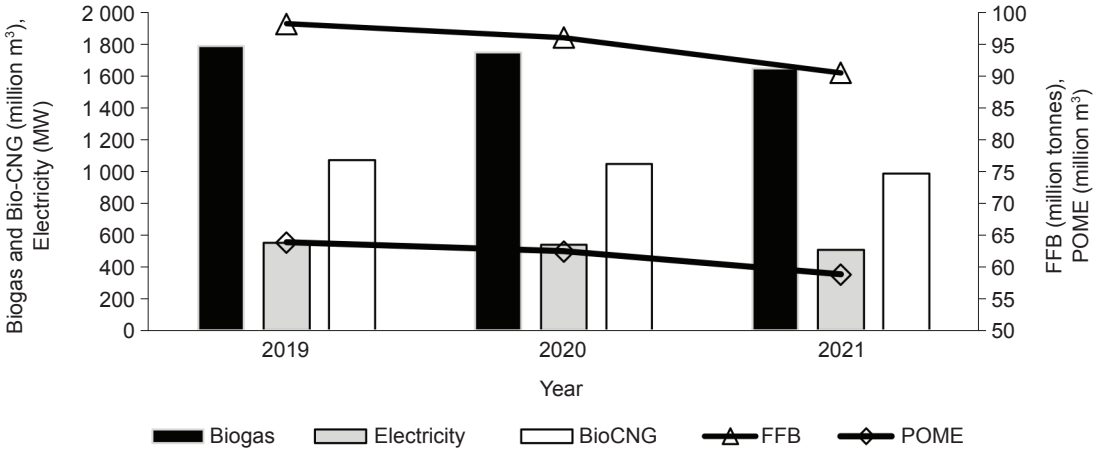


Figure 1. Estimated volume of palm oil mill effluent (POME), biogas and bio-compressed natural gas (Bio-CNG), and renewable electricity potential derived from fresh fruit bunches (FFB) processed in the Malaysian palm oil mills (2019-2021).

TABLE 3. ESTIMATED ANNUAL RENEWABLE ENERGY POTENTIAL FROM FRESH FRUIT BUNCHES (FFB) PROCESSED, PALM OIL MILL EFFLUENT (POME) AND BIOGAS GENERATION

Item	2019	2020	2021	135 mills with biogas plant (2021)
FFB processed, million tonnes	98.28	96.09	90.53	29.93
POME production, million m^3	63.88	62.46	58.84	19.45
Biogas generation, million m^3	1 789	1 749	1 648	545
Energy potential, million MJ	35 780	34 980	32 960	10 895
Diesel equivalent, million L	1 018	995	938	310
Natural gas equivalent, million m^3	1 022	1 000	942	311
Electricity (installed capacity), MW	552	539	508	168
Bio-CNG, million m^3	1 073	1 049	989	327

technologies (Muzzammil and Loh, 2020). If biogas is not captured in POMs, the potential RE is wasted. More critically, CH_4 and CO_2 in biogas are emitted to the atmosphere contributing to GHG emissions and causing global warming. The capturing facilities established from 135 mills could prevent about 545 million m^3 biogas from being released to the atmosphere, which means 33% RE potential have been tapped from the overall potential in 2021.

Renewable Energy (Biogas) Potential from Palm Oil Mill Effluent

Table 3 summarises the potential of various types of RE that can be derived from biogas. Biogas contains an average of 60%-70% CH_4, 30%-40% CO_2 and 800-1500 ppm H_2S (Loh *et al.*, 2017). Energy potential or calorific value of biogas relies on CH_4 content as a combustible gas. The calorific value of biogas containing 55%-65% CH_4 is typically between 19.7-23.3 MJ m^{-3} (Kaparaju and Rintala, 2013). Assuming that biogas from POME has a calorific value of 20 MJ m^{-3}, the total annual energy potential from the generated biogas has decreased from 35 780 MJ in 2019 to 32 960 MJ in 2021. More importantly, these values are equivalent to more than 938 million L diesel or 942 million m^3 natural gas annually, if the biogas is fully harnessed as an alternative to fossil fuels. Biogas is typically used for heat or power generation, or by combining both the energy sources in a combined heat and power (CHP) plant via combustion process. A direct method to exploit biogas as RE in the forms of heat or steam is through either package boiler, burner or cofiring with biomass in palm oil mill boiler (Loh *et al.*, 2017).

Internal combustion engine or gas engine is commonly deployed for commercial electricity generation from biogas. Raw biogas is pre-treated to remove H_2S and moisture prior to being burnt in the gas engine. The heat generated from this conversion system can be recovered and used as energy. Other energy conversion systems for biogas to electricity generation are gas or micro gas turbine, diesel generator (via cofiring) and fuel cell (Kaparaju and Rintala, 2013). The potential annual electricity generation from POME-based biogas is

estimated to be 3.65-3.97 million MWhr or 508-552 MW installed capacity if all the captured biogas is used for electricity generation. Power generation capacity is dependent on the thermal efficiency of a gas engine. Studies reported that thermal efficiencies of natural gas-based and biogas-based engines can range between 38%-42% and 28%-30%, respectively (Firdaus *et al.*, 2017). The country's total installed capacity for electricity generation in 2019 was 36 182.8 MW, consisted mainly of fossil-based power (78.1%), hydropower (17.1%) and renewables (4.8%) including 0.4% from biogas (Suruhanjaya Tenaga, 2021). Current scenario indicates that electricity potential of biogas from POME could contribute about 1.4%-1.5% to the national installed capacity mix and about 4.0% to the RE share (12 916.0 MW) target by 2025 under the Malaysia Renewable Energy Roadmap (SEDA, 2022). The roadmap also targets 40.0% RE share or 17 996.0 MW in 2035.

An emerging RE potential of biogas is the upgraded methane-rich Bio-CNG, a natural gas like fuel which is more versatile for effective and wider applications. The process involves multi-stage procedures by primarily removing CO_2, H_2S and moisture in raw biogas to ultra-low purification level using physical, chemical and biological methods, which leads to CH_4 enrichment. H_2S removal from POME-based biogas for Bio-CNG production has been carried out using a combined biological and physical adsorption of activated carbon, followed by chemical absorption to achieve 99% of removal efficiencies (Nasrin *et al.*, 2020; Park, 2021). Membrane technology used for CO_2 removal from POME-based biogas has enabled 94% of removal efficiencies with 98% CH_4 content in the resultant Bio-CNG (Park, 2021). Other major CO_2 removal technologies are pressurised water scrubber, pressure and vacuum swing adsorption, *etc*.

Potential of Bio-CNG from POME was estimated to be about 1073, 1049 and 989 million m^3 in 2019-2021. These values are equivalent to 35-38 million MMBTU Bio-CNG per year. In 2018, natural gas consumption from pipelines supplied by Gas Malaysia Berhad and Sabah Energy Corporation Sdn. Bhd. was 201 MMBTU (Suruhanjaya Tenaga, 2021). Assuming that all the captured biogas is upgraded to Bio-CNG and supplied to the natural gas pipelines nationwide, about 17%-19% of the piped gas can be potentially supplied to consumers. Feeding and funding mechanisms, infrastructure and logistic supports as well as the governmental frameworks are needed to further accelerate the development of Bio-CNG plant and natural gas blending via the pipelines.

The potential RE, as technically estimated above, can only be realised if all 451 POMs were installed with biogas capturing facilities while treating POME at the same time to meet the regulatory discharge limits. As of December 2021, some 135 POMs installed and captured biogas for various energy utilisation including just flared the captured biogas. This represents about 30% from the total number of POMs operated in 2021. *Table 3* shows the potential energy, electricity and Bio-CNG of 10 895 million MJ, 168 MW and 327 million m^3, respectively from 135 mills equipped with biogas facilities, based on 29.93 million tonnes FFB processed and 19.45 million m^3 POME generated. These values represented 33% of the total RE potential available from POME generated in 2021, and thus huge biogas potential is untapped in the country.

Greenhouse Gases (GHG) Emissions and Potential GHG Savings

Table 4 summarises the estimated GHG emissions from conventional POME treatment system from 2019 to 2021. The amount of CH_4 generated from AD of POME was 814 496, 796 346 and 750 268 t yr^{-1}, respectively. These values are equivalent to 18.76-20.36 million tonnes CO_2eq yr^{-1} nationwide, based on 25 times greater global warming potential of CH_4 than CO_2. It is slightly higher than the life cycle GHG emissions of 17.80, 17.15 and 16.24 million tonnes CO_2eq yr^{-1} calculated based on 896.48 kg CO_2eq t^{-1} CPO (Subramaniam *et al.*, 2010). The total GHG emissions from POME nationwide contributed about 6.8%-7.5% to the country's total GHG emissions in 2020 (272.61 million tonnes CO_2eq) (Ritchie *et al.*, 2020).

Uncaptured biogas is one of the dominant contributors of GHG emissions along the palm oil supply chain. It contributes about 50% to the total GHG emissions of CPO production (Krishnan *et al.*, 2017), with the remaining dominated by chemical fertilisers produced and used in oil palm plantations (Subramaniam *et al.*, 2021). Biogas trapping facilities give huge savings and greatly address the GHG emissions from POMs. The potential to generate and capture CH_4 from biogas plants operated in 135 POMs was 247 988 t yr^{-1} or about 33.1% from the total CH_4 emitted nationwide. Thus, 66.9% of biogas was still released to the atmosphere in 2021. Biogas production is proportionate to GHG emissions and likewise for biogas capturing *vis-à-vis* GHG savings. The higher amount of biogas is produced and captured, the more GHG emissions is mitigated, so does the GHG savings.

Capturing biogas for energy recovery provides two types of savings, namely avoiding biogas from emitting to the atmosphere and substituting fossil fuel with biogas fuel (Subramaniam *et al.*, 2021). If all mills were equipped with biogas plants, the GHG savings potential could be approximately 15.0-16.3 million tonnes CO_2eq annually. These values can be translated into 5.5%-6.0% potential avoided CO_2 emissions from the country's total GHG emissions in 2020 (Ritchie *et al.*, 2020). The calculated actual

TABLE 4. TOTAL METHANE AND GREENHOUSE GASES (GHG) EMISSIONS, AND POTENTIAL GHG SAVINGS FROM PALM OIL MILLS (POMS) IN MALAYSIA

	POMs nationwide			135 POMs with biogas plant
Year	**2019**	**2020**	**2021**	**2021**
Methane emissions, t yr^{-1}	814 496	796 346	750 268	(247 988)
GHG emissions, million tonnes CO_2eq yr^{-1}	20.36	19.91	18.76	(6.20)
Potential GHG savings, million tonnes CO_2eq yr^{-1}	16.29	15.93	15.00	4.96

potential of GHG savings from 135 mills was 4.96 million tonnes CO_2eq yr^{-1}, equivalent to about 1.8% of the country's GHG emissions in 2020, compared to 1.6% emission reduction in 2013 (Susskind *et al.*, 2020). Thus, biogas capture is an established GHG mitigation initiative, which also facilitates the country's commitment to reduce carbon emissions intensity per unit of gross domestic product (compared to 2005 levels) by 45% in 2030 (SEDA, 2022). *Table 5* summarises the potential of GHG savings via displacement of fossil fuel for electricity generation using biogas from POME.

Table 5 shows that an additional 1.89 million tonnes CO_2eq yr^{-1} of GHG savings could be accomplished through fossil fuel displacement if all POMs in the country capture biogas to generate electricity. Specifically, the 135 mills operated with biogas plant contribute to 0.66 million tonnes CO_2eq yr^{-1} GHG savings through electricity generation. In total, the country could potentially mitigate 16.89 and 5.62 million tonnes CO_2eq yr^{-1} of GHG associated with POME-based biogas capture for electricity utilisation from 451 mills and 135 biogas-based mills, respectively. Potential GHG savings from biogas utilisation as electricity is relatively lower than activity in biogas capture itself, depending much on emission factor of the displaced fossil fuels.

Status of Biogas Capture and Utilisation Technology Used for Biogas Capture in Palm Oil Mills

Based on the latest figure of 135 mills equipped with biogas plant in 2021, two type of biogas capture technology commercially used are closed digester tank (66 mills, 49%) and covered lagoon technology (65 mills, 48%). The remaining 4 mills opted for a combined technology (hybrid system, 3%). These findings indicated a relatively similar deployment of closed digester tank and covered lagoon technology due to growing interests in the latter. For the past 10 years, covered lagoon technology has been improvised in terms of design and process efficiency, leading to better operation and yield performance, compared to the basic system that was widely promoted during the Clean Development Mechanisms (CDM) period (2005-2012) (Loh *et al.*, 2017).

AD of POME using an improved covered lagoon technology has fetched high COD removal efficiencies of >85% (Yap *et al.*, 2020). These values are comparable to the typical continuous stirred tank reactor technology (CSTR) (Irvan *et al.*, 2018). The technology is also capable of generating 25-30 m^3 biogas m^{-3} POME, which is within the range offered by the CSTR technology (Muzzammil and Loh, 2020). High treatment efficiency can be accomplished by improving the mixing mechanisms via either sludge return, gas recirculation or multiple feeding system. Other factors such as lower capital expenditure (CAPEX) and operational expenditure (OPEX), and higher POME and biogas storage capacity are

TABLE 5. POTENTIAL OF GREENHOUSE GASES (GHG) SAVINGS VIA BIOGAS CAPTURE AND ELECTRICITY GENERATION FROM PALM OIL MILLS (POMS) IN 2021

Item	451 POMs nationwide	135 POMs with biogas plant
Potential savings (biogas capture), million tonnes CO_2eq.	15.00	4.96
Potential savings from electricity generation at 7200 hr yr^{-1}, million tonnes CO_2eq $MWhr^{-1}$		
Peninsular Malaysia (EF: 0.585)	1.18 (279 MW)	0.47 (112 MW)
Sabah (EF: 0.525)	0.45 (119 MW)	0.14 (37MW)
Sarawak (EF: 0.330)	0.26 (110 MW)	0.05 (19 MW)
Saving from fossil fuel displacement, million tonnes CO_2eq yr^{-1}	1.89 (508 MW)	0.66 (168 MW)
Total (million tonnes CO_2eq yr^{-1})	16.89	5.62

Note: EF - Emission factor.

considered as an added advantage to the covered lagoon technology. Nevertheless, the closed digester tank is still the preferred technology for mills with limited land areas. The survey also showed that 4 mills deployed a hybrid system, *i.e.*, by combining both the technologies to produce and capture the biogas. The hybrid AD system is operated either in series or parallel mode. Apart from yield maximisation, this approach is undertaken by developers to upgrade the biogas plant for better performance.

Biogas Utilisation in Palm Oil Mills

Figure 2 summarises major utilisation pathway of biogas capture in POMs. Out of 135 mills with biogas plant, 87 plants (64%) venture into electricity generation, 15 plants (11%) utilise the biogas for steam/heat or CHP generation, 32 plants (24%) have yet to use the biogas for energy generation and one plant upgrades and purifies the raw biogas for Bio-CNG production only. As of December 2021, the total installed capacity of POME-based biogas power plants was 138.51 MW, compared to the total potential of 168 MW estimated from 135 mills with biogas plant (*Table 3*). For this purpose, all the plants deployed a typical internal combustion engine, except one mill which opted for a micro-gas turbine to generate electricity for internal or off-site uses. For the 87 mills producing electricity from biogas, several utilisation configurations and multiple uses have been adopted. *Figure 3* shows a detailed utilisation breakdown of generated electricity from the POME-based biogas power plant in Malaysia.

Of the 87 mills with biogas plant for electricity generation, 43 plants are grid-connected under the national Feed-in Tariff (FiT) program including three plants which also channel part of the electricity generated to the mills for internal use, two plants for rural electrification, 35 plants for internal use

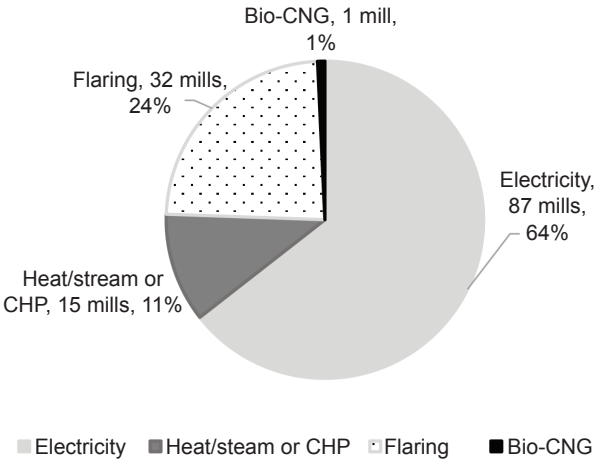


Figure 2. Major biogas utilisation in palm oil mills in Malaysia.

in the mills or integrated palm oil complexes and another seven mills for a combined electricity and steam generation. POME-based biogas plant for FiT has made up 57.5% or 79.69 MW of the total capacity realised nationwide. Biogas from POME contributes the biggest share, approximately 72%, to the cumulative installed grid-connected biogas plant capacity of 110.59 MW in 2020 (SEDA, 2021). Currently, electricity generation for FiT is the most deployed biogas utilisation option by the millers, mainly driven by the attractive 16-year fixed basic FiT rate and bonuses.

Previously, the maximum FiT rate was RM0.4669 $kWhr^{-1}$ consisting of RM0.3184 $kWhr^{-1}$ for basic rate and additional bonuses of RM0.1485 $kWhr^{-1}$, where applicable (Loh *et al.*, 2017). SEDA has introduced e-bidding exercise in 2018 for securing the lowest possible basic FiT rate of biogas. As of 2020, 3 e-bidding exercises have been held with an average basic FiT bid rate of RM0.2567-RM0.2599 $kWhr^{-1}$ (SEDA, 2021). The FiT quota for biogas is limited and competitive, mainly relied on the RE fund collected from electricity consumers nationwide, except for Sarawak. Besides, the potential of POMs for grid connection is also limited, depending mainly on the distance of the mills to the interconnection point, local load demand and safety aspects. Preliminary feasibility study is needed prior to conducting a full power system study which is very costly and may not be worthy of effort if the outcome is not promising (Loh *et al.*, 2017).

Two biogas power plants with a combined capacity of 2.8 MW have been operated by FGV Holdings Berhad in two of their POMs, which supply the generated electricity to the nearby settlement areas and townships at Felda Umas and Felda Sahabat in Sabah (FGV, 2020). This initiative reduces dependency on high-cost diesel-generated electricity for rural areas. To date, the total installed capacity from the POME-based biogas for off-site uses via the FiT and rural electrification programme was 82.49 MW, which was equivalent to 60% of the total installed capacity nationwide in 2021. This indicates that biogas from POME has huge potential for off-site electricity generation. It is anticipated that more POME-based biogas power plants will be built and connected either to the national or local grids in the future, if additional FiT quota or incentives for rural electrification is made available for deployment by palm oil millers.

The electricity generated from biogas has also been widely used internally for operation of POMs, and more so via integration of palm oil complexes consisting of mill, estates, workshop, downstream business activities (including Bio-CNG), workers housing and community areas. This approach could cater for the energy required to spur

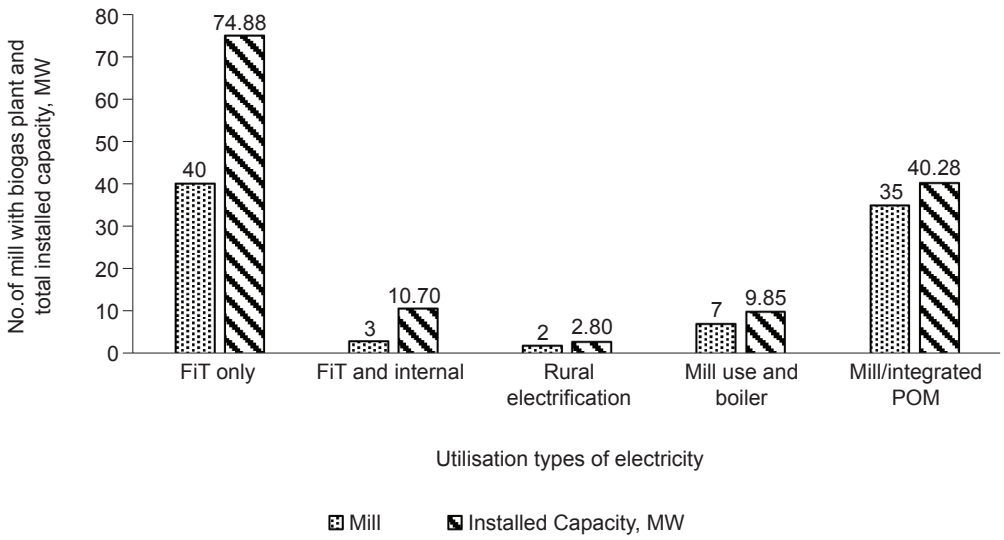


Figure 3. Utilisation configuration for electricity generation from biogas in the palm oil mills in Malaysia.

economic activities and improve livelihoods of the communities within mill vicinity. Currently, seven mills have adopted multiple uses for the captured biogas, *i.e.*, by combining electricity generation and biogas cofiring, for achieving better economic viability. Briefly, the electricity generated in these mills has been used mainly to support milling operation during start-up and shutdown as well as for non-processing period. Any biogas in excess is supplied to the biomass-fired boiler during processing hours.

The captured biogas is also used as fuel displacement to generate steam, heat or CHP, as deployed by 15 plants in 2021. Typically, biogas is cofired in biomass boilers (serve as a CHP plant) to generate steam and electricity for milling process. The process displaces biomass fuel, particularly palm kernel shell which can be sold as a solid fuel and feedstock for value-added products, and at the same time facilitates reduction of particulate emissions from boiler chimney. For those mills integrated with palm oil refinery, biogas is used in package boiler or chiller to generate steam and chilled water for refining process (Loh *et al.*, 2017). This kind of activity has resulted in substantial cost savings on fossil fuel. Besides, raw biogas can be sold to nearby industry that requires fuel for heat generation. This has been commercially demonstrated by BBC Palm Oil Mill in Sarawak for supplying the raw biogas to the brick factory located next to the mill (Lim and Biswas, 2019).

Currently, 32 mills are not utilising the captured biogas and opted to merely flare it. Most of these plants were developed during the CDM period (2005-2012) with profitable earning of certified emission reduction credits (Loh *et al.*, 2017). This activity continues to be business as usual post-CDM commitment. Biogas flaring is typically a temporary option for those newly-commissioned or long-established biogas plants in order to comply with existing licensing criteria mandated for new mills and mills requiring capacity expansion. These mills have yet to finalise their utilisation option or may not even opt for any energy recovery soon due to constraints such as low biogas yield or small plant capacity, and thus is deemed economically infeasible. For future deployment of captured biogas, four plants will commit to FiT, four plant will generate electricity for internal use and another plant for CHP.

Limited onsite utilisation within a mill also contributes to slow development of biogas capturing facility as well as underutilised or wasted biogas energy recovery (Loh *et al.*, 2022). One of the promising ways to optimise and diversify biogas uses for off-site applications is by upgrading raw biogas to Bio-CNG or biomethane (Tan and Lim, 2019). To date, two commercial Bio-CNG plants from POME have been installed at POMs to demonstrate their commercial potential. Each plant has the capacity to produce 9600 and 5000 m^3 day^{-1} concentrated compressed CH_4, respectively (Loh *et al.*, 2017). Bio-CNG is an emerging alternative to typical biogas utilisation option, in particular for those mills located near to industrial area or natural gas pipelines, and infeasible for grid connection. The product can be used either on-site, transported using compressed natural gas trailer to potential users' site (mobile pipeline), injected to gas pipeline and as alternative to vehicle fuel. Since biogas upgrading involves an advanced technology, high CAPEX and OPEX are required

compared to other biogas utilisation routes. It is anticipated that more Bio-CNG plants will be developed and injected to the natural gas pipelines with the implementation of third party access in the Gas Supply (Amendment) Act 2016, as part of the country's natural gas market liberation initiatives (Hoo *et al.*, 2020).

Limitations and Improvements of Biogas Utilisation: Safety, Environmental and Economic

Potential of biogas capture system for various energy applications is promising but there are still limitations that need to be addressed from safety, environmental and economic perspectives. Current biogas plants have only minimal safety feature such as flame arrestor and safety relief valve without sophisticated risk management tool, and thus it is important for developers to ensure the highest possible level of safety or minimum risks to human health and safety, and the environment (Gomez, 2013). There are adequate dedicated Malaysian Standard (MS), namely MS 2581:2014 on production of biogas - code of practice or guidelines on safety that are available for adoption in this business (Loh *et al.*, 2017). The existing MS or other guidelines can be improved further while new MS on safety of biogas utilisation also should be developed. As safety risks and hazards may also be associated with the operators, safety training modules and awareness programme must be regularly improved and conducted (Gomez, 2013).

Environmental benefits of biogas capture and utilisation are manifold and significant. However, the resultant environmental performance may be limited or jeopardised due to inefficiency of biogas plant operation, possible emissions from inefficient capturing facilities, leakages, poor POME handling during pre- and post-AD treatment from open ponding system and odour emissions (Chin *et al.*, 2013; Mahmod *et al.*, 2023). CH_4 slip may also occur during incomplete combustion of gas engine and off-gas from Bio-CNG plant (Gomez, 2013). The environmental performance related to biogas plant efficiencies can be improved by adopting the most efficient latest technology including to fully automatise and digitalise the biogas plant not just on the operation, but also process monitoring and quality control via the Fourth Industrial Revolution concepts, *i.e.*, internet of things, artificial intelligence, *etc.* (Cinar *et al.*, 2021). Adoption of these concepts also can contribute to better economic and improved safety aspects towards smart biogas plant in POMs.

Despite numerous end-use applications with varying level of economic returns, biogas utilisation either in POMs or for off-site uses is limited. This is mainly attributed to lack of energy needs and surplus biomass energy in typical POMs, logistics issues and limited infrastructures for off-site applications (Nasrin *et al.*, 2022; Tan and Lim, 2019). Grid-connected biogas plant is dependent on FiT quota which is very limited and only eligible for 16 years (Tan and Lim, 2019). Besides, the FiT programme is not available in Sarawak (Chin *et al.*, 2013). Economic returns are subjected to economic of scale which is dependent on the capacity of the biogas plant or the mills, types of biogas utilisation or pathway and location of the mills to the end users. Therefore, biogas utilisation path needs to be diversified and extensively exploited to expand potential application and improve economic returns. Business model of biogas plant needs to be strategised considering all the economic factors including to factor in environmental cost mechanism such as carbon credit scheme for an attractive revenue (Sharvini *et al.*, 2022). Improvement of the governmental frameworks, supports, incentives and infrastructures are required, in particular in new business opportunity such as Bio-CNG.

CONCLUSION

The mitigation activity via biogas capture and utilisation improves sustainability performance of the palm oil industry and facilitates the understanding and commitment on global issues related to energy crisis and global warming. In this study, biogas from POME shows huge potential RE and GHG savings. The palm oil industry could contribute approximately 1.5% and 4.0% to the national installed capacity and the RE share target in Malaysia by the year 2025, respectively with substantial GHG savings of 15 million tonnes CO_2eq yr^{-1} if all POMs capture and utilise the biogas. At present, 30.0% of POMs have installed biogas plants with 33.0% energy recovery rate from the overall estimated potential. More proactive and synergised efforts are required from the industry players to harness the huge untapped potential of RE from biogas in enhancing sustainable image of the industry. Future research should emphasis on new and emerging biogas end-uses such as Bio-CNG, liquefaction and biohydrogen for commercial adoption. This kind of new business opportunities could only be expediated by strengthening the governmental frameworks and supports such as infrastructure and incentives.

ACKNOWLEDGEMENT

The authors would like to thank the University of Malaya for supporting this work and the Director-General of the MPOB for permission to publish this article.

REFERENCES

Akhbari, A; Kutty, P K; Chuen, O C and Ibrahim, S (2020). A study of palm oil mill processing and environmental assessment of palm oil mill effluent treatment. *Environ. Eng. Res., 25(2)*: 212-221. DOI: 10.4491/eer.2018.452.

Bello, M M and Raman, A A A (2017). Trend and current practices of palm oil mill effluent polishing: Application of advanced oxidation processes and their future perspectives. *J. Environ. Manag., 198*: 170-182. DOI: 10.1016/j.jenvman.2017.04.050.

Chia, W Y; Chong, Y Y; Chew, K W; Vimali, E; Jayaram, M; Selvarajoo, A; Muthuvelu, K S; Varalakshmi, P; Show, P L and Arumugasamy, S K (2020). Outlook on biorefinery potential of palm oil mill effluent for resource recovery. *J. Environ. Chem. Eng., 8(6)*: 104519. DOI: 10.1016/j.jece.2020.104519.

Chin, M J; Poh, P E; Tey, B T; Chan, E S and Chin, K L (2013). Biogas from palm oil mill effluent (POME): Opportunities and challenges from Malaysia's perspective. *Renew. Sust. Energ. Rev., 26*: 717-726. DOI: 10.1016/j.rser.2013.06.008.

Choong, Y Y; Chou, K W and Norli, I (2018). Strategies for improving biogas production of palm oil mill effluent (POME) anaerobic digestion: A critical review. *Renew. Sust. Energ. Rev., 82*: 2993-3006. DOI: 10.1016/j.rser.2017.10.036.

Cinar, S; Cinar, S O; Wieczorek, N; Sohoo, I and Kuchta, K (2021). Integration of artificial intelligence into biogas plant operation. *Processes, 9(1)*: 85. DOI: 10.3390/pr9010085.

FGV (2020). Sustainability report 2018/2019. https://www.fgvholdings.com/wp-content/uploads/2020/06/FGV-Sustainability-Report-2018-2019.pdf, accessed on 25 May 2022.

Firdaus, N; Prasetyo, B T; Sofyan, Y and Siregar, F (2017). Part I of II: Palm oil mill effluent (POME): Biogas power plant. *Distrib. Gener. Altern. Energy J., 32(2)*: 73-79. DOI: 10.1080/21563306.2017.11869110.

Gomez, C D C (2013). Biogas as an energy option: An overview. *The Biogas Handbook - Science, Production and Applications* (Wellinger, A; Murphy, J and Baxter, D eds.). Woodhead Publishing, UK. p. 1-16.

Hasanudin, U and Haryanto, A (2018). Palm oil mill effluent recycling system for sustainable palm oil industries. *Asian J. Environ. Biotechnol., 2(2)*: 52-62.

Hoo, P Y; Hashim, H and Ho, W S (2020). Towards circular economy: Economic feasibility of waste to biomethane injection through proposed feed-in tariff. *J. Clean. Prod., 270*: 122160. DOI: 10.1016/j.jclepro.2020.122160.

Irvan, I; Trisakti, B; Maulina, S and Daimon, H (2018). Production of biogas from palm oil mill effluent at pilot scale: Effect of recycle sludge. *Orient. J. Chem., 34(1)*: 161-168. DOI: 10.13005/ojc/340118.

Kaparaju, P and Rintala, J (2013). Generation of heat and power from biogas for stationary applications: Boilers, gas engines and turbines, combined heat and power (CHP) plants and fuel cells. *The Biogas Handbook - Science, Production and Applications* (Wellinger, A; Murphy, J and Baxter, D eds.). Woodhead Publishing, UK. p. 404-427.

Kospa, H S D; Lulofs, K R; Asdak, C and Rahim, S E (2017). Strategies to reduce water footprint in palm oil production: A case of PTP Mitra Ogan, Baturaja, South Sumatra. *MATEC Web of Conferences, 97:* 1-12. DOI: 10.1051/matecconf/20179701122.

Krishnan, Y; Bong, C P C; Azman, N F; Zakaria, Z; Abdullah, N; Ho, C S; Lee, C T; Hansen, S B and Hara, H (2017). Co-composting of palm empty fruit bunch and palm oil mill effluent: Microbial diversity and potential mitigation of greenhouse gas emission. *J. Clean. Prod., 146*: 94-100. DOI: 10.1016/j.jclepro.2016.08.118.

Lee, M K; Hashim, H; Lim, J S and Taib, M R (2019). Spatial planning and optimisation for virtual distribution of BioCNG derived from palm oil mill effluent to meet industrial energy demand. *Renew. Energy, 141*: 526-540. DOI: 10.1016/j.renene.2019.03.097.

Lim, C I and Biswas, W K (2019). Sustainability implications of the incorporation of a biogas trapping system into a conventional crude palm oil supply chain. *Sustainability, 11(3)*: 1-19. DOI: 10.3390/su11030792.

Loh, S K; Lai, M E; Ngatiman, M; Lim, W S; Choo, Y M; Zhang, Z and Salimon, J (2013). Zero discharge treatment technology of palm oil mill effluent. *J. Oil Palm Res., 25(3)*: 273-281.

Loh, S K; Nasrin, A B; Azri, S M; Adela, B N; Muzzammil, N; Jay, T D; Eleanor, R A S; Lim, W S; Choo, Y M and Kaltschmitt, M (2017). First report on Malaysia's experiences and development in biogas capture and utilization from palm oil mill effluent under the economic

transformation programme: Current and future perspectives. *Renew. Sust. Energ. Rev., 74*: 1257-1274. DOI: 10.1016/j.rser.2017.02.066.

Loh, S K; Nasrin, A B; Sukiran, M A; Bukhari, N A and Subramaniam, V (2022). Oil palm biomass value chain for biofuel development in Malaysia: Part II. *Value-Chain of Biofuels - Fundamentals,Technology and Standardisations* (Yusup, S and Rashidi, N A eds.). Elsevier, Amsterdam. p. 505-534.

Mahmod, S S; Takriff, M S; AL-Rajabi, M M; Abdul, P M; Gunny, A A N; Silvamany, H and Jahim, J M (2023). Water reclamation from palm oil mill effluent (POME): Recent technologies, by-product recovery, and challenges. *J. Water Process. Eng., 52*: 103488. DOI: 10.1016/j.jwpe.2023.103488.

MGTC (2019). 2017 CDM electricity baseline for Malaysia. https://www.mgtc.gov.my/wp-content/uploads/2019/12/2017-CDM-Electricity-Baseline-Final-Report-Publication-Version.pdf, accessed on 28 March 2022.

MPOB (2022). Economic and Industry Development Division. https://bepi.mpob.gov.my/index.php/en/, accessed on 23 February 2022.

Mundi, I (2021). Index Mundi-commodities glosary. https://www.indexmundi.com/commodities/glossary/mmbtu#:~:text=1%20MMBtu%20%3D%2028.263682%20m3,at%20defined%20temperature%20and%20pressure, accessed on 2 April 2022.

Muzzammil, N and Loh, S K (2020). Pilot scale integrated anaerobic-aerobic treatment of palm oil mill effluent. *J. Oil Palm Res., 32(2)*: 286-293. DOI: 10.21894/jopr.2020.0030.

Nasrin, A B; Raman, A A A; Bukhari, N A; Sukiran, M A; Buthiyappan, A; Subramaniam, V; Aziz, A A and Loh, S K (2022). A critical analysis on biogas production and utilisation potential from palm oil mill effluent. *J. Clean. Prod., 361*: 132040. DOI: 10.1016/j.jclepro.2022.132040.

Nasrin, A B; Raman, A A A; Loh, S K; Sukiran, M A; Bukhari, N A; Aziz, A A; Saad, M F M; Kamarudin, M K M and Buthiyappan, A (2020). Characteristics and techno-economic potential of bio-compressed natural gas (Bio-CNG) from palm oil mill effluent (POME). *IOP Conf. Ser.: Mater. Sci. Eng., 736(2)*: 022060. DOI: 10.1088/1757-899X/736/2/022060.

Park, Y G (2021). Study for the Bio-CNG recovery of methane gas in the anaerobic co-digestion using Malaysian POME (palm oil mill effluent). *Biotechnol. Bioproc. E., 26(3)*: 435-446. DOI: 10.1007/s12257-019-0401-2.

Parveez, G K A; Tarmizi, A H A; Sundram, S; Loh, S K; Ong-Abdullah, M; Palam, K D P; Salleh, K M; Ishak, S M and Idris, Z (2021). Oil palm economic performance in Malaysia and R&D progress in 2020. *J. Oil Palm Res., 33*: 181-214. DOI: 10.21894/jopr.2021.0026.

Ritchie, H; Roser, M and Rosado, P (2020). CO_2 and greenhouse gas emissions. https://ourworldindata.org/co2-and-other-greenhouse-gas-emissions, accessed on 3 July 2022.

Sarwani, M K I; Fawzi, M; Osman, S A and Nasrin, A B (2019). Bio-methane from palm oil mill effluent (POME): Transportation fuel potential in Malaysia. *J. Adv. Res. Fluid Mech. Thermal Sci., 63(1)*: 1-11.

SEDA (2021). Annual Report 2020 Sustainable Energy Development Authority (SEDA). https://www.seda.gov.my/wp-content/uploads/2022/01/SEDA-KWSM-Annual-Report-2020_2.pdf, accessed on 30 May 2022.

SEDA (2022). Malaysia Renewable Energy Roadmap (MyRER). https://www.seda.gov.my/reportal/myrer/, accessed on 1 June 2022.

Sharvini, S; Noor, Z; Stringer, L; Afionis, S and Chong, C (2022). Energy generation from palm oil mill effluent: A life cycle cost-benefit analysis and policy insights. *Renew. Sust. Energ. Rev., 156*: 111990. DOI: 10.1016/j.rser.2021.111990.

Subramaniam, V; Loh, S K and Aziz, A A (2021). GHG analysis of the production of crude palm oil considering the conversion of agricultural wastes to by-products. *Sustain. Prod. Consum., 28*: 1552-1564. DOI: 10.1016/j.spc.2021.09.004.

Subramaniam, V; Ma, A and Choo, Y (2010). Capturing biogas: A means to reduce green house gas emissions for the production of crude palm oil. *Amer. J. Geoscience, 1(1)*: 1-6.

Suruhanjaya Tenaga (2021). *Malaysia Energy Statistics Handbook 2020*. Suruhanjaya Tenaga. Putrajaya. 88 pp.

Susskind, L; Chun, J; Goldberg, S; Gordon, J A; Smith, G and Zaerpoor, Y (2020). Breaking out of carbon lock-in: Malaysia's path to decarbonization. *Front. Built Environ., 6*: 1-14. DOI: 10.3389/fbuil.2020.00021.

Tan, Y D and Lim, J S (2019). Feasibility of palm oil mill effluent elimination towards sustainable Malaysian palm oil industry. *Renew. Sust. Energ. Rev., 111*: 507-522. DOI: 10.1016/j.rser.2019.05.043.

United Nations (2022). United Nations - Sustainable Development. https://sdgs.un.org/goals, accessed on 1 June 2022.

Yap, C C; Chan, Y J; Loh, S K; Sypramaniam, C V; Soh, A C; Chong, M F; Chew, C L and Lim, K L (2020). Comparison of different industrial scale palm oil mill effluent anaerobic systems in degradation of organic contaminants and kinetic performance. *J. Clean. Prod., 262*: 121361. DOI: 10.1016/j.jclepro.2020.121361.



Journal of Oil Palm Research Vol. 36 (3) September 2024 p. 469-483
DOI: https://doi.org/10.21894/jopr.2023.0042

EVALUATION OF OIL PALM FROND FOR BIOBUTANOL PRODUCTION BY DIFFERENT *Clostridia* SPECIES

ABDURRAHMAN ABUBAKAR[1,2]; MADIHAH MD SALLEH[1]*; ADIBAH YAHYA[1]; HUSZALINA HUSSIN[1]; CHONG CHUN SHIONG[1]; SHAZA EVA MOHAMAD[1] and SURAINI ABD AZIZ[3]

ABSTRACT

Ideal substrates and biobutanol producers are the key and most important ingredients for efficient biobutanol production. In this research, we evaluated the composition of oil palm fronds based on the different ages of the plant. Fresh oil palm frond (OPF) juice was found to be the most potent OPF component for biobutanol production and was pressed from 5, 10, 15 and 20 years old trees using a sugarcane pressing machine. The total sugar concentrations were estimated by the use of a DNS and spectrophotometer and were found to be decreasing with the increasing age of the palm oil tree, with the highest sugar obtained at OPF ages 5 and 10. HPLC analysis revealed that glucose was the highest fraction in the juice, accounting for 57% to 66%, while fructose (12%-17%) and sucrose (19%-25%) made up the remaining percentage. Fermentation inhibitors like gallic and ferulic acids were also detected in the juice using the HPLC technique, and their concentrations also increased with age. Therefore, the research screened for a robust bacterial strain that can tolerate these phenolics in the hydrolysate for biobutanol production. Out of the 11 strains of Clostridium *screened, strain A1 was found to successfully utilise the hydrolysate and yield the highest concentration of biobutanol at 2.32 g/L with the productivity of 0.064 g/L/hr. The strain was identified as* Clostridium *strain A1 based on 16S rRNA gene sequencing techniques.*

Keywords: biobutanol, *Clostridia* sp., OPF age, phenolic compound, sugar.

Received: 24 February 2023**; Accepted:** 1 July 2023**; Published online:** 30 August 2023.

INTRODUCTION

The reliance of most countries in the world on the existing energy source (fossil fuels) as their main supply has resulted in several detrimental environmental consequences, including global warming and air pollution, which create a lot of health issues as well as social and economic concerns (Jacobson *et al*., 2022). Moreover, beside its price fluctuation and hiking, there is a depletion of non-renewable resources, which may be scarce or non-existent in future generations. As a result, the energy source is shifting from non-renewables like fossil fuels (coal, gas and oil) to renewable energy sources like bioethanol and biobutanol. Consequently, the world's attention is increasingly focused on developing and using chemicals and fuels from renewable resources. Among the alternative sources of energy, biobutanol is considered the most attractive biofuel. It undoubtedly possesses superior properties relative to ethanol and others, owing to its higher energy density, low volatility, hygroscopicity and low greenhouse gas emissions (Grande *et al*., 2021). Apart from being a solvent for various industrial applications, biobutanol is an essential chemical precursor for producing paints, polymers and plastics (Zhen *et al*., 2020).

[1] Department of Biosciences,
Faculty of Sciences, Universiti Teknologi Malaysia,
81310 Skudai, Johor, Malaysia.

[2] Department of Biological Sciences,
Faculty of Science, Federal University of Kashere, Gombe,
Gombe State P.M.B. 0182, Nigeria.

[3] Department of Bioprocess Technology,
Faculty of Biotechnology and Biomolecular Sciences,
Universiti Putra Malaysia, 43400 Seri Kembangan,
Selangor, Malaysia.

* *Corresponding author e-mail: madihah@fbb.utm.my*

Although biobutanol can be produced by fermenting several carbohydrate derivatives derived from agricultural and forest residues, substrate sustainability is one of the most difficult aspects of biofuel development in general, including biobutanol production (Rafieisakhaei and Barazandeh, 2017). Resources with high carbohydrate content, an effective conversion method, and an available and low-cost source are required. Therefore, the efficiency, economy, and sustainability of biobutanol production are primarily influenced by the availability of raw materials. Many substrates have been described as feedstock for biobutanol production, and few studies in recent years have reported the laboratory-scale production of biobutanol from oil palm frond (OPF) juice, yet those studies mostly focused on the characterisation of the OPF juice as fermentation substrate for biobutanol production (Asri *et al*., 2019). It is reported that OPF juice meets all the conditions for a useful fermentation substrate due to its renewability, accessibility, and constant availability (Rafieisakhaei and Barazandeh, 2017). According to a report by the Malaysian Palm Oil Board (MPOB), approximately 51.80 million tonnes of biomass are generated annually from oil palm industries, with OPF biomass accounting for the majority; only a small portion of this is used as animal feed, with the remainder simply left in the plantation sites (Abubakar *et al*., 2022). Moreover, juice extracted from OPF is less toxic to microbial growth and product formation since it contains low impurities. A study conducted on the production of biobutanol from oil palm frond (OPF) juice by *Clostridium acetobutylicum* ATCC 824 in a 2 L batch culture using 50 g/L OPF juice yielded as high as 9.3 g/L of butanol (Huzir *et al*., 2019), but the research did not indicate the age of the oil palm frond juice used for the production. However, accumulations of both primary and secondary metabolites in plants are affected by several factors, including their developmental stage (age), this scenario has been neglected by most scientists while considering substrates as feedstock for biobutanol production. Therefore, the current study focused on the analysis and utilisation of different ages of OPF juice as a fermentation substrate for biobutanol production in batch fermentation mode.

Besides, different microorganisms participate in converting sugar-rich hydrolysate to biobutanol by acetone-butanol-ethanol (ABE) fermentation. A variety of *Clostridia* species were reported to have been used to produce solvent mixtures, usually in the ratio of 3:6:1 acetone-butanol-ethanol, respectively (Jiang *et al*., 2022). However, the capacity of the fermentation microbe to achieve a high yield of fermentation products despite the presence of phenolic inhibitors and the fermentation products as well as the ability to utilise both hexose and pentose is one of the significant factors leading to the production economy and sustainability. Currently, the main natural butanol producers are the *Clostridia* species, but due to their poor tolerance to butanol, a very low titre values are usually obtained in ABE fermentation broth. It is reported that, the maximum butanol that can be tolerated by *Clostridia acetobutylicum* is 2.0% and only less than 1.8% can be tolerated by *C. beijirankii* (Russmayer *et al*., 2019).

Genetic engineering to enhance the butanol tolerance in those species proved to be a very complicated step since the butanol tolerance is controlled by the action of many genes. Therefore, the other option like searching for robust and tolerant strains became a good alternative for enhanced microbial butanol production. However, this remains an obstacle to realising sufficiently high butanol fermentation and product recovery levels (Liu *et al*., 2017). So, to progress in the scale-up of the production of biobutanol, some of the significant factors are that toxicity tolerance needs to be demonstrated in the fermentative strain and a considerable enhancement in the development of strains with the capability to ferment the variety of carbohydrate fractions of biomass hydrolysate to produce biobutanol. Therefore, the current research initially analysed the chemical composition of different segments of OPF and selected the best portion for biobutanol production, and finally screened and identified *Clostridium* species that can efficiently convert the substrate to biobutanol.

MATERIALS AND METHODS

Oil Palm Frond Collection and Preparation

Fresh and basal parts of OPF petioles with an average length of 1.0-1.5 m were collected during the monsoon period from Kampung Terjun Rimba Pontian, Johor Bahru, Malaysia, located at latitude 1°27′59.20″N and longitude 103°27′20.50″E. The location was chosen because of its abundance of different ages of palm trees and because it is also close to a juice extraction site. To avoid the influence of external factors, the samples were collected in duplicate from palm trees (*Elaeis guineensis*) of varying ages (5, 10, 15 and 20 years old). To minimise the intrusion of microbes and dirt, freshly harvested petioles were cut at both edges and spread with 40% (v/v) of ethanol just before being put in sealed plastic bags and immediately transported to the juice processing site for juice extraction. The leaves from the fronds were also collected for elemental compositional analysis using plastic bags. To obtain the juice, a sugarcane juicing machine

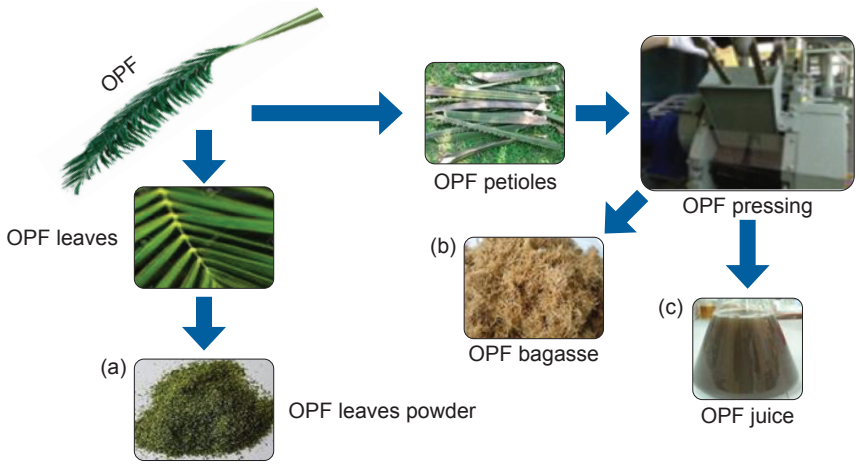


Figure 1. Sample collection and preparation.

(Hisaki, TFS3777) was used to press the OPF petiole repeatedly until the juice content was completely removed. To collect the juice from different plant ages, 1 L sterilised Scott bottles were used. However, the juice-free bagasse and the leaflets from the various oil palm fronds of varying ages were processed by oven-drying at a temperature of 70°C until the moisture content was less than 10% for subsequent analysis (Mat Rozi *et al*., 2021). *Figure 1* illustrates the sample collection and preparation.

Strain and Inoculum Development

The solvent-producing bacteria such as *Clostridium acetobutylicum* SR1 and other strains that include A1 and A2 (UPM), A1 and A2 (LM), A1 and A2 (June, 2011), L1, L2, WK and S1, which were previously isolated by Ramanathan *et al.* (2018), were screened for fermentable sugar utilisation for the production of biobutanol and tolerance towards phenolic compounds. Prior to the development of the inoculums, Reinforced Clostridial Medium (RCM) was prepared by adding g/L of meat extract (10 g), peptone (10 g), yeast extract (3 g), glucose (5 g), soluble starch (1 g), NaCl (5 g), and sodium acetate (3 g). The contents were sterilised by autoclaving at 121°C for 15 min. After cooling off the contents at room temperature, L-cysteine HCL (0.5 g), para-aminobenzoic acid (0.001 g), and biotin (0.008 g) were added separately via filter sterilisation using PTFE (0.2 m) (Fonseca *et al*., 2020). The stock cultures of the various species that were maintained in RCM were first heat-shocked at 90°C for 90 s (Wani *et al*., 2018). 1 mL of the respective heat-shocked culture for each strain was transferred separately into freshly prepared modified RCM and incubated at 37°C without agitation. The growth of the bacteria was monitored using optical density (OD) at 600 nm after every 4 hr of incubation until the cells reached a stable exponential phase (24 hr).

ABE Fermentation

To ferment the OPF juice for the production of biobutanol, a batch culture mode was employed. Initially, 135 mL of sterilised P2 medium were transferred into separate 150 mL serum bottles, leaving a space of 15 mL to aseptically sparge the medium with oxygen-free nitrogen gas using the modified Hungate technique. This was done to remove oxygen from the medium for strict anaerobic metabolism. The production medium (P2) is a stock solution containing KH_2PO_4 (0.75 g/L), K_2HPO_4 (0.75 g/L), yeast extract (5.0 g/L), NH_4NO3 (2.0 g/L), $MgSO_4.7H_2O$ (0.4 g/L), $MnSO_4.H_2O$ (0.01 g/L), $FeSO_4.H_2O$ (0.01 g/L), NaCl (0.5 g/L), and 50 g/L reducing sugar from the OPF juice (Gomez-Flores *et al*., 2018). After autoclaving the media, a solution containing 0.001 g/L of para-aminobenzoic acid, thiamin, and biotin was filter-sterilised into the sample mixture, and the pH was adjusted to 6 by the addition of 1M NaOH. To inoculate the media, 10% (v/v) of the well-grown cells of the respective strains were first heat-shocked at 90°C for 90 s and inoculated separately into fermentation media using sterilised syringes and needles. Finally, the inoculated media were incubated at 37°C without agitation for 96 hr. Samples were taken at 8 hr intervals for ABE, acid formation, biomass formation, and residual sugar analysis. The data reported in the figure and tables are the mean values of duplicate analysis and the standard error was always lower than 5%.

Identification of the Isolate

The 16S rRNA partial gene sequence was used to identify bacteria. To conduct this experiment, genomic DNA (gDNA) was extracted from actively growing cells of the selected strain during its exponential phase using the basic steps and protocol described by Guerrero *et al*. (2021). The extracted DNA was sent to Apical Scientific Malaysia for

purification and sequencing services. The nucleotide sequences of the gene were determined using the genetic analyser by Homology Searching Tools (BLASTN) with the standard programme default (http://www.ncbi.nlm.nih.gov/BLASTN/, NCBI, Bethesda, Md., USA), which was conducted based on the previous method (Hirakawa *et al*., 2019). The unknown bacterium was identified based on the highest percentage of sequence similarity with the strains in GenBank. MEGA 11 software was used for the construction of a phylogenetic tree using the neighbour-joining method. The evolutionary relationship of the bacterial isolate strain A1 and other related bacteria obtained from the Gene Bank was analysed by the distance matrix calculated using neighbour-joining using an out-group with an accession number of NR 113246.1. A bootstrap value of 1000 datasets was used by the software to assess the stability of the relationship (Traverso *et al*., 2020).

Analytical Methods

Determination of sugar and phenolic compounds. The total reducing sugar concentration was determined via the dinitrosalicyclic (DNS) method (Deshavath *et al*., 2020). Glucose monohydrate was used as a standard solution, and the absorbance of both the samples and the standards was read at 540 nm. On the other hand, the Folin-Ciocalteu reagent was used to determine total phenolic compounds with an absorbance read at 765 nm by a spectrophotometer, and here, gallic acid was utilised as the benchmark. However, the concentration of individual sugars and phenolic compounds in the juice was determined using an Agilent 1100 series HPLC technique with Rezex RPM-monosaccharide Pb^{2+} columns and a lead ion (Pb^{2+}) as the stationary phase for sugar determination and a C18 column for phenolic compound determination. All the data generated were analysed by use of SPSS v.10 software (SPSS Inc, Chicago, IL). One-way analysis of variance between ages of OPF for each composition was determined, and $P<0.05$ was considered significant.

Determination of lignocellulose composition. The determination of oil palm frond leaves, and bagasse structural components were conducted following the standard technique proposed by Lin *et al.* (2010) by considering the OPF structure to consist majorly of extractives, lignin, hemicellulose, and cellulose (Ang *et al*., 2015). Quantification of the extractives was performed by taking the weight loss of the sample contents; after that, the dried OPF leaflet and bagasse were treated with 99.5% (v/v) acetone. The weight loss of the 99.5% (v/v) acetone-treated samples after incubation for 3.5 hr at 80°C was the amount of hemicellulose (Ang *et al*., 2015; Lin *et al*., 2010). The percentage of lignin was recorded as the amount of weight lost after treating the extractive-free sample with 98.0% (v/v) H_2SO_4. Lastly, the content of cellulose was measured by taking the differences between the weighted total of the other products (extractives, hemicellulose and lignin) and the initial weight of the OPF leaves and bagasse powder.

***Elemental analysis using X-ray fluorescence* (XRF).** XRF is an analytical technique used to determine the elemental composition of materials. This technique determines the chemistry of a sample by measuring the fluorescent (or secondary) X-ray emitted from a sample when it is excited by a primary X-ray source (Marguí *et al*., 2009). To conduct this analysis, leaflets from the various ages of oil palm fronds were processed by oven-drying at a temperature of 70°C until the moisture content was less than 10%. The dried leaves were ground into a powder with the help of a blending machine. The powdered samples were then placed on an X-ray beam for elemental composition determination.

***Determination of acids and solvents using Gas Chromatography* (GC).** The concentration of acids such as acetic acid and butyric acid and solvents such as acetone, butanol and ethanol was determined using gas chromatography equipped with a DB-WAX column and a Flame Ionised Detector (FID). The carrier gas was helium, with a flow rate of 25 mL/min. The temperatures of the oven was 200°C while for both column inlet and detector were set at 300°C (Abe *et al*., 2020). Prior to the GC analysis, solvent-solvent extraction was done to separate the products from the broth. At first, a drop of 5% HCl was used to acidify the broth to separate the culture from the sample, and the acidified sample was extracted with an equivalent amount of dichloromethane (DCM). The mixture was then centrifuged at 10 000 rpm for 30 min. The top layer was discarded and the bottom layer was kept, which was expected to contain the acids and solvents, including the DCM. Finally, 20 µL of the samples were injected into the column using auto-injection. Acids and solvents of analytical grade (Sigma Aldrich, USA) were used as standards. The concentrations of acids and solvents in the sample were determined by comparing the area peaks of each sample with the area of the reference sample (the standards for acids and solvents). Prior to the analysis, calibration curves for the ABE and acids were constructed by plotting the peak area ratios against concentrations. Excellent linearity of the acids and solvents with correlation coefficients in the range of

0.991-0.996 was obtained, and the precision of the method was determined from duplicate analyses of the same with relative standard deviations (RSDs) of less than 5%.

RESULTS AND DISCUSSION

Selection of Oil Palm Frond Component Based on Composition and Age of the Tree

One of the ultimate aims of this study was to select the best material from the OPF biomass that could be used as an economical and efficient substrate for biobutanol production. Two parameters were taken into consideration, which include segment composition and OPF age. The initial phase of the research, therefore, analysed the major segments of the oil palm frond for their lignocellulosic composition. This was very necessary because, to fulfil the demand as a promising substrate for bioenergy, it is very important that the feedstock contain a reasonable percentage of its primary metabolites [carbohydrate (simple sugar, cellulose, hemicelluloses, starch, *etc.*)] in high volume in the biomass, which later can be converted by the solvent producers to biofuels. The OPF is generally a highly fibrous lignocellulosic material that contains two major segments: Leaflets (tips) at the top and the basal portion (petioles). Both of the segments were analysed for the lignocellulose fraction, and the results are provided in this section based on the different ages of the palm tree.

Effect of Frond Age on the Lignocellulose and Elemental Composition

Since one of the aims of this study was to investigate the effect of ageing on economically important biobutanol traits, the profile of chemical composition of OPF leaflet ages was studied, and the results showed considerable differences at the 5% level of significance. Additionally, the environmental influences from chemical nutrients and soil type were minimised by sampling trees within a single plantation trial site. *Table 1* summarises the lignocellulose and elemental compositions of the different samples of OPF leaflets. The results indicated that the cellulose and hemicellulose fractions are generally low in all the OPF leaflet ages and frequently decrease with an increase in the age of the frond. The highest cellulose and hemicellulose percentages were 11.4 ± 2.04% and 13.7 ± 1.54% found in a 5 yr OPF leaflet, while the lowest percentages were detected in a 20 yr OPF leaflet, amounting to 10.2 ± 2.14% and 8.4 ± 1.61% for cellulose and hemicellulose, respectively. However, the percentage of cellulose and hemicellulose found in the OPF leaflet is far too low for the economical production of biobutanol. This is because, to date, no research has demonstrated a good butanol recovery from a substrate containing less than 30% holocellulose as a carbohydrate usable for butanol production. Moreover, the lignin fractions were found to be very high in all the OPF leaflet samples, which ranged from 52.4 ± 4.11% to 60.9 ± 3.08% (*Table 1*). The high amount of lignin in the OPF leaflets justifies the presence of abundant metals, which might be usable for many other industrial applications. Hence, the research went further to determine the elemental composition of the OPF leaflets.

Silicon was found to be the most abundant element in the entire powdered OPF leaflet samples, with relatively high levels compared to the other chemical elements present, such as calcium, potassium, and molybdenum, as determined by XRF analysis of their elemental composition. Even though some researchers reported a higher abundance of potassium in OPF leaves relative to silicon, this might be a result of the chemical constituents of the soil type in which the oil palm trees were grown. Other elements were found in trace quantities in OPF leaves, which include titanium, zinc, manganese, magnesium, aluminium, calcium and chlorine. Studies revealed that oil palm trees are good sources of silicon, potassium, and calcium, a fair source of microelements such as chlorine, magnesium, and sulphur, and a minor source of phosphorus (Alotaibi *et al*., 2019).

Another study reported that oil palm contains considerable amounts of calcium, magnesium, phosphorous, potassium, iron and zirconium (Mansir *et al*., 2017). From the results in *Table 1*, age was found to play a significant role in determining the amount of element present in the OPF leaflets, as it can be seen that the amount of silicon in the OPF leaflet samples is increasing with the increase in the age of the plant. The same trends were observed for manganese, aluminium, and chlorine, while for magnesium, zinc, and copper the reverse is the case. Based on our search, no reports are available in the literature for comparing the elemental composition of oil palm according to age, as determined in this study.

Effect of Frond Age on Lignocellulose Composition of OPF Bagasse

OPF petioles are reported as a good source of abundant unutilised carbohydrates, which consist of about 30%-50% cellulose, 20%-30% hemicellulose, and 20%-30% lignin and other extractive materials (Tnah *et al*., 2022). From the freshly harvested OPF, after the juice extraction, the composition of different ages of OPF bagasse was analysed for fractions of cellulose, hemicelluloses, lignin, and extractives. The weight percentages of each component per gramme of dry biomass

TABLE 1. LIGNOCELLULOSE AND ELEMENTAL COMPOSITION OF OPF LEAFLET

Composition		Samples of OPF leaflet (ppm)				*P*-value
		5 years	10 years	15 years	20 years	
Lignocellulose composition (%)	Cellulose	11.4 ± 2.04	10.9 ± 1.67	11.0 ± 0.84	10.2 ± 2.14	0.0447
	Hemicellulose	13.7 ± 1.54	11.5 ± 1.22	12.6 ± 2.00	8.4 ± 1.61	0.0034
	Lignin	52.4 ± 4.11	52.6 ± 2.34	60.9 ± 3.08	59.3 ± 2.44	0.0452
	Extractives	22.4 ± 1.56	24.6 ± 2.15	15.5 ± 2.64	22.1 ± 2.02	0.9621
Elemental analysis (ppm)	Mn	993 ± 21.4	1 790 ± 26.0	4 230 ± 43.5	3 190 ± 35	<0.0001
	Mg	1 300 ± 138	1 160 ± 138	1 200 ± 135	961 ± 128	<0.0001
	Al	1 050 ± 21.5	17 800 ± 22.8	21 700 ± 25.3	24 000 ± 19.6	<0.0001
	Si	836 000 ± 421	864 000 ± 660	754 000 ± 340	854 000 ± 504	0.0466
	Zn	232 ± 6.36	243 ± 4.64	206 ± 4.65	118 ± 3.15	0.0525
	Cu	302 ± 6.04	253 ± 7.83	228 ± 5.73	69 ± 3.08	0.0312
	Cl	2 800 ± 9.04	4 900 ± 28.0	5 750 ± 26.7	29 200 ± 30.5	<0.0001
	K	57 200 ± 298	26 500 ± 215	40 900 ± 280	34 800 ± 231	<0.0001
	Ca	8 560 ± 371	35 100 ± 201	39 500 ± 216	41 000 ± 212	<0.0001
	Mo	5 700 ± 16.9	ND	35 300 ± 83.1	ND	<0.0001
	Ru	9 510 ± 43.4	ND	89 300 ± 136	ND	<0.0001

Note: ND - not determined, while the number before " ± " denotes mean values of three replicate and the number after " ± " denotes standard deviation. *P*-value less than 0.05 indicate significant difference, while *p*-value of 0.05 and above indicates that there is no significant difference in the composition across the different ages of palm tree.

are presented in *Table 2*. The highest fraction was found to be cellulose in 5, 10, 15 and 20 years of OPF bagasse, with the highest cellulose in the 5 year sample accounting for about 40.1 ± 2.13% of the total and the lowest percentage obtained in the 20 year sample (21.3 ± 2.35%).

The second most abundant fraction in the lignocellulose composition of OPF bagasse was hemicellulose, which amounts to 18% to 28% of the lignocellulose content. The percentages of cellulose and hemicelluloses in OPF bagasse in this study were quite comparable with the previously reported biomass material, including OPF itself (*Table 2*). However, this result shows slightly lower holocellulose content in comparison with 56.0% and 16.7% for cellulose and hemicelluloses, respectively (Khalil *et al*., 2012). Additionally, the percentage of holocellulose (cellulose and hemicellulose) in this study showed a decreasing trend as the oil palm plants grew older. The differences observed in the percentage of cellulose, hemicellulose, and lignin across the different ages of OPF (with a *p*-value of <0.0001, which indicated the difference between the four ages used at a 5% level of significance) might not be only due to the differences in the source used but also in the different maturity levels of the plants. According to Perlo *et al.* (2020), the chemical composition of lignocellulose biomasses may vary with plant age, plant height, and anatomical structure, which can limit or increase the cellulose, hemicellulose and lignin ratios.

The breakdown of lignocellulose material into reducing sugar as a product can still be maximised by effective pretreatment, even though OPF has a lower cellulose and hemicellulose content than other reported biomass materials. This is so because the effectiveness of enzymatic hydrolysis is heavily dependent on the biomass's digestibility. There are three major types of pretreatment methods in use today; physical, chemical, and biological methods, all aimed at breaking down the naturally resistant carbohydrate-lignin barrier that prevents enzymes from accessing holocellulose by disrupting the internal structure of holocellulose and increasing the reaction surface and porosity of biomass (Dutra *et al*., 2018; Rafieisakhaei and Barazandeh, 2017). However, pretreatment is the most critical need that must be addressed for this lignocellulosic biomass to become a commercially viable and cost-effective material for bio-based productions, such as biobutanol. It is reported that, out of the total cost of the bioconversion of biomass to biofuels, nearly 40% of the projected cost is connected with the release of sugars from cellulose and hemicellulose through the pretreatment operations (Zhang, 2019). Therefore, there is a need to continue research and development for an efficient pretreatment technology to produce low-cost fermentable sugar from the processing of OPF bagasse.

Effect of Frond Age on Total and Individual Fermentable Sugar of OPF Juice

The juices extracted from the oil palm frond samples were investigated for their total reducing sugar content via the DNS method, and the results are presented in *Table 3*. The results indicated a decreasing order of total fermentable sugar in OPF

TABLE 2. LIGNOCELLULOSE COMPOSITION OF OPF BAGASSE

Age of palm oil tree	Pretreatment type	Cellulose (%)	Hemicellulose (%)	Lignin (%)	Extractive (%)	References
5 years	Physical (Pressing)	38.7 ± 2.25	27.4 ± 1.84	24.8 ± 0.88	09.5 ± 1.55	
10 years	Physical (Pressing)	40.1 ± 2.13	24.5 ± 3.04	22.7 ± 2.41	12.7 ± 2.14	
15 years	Physical (Pressing)	30.3 ± 2.66	26.4 ± 2.30	31.4 ± 3.06	11.9 ± 1.41	This study
20 years	Physical (Pressing)	21.3 ± 2.35	18.4 ± 1.08	52.9 ± 1.20	07.5 ± 4.20	
p-value		<0.0001	<0.0001	<0.0001	<0.0001	
Report from other researches						
NA	Physical (Pressing)	43.6	8.22	10.4	NA	Rusli *et al*. (2016)
NA	Physical (Ball milling)	32.5	22.5	15.2	16.4	Zakaria *et al*. (2014)
NA	Physico-chemical	44.0	30.4	15.4	04.1	Sabiha-Hanim *et al*. (2011)
NA	Chemical	28.7	26.0	37.6	07.6	Sukri *et al*. (2014)
NA	Chemical	56.0	16.7	28.5	04.4	Khalil *et al*. (2012)
NA	Chemical	45.0	32.0	16.9	02.3	Megashah *et al*. (2018)
NA	Chemical	42.8	20.9	32.0	04.4	Dávila *et al*. (2016)

Note: The number before "±" denotes mean values of three replicate and the number after "±" denotes standard deviation. *P*-value less than 0.05 indicate significant difference exist in the lignocellulose composition across the different ages of palm tree.

juices as the plant increases in age, with 69.04 ± 1.14 g/L, 65.44 ± 0.55 g/L, 48.22 ± 2.46 g/L, and 43.59 ± 1.52 g/L for 5, 10, 15 and 20 years of OPF juice, respectively. However, all of the studied OPF juice samples contained total fermentable sugar contents higher than the minimum recommended level for a substrate intended for the production of biofuels. The relatively lower fermentable sugar found in the 15 and 20 year samples can be attributed to the negative correlation that exists between holocellulose and lignin. Plants usually become lignified as they grow older in defense against external factors, which invariably lower the level of cellulose and hemicellulose. Thus, the results of the current research indicated a significant relationship between the total amount of fermentable sugar and the age of the plant (with a *p*-value less than α, which indicated a significant interaction of the age and sugar contents), with the older plant having a lower sugar content compared with the younger plant (*Table 3*). The trend of the results is in agreement with the previously reported study, where they found that the content of sugar in OPT at 19 years is 6.6/350.0 kg of dried OPT, which is significantly higher than the OPT at 31 years with only 4.6/350.0 kg (Murai and Kondo, 2011).

To utilise the best oil palm frond juice as feedstocks for the bioenergy conversion process, knowledge on the variation of sugar types between the different ages of oil palm fronds is considered very important, as the compositional data of a feedstock is crucial to gaining an understanding of feedstock properties prior to selecting a processing or conversion technology. This is because not all types of sugars can be readily fermented by some microorganisms. According to Zwetsloot *et al*. (2020), specific sugar mixtures such as glucose, fructose, arabinose, galactose, mannose, xylose, *etc*., in the substrate determine the activity of the microbial communities and their utilisation. It is observed that the specific sugars (*e.g*., glucose and fructose) in sugar substrates are shown to positively associate with microbial growth and fermentation. For example, the presence of glucose in a substrate influences the growth of the abundant genera *Lactobacillus* and *Saccharomyces*, which are the most utilised microbial communities related to butanol fermentation (Wei *et al*., 2021). Meanwhile, glucose and fructose are the preferred substrates for anaerobic strains to produce acetone, butanol and ethanol in fermentation (Ezeji *et al*., 2007). Even though the proper combination of sugar mixture in a substrate and its ratio has a significant influence on microbial growth and fermentation, there is little or no information on the profile of sugar in OPF juice at the different maturity stages. Hence, the present study analyses the profiles of individual sugars in the juice samples extracted from OPF ages, and the results are shown in *Table 3*.

As can be observed in *Table 3*, differences exist in the concentration of individual sugars present in the various OPF juices extracted from different ages of oil palm trees. It is found that the fermentable sugars in the juices contain two monosaccharides (glucose and fructose) and one disaccharide (sucrose) in various proportions and concentrations. Among the individual sugars, glucose was found to have the highest percentage, ranging from 55% to 65% of the total sugar in all the OPF juice samples tested (63.17%, 60.43%, 56.95% and 64.46% for ages 5, 10, 15 and 20, respectively). The remaining percentage of the total fermentable sugar was made up of the

TABLE 3. TOTAL FERMENTABLE SUGAR CONTENT IN OPF JUICE SAMPLES

	Total fermentable sugar	Glucose		Sucrose		Fructose		References
		g/L	%	g/L	%	g/L	%	
5 years	69.03 ± 1.14 g/L	43.61 ± 1.6	63.17	16.53 ± 0.4	23.90	8.19 ± 2.1	12.0	This study
10 years	65.44 ± 0.55 g/L	39.55 ± 0.5	60.43	12.64 ± 1.3	19.32	8.02 ± 1.5	12.25	
15 **years**	48.22 ± 2.46 g/L	27.46 ± 1.1	56.95	12.14 ± 1.5	25.18	9.56 ± 0.2	19.8	
20 **years**	43.53 ± 3.52 g/L	28.06 ± 2.2	64.46	9. 69 ± 0.6	22.23	7.43 ± 2.6	17.06	
p-value		<0.0001		0.0086		<0.0357		
Reports from other studies								
NA	44.2 g/L	24.80	56.11	15.2	34.39	3.10	7.01	Tan *et al*. (2016)
NA	65.0 g/L	42.00	64.62	22.0	33.85	1.00	1.54	Zahari *et al*. (2014)
NA	76.1 g/L	53.95	70.00	20.46	27.00	1.68	3.00	Zahari *et al*. (2012)
NA	116.4 g/L	89.83	77.17	19.6	16.84	6.93	5.95	Abdullah *et al*. (2021)

Note: The number before " ± " denotes mean values of three replicate and the number after " ± " denotes standard deviation. *P*-value less than 0.05 indicate significant difference exist between the sugar compositions across the different ages of palm tree.

two sugar types detected in the samples, which were detected in relatively lower concentrations, with fructose ranging from 19% to 26% and sucrose from 12% to 20%. Even though the total fermentable sugar of all the OPF juice samples analysed in this study has significant differences across the various ages of the palm plants, fluctuations in the concentrations of individual sugars were also observed as the plant's age increased. It is noted that the sucrose percentage in the OPF juices increases as the plant's age increases, *i.e*., from a younger sample to the most matured sample tested, where glucose and fructose showed reverse gradients, with the younger plant sample having the higher percentage. These inherent fluctuations in the sugar composition of the oil palm plant with age have yet to be fully cleared. Some researchers hypothesised a similar situation on temperate fruit-bearing species such as the oil palm tree. They suggested that the variation in chemical composition with age and storage compartment could be as a result of the need for the plant to balance the unsatisfactory photosynthesis to sustain organ demands (Suryawan and Heru, 2019).

Effect of Frond Age on Total and Individual Phenolic Compounds of OPF Juice

The total phenolic content of the oil palm frond juice samples investigated was found to vary among the different ages of the juice samples. The concentrations of each of the total phenolic contents measured at the different ages of the studied samples are presented in *Table 4*. The result indicated a decreasing order of total phenolic compound concentration in the samples, *i.e*., younger oil palm fronds contained juice with higher phenolic compounds relative to the older. The juice from 5 years of OPF contains a total phenolic compound of 0.332 ± 0.01 g/L, which is higher than the concentration of phenolic compounds found in the 10, 15 and 20 years, with level of 0.317 ± 0.00, 0.282 ± 0.02 and 0.260 ± 0.01 g/L, respectively. This means that more phenolic compounds are accumulated in younger OPFs than in older ones. However, two previous studies suggested the reverse, such that phenolic contents in plants increase with plant age. For example, the research conducted on *Mentha* L. species on the variation of secondary metabolites, especially the polyphenols and tannins, based on the 1-4 years has indicated an improvement in the quantity of polyphenols and tannins as the plant gets older, with the highest polyphenols of 12.74% obtained in the 4 years, compared to only 11.98% and 9.44% obtained from the 3 and 2 years, respectively (Aleksic and Knezevic, 2014; Muyny and Chantarapanont, 2022).

Moreover, research conducted to compare the levels of secondary metabolites (phenols and flavonoids) and their distribution shows that the content of phenols is not only affected by the differences between the plant organs but also by the stage of plant growth (Fialová *et al*., 2015; Saffaryazdi *et al*., 2020). Their results showed significant differences in the flavonoid content between leaf and stem as well as with the change in growth stage. At the flowering stage, the flavonoid content of the leaves was five times higher than the value measured in the stems. However, during the vegetative stage, the measured flavonoid levels in the leaves were 1.3 times higher than their content in the stems. The research finally suggested that the changes in flavonoid content were also affected by both physiological and growth stages (Saffaryazdi *et al*., 2020). Therefore, the present study suggested that the differences in phenolic compound levels could be attributed to the influence of external factors (long-term weather before harvesting time, intensity of sunlight, pathogens, and time of harvesting).

TABLE 4. TOTAL AND INDIVIDUAL PHENOLIC CONTENT IN OPF JUICE SAMPLES

Phenolic compounds	Concentrations of phenolic compounds (mg/L)				
	5 years	10 years	15 years	20 years	*P*-value
Total phenolic content (g/L)	0.332 ± 0.01	0.317 ± 0.00	0.282 ± 0.02	0.260 ± 0.01	<0.0001
Gallic acids (g/L)	0.264 ± 0.02	0.251 ± 0.01	0.207 ± 0.00	0.194 ± 0.03	<0.0001
p-coumaric acids (g/L)	ND	ND	ND	ND	ND
Vanillic acids (g/L)	ND	ND	0.013 ± 0.04	0.017 ± 0.01	<0.0001
Ferulic acids (g/L)	0.061 ± 0.00	0.050 ± 0.01	0.064 ± 0.02	0.079 ± 0.02	<0.0001

Note: ND - Not detected, while the number before " ± " denotes mean values of three replicate and the number after " ± " denotes standard deviation. *P*-value less than 0.0001 indicate significant difference between the profiles of phenolic compound across the different ages of palm tree.

Table 4 presents the differences that exist in the concentration and profile of the various OPF juices extracted from different ages of oil palm trees. The results indicated that phenolic compounds such as gallic acid, ferulic acid, and vanillic acid were detected in the 15 and 20 year old juice samples, while only gallic acid and ferulic acid were detected in the 5 and 10 year old juice samples. Earlier, it was proposed that variations in the types and distribution of secondary metabolites across plant organs, maturity stage, and nutrient presence in the soil might account for the observed differences in phenolic compound types. However, beside the differences in the number of phenolic compounds detected, the concentrations of individual phenols differ. Gallic acid was discovered to be the most abundant individual phenol, accounting for approximately 80% of the total phenolic compound in the juices. However, the concentration of gallic acid decreases with an increase in the age of the palm tree. The second most abundant phenolic compound type is ferulic acid, which consists of about 18% of the total phenolic compound, and its concentration fluctuates across the ages of the palm tree. The other phenolic compound detected was found only in 15 and 20 years, with 0.01 3± 0.04 and 0.079 ± 0.01 g/L, respectively.

Depending on the type of phenolic compound, its concentration, and other physicochemical parameters of the culture medium, such as temperature and pH, the effects of a variety of phenolic compounds usually vary among the different organisms used in the fermentation process. For example, *C. beijerinckii* BA101 was less affected by acetates, furfural, and HMF at concentrations less than 1.9 g/L (Ezeji *et al*., 2007), while solvent production halted in *C. acetobutylicum*, especially when the cells were in a medium where acetic and butyric acids accumulated quickly and caused the pH to drop (Suryawan and Heru, 2019). Another study on the toxicity of various phenolic compounds found that phenolic compounds (coumaric acid, ferulic acid, and 4-hydroxybenzoic acid) at 1 g/L can inhibit the growth of most microorganisms by up to 70%, effectively inhibiting butanol production (Muyny and Chantarapanont, 2022). However, syringaldehyde and vanillin were reported to be less toxic to cell multiplication, even though butanol production can be highly inhibited (Aleksic and Knezevic, 2014). In general, phenolic compounds like ferulic acid were found to be more toxic to most *Clostridia* sp., followed by coumaric acid, especially at concentrations above 0.5 g/L (Fialová *et al*., 2015).

A correlation was established between the age of the OPF samples and their fermentable sugar levels and phenolic compounds. The fermentable sugars in the OPF juice tend to decrease as the oil palm tree gets older. The same trend was seen in the relationship between the age of oil palm trees and the level of fermentable sugar. Higher phenolic compounds in the OPF juices also show a decreasing pattern with the increase in the age of oil palm trees, as in the case of the concentration of fermentable sugar. Another correlation was observed between the total fermentable sugar and the lignocellulose composition of the OPF bagasse, such that the higher the sugar levels, the lower the level of cellulose and hemicellulose. For example, 5 year old OPF, which had the highest fermentable sugar, showed a decrease in the percentage of holocellulose, suggesting that the fermentable sugars are generated from the holocellulose. It is observed that there is a specific relationship between potassium availability and sugar composition and concentration; research shows that, in rachis, the sugar composition changed a lot under low potassium availability, irrespective of the age of the rachis, with a 60% increase in glucose (Cui *et al*., 2020). However, in this study also, the concentration of potassium detected in 5 year old OPF leaves is higher than what is observed in 10, 15 and 20 year old OPF leaves, showing strong agreement with the previously mentioned report because both potassium and total sugar are higher in 5 year old OPF leaves than they are in the older OPF leaves.

Screening and Identification of Potential Bacteria for ABE Fermentation Using OPF Juice

In an effort to improve the performance of biobutanol production via ABE fermentation using OPF juice, a strain screening process was employed to assist in the selection of the best and most robust strain of *Clostridium* for biobutanol production. Eleven potential bacteria were screened, including *Clostridium acetobutylicum* SR1, which was previously isolated from cow dung, L1 and L2 WK1, WK2, LM1, LM2, A1, A2 and S1, previously isolated and preserved in a -4°C refrigerator in the Biorefinery Research Laboratory, UTM. All the isolates were studied for tolerance towards phenolic compounds as well as their ability to utilise hydrolysate from OPF juice for ABE fermentation. Ten years old oil palm frond juice was used as the fermentation feedstocks, which contain 50 g/L reducing sugar (37 g/L glucose, 6 g/L fructose, and 7 g/L sucrose) as the sole carbon and energy source from the P2 medium.

Table 5 presented the results of bacterial screening for the biobutanol production using OPF juice. The results indicated that, eight out of the total of 11 strains screened have successfully thrived in the presence of phenolic compounds and were able to utilise the hydrolysate from oil palm frond juice for biobutanol production via ABE fermentation. Strains SR1, L2, A1, WK1, WK2, LM1, LM2 and S1 were able to produce certain amounts of butanol, while on the other hand, strains L1, A2 and A1 (UPM) were unable to ferment the reducing sugars in the hydrolysate to produce a significant amount of biobutanol.

The general fermentation kinetics of the strains screened for the production of butanol via ABE fermentation are presented in *Table 5*. It can be seen that the different strains have shown different abilities for both acid and solvent production. The strains also demonstrated dissimilar potentials during the fermentation process, as different end product concentrations were obtained. Strain A1 resulted in the highest production with a butanol concentration of 2.32 g/L and a productivity of 6.4×10^{-2} g/L/hr. This was followed by strains SR1 and L2, with butanol production of 2.04 g/L and 1.96 g/L, while other strains showed poor utilisation ability of the hydrolysate for the production of butanol, with the least production of butanol of 0.03 g/L by L1 and zero production from A2. However, other solvents, such as acetone and ethanol production, were also fairly high in the culture with the A1 strain. Acetone and ethanol production observed were 2.59 g/L and 1.53 g/L, respectively, with total solvent production of 6.44 g/L. Strain A1 also showed a considerably high acid production during ABE fermentation, with acetic acid and butyric acid concentrations of 0.185 g/L and 1.234 g/L, respectively, and a total acid production of 1.419 g/L produced. The higher solvent produced by A1 indicated that the strain can tolerate the highly acidic conditions caused by the production of organic acids during the acidogenic phase, and the nature of the waste, which contains high levels of undissociated organic acids and phenolic inhibitors.

During the 96 hr of batch culture fermentation, it was observed that the acidogenic phase of most of the strains was between 16 and 24 hr of the fermentation, where acetic acid and butyric acid were the main products produced, except for strains L2, WK1 and WK2, which could not produce the acids until after 30 hr of the fermentation. However, the production of total acids after 96 hr of fermentation by different strains was observed within the range of 0.001 to 2.781 g/L, with the highest being the S1. Unfortunately, this high production of acetic and butyric acid within 48 to 96 hr of ABE fermentation by strains S1 and LAMA1 could possibly be due to the incomplete phase transition from the acidogenic phase to the solventogenic phase, which later hinders solvent production. This is because the presence of organic acids at high concentrations that accumulated during fermentation decreased the capability of the microorganisms for uptake and recycling of both butyric and acetic acids, resulting in a very low ABE concentration.

After 96 hr of fermentation, A1 had used about 70% of the fermentable, leaving 13.4 g/L as the main residual sugars in the medium (*Figure 2*). This indicated that the isolate could utilise all the sugar types in the hydrolysate. The higher solvent production by strain A1 (*Table 5*) and good substrate utilisation ability of the strain can be directly related to the good biomass production. Efficient substrate utilisation indicates that the strain is able to use the carbon source provided, which results in an increase in microbial growth. As can be seen from *Table 5*, a total of 0.372 g/L of biomass was obtained in the culture of A1 at the end of the ABE fermentation with a doubling time of 1.61/hr. Other isolates, like LAMA1, displayed higher substrate utilisation relative to A1. However, this isolate could only produce a high amount of acids with a relatively lower solvent concentration, which might be because of the lower pH and other phenolic compounds and product inhibition (Capilla *et al*., 2021). The isolate LAMA2 was unable to use the substrate provided for new cell propagation, which could have aided in increased solvent production. The inability of the isolates to utilise the hydrolysate is proven based on the higher residual reducing sugar left in the culture at the end of the fermentation.

TABLE 5. FERMENTATION KINETICS OF THE STRAINS SCREENED FOR THE PRODUCTION OF BUTANOL VIA ABE FERMENTATION

Parameters	Strain SR1	L2	L1	A1	A2	WK 1	WK 2	LAMA 1	LAMA 2	S1	A1 (UPM)
Max. acetone (g/L)	0.38 ± 0.02	0.92 ± 0.04	0.11 ± 0.01	2.59 ± 0.03	0.00	0.07 ± 0.01	0.09 ± 0.02	0.26 ± 0.01	0.00	0.00	0.11 ± 0.05
Max. butanol (g/L)	1.96 ± 0.04	2.04 ± 0.01	0.03 ± 0.02	2.32 ± 0.05	0.00	0.35 ± 0.05	0.15 ± 0.01	0.40 ± 0.02	0.03 ± 0.05	0.04 ± 0.02	0.03 ± 0.01
Max. ethanol (g/L)	2.30 ± 0.06	1.67 ± 0.03	0.01 ± 0.00	1.53 ± 0.05	0.00	0.04 ± 0.03	0.00	0.43 ± 0.07	0.00	0.00	0.04 ± 0.08
Max. solvent (ABE) (g/L)	4.58 ± 0.11	4.63 ± 0.08	0.16 ± 0.04	6.44 ± 0.12	0.00	0.45 ± 0.06	0.24 ± 0.05	0.97 ± 0.06	0.03 ± 0.02	0.04 ± 0.02	0.16 ± 0.14
Max. acetic acid (g/L)	1.35 ± 0.04	0.25 ± 0.02	0.03 ± 0.01	2.19 ± 0.06	0.86 ± 0.00	0.02 ± 0.01	0.01 ± 0.02	0.22 ± 0.05	0.27 ± 0.03	1.14 ± 0.22	0.02 ± 0.01
Max. butyric acid (g/L)	2.90 ± 0.03	0.90 ± 0.06	0.07 ± 0.02	2.36 ± 0.04	0.13 ± 0.02	0.13 ± 0.03	0.01 ± 0.05	1.64 ± 0.11	0.16 ± 0.08	1.64 ± 0.24	0.06 ± 0.02
Max. acid (g/L)	4.25 ± 0.07	1.05 ± 0.08	0.09 ± 0.04	4.55 ± 0.10	0.99 ± 0.02	0.16 ± 0.03	0.02 ± 0.02	1.86 ± 0.16	0.43 ± 0.04	2.78 ± 0.41	0.09 ± 0.04
Acetone productivity (g/L/hr)	1.1×10^{-2}	1.9×10^{-2}	0.3×10^{-2}	5.3×10^{-2}	0.00	0.3×10^{-2}	03×10^{-2}	1.0×10^{-2}	0.00	0.00	0.2×10^{-2}
Butanol productivity (g/L/hr)	8.1×10^{-2}	5.6×10^{-2}	0.2×10^{-2}	6.4×10^{-2}	0.00	0.7×10^{-2}	0.6×10^{-2}	1.6×10^{-2}	0.1×10^{-2}	0.1×10^{-2}	0.1×10^{-2}
Ethanol productivity (g/L/hr)	9.5×10^{-2}	6.9×10^{-2}	0.1×10^{-2}	4.2×10^{-2}	0.00	0.1×10^{-2}	0.00	1.7×10^{-2}	0.00	0.00	0.1×10^{-2}
Acetic acid productivity (g/L/hr)	5.6×10^{-2}	0.9×10^{-2}	0.1×10^{-2}	6.0×10^{-2}	0.00	0.1×10^{-2}	0.04×10^{-2}	0.9×10^{-2}	0.7×10^{-2}	4.7×10^{-2}	0.05×10^{-2}
Butyric acid productivity (g/L/hr)	8.0×10^{-2}	1.8×10^{-2}	0.3×10^{-2}	4.9×10^{-2}	3.5×10^{-2}	0.5×10^{-2}	0.04×10^{-2}	1.0×10^{-2}	0.6×10^{-2}	6.8×10^{-2}	0.1×10^{-2}
Overall acetone productivity (g/L/hr)	0.5×10^{-2}	1.4×10^{-2}	0.2×10^{-2}	4.7×10^{-2}	1.0×10^{-2}	0.1×10^{-2}	0.1×10^{-2}	0.5×10^{-2}	0.00	0.00	0.2×10^{-2}
Overall butanol productivity (g/L/hr)	4.0×10^{-2}	4.2×10^{-2}	0.1×10^{-2}	4.4×10^{-2}	0.00	0.7×10^{-2}	0.3×10^{-2}	0.6×10^{-2}	0.00	0.00	0.06×10^{-2}
Overall ethanol productivity (g/L/hr)	3.9×10^{-2}	3.4×10^{-2}	0.02×10^{-2}	3.1×10^{-2}	0.00	0.1×10^{-2}	0.00	0.6×10^{-2}	0.00	0.00	0.05×10^{-2}
Overall total solvent productivity (g/L/hr)	7.1×10^{-2}	9.6×10^{-2}	0.4×10^{-2}	12×10^{-2}	0.00	1.3×10^{-2}	0.5×10^{-2}	2.0×10^{-2}	0.1×10^{-2}	0.00	0.3×10^{-2}
Overall acetic acid productivity (g/L/hr)	2.8×10^{-2}	0.5×10^{-2}	0.1×10^{-2}	4.5×10^{-2}	2.3×10^{-2}	0.08×10^{-2}	0.02×10^{-2}	0.4×10^{-2}	0.05×10^{-2}	1.0×10^{-2}	0.04×10^{-2}
Overall butyric acid productivity (g/L/hr)	6.0×10^{-2}	1.0×10^{-2}	0.15×10^{-2}	4.9×10^{-2}	0.4×10^{-2}	0.5×10^{-2}	0.02×10^{-2}	3.4×10^{-2}	0.3×10^{-2}	5.0×10^{-2}	0.07×10^{-2}
Overall total acids productivity (g/L/hr)	5.9×10^{-2}	2.1×10^{-2}	0.2×10^{-2}	9.4×10^{-2}	4.1×10^{-2}	0.3×10^{-2}	0.03×10^{-2}	3.9×10^{-2}	0.69×10^{-2}	5.1×10^{-2}	1.8×10^{-2}
Initial total fermentable sugar (g/L)	47.50	47.50	47.50	47.50	47.50	47.50	47.50	47.50	47.50	47.50	47.50
Final total fermentable sugar (g/L)	18.2	19.5	26.7	13.4	22.5	31.7	20.6	12.2	36.8	17.0	29.8
Percentage of sugar consumed (%)	66.7	59.1	45.3	69.1	52.6	33.2	56.6	74.3	22.5	64.2	37.3
Sugar utilisation rate (g/L/hr)	0.33	0.31	0.217	0.35	0.260	0.165	0.280	0.368	0.111	0.318	0.184
Xmax (g/L)	0.317	1.051	0.283	0.372	0.187	0.123	0.265	0.520	0.161	0.420	0.247
Doubling time td (hr^{-})	1.395	0.659	1.610	1.863	0.609	0.374	0.741	1.261	0.322	0.951	0.410

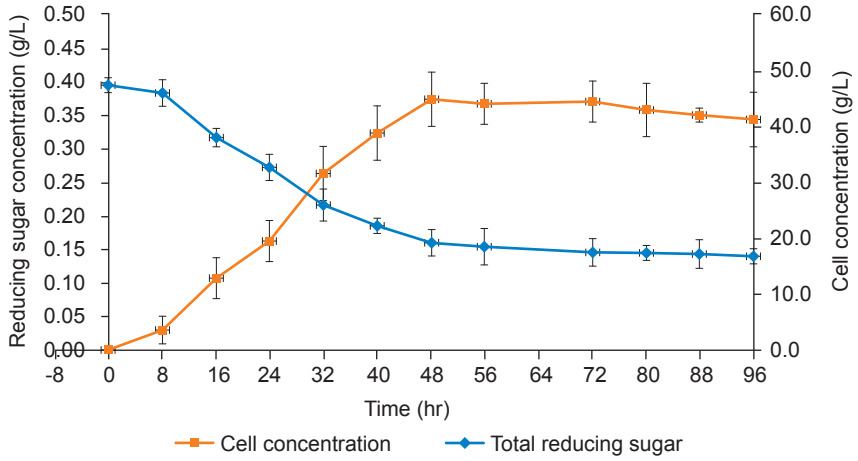


Figure 2. Time course for bacterial growth and sugar utilisation by Clostridium *strain A1 in P2 medium containing 70% of OPF hydrolysate.*

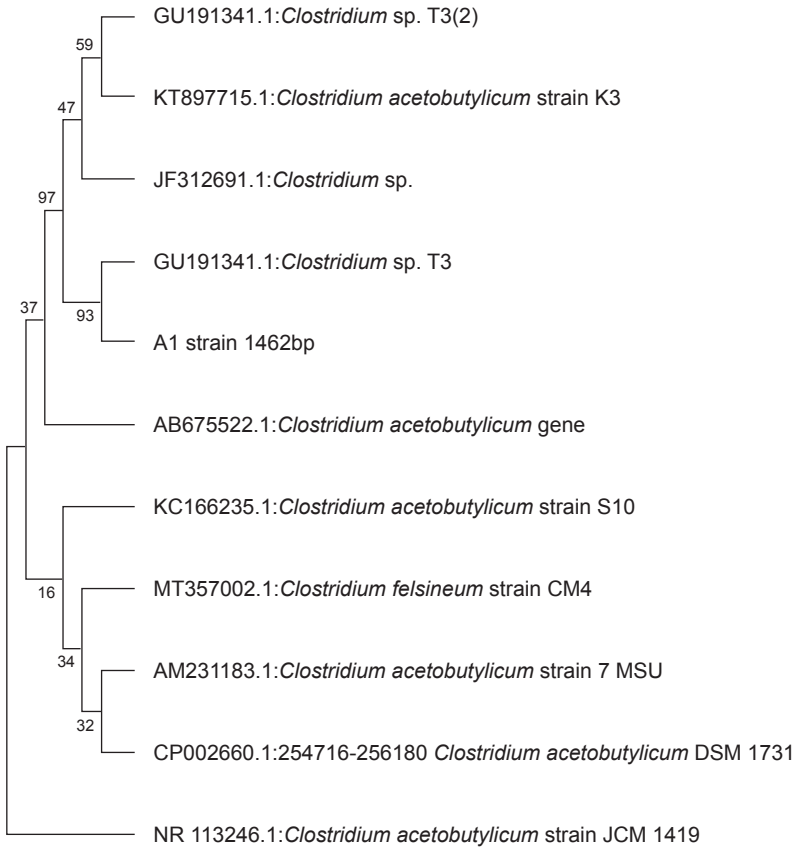


Figure 3. Phylogenetic tree based on 16S rRNA gene sequence link showing the relationship between bacteria of the genus Clostridium *sp. and the strain A1.*

Identification of the Strains

The 16S rRNA gene has been identified as roughly 1.55 kb in length and is composed of both variable and conserved regions with sufficient interspecific polymorphisms that can also be responsible for distinct and statistically accurate measurements (Al-Haideri, 2019). Apart from being the most conserved region among the three rRNA genes (16S, 23S and 5S), the 16S rRNA gene is highly conserved in bacteria, making it the best gene for comparing and identifying newly isolated bacteria. The 16S rRNA gene sequence analysis of the pure bacterium in this study revealed 1427 base pairs in the gene sequence. The bacteria's evolutionary history was investigated

by constructing a phylogenetic tree using the neighbor-joining technique (Hong *et al*., 2021). The P-distance method was used to calculate the evolutionary distance (Criscuolo, 2020). The 16S rRNA analysis with BLASTN indicated that the bacterial strain A1 belongs to the *Clostridium* species and is 99% identical to *Clostridium acetobutylicum* GXO1. As a result, the strain was given the name *Clostridium* strain A1. The phylogenetic tree in *Figure 3* depicts the relationship between closely related isolates with a higher similarity index.

The present research highlighted new developments in feedstock selection criteria and utilisation, microbial strain development, and fermentation process development, all of which significantly impact the production economy. This technology is hoped to offer a synergistic relationship for industry to capitalise on underutilised organic wastes such as OPF biomass for biobutanol production. Considering that the investigation of changes in biobutanol economic traits as trees age will inform optimal harvesting ages and biomass requiring fewer pretreatments to deconstruct biomass.

CONCLUSION

The current study evaluated the chemical composition of OPF leaflets, bagasse, and juice at different ages for its potential application for biobutanol production. Relative to leaflets and bagasse, pressed juices from different ages of OPF are indicated to contain a higher amount of renewable sugars, including glucose, sucrose, and fructose. However, an increase in palm age was seen to significantly decrease the concentration of both fermentable sugars and total phenolic compounds in the juice. Thus, juice from 10-year-old OPF containing 65.44 g/L of total fermentable sugar and 0.317 g/L of phenolic compounds was selected and used for biobutanol production using 11 strains of *Clostridia* species. Despite the presence of phenolic compound inhibitors, strain A1 was found to be the most successful strain that tolerated the inhibitors and utilised the sugars in the hydrolysate to produce 2.32 g/L of biobutanol. The strain was identified as *Clostridium* strain A1 based on 16S rRNA gene sequencing. Therefore, the research recommends optimising biobutanol production from 10-year-old OPF juice using *Clostridium* strain A1 as the fermentation microorganism.

ACKNOWLEDGEMENT

This study was funded by the UTM High Impact Research grant (Q.J130000.2454.09G06), under the Universiti Teknologi Malaysia. The first author also acknowledged TETFund, Nigeria for financial assistance during his PhD studies.

REFERENCES

Abe, K; Hori, Y and Myoda, T (2020). Characterization of key aroma compounds in aged garlic extract. *Food Chem., 312*: 126081.

Abubakar, A; Ishak, M Y and Makmom, A A (2022). Nexus between climate change and oil palm production in Malaysia: A review. *Environ. Monit. Assess., 194*: 1-22.

Al-Haideri, H (2019). Gene expression of blaOXA-51-like and blaOXA-23 in response to β-lactam antibiotic in clinically isolated *Acinetobacter baumannii* and *Acinetobacter lowffii* from urine samples. *Iraqi J. Agric. Sci., 5.*

Aleksic, V and Knezevic, P (2014). Antimicrobial and antioxidative activity of extracts and essential oils of *Myrtus communis* L. *Microbiol. Res., 169*: 240-254.

Alotaibi, M D; Alshammari, B A; Saba, N; Alothman, O Y; Sanjay, M; Almutairi, Z and Jawaid, M (2019). Characterization of natural fiber obtained from different parts of date palm tree (*Phoenix dactylifera* L.). *Intl. J. Biol. Macromol., 135*: 69-76.

Ang, S; Yahya, A; Abd Aziz, S and Md Salleh, M (2015). Isolation, screening, and identification of potential cellulolytic and xylanolytic producers for biodegradation of untreated oil palm trunk and its application in saccharification of lemongrass leaves. *Prep. Biochem. Biotechnol., 45(3)*: 279-305.

Asri, F; Masngut, N and Zahari, M (2019). Biobutanol production from oil palm frond juice in 2 L stirred tank bioreactor with in situ gas stripping recovery. *IOP Conf. Ser.: Mater. Sci. Eng., 702*: 012004. IOP Publishing.

Capilla, M; San-Valero, P; Izquierdo, M; Penya-roja, J and Gabaldón, C (2021). The combined effect on initial glucose concentration and pH control strategies for acetone-butanol-ethanol (ABE) fermentation by *Clostridium acetobutylicum* DSM 792. *Biochem. Eng. J., 167*: 107910.

Criscuolo, A (2020). On the transformation of MinHash-based uncorrected distances into proper evolutionary distances for phylogenetic inference. *F1000Res., 9*: 1309.

Cui, J; Lamade, E and Tcherkez, G (2020). Potassium deficiency reconfigures sugar export and induces

catecholamine accumulation in oil palm leaves. *Plant Sci., 300*: 110628.

Deshavath, N N; Mukherjee, G; Goud, V V; Veeranki, V D and Sastri, C V (2020). Pitfalls in the 3, 5-dinitrosalicylic acid (DNS) assay for the reducing sugars: Interference of furfural and 5-hydroxymethylfurfural. *Intl. J. Biol. Macromol., 156*: 180-185.

Dutra, E D; Santos, F A; Alencar, B R A; Reis, A L S; de Souza, R d F R; da Silva Aquino, K A; Morais Jr, M A and Menezes, R S C (2018). Alkaline hydrogen peroxide pretreatment of lignocellulosic biomass: Status and perspectives. *Biomass Convers. Biorefin., 8*: 225-234.

Ezeji, T C; Qureshi, N and Blaschek, H P (2007). Bioproduction of butanol from biomass: From genes to bioreactors. *Curr. Opin. Biotechnol., 18*: 220-227.

Fialová, S; Tekeľová, D; Rendeková, K; Klinčok, J; Kolárik, M; Kurucová, K and Grančai, D (2015). Phenolic compounds variation in *Mentha* L. species in the course of a four-years period. *Eur. J. Pharm. Sci., 62*: 2-7.

Fonseca, B C; Bortolucci, J; da Silva, T M; dos Passos, V F; de Gouvêa, P F; Dinamarco, T M and Reginatto, V (2020). Butyric acid as sole product from xylose fermentation by a non-solventogenic *Clostridium beijerinckii* strain under controlled pH and nutritional conditions. *Bioresour. Technol. Rep., 10*: 100426.

Gomez-Flores, R; Thiruvengadathan, T N; Nicol, R; Gilroyed, B; Morrison, M; Reid, L M and Margaritis, A (2018). Bioethanol and biobutanol production from sugarcorn juice. *Biomass Bioenergy, 108*: 455-463.

Grande, L; Pedroarena, I; Korili, S A and Gil, A (2021). Hydrothermal liquefaction of biomass as one of the most promising alternatives for the synthesis of advanced liquid biofuels: A review. *Materials, 14*: 5286.

Guerrero, K; Gallardo, R; Paredes, I; Quintero, J; Mau, S; Conejeros, R; Gentina, J C and Aroca, G (2021). Continuous biohydrogen production by a degenerated strain of *Clostridium acetobutylicum* ATCC 824. *Intl. J. Hydrog. Energy, 46*: 5100-5111.

Hirakawa, H; Sumitomo, K; Hisamatsu, T; Nagano, S; Shirasawa, K; Higuchi, Y; Kusaba, M; Koshioka, M; Nakano, Y and Yagi, M (2019). *De novo* whole-genome assembly in *Chrysanthemum seticuspe*, a model species of Chrysanthemums, and its application to genetic and gene discovery analysis. *DNA Res., 26*: 195-203.

Hong, Y; Guo, M and Wang, J (2021). ENJ algorithm can construct triple phylogenetic trees. *Mol. Ther. Nucleic Acids, 23*: 286-293.

Huzir, N M; Aziz, M A; Ismail, S; Abdullah, B; Mahmood, N A N; Umor, N A and Muhammad, S A F a S (2019). Next generation of agro-industrial lignocellulosic residues to eco-friendly biobutanol. *Fossil Free Fuels*. CRC Press. p. 1-18.

Jacobson, M Z; von Krauland, A-K; Coughlin, S J; Dukas, E; Nelson, A J; Palmer, F C and Rasmussen, K R (2022). Low-cost solutions to global warming, air pollution and energy insecurity for 145 countries. *Energy Environ. Sci., 15*: 3343-3359.

Jiang, Y; Li, J; Ni, Y; Tang, Y; Wu, M; Zhang, W; Xin, F and Jiang, M (2022). High butanol production from galactose riched red seaweed *Gracilaria lemaneiformis* by solventogenic *Clostridium* sp. strain NJ4. *Fuel, 307*: 121867.

Khalil, H A; Jawaid, M; Hassan, A; Paridah, M and Zaidon, A (2012). Oil palm biomass fibres and recent advancement in oil palm biomass fibres based hybrid biocomposites. *Composites and Their Aplications* (Hu, N ed.). IntechOpen. 440 pp.

Lin, L; Yan, R; Liu, Y and Jiang, W (2010). In-depth investigation of enzymatic hydrolysis of biomass wastes based on three major components: Cellulose, hemicellulose and lignin. *Biores. Technol., 101(21)*: 8217-8223.

Liu, S; Qureshi, N and Hughes, S R (2017). Progress and perspectives on improving butanol tolerance. *World J. Microbiol. Biotechnol., 33*: 1-5.

Mansir, N; Taufiq-Yap, Y H; Rashid, U and Lokman, I M (2017). Investigation of heterogeneous solid acid catalyst performance on low grade feedstocks for biodiesel production: A review. *Energy Convers. Manag., 141*: 171-182.

Marguí, E; Queralt, I and Hidalgo, M (2009). Application of X-ray fluorescence spectrometry to determination and quantitation of metals in vegetal material. *Trends Analyt. Chem., 28*: 362-372.

Mat Rozi, N; Hamid, H A; Hossain, M S; Khalil, N A; Ahmad Yahaya, A N; Syimir Fizal, A N; Haris, M Y; Ahmad, N and Zulkifli, M (2021). Enhanced mechanical and thermal properties of modified oil palm fiber-reinforced polypropylene composite via multi-objective optimization of in situ silica sol-gel synthesis. *Polymers, 13*: 3338.

Murai, K and Kondo, R (2011). Extractable sugar contents of trunks from fruiting and nonfruiting oil palms of different ages. *J. Wood Sci., 57*: 140-148.

Muyny, C and Chantarapanont, W (2022). Drying effect on physical characteristics and total phenolic content with subsequent effect on antioxidant and antidiabetic activities of galangal (*Alpinia galanga* L.) rhizomes and holy basil (*Ocimum sanctum* L.) leaves. Kasetsart University.

Perlo, V; Botha, F C; Furtado, A; Hodgson-Kratky, K and Henry, R J (2020). Metabolic changes in the developing sugarcane culm associated with high yield and early high sugar content. *Plant Direct, 4*: e00276.

Rafieisakhaei, M and Barazandeh, B (2017). The effects of oil market events on carbon emissions: A 2016 case study. *SPE Health, Safety, Security, Environment, & Social Responsibility Conference-North America*. Society of Petroleum Engineers.

Russmayer, H; Marx, H and Sauer, M (2019). Microbial 2-butanol production with *Lactobacillus diolivorans*. *Biotechnol. Biofuels, 12*: 1-11.

Saffaryazdi, A; Ganjeali, A; Farhoosh, R and Cheniany, M (2020). Variation in phenolic compounds, α-linolenic acid and linoleic acid contents and antioxidant activity of purslane (*Portulaca oleracea* L.) during phenological growth stages. *Physiol. Mol. Biol. Plants, 26*: 1519-1529.

Ramanathan, S; Salleh, M M; Yahya, A; Hussin, H; Wan Dagang, W R; Mohamad, S E and Syed Yaacob, S N (2018). Potential lignocellulosic biomass resources in ASEAN countries. *Emerging Areas in Bioengineering, 1*: 163-172.

Suryawan, A and Heru, B (2019). A review on the floating net cage waste management for the sustainability of Cirata Reservoir service life. *IOP Conf. Ser.: Earth and Environ. Sci., 407*: 012003. IOP Publishing.

Tnah, S K; Wu, T Y; Ting, D C C; Chow, H K; Shak, K P Y; Subramonian, W; Procentese, A; Cheng, C K; Teoh, W H and Jahim, J M (2022). Effect of chlorine atoms in choline chloride-monocarboxylic acid for the pretreatment of oil palm fronds and enzymatic hydrolysis. *Renew. Energy, 182*: 285-295.

Traverso, A; Kazmierski, M; Zhovannik, I; Welch, M; Wee, L; Jaffray, D; Dekker, A and Hope, A (2020). Machine learning helps identifying volume-confounding effects in radiomics. *Phys. Med., 71*: 24-30.

Wani, N; Wani, S A; Munshi, Z; Ahmad, S; Shah, M R; Hussain, A; Kashoo, Z and Nabi, N (2018). Isolation and virulence gene profiling of *Clostridium perfringens* from freshwater fish. *J. Entomol. Zool. Stud., 6*: 176-181.

Wei, J; Du, H; Zhang, H; Nie, Y and Xu, Y (2021). Mannitol and erythritol reduce the ethanol yield during Chinese Baijiu production. *Intl. J. Food Microbiol., 337*: 108933.

Zhang, C (2019). Lignocellulosic ethanol: Technology and economics. *Alcohol Fuels-Current Technologies and Future Prospect*. IntechOpen, London. 21 pp.

Zhen, X; Wang, Y and Liu, D (2020). Bio-butanol as a new generation of clean alternative fuel for SI (spark ignition) and CI (compression ignition) engines. *Renew. Energy, 147*: 2494-2521.

Zwetsloot, M J; Ucros, J M; Wickings, K; Wilhelm, R C; Sparks, J; Buckley, D H and Bauerle, T L (2020). Prevalent root-derived phenolics drive shifts in microbial community composition and prime decomposition in forest soil. *Soil Biol. Biochem., 145*: 107797.

Journal of Oil Palm Research Vol. 36 (3) September 2024 p. 484-494
DOI: https://doi.org/10.21894/jopr.2023.0040

EFFECT OF REACTION TIME ON VARIOUS PROPERTIES OF PALM OIL BIODIESEL IN CONTINUOUS BIODIESEL REACTOR

V PALANISELVAM[1]*; S SINDHUJA RAJAN[1]; S SRIRAMAJAYAM[1] and D RAMESH[1]

ABSTRACT

Biodiesel consists of the fatty acid esters of simple alcohols, which pave the way to replace fossil diesel fuel with biodiesel in transportation. Using a continuous flow transesterification process is the viable option to produce biodiesel with reduced time and cost. In this study, different concentrations of catalyst potassium hydroxide at 1.0%, 1.5% and 2.0% were experimented to determine the higher recovery of biodiesel from palm oil. By increasing the methanol concentration 2-3 times higher than the stoichiometric requirement with respect to the catalyst concentration, the methyl ester yield increase gradually at a ratio of 0.5%. The maximum methyl ester yield was 96.0% for a 7.5:1.0 molar ratio. The samples taken at 10 min intervals were analysed for kinematic viscosity and specific gravity. In comparison with methyl ester yield, the maximum yield (96.0%) was obtained at 7.5:1.0 molar ratio and 2.0% catalyst concentration, which has minimum kinematic viscosity. For continuous transesterification of palm oil using static mixer, the optimum condition for maximum methyl ester yield (96.0%) was 7.5:1.0 molar ratio and 2.0% catalyst concentration.

Keywords: biodiesel, continuous reactor, palm oil, transesterification.

Received: 1 March 2023; **Accepted:** 5 July 2023; **Published online:** 29 August 2023.

INTRODUCTION

In developed and developing nations, the energy demand of the growing world population pressurises researchers to adopt and improve technical means and ways to fulfil the thirst for energy and improve the standard of living. Several studies showed that biodiesel is a better alternative fuel than fossil-based diesel in terms of engine performance, emission reduction and environmental benefits (Canakci and Van Gerpen, 2000; Kusumo *et al.*, 2017; Peterson *et al.*, 1997; Yun *et al.*, 2016). Biodiesel is a fuel that can be produced straight from vegetable oils (edible and non-edible), recycled waste cooking oil, and animal fats for use in compression ignition (diesel) engines (Krawczyk, 1996); it can be produced locally, thus helping to reduce the country's dependence on imported crude oil. The cost of cooking oils used as raw material for biodiesel production, the viability of a continuous transesterification process and the recovery of high-quality glycerol as a biodiesel by-product are primary options to be considered to lower the cost of biodiesel (Ma and Hanna, 1999). Direct use of vegetable oils and their blended oil fuels has several problems. In the early transesterification stage, the reaction is limited by the mass transfer of alcohol to the vegetable oil phase (Van Gerpen *et al.*, 2004). Considering the characteristics of the transesterification reaction, a laboratory-scale continuous-flow reactor system using a static mixer method was developed and investigated (Thompson and He, 2007). Several alternative energy resources have been explored worldwide to meet the growing energy requirements. The search for alternate fuels for the use of transport and other sectors

[1] Department of Renewable Energy Engineering, Agricultural Engineering College and Research Institute, Tamil Nadu Agricultural University, Coimbatore, 641003 Tamil Nadu, India.

* *Corresponding author e-mail: palaniselvam.v@tnau.ac.in*

globally need more research on biofuels (Khairil *et al.*, 2018; Silitonga *et al.*, 2018). Most biodiesel production systems available in the market are batch-type only. Hence, the biodiesel production as a continuous system needs more attention and requires high-quality result-oriented research on the continuous production of biodiesel system. The biodiesel as a partial/complete replacement of diesel in compression-ignition type engines significantly decreased the CO and HC emission, which is likely since this blend promotes complete combustion, whereas there is a slight increase in NOx emissions due to higher oxygen contents (Damanik *et al.*, 2019). Among the vegetable and tree born oils, palm oil has excellent resistance to oxidation and high heat exposure for an extended period of time (Kurnia *et al.*, 2016; Mahlia *et al.*, 2019). In this study, the effect of different properties at various molar ratios of the higher recovery of biodiesel from palm oil using continuous reactor with static mixer was experimented and optimised.

MATERIALS AND METHODS

The biodiesel feedstock used for this study was palm oil and it was procured from local oil mill, Chinthamani Pudhur, Coimbatore district, Tamil Nadu. Various properties of palm oil biodiesel were studied using ASTM standards.

Kinematic Viscosity

The kinematic viscosity of the sample was determined by Redwood Viscometer using ASTM: 445-72 procedure. The water bath in the viscometer was heated to the testing temperature of 40ºC. The sample was filtered in a B_{200} mesh and poured into the oil cup of the viscometer. The sample was stirred to make it homogenous and adjusted to achieve the testing temperature. A 50 mL measuring cylinder was placed below the jet of the viscometer. The time taken for filling 50 mL of sample was noted with a stopwatch. The sample's kinematic viscosity was calculated by using Equation (1) and (2). The experiment was replicated three times and average values were reported.

Kinematic viscosity of test sample,

$$V\ (mm^2/s) = 0.26 \times t - 179/t \text{ for } 34 < t > 100s \quad (1)$$

$$V\ (mm^2/s) = 0.24 \times t - 179/t \text{ for } 34 < t > 100s \quad (2)$$

where, t is the time taken for filling 50 mL of oil sample, s.

Specific Gravity

The specific gravity was determined using a specific gravity bottle (IS: 1448-1972). The specific gravity bottle was washed in acetone and dried in an autoclave. The empty weight of the specific gravity bottle with a lid was weighed using a weighing balance. The water weight and the specific gravity of the bottle with lid were weighed and taken. The specific gravity of the bottle was again washed with acetone and dried in autoclave. The weight of the sample and specific gravity bottle with lid was weighed. The experiments were conducted at 40°C. The sample's specific gravity was calculated, the experiment was replicated three times, and average values were reported.

Flash Point

Pensky Martens, a semi-automatic flash point tester was used to determine the flash point of biodiesel (IS: 1448-1992 method) in the range of 25°C to 400°C. The test was performed by filling biodiesel up to a definite mark, fixing the cover and heating the biodiesel at a rate of 5°C/min to 6°C/min. A stirrer was used to ensure uniform temperature distribution in the test sample. The flash point was recorded at the time of distinct flash in the interior of the biodiesel cup by reading the temperature.

Cloud Point

The cloud point and pour point apparatus were used to measure the cloud point of test samples. The ASTM D-97/57 method was adopted for this experiment. The test jar with oil was heated to 46.0°C and then cooled to 15.5°C in a water bath maintained at 7°C. After this pretreatment, the ring jacket was placed at 25 mm from the bottom of the test jar and was kept in the jacket. The capillary thermometer was immersed 3 mm above the bottom of the test jar, and the jacket was cooled between -1°C and 2°C. The sample was frequently inspected at 3°C intervals by removing the test jar from the jacket and observing crystal formation in the sample due to the cooled bath in the apparatus, and that temperature was recorded as the cloud point of the test sample. Each inspection was completed within 5 s.

Pour Point

The pour point of the test sample was determined by the same procedure followed for the cloud point except for the position of the thermometer. The thermometer was immersed to 3 mm below the surface of the test sample. The inspection continued until there was no sample movement at the horizontal position of the test

jar for 5 s. The temperature recorded under these conditions was taken as the pour point of the test sample.

Free Fatty Acid

Association of Official Chemists Society (AOCS) Method, Ca 5a-40 was used to determine the Free Fatty Acid (FFA) of oil. An oil sample of 7.05 ± 0.5 g was weighed in a conical flask. 75 mL of ethanol and 2 mL of phenolphthalein were added to the sample. The oil sample was titrated against 0.25 N sodium hydroxide, shaking the flask vigorously until the appearance of the first permanent pink colour persisted for 30 s. The FFA content was calculated as oleic acid as given below in Equation (3).

$$\text{FFA as oleic acid (\%)} = \frac{\text{Volume of alkali consumed (mL)} \times \text{Normality} \times 28.2}{\text{Weight of sample (g)}} \quad (3)$$

Performance Evaluation of Continuous Transesterification System

For optimising the parameters used in the continuous transesterification system, the catalyst amount and molar ratio were considered. Up to 5% FFAs, the transesterification reaction can be done with an alkaline catalyst. The FFA of raw oil used for this study was less than 5%, and hence potassium hydroxide was selected as a catalyst.

Catalyst Amount

The FFA of palm oil was found as 3.3%, which is lesser than 5.0% and so as the first stage of experiments, three different levels of concentration of potassium hydroxide were used (1.0%, 1.5% and 2.0%) in this work to determine the higher recovery of biodiesel if the yield is less, higher concentration of catalyst will be used to carry out the study.

Molar Ratio

The molar ratios for this study were taken by different methanol to oil ratios of 4.5:1.0, 6.0:1.0 and 7.5:1.0 to study their effects on biodiesel yield. The molecular weight of the oil was calculated based on the fatty acid composition of the oil.

Reaction Temperature

At the beginning of the experiment, the water bath temperature was fixed at 50ºC. Then the heat discharged from the pump raises the temperature to the required temperature of 60ºC. The primary advantage of the higher temperatures influences shorter reaction time. Sometimes the higher reaction temperature also causes the methanol to vaporise, resulting in decreased yield (boiling point 65°C). When the temperature decreases, the reaction rate also decreases. The sample was collected for every 10 min interval, which was subsequently evaluated for certain properties such as specific gravity and kinematic viscosity.

Biodiesel Yield

The quantity of biodiesel was measured after each experimental trial based on molar ratio, reaction temperature and time. The measured quantity was weighed and the following Equation (4) was used to calculate the biodiesel yield.

$$\text{Biodiesel yield (\%)} = \frac{\text{Wight of the biodiesel}}{\text{Weight of the oil}} \times 100 \quad (4)$$

Fatty Acid Methyl Ester Composition

For confirmation of fatty acid methyl ester (FAME) of palm oil biodiesel, MS spectra of the unknown sample were compared with MS spectra from the NIST mass spectral library provided with the GC/MS system. The samples were prepared by diluting ester in hexane and used in a gas chromatography-mass spectrometer (GC-MS, Agilent 7890B-5977A model). The condition maintained for analysing the biodiesel quality is given below.

GC column	:	DB-5 ms
Carrier gas	:	Helium gas
Carrier gas flow rate	:	1.0 mL/min
Injection mode	:	splitless
Purge flow to split vent	:	20 mL/min
Mass spectrometer conditions		
Injection port temperature	:	250°C
Source temperature	:	200°C
Inference temperature	:	230°C
Data collection mode	:	scan

The column was heated at 50°C for 5 min and then the temperature was increased to 200°C at 15°C/min and held at 200°C for 45 min.

RESULTS AND DISCUSSION

The continuous transesterification system was developed to produce biodiesel from palm oil (*Figure 1*). The reaction mixture (potassium

hydroxide, methanol and raw oil) was circulated with the help of the pump at higher pressure to make the turbulent flow inside the reactor. The samples were drawn from the system at different intervals to analyse the biodiesel yield and the selected properties. The value of the FFA present in the selected oil was 3.3%. For optimising the operational parameters for higher biodiesel yield from selected palm oil, three different levels of molar ratio (4.5:1.0, 6.0:1.0 and 7.5:1.0), catalyst concentration (1.0%, 1.5% and 2.0%) and reaction time (20-60 min) were selected. The catalyst and alcohol used in this study were potassium hydroxide and methanol. The experiment was continued until it reached the constant value of specific gravity and kinematic viscosity of the produced biodiesel (*Table 1*).

TABLE 1. METHYL ESTER YIELD IN CONTINUOUS TRANSESTERIFICATION SYSTEM

Trials	Reaction temperature maintained at 50°C		
	Molar ratio	Catalyst concentration (%)	Methyl ester yield (%)
T1	4.5:1.0	1.0	93.00
		1.5	93.50
		2 .0	94.00
T2	6.0:1.0	1.0	94.50
		1.5	94.75
		2.0	95.00
T3	7.5:1.0	1.0	95.50
		1.5	95.75
		2 .0	96.00

Effect of Properties of Palm Oil Biodiesel at Different Molar Ratio

Fuel properties such as specific gravity and kinematic viscosity as detailed in the methodology were studied for raw oil and biodiesel produced in a continuous transesterification process using a static mixer. In continuous production, for analysing the above properties after 30 min run on batch mode, the samples were taken at 10 min intervals.

Effect of Kinematic Viscosity at 4.5:1.0 Molar Ratio

The kinematic viscosity of the palm oil was 30.3 mm^2/s. The combination of the molar ratio at 4.5:1.0 and 1.0% concentration of catalyst, the kinematic viscosity of palm oil biodiesel produced were reduced to 10.07, 9.75, 8.01, 7.37, 6.21 and 5.76 mm^2/s for the reaction time of 10, 20, 30, 40, 50 and 60 min respectively. From the graph, it was noted that the kinematic viscosity of palm biodiesel was 5.76 mm^2/s at 60 min reaction time and the viscosity of biodiesel produced was stabilised. The reduction in the kinematic viscosity of the oil was 81.0% at 60 min, as compared to palm oil. The combination of the molar ratio of 4.5:1.0 and 1.5% concentration of catalyst, the kinematic viscosity of palm oil biodiesel produced was reduced to 9.42, 8.41, 7.72, 7.37, 6.29 and 5.55 mm^2/s for the reaction time of 10, 20, 30, 40, 50 and 60 min, respectively. The kinematic viscosity of palm biodiesel was 5.55 mm^2/s at 60 min reaction time and the viscosity of biodiesel produced was stabilised after this reaction time. The reduction in kinematic viscosity of the oil was 81.5% at 60 min reaction time, as compared to that of palm oil. At the molar ratio 4.5:1.0 and 2.0% concentration of



Figure 1. Continuous transesterification rector.

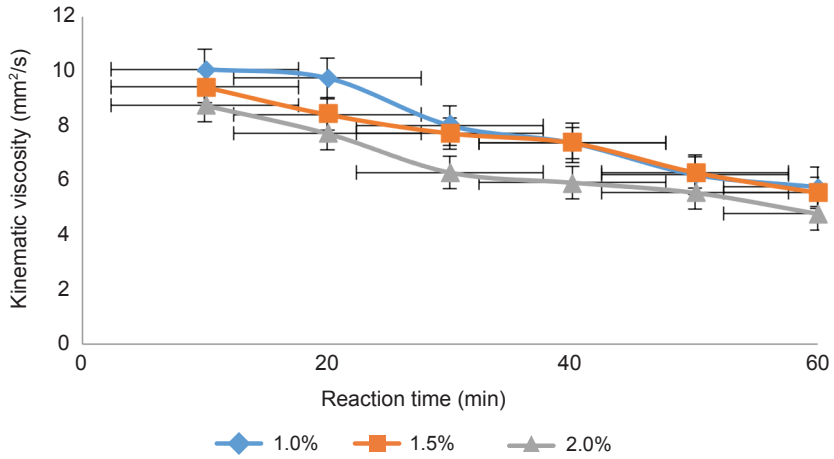


Figure 2. Effect of reaction time on kinematic viscosity of biodiesel produced at 4.5:1.0 molar ratio.

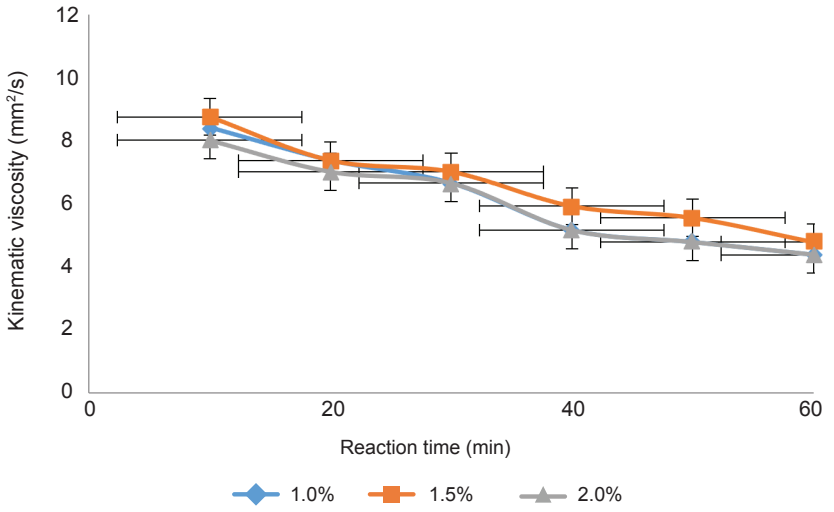


Figure 3. Effect of reaction time on kinematic viscosity of biodiesel produced at 6.0:1.0 molar ratio.

catalyst, the kinematic viscosity of palm oil biodiesel produced was reduced from 8.75 to 4.78 mm^2/s for the reaction time of 10 to 60 min respectively. The kinematic viscosity of palm biodiesel was reduced with respect to an increase in reaction time. At 60 min time intervals the reduction in kinematic viscosity of the oil was 84.0% as compared to palm oil (*Figure 2*).

Effect of Kinematic Viscosity at Molar Ratio of 6.0:1.0

The kinematic viscosity of palm oil biodiesel was reduced from 8.41 to 4.38 mm^2/s for the reaction time of 10 to 60 min, respectively. The kinematic viscosity of palm biodiesel was reduced with respect to the increase in reaction time. The kinematic viscosity of the biodiesel produced was stabilised. The kinematic viscosity of palm biodiesel was 4.38 mm^2/s at 60 min reaction time. The reduction in kinematic viscosity of the oil was reduced to 85.4% at 60 min reaction time, as compared to that of palm oil. The combination of molar ratio 6.0:1.0 at 1.5% concentration of catalyst, the kinematic viscosity of palm oil biodiesel was reduced to 8.75, 7.37, 7.01, 5.92, 5.55 and 4.78 mm^2/s for the reaction time of 10, 20, 30, 40, 50 and 60 min respectively. The reduction in kinematic viscosity of the oil was 84.1% at 60 min, as compared to that of palm oil. With the 2.0% catalyst concentration, the kinematic viscosity of palm oil biodiesel produced was reduced from 8.01 to 4.38 mm^2/s for the reaction time of 10, 20, 30, 40, 50 and 60 min respectively. The reduction percentage in kinematic viscosity of the oil was 85.4 mm^2/s at 60 min reaction time, compared to palm oil (*Figure 3*).

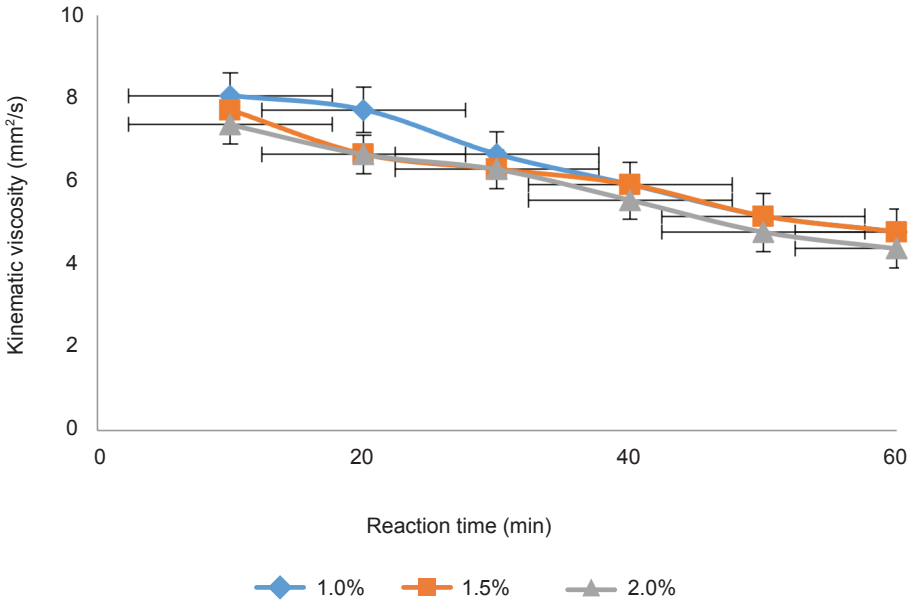


Figure 4. Effect of reaction time on kinematic viscosity of biodiesel produced at 7.5:1.0 molar ratio.

Effect of Kinematic Viscosity at Molar Ratio 7.5:1.0

The kinematic viscosity of palm oil biodiesel was reduced to 8.06, 7.72, 6.65, 5.92, 5.16 and 4.78 mm^2/s for the reaction time of 10, 20, 30, 40, 50 and 60 min, respectively. It was noted that the kinematic viscosity of palm biodiesel of 4.78 mm^2/s at 60 min reaction time the viscosity was stabilised. The reduction in kinematic viscosity of the oil was 84.07% at 60 min of the process as compared to palm oil. At a 1.5% catalyst concentration of 7.5:1.0 molar ratio, the kinematic viscosity of palm oil biodiesel produced was reduced from 7.72 to 4.78 mm^2/s for the reaction time of 10, 20, 30, 40, 50 and 60 min respectively. The reduction in kinematic viscosity of the oil was 84.1%. The molar ratio of 7.5:1.0 at a 2.0% concentration of catalyst, the kinematic viscosity of palm oil biodiesel produced was reduced from 7.37 to 4.38 mm^2/s for the reaction time from 10 to 60 min. The kinematic viscosity of palm biodiesel was reduced due to increase in reaction time. The reduction in kinematic viscosity of the oil was 85.4% at 60 min, as compared to palm oil (*Figure 4*).

From the results, it is concluded that the kinematic viscosity decreases with an increase in reaction time. The kinematic viscosity obtained at these concentrations met with the fuel standard of IS:9466-1980 (3.5-5.0 mm^2/s). The minimum kinematic viscosity 4.38 mm^2/s was obtained at 6.0:1.0 and 7.5:1.0 molar ratio at 2.0% catalyst concentration. Compared with methyl ester yield, the maximum methyl ester yield of 96% was obtained at a 7.5:1.0 molar ratio and 2.0% catalyst concentration, which has a minimum kinematic viscosity of 4.38 mm^2/s. Similar results were observed by Dhanasekaran and Dharmendirakumar (2014) that minimum kinematic viscosity of 4.1 mm^2/s was achieved at 6:1 molar ratio at 2.0% catalyst. It indicated the completion of the reaction process and the removal of heavy glycerin.

Effect of Specific Gravity at 4.5:1.0 Molar Ratio

The specific gravity of palm oil was observed as 0.901. Similar to kinematic viscosity, the specific gravity of the oil also decreased with an increase in reaction time. *Figure 5* shows the effect of the catalyst on the specific gravity of biodiesel at 4.5:1.0 molar ratios. At 1.0% catalyst concentration, the specific gravity was 0.883 at the initial stage; as the reaction time increases, the specific gravity decreases gradually to 0.877. Initially, at 1.5% of the catalyst concentration, the specific gravity was 0.882 and decreased to 0.877. Similarly, at 2.0% catalyst concentration, the initial specific gravity was 0.880; as the reaction time increased, the specific gravity gradually decreased to 0.874. The minimum specific gravity of 0.874 was obtained at 2.0% catalyst for a 4.5:1.0 molar ratio. The percentage reduction of specific gravity for the 4.5:1.0 molar ratio at 1.0%, 1.5% and 2.0% catalyst concentration was from 2.6% to 3.0%.

Effect of Specific Gravity at 6.0:1.0 Molar Ratio.

The effect of the catalyst on the specific gravity of biodiesel for 6.0:1.0 molar ratio at different catalyst

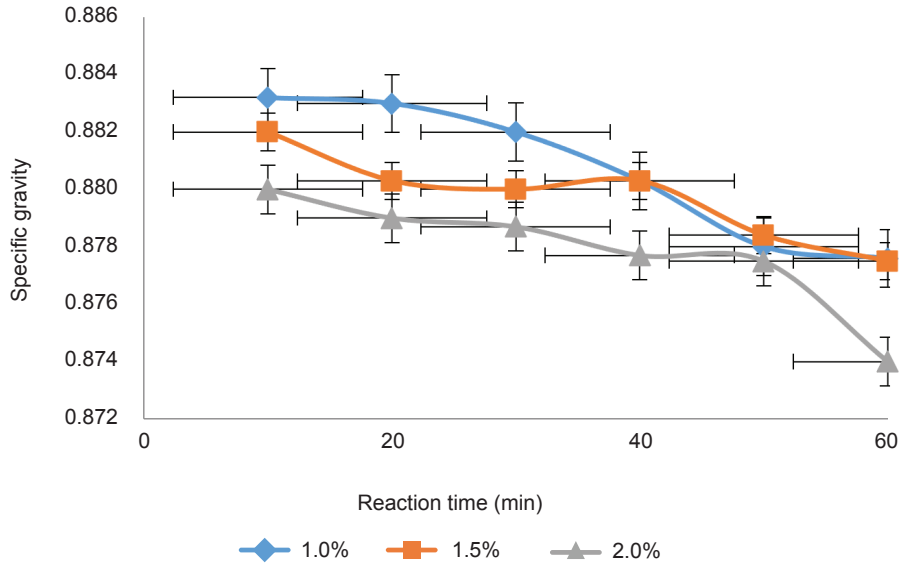


Figure 5. Effect of reaction time on specific gravity of biodiesel produced at 4.5:1.0 molar ratio.

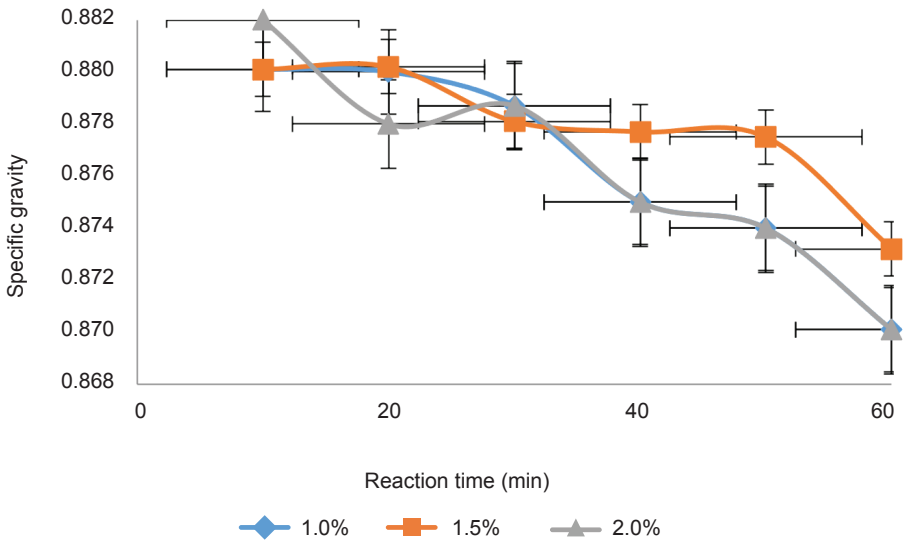


Figure 6. Effect of reaction time on specific gravity of biodiesel produced at 6.0:1.0 molar ratio.

concentrations, as shown in *Figure 6* indicates that, at 1.0% catalyst concentration, the specific gravity of 0.880 was decreased to 0.870. Initially, at 1.5% catalyst concentration, the specific gravity was 0.880 and decreased to 0.873. The specific gravity for 2.0% catalyst concentration was 0.882, as the reaction time increases, the specific gravity decreased gradually to 0.873. For 6.0:1.0 molar ratio, the minimum specific gravity of 0.870 was obtained at 1.5% catalyst. The percentage reduction in specific gravity for the above molar ratio was around 3.4%.

Effect of Specific Gravity at 7.5:1.0 Molar Ratio

The specific gravity of biodiesel for 7.5:1.0 molar ratio at different reaction times and catalyst concentration effect is shown in *Figure 7*. It indicated that the specific gravity was 0.880 and decreased to 0.874. At 1.5% catalyst concentration, the specific gravity was 0.880 and decreased gradually to 0.874. Similarly, at 2.0% catalyst concentration, the specific gravity was 0.880 and decreased to 0.870. For all the catalyst concentrations at the initial stage, the

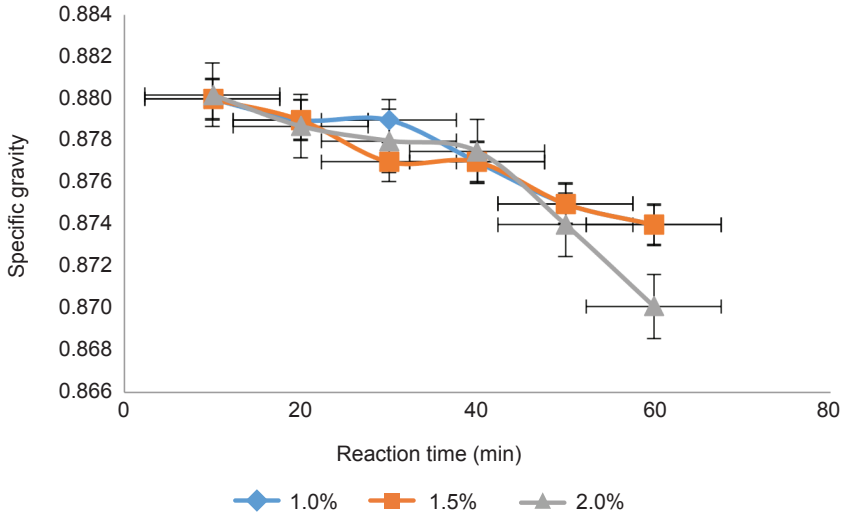


Figure 7. Effect of reaction time on specific gravity of biodiesel produced at 7.5:1.0 molar ratio.

specific gravity also decreased when the reaction time increased. The minimum specific gravity of 0.870 was obtained at 2.0% catalyst. The reduction of specific gravity in this molar ratio at three different catalyst levels was from 3.0% to 3.4%.

From the above results, it is concluded that at the 7.5:1.0 molar ratio, the specific gravity decreased gradually with increase reaction time. The specific gravity obtained at this concentration met with the fuel standard of IS:1448-1972 as specified by the Indian standards (0.87-0.90). The minimum specific gravity (0.870) was obtained at 6.0:1.0 and 7.5:1.0 molar ratio for 2.0% catalyst concentration. Compared with methyl ester yield, the maximum yield of 96.0% was obtained at a 7.5:1.0 molar ratio and 2.0% catalyst with minimum specific gravity (*Figure 8*).

Similar results were observed by Padmarag and Kavita (2012) and results indicated that a lower value of specific gravity of (0.866) is an indication of the completion of the reaction process and the removal of heavy glycerin.

The experimental trials concluded that the combination of a 6.0:1.0 molar ratio and 1.0% catalyst concentration performed better for higher recovery of biodiesel yield and fuel properties. The kinematic viscosity of biodiesel produced at a molar ratio of 4.5:1.0 and 2.0% catalyst concentration was equivalent to the viscosity of biodiesel produced at other higher molar ratios. The catalyst used under these conditions was higher than that, leading to more catalysts present in the biodiesel. During the water washing of biodiesel, the biodiesel yield will be reduced due to repeated washing to neutralise the biodiesel. In the case of a 7.5:1.0 molar ratio with three levels of catalyst concentration (1.0%, 1.5% and 2.0%), the biodiesel yield was greater than 95.0%. The higher biodiesel yield recorded under this condition is due to 150 times higher than the stoichiometric requirement (*i.e.*, 3:1), and also, the excess amount of methanol used in the transesterification process must be recovered before washing the product (*i.e.*, raw biodiesel).

The biodiesel yield for the combination of 6.0:1.0 at three different catalyst levels was 94.5% to 95.0%. Among the three combinations, 6.0:1.0 with 1.0% catalyst concentration was selected for biodiesel production. Therefore, for the other two higher concentrations of catalyst amount, the biodiesel yield was closer to that of 1.0% catalyst concentration. Furthermore, the reduction in kinematic viscosity was 85.0%, which was higher than the other two catalyst combinations.

From the study, the optimised condition for the continuous transesterification system for the tested palm oil was a 6.0:1.0 molar ratio with 1.0% catalyst concentration operated for 30 min in batch mode and then converted into a continuous mode for 60 min. The properties of biodiesel derived from palm oil at optimised conditions are presented in *Table 2*.

TABLE 2. PROPERTIES OF PALM OIL BIODIESEL

No.	Particulars	Palm oil biodiesel
1	Kinematic viscosity @ 40°C, mm^2/s	5.92
2	Specific gravity @ 40°C	0.877
3	Flash point, °C	165.00
4	Cloud point, °C	10.00
5	Pour point, °C	7.00
6	Energy content, MJ	330.87

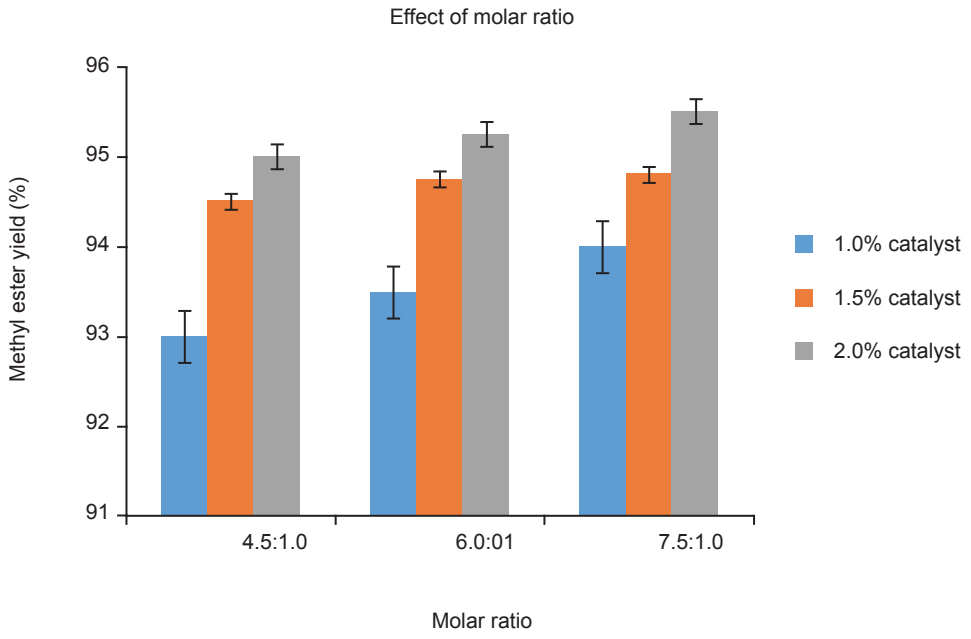


Figure 8. Methyl ester yield of palm oil in continuous transesterification system.

The kinematic viscosity of the biodiesel produced was 5.92 mm^2/s which was the same as that of the values obtained from waste cooking palm oil biodiesel (4.77 mm^2/s) (Hussanai Sukkathanyawat and Kittisak Wichianwat, 2023).

Flash Point

The flash point of biodiesel is higher than diesel fuel (Mofijur *et al.*, 2017). Furthermore, the flash point of palm oil biodiesel (165°C) was three times higher than diesel fuel (55°C). The higher flash point indicates the in-volatile nature of oils. The flash point obtained for maximum methyl ester yield met with the fuel standard of (IS:1448-1992 method). The flash point of the Waste cooking palm oil biodiesel is 166°C (Hussanai Sukkathanyawat and Kittisak Wichianwat, 2023).

Cloud Point

The cloud point of the palm oil biodiesel for maximum methyl ester (96%) was 10°C. The cloud point obtained for maximum methyl ester yield met the fuel standard of ASTM D-97/57 (-3°C to 12°C). Most of the fuel properties of biodiesel compare well with fossil diesel except cloud point. One major disadvantage of biodiesel is its relatively poor cold flow properties, affecting an engine's performance in cold weather, *i.e.*, moderate temperature climates (Robert, 2018). The cloud point of the Waste cooking palm oil biodiesel is 7°C (Hussanai Sukkathanyawat and Kittisak Wichianwat, 2023).

Pour Point

Pour point of the palm oil biodiesel for maximum methyl ester was found as 7°C. The cloud point obtained for maximum methyl ester yield met with the fuel standard of ASTM D-97/57 (-15°C to 10°C). The higher pour point of edible oils than diesel fuel indicates the poor flow characteristics of oil at lower temperatures. Generally, the pour point of vegetable oils was higher than diesel fuel, which indirectly correlates to the poor flow characteristics of oil at lower temperatures (Bazooyar *et al.*, 2015). From the waste cooking palm oil biodiesel, the pour point is 6°C as equivalent as that of palm oil biodiesel produced in this experimental analysis (Hussanai Sukkathanyawat and Kittisak Wichianwat, 2023).

Fatty Acid Methyl Ester Composition

Gas chromatography-mass spectrometry (GC-MS) was used to determine the fatty acid composition of palm oil biodiesel. For confirmation of fatty acid methyl ester (FAME) of palm oil biodiesel, MS spectra of the unknown sample were compared with MS spectra from the NIST mass spectral library provided by GC/MS system. The palm oil fatty acid methyl ester (POFAME) consist of palmitic acid methyl ester ($C_{16:0}$), caprylic acid methyl ester ($C_{8:0}$), capric acid methyl ester ($C_{10:0}$), undecylenic acid ($C_{11:0}$), pelargonic acid ($C_{9:0}$), arachidic acid methyl ester ($C_{20:0}$), palmitoleic acid ($C_{16:1}$), and their quantity are represented in *Table 3*.

TABLE 3. FATTY ACID METHYL ESTER OF PALM OIL BIODIESEL

Compositions	Values (%)
Caprylic acid ($C_8H_{16}O_2$)	0.10
Capric acid ($C_{10}H_{20}O_2$)	5.96
Undecylenic acid ($C_{11}H_{20}O_2$)	0.12
Palmitic acid ($C_{16}H_{32}O_2$)	41.50
Pelargonic acid (3(CH_2) 7CO 2H)	1.57
Arachidic acid ($C_{20}H_{32}O_2$)	1.13
Mystric acid ($CH_3(CH_2)_{12}COOH$)	1.40
Stearic acid ($C_{18}H_{36}O_2$)	38.60
Methyl 8-methyl-nonanoate ($C_{11}H_{22}O_2$)	5.96
18-Nonadecen-1-ol ($C_{19}H_{38}O$)	2.43
Cyclododecanemethanol ($C_{13}H_{26}O$)	1.23
Total	**100**

Comparing the GC-MS analysis of fish oil biodiesel, the major esters were identified as methyl esters of palmitic acid, linoleic acid, oleic acid, linolenic acid, and stearic acid for biodiesel produced in the present study (Whetstine, 2020).

CONCLUSION

The effect of reaction time on various properties of palm oil biodiesel in a continuous biodiesel reactor was studied, and the optimised condition for continuous transesterification system for the tested palm oil was found as a 6.0:1.0 molar ratio with 1.0% catalyst concentration operated for 30 min as batch mode and then converted into a continuous mode for 60 min. The biodiesel yield for the molar ratio combination of 6.0:1.0 at three different catalyst levels was 94.5% to 95.0%. Other two higher concentrations of catalyst amount, the biodiesel yield was closer to that of 1.0% catalyst concentration. Moreover, the reduction in kinematic viscosity was 85.0%, which was higher than the other two catalyst combinations with a biodiesel yield of 94.75%.

The optimised condition identified for the continuous biodiesel production by this research was using a 6.0:1.0 molar ratio with a minimum of 1.0% catalyst concentration. This is to recommend that future work on the process optimised by this study will be tested in the large high-capacity continuous reactor of more than 100 L/hr will give good results in producing biodiesel from palm oil. The continuous biodiesel production is a novel idea to produce raw palm oil into biodiesel using a transesterification reactor under the optimised condition. The present article will give more hope and knowledge about biofuels from palm oil using different conditions to the readers in the oil palm industry.

ACKNOWLEDGEMENT

The authors acknowledged to thank the ICAR, New Delhi, and Tamil Nadu Agricultural University, Coimbatore, for carrying out the research on Continuos biodiesel production system in the Department of Renewable Energy Engineering, Agricultural Engineering College and Research Institute, Coimbatore, for rendering necessary help during the period of experimental study.

REFERENCES

Bazooyar, B; Ghorbani, A and Shariati, A (2015). Physical properties of methyl esters made from alkali-based transesterification and conventional diesel fuel. *Energy Sources A: Recovery, Util. Environ. Eff., 37(5)*: 468-476. DOI: 10.1080/15567036.2011.586975.

Canakci, M and Van Gerpen, J (2000). Biodiesel production from oils and fats with high free fatty acids. *American Society of Agricultural Engineering, 44(6)*: 1429-1436. DOI: 10.13031/2013.7010.

Damanik, N; Ong, H C; Mofijur, M; Tong, C W; Silitonga, A S; Shamsuddin, A H; Sebayang, A H; Mahlia, T M I; Wang, C T and Jang, J H (2019). The performance and exhaust emissions of a diesel engine fuelled with *Calophyllum inophyllum*-palm biodiesel. *Processes, 7*: 597. DOI: 10.3390/pr7090597.

Dhanasekaran, K and Dharmendirakumar, M (2014). Biodiesel characterization and optimization study of used frying palm oil. *Int. J. Curr. Res. Acad. Rev., 2(1)*: 105-120.

Hussanai Sukkathanyawat and Kittisak Wichianwat (2023). Optimisation of fame production from waste cooking palm oil with koh catalyst supported on palm kernel shells ash (PKSA) using response surface methodology (RSM). *J. Oil Palm Res., 35(4)*: 668-681. DOI: 10.21894/jopr.2023.0005.

Khairil, R A; Iskandar, J; Silitonga, A S; Masjuki, H H and Mahlia, T M I (2018). The potential biodiesel production from *Cerbera odollam* oil (Bintaro) in Aceh. *MATEC Web of Conferences, 159*: 01049.

Krawczyk, T (1996). Biodiesel-alternative fuel makes in roads but hurdles remain. *INFORM, 7*: 801-815.

Kurnia, J C; Jangam, S V; Akhtar, S; Sasmito, A P and Mujumdar, A S (2016). Advances in biofuel production from oil palm and palm oil processing wastes: A review. *Biofuel Res. J., 3*: 332-346. DOI: 10.18331/BRJ2016.3.1.3.

Kusumo, F; Silitonga, A; Masjuki, H; Ong, H C; Siswantoro, J and Mahlia, T (2017). Optimization of transesterification process for *Ceiba pentandra* oil: A comparative study between kernel-based extreme learning machine and artificial neural networks. *Energy, 134*: 24-34. DOI: 10.1016/j.energy.2017.05.196.

Ma, F and Hanna, M A (1999). Biodiesel production: A review. *Biores. Technol., 70*: 1-15. DOI: 10.1016/S0960-8524(99)00025-5.

Mahlia, T M I; Ismail, N; Hossain, N; Silitonga, A S and Shamsuddin, A H (2019). Palm oil and its wastes as bioenergy sources: A comprehensive review. *Environ. Sci. Pollut. Res., 26*: 14849-14866. DOI: 10.1007/s11356-019-04563.

Mofijur, M; Rasul, M G; Hassan, N M S; Masjuki, H H; Kalam, M A and Mahmudul, H M (2017). Chapter fourteen-assessment of physical, chemical, and tribological properties of different biodiesel fuels. *Clean Energy for Sustainable Development* (Mohammad, G R; Abul, K A and Subhash, C S eds.). *Academic Press*. p. 441-463.

Padmarag, D and Kavita, K (2012). Production and evaluation of biodiesel from palm oil and ghee (clarified butter). *Proc. of the International Institute for Science, Technology and Education conference-Chemical and Process Engineering Research Nigeria.* p. 2225-0913.

Peterson, C L; Wagner, G L and Auld, D L (1983). Vegetable oil substitutes for diesel fuel. *Trans. ASABE, 26(2)*: 322-327.

Robert, O D (2018). Correlating the cloud point of biodiesel to the concentration and melting properties of the component fatty acid methyl esters. *Energy Fuels, 32(1)*: 455-464. DOI: 10.1021/acs.energyfuels.7b02935.

Silitonga, A S; Masjuki, H H; Ong, H C; Sebayang, A H; Dharma, S; Kusumo, F; Siswantoro, J; Milano, J; Daud, K; Mahlia, T M I; Chen, W H and Sugiyanto, B (2018). Evaluation of the engine performance and exhaust emissions of biodiesel-bioethanol-diesel blends using kernel-based extreme learning machine. *Energy, 159*: 1075-1087. DOI: 10.1016/j.energy.2018.06.202.

Thompson, J C and He, B B (2007). Biodiesel production using static mixers. *Trans ASABE, 50(1)*: 161-165. DOI: 10.13031/2013.22389.

Van Gerpen, J; Shanks, B; Pruszko, R; Clements, D and Knothe, G (2004). Biodiesel production technology. *National Renewable Energy Laboratory, 1617*: 80401-3393.

Whetstine, C R (2020). GC-MS analysis of synthesized biodiesel. *Forensic Science Master's Projects*. https://digitalcommons.buffalostate.edu/forensic_science_projects/1, accessed on 1 February 2020.

Yun, H S; Ji, M K; Park, Y T; Salama, E S and Choi, J (2016). Microalga, *Acutodesmus obliquus* KGE 30 as a potential candidate for CO_2 mitigation and biodiesel production. *Environ. Sci. Pollut. Res., 23*: 17831-17839. DOI: 10.1007/s11356-016-6971-z.

Journal of Oil Palm Research Vol. 36 (3) September 2024 p. 495-509
DOI: https://doi.org/10.21894/jopr.2023.0049

SELECTIVE CYTOTOXICITY EFFECTS OF *R*-GLYCIDOL AND *S*-GLYCIDOL ON VERO AND HCT 116 CELLS IN EVALUATING THE INCIDENCE OF GLYCIDYL ESTERS IN EDIBLE OILS AND FATS

SITI NUR SYAHIRAH NOR MAHIRAN[1]; NANTHINI RAVI[3]; ALAM MAHBOOB[4]* and NURUL HUDA ABD KADIR[1,2]*

ABSTRACT

Despite their feasibility as food flavouring, glycidol is classified as a probable carcinogen under group 2A by WHO. The cytotoxicity effects of isomers of R- *and* S-*glycidol on African green monkey kidney normal cell lines (Vero) and human colon cancer cell line (HCT 116) remain unclear. Cell viability of the treated Vero and HCT 116 cells was determined using the AlamarBlue® assay. Dichlorodihydrofluorescein diacetate (DCFDA) was used to evaluate reactive oxygen species (ROS) activity. Protein expressions of ERK ½, p-ERK, Bcl-2 and caspase-3 were investigated using western blotting technique. The findings indicated that* R- *and* S-*glycidol (1.16 µg/mL) exposure dramatically reduced the cell viability of the treated HCT 116 cells but was slightly cytotoxic to Vero cells, hence triggering ROS activity.* R- *and* S-*glycidol cause down-regulation of ERK ½, p-ERK, and BCL-2 protein expression at 48 hr of treatment. Furthermore, both* R- *and* S-*glycidol possess close interaction in proximity to 3D-structure of human ERK and p-ERK protein receptors. In conclusion,* R- *and* S-*glycidol potentially triggered oxidative stress and affected ERK protein phosphorylation, leading to caspase-3 independent cell death of the treated HCT 166 cells, suggesting that lower doses (<1.16 µg/mL) of* R- *and* S-*glycidol are safe for human consumption.*

Keywords: cooking oil and lipids, food contaminants, molecular toxicology, safety.

Received: 30 November 2022**; Accepted:** 25 June 2023**; Published online:** 27 September 2023.

INTRODUCTION

Glycidol is widely employed in industrial applications such as the production of sweetening, flavouring compounds, diluent, and dye-levelling agents due to oxiran ring of glycidol that may function as an alkylating agent and contributes to some of its reactivity (Foroumadi and Emami, 2014). Natural oils and vinyl polymers are both produced using glycidol as a stabiliser (Foroumadi and Emami, 2014). Glycidols have become an important key intermediate as substitute dendrimers for the preparation of chemicals, pharmaceuticals, bioactive compounds and food products (Tollini *et al.*, 2022). Mahapatra and Tysoe (2015) have stated that glycidols exist in two stereoisomeric forms, namely, *R*- and *S*-glycidol enantiomers and the difference between the two compounds is only chirality (EFSA Panel on Contaminants in the Food Chain (CONTAM), 2016). Due to biocompatibility with human cells, *R*- and *S*-glycidol have been investigated for their potential as replacement dendrimers for biomedical applications. Dendrimers are hyper-

[1] Faculty of Science and Marine Environment, Universiti Malaysia Terengganu, 21030 Kuala Terengganu, Malaysia.

[2] BIOSES group, Universiti Malaysia Terengganu, 21030 Kuala Terengganu, Malaysia.

[3] Clinical Research, Beacon Hospital, 46050 Petaling Jaya, Selangor, Malaysia.

[4] Division of Chemistry and Biotechnology, Dongguk University, 123 Dongdae-ro, Gyeongju, Republic of Korea.

* *Corresponding author e-mail: nurulhuda@umt.edu.my; mahboobchem@gmail.com*

branched macromolecules which can be functionalised. In order to express explicit biological traits such as lipid bilayer interactions, cytotoxicity, and others, changing their physicochemical properties has made it a suitable delivery vehicle (Abbasi *et al.*, 2014). The benefits of many drugs cannot be exploited because of their poor solubility, toxicity, or stability problems. The use of dendrimers as carriers of bioactive compounds can solve many problems in biomedical approaches and have an advantage in improving their usage for clinical applications (Aurelia *et al.*, 2020). The utilisation of drug combinations based on their targeted administration or drug delivery materials has become a new trend to optimise the therapeutic effects of the drugs with a reduction in adverse effects and potentially becomes a new strategy in the search for successful cancer therapy (Wróbel *et al.*, 2022). In addition, according to a study by Wróbel *et al.* (2022), 2- and 3-poly(amidoamine) (PAMAM G2 and G3) dendrimers covered with *R*-glycidol could penetrate cells faster and exhibited higher toxicity for cancerous cells than for normal cells compared to *S*-glycidol covered analogues. Interestingly, the chirality and functional group of the stereoisomers were reported to alter the physiological of human cells that may contribute to either harmful or harmless effects (Mäder and Kattner, 2020; Moreno-Yruela *et al.*, 2022).

Contradictory, reports by EFSA CONTAM (2016) and Hartwig *et al.* (2020) stated that glycidol is genotoxic (damages DNA) and carcinogenic (causes cancer). The chemicals have the ability to cause adverse effects in rodents (Spungen *et al.*, 2018) that may contribute to genotoxic and mutagenic effects on rats (Bakhiya *et al.*, 2011 and EFSA CONTAM, 2016). Given that the research on glycidol in human is limited, Schilter *et al.* (2011) conducted carcinogenicity bioassays on glycidol in mice and rats in various tissues and found that glycidol induced dose-related increases in the rates of neoplasms. According to Akane *et al.* (2013), adult rats axon injury in the central and peripheral nervous systems were damaged by glycidol, which suggests that it targets the developing nerve terminals of immature granule cells and inhibits late-stage hippocampal neurogenesis. The studies on evaluation of the food contaminant isomers especially the toxicological effect of *R*-glycidol or *S*-glycidol on human cells are limited (EFSA CONTAM, 2016).

Moreover, foods such as infant food formula, margarine, potato crisp, cookies, hot surface cooked pastries, short crusts, fried, roast meat and chocolate spreads were reported to contain harmful food contaminants especially glycidol (EFSA CONTAM, 2016 and Bakhiya *et al.*, 2011). Goh *et al.* (2021) stated that glycidyl esters contamination in palm-based cooking oil were in the range of 1.338 to 18.362 mg/kg. However, the permissible daily glycidol exposure from refined dietary oils and fats is 1.33 g/kg/day (maximum daily fat intake: 80 g) for adult individuals weighing 60 kg (Bakhiya *et al.*, 2011). This controversial toxicological effects of glycidols need to be investigated in order to understand underlying mechanism on the safety of the chemical to human normal and cancer cells especially *R*- and *S*-glycidols isomers. Furthermore, limited studies were reported on the genotoxic, mutagenic and cytotoxic effect of glycidols in human normal and cancer cells.

Trans and *cis* fat are example of isomers that have different effects on human cells where *trans*-fat may contribute to carcinogenesis and cancer risk (Matta *et al.*, 2021) but *cis*-fat is considered to be safe to human as it plays important roles as energy source, a component of cellular membranes, and a regulator of different biological process (Hirata, 2021). Despite the fact that the all-*trans* isomer of astaxanthin (AST) is a potent antioxidant predominates in nature, certain studies have indicated that the cis isomer of AST, particularly the 9-*cis* AST, demonstrated a higher antioxidant potency than the all *trans* isomer (Liu *et al.*, 2016). Furthermore, α-tocopheryl succinate (α-TOS) is selective for cancer cells at least in part due to the lower esterase activity and reduced antioxidant defences expressed by these malignant cells when compared to their normal (non-malignant) counterpart than the others isomers of tocopherols (Constantinou *et al.*, 2008). Lim *et al.* (2014) has suggested that different tocotrienol isomers might exhibit a different cellular mechanism of cell death in different cancer types but specific mechanisms induced by alpha-, gamma- and delta-tocotrienols in both brain and lung cancers are still unclear.

According to Brooks *et al.* (2011) chirality is one of the important factors that plays a role in determining the chemicals interaction with the cancer protein receptors which results in dichotomous effects in normal and cancer human cells. Oxaliplatin isomers of (*R, R*)-cyclohexane-1,2-diamine and (*S, S*)-cyclohexane-1,2-diamine have different roles in inducing cytotoxic effects on leukaemia, lung, colon, breast, renal, melanoma and ovarian human tumour cells. (*S, S*)-cyclohexane-1,2-diamine platinum antineoplastic compound is more biologically active in comparison with (*R, R*)-cyclohexane-1,2-diamine (Arnesano *et al.*, 2015). Toxicological assessment of the glycidol isomers on human cells are limited. Thus, the objectives of this study are to elucidate selective toxicological effects of *R*- and *S*-glycidol in normal and cancer cells. This finding may lead to better understanding of selective cytotoxicity of *R*- and *S*-glycidol in normal cells (monkey) and cancer cells (human), which may be beneficial for safety evaluation of glycidols exposure in food.

MATERIALS AND METHODS

Chemicals

R- and *S*-glycidol were purchased from Sigma Aldrich, USA. RPMI 1640, penicillin-streptomycin and accutase were purchased from Apical Scientific (Gibco, USA). Fetal bovine serum (FBS) was purchased from Apical Scientific (Tico Europe, Netherlands). AlamarBlue® was purchased from Bio-Diagnostics (Invitrogen, Scotland, UK). NucleoSpin® RNA/Protein extraction kit was purchased from Apical Scientific (Macherey-Nagel, Germany). The primary mouse monoclonal ERK ½ (SC-514302), p-ERK (SC-7383), BCL-2 (SC-7382), Caspase (SC-7272) and GAPDH (SC-47724) antibodies were purchased from Santa Cruz Biotechnology (Santa Cruz, CA) and HRP conjugated anti-mouse secondary antibody (A16072) (Life Technologies, USA).

Cell Culture of African Green Monkey Kidney Cell Lines, Vero and HCT 116 Cells

Vero cell line was obtained from Universiti Sultan Zainal Abidin (UNISZA) and HCT 116 cells were obtained from Imperial College London. Vero and HCT 116 cells were maintained in RPMI 1640 media (Gibco, USA), 1% penicillin-streptomycin (Gibco, USA) and 10% FBS (Tico Europe, Netherlands). The flasks were incubated in 37°C humidified incubator supplemented with 5% CO_2. After the cells reached 80%-90% confluency, the cells were trypsinised. The cultures were examined using inverted microscope to check for signs of contamination; old media were discarded. The flasks were rinsed with PBS (3 mL) for three times to discard traces of serum, thereby inhibiting the action of accutase. Accutase (1 mL) was added for trypsinisation process and the flasks were incubated at 3°C and 5% humidified incubator for 5 min to detach the cells. Complete medium (3 mL) was added, and the solutions were transferred into 15 mL centrifuge tubes before spinning down at 2500 rpm for 5 min. The supernatants were discarded, and the pellet of Vero and HCT 116 cell lines was used for the next procedure. The cells and media (10 µL) were transferred immediately to the edge of the hemocytometer chamber, and the slide was viewed under inverted microscope. The cells were counted within the four corners of the grid. Non-viable cells were stained blue (Kim *et al.*, 2016).

The final volume of fresh media and treatment solution (1 µL) was 100 µL in each plate. The 96-well plate that contains 99 µL of seeded cells and fresh complete medium was incubated overnight in 37°C humidified incubator supplemented with 5% CO_2 (Kadir *et al.*, 2009).

AlamarBlue® Assay by Using Vero and HCT 116 Cell Lines

Different concentrations of *R*- and *S*-glycidol (0.000116, 0.00116, 0.0116, 0.116 and 1.16 µg/mL) were used to treat the Vero and HCT 116 cell lines. Four replicates of the treatment were conducted on 96-well plates and incubated in 37°C humidified incubator supplemented with 5% CO_2 for 24, 48 and 72 hr. AlamarBlue® reagent (10 µL was added into each well and immediately incubated back in the same condition for 4 hr. Resazurin (opaque blue) in AlamarBlue® reagent was converted to resorufin (fluorescence pink) via the reduction reactions of metabolically active cells. The absorbance values were measured at 570 nm excitation wavelength value and 590 nm emission wavelength value by using microplate reader (Thermo Fisher Scientific, USA) (Bonnier *et al.*, 2015).

ROS by Using 2,7-dichlorofluorescin Diacetate (DCFDA) Dye

The cells were seeded in 24-well plate, and 1×10^5 cells were seeded in each well. The 24-well plates containing cells were incubated overnight. Dichlorodihydrofluorescein diacetate (DCFDA) powder (Sigma Aldrich, USA) was used to measure ROS activity in treated HCT 116 cells. 5 mg of DCFDA was mixed with dimethylsulfoxide (DMSO) (4.104 mL). DCFDA (2.5 µL) was added to the wells containing cells and incubated in an incubator for 30 min. After 30 min, the medium in each well was discarded carefully and washed with PBS. The media were added in each well and treated with different concentrations of *R*- and *S*-glycidol. 5 µL of the treatment solutions was aliquoted in media containing HCT 116 cells (500 µL) that were pre-treated with DCFDA. The treated cells were immediately incubated at 37°C with 5% CO_2. The samples were measured for every 1 hr by using microplate reader. The absorbance values were measured fluorometrically at excitation of 520 nm and emission of 550 nm (Wu and Yotnda, 2015).

Protein Extraction

2.5×10^5 of HCT 116 cells were seeded in six-well plate and treated with 500 mM to obtain final concentration of 5 mM for 24 and 48 hr. The seeded cells that were treated with 0.01% DMSO was used as a negative control for both time points. The cells were incubated for 24 and 48 hr prior to treatment with *R*-glycidol and *S*-glycidol and trypsinisation. The cell pellets were washed with 3 mL PBS and centrifuged at 3000 rpm for 5 min. The supernatants were completely discarded by pipetting, and the pellets were stored in -80°C until the next procedure was conducted. Proteins from the samples of treated

cells were extracted using NucleoSpin® RNA/ Protein (Macherey-Nagel) protocol with slight modifications. Bradford assay was performed using Bio-Rad Protein Assay (Bio-Rad, USA) to determine protein concentrations. The absorbance of the samples was measured at 595 nm by using ELISA plate reader (Bio-Rad, USA) (Sinkala *et al.*, 2017).

Western Blotting, Blocking and Gel Dot

Loading samples of the treated HCT 116 cells with *R*- and *S*-glycidol were prepared according to manufacturer's instructions (Pub. Part No. IM-8042). 20.0 μg/μL protein samples, 3.75 μL NuPAGE® LDS sample buffer (4X), 0.75 μL BME and deionised water were mixed together with the total volume of 15 μL. The mixture was heated at 72°C for 10 min at 500 rpm. 1X SDS running buffer was poured in XCell SureLock™ Mini-Cell electrophoresis tank. Protein samples (15 μL) from section 2.5 were loaded in NuPAGE 4%-12% Bris-Tris gel (Novex, Life Technologies, USA) by using loading tips. The system was run at voltage 200 V and 100-125 mA for 1 hr and 30 min. After that, the gel was taken out from its cassette and washed three times with ultrapure water. The SDS-PAGE gel was then stained with SimplyBlue® safe stain for 2 hr. The gel was destained by ultrapure water overnight. The image was observed by using gel imager (Gel Doc XR + system, Bio-Rad, USA). After separating the protein mixture, it was transferred to a PVDF membrane.

The PVDF membrane was soaked in a blocking buffer (5% of non-fat dry milk) for 2 hr. The membrane was incubated overnight with primary mouse monoclonal ERK ½ at 4ºC. Subsequently, the membrane was incubated with HRP conjugated anti-mouse secondary antibody (1:2200 dilution) for 4 hr. The membrane was washed with Tris-buffered saline with Tween 20 (TBST) buffer (20 mM Tris pH 7.5, 150 mM NaCl, 0.1% Tween 20) for three times. The bounded antibody was detected by using chromogenic peroxidase substrate (Life technologies, USA). Gel dot was used to measure band intensity. The image was analysed by using ImageJ software.

Then, the membrane was washed with TBST for 3 hr before it was soaked with other antibody and blocking buffer (5% of non-fat dry milk) for 2 hr. The same step was repeated for another antibody, namely, p-ERK (1:1000 dilution), BCL-2 (1:1000 dilution), Caspase-3 (1:1000 dilution), GAPDH (1:5000 dilution). Whereas, GAPDH protein expression was used as loading controls.

Molecular Docking Study

AutoDock 4.2 and AutoDock Tools (Morris *et al.*, 2009) were used to examine the nonbonding interaction of the 3D-structure of human ERK2 (PDB: 4FMQ) and Phosphorylated Map Kinase ERK2 (PDB: 2ERK) with *R*- and *S*-glycidol through molecular docking study (Aral *et al.*, 2012). The crystal structures were downloaded from the RCSB PDB and prepared for molecular docking in two steps. The protein data bank (PDB) files (4FMQ and 2ERK) were separately imported into AutoDock Tools (ADT), the graphical user interface for AutoDock, as the first step. Water molecules, ligands, and any associated molecules were removed from the receptor (protein) structure (PDB: 4FMQ and 2ERK) during this process. Next, the receptor was prepared by adding missing hydrogen atoms, residues, and charges. The *R*- and *S*-glycidol structure were retrieved from PubChem and the energy of the molecules was minimised for optimal geometrical parameters for docking with AutoDock 4.2. The best dock poses obtained from docking simulations were used for visualisation using Discovery Studio software (BIOVIA Discovery Studio 2016).

Statistical Analysis

GraphPad Prism V was used to analyse cell viability, ROS level and western blot analysis value. One-way ANOVA analysis with Dunnet post-test and two-way ANOVA with Bonferroni multiple comparison test were used to determine significant difference of cell viability and ROS at $p<0.05$ of the treated HCT 116 with *R*- and *S*-glycidol. However, unpaired t-test was used to determine significant difference of protein expression in the treated human colon, HCT 116 cell lines.

RESULTS AND DISCUSSION

Cytotoxicity Effect of *R*- and *S*-glycidol on Vero and HCT 116 Cell Lines

In order to determine the toxicity of *R*- and *S*-glycidol, Alamar blue was performed on normal and cancer cell lines. *Figure 1 [i(a)]; [ii(a)]; [iii(a)]; [i(b)]; [ii(b)]* and *[iii(b)]* shows percentage cell viability of Vero and HCT 116 after treatment with *R*-glycidol and *S*-glycidol. Based on our result, *R*- and *S*-glycidol caused the inhibition of cell viability at 24, 48 and 72 hr of the treatment for HCT 116 but not for the Vero cells. *R*- and *S*-glycidol showed a slight cytotoxicity effect on Vero cells persistent with the increased time points. However, the inhibition activity of treated HCT 116 cells were more cytotoxic and prominent when the cells were exposed to *R*- and *S*-glycidol at higher dose and time of the exposure, suggesting that the cytotoxicity effect were dose and time dependent. This interesting results on cell viability of the treated Vero and HCT 116 cells has proven the selectivity on cytotoxicity effects of *R*- and *S*-glycidol exposure. Based on our findings, 50%

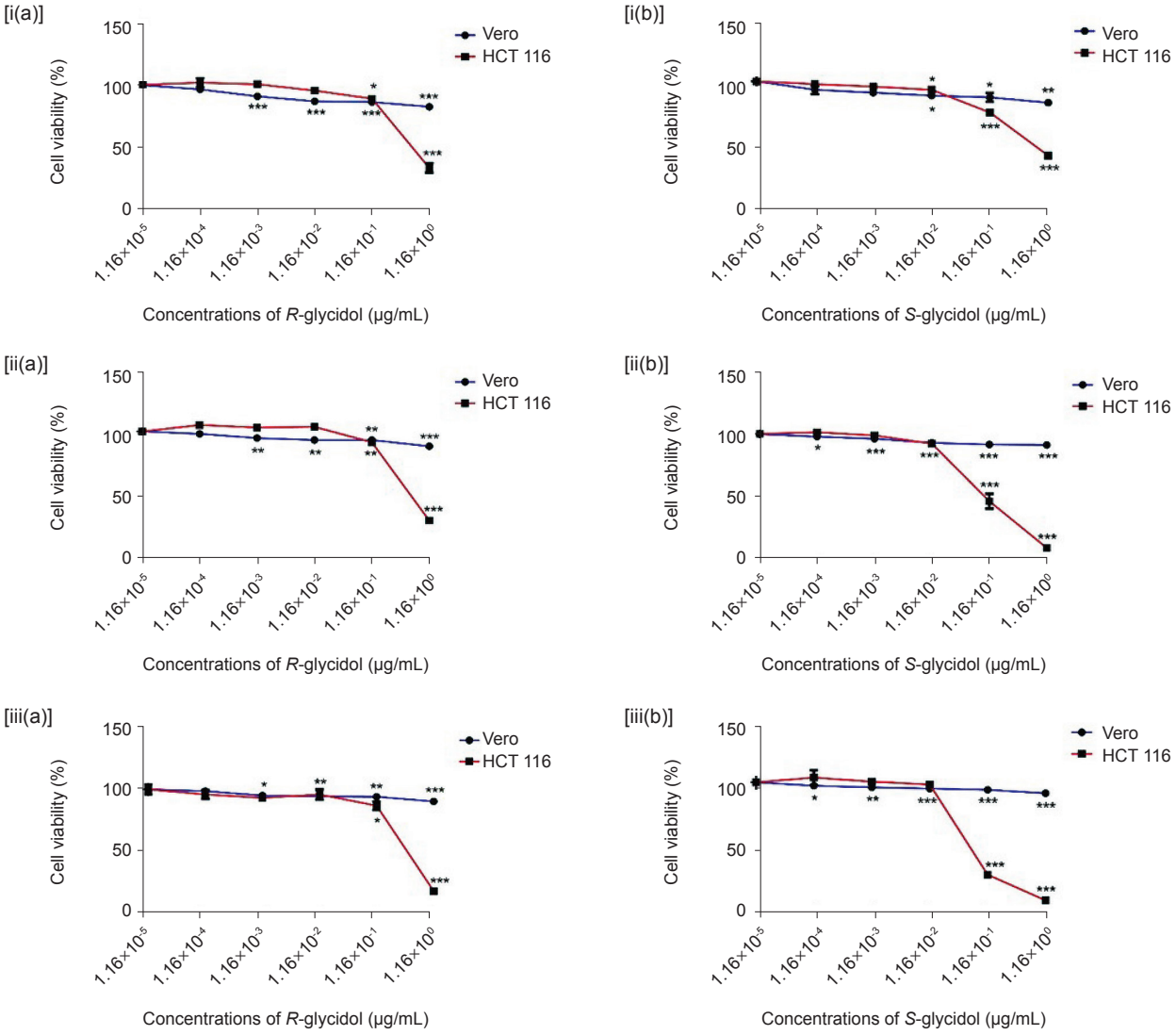


Figure 1. Cytotoxicity effect of Vero and HCT 116 cells after 24 (1), 48 (2) and 72 (3) hr of treatment with R*-glycidol (a) and* S*-glycidol (b). The analysis was performed using GraphPad Prism V and one-way ANOVA analysis with Dunnet post-test were done. * indicates* $p<0.05$*, ** indicates* $p<0.01$*, *** indicates* $p<0.001$ *significant difference of the concentration towards the control.*

of inhibition concentration (IC_{50}) values *R*-glycidol of the treated HCT 116 cells were 5.0, 4.5 and 3.4 µg/mL at 24, 48 and 72 hr of treatment, respectively. Whereas IC_{50} values of the treated HCT 116 cells with *S*-glycidol were 4.8, 0.7 and 0.4 µg/mL at 24, 48 and 72 hr of treatment, respectively. Interestingly, the exposure of *R*- and *S*-glycidol on Vero cells did not exceed 50% of cell inhibition indicating that the chemicals were less toxic to normal cells. Moreover, the cell cytotoxicity effects of both chemicals have shown similar trend of cells inhibition, suggesting that the isomers of glycidols did not contribute much on the cytotoxic effects.

Reactive Oxygen Species (ROS) Expression

In ROS level was determined to evaluate the oxidative stress event after the exposure *R*- and *S*-glycidol on HCT 116 cells. *Figure 2a* shows significant increase at concentration of 10 mM of the treatments compared to control at time points 6 and 24 hr, but other concentrations of *R*- and *S*-glycidol treatments had negligible effect. The data suggested that the highest concentration of *R*-glycidol (1.16 µg/mL) exposure resulted in significant increase in ROS level of the treated HCT 116 cells, whereas other concentrations of the treatment showed slight increase in ROS level of the treated HCT 116 cells with *R*- and *S*-glycidol, suggesting that oxidative stress was expressed after the exposure of *R*-glycidol to HCT 116 cells at 24 hr. *Figure 2b* shows significant increase in ROS production after the treatment with *S*-glycidol (1.16 µg/mL) compared to control. However, other concentrations of the treatments showed negligible effect. The data suggested that the highest concentration of *R*- and *S*-glycidol may

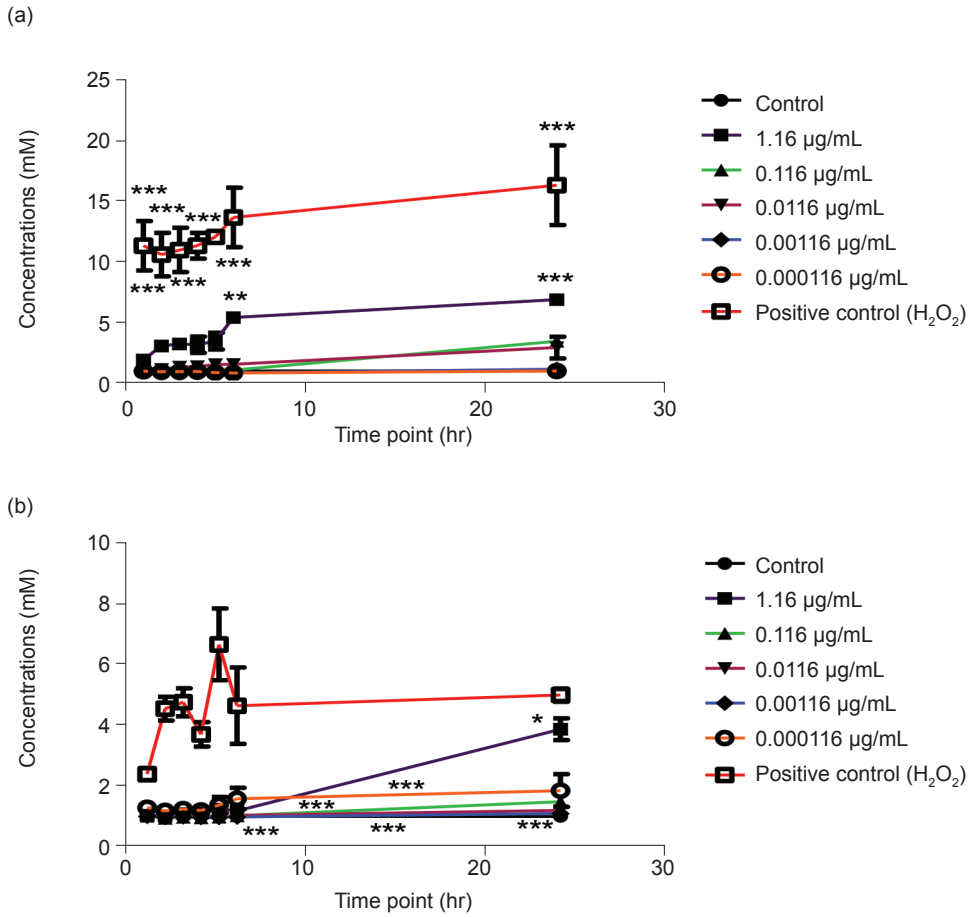


Figure 2. ROS expression of HCT 116 cells after 24 hr treatment of (a) R*-glycidol, and (b)* S*-glycidol. Two-way ANOVA with Bonferroni multiple comparison test were done and * indicates* p*<0.05, ** indicates* p*<0.01, *** indicates* p*<0.001 significant difference of the concentration towards the control.*

induce significant increase in ROS level of the treated HCT 116 cells. Whilst, the other concentrations of the treatment of both chemicals showed slight increase in ROS level in the treated HCT 116 cells, suggesting that oxidative stress was expressed after the exposure of *R*- and *S*-glycidol. We speculated that oxidative stress might be the main cause of the cytotoxic effect in the HCT 116 cells after the exposure with *R*- and *S*-glycidol.

Western Blot Analysis of the Protein Expressions

ERK ½ is a protein in MAPK pathway that may contribute to oxidative stress event in cells. Furthermore, the expression of ERK ½ protein (42 kD), p-ERK protein (43-55 kD), BCL-2 protein (26 kD), Caspase-3 (35 kD) and GAPDH (36 kD) using western blotting technique were done to elucidate the mechanism in the cells. The expression of ERK ½ protein (42 kD), p-ERK protein (43-55 kD), BCL-2 protein (26 kD), Caspase-3 (35 kD) and GAPDH (36 kD) expression of the treated HCT 116 cells with *R*- and *S*-glycidol at 24 and 48 hr treatments are shown in *Figure 3a* and *3b*, respectively. Protein bands were intensely expressed on the PVDF membrane of the treated HCT 116 cells with *R*- and *S*-glycidol (1.16 µg/mL) compared to control at 24 and 48 hr of the exposure.

As shown in *Figure 3c*, there was no significant difference between the ERK ½ protein expression of the treated HCT 116 cells with *R*-glycidol compared to control after 24 hr of the treatment. However, after 48 hr of exposure, HCT 116 treated with *R*-glycidol showed a marginal decrease compared to control with significant difference at $p<0.05$. On the other hand, *S*-glycidol exposure to HCT 116 cells showed significant down regulation ($p<0.01$) at 48 hr exposure of the ERK ½ protein expression, but the expression of ERK ½ protein at 24 hr showed no significant difference, suggesting that the expression of ERK ½ protein of *R*- and *S*-glycidol treatments in HCT 116 cells took longer time of exposure to show the effect. The p-ERK protein expression of the treated HCT 116 cells with *R*- and *S*-glycidol showed no significant difference compared to control at 24 hr treatment, but at 48 hr treatment, it showed significant decrease ($p<0.01$) (as shown in *Figure 3d*). Interestingly, BCL-2 protein expression

in *Figure 3e* was down-regulated compared with the control with significant difference of $p<0.05$ at 48 hr but no significance at 24 hr after *R*- and *S*-glycidol exposure. This finding suggested that pro-apoptotic event might occur during 48 hr of the exposure. However, caspase-3 protein expression of the HCT 116 cells showed no significant difference compared to control after the treatment with free *R*-glycidol at 24 and 48 hr (*Figure 3f*). Whereas caspase-3 protein expression of the treated HCT 116 cells with free *S*-glycidol was significantly down-regulated ($p<0.001$) compared to the control at 48 hr of exposure but no significance at 24 hr of *S*-glycidol exposure. This finding suggested that cell death induced by *R*-glycidol was caspase-3 independent.

Relative density ratio of p-ERK and ERK ½ and proteins was calculated to assess the phosphorylation event of ERK. The results in *Figure 4a* and *4b* indicate that the relative density ratio p-ERK/ERK ½ of the HCT 116 cells treated with *R*-glycidol was significantly lower than the control at 48 hr of exposure but not significant at 24 hr of exposure. Meanwhile, relative density ratio p-ERK/ERK ½ of the HCT 116 cells treated with *S*-glycidol *(Figure 4c* and *4d)* showed no significant difference at both 24 and 48 hr of the exposure. The findings suggest that the cytotoxicity and oxidative stress in the treated cells with *R*-glycidol were likely due to phosphorylation event of ERK protein.

Molecular Docking Analysis

In silico study was conducted to support protein expression data, and the molecular docking result showed an interaction between *R*- and *S*-glycidol *[Figure 5(c,d); Figure 6(c,d)]* and ERK2 *(Figure 5a)* and phosphorylated Map Kinase ERK2 *(Figure 6a)* protein receptor. A molecular docking simulation involving two receptors (PDB: 4FMQ and 2ERK) and two compounds (*R*- and *S*-glycidol) was performed using AutoDock 4.2. The top four docking poses in this simulation were selected based on their binding energies, which ranged from -3.42 to -4.0 kcal/mol. These selected poses were further investigated in Discovery Studio to investigate the interactions of *R*- and *S*-glycidol with the 3D structures of the human ERK2 protein (PDB: 4FMQ) and pERK2 (PDB: 2ERK). The results are shown in *Figure 5* and *6*. In *Figure 5(d,e)*, the active amino acid residues form a cavity that resembles a sphere around the molecule. The presence of glycidol is close to the hydrophobic and hydrophilic radicals, leading to different secondary forces, such as Van der Waals contacts and hydrogen bonding. This hydrophobic contact, hydrogen bonding and Van der Waals forces contribute in the binding interaction between chemical compounds and active amino residues of the receptor. *R*- and *S*-glycidol formed two hydrogen bonds with MET108 and ASP106 with distances of 1.62276-2.30747 Å, as well as Van der Waals contacts with the amino acid residues LEU017, ALA52, LEU156, ILE84 and GLN105 as represented in *Figure 5h, 5i.* These binding interactions allow the drug to connect closely with the receptor, inhibiting the activity of the cells in the system. The hydrophobic receptor residues involved in interactions with compounds, such as LEU, ILE, and ALA, as well as the hydrophilic amino acid GLN, provide extra strength inside the active pocket. This condition allows for a better mutual relationship between the ligand and the receptor, paving the way for inhibitory drug development. The binding details and bond lengths achieved through molecular docking are shown in *Table 1.* Docking analysis (*Table 1*) revealed that *R*- and *S*-glycidol interacted with the protein in the best possible orientation to stabilise the structures by making close contact with the receptor cavities. As a result, at their best docked positions, both compounds exhibit similar interactions and approximately similar binding energies, culminating in similar inhibition activities in experimental studies for both compounds (*R*- and *S*-glycidol).

Discussion

A study by Abraham *et al.* (2011), indicated that different isomers may provide different effects, and the induction mechanism in human cells should be studied. Two enantiomers from same chemical composition that has different chirality could react differently in biochemical process or biological reaction of cells (Fanali *et al.*, 2019). At the low concentration less than 5 μg/mL of glycidol, it did not show any toxicity effects on Chinese hamster ovary (CHO) cells as the cell toxicity treated with glycidol never exceeded more than 8% in CHO as measured by trypan blue dye exclusion (El Ramy *et al.*, 2007). Based on our findings, IC_{50} values of cell viability of treated HCT 116 cells with *R*- and *S*-glycidol at 24, 48 and 72 hr were 5.0, 4.5, 3.4 μg/mL and 4.8, 0.7, 0.4 μg/mL, respectively. This result has shown that the cytotoxicity effect of both glycidols are dose and time dependant. Our finding is supported by Senyildiz *et al.* (2017), who stated that cytotoxicity of glycidols and 3-MCPD were dose and time dependant. Ozcagli *et al.* (2016) found that 3-MCPD, glycidol and β-chlorolactic acid also reduced the cell viability of human embryonic kidney cells (HEK-293) and kidney epithelial cell lines (NRK-52E) at 24 hr treatment by using MTT assay. Furthermore, Liu *et al.* (2021) indicated that glycidol at different doses of treatments using NRK-52E cells induced a significant cytotoxicity effect in a dose and time dependent.

The glycidol induce ROS by damaging DNA and proteins in the cells as the epoxide group of the glycidol may react with the macromolecules in the

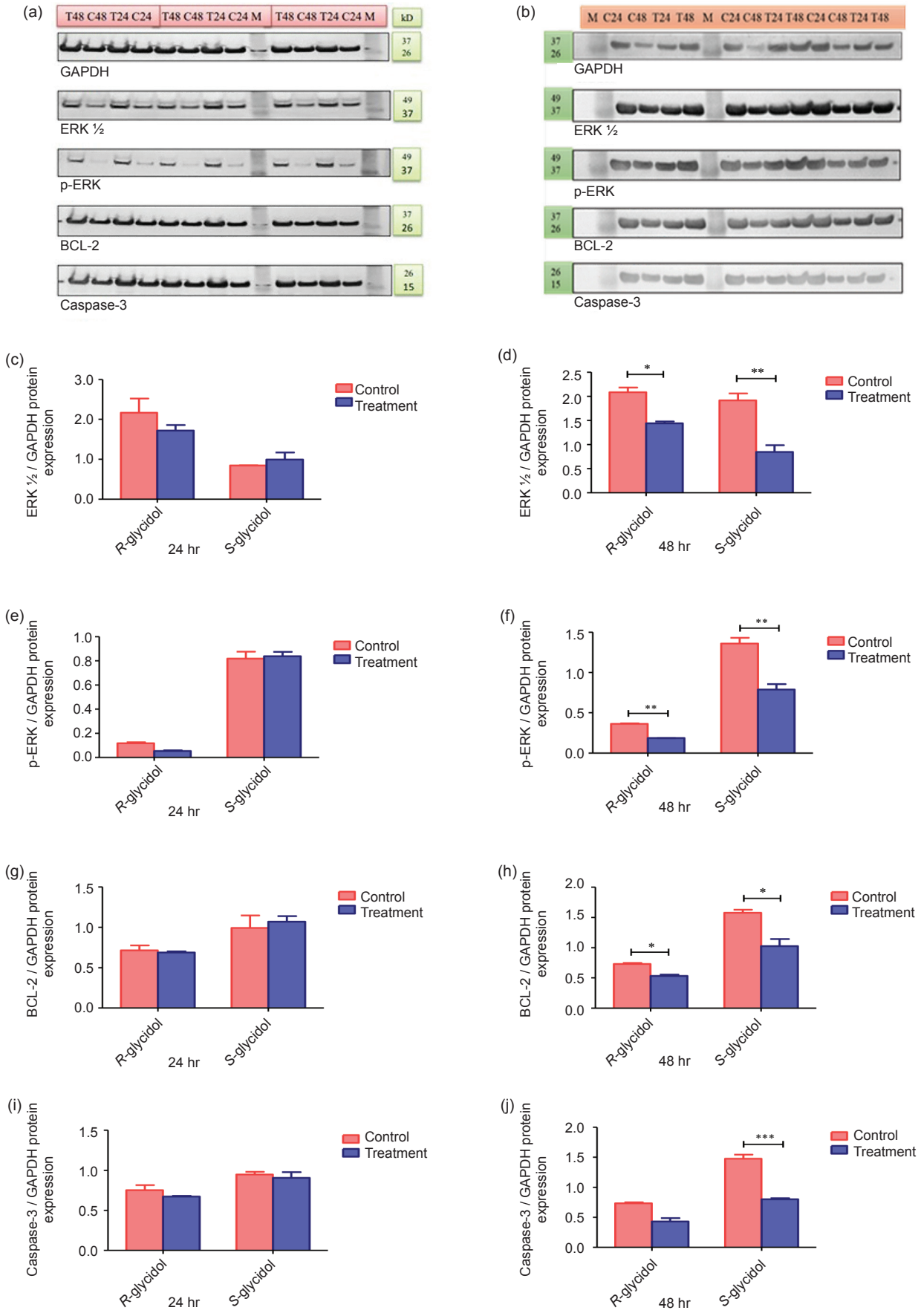


Figure 3. (a) R-*glycidol, and (b)* S-*glycidol protein bands of targeted protein located between 15 kD and 49 kD on PVDF membrane using western blot technique. (M) protein marker; (C24) Control 24 hr; (T24)* IC_{50} *24 hr; (C48) Control 48 hr; (T48)* IC_{50} *48 hr. Intensity area (c, d, e and f) of the targeted protein mitogen-activated protein kinase of* R- *and* S-*glycidol at 24 and 48 hr. The analysis was done by using ImageJ software.*

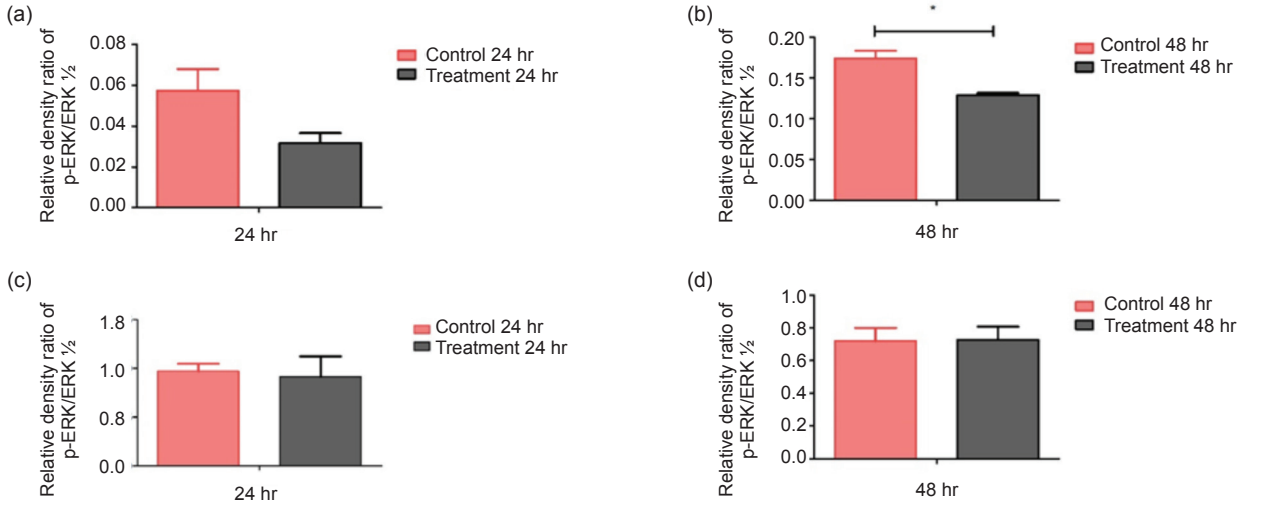


Figure 4. Relative density ratio of p-ERK/ERK ½ proteins of the treated HCT 116 cells with (a, b) R*-glycidol and (c, d)* S*-glycidol at 24 and 48 hr treatments, respectively.*

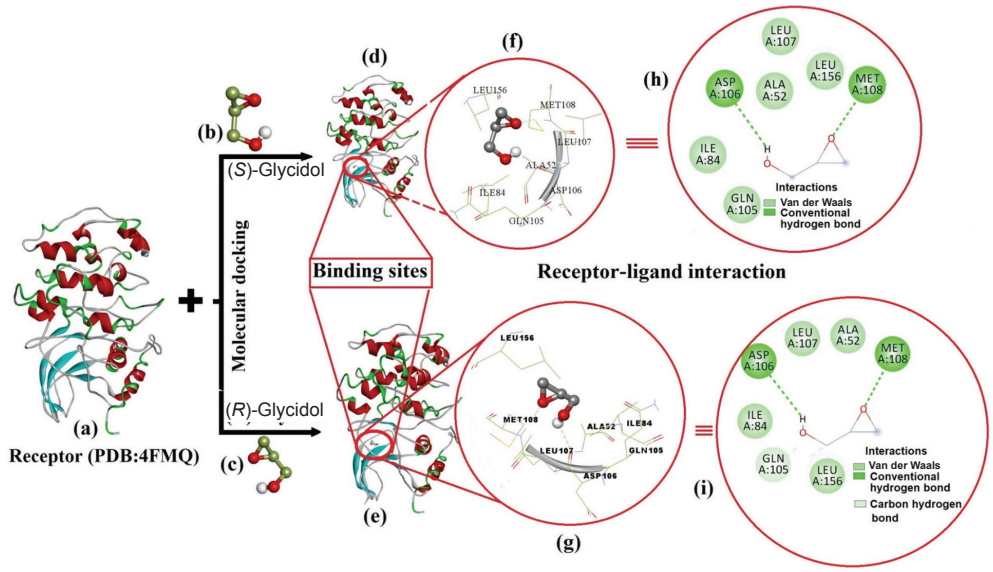


Figure 5. Molecular docking study of (a) human ERK2, (b, c) S*- and* R*-glycidol, (d, e) active pocket of receptor shown by sphere around compounds, (f, g) involvement of various hydrophobic amino acids including a hydrophilic amino acid with the studied compounds, and (h, i) 2D representation for the buried compound inside cavity of receptor showing hydrogen bond, Van der Waals, and other secondary forces.*

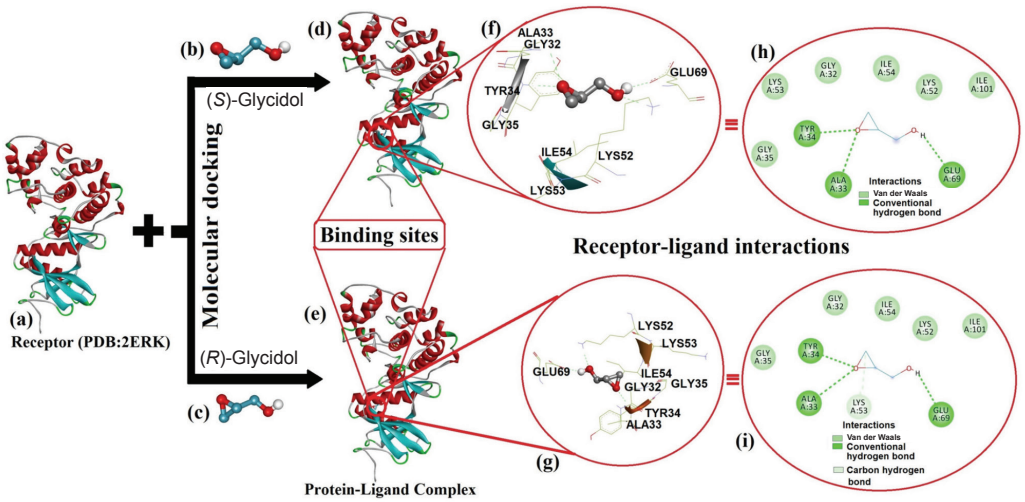


Figure 6. Molecular docking study of (a) Phosphorylated Map Kinase ERK2, (b, c) S*- and* R*-glycidol, (d, e) active pocket of receptor shown by sphere around compounds, (f, g) involvement of various hydrophobic amino acids including a hydrophilic amino acid with the studied compounds, and (h, i) 2D representation for the buried compound inside cavity of receptor showing hydrogen bond, Van der Waals, and other secondary forces.*

TABLE 1. THE BINDING OF *R*- AND *S*-GLYCIDOL WITH RECEPTORS (PDB: 4FMQ AND 2ERK) RESULTED FROM MOLECULAR DOCKING WITH THEIR MODE OF BINDING

Receptor	*R*-glycidol		*S*-glycidol	
	HB distance (A°)	Nature of interaction	HB distance (A°)	Nature of interaction
Human ERK2 complexed with a MAPK (PDB: 4FMQ)	1.64289 2.21280	MET108:R-Lig (HB) S-Lig:ASP106 (HB) LEU107-R-Lig (vdW) LEU156-R-Lig (vdW) ALA52-R-Lig (vdW) ILE84-R-Lig (vdW) GLN105-R-Lig (CHB)	1.62276 2.08040	MET108:S-Lig (HB) S-Lig:ASP106 (HB) LEU107-S-Lig (vdW) LEU156-S-Lig (vdW) ALA52-S-Lig (vdW) ILE84-S-Lig (vdW) GLN105-S-Lig (vdW)
Phosphorylate-Map Kinase ERK2 (PDB: 2ERK)	1.89862 1.77878 1.94482	TYR34:R-Lig (HB) ALA33:R-Lig (HB) R-Lig:GLU69 (HB) GLY35-R-Lig (vdW) GLY32-R-Lig (vdW) ILE54-R-Lig (vdW) LYS52-R-Lig (vdW) LYS53-R-Lig (CHB)	1.96735 2.40056 1.88987	TYR34:S-Lig (HB) ALA33:S-Lig (HB) S-Lig:GLU69 (HB) GLY35-S-Lig (vdW) GLY32-S-Lig (vdW) ILE54-S-Lig (vdW) LYS52-S-Lig (vdW) LYS53-S-Lig (vdW)

Note: HD - hydrogen bond; vdW - Van der Waals forces; CHB - carbon hydrogen bond; *S*-Lig-*S*-glycidol; *R*-Lig-*S*-glycidol.

cells (Sevim *et al.*, 2021). The epoxide group of the glycidol have the ability to react with the nucleophilic biomolecules such as protein in the cells that may triggers ROS production (Inagaki *et al.*, 2019). ROS level of treated 116 cells with *R*- and *S*-glycidol (*Figure 2*) had shown that both chemicals are able to induce oxidative stress. This may be due to ROS levels have been found to be elevated in almost all cancers, promoting several aspects of tumour formation and progression (Liou and Storz, 2010). The increase in ROS production (oxidative stress) might mediate changes in the biological response that cause cell and tissue damage (NavaneethaKrishnan *et al.*, 2019; Pizzino *et al.*, 2017; Snezhkina *et al.*, 2019). In addition, the oxidative stress event may cause the induction of mitochondrial cytochrome C which triggered by the ROS (Ji *et al.*, 2017). Our results also supported by Mossoba *et al.* (2020) who reported that HK-2 cells that were treated with 3-MCPD and its esters have shown slightly increased in ROS levels with the increasing concentrations of the treatment. ROS are a typical by product of oxidative energy metabolism and are thought to have a role in various intracellular signalling pathways, including the MAPK pathway (Rezatabar *et al.*, 2019). According to Circu and Aw (2010), concentrations of compound are the most important factors that affect ROS production because it is a product of normal metabolism during xenobiotic exposure. Increasing ROS production can occur when mutation in mitochondrial genes is observed (Redza-Dutordoir and Averill-Bates, 2016). The formation of superoxide can occur when the electron transfer is inhibited along the electron transport chain (ETC). Thus, this radical yielding hydrogen peroxide (H_2O_2) by diffusion into cell nucleus and DNA attack leads to the genetic instability (Schumacker, 2006). At low level, ROS can function as redox messenger in most intracellular signalling. Otherwise, excessive or high production of ROS would induce oxidative stress of cellular macromolecules that might inhibit protein function and promote cell death that could lead to DNA damage, apoptosis and cancer development (Fu *et al.*, 2014).

The results in *Figure 3* showed that high concentration of *R*- and *S*-glycidol compound affected protein expressions of ERK ½, p-ERK, BCL-2 and caspase-3. This effect was due to phosphorylation event of ERK ½ that might be responsible in inducing oxidative stress and further led to cell death (Liou and Storz, 2010). Furthermore, docking results *(Figure 5* and *6)* shows that *R*- and *S*-glycidol have similar interactions and relatively similar binding energies, resulting in similar inhibition activities of ERK ½, p-ERK proteins after the treatment with both compounds. We speculated that the down regulation of ERK ½ and p-ERK protein expression for HCT 116 cells treated with both *R*- and *S*-glycidol might activate the phosphorylation event of ERK protein (*Figure 4*) when ROS is elevated (*Figure 2*), thereby leading to oxidative stress that may contribute to cytotoxic effect. The cell death mechanism of *R*- and *S*-glycidol is shown in *Figure 7.* As in human cells, the Raf/MEK/ERK module was activated through MAPK pathway as shown in *Figure 7. R*- and *S*-glycidol potentially induce the production of ROS by triggering the MAPK pathway that involves ERK ½, p-ERK, BCL-2 and caspase-3. In the nucleus, DNA alteration occur as the phosphorylated ERK and BCL-2 were activated that might lead to the DNA damage and cell death. ERK ½ requires simultaneous phosphorylation at conserved threonine (Thr) and

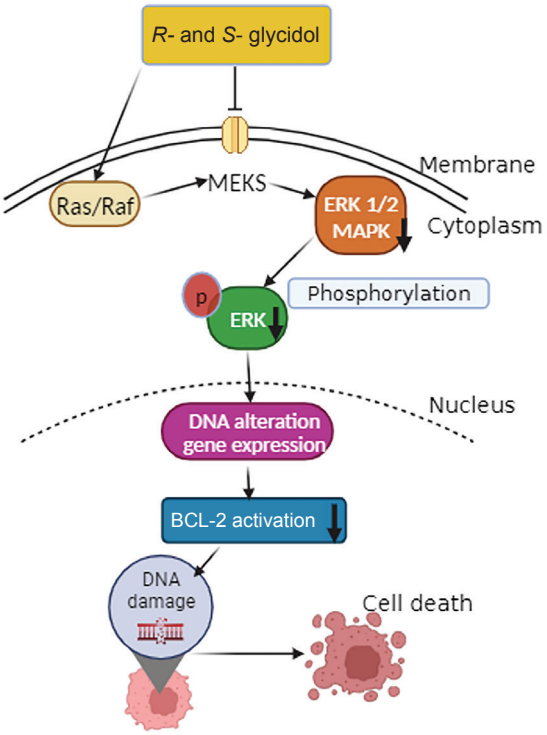


Figure 7. Schematic diagram of cell death mechanism after treatment with R- *and* S-*glycidol in HCT 116 cells.*

tyrosine (Tyr) residues to be fully activated. As the result of the phosphorylation event, the ERK ½ kinase protein undergoes conformational changes, domain rotation and remodelling which allowing substrates to bind and be phosphorylated by ERK ½ kinase (Takahashi *et al.*, 2012).

Caspase-mediated intrinsic signalling system, which is mostly regulated by the BCL-2 family of intracellular proteins, or an extrinsic signalling pathway, which is primarily regulated by the tumour necrosis factor (TNF) receptor family, can both cause apoptosis (Lu *et al.*, 2020). Apoptosis dysregulation is linked to uncontrolled cell proliferation, cell growth, and cancer development (Takahashi *et al.*, 2012). Based on our findings, BCL-2 protein expression for both *R*- and *S*-glycidol were down regulated as the time exposure increased (*Figure 3*). We postulated that the down regulation of BCL-2 contributes to cell death of treated HCT 116 cells after *R*- and *S*-glycidol treatments. According to Ji *et al.* (2017), the decreasing BCL-2 protein expression after exposure of 3-MCPD resulted in activation of mitochondrial apoptosis pathway. In order to prove whether early apoptotic event occurred or not, caspase-3 protein expression was conducted and caspase-3 protein expression showed no significant difference compared to control after treated with *R*- and *S*-glycidol in the HCT 116 cells *(Figure 3)*. This event suggested that induction of cell death by *R*- and *S*-glycidol in the treated HCT 116 cells was caspase independent. A study by Kim *et al.* (2021), indicated that cytotoxic effects on human lung cells after treated with mercury chloride ($HgCl_2$), subsequently leading to the cell death via caspase-3 independent pathway. Previous studies also indicated that cell death event in various types of cells (*in vitro)* which mediated cell death via caspase-3 independent (Cregan *et al.*, 2013; Mallepogu *et al.*, 2017; Nowak *et al.*, 2020). In addition, glycidol has an ability to induce immunoreactivity which may lead to the apoptosis in the Albino rat brain cells (Sevim *et al.*, 2021). Furthermore, epoxide functional group in the chemical structure of metabolites (chemicals undergo xenobiotic metabolism) has high reactivity that was proven to promote high toxicity than the parent compound (Obach and Kalgutkar, 2010). The epoxide of the glycidol was believed the cause of DNA damage in human cells that mediated cell death (Liu *et al.*, 2021). The free glycidol was discovered to induce cell cycle arrest and apoptosis event with the involvement MAPK. RAS/RAF/MEK/ERK proteins are proteins in MAPK pathway, which are the most common proteins in cancer cell biology especially in oxidative stress event of the cancer cells (De Luca *et al.*, 2012). McCubrey *et al.* (2012), reported that activated ERK ½ S/T kinases phosphorylated and activated various substrates, and this pathway was involved in cancer development. Furthermore, ERK MAPK overexpression and activation have a role in the proliferation and progression of cancer cells development (Fang and Richardson, 2005). RAS protein or originally known as Rat Sarcoma Virus (RAS) protein can be found in human. The RAS protein mediates the ERK pathway, which subsequently activates rapidly accelerated fibrosarcoma 1 (RAF1), triggering a cascade involving MEK and then ERK activation, which was involved in the pathogenesis, progression, and oncogenic behaviour of human colorectal cancer (Fang and Richardson, 2005; Rezatabar *et al.*, 2019). Nappi *et al.* (2020) and Vidri and Fitzgerald (2020) have stated that the function of enhanced signalling in colorectal cancer through the Ras/Raf/MEK/ERK has become one of the prominent pathway to investigate the cytotoxicity and oncogenic events of xenobiotic such as glycidols in human cells (as provided in *Figure 7*).

CONCLUSION

R- and *S*-glycidol compounds were found less toxic to Vero (normal cells) but it induces cell death in HCT 116 cells. The cytotoxic event of the chemicals has proven that it was due to phosphorylation of ERK ½ proteins that may activate MAPK pathway which activated ROS production and leads to oxidative stress. Furthermore, the docking study showed that the interactions between glycidol and the 3D-structure of human ERK2 predominantly

include hydrogen bonds, Van der Waals interactions and hydrophobic contacts with amino acids, leading to the formation of binding pockets and the stabilisation of protein-ligand complex to support the down regulation event of ERK ½ and p-ERK proteins. In this study, toxicological effects of *R*- and *S*-glycidol were investigated. This finding has shown the similarity of cell death mechanism of treated HCT 116 cells after the exposure of *R*- and *S*-glycidol compounds. However, further investigation should be carried out to elucidate toxicological effects of lower dose *R*-glycidol and *S*-glycidol in *in vivo* study for further safety evaluation.

ACKNOWLEDGEMENT

Laboratory works were carried out at the Centre of Research and Field Service (CRAFT), Universiti Malaysia Terengganu and many thanks to the CRAFT's staff for their contribution in this project. This work was supported by the Ministry of Higher Education Malaysia (FRGS/1/2018/WAB11/UMT/02/1) and UMT for the funding [Fundamental Research Grant Scheme (Vot. 59539)].

REFERENCES

Abbasi, E; Aval, S F; Akbarzadeh, A; Milani, M; Nasrabadi, H T; Joo, S W; Hanifehpour, Y; Nejati-Koshki, K and Pashaei-Asl, R (2014). Dendrimers: Synthesis, applications, and properties. *Nanoscale Res. Letters., 9(1)*: 1-10. DOI: 10.1186/1556-276X-9-247.

Abraham, K; Andres, S; Palavinskas, R; Berg, K; Appel, K E and Lampen, A (2011). Toxicology and risk assessment of acrolein in food. *Mol. Nutr. Food Res., 55(9)*: 1277-1290. DOI: 10.1002/mnfr.201100481.

Akane, H; Shiraki, A; Imatanaka, N; Akahori, Y; Itahashi, M; Ohishi, T; Mitsumori, K and Shibutani, M (2013). Glycidol induces axonopathy by adult-stage exposure and aberration of hippocampal neurogenesis affecting late-stage differentiation by developmental exposure in rats. *Toxicol. Sci., 134(1)*: 140-154. DOI: 10.1093/toxsci/kft092.

Aral, T; Karakaplan, M and Hosgoren, H (2012). Asymmetric organocatalytic efficiency of synthesized chiral beta-amino alcohols in ring-opening of glycidol with phenols. *Catal. Lett., 142(6)*: 794-802. DOI: 10.1007/s10562-012-0814-4.

Arnesano, F; Pannunzio, A; Coluccia, M and Natile, G (2015). Effect of chirality in platinum drugs. *Coordination Chem. Rev., 284*: 286-297. DOI: 10.1016/j.ccr.2014.07.016.

Aurelia, A C; Dobrea, C; Morgovan, C; Arseniu, A M; Rus, L L; Butuca, A; Juncan, A M; Totan, M; Vonica-Tincu, A L; Cormos, G; Muntean, A C; Muresan, M L; Gligor, F G and Frum, A (2020). Applications and limitations of dendrimers in biomedicine. *Molecules., 25(17)*: 3982. DOI: 10.3390/molecules25173982.

Bakhiya, N; Abraham, K; Gürtler, R; Appel, K E and Lampen, A (2011). Toxicological assessment of 3-chloropropane-1, 2-diol and glycidol fatty acid esters in food. *Mol. Nutr. Food Res., 55(4)*: 509-521. DOI: 10.1002/mnfr.201000550.

Bonnier, F; Keating, M E; Wróbel, T P; Majzner, K; Baranska, M; Garcia-Munoz, A; Blanco, A and Byrne, H J (2015). Cell viability assessment using the Alamar blue assay: A comparison of 2D and 3D cell culture models. *Toxicol. In Vitro., 29(1)*: 124-131. DOI: 10.1016/j.tiv.2014.09.014.

Brooks, W H; Guida, W C and Daniel, K G (2011). The significance of chirality in drug design and development HHS public access. *Curr. Top. Med. Chem., 11(7)*: 760-770. DOI: 10.2174/156802611795-165098.

Circu, M L and Aw, T Y (2010). Reactive oxygen species, cellular redox systems and apoptosis. *Free Radic. Biol. Med., 48(6)*: 749-762. DOI: 10.1016/j.freeradbiomed.2009.12.022.

Constantinou, C; Papas, A and Constantinou, A I (2008). Vitamin E and cancer: An insight into the anticancer activities of vitamin E isomers and analogs. *Int. J. Cancer., 123(4)*: 739-752. DOI: 10.1002/ijc.23689.

Cregan, I L; Dharmarajan, A M and Fox, S A (2013). Mechanisms of cisplatin-induced cell death in malignant mesothelioma cells: Role of inhibitor of apoptosis proteins (IAPs) and caspases. *Int. J. Oncol., 42(2)*: 444-452. DOI: 10.3892/ijo.2012.1715.

De Luca, A; Maiello, M R; D'Alessio, A; Pergameno, M and Normanno, N (2012). The RAS/RAF/MEK/ERK and the PI3K/AKT signalling pathways: Role in cancer pathogenesis and implications for therapeutic approaches. *Expert Opin. Ther. Targets., 16*: 17-27. DOI: 10.1517/14728222.2011.639361.

EFSA Panel on Contaminants in the Food Chain (CONTAM) (2016). Risks for human health related to the presence of 3- and 2-monochloropropanediol (MCPD), and their fatty acid esters, and glycidyl fatty acid esters in food. *EFSA J., 14(6)*: 04426. DOI: 10.2903/j.efsa.2016.4426.

El Ramy, R; Ould Elhkim, M; Lezmi, S and Poul, J M (2007). Evaluation of the genotoxic potential of 3-monochloropropane-1,2-diol (3-MCPD) and its metabolites, glycidol and β-chlorolactic acid, using the single cell gel/comet assay. *Food Chem. Toxicol., 45(1)*: 41-48. DOI: 10.1016/j.fct.2006.07.014.

Fanali, C; D'Orazio, G; Gentili, A and Fanali, S (2019). Analysis of enantiomers in products of food interest. *Molecules., 24(6)*: 1119. DOI: 10.3390/molecules24061119.

Fang, J Y and Richardson, B C (2005). The MAPK signalling pathways and colorectal cancer. *Lancet Oncol., 6(5)*: 322-327. DOI: 10.1016/S1470-2045(05)70168-6.

Foroumadi, A and Emami, S (2014). Glycidol. *Encyclopedia of Toxicol*. 3rd edition. p. 757-761.

Fu, P P; Xia, Q; Hwang, H M; Ray, P C and Yu, H (2014). Mechanisms of nanotoxicity: Generation of reactive oxygen species. *J. Food Drug Anal., 22(1)*: 64-75. DOI: 10.1016/j.jfda.2014.01.005.

Goh, K M; Wong, Y H; Tan, C P and Nyam, K L (2021). A summary of 2-, 3-MCPD esters and glycidyl ester occurrence during frying and baking processes. *Curr. Res. Food Sci., 4*: 460-469. DOI: 10.1016/j.crfs.2021.07.002.

Hartwig, A; Arand, M; Epe, B; Guth, S; Jahnke, G; Lampen, A; Martus, H J; Monien, B; Rietjens, I M C M; Schmitz-Spanke, S; Schriever-Schwemmer, G; Steinberg, P and Eisenbrand, G (2020). Mode of action-based risk assessment of genotoxic carcinogens. *Arch. Toxicol., 94(6)*: 1787-1877. DOI: 10.1007/s00204-020-02733-2.

Hirata, Y (2021). *Trans*-fatty acids as an enhancer of inflammation and cell death: Molecular basis for their pathological actions. *Biol. Pharm. Bull., 44(10)*: 1349-1356. DOI: 10.1248/bpb.b21-00449.

Inagaki, R; Uchino, K; Shimamura, Y and Masuda, S (2019). Investigation of DNA damage of glycidol and glycidol fatty acid esters using FPG-modified comet assay. *Fundam. Toxicol. Sci., 6(1)*: 9-14. DOI: 10.2131/fts.6.9.

Ji, J; Zhu, P; Sun, C; Sun, J; An, L; Zhang, Y and Sun, X (2017). Pathway of 3-MCPD-induced apoptosis in human embryonic kidney cells. *J. Toxicol. Sci., 42(1)*: 43-52. DOI: 10.2131/jts.42.43.

Kadir, N H A; Rossiter, J T and Gooderham, N J (2009). *In vitro* toxicology of 2-propenyl and 3-butenyl glucosinolate derivatives. *Toxicol., 262(1)*: 15-16. DOI: 10.1016/j.tox.2009.04.016.

Kim, M J; Park, J; Kim, J; Kim, J Y; An, M J; Shin, G S; Lee, H M; Kim, C H and Kim, J W (2021). Transcriptome analysis reveals $HgCl_2$ induces apoptotic cell death in human lung carcinoma H1299 cells through caspase-3-independent pathway. *Int. J. Mol. Sci., 22(4)*: 2006. DOI: 10.3390/ijms22042006.

Kim, S I; Kim, H J; Lee, H J; Lee, K; Hong, D; Lim, H; Cho, K; Jung, N and Yi, Y W (2016). Application of a non-hazardous vital dye for cell counting with automated cell counters. *Anal. Biochem., 492*: 8-12. DOI: 10.1016/j.ab.2015.09.010.

Lim, S W; Loh, H S; Ting, K N; Bradshaw, T D and Zeenathul, N A (2014). Cytotoxicity and apoptotic activities of alpha-, gamma- and delta-tocotrienol isomers on human cancer cells. *BMC Complement. Altern. Med., 14(1)*: 1-18. DOI: 10.1186/1472-6882-14-469.

Liou, G Y and Storz, P (2010). Reactive oxygen species in cancer. *Free Radic. Res., 44(5)*: 479-496. DOI: 10.3109/10715761003667554.

Liu, P W; Li, C I; Huang, K C; Liu, C S; Chen, H L; Lee, C C; Chiou, Y Y and Chen, R J (2021). 3-MCPD and glycidol coexposure induces systemic toxicity and synergistic nephrotoxicity via NLRP3 inflammasome activation, necroptosis and autophagic cell death. *J. Hazard. Mater., 405*: 124241. DOI: 10.1016/j.jhazmat.2020.124241.

Liu, X; Luo, Q; Rakariyatham, K; Cao, Y; Goulette, T; Liu, X and Xiao, H (2016). Antioxidation and anti-ageing activities of different stereoisomeric astaxanthin *in vitro* and *in vivo*. *J. Funct. Foods., 25*: 50-61. DOI: 10.1016/j.jff.2016.05.009.

Lu, Y; Liu, B; Liu, Y; Yu, X and Cheng, G (2020). Dual effects of active ERK in cancer: A potential target for enhancing radiosensitivity. *Oncol. Lett., 20(2)*: 993-1000. DOI: 10.3892/ol.2020.11684.

Mäder, P and Kattner, L (2020). Sulfoximines as rising stars in modern drug discovery? Current status and perspective on an emerging functional group in medicinal chemistry. *J. Med. Chem., 63(23)*: 14243-14275. DOI: 10.1021/acs.jmedchem.0c00960.

Mahapatra, M and Tysoe, W T (2015). Chemisorptive enantioselectivity of chiral epoxides on tartaric-acid modified Pd (111): Three-point bonding. *Phys. Chem. Chem., 17(7)*: 5450-5458. DOI: 10.1039/c4cp05611f.

Mallepogu, V; Jayasekhar, P B; Doble, M; Suman, B; Nagalakshmamma, V; Chalapathi, P V and Thyagaraju, K (2017). Effects of acrylamide on cervical cancer (HeLa) cells proliferation and few marker enzymes. *Austin J. Biotechnol. Bioeng., 4*: 1087.

Matta, M; Huybrechts, I; Biessy, C; Casagrande, C; Yammine, S; Fournier, A; Olsen, K S; Lukic, M; Gram, I T; Ardanaz, E; Sánchez, M J; Dossus, L; Fortner, R T; Srour, B; Jannasch, F; Schulze, M B; Amiano, P; Agudo, A; Colorado-Yohar, S; Quirós, J R; Tumino, R; Panico, S; Masala, G; Pala, V and Murphy, N (2021). Dietary intake of trans fatty acids and breast cancer risk in 9 European countries. *BMC Med., 19(1)*: 1-11. DOI: 10.1186/s12916-021-01952-3.

McCubrey, J A; Steeman, L; Chappell, W; Abrams, S; Montalto, G; Cervello, M; Nicoletti, F; Fagone, P; Malaponte, G; Mazzarino, M; Candido, S; Libra, M; Basecke, J; Mijatovic, S; Maksimovic-Ivanic, D; Milella, M; Tafuri, A; Cocco, L; Evangelisti, C; Chiarini, F and Martelli, A (2012). Mutations and deregulation of Ras/Raf/MEK/ERK and PI3K/PTEN/Akt/mTOR cascades which alter therapy response. *Oncotarget., 3(9)*: 954-987. DOI: 10.18632/oncotarget.652.

Moreno-Yruela, C; Bæk, M; Monda, F and Olsen, C A (2022). Chiral posttranslational modification to lysine ϵ-amino groups. *Acc. Chem. Res., 55(10)*: 1456-1466. DOI: 10.1021/acs.accounts.2c00115.

Morris, G M; Huey, R; Lindstrom, W; Sanner, M F; Belew, R K; Goodsell, D S and Olson, A J (2009). AutoDock4 and AutoDockTools4: Automated docking with selective receptor flexibility. *J. Comput. Chem., 30(16)*: 2785-2791. DOI: 10.1002/jcc.21256.

Mossoba, M E; Mapa, M S T; Araujo, M; Zhao, Y; Flannery, B; Flynn, T; Sprando, J; Wiesenfeld, P and Sprando, R L (2020). *In vitro* toxicological assessment of free 3-MCPD and select 3-MCPD esters on human proximal tubule HK-2 cells. *Cell Biol. Toxicol., 36(3)*: 209-221. DOI: 10.1007/s10565-019-09498-0.

Nappi, A; Nasti, G; Romano, C; Berretta, M and Ottaiano, A (2020). Metastatic colorectal cancer: Prognostic and predictive factors. *Curr. Med. Chem., 27(17)*: 2779-2791. DOI: 10.2174/09298673266661906 20110732.

NavaneethaKrishnan, S; Rosales, J L and Lee, K Y (2019). ROS-mediated cancer cell killing through dietary phytochemicals. *Oxid. Med. Cell. Longev., 2019*: 9051542. DOI: 10.1155/2019/9051542.

Nowak, A; Zakłos-Szyda, M; Żyżelewicz, D; Koszucka, A and Motyl, I (2020). Acrylamide decreases cell viability, and provides oxidative stress, DNA damage, and apoptosis in human colon adenocarcinoma cell line Caco-2. *Molecules., 25(2)*: 368. DOI: 10.3390/molecules25020368.

Obach, R S and Kalgutkar, A S (2010). Reactive electrophiles and metabolic activation. *Comprehensive Toxicology.* 2nd edition. Elsevier. p. 309-347. DOI: 10.1016/B978-0-08-046884-6.00115-9.

Ozcagli, E; Alpertunga, B; Fenga, C; Berktas, M; Tsitsimpikou, C; Wilks, M F and Tsatsakis, A M (2016). Effects of 3-monochloropropane-1, 2-diol (3-MCPD) and its metabolites on DNA damage and repair under *in vitro* conditions. *Food Chem. Toxicol., 89*: 1-7. DOI: 10.1016/j.fct.2015.12.027.

Pizzino, G; Irrera, N; Cucinotta, M; Pallio, G; Mannino, F; Arcoraci, V; Squadrito, F; Altavilla, D and Bitto, A (2017). Oxidative stress: Harms and benefits for human health. *Oxid. Med. Cell. Longev., 2017*: 8416763. DOI: 10.1155/2017/8416763.

Redza-Dutordoir, M and Averill-Bates, D A (2016). Activation of apoptosis signalling pathways by reactive oxygen species. *Biochimica et Biophysica Acta (BBA) Molecular Cell Res., 1863*: 2977-2992. DOI: 10.1016/j.bbamcr.2016.09.012.

Rezatabar, S; Karimian, A; Rameshknia, V; Parsian, H; Majidinia, M; Kopi, T A; Bishayee, A; Sadeghinia, A; Yousefi, M; Monirialamdari, M and Yousefi, B (2019). RAS/MAPK signaling functions in oxidative stress, DNA damage response and cancer progression. *J. Cell. Physiol., 234*: 14951-14965. DOI: 10.1002/jcp.28334.

Schilter, B; Scholz, G and Seefelder, W (2011). Fatty acid esters of chloropropanols and related compounds in food: Toxicological aspects. *European J. Lipid Sci. Technol., 113(3)*: 309-313. DOI: 10.1002/ejlt.201000311.

Schumacker, P T (2006). Reactive oxygen species in cancer cells: Live by the sword, die by the sword. *Cancer Cell., 10(3)*: 175-176. DOI: 10.1016/j.ccr.2006.08.015.

Senyildiz, M; Alpertunga, B and Ozden, S (2017). DNA methylation analysis in rat kidney epithelial cells exposed to 3-MCPD and glycidol. *Drug Chem. Toxicol., 40(4)*: 432-439. DOI: 10.1080/01480545.2016.1255951.

Sevim, C; Özkaraca, M; Kara, M; Ulaş, N; Mendil, A S; Margina, D and Tsatsakis, A (2021). Apoptosis is induced by sub-acute exposure to 3-MCPD and glycidol on Wistar Albino rat brain cells. *Environ. Toxicol. and Pharmacology., 87*: 103735. DOI: 10.1016/j.etap.2021.103735.

Sinkala, E; Sollier-Christen, E; Renier, C; Rosàs-Canyelles, E; Che, J; Heirich, K; Duncombe, T A; Vlassakis, J; Yamauchi, K A; Huang, H; Jeffrey, S S and Herr, A E (2017). Profiling protein expression in circulating tumour cells using microfluidic western

blotting. *Nat. Commun., 8*: 14622. DOI: 10.1038/ncomms14622.

Snezhkina, A V; Kudryavtseva, A V; Kardymon, O L; Savvateeva, M V; Melnikova, N V; Krasnov, G S and Dmitriev, A A (2019). ROS generation and antioxidant defense systems in normal and malignant cells. *Oxid. Med. Cell. Longev., 2019*: 6175804. DOI: 0.1155/2019/6175804.

Spungen, J H; MacMahon, S; Leigh, J; Flannery, B; Kim, G; Chirtel, S and Smegal, D (2018). Estimated US infant exposures to 3-MCPD esters and glycidyl esters from consumption of infant formula. *Food Addit. Contam. Part A Chem. Anal., Control Expo. Risk Assess., 35(6)*: 1085-1092. DOI: 10.1080/19440049.2018.1459051.

Takahashi, T; Steinberg, G K and Zhao, H (2012). Phosphorylated MAPK/ERK1/2 may not always represent its kinase activity in a rat model of focal cerebral ischemia with or without ischemic preconditioning. *Neuroscience., 209*: 155-160. DOI: 10.1016/j.neuroscience.2012.02.005.

Tollini, F; Occhetta, A; Broglia, F; Calemma, V; Carminati, S; Storti, G; Sponchioni, M and Moscatelli, D (2022). Influence of pH on the kinetics of hydrolysis reactions: The case of epichlorohydrin and glycidol. *React. Chem. Eng., 7(10)*: 2211-2223. DOI: 10.1039/D2RE00191H.

Vidri, R J and Fitzgerald, T L (2020). GSK-3: An important kinase in colon and pancreatic cancers. *Biochimica et Biophysica Acta (BBA) Molecular Cell Res., 1867(4)*: 118626. DOI: 10.1016/j.bbamcr.2019.118626.

Wróbel, K; Wołowiec, S; Markowicz, J; Wałajtys-Rode, E and Uram, Ł (2022). Synthesis of biotinylated PAMAM G3 dendrimers substituted with *R*-glycidol and celecoxib/simvastatin as repurposed drugs and evaluation of their increased additive cytotoxicity for cancer cell lines. *Cancers., 14(3)*: 714. DOI: 10.1186/1556-276X-9-247.

Wu, D and Yotnda, P (2015). Production and detection of reactive oxygen species (ROS) in cancers. *J. Vis. Exp., 57*: 3357. DOI: 10.3791/3357.

Journal of Oil Palm Research Vol. 36 (3) September 2024 p. 510-523
DOI: https://doi.org/10.21894/jopr.2023.0045

COMPARATIVE STUDY OF PALM-BASED MILK YOGHURT WITH DAIRY AND COCONUT MILK YOGHURT BASED ON PROXIMATE, TEXTURE AND AMINO ACID ANALYSIS

HADI AKBAR DAHLAN[1]* and NORRAKIAH ABDULLAH SANI[1]

ABSTRACT

Palm-based milk is one of the derivative products of the local palm oil industry. Currently, it is being sold as an alternative ingredient to coconut milk. However, palm-based milk is a potential ingredient and can be utilised to make new food products. This is in line with the Sustainable Development Goal (SDG) of using local resources to make food products. In this preliminary study, palm-based milk is being developed into a plant-based yoghurt. To assess the feasibility of the palm-based milk yoghurt, seven formulations consisting of a combination of three types of common yoghurt starter cultures were made. These seven formulations of palm-based milk yoghurts will be compared against dairy yoghurts and coconut milk yoghurts of the same formulation. Based on the result, palm-based milk yoghurt has the highest lipid content among the three types of yoghurt. As such, it can be marketed as an energy-dense yoghurt. However, it is lacking in several aspects of proximate and amino acid content, viscosity and high rate of syneresis when compared to the other yoghurt types in this study. Suggestions for mitigating this issue in palm-based milk yoghurt are also given in this study.

Keywords: amino acids, palm-based milk, proximate analysis, yoghurt.

Received: 25 November 2022; **Accepted:** 25 June 2023; **Published online:** 8 September 2023.

INTRODUCTION

The Sustainable Development Goals (SDGs) are a blueprint for peace and prosperity for the people and the planet that was adopted by all United Nations Member states in 2015 (United Nations, 2015a). Among the 17 goals, two goals stress the need for developing sustainable food production using domestic resources, specifically Target 2.4 and Target 9.b. Target 2.4 of SDG Goal 2 is to ensure sustainable food production systems (United Nations, 2015b) while Target 9.b of SDG Goal 9 is to support domestic technology development (United Nations, 2015c). Therefore, research on developing new food products using local resources or products is an effort that followed the SDGs.

Malaysian palm oil is a sustainable resource (Hanafiah *et al.*, 2022) but still lacking in economic, environmental and social strategies (Wardhani and Rahadian, 2021). One underutilised palm oil product is palm-based milk (called *Santan* in the Malay language) which was developed by the Malaysian Palm Oil Board (MPOB). The palm-based milk is made with palm oil, emulsifier and coconut flavourings (Zainal *et al.*, 1997). Presently, palm-based milk is marketed in Malaysia as a raw material and healthier coconut milk replacement. The utilisation of palm-based milk as a replacement for coconut milk in one Malaysian rice dish was similar in the majority of its sensory attributes (Rafidah *et al.*, 2013). If a derivative food product can be made from palm-based milk, then a small food industry can be developed, and this should strengthen the palm oil industry in Malaysia.

[1] Department of Food Sciences,
Faculty of Science and Technology,
Universiti Kebangsaan Malaysia,
43600 UKM Bangi, Selangor, Malaysia.

* *Corresponding author e-mail: hadiukm@gmail.com*

One potential derivative product from palm-based milk is palm-based yoghurt, a plant-based yoghurt. Non-dairy yoghurt is part of the non-dairy probiotic product market which involves inoculating prebiotic starter culture to non-dairy substrates (Kumar *et al.*, 2015). Examples of plant-based yoghurt such as coconut yoghurt (Yaakob *et al.*, 2012), and yoghurt-like beverages from mixture of cereal, soy and grape must (Coda *et al.*, 2012). Lactic acid bacteria had been found to be able to grow in non-dairy milk based on previous studies. Coconut milk was been found to be able to ferment lactic acid bacteria (Mauro and Garcia, 2019). Palm-based milk can also be developed into non-dairy yoghurt because yoghurt starter culture has been found to be able to grow within the palm-based milk. The lactic acid bacteria had been found to grew up to 8-9 log cfu/mL within the palm-based milk (Dahlan *et al.*, 2017). Mixed starter culture of lactic acid bacteria had been found to affect the physical quality of dairy milk (Dahlan and Sani, 2017). However, study regarding the comparison of proximate quality of dairy yoghurts, coconut milk yoghurts and palm-based milk yoghurts formed by mixed lactic acid bacteria cultures into their proximate contents had not been performed. Thus, the objective of this study is to perform a preliminary study on the proximate, texture and amino acid intensity of palm-based milk yoghurt against dairy yoghurt and coconut yoghurt.

MATERIALS AND METHODS

Base Material for Yoghurt Production

Three types of yoghurt were made in this study, namely dairy yoghurt for control comparison, coconut milk yoghurt for comparison with alternative plant-based yoghurt and palm-based milk yoghurt. The dairy milk for dairy yoghurt was made with Farm Fresh Dairy Milk (Farm Fresh, Selangor, Malaysia). M&S brand of ultrahigh temperature (UHT) treated coconut milk was used for coconut milk yoghurt production. Khalis brand (Khalis Santan, Selangor, Malaysia) of palm-based milk was used for palm-based milk yoghurt. All three types of yoghurt base material were commercially available and were bought from a grocery store at Bandar Baru Bangi, Selangor, Malaysia.

Yoghurt Production

Yoghurt formulations for all three substrates were based on seven formulations shown in *Table 1*. The formulation was based on a combination of three yoghurt starter cultures: *Lactobacillus acidophilus*, *L. delbrueckii* sbsp. *bulgaricus* and *Streptococcus thermophilus*. All starter cultures were obtained commercially (Custom Probiotics, California USA). All yoghurts were incubated at 37°C for 20 hr with Trio Yoghurt Maker (Trio Sdn. Bhd., Selangor, Malaysia). All yoghurts were analysed within 3 days after incubation was completed.

Protein Analysis

Protein content of the yoghurt was analysed according to Kjedahl method (Chang, 2010). 1 g of yoghurt sample was placed in a Kjeldahl flask. Concentrated sulphuric acid (98%) was added into the flask and was soaked for 2 hr at 420°C. After digestion, a concentrated sodium hydroxide solution (40%) was added for neutralisation. It was filtrated after 5 min using the filtration system. The filtrate then underwent titration with 0.1 N hydrochloric acid. The titration will determine the nitrogen content. The percentage of nitrogen can be calculated using the following Equation (1):

TABLE 1. THREE COMPONENT MIXTURE DESIGN FOR SEVEN YOGHURT FORMULATION

Sample: 100 mL substrate (dairy/coconut/palm milk)
Volume of inoculation: 1 g

Formulation	*Lactobacillus acidophilus*	*Lactobacillus delbrueckii* sbsp. *bulgaricus*	*Streptococcus thermophilus*
1	1	0	0
2	0	1	0
3	0	0	1
4	1/2	1/2	0
5	1/2	0	1/2
6	0	1/2	1/2
7	1/3	1/3	1/3

$$\text{Nitrogen content} = \frac{0.1\ \text{N HCl} \times (\text{mL 0.1 N HCl in sample - mL 0.1 N HCl blank}) \times 14 \times 100)}{(\text{Sample weight} \times 1000)} \quad (1)$$

The protein content can be determined by multiplying the nitrogen content with protein factor for dairy product 6.38.

Lipid Analysis

Lipid analysis was done according to the Rose-Gottlieb method (Min and Ellefson, 2010) for both yoghurt products. The lipid was extracted using ether petroleum. 1 g of yoghurt sample was placed inside a Mojonnier flask and was added with 6 mL of boiling water. The mixture was homogenised via vortex until it reached room temperature. After that, 1 mL of ammonia (25% concentrated) was added to the mixture and homogenised for 2 min.

After that, 7.5 mL methanol was added into the mixture and homogenised via vortex for 2 min. 17 mL of diethyl ether was added followed by 17 mL of petroleum ether. The ether mixture was then poured into Mojonnier bowl. The mixture was left to dry on top of a hot plate (C-Mag HP 7, IKA) at a temperature reaching 100°C. The dried matter was weighed after complete drying. The lipid determination was calculated in Equation (2) as follows:

$$\text{Lipid content} = 100 \times \left[\frac{(\text{Weight of Mojonnier bowl + Sample}) - (\text{Weight of Mojonnier bowl})}{\text{Weight of yoghurt sample}}\right] \quad (2)$$

Crude Fibre Analysis

About 2-3 g of the yoghurt samples were taken and defatted by soaking in acetone (Sigma Aldrich, United States). After that, the sample was dried and placed into 200 mL of sulphuric acid. The flask was then connected to a condenser at boiling temperature for 30 min. The solution in the flask was whirled throughout the heating process.

The solution in the flask was filtered through a Buchner funnel equipped with filter paper. Residue from the filter paper was then placed into a flask containing 200 mL NaOH at boiling temperature for 30 min. The mixture was then filtered again and washed with boiling water and HCl solution in sequence three times. The final wash was done by washing with petroleum ether. The residue was then heated in the oven at 105°C for 12 hr before weighing (BeMiller, 2010).

Ash Content Determination

Ash content in the yoghurt sample was determined by calcination. About 5-10 g of yoghurt sample was placed in a clay bowl before being heated in a furnace oven (Lindberg/Blue M, Thermo Scientific) at 480°C overnight. The sample was weighed after it had cooled down to room temperature (Marshall, 2010).

Carbohydrate Content Determination

The carbohydrate content of yoghurt samples was determined through calculation. The carbohydrate content calculation which is also known as nitrogen free extract (NFE) calculation in Equation (3) as follows:

$$\text{Carbohydrate content} = 100 - (\text{Protein content + Lipid content + Ash content + Moisture content}) \quad (3)$$

Carbohydrate content calculated by NFE means carbohydrates that are not crude fibres. Monosaccharides and disaccharides are examples of non-crude fibres (Charalampopoulos *et al.*, 2002).

Moisture Content

The moisture content in yoghurt samples was determined through the drying process via a drying oven. A total of 5-10 g of yoghurt samples were placed in a clay bowl before being dried in a drying oven at 100°C overnight. After overnight, the weight of the clay bowl was measured to determine the total water content of the yoghurt sample.

Amino Acid Analysis

Amino acid content was determined through acid hydrolysis according to Waters™ accQ.Tag method (Nancy Astephen, 1993). Approximately 0.3 g of sample was poured into a glass stoppered test tube and hydrolysed with 5 mL of 6 N HCl at 110°C for 24 hr. The sample was cooled to room temperature before it was filtered through a filter paper (Sartorius grade 292) into 100 mL volumetric flask. The internal standard (400 µL) (50 µmol/mL α-Aminobutyric Acid (AABA) in 0.1 M HCl) was added and made up to 100 mL with distilled water. The aliquot was filtered through 0.20 mm nylon microfilter.

As for derivatisation, 10 µL of filtered hydrolysated samples or standard were transferred into a 1.5 mL glass vial and 70 µL of borate buffer solution was added and mixed well. Then, 20 µL of AccQ Flour reagent (3 mg/mL in acetonitrile) was added to the mixture and thoroughly mixed

through vortex for several seconds. 10 µL of samples and standards were injected into the HPLC (Waters 2475, Waters Co., Milford, MA, USA) and the flow rate was set at 1 mL/min. Analysis of the amino acids was performed with AccQ Tag (3.9×150 mm) column. The mobile phase A was Eluent A (200 mL AccQ Tag to 2 L of Milli-Q water) and mobile phase B, was Eluent B (60% acetonitrile).

Yoghurt Viscosity

A rotational viscometer (Brookefield, model DV II, USA) was used to measure the viscosity of the dairy, coconut and palm-based milk yoghurts. Approximately 50 mL of yoghurt in a 50 mL beaker was used as sample during measurement. The viscosity measurements were made at room temperature (27°C) using 10 rpm. The spindle used was Brookefield LV spindle No. 4.

Yoghurt Syneresis

Syneresis is the ability of retaining water in food. About 10-20 g of yoghurt samples were taken and put into centrifuge tubes for analysis. The syneresis was done via centrifuge (Kubota, Japan) at 3300× rpm for 15 min at 4°C. Liquid that was separated from the yoghurt after the centrifugation was taken for weighting. The syneresis percentages were calculated by dividing the weight of separating liquid and weight of the sample and then multiplied by 100 (Morell *et al.*, 2015).

pH Value Determination

The pH analysis was carried out using a Benchtop pH meter (Mettler Toledo Inc., Parkway, USA). The pH meter was calibrated prior to yoghurt pH measurement. Yoghurt samples were measured immediately after the end of the incubation period (Sadler and Murphy, 2010).

Statistical Analysis

Analysis of variance (ANOVA) was performed with Tukey-test using Minitab version 17 (Minitab Pty. Ltd., Sydney). Principal component analysis (PCA) was performed with SIMCA-P+ version 13 (Umetrics, Sweden). All analysis were done in triplicates except for amino acid analyses which were done in duplicate.

RESULTS AND DISCUSSION

Proximate and Texture Comparison

Three types of substrates namely palm-based milk, coconut milk and dairy milk were made into yoghurt by inoculating seven formulations of three types of yoghurt starter culture: *Lactobacillus acidophilus*, *L. delbrueckii* sbsp. *bulgaricus* and *Streptococcus thermophilus* (*Table 1*). The objective for comparing with dairy yoghurt is to compare the proximate and texture characteristics between palm-based milk and normal-type yoghurts (dairy yoghurts). The reason for comparing with coconut milk yoghurt is to observe the differences between palm-based milk yoghurt with another plant-based yoghurt (coconut milk yoghurt).

All seven formulations for each three types of substrates underwent proximate analysis which includes protein, lipid, ash, carbohydrate, and crude fibre content. Besides proximate, the yoghurt samples also underwent yoghurt texture analysis which include viscosity, moisture content, syneresis percentage and pH measurement. Yoghurt viscosity is a non-Newtonian fluid with shear-thinning characteristics (Loveday *et al.*, 2013). Since yoghurt viscosity is usually associated with dairy yoghurt, additional measurements such as moisture content, syneresis percentage and pH measurement will be complementary to the texture description of both coconut and palm-based milk yoghurts. Syneresis is described as the expulsion of liquid from the gel matrix that forms the yoghurt texture (Walstra *et al.*, 1993). A high syneresis percentage means that gel within the yoghurt structure could not hold liquid and requires additional ingredients such as an emulsifier. The pH of the yoghurt affected the yoghurt texture (Ozcan *et al.*, 2015). Lower pH in dairy yoghurts usually indicates the formation of micelle globules that form the texture. It is possible that a similar trend can be seen in non-dairy yoghurts.

To visualise the overall results of proximate and texture among the 21 types of yoghurts, principal component analysis (PCA) was utilised. PCA is a proven dimensional reduction technique to visualise complex data sets into easier interpretation and discussion (Granato *et al.*, 2018). *Figure 1* shows the PCA score and loading plot of all three types of yoghurts.

The PCA score plot (*Figure 1a*), shows three clusters of yoghurt samples separated along the PC1. The separation is based on the type of yoghurt (dairy yoghurt, coconut milk yoghurt, and palm-based milk yoghurt). The PCA loading plot (*Figure 1b*) indicates the variables of the analysis. The variables are the proximate and textural analysis performed in this study. The position of the variables in the loading plot corresponds to the position of clusters in the score plot. Based on the loading plot, dairy yoghurts formulations had the highest protein, carbohydrate, viscosity, moisture, and ash content. This can be seen based on the position of the selected variables

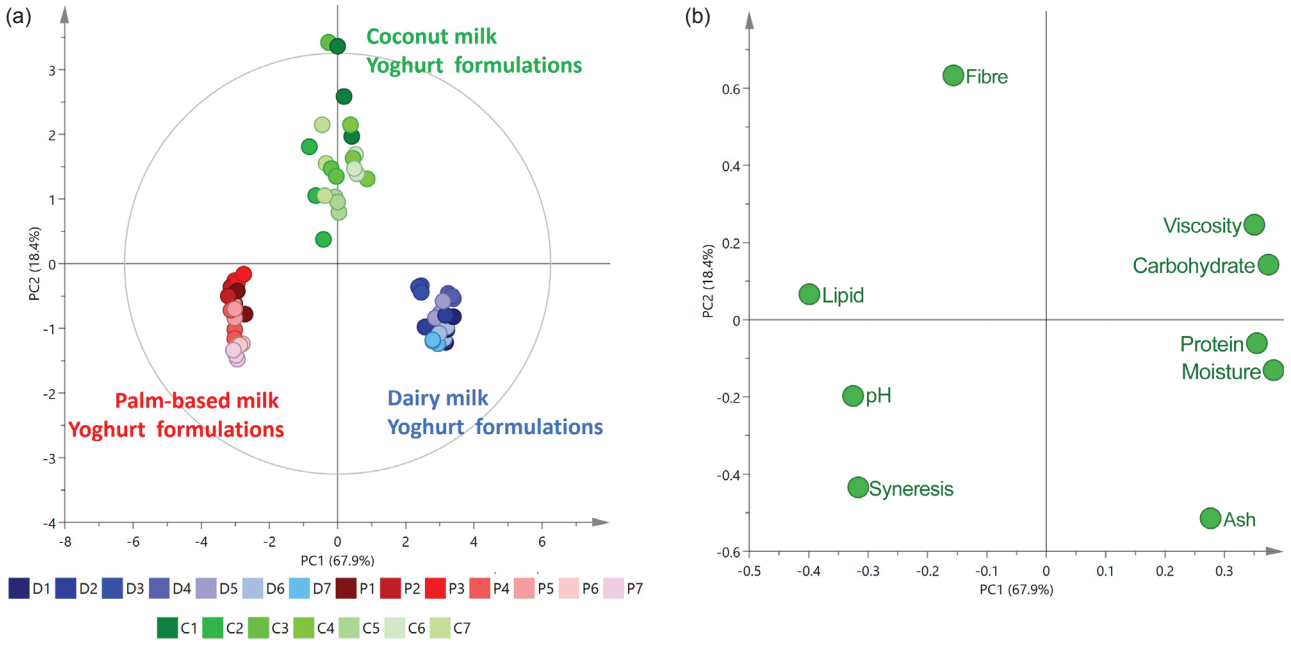


Figure 1. (a) PCA score and, (b) loading plot of all seven yogurt formulations for each dairy yoghurt, coconut milk yoghurt and palm-based milk yoghurt.

at the positive axis of PC1, which correspond to the position of the dairy yoghurts cluster in the score plot.

The loading plot also showed that coconut milk yoghurt formulations had higher fibre content (*Figure 1b*). This indicates that among the palm-based milk yoghurts and coconut milk yoghurts, coconut milk yoghurts had higher fibre content. Dairy milk yoghurts do not contain any fibre content. Palm-based milk yoghurts had the highest lipid content, pH and syneresis percentage. This indicates that palm-based milk yoghurts would be an energy-dense yoghurt but have less acidity and possibly watery. The axis of PC2 in the score plot also showed a trend among the three yoghurts clusters. Based on the clustering, yoghurts formulations with single starter culture inoculation (darker colour) were positioned on the upper part of each cluster. Meanwhile, the mixed starter culture inoculations trailed below in each yoghurt cluster. This indicates that starter culture formulation contributes to the variations of the proximate content and textural properties of the yoghurt. To observe the effect of starter culture formulations, single PCA plots for each yoghurt base were plotted.

The Effect of Starter Culture Formulations

The seven formulations of each yoghurt base influenced the proximate and starter culture. *Figure 2* shows the PCA of all seven formulations of dairy yoghurts and the individual bar graph of all proximate and measured texture parameters. Based on the score plot (*Figure 2a*), all single starter culture of *L. acidophilus* (D1), *L. delbrueckii* sbsp. *bulgaricus* (D2) and *S. thermophilus* (D3) are clustered separately in both PC1 and PC2 axis. This indicates that these starter cultures' ability to grow differed from each other in dairy milk. The capability of these single starter cultures to change the sensory quality and indirectly the proximate and texture quality of dairy yoghurt had been established (McSweeney and Sousa, 2000; Smit *et al.*, 2005). Meanwhile, the mix starter culture formulations (D4 to D7) are positioned from the central axis toward the positive axis of PC1 and PC2. The loading plot (*Figure 2b*) showed that the individual starter culture and mixtures of these starter cultures influenced the proximate and the measured textural qualities.

In this study, formulation 1 (D1) has the highest ash content (*Figure 2f*), viscosity (*Figure 2h*), and lowest syneresis (*Figure 2i*). Meanwhile, formulation 2 (D2) has the highest protein content (*Figure 2c*) and lowest pH (*Figure 2j*). Formulation 3 (D3) has the highest carbohydrate content (*Figure 2e*) but it has the highest syneresis percentage (*Figure 2i*). Formulations 4-7 (D4 to D7) are a mixture of starter cultures (*Table 1*) and each formulation led to different effects. Formulation 7 was a mixture of all starter cultures in the dairy yoghurt that had the highest lipid content (*Figure 2d*). Some starter cultures might have a dominant effect in the mixed formulation.

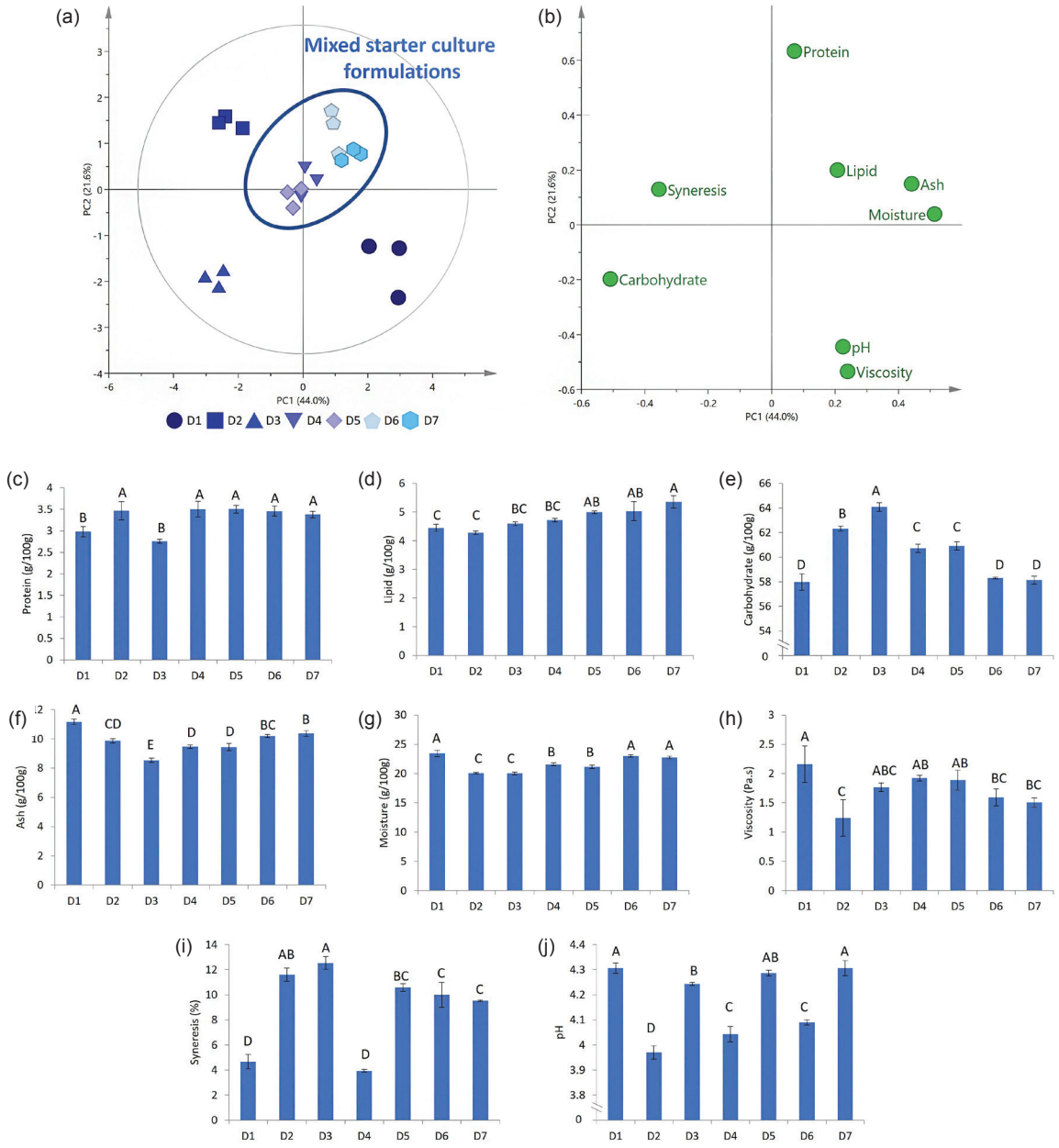


Figure 2. (a) PCA score and, (b) loading plot of all seven yogurt formulations of dairy yoghurts. Bar graph (c) to (j) shows the proximate and texture variables. Different letters between the bar graph denotes significant differences ($p<0.05$) *via Tukey's test.*

For example, D4 contained *L. acidophilus* has lowered syneresis percentage similar to D1. Another example is formulations that contained *L. delbrueckii* sbsp. *bulgaricus* had lowered pH values (D2, D4 and D6).

Figure 3 shows the PCA of all seven formulations of coconut milk yoghurts and the individual bar graph of all proximate and measured texture parameters. Single starter culture formulations (C1 to C3) were positioned on the negative axis of PC1. The difference of single starter culture was separated along the axis of PC2. Meanwhile, the mixed formulations (C4 to C7) were positioned from the central axis to the positive axis of PC1. Based on the loading plot (*Figure 3b*), the formulation of the starter culture influences the proximate and texture quality. However, based on single bar graphs of the proximate analysis (*Figure 3c-k*), the formulation variation does not affect protein content (*Figure 3c*), fibre (*Figure 3f*), and ash (*Figure 3g*) significantly ($p>0.05$).

Single starter culture affects the lipid content of the coconut milk yoghurts. Among the three types of starter culture, C2 yoghurt contains only *L. delbrueckii* sbsp. *bulgaricus* had the lowest lipid content (*Figure 3d*). However, C2 yoghurt had the highest carbohydrate content (*Figure 3e*) and pH above 5 (*Figure 3k*). Yoghurt C3 which contains *S. thermophiles* had the highest syneresis percentage (*Figure 3j*) when compared to the other single starter

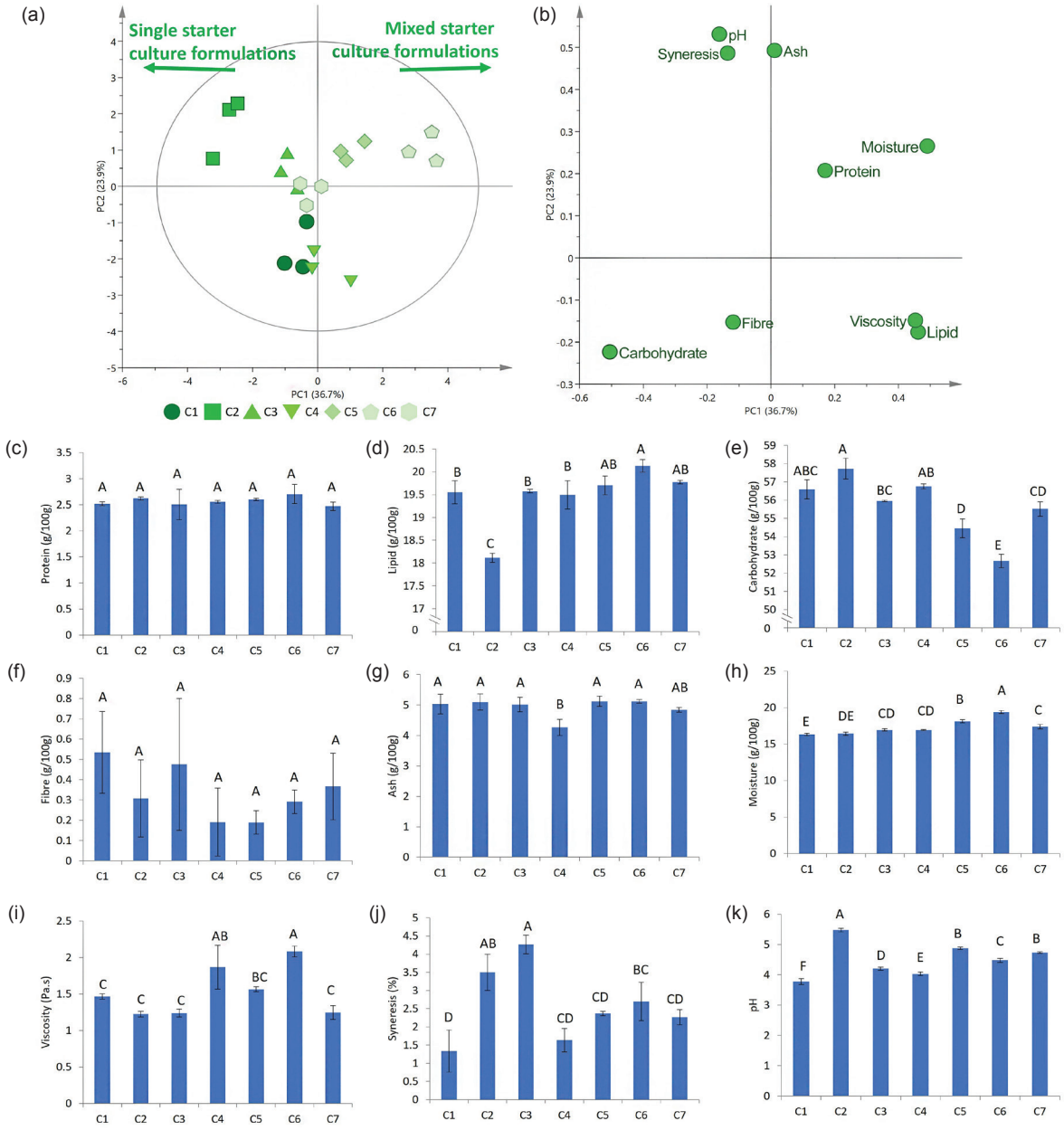


Figure 3. (a) PCA score and, (b) loading plot of all seven yogurt formulations of coconut milk yoghurts. Bar graph (c) to (k) shows the proximate and texture variables. Different letters between the bar graph denotes significant differences ($p<0.05$) *via Tukey's test.*

culture formulations. Based on the bar graphs, the mixed starter culture yoghurts have higher lipid content (C6 in *Figure 3d*), moisture content (C6 in *Figure 3h*), contributing toward yoghurt viscosity (C4 and C6 in *Figure 3i*) and lowered syneresis percentage (*Figure 3j*).

Figure 4 shows the PCA of all seven formulations of palm-based milk yoghurts and the individual bar graph of all proximate and measured texture parameters. Based on the score plot (*Figure 4a*), all three single starter culture formulations (P1 to P3) were positioned on the positive axis of PC1. The majority of the mixed starter culture formulations (P4 to P7) were positioned on the negative axis of PC1. Similar to coconut milk yoghurts, the single starter culture formulation was separated along the axis of PC2.

Based on the bar graphs, the variation in starter culture formulation does not affect carbohydrate (*Figure 4e*) and ash content (*Figure 4g*) significantly ($p>0.05$). Single starter culture formulation of palm-based milk yoghurt (P1 to P3) had the highest protein content (*Figure 4c*) and was higher in fibre content (*Figure 4f*) than the mixed culture formulation yoghurts. Among the three types of starter culture, formulation with *L. delbrueckii* sbsp. *bulgaricus* (P2) has the highest lipid content (*Figure 4d*). However, P2 was also the yoghurt with the highest syneresis

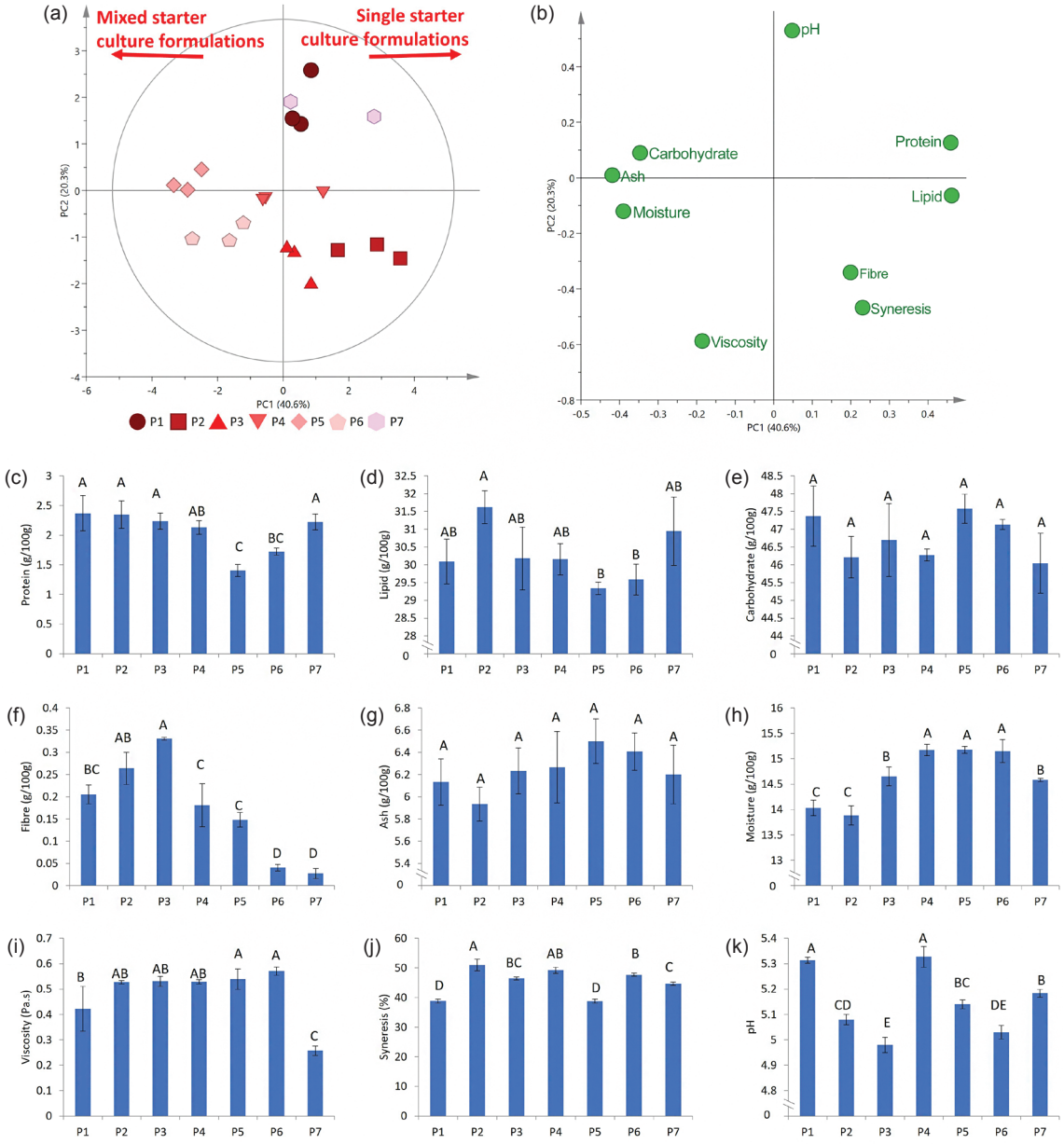


Figure 4. (a) PCA score and, (b) loading plot of all seven yogurt formulations of palm-based milk yoghurts. Bar graph (c) to (k) shows the proximate and texture variables. Different letters between the bar graph denotes significant differences (p<0.05) via Tukey's test.

percentage (*Figure 4j*). The mixture of starter culture (P4 to P6) except P7 generally had low protein (*Figure 4c*), lipid (*Figure 4d*) and fibre content (*Figure 4f*). The mixture of starter culture (P4 to P6) also has a higher moisture content (*Figure 4h*), viscosity (*Figure 4i*) and lower pH (*Figure 4k*). Yoghurt P7 which contains all three types of starter culture equivalently (*Table 1*) had an inverse result to other mixed formulation yoghurts (P4 to P6).

Based on the PCA of each yoghurt type, starter culture formulation can influence the proximate content and the textural quality of yoghurts including palm-based milk yoghurts. The next section will discuss the comparison of amino acid contents in palm-based milk yoghurts against both dairy yoghurt and coconut milk yoghurt.

Amino Acid Content Analysis

The amino acid analysis of the yoghurt samples in this study detected 16 types of amino acids. The 16 amino acids are lysine, isoleucine, methionine, leucine, valine, threonine, tyrosine, histidine, serine, phenylalanine, glutamic acid, proline, aspartic acid, alanine, glycine, and arginine. *Figure 5* shows the PCA plot amino acid analysis. The score plot (*Figure 5a*) shows that three types

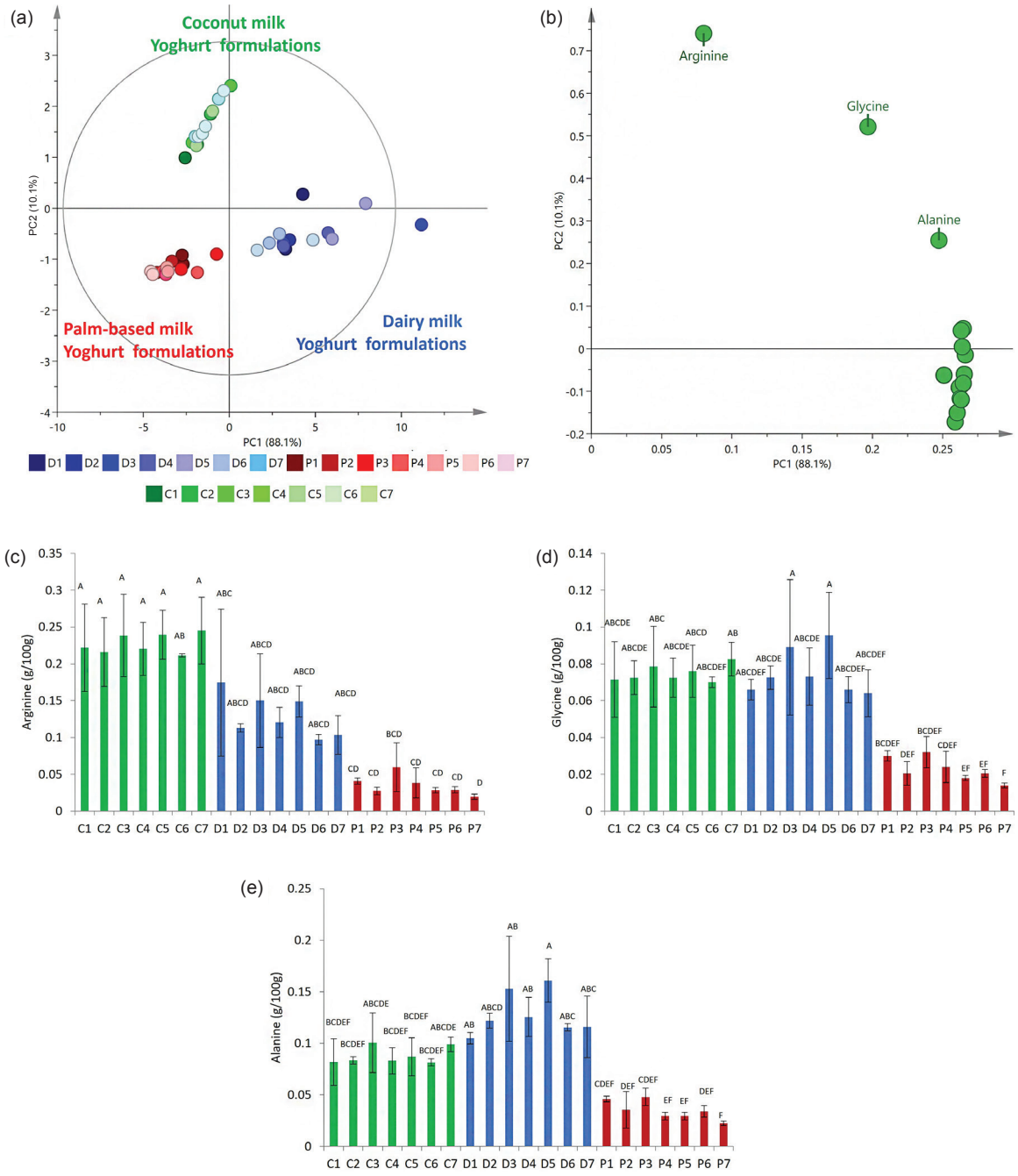


Figure 5. (a) PCA score and, (b) loading plot of amino acid analysis in all yoghurt samples. Bar graphs show selected amino acid of (c) arginine, (d) glycine and (e) alanine. Different letters between the bar graph denotes significant differences ($p<0.05$) *via Tukey's test.*

of yoghurt were different based on the separation along both PC1 and PC2. The dairy yoghurts were positioned on the positive axis of PC1 while both coconut milk yoghurts and palm-based milk yoghurts were positioned on the negative axis of PC1. The axis PC2 separates the coconut milk yoghurts and palm-based milk yoghurts. The yoghurt samples of the same base substrate (dairy, coconut milk or palm-based milk) had similar amino acid profiles. This is shown when the formulations of the same base substrate were clustered together.

Based on the loading plot (*Figure 5b*), the majority of the detected amino acids were positioned on the positive axis of PC1. This indicates that dairy yoghurts have the highest intensity for these amino acids. Only arginine, glycine and alanine were positioned separately from the clusters of amino acids at the positive axis of PC1. The reason for deviation from the majority amino acid cluster can be seen in the bar graph (*Figure 5c-e*). Arginine (*Figure 5c*) content in the majority of coconut milk yoghurt formulations was found to be significantly

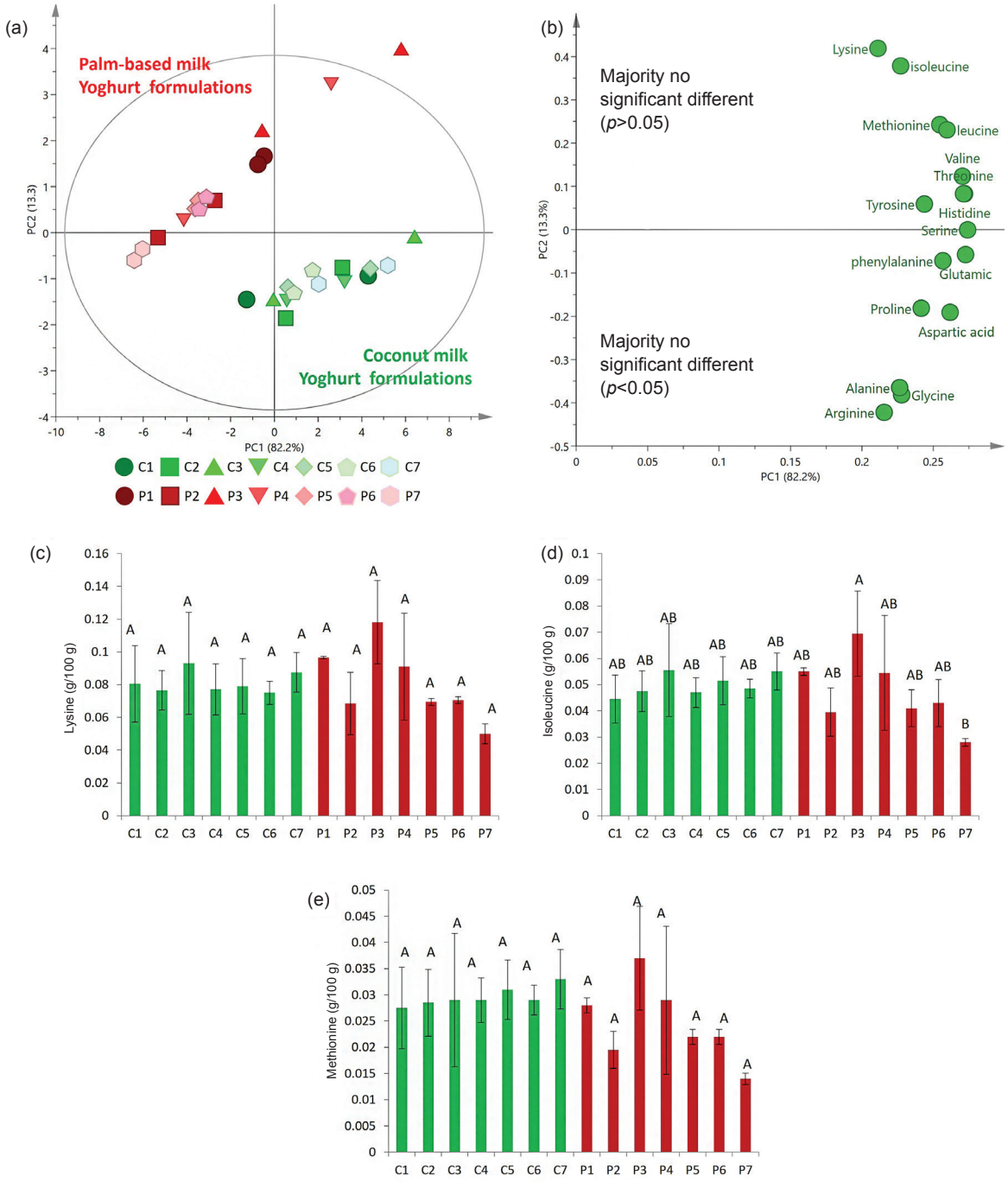


Figure 6. (a) PCA score and, (b) loading plot of amino acid analysis of non-dairy yoghurt samples in this study. Bar graphs show selected amino acid of (c) lysine, (d) isoleucine and (e) methionine. Different letters between the bar graph denotes significant differences (p<*0.05) via Tukey's test.*

higher (p<0.05) than the dairy yoghurts. This result can be expected since coconut had been found to have higher arginine content (Nandanie, 1996; Salil *et al.*, 2011). However, this study is among the first to report this observation in a fermented coconut milk product. Both glycine (*Figure 5d*) and alanine (*Figure 5e*) in the majority of coconut milk yoghurts were found to be not significant (p>0.05) with the majority of dairy yoghurt formulations.

To observe the comparison of amino acid content between non-dairy yoghurts, the PCA of coconut milk yoghurts and palm-based milk yoghurts were plotted (*Figure 6*). The score plot shows that there is a separation between clusters of coconut milk yoghurts and clusters of palm-based milk yoghurts along PC1 and PC2 (*Figure 6a*). The separation between the clusters showed that there are differences in amino acid profiles for both types of yoghurts.

The loading plot (*Figure 6b*) shows that the amino acids were positioned on the positive side of the PC1 axis and spread throughout the PC2 axis. Amino acids on the positive side of the PC2 axis were found to be amino acids that are not significantly different ($p>0.05$) between the majority of palm-based milk and coconut milk yoghurt formulations. This is shown in the bar graph of lysine (*Figure 6c*), isoleucine (*Figure 6d*) and methionine (*Figure 6e*). Alternatively, amino acids on the negative axis of PC2 were found to be significantly higher ($p<0.05$) in coconut milk yoghurts. This can be seen in the bar graph of arginine (*Figure 5c*), glycine (*Figure 5d*) and alanine (*Figure 5e*). From the result, dairy yoghurts contain the highest intensity for the majority of amino acids except for arginine. Although palm-based yoghurts were found to be the least favourable in terms of amino acid intensity profile, half of the amino acids in palm-based milk yoghurts were comparable to coconut milk yoghurt's amino acid profile.

Suggestions for Palm-based Milk Yoghurt Improvement

Based on the United States Food and Drug Agency regulation for yoghurt, the majority of the palm-based milk yoghurt formulations can be

TABLE 2. PROXIMATE AND AMINO ACID ANALYSIS OF PALM-BASED MILK YOGHURT RECOMMENDED FORMULATION

Analysis	Formulation		
	P1	P2	P3
Protein (g/100 g)	2.371 ± 0.297	2.346 ± 0.233	2.237 ± 0.136
Lipid (g/100 g)	30.093 ± 0.632	31.624 ± 0.464	30.179 ± 0.882
Carbohydrate (g/100 g)	47.371 ± 0.846	46.212 ± 0.586	46.698 ± 1.027
Fibre (g/100 g)	0.205 ± 0.021	0.264 ± 0.036	0.331 ± 0.003
Ash (g/100 g)	6.133 ± 0.208	5.933 ± 0.153	6.233 ± 0.208
Moisture (g/100 g)	14.032 ± 0.153	13.884 ± 0.188	14.653 ± 0.185
Viscosity (Pa.s)	0.420 ± 0.090	0.530 ± 0.010	0.530 ± 0.020
Syneresis (%)	38.800 ± 0.720	50.970 ± 1.950	46.470 ± 0.500
pH	5.310 ± 0.010	5.080 ± 0.020	4.980 ± 0.030
Aspartic acid (g/100 g)	0.096 ± 0.004	0.064 ± 0.016	0.105 ± 0.023
Serine (g/100 g)	0.063 ± 0.005	0.044 ± 0.011	0.084 ± 0.023
Glutamic (g/100 g)	0.225 ± 0.023	0.167 ± 0.045	0.311 ± 0.074
Glycine (g/100 g)	0.030 ± 0.003	0.021 ± 0.006	0.032 ± 0.008
Histidine (g/100 g)	0.028 ± 0.002	0.020 ± 0.004	0.041 ± 0.012
Arginine (g/100 g)	0.041 ± 0.004	0.028 ± 0.005	0.059 ± 0.033
Threonine (g/100 g)	0.051 ± 0.001	0.034 ± 0.009	0.06 ± 0.013
Alanine (g/100 g)	0.046 ± 0.003	0.036 ± 0.018	0.048 ± 0.008
Proline (g/100 g)	0.104 ± 0.013	0.079 ± 0.015	0.116 ± 0.083
Tyrosine (g/100 g)	0.036 ± 0.009	0.027 ± 0.008	0.051 ± 0.037
Valine (g/100 g)	0.071 ± 0.007	0.052 ± 0.011	0.093 ± 0.026
Methionine (g/100 g)	0.028 ± 0.001	0.019 ± 0.004	0.037 ± 0.01
Lysine (g/100 g)	0.097 ± 0.001	0.069 ± 0.019	0.118 ± 0.025
Isoleucine (g/100 g)	0.055 ± 0.001	0.040 ± 0.009	0.070 ± 0.016
Leucine (g/100 g)	0.096 ± 0.003	0.069 ± 0.016	0.130 ± 0.038
Phenylalanine (g/100 g)	0.052 ± 0.002	0.038 ± 0.007	0.072 ± 0.023

Note: Mean ± standard deviation; P1 - *Lactobacillus acidophilus*; P2 - *L. delbrueckii* sbsp. *bulgaricus*; P3 - *Streptococcus thermophiles.*

defined as yoghurt. This is because the regulation requires the yoghurt before additional ingredients are added to contain lipids not less than 3.25% and a pH of 4.6 or lower (U.S. Food and Drug Administration, 2022). This can be considered acceptable unless a new ruling regarding the origin of the milk or non-dairy yoghurt will be enacted in the future. However, extensive modifications will be needed to improve the quality of yoghurt.

The proximate contents of palm-based milk yoghurts are lacking when compared to both dairy milk yoghurt and coconut milk yoghurts. The reason for lacking in proximate content is due to the deficiency within the base material itself. From comparison of ash content between non-dairy yoghurts, coconut milk yoghurts had higher ash content than palm-based milk yoghurts. This is because coconut milk itself had higher mineral contents (Santos *et al.*, 2014) and more variety of vitamins (Vitamin A, D and E) (Drewnowski, 2021) than palm oil, which contain lower intensity of mineral content (Li, 2020) and vitamin E (Gapor, 1990). Based on the proximate analysis, starter culture formulations do not affect carbohydrate and ash content. Among the seven formulations, single starter culture formulations (P1-P3) were among the recommended due to these formulations had high protein and fibre content. If palm-based milk yoghurt were to be developed into an energy-dense yoghurt, then formulation with *L. delbrueckii* sbsp. *bulgaricus* (P2) will be the recommended starter culture.

Since palm-based milk yoghurt had a low amino acid intensity profile, it should not be marketed to be comparable to the level of dairy yoghurt. This is because palm-based milk yoghurt is a non-dairy yoghurt, and the majority of its amino acid intensity was similar to coconut milk yoghurt, another alternative to dairy yoghurt. As such, it is highly recommended that palm-based milk yoghurt be fortified with other nutrients or enriched with amino acids for it to be on par with coconut milk yoghurts. *Table 2* shows the average and standard deviation of each analysis for the recommended formulation (P1 to P3).

Sensory evaluation was not conducted at this stage because palm-based milk yoghurts are very different from the dairy yoghurts and coconut milk yoghurts. This can be seen from the viscosity of the yoghurts themselves, in which the viscosity of the palm-based milk yoghurts are lesser than 1 Pa.s and significantly lesser than both dairy yoghurts and coconut milk yoghurts [both types has more viscosity (>1 Pa.s)]. As such, sensory evaluation for the three types of yoghurt formulation was not perform because sensory evaluation between similar type of food samples that have clear physical differences between them will have apparent bias among the panelist and influence the final result (Kemisola and Olaide, 2021). To improve the textural quality of the palm-based yoghurt, it is recommended that a suitable emulsifier be added to mitigate the low viscosity and high syneresis.

Based on these preliminary analyses and suggestions for improvement, palm-based milk yoghurt is feasible to be developed into a new food product. Successful development of the palm-based milk yoghurt into the market will be a contribution toward sustainable food production by the Malaysian palm oil industry. Since palm-based milk yoghurt utilised local derivative palm oil by-product, this will also contribute toward United Nation's SDG, specifically Goal 2 and 9 of the SDG.

CONCLUSION

This is the first study to report the effect of various starter culture formulations in the development of palm-based milk yoghurt against dairy yoghurt and coconut milk yoghurt in terms of proximate analysis, texture quality and amino acid intensity. Based on the result, palm-based milk yoghurt has the highest lipid content among the three types of yoghurt. However, it is lacking in protein, ash, carbohydrate, fibre contents, viscosity, and high rate of syneresis when compared to the other yoghurt types in this study. The majority of palm-based milk yoghurt's amino acid profiles were comparable to coconut milk yoghurt's amino acid profile. Suggestions for improvement of palm-based milk yoghurt quality include adding a suitable emulsifier to mitigate low viscosity and high rate of syneresis and fortifying the yoghurt with a new nutrient or enriching the amino acids. Successful development of palm-based milk yoghurt into the market is an effort contributing toward the production of new food product using unconventional resources.

REFERENCES

BeMiller, J N (2010). Carbohydrate analysis. *Food Analysis.* Boston, MA, Springer US.

Chang, S K C (2010). Protein analysis. *Food Analysis.* Boston, MA, Springer US.

Charalampopoulos, D; Wang, R; Pandiella, S and Webb, C (2002). Application of cereals and cereal components in functional foods: A review. *Int. J. Food Microbiol., 79*: 131-141.

Coda, R; Lanera, A; Trani, A; Gobbetti, M and Di Cagno, R (2012). Yogurt-like beverages made of a mixture of cereals, soy and grape must: Microbiology,

texture, nutritional and sensory properties. *Int. J. Food Microbiol., 155*: 120-127. DOI: 10.1016/j.ijfoodmicro.2012.01.016.

Dahlan, H A and Sani, N A (2017). The interaction effect of mixing starter cultures on homemade natural yogurt's pH and viscosity. *Int. J. Food Stud., 6*.

Dahlan, H A; Sani, N A and Dahlan, I (2017). Logistic-like growth model of *Lactobacillus acidophilus*, *Lactobacillus delbrueckii* subsp. *bulgaricus* and *Streptococcus thermophilus* in Palm Oil *Santan*. *Japan J. Food Eng., 18*: 155-159. DOI: 10.11301/jsfe.16474.

Drewnowski, A (2021). Plant-based milk alternatives in the USDA branded food products database would benefit from nutrient density standards. *Nat. Food, 2*: 567-569. DOI: s43016-021-00334-5.

Gapor, A (1990). Content of vitamin E in palm oil and its antioxidant activity. *Palm Oil Dev., 12*: 25-27.

Granato, D; Santos, J S; Escher, G B; Ferreira, B L and Maggio, R M (2018). Use of principal component analysis (PCA) and hierarchical cluster analysis (HCA) for multivariate association between bioactive compounds and functional properties in foods: A critical perspective. *Trends Food Sci. Technol., 72*: 83-90. DOI: 10.1016/j.tifs.2017.12.006.

Hanafiah, K M; Mutalib, A H A; Miard, P; Goh, C S; Sah, S A M and Ruppert, N (2022). Impact of Malaysian palm oil on sustainable development goals: Co-benefits and trade-offs across mitigation strategies. *Sustain. Sci., 17*: 1639-1661. DOI: 10.1007/s11625-021-01052-4.

Kemisola, A and Olaide, A (2021). Understanding sensory evaluation of food (*Oluwatosin Ademola, I ed.). Food Science and Technology.* Berlin, Boston: De Gruyter.

Kumar, B V; Vijayendra, S V N and Reddy, O V S (2015). Trends in dairy and non-dairy probiotic products - A review. *J. Food Sci. Technol.*, *52(10)*: 6112-6124.

Li, S (2020). Analysis of trace elements in palm oil using ICP-OES. *Agilent Application Brief.* Agilent Technologies, Inc. USA.

Loveday, S M; Sarkar, A and Singh, H (2013). Innovative yoghurts: Novel processing technologies for improving acid milk gel texture. *Trends Food Sci. Technol., 33*: 5-20. DOI: 10.1016/j.tifs.2013.06.007.

Marshall, M R (2010). Ash analysis. *Food Analysis.* Springer US. Boston, USA.

Mauro, C S I and Garcia, S (2019). Coconut milk beverage fermented by *Lactobacillus reuteri*: Optimization process and stability during refrigerated storage. *J. Food Sci. Technol., 56*: 854-864. DOI: 10.1007/s13197-018-3545-8.

McSweeney, P L and Sousa, M J (2000). Biochemical pathways for the production of flavour compounds in cheeses during ripening: A review. *Le Lait, 80*: 293-324.

Min, D B and Ellefson, W C (2010). Fat analysis. *Food Analysis.* Boston, MA, Springer US.

Morell, P; Piqueras-Fiszman, B; Hernando, I and Fiszman, S (2015). How is an ideal satiating yogurt described? A case study with added-protein yogurts. *Food Res. Int., 78*: 141-147. DOI: 10.1016/j.foodres.2015.10.024.

Nancy Astephen (1993). *WatersAccQ.Tag Method for Hydrolysate Amino Acid Analysis*. 1st edition. Milford USA: Milipore Corporation.

Nandanie, D E (1996). King coconut. *CORD, 12(2)*: 34. DOI: 10.37833/cord.v12i02.304.

Ozcan, T; Horne, D S and Lucey, J A (2015). Yogurt made from milk heated at different pH values. *J. Dairy Sci., 98*: 6749-6758. DOI: 10.3168/jds.2015-9643.

Rafidah, A H; Zaida, Z; Nur, I and Miskandar, M S (2013). A comparative study of the effects of processing conditions and formulations on the physical and sensory properties of frozen nasi lemak made of palm-based santan and coconut santan. *J. Oil Palm Res., 25*: 170-179.

Sadler, G D and Murphy, P A (2010). pH and titratable acidity. *Food Analysis.* Springer US. Boston, USA.

Salil, G; Nevin, K G and Rajamohan, T (2011). Arginine rich coconut kernel protein modulates diabetes in alloxan treated rats. *Chem. Biol. Interact., 189*: 107-111. DOI: 10.1016/j.cbi.2010.10.015.

Santos, D C M B; Carvalho, L S B; Lima, D C; Leão, D J; Teixeira, L S G and Korn, M G A (2014). Determination of micronutrient minerals in coconut milk by ICP OES after ultrasound-assisted extraction procedure. *J. Food Composit. Anal., 34*: 75-80. DOI: 10.1016/j.jfca.2014.02.008.

Smit, G; Smit, B A and Engels, W J (2005). Flavour formation by lactic acid bacteria and biochemical

flavour profiling of cheese products. *FEMS Microbiol. Rev., 29*: 591-610.

U.S. Food and Drug Administration (2022). Sec. 131.200 Yogurt. *Code of Federal Regulations Title 21*. USA.

United Nations (2015a). *The 17 Goals*. New York, United States: United Nations. https://sdgs.un.org/goals, accessed on 30 October 2022.

United Nations (2015b). (Goal 2 - End hunger, achieve food security and improved nutrition and promote sustainable agriculture.) https://www.un.org/sustainabledevelopment/hunger/, accessed on 27 October 2022.

United Nations (2015c). *Goal 9* - Build resilient infrastructure, promote inclusive and sustainable industrialization and foster innovation. https://www.un.org/sustainabledevelopment/infrastructure-industrialization/, accessed on 27 October 2022.

Walstra, P; Noomen, A and Geurts, T (1993). Ducth-type varieties. *Cheese: Chemistry, physics and microbiology* (Fox, P ed.). Chapman and Hall. London. p. 39-82.

Wardhani, R and Rahadian, Y (2021). Sustainability strategy of Indonesian and Malaysian palm oil industry: A qualitative analysis. *Sustain. Account. Manag. and Policy J., 12*: 1077-1107. DOI: 10.1108/SAMPJ-07-2020-0259.

Yaakob, H; Ahmed, N R; Daud, S K; Malek, R A and Rahman, R A (2012). Optimization of ingredient and processing levels for the production of coconut yogurt using response surface methodology. *Food Sci. Biotechnol., 21*: 933-940.

Zainal, Z; Yusoff, M S A; Habi, N L; Omar, M N and Salam, B A (1997). Production and caharacterization of palm-based santan powder. *PORIM Information Series,* PORIM TT No. 45.

Journal of Oil Palm Research Vol. 36 (3) September 2024 p. 524-533
DOI: https://doi.org/10.21894/jopr.2023.0038

N-ALKANE PROFILES OF LARD AND VEGETABLE OILS, AND THEIR CHEMOMETRICS DIFFERENTIATION

NUR AIN SYAQIRAH SAPIAN[1,2]; MUHAMAD AIDILFITRI MOHAMAD ROSLAN[1,2,3]; AMALIA MOHD HASHIM[1,4]; YANTY NOORZIANNA ABDUL MANAF[5]; MOHD NASIR MOHD DESA[1]; MURNI HALIM[2]; MUHAMAD SHIRWAN ABDULLAH SANI[6]; MOHD TERMIZI YUSOF[4]; MOHD SABRI PAK DEK[7] and HELMI WASOH[1,2]*

ABSTRACT

This research aims to examine fat from various vegetable oils using n-alkane profiles, as well as chemometrics and machine learning. Unsaponifiable vegetable oils (coconut, peanut, palm and soybean oils) were separated and analysed using gas chromatography-mass spectrometry (GC-MS) to investigate the n-alkane profiles of each fat. The authenticity of the detected n-alkane profiles was determined by comparing to the retention time of C_7-C_{40} n-alkane standards. The test designs were developed using Principal Component Analysis (PCA), Hierarchical Clustering Analysis (HCA), Partial Least Squares-Discriminant Analysis (PLS-DA), and Random Forest (RF). Both PCA and HCA appeared to provide a clear distinction between each of the vegetable oil tests. Based on the PLS-DA and RF determination, tetracosane (C_{24}) and octadecane (C_{18}) are proposed as the key n-alkane markers for separating lard from vegetable oils. These findings suggest that additional work may be required to achieve and determine the different characteristics across oils in numerous statistical applications, notably chemometrics and machine learning.

Keywords: chemometrics, lard, n-alkane, principal component analysis, random forest.

Received: 1 January 2023**; Accepted:** 5 July 2023**; Published online:** 22 August 2023.

[1] Halal Products Research Institute, Universiti Putra Malaysia, 43400 UPM Serdang, Selangor, Malaysia.

[2] Department of Bioprocess Technology, Faculty of Biotechnology and Biomolecular Sciences, Universiti Putra Malaysia, 43400 UPM Serdang, Selangor, Malaysia.

[3] Institute of Systems Biology (INBIOSIS), Universiti Kebangsaan Malaysia, 43600 UKM Bangi, Selangor, Malaysia.

[4] Department of Microbiology, Faculty of Biotechnology and Biomolecular Sciences, Universiti Putra Malaysia, 43400 UPM Serdang, Selangor, Malaysia.

[5] Halal Research Group, Faculty of Food Science and Nutrition, Universiti Malaysia Sabah, Jalan UMS, 88400 Kota Kinabalu, Sabah, Malaysia.

[6] International Institute for Halal Research and Training, International Islamic University Malaysia, 53100 Kuala Lumpur, Malaysia.

[7] Department of Food Science, Faculty of Food Science and Technology, Universiti Putra Malaysia, 43400 UPM Serdang, Selangor, Malaysia.

* *Corresponding author e-mail: helmi_wmi@upm.edu.my*

INTRODUCTION

Lard is one of the cheapest semisolid fats widely used in food production to give food a rich flavour and creamy texture. Due to this reason, it has been subjected as a potential source for adulteration to other fats and oils. Since the use of lard and its by-products are prohibitive under the Kosher and Halal regulations (Al-Kahtani *et al.*, 2017), it is important to explore techniques for clear discrimination between lard and other permissible ingredients (Azir *et al.*, 2017). Each fat and oil exhibit specific components and their presence should be considered as an important detection tool. Mainly, fats and oils are composed of triglycerides (TAGs), while the remaining consists of minor components such as hydrocarbons, fatty acids (FAs), natural compounds, unsaponifiable and polar lipids (Ferreira *et al.*, 2021).

Hydrocarbons can be found in the unsaponifiable fraction and they are the least polar compounds, made up of only carbon (C) and hydrogen (H) (Giuffrè and Capocasale, 2016).

Single-chain hydrocarbons are known as normal alkanes (n-alkanes), with the formula C_nH_{2n+2} (Zenkevich, 2006). To date, several methods are employed to detect lard adulterants such as electronic nose, polymerase chain reaction (PCR), Fourier transform infrared spectroscopy (FTIR) (Salleh *et al.*, 2018), differential scanning calorimetry and other different chromatographic-based techniques (such as HPLC, GLC, LC-MS, GC-FID and GC-TOF-MS) (Azir *et al.*, 2017). The HPLC and GC-based detection techniques could, however, become more difficult if the TAG or FAs composition of the adulterant exhibit close similarity to that of the tested oils. Several analytical approaches have been developed to analyse the n-alkane quantitatively (Troya *et al.*, 2015). Previous research reported that the n-alkane composition could potentially be used to discriminate against a group of vegetable oils (Mihailova *et al.*, 2015; Troya *et al.*, 2015). Quantitative data considering the whole n-alkanes profile might serve better as a characteristic 'fingerprint' of the oil. If such profiles are to be used to study the effect caused by the adulteration, powerful statistical methods to deal with the multivariate data are recommended (Yousefinejad *et al.*, 2018) to consider the differences taking place in the whole chromatogram. It has now been realised that the qualitative analysis using mainly single-component species may be inadequate (Sharin *et al.*, 2021).

The objective of PCA and PLS-DA is to achieve a linear transformation that converts data to a very low dimensional condition with an error as minimum as possible. For PCA, in its first principal component (PC), the transformation preserves as much variance as possible, however, PLS-DA preserves as much covariance as possible between the original and labelling data. Both can be described as iterative processes as the rest of the variance and error are preserved to define the next PC (Ruiz-Perez *et al.*, 2020). Besides its use for dimensionality reduction, it can be adapted to be used for feature selection (Christin *et al.*, 2013) as well as for classification (Botella *et al.*, 2009). Yousefinejad *et al.* (2018) reported that the m-dimensional space of a matrix D (from the PCA result) can be reduced to a significantly lower-dimensional space of principal components (PCs): D = TP' + E. Where, T is the score matrix (containing PCs in the direction of the samples), P is the loading matrix (carrying in the direction of the wavenumbers) and E is the residual matrix. The superscript (') denotes the matrix transpose. The calculated PCs represent the compressed information, demonstrating the fine difference in the instrumental signal relating to various samples for discrimination purposes. PLS-DA can be assumed as a "supervised" version of PCA in the sense that it achieves dimensionality reduction but with full awareness of the class labels (Ruiz-Perez *et al.*, 2020). Previously, PCA and PLS-DA were successfully used for the blood-volatile organic compound in an animal study (Ataabadi *et al.*, 2023) and the solvent-electrochemical interactions of anthraquinones (Aq) in different organic media (Yousefinejad *et al.*, 2019).

The PLS-DA showed a good performance in the calibration step (Yousefinejad *et al.*, 2018) as a further consideration for classification. The other multivariate techniques such as hierarchical cluster analysis (HCA) can be further applied due to their high sensitivity. Variable Importance in Projection (VIP) scores estimate the importance of each variable in the projection used in the PLS model. In any proposed model, a variable with VIP Score close to one can be considered important. Variables with a score of less than one can be considered as less important and potential for exclusion (Chong and Jun, 2005). In PLSDA**,** Cocchi *et al.* (2018) introduced a filter method which is independent of the modelling step and does not require additional validation nor increase the adjustable model parameters (by referring to the VIP variables ranking). If R^2 and Q^2 are acceptable and the model is interpretable, thus, the suggested model can be improved by deleting unimportant terms, such as the variables with low VIP values. Thereafter a final model is developed, interpreted and thus, better predictions can be concluded (Wold *et al.*, 2001). In this case, less complex statistical applications can be applied due to the advantage to exclude unimportant items (Cocchi *et al.*, 2018). Therefore, this criterion is reasonable with good potential to discard irrelevant variables. To date there is no report has been published on the application of GC-MS in combination with multivariate analysis. Therefore, sophisticated methods need to be given due consideration and the present study aimed at developing an advanced and effective methodology for the study of lard adulteration by using the GC-MS. As such, the objective was coupled with multivariate data analysis, as a means for distinguishing lard from other vegetable oils.

MATERIALS AND METHODS

Reagents

Chemicals for column chromatography *i.e.*, potassium hydroxide, methanol, ethanol, anhydrous sodium sulphate, silica gel 60 and n-hexane were purchased from Merck (Germany). Saturated alkanes standard of C_7-C_{40} (1000 µg/mL, in hexane) for every component were purchased from Supelco (Bellefonte, PA, USA). All the reagents were of analytical grade.

Sample Preparation

Lard and vegetable oils including coconut, peanut and soybean oils were obtained from the Laboratory of Halal Science Research (Halal Products Research Institute, Universiti Putra Malaysia), while palm oil was obtained from the Malaysian Palm Oil Board (MPOB). Lard was made by rendering pig adipose tissue at 100ºC for 2 hr. To remove contaminants, the oils were filtered using a muslin cloth and then stored at -20ºC until use.

Extraction of Unsaponifiable Fraction

The n-alkane fractions of vegetable oils were created with slight adjustments according to Troya *et al.* (2015). The standard saponification process was used to extract the unsaponifiable fraction of each fat. The preferred fat samples (5 g) were saponified using a reflux condenser and heating mantle for 20 min at 70ºC with an ethanolic potassium hydroxide solution (10%, 19 mL). The solution was allowed to cool before being added to a separating funnel with 25 mL of distilled water. Using 25 mL of n-hexane, the non-saponifiable materials were extracted twice. The hexane extracts were mixed and added to a new separating funnel, which were then washed three times with an ethanol-water mixture in a similar ratio (12.5 mL). The extracts were dried over an anhydrous sodium sulphate and evaporated at 30ºC under vacuum using a rotary evaporator (EYELA, Japan). For separation, the residues were dissolved in 2 mL n-hexane.

Separation procedure using solvents and column chromatography was used to separate the hydrocarbon fraction and impurities from the unsaponifiable materials obtained. The stationary phase was created using a silica gel-filled glass column with an internal diameter of 1.5 cm and a length of 40.0 cm (15 g in n-hexane). A chromatographic elution technique was used with 40 mL of n-hexane as the mobile phase, and the eluate (20 mL) was regarded as an n-alkane fraction and subjected to further investigation. The eluate was evaporated under vacuum in a rotary evaporator (EYELA, Japan) at 30ºC to remove the solvent. The resulting sample was immediately diluted in 0.5 mL of n-hexane and stored in a chiller at 4ºC prior further analysis with gas chromatography-mass spectrometry (GC-MS).

Gas Chromatography-Mass Spectrometry Analysis

The n-alkane composition of lard and other animal fats was analysed using the Agilent 7890A gas chromatography paired with the Agilent 5975C mass spectrometry detector in a selected ion monitoring (SIM) mode (Agilent, USA). The HP-5MS (30 m × 0.25 μm × i.d., 0.25 μm film thickness) was used as the analytical capillary column. The oven temperature was set to 35ºC for 2 min, then increased to 250ºC (10º/min), and eventually to 300ºC for 23 min (20º/min). The detector temperature was 300ºC. The MS interface was kept at a constant temperature of 300ºC. The injection volume was 1 μL and operated in the split mode (at a split ratio of 1:10). Helium was used as the carrier gas at a flow rate of 1 mL/min. The compounds were identified by comparing the data with NIST 11 mass spectral library and C_7-C_{40} saturated alkanes standard (supplied by Supelco, Bellefonte, PA, USA). The composition of each identified n-alkane was determined by calculating the peak area of each alkane to the total peak area of all alkanes in the sample (Hassan *et al.*, 2010).

Chemometric Analysis and Machine Learning

Data analysis was performed using statistical online software packages; MetaboAnalyst 5.0 (Parasitology Building, 21111 Lakeshore Road Ste. McGill University, Anne de Bellevue, QC, Canada; http://www.metaboanalyst.ca) software. A total of 12 samples were analysed in triplicates. Prior to chemometric analysis, data were pre-tested using Kruskal-Wallis *post-hoc* test at $p<0.05$ to determine the significant differences in the means of peak area of each fat sample (Chong *et al.*, 2019). The data matrix was then normalised to a constant sum and scaled by Pareto scaling to modify the variance of spectral data so that the peaks are equally weighted in order to build multivariate models (Höjer Holmgren *et al.*, 2018). Clustering of oils' n-alkanes was accomplished using unsupervised methods, PCA and Hierarchical Clustering Analysis (HCA). Supervised approaches were used to classify oil samples, including the partial least squares-discriminant analysis (PLS-DA) and the Random Forest (RF) of the machine learning algorithm. The performance of the PLS-DA model was evaluated using a 10-fold cross-validation (Van Ruth *et al.*, 2010).

During the initial stage, it is unclear which value of the diagnostic statistics was really corresponding to discrimination between groups (Westerhuis *et al.*, 2008). Permutation tests assumed that there is no difference between two random groups (Westerhuis *et al.*, 2008). Furthermore, the labels of all samples were randomly permuted followed by the calculation of a new classification model (Lindgren *et al.*, 1996). By repeating the procedure N times, a null distribution of H_0 was obtained (Preece, 1990). The significance of the PLS-DA model was then assessed by relating the values of the calculated model to the H_0 distribution of the permuted data sets. From these classifications, H_0 distributions for Q^2 and regression coefficients and others were obtained. As the groups were formed in a random way, therefore, no difference between group was used as an assumption.

PLS-DA classifies lard from other animal fats by highlighting the important variables in term of VIP scores, and according to Cocchi *et al.* (2018) the score can be potentially applied especially for variable selection**.** The RF classification was performed using Metaboanalyst 5.0 software, and the model's performance was confirmed by using the RF package in the RStudio. In this study, the normalised data were randomly divided between training (90%) and test (10%) groups. A confusion matrix was generated to determine the RF model's prediction accuracy.

RESULTS AND DISCUSSION

Profiles of n-Alkane

The n-alkane fractions of lard and all tested vegetable oils were subjected to GC-MS analysis to determine their individual composition. A total of 17 n-alkanes ranging from C_8 to C_{27} were identified (*Figure 1*).

Some vegetable oils showed a similar pattern of n-alkane composition, where alkanes with chain lengths of C_{12}, C_{14}, C_{15} and C_{16} were the most abundant, except for peanut oil (C_{10}, C_{12}, C_{14} and C_{15}). For coconut, palm and soybean oils, the C_{14} was found with the highest abundance, composed of 21.46%, 19.78% and 21.06%, respectively. Meanwhile, for peanut oil, C_{12} was the most significant, with 23.49% of the total composition. Compared to lard, the most predominant alkanes are C_{24}, followed by C_{16}, C_{15}, C_{14} and C_{18}, composed of 15.72%, 14.84%, 14.05%, 13.60% and 9.94%, respectively. Among the long chain alkanes (C_{14}-C_{18}), the C_{18} (9.94%) contributed to the highest increase (0.44-fold) when compared to the nearest competitor (palm oil, 5.58%). The C_{16} and C_{15} only contributed to 0.18 and 0.15-fold, respectively (compared to the nearest competitor). The n-alkane C_{24} (15.72%) was notable for lard since this alkane was absent (or present at low percentage) in coconut, palm, peanut and soybean oils.

Clustering Analysis of Lard and Vegetable Oils

Only 14 significant n-alkanes (p<0.05) were chosen from the 17 discovered (*Figure 2a*). The clustering of lard from vegetable oils was done using unsupervised PCA and HCA methods. PCA is the most often used unsupervised technique in the chemometrics research, and it analyses the pattern identification by using the correlation between the examined data (Ruiz-Perez *et al.*, 2020). PCA score plot of lard and vegetable oil samples (coconut, palm, peanut and soybean oils) involving the first (PC1) and second (PC2) components, with 83.0% variations were explained. PC1 explained 68.5% of the variance, while PC2 explained 14.5% of the variance.

Figure 2b shows the PCA biplot of the samples as a combination of the score plot and loading plot. Variables with weights (loading) close to 1 or -1 have a strong influence on sample clustering (Azizan *et al.*, 2021), while those with almost no weight have a minor impact (Schaettler *et al.*, 2022). Based on the PCA biplot, C_{24} had a positive contribution towards lard clustering with the loading of -0.27277 and -0.48868 toward PC1 and PC2, respectively. The alkanes that contributed to the clustering of all vegetable oils at a positive score of PC2 are C_{10}, C_{12}, C_{14} and C_{15}. The influence of the variables in the biplot was supported in the heatmap of HCA (*Figure 2c*).

Consistent with the PCA result, HCA also clustered the samples into two groups, *i.e.*, lard and vegetable oils (coconut, palm, peanut and soybean oils). This clustering result was achieved through the combination of Euclidean distance measure and Ward's linkage algorithm. Based on the heatmap,

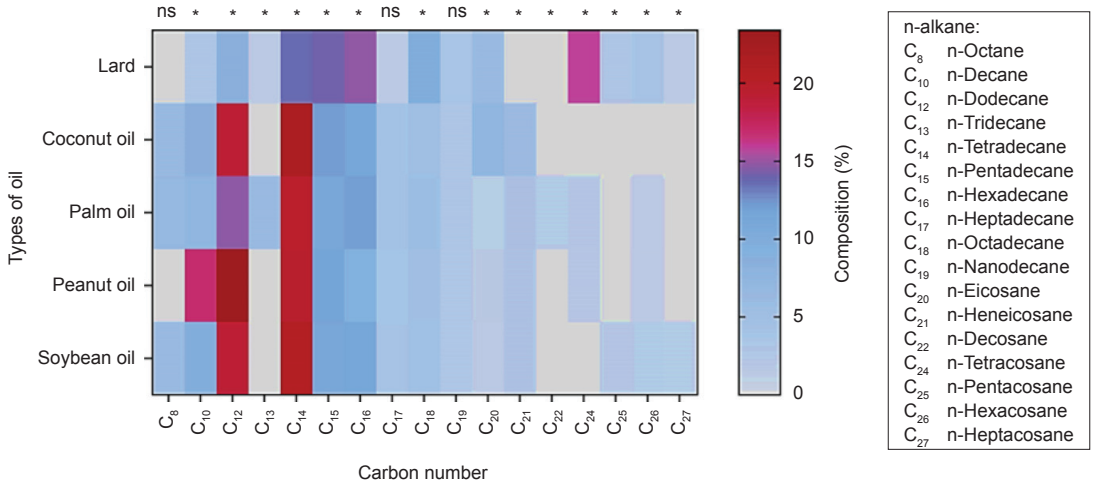
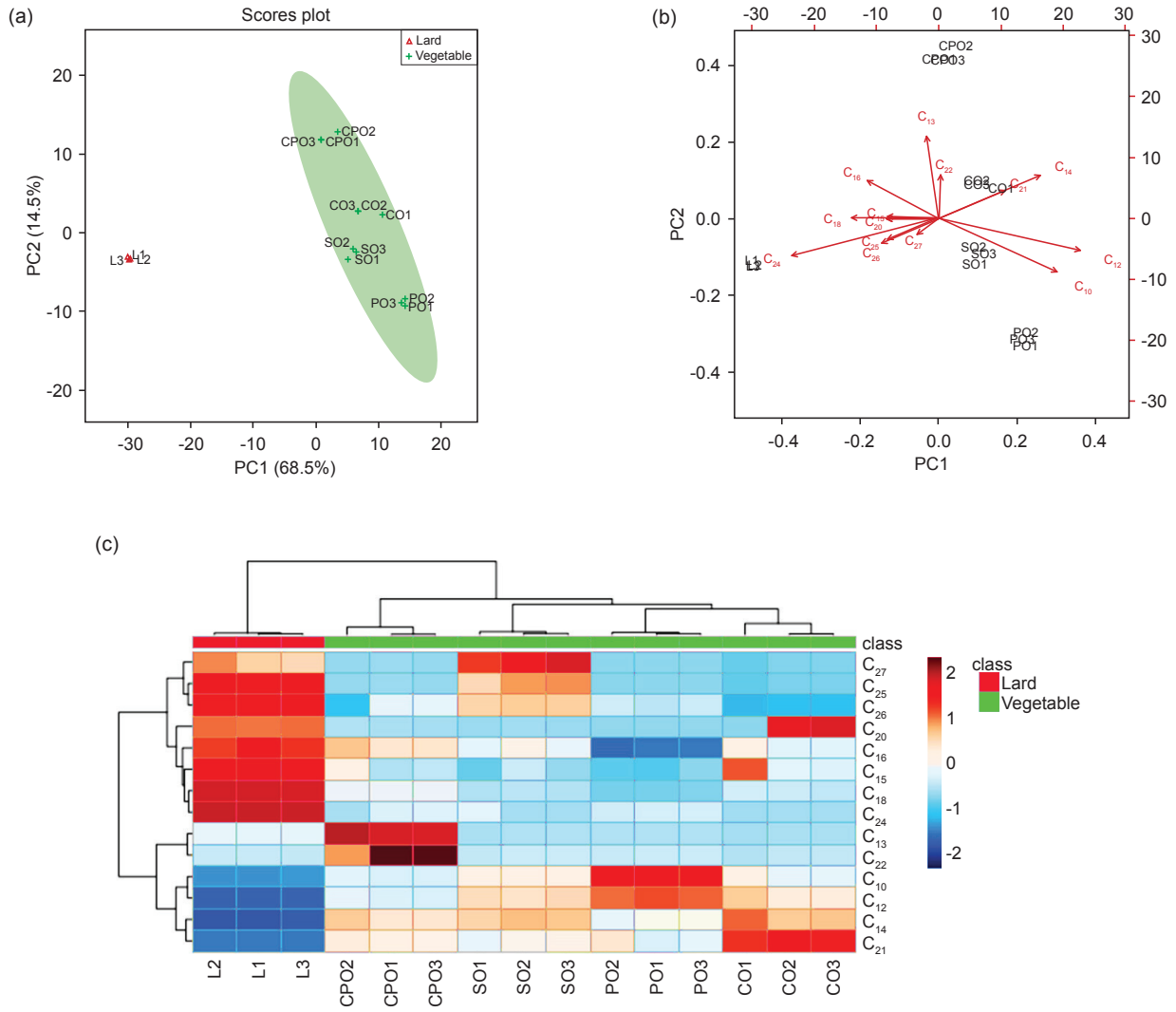


*Figure 1. Heatmap of n-alkane composition (%) of lard and vegetable oils supported by Kruskal-Wallis Test; * - significant difference* (p<*0.05); ns - non-significant difference* (p>*0.05).*



Note: CO - coconut oil; CPO - palm oil; PO - peanut oil; SO - soybean oil.

Figure 2. (a) PCA score plot, (b) PCA biplot, and (c) dendrogram heatmap of lard and other vegetable oils based on 14 significant n-alkanes profile.

all vegetable oil samples were grouped together in a cluster but separated distinctly into 4 sub-clusters based on the type of oils. The heatmap presents individual values contained in a matrix in the form of colours (Zhao *et al.*, 2014). The correlation of C_{18} and C_{24} was detected in high levels in lard but absent in the vegetable oil samples. The distribution of n-alkanes in vegetable oils was more closely related to each other. The heatmap shows that C_{10}, C_{12}, C_{14} and C_{21} contribute to the clustering of all vegetable oils distinctly from the lard. Meanwhile, C_{13} and C_{22} were notable and unique to palm oil as both alkanes were found in low amounts or absent in lard and other vegetable oils.

Classification Analysis of Lard and Vegetable Oils

The same dataset of 14 significant alkanes was used for the classification analysis using supervised methods of PLS-DA model and RF machine learning. Lard and vegetable oil samples were classified using the PLS-DA model with variance explanation of 68.3% (component 1) and 14.3% (component 2) (*Figure 3a*).

Because this model is prone to overfitting, cross validation (CV) was used to assess its performance. In this work, 10-fold cross-validation was used to establish the appropriate number of components needed to construct the PLS-DA model (*Figure 3b*). Based on three popular performance criteria, such as prediction accuracy, R^2 and Q^2 values, the three-component model was deemed to as the best classifier. The PLS-DA model's predictability can be rated excellent if $Q^2 \geq 0.90$ (Idris *et al.*, 2022). Using the 14 significant alkanes, a 10-fold cross-validation found an accuracy of 1.0, variance repeated in cross-validation (Q^2 value) of 0.99, and endpoint variation incorporated in the regression model (R^2 value) of 1.0. Based on the result, there were no outlier and overfitting occurred for the PLS-DA model as indicated by the value difference of R^2 and Q^2 (<0.01).

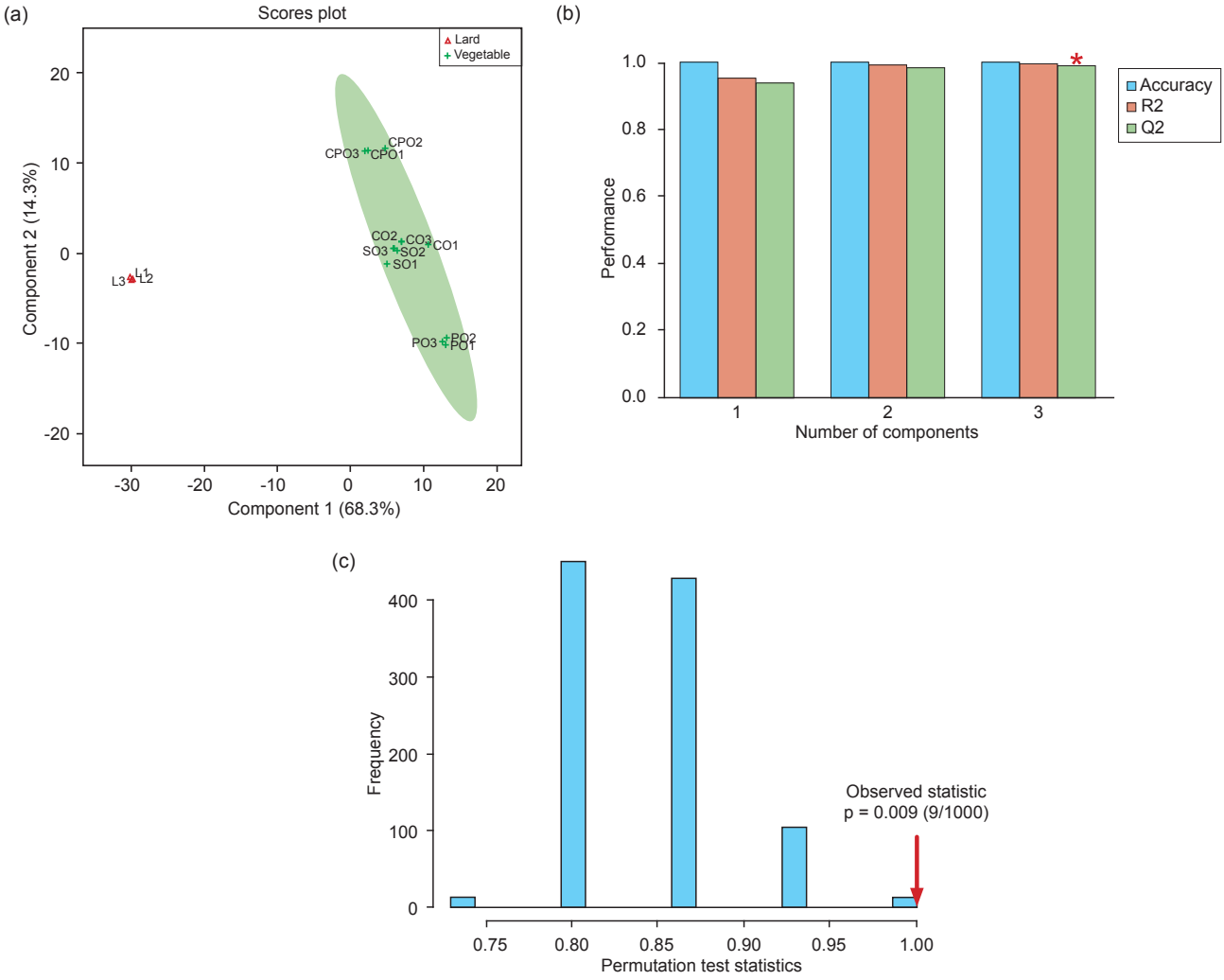


*Figure 3. 2-D PLS-DA model (a) of lard and other vegetable oil samples based on n-alkane profile with 82.6% of explained variance, 10-fold cross-validation (b) determined the best classifier for the PLS-DA model, marked with an asterisk (*), and permutation test of PLS-DA model (c) with 1000 random permutations (*p<0.009).

The performance of the developed PLS-DA model was further evaluated. A permutation test using 1000 random permutations was conducted to determine the overfitting possibility. Despite the common use of PLS-DA for assessing the discriminatory and predictive ability of oils and alkanes, it seems that the developed models are too closely fitted to the current data. Such argument can be referred to the value of C_{24} (0.049) which is close to 0.050 by using Kruskal-Wallis test (*Figure 1*). In this study, the permutation test indicated a possibility of such accuracy (*Figure 3c*) due to potential overfitting since the *p*-value obtained was 0.009. Therefore, the permutation test can be considered as a very sensitive method for classification. Golland *et al.* (2005) reported that the number of permutations needs to be "large enough" to sample both tails of the available distribution dataset. A permutation test can be used to evaluate whether the specific classification of the individual group (within a pair of groups) is better than any other random classification group (Mielke and Berry, 2007). Hemmateenejad *et al.* (2011) also reported that the cross validation and permutation test are very promising statistical tools to evaluate the prediction ability of the proposed model.

Another classification approach using RF machine learning was performed using Metaboanalyst 5.0 and then validated by the R package in the R Studio. The same 14 pre-processed datasets were utilised in this classification analysis. The samples were grouped correctly into their respective classes, therefore producing an "out-of-bag" (OOB) error of 0 for all classes (*Table 1*). The RF model revealed the significant variables in terms of mean decrease accuracy values, where the importance of the variables was indicated in descending order (*Figure 4*). Consequently, random forest highlighted C_{18}, C_{24} and C_{16} as the top three significant alkanes in the classification of lard from the selected vegetable oil, with the values of 0.033743, 0.031867 and 0.030652, respectively.

According to Hengl *et al.* (2018), an RF model does not require cross validation since this

algorithm already makes an unbiased estimation internally through the OOB error estimation. In this study, an additional 10-fold cross-validation was implemented to calculate the prediction accuracy of the developed RF model. Classification accuracy was measured based on how many times the predictions accuracy made by the model were correct. This additional cross-validation step indicated a prediction accuracy of 1.0 that is acceptable criteria for model predictability.

TABLE 1. CONFUSION MATRIX OF SAMPLE CLASSIFICATION FOR LARD AND VEGETABLE OIL BY RANDOM FOREST

Item	Lard	Vegetable oil	Class error
Lard	3.00	0.00	0.00
Vegetable oil	0.00	12.00	0.00

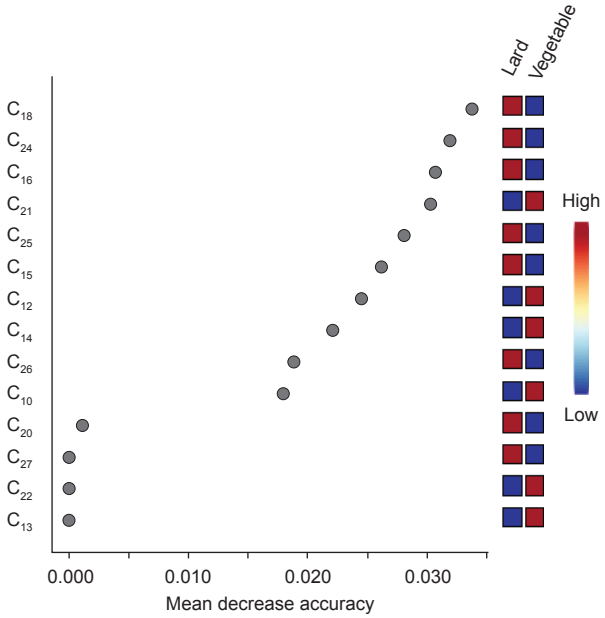


Figure 4. Random forest highlighted significant variables in sample classification in decreasing order of mean decrease accuracy.

Identification of Potential n-alkane Markers

Potential n-alkane marker of lard was identified after analysing the outcome and performance of the developed models to each other. *Table 2* shows the summary of loading scores of the PCA model, the mean decrease accuracy value determined by the RF, and the total abundance of selected significant n-alkanes in the differentiation of lard from vegetable oils. RF highlighted C_{18}, C_{24} and C_{16} as the top three significant alkanes in the differentiation of lard from the selected vegetable oils with mean decrease accuracy of 0.0337, 0.0319 and 0.0307, respectively. In the PCA model, C_{18} and C_{16} were located on the negative side of PC1 and the positive side of PC2, while C_{24} located on the negative sides of both PCs to indicate the distinctive clustering of lard samples (*Figure 2a*).

Even though, at first, the model for classification result was considered invalid since the PLS-DA developed in this study was overfit, however, further classification by the RF provides an acceptable prediction accuracy of 1.0. Consequently, tetracosane (C_{24}) and octadecane (C_{18}) were proposed as the potential lard markers based on the RF feature selection and their contribution to lard clustering in the PCA model. The C_{24} alkane was detected to be the most abundant in lard (15.72%) and the C_{18} was considered to be given the highest increase if compared to the close highest alkane value (0.44-fold). PLS-DA and RF are popular machine learning tools with useful selector and classifier features (Ruiz-Perez *et al.*, 2020). Since the PLS-DA was able to strengthen the PCA finding, the multitude tools available and the use of different methods depending on the dataset is an advantage. It is important to note that the PLS-DA role in the discriminant analysis can be easily misinterpreted (Brereton *et al.*, 2014). As the PLS-DA is prone to overfitting, it is important to further verify its function by using CV (Kjeldahl and Bro, 2010). To refine the result, the RF was trained and validated using a separate unrelated group data (Broughton-Neiswanger *et al.*, 2020; Sharin *et al.*, 2021). The developed methodology can be helpful in early routine laboratories practice (Felipe Bachion *et al.*, 2018) supposedly for the screening analysis of different oils.

TABLE 2. SUMMARY OF PCA LOADING SCORES, MEAN DECREASE ACCURACY VALUE AND TOTAL ABUNDANCE OF SELECTED SIGNIFICANT N-ALKANES FOR LARD CLASSIFICATION FROM OTHER FATS

n-alkanes	PCA loading scores (PC1, PC2)	Mean decrease accuracy[1]	Decrease abundance of alkane in lard[2] (%)
C_{18}	-0.26319, 0.34170	0.0337	9.94
C_{24}	-0.27277, -0.48868	0.0319	15.72
C_{16}	-0.06548, 0.21531	0.0307	14.84

Note: [1] Mean decrease accuracy determined by random forest.
[2] Abundance of n-alkane in percentage calculated by the following formula: (Peak area of single alkane / Total peak area of n-alkanes) × 100.

CONCLUSION

Through GC-MS and multivariate analysis, lard and vegetable oil samples (coconut, palm, peanut, and soybean oils) were differentiated based on n-alkane profiles using unsupervised method (PCA and HCA) and verified by supervised method (PLS-DA and RF). Only 14 significant n-alkanes (p<0.05) were chosen from the 17 original n-alkanes

for detailed classification. The PCA score plot (PC1 and PC2) was indicated by 83% variation with C_{24} having a major positive contribution towards lard clustering. Similar to PCA, the HCA separated lard and vegetable oils into two different clusters. Due to overfitting, PLS-DA and RF were further used to verify the PCA result and 82.6% of variance was obtained for both components 1 and 2. With a prediction accuracy of 1.0, the generated RF model was considered as acceptable categorisation. A cross-validation (accuracy of 1.0), variance repeated in cross-validation (Q^2 of 0.99) and endpoint variation incorporated in the regression model (R^2 of 1.0) concluded no outlier and overfitting occurred for the PLS-DA model (R^2 and Q^2<0.01). For distinguishing lard from other vegetable oils, the tetracosane (C_{24}) and octadecane (C_{18}) were chosen as the potential indicators because of their high influence on the sample clustering in the PCA and PLS-DA models, high abundance in lard, and prominence as the first and second most significant variables in the RF model.

ACKNOWLEDGEMENT

The authors would like to acknowledge the Universiti Putra Malaysia for financial support under the Putra Grant Scheme [Grant number 9646800] and the Ministry of Higher Education, Malaysia (KPT reference code: FRGS/1/2020/STG01/UPM/02/14) under the Fundamental Research Grant Scheme [Grant number 5540357].

REFERENCES

Al-Kahtani, H A; Ahmed M A; Abou-Arab, A A and Hayat, K (2017). Identification of lard in vegetable oil binary mixtures and commercial food products by FTIR. *Qual. Assur. Saf. Crops Foods*, *9(1)*: 11-22. DOI: 10.3920/QAS2015.0692.

Ataabadi, M S; Bahmanpour, S; Yousefinejad, S and Alaee, S (2023). Blood volatile organic compounds as potential biomarkers for poly cystic ovarian syndrome (PCOS): An animal study in the PCOS rat model. *J. Steroid Biochem. Molecul. Biol.*, *226*: 106215. DOI: 10.1016/j.jsbmb.2022.106215.

Azir, M; Abbasiliasi, S; Tengku Ibrahim, T; Manaf, Y; Sazili, A and Mustafa, S (2017). Detection of lard in cocoa butter - Its fatty acid composition, triacylglycerol profiles and thermal characteristics. *Foods*, *6(11)*: 98. DOI: 10.3390/foods6110098.

Azizan, N I; Mokhtar, N F K; Arshad, S; Sharin, S N; Mohamad, N; Mustafa, S and Hashim, A M (2021). Detection of lard adulteration in wheat biscuits using chemometrics-assisted GCMS and random forest. *Food Analyt. Met.*, *14(11)*: 2276-2287. DOI: 10.1007/s12161-021-02046-9.

Botella, C; Ferré, J and Boqué, R (2009). Classification from microarray data using probabilistic discriminant partial least squares with reject option. *Talanta*, *80(1)*: 321-328. DOI: 10.1016/j.talanta.2009.06.072.

Brereton, R G and Lloyd, G R (2014). Partial least squares discriminant analysis: Taking the magic away. *J. Chemom.*, *28(4)*: 213-225. DOI: 10.1002/cem.2609.

Broughton-Neiswanger, L E; Rivera-Velez, S M; Suarez, M A; Slovak, J E; Hwang, J K and Villarino, N F (2020). Pharmacometabolomics with a combination of PLS-DA and random forest algorithm analyses reveal meloxicam alters feline plasma metabolite profiles. *J. Vet. Pharmacol. Ther.*, *43(6)*: 591-601. DOI: 10.1111/jvp.12884.

Chong, I-G and Jun, C-H (2005). Performance of some variable selection methods when multicollinearity is present. *Chemometr. Intell. Lab. Syst.*, *78(1-2)*: 103-112. DOI: 10.1016/J.CHEMOLAB.2004.12.011.

Chong, J; Yamamoto, M and Xia, J (2019). MetaboAnalystR 2.0: From raw spectra to biological insights. *Metabolites*, *9(3)*: 57. DOI: 10.3390/metabo9030057.

Christin, C; Hoefsloot, H C; Smilde, A K; Hoekman, B; Suits, F; Bischoff, R and Horvatovich, P A (2013). Critical assessment of feature selection methods for biomarker discovery in clinical proteomics. *Mol. Cell Proteomics*, *12(1)*: 263-276. DOI: 10.1074/mcp.M112.022566.

Cocchi, M; Biancolillo, A and Marini, F (2018). Chemometric methods for classification and feature selection. *Compr. Anal. Chem.*, *82*: 265-295. DOI: 10.1016/bs.coac.2018.08.006.

Felipe Bachion, S; Sarmento, M; Lucas, G; Waldomiro, N and Ronei, P (2018). Rapid discrimination between authentic and adulterated andiroba oil using FTIR-HATR spectroscopy and random forest. *Food Analyt. Met.*, *11*: 1927-1935. DOI:10.1007/s12161-017-1142-5.

Ferreira, G F; Ríos Pinto, L F; Carvalho, P O; Coelho, M B; Eberlin, M N; Maciel Filho, R and Fregolente, L V (2021). Biomass and lipid characterization of microalgae genera *Botryococcus, Chlorella*, and *Desmodesmus* aiming

high-value fatty acid production. *Biomass Convers. Biorefin.*, *11(5)*: 1675-1689. DOI: 10.1007/s13399-019-00566-3.

Giuffrè, A M and Capocasale, M (2016). N-Alkanes in tomato (*Solanum lycopersicum* L.) seed oil: The cultivar effect. *Int. Food Res. J.*, *23(3)*: 979-985.

Golland, P; Liang, F; Mukherjee, S and Panchenko, D (2005). Permutation tests for classification. *COLT*, *5*: 501-515.

Hassan, J; Farahani, A; Shamsipur, M and Damerchili, F (2010). Rapid and simple low density miniaturized homogeneous liquid-liquid extraction and gas chromatography/mass spectrometric determination of pesticide residues in sediment. *J. Hazard. Mater.*, *184(1-3)*: 869-871. DOI: 10.1016/j.jhazmat.2010.08.008.

Hemmateenejad, B; Yousefinejad, S and Mehdipour, A R (2011). Novel amino acids indices based on quantum topological molecular similarity and their application to QSAR study of peptides. *Amino Acids*, *40*: 1169-1183. DOI: 10.1007/s00726-010-0741-x.

Hengl, T; Nussbaum, M; Wright, M N; Heuvelink, G B and Gräler, B (2018). Random forest as a generic framework for predictive modeling of spatial and spatio-temporal variables. *PeerJ*, *6*: p.e5518. DOI: 10.7717/peerj.5518.

Höjer Holmgren, K; Hok, S; Magnusson, R; Larsson, A; Åstot, C; Koester, C; Mew, D; Vu, A K; Alcaraz, A; Williams, A M; Norlin, R and Wiktelius, D (2018). Synthesis route attribution of sulfur mustard by multivariate data analysis of chemical signatures. *Talanta*, *186*: 615-621. DOI: 10.1016/j.talanta.2018.02.100.

Idris, M H H; Abdullah Sani, M S; Mohd Hashim, A; Mohd Zaki, N N; Abdul Manaf, Y N; Mohd Desa, M N; Arshad, S; Yuswan, M H; Hassan, M S; Yusof, Y A; Kamaruddin, M S and Mustafa, S (2022). Forensic feed strategy: Incorporation of multivariate and instrumental analyses for authentication of fish feed sources. *J. Halal Industry and Services*, *5(1)*: a0000293. DOI: 10.36877/jhis.a0000293.

Kjeldahl, K and Bro, R (2010). Some common misunderstandings in chemometrics. *J. Chemom.*, *24(7-8)*: 558-564. DOI: 10.1002/cem.1346.

Lindgren, F; Hansen, B; Karcher, W; Sjöström, M and Eriksson, L (1996). Model validation by permutation tests: Applications to variable selection. *J. Chemom.*, *10(5-6)*: 521-532.

Mielke, P W and Berry, K J (2007). *Permutation Methods: A Distance Function Approach*. New York: Springer.

Mihailova, A; Abbado, D and Pedentchouk, N (2015). Differences in n-alkane profiles between olives and olive leaves as potential indicators for the assessment of olive leaf presence in virgin olive oils. *Eur. J. Lipid Sci. Technol.*, *117(9)*: 1480-1485. DOI: 10.1002/ejlt.201400406.

Preece, D (1990). RA Fisher and experimental design: A review. *Biometrics*: 925-935. DOI: 10.2307/2532438.

Ruiz-Perez, D; Guan, H; Madhivanan, P and Narasimhan, G (2020). So you think you can PLS-DA?. *BMC Bioinform.*, *21(2)*: 1-10. DOI: 10.1186/s12859-019-3310-7.

Salleh, N A M; Hassan, M S; Jumal, J; Harun, F W and Jaafar, M Z (2018). Differentiation of edible fats from selected sources after heating treatments using fourier transform infrared spectroscopy (FTIR) and multivariate analysis. *AIP Conf. Proc.*, *1972*(*1*): 030015. DOI: 10.1063/1.5041236.

Schaettler, M O; Richters, M M; Wang, A Z; Skidmore, Z L; Fisk, B; Miller, K E; Vickery, T L; Kim, A H; Chicoine, M R; Osbun, J W; Leuthardt, E C; Dowling, J L; Zipfel, G J; Dacey, R G; Lu, H-C; Johanns, T M; Griffith, O L; Mardis, E R; Griffith, M and Dunn, G P (2022). Characterization of the genomic and immunologic diversity of malignant brain tumors through multisector analysis. *Cancer Discov.*, *12(1)*: 154-171. DOI: 10.1158/2159-8290.CD-21-0291.

Sharin, S N; Sani, M S A; Jaafar, M A; Yuswan, M H; Kassim, N K; Manaf, Y N; Wasoh, H; Zaki, N N M and Hashim, A M (2021). Discrimination of Malaysian stingless bee honey from different entomological origins based on physicochemical properties and volatile compound profiles using chemometrics and machine learning. *Food Chem.*, *346*: 128654. DOI: 10.1016/j.foodchem.2020.128654.

Troya, F; Lerma-García, M J; Herrero-Martínez, J M and Simó-Alfonso, E F (2015). Classification of vegetable oils according to their botanical origin using n-alkane profiles established by GC-MS. *Food Chem.*, *167*: 36-39. DOI: 10.1016/j.foodchem.2014.06.116.

Van Ruth, S M; Villegas, B; Akkermans, W; Rozijn, M; van der Kamp, H and Koot, A (2010). Prediction of the identity of fats and oils by their fatty acid, triacylglycerol and volatile compositions using

PLS-DA. *Food Chem.*, *118(4)*: 948-955. DOI: 10.1016/j.foodchem.2008.10.047.

Westerhuis, J A; Hoefsloot, H C; Smit, S; Vis, D J; Smilde, A K; van Velzen, E J; van Duijnhoven, J P and van Dorsten, F A (2008). Assessment of PLSDA cross validation. *Metabolomics*, *4*: 81-89. DOI: 10.1007/s11306-007-0099-6.

Wold, S; Sjöström, M and Eriksson, L (2001). PLS-regression: A basic tool of chemometrics. *Chemom. Intell. Lab. Syst.*, *58*: 109-130.

Yousefinejad, S; Bahram, M and Baheri, T (2018). Classification of methamphetamine seized in different regions of Iran using GC-MS and chemometrics. *J. Iran Chem. Soc.*, *15*: 163-170. DOI: 10.1007/s13738-017-1219-5.

Yousefinejad, S; Honarasa, F; Fararouei, M and Moosavi-Movahedi, A A (2019). Structure-electrochemistry relationship for monovalent alkaline metals in non-aqueous solutions. *Phys. Chem. Liquids, 57(5)*: 600-620. DOI: 10.1080/00319104.2018.1507031.

Zenkevich, I G (2006). Use of recurrence relations for approximating properties of any homologs of organic compounds. *Russ. J. Gen. Chem.*, *76*: 1742-1752. DOI: 10.1134/S1070363206110120.

Zhao, S; Guo, Y; Sheng, Q and Shyr, Y (2014). Heatmap3: An improved heatmap package with more powerful and convenient features. *BMC Bioinform.*, *15(S10)*: P16. DOI: 10.1186/1471-2105-15-S10-P16.

SHORT COMMUNICATION

Journal of Oil Palm Research Vol. 36 (3) September 2024 p. 534-546
DOI: https://doi.org/10.21894/jopr.2023.0056

PALM OIL MILL EFFLUENT (POME) AS A SOURCE OF BIOFUELS AND VALUE-ADDED PRODUCTS VIA OIL RECOVERY: A REVIEW

YEE MUN TANG[1]; KOK TAT TAN[2] and LAI PENG WONG[1]*

ABSTRACT

Large scale palm oil production will inevitably generate a vast amount of liquid waste, particularly palm oil mill effluent (POME), that has adverse environmental impacts. While most studies concentrate on the organic removal from POME, the recovery of valuable resources from the effluent is infrequently described. The rising awareness of sustainability has motivated palm oil millers and academics to enhance waste management while also placing cognisance need for the resource's recovery. POME possesses a substantial amount of oil and grease (O&G), which can be valorised into value-added products such as biofuels or phytonutrients via oil recovery. Recovering oil loss through POME not only prevents income loss but also improves downstream treatment effectiveness. In this article, the perspective of oil recovery from POME, focusing on technologies like physical separation, chemical extraction, and ultrasonic irradiation as a pre-treatment will be discussed, along with their effectiveness and limitations. Additionally, future opportunities as well as the economic viewpoint will be looked upon to provide a comprehensive outlook. Overall, this article will provide the readers with an understanding of the significance of recovering oil from POME and its potential as a sustainable resource, contributing to effective waste management and supporting a circular economy.

Keywords: biofuel, oil recovery, palm oil mill effluent, sustainable, valorisation.

Received: 9 February 2023; **Accepted:** 27 August 2023**; Published online:** 26 October 2023.

INTRODUCTION

Malaysia is recognised as the world's second-largest producer and exporter of palm oil after Indonesia, accounting for 25.8% and 34.3% of global palm oil production and exports, respectively, with more than 18 million tonnes of crude palm oil (CPO) produced in 2022 (MPOB, 2022a). While Malaysia benefits economically from its massive palm oil production, it also generates a large quantity of industrial wastewater known as palm oil mill effluent (POME), a high-strength acidic contaminant with substantial solids and organic contents. Despite enhanced extraction efficiency in the palm oil mills, a significant amount of oil and grease (O&G) was unavoidably discovered in the effluent as oil losses. Studies have shown that the average oil loss in POME is around 4000 to 6000 mg/L (Choong *et al.*, 2018; Lee *et al.*, 2019), which has been largely neglected by the industry without realising the effects and potentials that might be generated.

Conventional POME treatment via biological process focuses primarily to avoid penalties from non-conformance with the government regulations by adhering to the stringent discharge limits. However, they have frequently overlooked the resource recovery from POME for higher value-added products. Resource recovery from waste is far more than just being sustainable, as it would concurrently lead to less environmental impacts and promotes economic development in the industry.

[1] Department of Environmental Engineering, Faculty of Engineering and Green Technology, Universiti Tunku Abdul Rahman, Jalan Universiti Bandar Barat, 31900 Kampar, Perak, Malaysia.

[2] Department of Petrochemical Engineering, Faculty of Engineering and Green Technology, Universiti Tunku Abdul Rahman, Jalan Universiti Bandar Barat, 31900 Kampar, Perak, Malaysia.

* *Corresponding author e-mail: wonglp@utar.edu.my*

These practices would also act as a cradle for green industry practices such as harnessing renewable energy sources, and reducing dependency on the depletable fossil fuels, while minimising negative impact on the planet all at one go.

The whole objective of this article aims to concisely review and report on the oil management strategies from POME that have not previously been compiled to acquire insight for better effluent management. As the current scenario in palm oil research focuses on resource recovery, this article introduces technologies for oil recovery from POME, along with their mechanisms of action, advantages, and disadvantages, while also presenting a green technology for enhancing oil recovery from POME via ultrasonication. Future opportunities in terms of environmental, social, and governance (ESG) as well as the economic viewpoint were looked upon. This strategy will pave the way for waste recovery and resource valorisation, which will not only effectively reduce pollution degree, but also greatly reduce the usage of non-renewable sources, moving the palm oil industries towards a sustainable development.

PALM OIL MILL EFFLUENT

Over the past 60 years, palm oil production has increased substantially as a result of expanding global population and driving demand from the food and beverage, oleochemical and biodiesel industries. Global palm oil production in 2022 reached a new high of 77 million tonnes, which is 40 times the output from 1970 (Edi, 2022). Nonetheless, the continual expansion of palm oil production will undeniably generate massive volumes of waste. A typical extraction operation of 1 t of CPO would require 5.0-7.5 t of water, with over half of it ending up as liquid waste (Mohammad *et al*., 2021). POME is the most prominent oily pollutant in palm oil mills derived from the mixture of steriliser condensate, crude oil clarification, and hydro-cyclone effluent. Not to mention that various boiler blowdown, tank and decanter drains, water used for maintenance and cleaning also resulted in POME generation.

Due to the heterogeneity of POME, no fixed values are provided for its attributes, as they fluctuate significantly in response to starting material qualities and processing variations. *Table 1* summarises the general physicochemical properties of raw POME along with the established regulatory limits to the discharge of POME. The raw POME characteristics were found to be non-compliant with the discharge limits.

POME is a solid-liquid effluent composed primarily of fine cellulosic materials as well as water-soluble oil palm components. Commonly, POME is a dense, brownish underutilised agro-industrial wastewater discharged at high temperatures and with a low pH value. Owing to the elevation of solids, O&G, and organic contents, indiscriminate discharge of untreated POME on land and into waterway can be concomitantly sensitive to environmental issues. POME is also eutrophic and emits an unpleasant odour due to its rich mineral content.

Presence of Oil and Grease in POME

Section 304(a) of the Clean Water Act (CWA) classifies O&G as conventional pollutants. In recent years, biological treatment has been the most prevalent approach for the treatment of POME (Cheng *et al*., 2021; Yashni *et al*., 2020). Despite POME's biodegradability ability, oil is notoriously difficult to be degraded biologically since not all microorganisms generate lipase enzymes that are capable of decomposing triglycerides. Oil film deposition surrounding the microbes would interfere with the existing biological treatment by hindering the transmission of oxygen and soluble substrate for microbial degradation. This will ultimately result in a decrease in the efficacy of treatment process and an increase in the operational treatment cost.

The oil droplets in POME exist in two phases being either floating in the supernatant or embedded in the solids. Due to the harsh mechanical processing, residual oil in POME is mostly in emulsified and dispersed form (<150 μm). In addition, the presence of natural surfactants in POME, such as glycolipids and phospholipids, increases the oil's stability, making it more resistant to coalescence and more challenging to be separated by natural means. POME is also highly complicated in nature due to the involvement of a diverse structure of cellulose, hemicellulose, and lignin (Hii *et al*., 2012). The carbohydrate-rich particles in POME encapsulate bulk of the oil droplets due to their amphiphilic properties, with predominating lipophilic capabilities (Wan Sharifudin *et al*., 2015). In brief, the oil is believed to be primarily trapped in the suspended solids and inseparable mechanically from the multiphase system, contributing to poor recovery and resource wastefulness in the long term.

OIL MANAGEMENT STRATEGIES FROM POME

Although biological treatment shows a certain level of efficiency in treating POME, it frequently disregards the resource recovery from POME. Resource recovery is one of the most desirable environmental options for handling oily sludge. It not only enables the palm oil industry to reprocess and reformulate the recovered oil for energy recovery, but it also significantly reduces the volume of waste and alleviates the negative impact.

TABLE 1. GENERAL CHARACTERISTICS OF RAW POME AND REGULATORY DISCHARGE LIMITS FOR POME

Parameters	Concentration range	Standard discharge limit
pH	3.3-5.7	5-9
Temperature	80°C-90°C	45°C
Total solids (TS)	11 500-78 000 mg/L	N/A
Suspended solids (SS)	5 000-54 000 mg/L	400 mg/L
Biochemical oxygen demand (BOD)	10 250-43 750 mg/L	100 mg/L
Chemical oxygen demand (COD)	15 000-100 000 mg/L	N/A
Total nitrogen (TN)	180-1 400 mg/L	200 mg/L
Ammoniacal nitrogen (NH_3-N)	4-80 mg/L	150 mg/L
Oil and greases (O&G)	130-18 000 mg/L	50 mg/L

Note: N/A – not applicable.

Source: Department of Environment Malaysia, 1977; Kamyab *et al.*, 2018; Loh *et al.*, 2017; Mahmod *et al.*, 2021.

Oil recovery is identical to oil extraction, with the key distinction being that when a virgin source is employed, it is commonly referred to as 'extraction'. 'Oil recovery', on the other hand, is usually used to define oil extraction from waste or subsequent oil extraction. Mechanisms employed in extracting oil from virgin sources have also been applied in the oil recovery process. Since oil recovery from POME has received less attention from the industry, this section intends to concisely review the oil management techniques that have been explored from POME on a laboratory scale to acquire insight for better effluent management. Various oil recovery methods, including physical, chemical, as well as physicochemical, have been investigated as one of the waste management approaches for POME.

Physical Methods

Oil recovery from POME could be accomplished by using trapping and skimming techniques. This entails the collection of all liquid effluent from the processing stages in a container and allowing it to stand for days until the oil components float to the surface and are skimmed off due to density differences. Commonly, this phenomenon is known as gravity separation. As Stoke's Law states, there are several factors that affect the physical separation, such as the medium viscosity, density, and particle sizes.

To improve the efficiency of oil recovery for gravity separation, researchers had incorporated dissolved air flotation (DAF) into the oil skimming process. When pressurised air is supplied at the bottom of an open container, the resulting air bubbles will adhere to the microscopic oil droplets, causing them to float to the surface and be recovered by the skimming equipment. Faisal *et al.* (2016) studied the optimal DAF parameters and the result shows that 52.6% of the O&G in POME could be removed with an airflow of 11 L/min and a treatment time of 5 days. This represents a 39.9% improvement over conventional separation. By integrating a membrane separation (MS) unit, the oil recovery rate improved to 99.9%. Albeit improved efficiency, the incorporation of DAF and MS units incurred substantial operating and maintenance expenses due to the requirement to generate a continual stream of bubbles and high tendency of membrane clogging.

Mechanical centrifugation is another method of recovering oil by physical means. During centrifugal operation, the force of centrifugation generated by high-speed rotation causes particles in oily sludge to move radially toward the bottom of the centrifugal device. Upon stratification of oily sludge, the top layer of oil-water emulsion liquid can be recovered for value-added products, while the bottom layer of solid particles can be processed for further uses. Laohaprapanon *et al.* (2005) compared gravity separation and mechanical centrifugation to physically separate oil from POME. It was discovered that centrifugation at 7000 rpm for 15 min yielded comparable oil recovery to gravity settling at 55°C for 1 day. Centrifugal efficiency is influenced by a number of factors, including centrifugal speed, power, temperature, and duration (Philemon and Benoît, 2013). Despite its superior performance to gravity separation in terms of space and time, mechanical centrifugation still has a relatively low efficiency.

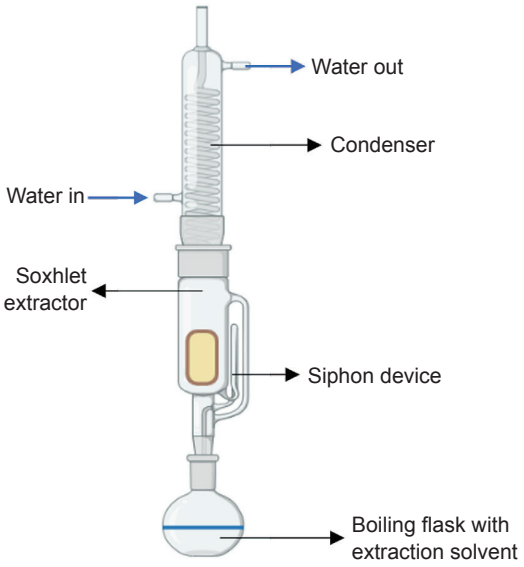
Conventionally, physical separation is the most common and simplest method to adopt. Despite its relatively simple design and low operating expenses, it is inefficient as it necessitates a huge setup area and is only able to recover 35%-55% oil layer on the surface (Loh *et al.*, 2013; Wang *et al.*, 2015). In contrast, the oil encapsulated within the remnant source cannot be freed and will be discharged as sludge. Consequently, the oil from the wastewater is not effectively recovered, necessitating a better recovery method or pre-conditioning of sample.

Chemical Methods

Solid-liquid extraction (SLE), commonly known as Soxhlet extraction, developed by Franz Von Soxhlet in the mid-18th century, has been used to separate various compounds from solid samples. A typical Soxhlet apparatus mainly consists of a boiling flask, a Soxhlet extractor, and a condenser, as illustrated in *Figure 1*.

The process begins with the addition of extraction solvent into the boiling flask. As the flask is steadily heated, the solvent vaporises as it reaches its boiling point. Through the siphon device and condenser, the vaporised solvent condenses and drains into the Soxhlet extractor. The analyte is extracted when the warm solvent contacts the oil source. When the extractor is full, the analyte-containing solvent floods back into the boiling flask. Repetition of cycles will result in complete extraction. Suwanno *et al.* (2017) employed a laboratory-scale Soxhlet technique to recover residual oil from POME. They discovered that 80% of the oil was recovered after 1 hr of reaction at 100°C with a sample-to-solvent ratio of 1:6.

Soxhlet extraction is a less commonly used method for oil recovery from POME on an industrial scale due to several limitations. One of the major drawbacks is that this technique is only applicable to solid samples. With the overwhelming presence of liquid phase in POME, a pre-treatment by drying is required prior to oil recovery. This will undoubtedly result in extended treatment time and higher production costs. Additionally, prolonged high-temperature exposure may also result in lipid peroxidation and deterioration of recovered products (López-Bascón and Luque de Castro, 2020).



Source: López-Bascón and Luque de Castro (2020).

Figure 1. Soxhlet apparatus setup.

On the other hand, liquid-liquid extraction (LLE), often termed as chemical extraction or solvent extraction, is currently widely employed in the food, pharmaceutical, and petrochemical sectors for the extraction process. Analytes are isolated based on their relative solubility in two immiscible solutions. LLE differs from Soxhlet extraction in that it does not entail any heating. *Figure 2* depicts the mechanisms of LLE, which consists of three fundamental steps: Interaction, separation, and recovery of solvent.

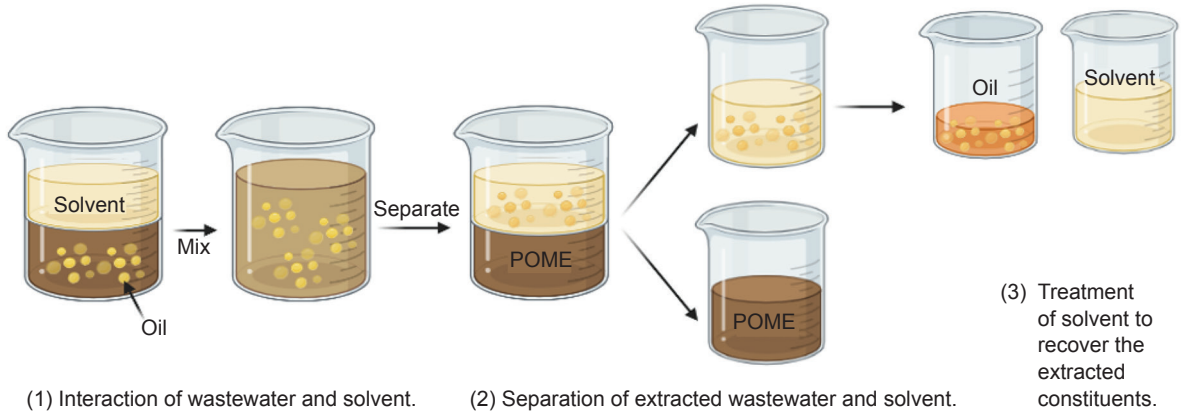
In POME, residual oil can be chemically recovered using non-polar organic solvents like n-hexane, n-heptane, pentane, petroleum ether, and benzene. Among various solvents, n-hexane is the most popular choice due to its superior oil extraction performance. The fundamental properties for the selection of extraction solvent include the solubility, hydrophobicity, molecular weight, vapor pressure, and acid dissociation (Wells, 2003).

Zulqarnain *et al.* (2021) conducted a study on the impact of various solvent extraction parameters on POME oil recovery efficiency. The parameters assessed included the solvent type, sample-to-solvent ratio, mixing time, agitation speed, and pH. The results revealed that the highest oil recovery from POME was 90% under the conditions of a POME-to-hexane ratio of 1:1 for 25 min at an agitation speed of 500 rpm and a pH of 10. Additionally, there are ongoing efforts being undertaken to commercialise solvent extraction as a viable method for POME oil recovery. One notable example is Mecpro Heavy Engineering Limited (2022), a reputable company specialising in process engineering for the palm oil industry, which has recently developed an innovative solvent extraction system known as the Mecpro Multi extraction system. This system is designed to recover both floating and emulsified oil from POME as well as wet mesocarp fibre simultaneously, leading to an oil extraction rate (OER) increase of more than 1%.

As a matter of fact, chemical extraction is considered as one of the most efficient means of separating residual oil from oily sludge. Unlike physical separation, this method requires organic extraction solvents. In addition to sourcing green solvents to reduce environmental pollution, future research may also focus on improving the efficiency of chemical extraction process by reducing the size of substrates, which increases their surface area and facilitates better solvent-substrate contact.

Physicochemical Methods

Progressive freezing concentration (PFC) is a process of concentrating a solution that entails freezing or solidifying one liquid component to form a pure solid, and then separating the solidified fragment from the mother liquor. The PFC process



Source: Suzuki *et al.* (2020).

Figure 2. Mechanisms of LLE.

is affected by several factors, including temperature, duration, freezing rate, oil-water phase, and impurities (Hui *et al.*, 2020). Mohamed Anuar *et al.* (2020) discovered that the PFC technique could recover 67.9% of O&G from POME after 1 hr at a coolant temperature of 6°C. One of the main advantages of PFC is that it is a green technology that operates at low process temperature, which can help maintain thermally sensitive elements of the solution. However, the productivity of PFC is relatively poor, and the energy requirements for the process can be high, making it less economically viable in warm climates. Nevertheless, there is a potential for application of this method in cold winter regions where low temperatures are prevalent.

Adsorption is one of the most popular techniques adopted for oil separation from oily wastewater. Adsorption is a surface-related phenomenon in which the sorbate molecules adhere to the sorbent without penetrating it. Adsorbent materials can be either synthetic or natural. Several sorbents have been reported for the adsorption of oil from POME; including synthetic rubber powder (Ahmad *et al.*, 2005a), chitosan (Ahmad *et al.*, 2005b), palm shell activated carbon magnetic composite (Ngarmkam *et al.*, 2011), modified oil palm leaf (Jahi *et al.*, 2015), esterified sago bark fibre waste (Wahi *et al.*, 2017), as well as polypropylene micro/nanofiber (PP-MNF) (Semilin *et al.*, 2021). The efficiency of oil adsorption ranged from 80% to 99%, with the esterified sago bark fibre waste achieving the lowest efficiency, and chitosan powder achieving the highest. The efficiency of the oil-water adsorption process is determined by the properties of sorbent, the most important of which are the hydrophobic and oleophilic properties. These studies have shown that the adsorption efficiency can be improved by optimising the processing conditions, such as dosage, contact time, pH, and temperature. Physical pressing, chemical extraction, or supercritical carbon dioxide techniques can be used to recover the adsorbed oil from the sorbent. Adsorption is widely utilised for its benefits, such as high efficiency, ease of operation, and environmental friendliness. However, the concern over the reusability of adsorbent and post-adsorption treatment to recover the adsorbed oil is a huge disincentive to this technology as it will certainly increase the expenditure.

Table 2 provides an overview of various oil management strategies for POME, along with their advantages and disadvantages. Among those, chemical extraction would be the preferred option due to its high recoverability efficiency and industrial-scale practicability.

ULTRASONICATION TECHNIQUE – A GREEN TECHNOLOGY TO ENHANCE OIL RECOVERY

The primary drawback of oil recovery from POME is the oil-bearing cell, and most oil recovery systems are geared only toward recovery, with little attempt made to enhance the recovery yields. As approaches outlined above have limitations in extracting the entrapped lipids, research has demonstrated that the incorporation of ultrasound pre-treatment can transcend these barricades.

Ultrasound is a cyclic sound pressure with a frequency greater than 20 kHz. Ultrasonication technique is often regarded as a 'green technology', as evidenced by its numerous advantages such as high efficiency, low equipment requirement, short operation duration (seconds to minutes), and ability to operate under atmospheric pressure and ambient temperature. Most notably, ultrasonication does not require any chemical enhancers to increase yield, which exhibits the benefit of being non-hazardous to the environment and contributes to waste reduction. In recent years, ultrasound technology has acquired

TABLE 2. OVERVIEW OF OIL MANAGEMENT STRATEGIES FOR POME

Oil recovery method	Advantages	Disadvantages
Trapping and skimming	Simple design Low cost Does not require chemicals	Only able to remove free oil Slow removal process Huge setup area
Dissolved air flotation and membrane separation	Improved efficiency compared to gravity separation Does not require chemicals	High operating costs Tendency of membrane clogging
Mechanical centrifugation	Reduced time and space compared to gravity separation	Emulsified and entrapped oil cannot be recovered High maintenance cost
Soxhlet extraction	Large selectivity High yield	Necessitate pre-treatment of drying and chemicals Adverse thermal effects
Chemical extraction	Industrial practicability High recoverability efficiency	Require chemicals
Progressive freezing concentration	Maintain thermally sensitive element	Low productivity Unsuitable for warm climates
Adsorption	High removal efficiency Ease of operation	Post-adsorption treatment is required Concern over reusability

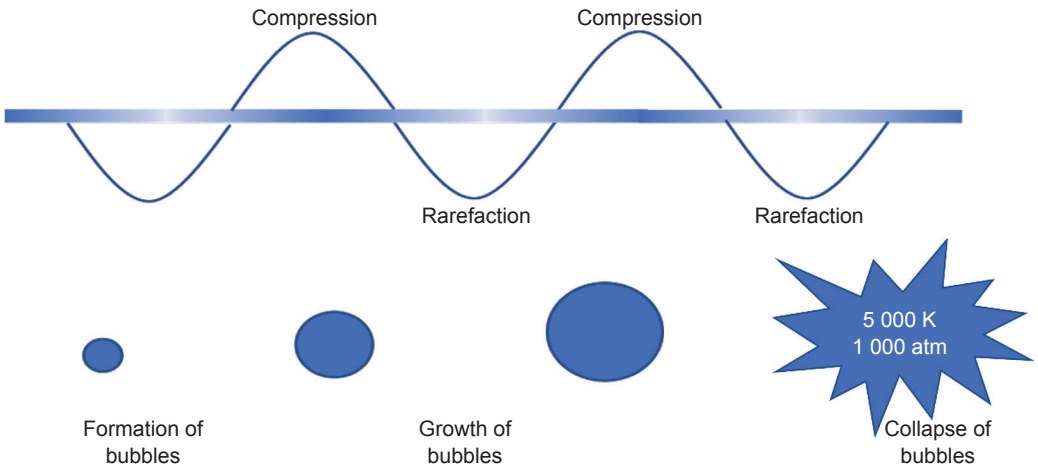
greater application in almost all disciplines, including the fields of medical and therapy, food and beverage, material cleaning, nanotechnology, industrial welding, and environmental applications (Mohammed and Alhajhoj, 2020).

When ultrasound wave propagates in the sample, it generates a series of cycles known as compression and rarefaction, which impose positive pressure by pushing the molecules together and negative pressure by pulling them apart. As a result of instantaneous and enormous pressure difference, microbubbles occur in the rarefaction region. These microbubbles expand in successive cycles by absorbing the ultrasonic energy and collapse violently upon reaching an unstable diameter. This phenomenon is known as acoustic cavitation and is represented in *Figure 3*.

The detonation of cavitation bubbles induces shock waves, which in turn create intense localised heating (5000 K), high pressure (500 atm), and a high heating and cooling rate (10^9 K/s) at the liquid-gas interface turbulence over a few microseconds (Suslick, 1998). Such extreme conditions create other physical and mechanical effect, namely hydromechanical shear forces created by liquid jet stream travelling at a speed of 400 km/hr. These effects can cause breakdown of cell wall and exudation of cellular content, all of which contribute to an increase in yield. In addition, ultrasonication has been associated with sonochemistry reactions. The heat generated by the cavity implosion dissociates the water (H_2O) molecules into highly reactive hydroxide radicals ($OH\cdot$) and hydrogen (H^+) atoms. These radicals recombine during the rapid cooling phase to form hydrogen peroxide (H_2O_2) and molecular hydrogen (H_2). These reactive oxygen species will oxidise and degrade the solutes. Overall, ultrasonic irradiation is an emerging technology with a combination of physical (pyrolysis and shearing) and chemical effects (radical reaction).

Tang *et al.* (2021) studied the use of low-frequency ultrasound to enhance the oil recovery from POME. The oil content after subjecting POME to ultrasound pre-treatment was compared to the oil content from corresponding sample without ultrasound pre-treatment. The results reveal that low-frequency ultrasound pre-treatment improved extractability by 39.17% additional oil content, with the highest extractability achieved under the conditions of 150 W and 15 s. In addition, ultrasonic irradiation on POME could also enhance the organic solids solubilisation, which will be an added advantage for subsequent biological treatment (Isa *et al.*, 2020; Wong *et al.*, 2019).

Essentially, the ultrasound intervention on POME not only allows for potentially higher oil recovery and increases economic returns for palm oil mills, but also appreciably reduces the treatment operation footprint through enhanced organic solubilisation. Although ultrasound pre-treatment exhibited numerous benefits, concerns regarding energy consumption and the possibility of oxidation on recovered products should be considered.



Source: Perera and Alzahrani (2021).

Figure 3. Mechanisms of ultrasonic irradiation.

POTENTIAL PRODUCTS FROM POME-RECOVERED OIL

Table 3 shows the characteristics of residual oil recovered from POME with that of CPO. The attributes of residual oil recovered from POME are comparable to CPO, but with a slightly higher free fatty acids (FFA) and peroxide value (PV). *Figure 4* illustrates the potential products from POME-recovered oil. The recovered oil from POME can be valorised as feedstock for biodiesel production, burner fuel, sustainable aviation fuel, as well as in nutritional platform.

Biodiesel

The imminent depletion of fossil fuel reserves, combined with environmental concerns, has fuelled the desire to achieve greater energy independence by encouraging more research on ecologically friendly and sustainable biofuels. Biodiesel, a renewable liquid fuel, has been advocated as a promising fuel for the future. It outperforms petroleum-based fuels in several aspects, including being biodegradable, non-toxic, and emitting fewer harmful pollutants (Ogunkunle and Ahmed, 2019). Commonly, edible oil is the leading resources for the manufacturing of biodiesel. Nevertheless, the utilisation of edible oil invariably sparks controversy and establishes a conflict between the availability of food and fuel. To alleviate the issue, academics and stakeholders strive to transform the processed-palm-oil waste into biofuel, while reutilising the residual oil recovered from POME for biodiesel production came on top of the plan. Zulqarnain *et al.* (2021) reviewed the biodiesel production process and discussed the research gaps related to valorising POME as a substrate. The authors emphasised that although POME demonstrated a great potential as a feedstock for green fuels, there is a need for more research to improve the efficiency and cost-effectiveness of POME-based biodiesel production.

Burner Fuel

Alternatively, residual oil from POME can be valorised directly as a fuel substitute in a burner without undergoing any refining process. According to Zuber *et al.* (2018), the viscosity of residual oil from POME is 15 times higher than that of conventional diesel, preventing it from flowing or spraying efficiently without any treatment. Through heating, its viscosity can be reduced significantly, while its flowability can be enhanced. Compared with conventional diesel, it has been reported that the use of residual oil from POME in a burner reduces emissions of carbon monoxide (CO) and nitrogen oxides (NOx) by 34% and 90%, respectively, indicating its feasibility as burner fuel.

Sustainable Aviation Fuel

In conjunction with the global commitment in reducing emissions in the aviation sector, conversion of residual oil from POME into sustainable aviation fuel (SAF) with hydrotreated vegetable oil (HVO) technology could be one of the most effective strategies. Yeoh and Goh (2022) presented a review on current state of HVO production from POME along with its opportunities and challenges. The study also highlights the benefits it could bring to the aviation industry. The conversion of POME into SAF can reduce the carbon footprint of aviation by up to 80% compared to conventional jet fuel. It can also improve energy security by reducing reliance on fossil fuels and diversifying fuel sources.

TABLE 3. CHARACTERISTICS COMPARISON OF POME-RECOVERED OIL AND CPO

Item	Residual oil from POME	Crude palm oil
Free fatty acids, FFA (%)	5-45	Max 5
Iodine value, IV	40-100	50.40-53.70
Peroxide value, PV (meq/kg)	1.36-21.81	Max 3
Fatty acid composition (%)		
Myristic (C14:0)	1.08-1.20	0.90-1.50
Palmitic (C16:0)	45.00-46.20	39.20-45.80
Stearic (C18:0)	3.70-4.45	3.70-5.10
Oleic (C18:1)	37.99-39.80	37.40-44.10
Linoleic (C18:2)	9.80-9.85	8.70-12.50
Linolenic (C18:3)	0.02-0.40	0.00-0.60

Source: Hayyan *et al.*, 2011; Malaysia Department of Standards, 2007; Putri Primandari *et al.*, 2013.



Figure 4. Potential products from POME-recovered oil.

Additionally, the production of SAF from POME can create new economic opportunities by providing an additional source of income for palm oil producers.

Phytonutrients

Phytonutrients are bioactive compounds that have beneficial effects on human health. These extracts have been shown to have antioxidant, anti-inflammatory, and anti-cancer properties, which can be employed as cosmeceuticals additives, colouring agents, as well as nutritional supplements within the pharmaceutical and food industries. Recent studies revealed that POME-recovered oil possesses high nutritional value, prompting the nutraceutical investors to venture in technologies for the valorisation of essential bioactive compounds. In a study conducted by Teh *et al.* (2017), it was reported that POME-recovered oil is rich in various phytonutrients, containing 161 ppm of sterols, 706 ppm of vitamin E (tocotrienol and tocopherols), 569 ppm of pro-vitamin A (carotenoids), as well as 514 ppm of squalene. Sterols are plant-based compounds that have cholesterol-lowering properties, while vitamin E is a group of fat-soluble compounds that act as an antioxidant. Carotenoids are essential for maintaining healthy vision, skin, and immune function, and squalene is a natural antioxidant that can enhance skin health and reduce the risk of chronic diseases. The study also revealed that the phytonutrient contents of POME-recovered oil are comparable to those of CPO, suggesting the possibility for valorisation as a reliable source of nutritional products. Furthermore, Chen *et al.* (2019) provided a comprehensive review of the challenges related to recovering high-value nutrients from POME, including safety, technology, regulations, and cost-effectiveness.

FUTURE OPPORTUNITIES

With the rising generation of POME, there is a need for research to be conducted to intensify the performance of current oil recovery techniques from POME. Given the possibility of industry's reliance on solvent extraction method, an alternative of low-cost green solvent is also one of the highly anticipated opportunities. Methods like supercritical fluid extraction (SFE) or aqueous extraction process (AEP), which involve the use of green solvents such as carbon dioxide or water, could be explored. The massive volume of POME could be a trade-off between the environmental benefits and the cost of the associated technology. Besides, palm oil millers could also look into the incorporation of other green technologies like microwave-assisted or enzymatic hydrolysis as a pre-treatment or polishing step to improve the oil recovery process, as certain treatment methods are insufficient to stand alone. As for the ultrasound pre-treatment in enhancing oil recovery from POME, a thorough study of the system design, ultrasound field patterns, cost-benefit analysis, as well as quality assessment on the recovered products could be undertaken.

A more scientific approach in the entire palm oil industry is necessary for the future growth of the industry, both in terms of efficiency and economics. Biodiesels are one of the potential outcomes for recovered oil from POME. An effective conversion technology with the lowest possible production cost and environmental impact should be designed by conducting economic assessment and life cycle analysis. Besides, a comprehensive strategy for connecting and transporting the effluent from its source to biodiesel manufacturing facility could be devised. Aside from enhancing the conversion and recovery process, researchers can also expand their horizons and explore new possibilities and applications for the recovered oil.

Environmental Aspect of the Residual Oil Recovery Practice

Oil palms were cultivated as a strategy to minimise the country's economic reliance on tins and rubber as early as 1960. The decision to cultivate oil palm is often linked to the negative impacts on the environments which include mass scale deforestation and emission of greenhouse gases (GHG). Another controversial issue of the palm oil industry is the discharge of POME into open water bodies. The water consumption in the palm oil industry is so huge, that POME has become one of the largest contributors to the wastewater in Malaysia.

Both government and private organisations have been encouraged to undertake all development projects with a focus on sustainable development. The implementation of best-developed practices (BDPs) with a 'zero waste' philosophy that emphasises the recycling and utilisation of all waste and by-products from the entire palm oil sector, is promoting the palm oil industry to become more environmental-friendly.

Rather than new forest land exploration that lead disturbance of forest system, loss of animal habitats, and pesticide pollution in maintaining the plantation, researchers can divert their efforts to increase the oil production through adoption of residual oil recovery from processed palm-oil waste as one of its waste management strategies. The adoption of these practices will greatly drive the sector towards cleaner production, with benefits such as reduced waste generation, efficient utilisation of waste, and cost-effective improvements to end-of-pipe solutions when integrated into current production processes.

Along with the country's commitment to the Paris Agreement, the Malaysian government recently declared that carbon tax would be incorporated in the 12th Malaysia Plan (2021-2025). Through introducing the carbon tax, palm oil millers will be obliged to seek into alternative energy source as a method to reduce and offset the carbon footprints from the process. One example is that the residual oil recovered from POME can be used for biodiesel production, which acts as a renewable substitute for petroleum fuel. Advanced feedstocks derived from waste and achieving greater GHG savings are double counted towards transport fuel mandates under the new European Union Renewable Energy Directive (EU RED) II, and POME has been included as one of the sources, which would offer a significant incentive in the field.

Social Aspect of the Residual Oil Recovery Practice

The palm oil industry is currently a hot topic in the society and communities, and the recovery of residual oil from POME is viewed as a potential solution to the sector's social issues. The implementation of residual oil recovery practices could potentially result in the creation of new job opportunities in waste management, oil recovery, and renewable energy production. As the demand for sustainable palm oil grows, there will be a need for more skilled personnel in these areas, which could contribute to the development of local communities. Furthermore, integrating these communities in the process can lead to environmental education and awareness, promoting sustainable practices.

The recovery of residual oil from POME could also result in new partnerships between palm oil producers and other industries, like biofuel industry. This could help strengthen the supply chain and open new avenues for collaboration. The Malaysian government's launch of PEMERKASA stimulus

package and Workforce Recalibration Programme could contribute to the social sustainability by encouraging investment in the palm oil industry and providing legal status to foreign workers (Nur Aisha, 2021). These initiatives encourage technology transfer and fair labour practice, resulting in a more socially responsible and sustainable industry.

Overall, the residual oil recovery practice offers a range of opportunities for employment creation, community development, environmental education, and partnership development. By prioritising these social aspects, the palm oil industry can progress towards a more sustainable future, fulfilling the growing demand for sustainable palm oil while benefiting communities and the environment.

Governance Aspect of the Residual Oil Recovery Practice

Governance factors refer to a country's norms or standards, allowing investors to screen for proper governance practices in the same manner that they do for the environmental and social aspects. The European market is already shifting from voluntary standards to enforcing sustainability by law, and this process is being expedited by the global climate ambitions, which have turned the Paris Climate Agreement into European Green Deal, with the goal of achieving EU climate neutral by 2050. Malaysia has also developed its own mandatory certification scheme known as Malaysia Sustainable Palm Oil (MSPO) for the palm oil industry stakeholders, with the goal of promoting and ensuring the industry's sustainability. However, the EU's failure to recognise the importance of MSPO had ushered for further improvement. Hence, governments over the countries should work together to enable a feasible two-way collaboration.

To achieve a greener future, governments have also introduced renewable fuel policies such as subsidies, incentives, mandates, and taxes to boost the biodiesel sector. One example is the Malaysian and Indonesian governments' announcement of the objective in promoting biodiesel blend B20 and B40 mandates by the end of 2022 (Ajeng Dinar, 2022). Since POME is abundantly generated, cheap, and challenging to dispose of, one of the research areas that can be investigated for sustainability is recovering the residual oil from POME and utilising it for biodiesel production. Without the cooperation by government and industry players, this approach would not be a success.

ECONOMIC VIEWPOINT

Oil recovery from POME could be an appealing alternative as it demonstrated a considerable reduction in organic content in POME, making subsequent treatment more efficient. Research has shown that removing oil from raw sludge reduces COD content by 10%-15% (Liew *et al*., 2017). Additionally, de-oiling contributes positively to anaerobic digestion rate and biomethane yield, which is advantageous for subsequent biological treatment (Aziz *et al*., 2020). Moreover, the recovered oil from POME can be sold for 40%-60% of the typical CPO price, revealing a new economic opportunity. The market price/t of CPO in 2022 ranges from RM3682 to RM6873 (MPOB, 2022b). With the assumption of recovered oil from POME is sold at 50% of the average market price of CPO (RM5126/t), the selling price of residual oil recovered from POME is approximately RM2563/t.

In 2022, global production of palm oil reached 77 million tonnes, resulting in 231 million tonnes of POME being produced. Not only did the process generate a considerable volume of effluent, but a rough speculation also indicates that the POME discharged contains approximately 1.16 million tonnes of residual oil that can be recovered. This could result in an additional revenue of RM2.9 billion/yr for the industry if the recovery of residual oil from POME is properly implemented. Additionally, this would also support the government's Economic Transformation Program (ETP) and its goal of boosting OER through Entry Point Projects (EPP) 4.

It is crucial to factor in the costs, particularly the equipment cost, to accurately determine the net economic benefit when considering the implementation of oil recovery technology. The cost of adding equipment can vary depending on the specific technology employed and the scale of operation. Some of the other expenses associated with implementing oil recovery technology include the installation cost of equipment, maintenance cost, operation cost, as well as infrastructure improvement cost. While the adoption of oil recovery practice from POME does incur some costs, these expenses can be offset by the value of recovered oil and other benefits. Therefore, a thorough analysis of the associated costs and benefits with the implementation of oil recovery technology is essential for making an informed decision.

CONCLUSION

The huge amounts of waste produced by the palm oil sector have sparked public concern. As a results, efforts are being made to study ways to effectively manage and utilise this waste to mitigate its negative effects on the environment. This review article outlines the valorisation of liquid palm oil waste via oil recovery. Various techniques along with research gaps for oil recovery from POME were looked upon, while also presenting the green technology

such as ultrasonic irradiation as a pre-treatment to enhance the efficiency of oil recovery. This review also highlights the use of recovered oil from POME as a renewable and sustainable source of material for producing value-added products, diversifying the utilisation of POME beyond traditional ponding systems. The future opportunities in terms of environmental, social, and governance aspects of residual oil recovery practice were critically evaluated. Overall, the implementation of techniques to recover residual oil from POME is highly recommended as an effective and sustainable waste management solution. It not only helps to conserve the environment, but also creates a new economic opportunity for palm oil millers. Additionally, the utilisation of recovered oil as a sustainable resource can provide industrial symbiosis possibilities and contributes to the circular economy.

ACKNOWLEDGEMENT

This research was financially supported by Universiti Tunku Abdul Rahman Research Fund (UTARRF) (Project Number: IPSR/RMC/UTARRF/2020-C1-W01).

REFERENCES

Ahmad, A L; Bhatia, S; Ibrahim, N and Sumathi, S (2005a). Adsorption of residual oil from palm oil mill effluent using rubber powder. *Brazilian J. Chem. Eng.*, *22(3)*: 371-379.

Ahmad, A L; Sumathi, S and Hameed, B H (2005b). Adsorption of residue oil from palm oil mill effluent using powder and flake chitosan: Equilibrium and kinetic studies. *Water Res.*, *39(12)*: 2483-2494.

Ajeng Dinar, U (2022). Indonesia, Malaysia commit to biodiesel mandates despite higher prices. *Reuters*. https://www.reuters.com/business/sustainable-business/indonesia-malaysia-commit-biodiesel-mandates-despite-higher-prices-2022-03-24/, accessed on 20 April 2023.

Aziz, M M A; Kassim, K A; El-Sergany, M; Anuar, S; Jorat, M E; Yaacob, H; Ahsan, A; Imteaz, M A and Arifuzzaman (2020). Recent advances on palm oil mill effluent (POME) pretreatment and anaerobic reactor for sustainable biogas production. *Renew. Sustain. Energy Rev.*, *119*: 109603. DOI: 10.1016/j.rser.2019.109603.

Cheng, Y W; Chong, C C; Lam, M K; Ayoub, M; Cheng, C K; Lim, J W; Yusup, S; Tang, Y and Bai, J (2021). Holistic process evaluation of non-conventional palm oil mill effluent (POME) treatment technologies: A conceptual and comparative review. *J. Hazard. Mater., 409*. DOI: 10.1016/j.jhazmat.2020.124964.

Chen, H; Zhang, H; Tian, J; Shi, J; Linhardt, R J; Ye, T D X and Chen, S (2019). Recovery of high value added nutrients from fruit and vegetable industrial wastewater. *Compr. Rev. Food Sci. Food Saf., 18(5)*: 1388-1402. DOI: 10.1111/1541-4337.12477.

Choong, Y Y; Chou, K W and Norli, I (2018). Strategies for improving biogas production of palm oil mill effluent (POME) anaerobic digestion: A critical review. *Renew. Sustain. Energy Rev., 82(August)*: 2993-3006. DOI: 10.1016/j.rser.2017.10.036.

Department of Environment Malaysia (1977). Environmental Quality (Prescribed Premises) (Crude Palm Oil) (Amendment) Regulation 1977. *Environ. Qual. Act 1974 (Act 127)*.

Edi, S (2022). Varying sustainability standards polarize vegetable oil market. ANN Asia News. https://asianews.network/varying-sustainability-standards-polarize-vegetable-oil-market/, accessed on 11 October 2023.

Faisal, M; Machdar, I; Gani, A and Daimon, H (2016). The combination of air flotation and a membrane bioreactor for the treatment of palm oil mill effluent. *Int. J. Technol.*, *7(5)*: 767-777. DOI: 10.14716/ijtech.v7i5.3163.

Hayyan, A; Alam, M Z; Mirghani, M E S; Kabbashi, N A; Hakimi, N I N M; Siran, Y M and Tahiruddin, S (2011). Reduction of high content of free fatty acid in sludge palm oil via acid catalyst for biodiesel production. *Fuel Process. Technol.*, *92(5)*: 920-924. DOI: 10.1016/j.fuproc.2010.12.011.

Hii, K L; Yeap, S P and Mashitah, M D (2012). Cellulase production from palm oil mill effluent in Malaysia: Economical and technical perspectives. *Eng. Life Sci.*, *12(1)*: 7-28. DOI: 10.1002/elsc.201000228.

Hui, K; Tang, J; Lu, H; Xi, B; Qu, C and Li, J (2020). Status and prospect of oil recovery from oily sludge: A review. *Arab. J. Chem.*, *13(8)*: 6523-6543. DOI: 10.1016/j.arabjc.2020.06.009.

Isa, M H; Wong, L P; Bashir, M J K; Shafiq, N; Kutty, S R M; Farooqi, I H and Lee, H C (2020). Improved anaerobic digestion of palm oil mill effluent and biogas production by ultrasonication pretreatment. *Sci. Total Environ.*, *722:* 137833. DOI: 10.1015/j.scitotenv.2020.137833.

Jahi, N; Ling, E S; Othaman, R and Ramli, S (2015). Modification of oil palm plantation wastes as oil adsorbent for palm oil mill effluent (POME). *Malaysian J. Anal. Sci.*, *19(1)*: 31-40.

Kamyab, H; Chelliapan, S; Din, M F M; Rezania, S; Khademi, T and Kumar, A (2018). Palm oil mill effluent as an environmental pollutant. *Palm Oil*, *(2)*: 13-28.

Laohaprapanon, T; Prasertsan, P and Kittikun, A H (2005). Physical and chemical separation of oil and suspended solids from palm oil mill effluent. *Asian J. Energy Environ.*, *6(1)*: 39-55.

Lee, Z S; Chin, S Y; Lim, J W; Witoon, T and Cheng, C K (2019). Treatment technologies of palm oil mill effluent (POME) and olive mill wastewater (OMW): A brief review. *Environ. Technol. Innov., 15*: 100377. DOI: 10.1016/j.eti.2019.100377.

Liew, A S B; Hadi, N A; Halim, R M; Yap, A and Rahman, Z A (2017). Methane avoidance via zero effluent discharge using aquaeco plant. *Proc. of PIPOC*. p. 1-15.

Loh, S K; Lai, M E; Ngatiman, M; Lim, W S; Choo, Y M; Zhang, Z and Salimon, J (2013). Zero discharge treatment technology of palm oil mill effluent. *J. Oil Palm Res.*, *25(3)*: 273-281.

Loh, S K; Nasrin, A B; Mohamad Azri, S; Nurul Adela, B; Muzzammil, N; Daryl Jay, T; Stasha Eleanor, R A; Lim, W S; Choo, Y M and Kaltschmitt, M (2017). First report on Malaysia's experiences and development in biogas capture and utilization from palm oil mill effluent under the Economic Transformation Programme: Current and future perspectives. *Renew. Sustain. Energy Rev.*, *74*: 1257-1274. DOI: 10.1016/j.rser.2017.02.066.

López-Bascón, M A and Luque de Castro, M D (2020). Soxhlet extraction. *Liquid Phase Extraction: Handbook in Separation Science.* University of Cardoba, Spain. p. 327- 327-354. DOI: 10.1016/B978-0-12-816911-7.00011-6.

Mahmod, S S; Arisht, S N; Jahim, J M; Takriff, M S; Tan, J P; Luthfi, A A I and Abdul, P M (2021). Enhancement of biohydrogen production from palm oil mill effluent (POME): A review. *Int. J. Hydrogen Energy*, *47(96)*: 40637-40655. DOI: 10.1016/j.ijhydene.2021.07.225.

Malaysia Department of Standards (2007). MS 814:2007 Palm oil - Specification (second revision). *Malaysian Stand.*, *814(MS 814:2007)*: 12.

Mecpro Heavy Engineering Limited (2022). Palm oil mill - Oil recovery from effluent water. https://www.mecpro.com/oil-recovery-from-pome.html, accessed on 14 June 2021.

Mohamed Anuar, M A; Amran, N A and Ruslan, M S H (2020). Effect of stirring rate and freezing time on the percentage of recovery of residual oil from palm oil mill effluent via a stirred freeze crystallizer. *IOP Conf. Ser. Mater. Sci. Eng.*, *778(1)*: 012171.

Mohammad, S; Baidurah, S; Kobayashi, T; Ismail, N and Leh, C P (2021). Palm oil mill effluent treatment processes -A review. *Processes*, *9(5)*: 1-22.

Mohammed, M E and Alhajhoj, M R (2020). Importance and applications of ultrasonic technology to improve food quality. *Food Process.*: 1-16. DOI: 10.5772/intechopen.88523.

MPOB (2022a). Production of crude palm oil in 2022. https://bepi.mpob.gov.my/index.php/production/286-production-2022/1092-production-of-crude-oil-palm-2022, accessed on 16 January 2023.

MPOB (2022b). MPOB daily malaysia prices of crude palm oil. https://bepi.mpob.gov.my/admin2/price_local_daily_view_cpo_msia.php?more=Y&jenis=1Y&tahun=2022, accessed on 28 June 2022.

Ngarmkam, W; Sirisathitkul, C and Phalakornkule, C (2011). Magnetic composite prepared from palm shell-based carbon and application for recovery of residual oil from POME. *J. Environ. Manage.*, *92(3)*: 472-479. DOI: 10.1016/j.jenvman.2010.08.031.

Nur Aisha, A W (2021). MPOB: Palm oil industry remains resilient under MCO. *Malay Mail*. https://www.malaymail.com/news/malaysia/2021/08/28/mpob-palm-oil-industry-remains-resilient-under-mco/2001119, accessed on 20 April 2023.

Ogunkunle, O and Ahmed, N A (2019). A review of global current scenario of biodiesel adoption and combustion in vehicular diesel engines. *Energy Reports*, *5*: 1560-1579. DOI: 10.1016/j.egyr.2019.10.028.

Perera, C O and Alzahrani, M A J (2021). Ultrasound as a pre-treatment for extraction of bioactive compounds and food safety: A review. *LWT, 142*: 111114. DOI: 10.1016/j.lwt.2021.111114.

Philemon, Z B 'o and Benoît, N M (2013). Treatment of conditioned oily sludge from Cameroon petroleum refinery by centrifugation. *Int. J. Environ. Sci.*, *3(5)*: 1373-1382.

Putri Primandari, S R; Yaakob, Z; Mohammad, M and Mohamad, A B (2013). Characteristics of residual oil extracted from palm oil mill effluent (POME). *World Appl. Sci. J.*, *27(11)*: 1482-1484.

Semilin, V; Janaun, J; Chung, C H; Touhami, D; Haywood, S K; Chong, K P; Yaser, A Z and Zein, S H (2021). Recovery of oil from palm oil mill effluent using polypropylene micro/nanofiber. *J. Hazard. Mater.*, *404*: 124144. DOI: 10.1016/j.jhazmat.2020.124144.

Suslick, K S (1998). Sonochemistry. *Jirk-Othmer Encyclodpedia of Chemical Technology.* 4th edition. New York: John Wiley & Sons, Inc. p. 516-541.

Suwanno, S; Rakkan, T; Yunu, T; Paichid, N; Kimtun, P; Prasertsan, P and Sangkharak, K (2017). The production of biodiesel using residual oil from palm oil mill effluent and crude lipase from oil palm fruit as an alternative substrate and catalyst. *Fuel*, *195*: 82-87. DOI: 10.1016/j.fuel.2017.01.049.

Suzuki, D; Sato, Y; Kamasaka, H; Kuriki, T and Tamura, H (2020). Oiling-out effect improves the efficiency of extracting aroma compounds from edible oil. *NPJ Sci. Food*, *4(18)*: 1-11. DOI: 10.1038/s41538-020-00079-8.

Tang, Y M; Wong, W Y; Tan, K T and Wong, L P (2021). Enhanced oil recovery from palm oil mill effluent using ultrasonication technique. *IOP Conf. Ser. Earth Environ. Sci.*, *945(1)*: 012042.

Teh, S S; Ong, A S H and Mah, S H (2017). Recovery and utilization of palm oil mill effluent source as value-added food products. *J. Oleo Sci.*, *66(11)*: 1183-1191. DOI: 10.5650/jos.ess17078.

Wahi, R; Chuah Abdullah, L; Nourouzi Mobarekeh, M; Ngaini, Z and Choong Shean Yaw, T (2017). Utilization of esterified sago bark fibre waste for removal of oil from palm oil mill effluent. *J. Environ. Chem. Eng.*, *5(1)*: 170-177.

Wan Sharifudin, W S S A; Sulaiman, A; Mokhtar, N; Baharuddin, A S; Tabatabaei, M; Busu, Z and Subbian, K (2015). Presence of residual oil in relation to solid particle distribution in palm oil mill effluent. *BioResources*, *10(4)*: 7591-7603.

Wang, J; Mahmood, Q; Qiu, J P; Li, Y S; Chang, Y S; Chi, L N and Li, X D (2015). Zero discharge performance of an industrial pilot-scale plant treating palm oil mill effluent. *Biomed Res. Int.*, *2015*: 1-9. DOI: 10.1155/2015/617861.

Wells, M J M (2003). Principles of extraction and the extraction of semivolatile organics from liquids. *Sample Preparation Techniques in Analytical Chemistry*, *(2)*: 37-225.

Wong, L P; Isa, M H; Bashir, M J K and Guo, X X (2019). Optimization of ultrasound irradiation for palm oil mill effluent. *IOP Conf. Ser. Earth Environ. Sci.*, *344(1)*: 012008.

Yashni, G; Al-Gheethi, A; Radin Mohamed, R M S; Arifin, S N H and Mohd Salleh, S N A (2020). Conventional and advanced treatment technologies for palm oil mill effluents: A systematic literature review. *J. Dispers. Sci. Technol., 42(12)*: 1766-1784. DOI: 10.1080/01932691.2020.1788950.

Yeoh, M L and Goh, C S (2022). Hydrotreated vegetable oil production from palm oil mill effluents: Status, opportunities and challenges. *Biofuels, Bioprod. Biorefining*, *16(5)*: 1153-1158.

Zuber, M A; Ithnin, A M; Yahya, W J; Wahab, A D A and Ahmad, M A (2018). Performance of sludge palm oil combustion using waste oil burner. *J. Adv. Res. Fluid Mech. Therm. Sci.*, *49(1)*: 55-61.

Zulqarnain; Yusoff, M H M; Ayoub, M; Nazir, M H; Zahid, I; Ameen, M; Abbas, W; Shoparwe, N F and Abbas, N (2021). Comprehensive review on biodiesel production from palm oil mill effluent. *ChemBioEng Rev.*, *8(5)*: 439-462.

JOURNAL OF OIL PALM RESEARCH

GUIDE FOR AUTHORS

(for more details, kindly surf http://jopr.mpob.gov.my)

Type of Articles

1. **Regular Article**
   Full-length original empirical investigations, consisting of introduction, materials and methods, results and discussion, conclusions. Original work must provide references and an explanation on research findings that contain new and significant findings. Conclusion should be brief and focus on the research output, should not be in point form. These papers should not exceed 6000 words of text (including tables, figures and references) and generally not more than a total of 10 figures and tables. After peer-review, the article word count limit can be extended to a maximum of 8000 words to better address the reviewers' and editors' comments. Any additional figures or tables can be included in the supplementary data. Please note that papers submitted to JOPR will be sent back to authors because of poor figure resolution or exceeding the number of figures permitted.

2. **Short Communication**
   Significant new information to readers of the Journal in a short but complete form. Preferably not exceeding 3000 words (including tables, figures and references), and is intended for rapid publication. They are not intended for publishing preliminary results or to be a reduced version of regular article.

3. **Review Article**
   Critical evaluation of materials about current research that have already been published by organising, integrating, and evaluating previously published materials. Re-analyses as meta-analysis and systemic reviews are encouraged. Review articles provide systemic overview, evaluation and interpretation of research in a given field. They should not exceed 12 000 words (excluding references only) and should contain no more than a total of 20 figures and tables. Any additional figures or tables can be included in the supplementary data. Please note that papers submitted to JOPR will be sent back to authors because of poor figure resolution or exceeding the number of figures permitted. The same information should not be repeated in a figure and a table.

Language

Please write your text in good English (only British English is accepted). We do not accept American English or a mixture of these.

JOPR's Template

JOPR's template, which is a standard format that facilitates the manuscript writing and copyediting process. This template is created to provide a detail and clear house style of JOPR. The template is drafted according to JOPR's house style, but in standard word version format. When writing a paper, authors need to format their papers to fit into the journal's house style. To make this easier, Word templates are available for many of other established journals, ready for them to download and apply to their research paper format. It is crucial for author to write a research paper while considering formatting. Each journal has its own guidelines for formatting; hence, the template defines how an article will look when it is published online or in print.

JOPR's Aims & Scope

This is established to provide a detail and clear aims and scope for author reference. Authors should declare in the cover letter how the research fits the aims and scope of JOPR.

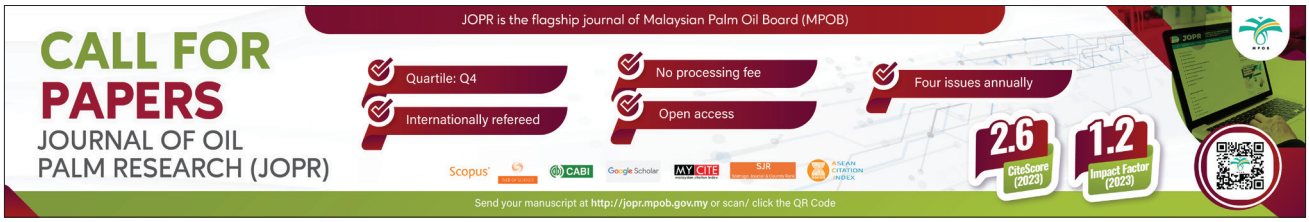
JOPR's House Style

A detail listing of JOPR's house style for authors and a checklist to facilitate the copyediting process and standardise the copyediting process. The JOPR's house style remains the same and is drafted into a detail version for author's reference.

Manuscript Submission

- Manuscripts should be submitted via: https://www2.cloud.editorialmanager.com/jopres/
- JOPR does not permit dual submission, publication and/or any archive platform (preprint) in violation of journal ethical practices.

For more details and to download the JOPR's House Style and Template, kindly surf http://jopr.mpob.gov.my



Contents of the Coming Issue
Journal of Oil Palm Research
Vol. 36 (4) December 2024*

- Patent Landscape Review on Modern Oil Palm Climatic Adaptation Strategies: Gaps and Opportunities
  Yeong Sheng Tey and Mark Brindal

- Biology and Behaviour of *Elaeidobius kamerunicus* Faust, 1898 (Coleoptera: Curculionidae) in Two Oil Palm Cultivars in Colombia
  Carlos Andrés Sendoya-Corrales; Norman Fabian Urrego-Morales; Jesús David Castaño-Martinez; Alex Enrique Bustillo and Anuar Morales Rodríguez

- Nutritive Screening and Forage Yield of Guinea and Hybrid Napier Grass Varieties Under Dense Shade of Mature Oil Palm Plantation
  Ramachandrudu Kummari; Narasimha Rao Bezawada and Manorama Kamireddy

- Structural Alteration of Oil Palm Empty Fruit Bunch by Peracetic Acid Combined with Ultrasonic Pretreatment for Xylanase Production by *Neosartorya* sp.
  Rama Mohan Poludasu; Benjamas Cheirsilp and Piyarat Boonsawang

- Determination of Triacylglycerol Composition and Its Content in Refined and Fractionated Palm Oil by Using LC-MS/MS with Multiple Neutral Loss Scan
  Seongeung Lee; Seungchul Baek; Siyoung Yang and Gyeonghweon Lee

- Development of Solid Fat Contentbased Predictive Model for Margarine Formula Design
  Jiajia Gong; Nanxi Shu; Xian Sun; Xinyu Cao; Yuanfa Liu and Yong-Jiang Xu

Note: * Subject to change.